WHY HAVE CORTICAL LAYERS? WHAT IS THE FUNCTION OF LAYERING? DO NEURONS IN CORTEX INTEGRATE INFORMATION ACROSS DIFFERENT LAYERS?

EDITED BY: Kathleen Rockland and Javier DeFelipe
PUBLISHED IN: Frontiers in Neuroanatomy

frontiers Research Topics

frontiers

ISSN 1664-8714
ISBN 978-2-88945-660-4
DOI 10.3389/978-2-88945-660-4

About Frontiers

Frontiers is more than just an open-access publisher of scholarly articles: it is a pioneering approach to the world of academia, radically improving the way scholarly research is managed. The grand vision of Frontiers is a world where all people have an equal opportunity to seek, share and generate knowledge. Frontiers provides immediate and permanent online open access to all its publications, but this alone is not enough to realize our grand goals.

Frontiers Journal Series

The Frontiers Journal Series is a multi-tier and interdisciplinary set of open-access, online journals, promising a paradigm shift from the current review, selection and dissemination processes in academic publishing. All Frontiers journals are driven by researchers for researchers; therefore, they constitute a service to the scholarly community. At the same time, the Frontiers Journal Series operates on a revolutionary invention, the tiered publishing system, initially addressing specific communities of scholars, and gradually climbing up to broader public understanding, thus serving the interests of the lay society, too.

Dedication to Quality

Each Frontiers article is a landmark of the highest quality, thanks to genuinely collaborative interactions between authors and review editors, who include some of the world's best academicians. Research must be certified by peers before entering a stream of knowledge that may eventually reach the public - and shape society; therefore, Frontiers only applies the most rigorous and unbiased reviews.
Frontiers revolutionizes research publishing by freely delivering the most outstanding research, evaluated with no bias from both the academic and social point of view. By applying the most advanced information technologies, Frontiers is catapulting scholarly publishing into a new generation.

What are Frontiers Research Topics?

Frontiers Research Topics are very popular trademarks of the Frontiers Journals Series: they are collections of at least ten articles, all centered on a particular subject. With their unique mix of varied contributions from Original Research to Review Articles, Frontiers Research Topics unify the most influential researchers, the latest key findings and historical advances in a hot research area! Find out more on how to host your own Frontiers Research Topic or contribute to one as an author by contacting the Frontiers Editorial Office: researchtopics@frontiersin.org

WHY HAVE CORTICAL LAYERS? WHAT IS THE FUNCTION OF LAYERING? DO NEURONS IN CORTEX INTEGRATE INFORMATION ACROSS DIFFERENT LAYERS?

Topic Editors:
Kathleen Rockland, Boston University School of Medicine, United States
Javier DeFelipe, Universidad Politecnica de Madrid and Instituto Cajal (CSIC), Spain

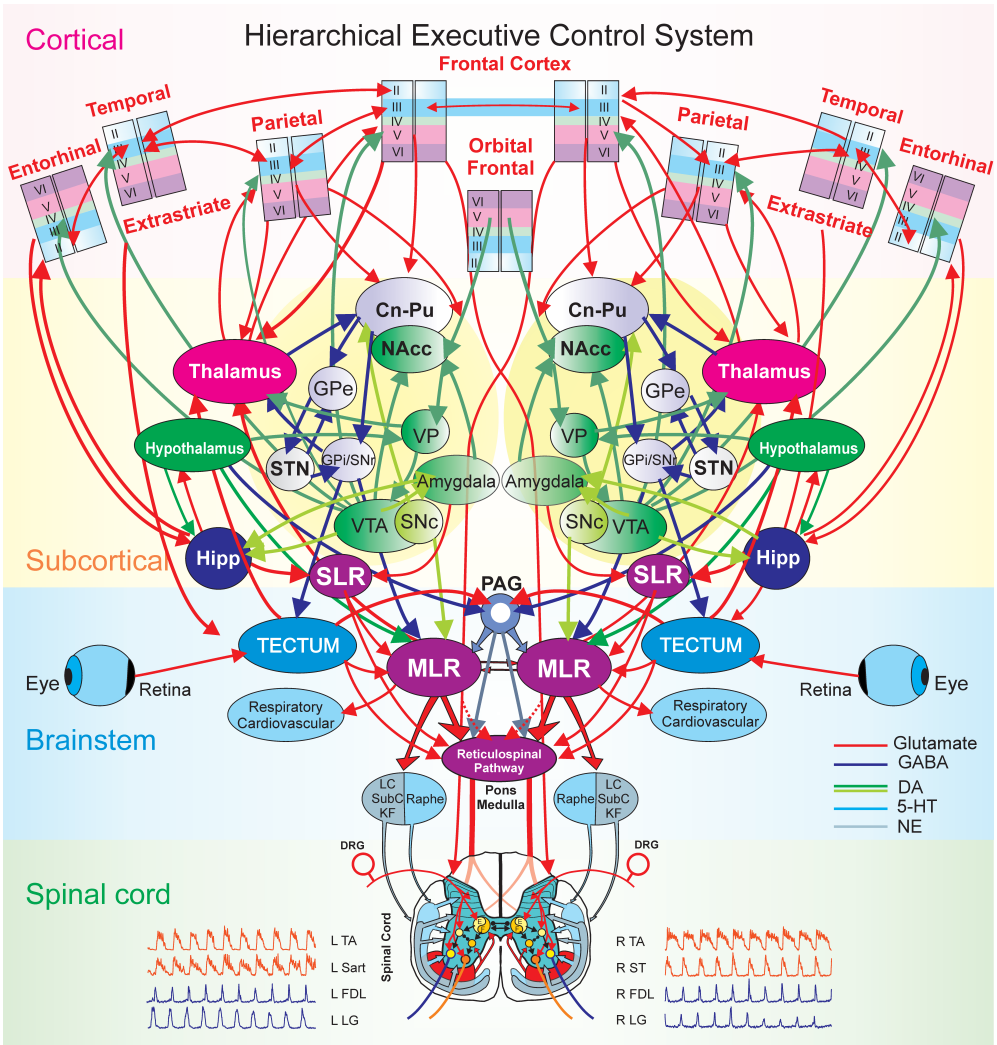

The hierarchical executive control system for movement. The executive control system is anatomically organized via a hierarchical architecture of cortical modules (layers, minicolumns with microcircuits), subcortical nuclei (basal ganglia and thalamus with cortical-subcortical-thalamic loops; hippocampus and hypothalamus), brainstem (midbrain, pons, medulla with cortical-brainstem networks), and spinal cord (locomotor central pattern generators, CPG). Figure from Opris I, Chang S and Noga BR (2017) What Is the Evidence for Inter-laminar Integration in a Prefrontal Cortical Minicolumn? *Front. Neuroanat.* 11:116. doi: 10.3389/fnana.2017.00116

Citation: Rockland, K., DeFelipe, J., eds (2018). Why Have Cortical Layers? What Is the Function of Layering? Do Neurons in Cortex Integrate Information Across Different Layers? Lausanne: Frontiers Media. doi: 10.3389/978-2-88945-660-4

Table of Contents

frontiers in Neuroanatomy

EDITORIAL
published: 09 October 2018
doi: 10.3389/fnana.2018.00078

Editorial: Why Have Cortical Layers? What Is the Function of Layering? Do Neurons in Cortex Integrate Information Across Different Layers?

Kathleen S. Rockland[1]* *and Javier DeFelipe*[2,3]*

[1] Anatomy and Neurobiology, School of Medicine, Boston University, Boston, MA, United States, [2] Universidad Politécnica de Madrid, Madrid, Spain, [3] Instituto Cajal, Madrid, Spain

Keywords: isocortex, insular cortex, olfactory, periallocortex, cell types, receptors, reeler, GABAergic connectivity

Editorial on the Research Topic

Why Have Cortical Layers? What Is the Function of Layering? Do Neurons in Cortex Integrate Information Across Different Layers?

This research topic brings together 14 articles dealing with the laminar organization of the neocortex. By convention, there are six cortical layers, but this organization may vary throughout the cerebral cortex of a given species or between species: many regions lack one or more layers, whereas in other regions there is good reason to consider more than six layers. An important perspective on neocortical lamination is thus the recognition that the cortical mantle is not homogeneous. With this in mind, we open with three articles discussing evolutionary comparisons of neocortex with non-neocortical, three-layer areas; namely, the hippocampal formation (Mercer and Thomson), periallocortical areas (Insausti et al.), and olfactory cortex (Shepherd and Rowe). Mercer and Thompson summarize and compare the development of the neocortex and hippocampus (mostly of the cat and monkey), the characteristics of their neurons, the circuits they form and the ordered, unidirectional flow of information from one hippocampal region, or one neocortical layer, to another. Insausti et al. focus on the main distinctions among the allocortex, periallocortex and isocortex, based on anatomical differences, in particular the number of layers, overall organization, appearance and connectivity. Finally, Shepherd and Rowe, discuss the possible existence of a basic cortical circuit that had its origin in the three-layer forebrain cortex of the ancestral amniote, that was conserved in non-avian reptiles, and that became elaborated in mammalian six-layer neocortex.

The laminar location of cortical neurons—their cell bodies—is determined during development. Two articles treat the developmental context. Popovitchenko and Rasin discuss transcriptional and post-transcriptional regulatory mechanisms related to pyramidal neuron genesis and migration in mice. González-Arnay et al. present new data on the derivation and migratory pathways of principal neurons in the insula cortex of fetal human brains, between 9 and 25 gestational weeks, including how these factors can relate to cytoarchitectonic diversity in the adult.

Cortical layers are deceptive—there and not there (as, the Cheshire Cat); conspicuously identifiable, but only when one stays within the classical cytoarchitectonic criteria of soma size and neuronal packing density. Notably, as reviewed by Narayanan et al. multiple cell types intermingle within the layers, and dendrites and local axons extend across multiple layers. These authors identify several cross-laminar patterns and propose 10 excitatory cell-type patterns with an orderly

OPEN ACCESS

Edited by:
Zoltan F. Kisvarday, University of Debrecen, Hungary

Reviewed by:
Noritaka Ichinohe, National Center of Neurology and Psychiatry, Japan

***Correspondence:**
Kathleen S. Rockland
krock@bu.edu
Javier DeFelipe
defelipe@cajal.csic.es

Received: *08 August 2018*
Accepted: *11 September 2018*
Published: *09 October 2018*

Citation:
Rockland KS and DeFelipe J (2018) Editorial: Why Have Cortical Layers? What Is the Function of Layering? Do Neurons in Cortex Integrate Information Across Different Layers? Front. Neuroanat. 12:78. doi: 10.3389/fnana.2018.00078

relation to laminar landmarks in rat barrel cortex. Larkum et al., reviewing fMRI data, similarly make a case that a simplified schema of "point neurons" is inadequate to convey the distributed functional properties of the neuronal arborization as this samples across layers.

Taking a global perspective, Opris et al. present data from biomorphic multielectrode arrays in support of laminar specific specializations for perceptual or executive circuits in the dorsolateral prefrontal cortex of nonhuman primates, and further argue on this basis for inter-laminar integration.

What about cortical connections? These are well-known to evince a laminar-specific bias, although important details, variability, and functional significance remain only sketchily understood. In their overview based on mouse visual cortex, D'Sousa and Burkhalter talk about layer-specific patterns of extrinsic connections, but suggest these might observe a gradient-like organization, rather than a sharp distinction of "feedforward" ("driving") and "feedback" properties (respectively, "driving" and "modulatory").

In the interaction of pre-synaptic inputs and their postsynaptic targets, receptors play an important role, and their orderly distribution is suggestive of layer-specific (or layer-biased) signaling mechanisms. These are discussed by Santana and Artigas (review: rat medial prefrontal cortex) and Zilles and Palomero-Gallagher (original research: human). These latter discuss the interesting result that receptor densities are not uniform across areas but segregate into definable area-specific clusters (a.k.a.,"fingerprints"). Radnikow and Feldmeyer further review layer- and cell-type specific differences in the effects of neuromodulator receptors on excitatory neurons of different cortical layers, with considerations of axonal projection patterns and their target structures.

Fish et al. use new quantitative fluorescent microscopy techniques to address the amount and type of GABAergic inhibition in different layers of human postmortem tissue of prefrontal cortex. Findings are discussed in the context of the laminar distribution of differentiable GAD+ terminations, GABAergic cell bodies, and their intracortical local connectivity.

Finally, in a paradoxical conclusion, Guy and Staiger review the relatively normal functioning of reeler mice, despite the severe disruption of their cortical lamination. They conclude that cortical layers *per se* are not an essential component for *basic* perception and cognition.

In summary, different cortical layers have distinct transcriptomic profiles, neurochemical attributes, connectivity patterns, number and types of synapses and many other structural attributes. There is evidence for cross-laminar integration. Nevertheless, results based on anatomy, or physiology or imaging leave largely unanswered, What is the function of each cortical layer? What do the different layers do? Thus, while lamination can be seen as inherent to neocortical organization, important questions remain open or only partially answered. Moving forward, can we refine these questions to be more approachable?

AUTHOR CONTRIBUTIONS

JD and KR collaborated together in initiating this Topic, and in writing the Editorial and Introduction.

Conflict of Interest Statement: The authors declare that the research was conducted in the absence of any commercial or financial relationships that could be construed as a potential conflict of interest.

frontiers in Neuroanatomy

REVIEW
published: 26 September 2017
doi: 10.3389/fnana.2017.00083

Cornu Ammonis Regions–Antecedents of Cortical Layers?

Audrey Mercer and Alex M. Thomson**

Department of Pharmacology, School of Pharmacy, University College London, London, United Kingdom

Studying neocortex and hippocampus in parallel, we are struck by the similarities. All three to four layered allocortices and the six layered mammalian neocortex arise in the pallium. All receive and integrate multiple cortical and subcortical inputs, provide multiple outputs and include an array of neuronal classes. During development, each cell positions itself to sample appropriate local and distant inputs and to innervate appropriate targets. Simpler cortices had already solved the need to transform multiple coincident inputs into serviceable outputs before neocortex appeared in mammals. Why then do phylogenetically more recent cortices need multiple pyramidal cell layers? A simple answer is that more neurones can compute more complex functions. The dentate gyrus and hippocampal CA regions—which might be seen as hippocampal antecedents of neocortical layers—lie side by side, albeit around a tight bend. Were the millions of cells of rat neocortex arranged in like fashion, the surface area of the CA pyramidal cell layers would be some 40 times larger. Even if evolution had managed to fold this immense sheet into the space available, the distances between neurones that needed to be synaptically connected would be huge and to maintain the speed of information transfer, massive, myelinated fiber tracts would be needed. How much more practical to stack the "cells that fire and wire together" into narrow columns, while retaining the mechanisms underlying the extraordinary precision with which circuits form. This demonstrably efficient arrangement presents us with challenges, however, not the least being to categorize the baffling array of neuronal subtypes in each of five "pyramidal layers." If we imagine the puzzle posed by this bewildering jumble of apical dendrites, basal dendrites and axons, from many different pyramidal and interneuronal classes, that is encountered by a late-arriving interneurone insinuating itself into a functional circuit, we can perhaps begin to understand why definitive classification, covering every aspect of each neurone's structure and function, is such a challenge. Here, we summarize and compare the development of these two cortices, the properties of their neurones, the circuits they form and the ordered, unidirectional flow of information from one hippocampal region, or one neocortical layer, to another.

Keywords: neocortex, hippocampus, pyramidal cells, interneurones, development, neuronal circuitry, neocortical columns

OPEN ACCESS

Edited by:
Javier DeFelipe,
Cajal Institute (CSIC), Spain

Reviewed by:
Tamas F. Freund,
Institute of Experimental Medicine (MTA), Hungary
Ricardo Insausti,
Universidad de Castilla-La Mancha, Spain

****Correspondence:***
Audrey Mercer
a.mercer@ucl.ac.uk
Alex M. Thomson
alex.thomson@ucl.ac.uk

Received: *01 June 2017*
Accepted: *08 September 2017*
Published: *26 September 2017*

Citation:
Mercer A and Thomson AM (2017) Cornu Ammonis Regions–Antecedents of Cortical Layers? Front. Neuroanat. 11:83. doi: 10.3389/fnana.2017.00083

On his deathbed in 1934, Santiago Ramón y Cajal wrote to his last student, Rafael Lorente de Nó, continuing a life-long discussion: *"the mouse is not a good choice for the study of cortical circuits because of its paucity of short-axon cells..."*[*].

[*]Ramón y Cajal S. Letter to Lorente. 1934. Courtesy of Dr Francisco Alvarez, translation by Rafael Yuste. Lorente de Nó, like many since, did not agree.

PRINCIPAL CELLS

Origins of Principal Cells in the Neocortex

This section draws heavily upon many excellent reviews (Nadarajah and Parnavelas, 2002; López-Bendito and Molnár, 2003; Cheung et al., 2007; Molnár et al., 2012; Tabata et al., 2012; Evsyukova et al., 2013; Tan and Shi, 2013; Sekine et al., 2014; Hoerder-Suabedissen and Molnár, 2015; Kawauchi, 2015; Molnár and Hoerder-Suabedissen, 2016). (Montiel et al., 2016, Figure 1; https://www.ncbi.nlm.nih.gov/pmc/articles/PMC4832283/figure/cne23871-fig-0001/).

Principal cells, i.e., glutamatergic, spiny excitatory pyramidal and spiny stellate cells are generated in the ventricular zone (VZ) from asymmetrical division of progenitor radial glial cells (Miyata et al., 2001; Noctor et al., 2001) or basal progenitors in the subventricular zone (Noctor et al., 2004; Shitamukai et al., 2011; Wang et al., 2011). Post-mitotic neurones then move to the multipolar cell accumulation zone (MAZ) just above VZ. There they stay (1–3 days: Kitazawa et al., 2014), extending and retracting multiple fine processes (Tabata and Nakajima, 2003; Tabata et al., 2009), until they begin to move toward the intermediate zone (IZ) below the cortical plate (CP, future gray matter). In IZ, the neurones become bipolar and "climb" through the CP toward the marginal zone (MZ), using the process of a single radial glial cell as a scaffold (Rakic, 1972; http://rakiclab.med.yale.edu/research/; Kawauchi, 2015 Figures 1, 2, https://www.ncbi.nlm.nih.gov/pmc/articles/PMC4595654/figure/F1/; https://www.ncbi.nlm.nih.gov/pmc/articles/PMC4595654/figure/F2/). Their leading process becomes anchored in MZ, they part company with their radial glial partners and their somata are pulled up to lie beneath MZ, or CP (Nadarajah et al., 2001; Sekine et al., 2011; Kitazawa et al., 2014).

The earliest born pyramidal cells form the deepest layer, L6. As later born neurones migrate, they pass through L6, forming sequentially more superficial layers. Phylogenetically, development of an additional germinal layer, the subventricular zone (SVZ) coincides with the appearance of L2-4 and emergence of the mammalian six layered neocortex (Noctor et al., 2004; Wu et al., 2005); the layers of phylogenetically older, three layered cortices being considered equivalent to L1, L5, and L6. The primate goes further, adding an additional germinal layer, the outer subventricular zone (OSVZ) (Lukaszewicz et al., 2005), which in the Macaque results in correspondingly deeper supragranular layers (Hoerder-Suabedissen and Molnár, 2015; Montiel et al., 2016). (Molnár et al., 2006, Figures 5, 7, https://www.ncbi.nlm.nih.gov/pmc/articles/PMC1931431/figure/F5/; https://www.ncbi.nlm.nih.gov/pmc/articles/PMC1931431/figure/F7/).

Origins of Principal Cells in the Hippocampus

Hippocampal CA regions are often considered to contain a single pyramidal cell layer, though developing CA regions also include neurones generated in SVZ (Kitazawa et al., 2014). Whether this population remains distinct from those arising in VZ is unclear. Likewise, whether there is an ordered, birth-date-dependent, inside-out layering of *stratum pyramidale* in hippocampal CA regions appears a matter for debate. However, while there may not be the wide range of pyramidal classes to be found in neocortex, CA1 pyramids are not all identical; to quote Lorente de Nò (1934) "*There are two types of pyramids, superficial and deep ones. The superficial are arranged in one or two very dense rows. The deep pyramids are grouped into several less dense rows below.…*"

"Deep" refers to the earliest born cells whose migration terminates close to the germinal layers, adjacent to the ventricles, cells destined to lie adjacent to *stratum oriens* (Supplementary Figure 1. http://uclsop.net/interneuron-reconstruction/ca1-pyramid). Superficial pyramids, lying adjacent to the future *stratum radiatum*, are born 1–2 days later, contain the calcium binding protein, Calbindin (Cb), Zinc (Slomianka and Geneser, 1997) and reelin and are more commonly dye-coupled, one with another (indicative of electrical gap junctions) than pyramids devoid of Cb (Baimbridge et al., 1991; Mercer et al., 2006; Mercer, 2012 for review). They also express different transcription factors (similar to deep/superficial expression in neocortex: Britanova et al., 2005; Dobreva et al., 2006; Leone et al., 2008); the deep cells expressing Sox5 and the superficial cells, SatB2 (Slomianka et al., 2011) and Zbtb20 (Xie et al., 2010), which may control Cb-expression (Nielsen et al., 2010). Even in CA regions disrupted by mutations, like Reeler, pyramids maintain separate identities, forming distinct—if mislocated—layers. Later born cells spend longer in MAZ; regions of IZ devoid of cell bodies, become filled with axons after early born cells have passed through (Kitazawa et al., 2014) and connections with these axons may delay migration of later born multipolar neurones (Altman and Bayer, 1990b). Later born superficial pyramids fire earlier, with higher probability during sharp wave ripples, while deep pyramids more frequently exhibit place fields, fields that are more plastic. Deep pyramidal firing correlates more with specific landmarks, superficial with general context (Geiller et al., 2017, for review).

The CA3 hippocampal plate (HP, future *stratum pyramidale*) becomes apparent at E18 (rat), expanding to adopt its pronounced curved profile by E22 (Altman and Bayer, 1990b). This expansion presents long migration paths for neurones generated in VZ, especially those destined to lie near the dentate gyrus. Radial movement from the tangential migratory stream into developing CA3 *stratum pyramidale* is promoted by Math2 (transcription factor), while continued tangential migration toward the developing dentate gyrus is promoted by Prox-1 (Sugiyama et al., 2014). CA3 pyramids are—on average—born earlier than CA1 neurones (E16-E20); with those that will lie close to CA1 born first (Bayer, 1980; Altman and Bayer, 1990b,a). Like CA1 pyramids, newly generated CA3 pyramidal

cells move from VZ to MAZ, becoming multipolar and waiting there longer than CA1 cells (Nakahira and Yuasa, 2005); possibly for innervation from dentate gyrus (Altman and Bayer, 1990b). That neurones born at the same time in dentate gyrus and CA regions, exhibit similar gene expression patterns and become preferentially connected with each other (Deguchi et al., 2011), has important implications for functional circuitry.

A distinct CA2 region, delineated by PCP4 immunostaining, is thought to emerge postnatally and to reach adult dimensions at P21 (San Antonio et al., 2014). Until relatively recently, rodent hippocampi were thought not to contain a CA2 region and further developmental detail has yet to materialize.

Sister Cells and Local Connectivity

Future neocortical pyramids climb radially, up a single, straight, radial glial process to reach their final destination. Sister cells, resulting from divisions of a single progenitor, therefore come to lie in a narrow, radially oriented "column." "The Radial Unit Hypothesis," proposed by Rakic (1988) as the anatomical basis for neocortical columnar architecture (Mountcastle, 1957), states that the position of a neurone's precursor in VZ determines its final horizontal coordinates, while its birth date determines its radial position.

In contrast, sister CA pyramids become distributed horizontally, often across large areas of *stratum pyramidale* (Kitazawa et al., 2014; Sugiyama et al., 2014). The leading processes of radial glial cells that direct migration here are not always straight, or radially oriented, as in neocortex. In CA1, they often curve, to run almost parallel with layer boundaries (Nakahira and Yuasa, 2005). In addition, migrating multipolar neurones continue to extend and retract processes in HP, contacting several radial glial cells, selecting one and migrating along a different path, in a "zig-zag" manner (Nowakowski and Rakic, 1979; Kitazawa et al., 2014; Xu et al., 2014; Hayashi et al., 2015, for review).

This raises an interesting question about local pyramidal interconnectivity. Neocortical pyramidal cells preferentially innervate their sisters (Yu et al., 2009; Costa and Hedin-Pereira, 2010), which exhibit, for example, similar orientation preferences in primary visual cortex, V1 (Li et al., 2012). Electrical coupling may precede sister-to-sister chemical synapse-formation since this similarity in orientation preference is lost when gap junctions are blocked from P1-7, or Cx26 (connexin 26) mutated (Li et al., 2012). If similar orientation preferences do not result solely from another influence, such as preferential innervation of sister-cells by common afferent axons, the physical separation of sister neurones may be a significant factor in determining whether they "wire together."

In both mature neocortex and CA regions, powerful electrical synapses form between closely neighboring pyramids (CA1, Baimbridge et al., 1991; CA1-3, neocortex, Mercer et al., 2006; Mercer, 2012); an average of 25% of steady state and 10% peak action potential (AP) voltage change transferring to the coupled cell. The resultant post-junctional "spikelets" can trigger overshooting APs. Quite unlike electrical junctions between interneurones (neocortex: Gibson et al., 1999; Tamás et al., 2000; Amitai et al., 2002; Simon et al., 2005; hippocampus: Fukuda and Kosaka, 2000; Meyer et al., 2002; Allen et al., 2011), these junctions form between somata and proximal apical dendrites; hence the very high electrical-coupling ratios. Vertically distributed neocortical sister-cells are, therefore, well positioned for such connections; horizontally distributed sister-CA pyramids are not (unless axon-axonic electrical junctions are also involved: Schmitz et al., 2001; Wang et al., 2010). However, other factors, such as the preferential innervation of CA1 pyramids by CA3 pyramids exhibiting similar gene expression patterns (Deguchi et al., 2011), may also contribute to the emergence of functionally related sister-cell groups across regions. Indeed, CA1 sister pyramids rarely develop electrical or chemical synapses with each other, but they do receive common input from nearby fast-spiking (FS, but not non-FS) interneurones and exhibit synchronous synaptic activity, indicative of common excitatory drive (Xu et al., 2014). During development, early born GABAergic "hub" neurones with long range connections (which later develop into projection interneurones: Picardo et al., 2011) facilitate such connectivity (Bonifazi et al., 2009; Villette et al., 2016). Spiny cells connected by chemical synapses receive common excitatory (Song et al., 2005; Yoshimura and Callaway, 2005; Kampa et al., 2006) and inhibitory inputs (Xu et al., 2014) and deliver coincident outputs, more frequently than unconnected cells, and input-convergence from electrically coupled pyramids via chemical synapses is high (5:11, Bannister and Thomson, 2007).

Development of the Wide Range of Neocortical Pyramidal Cell Classes

(**Table 1**; Cheung et al., 2007; Hoerder-Suabedissen and Molnár, 2012, 2013, 2015; Hayashi et al., 2015, for reviews).

Both the inside out, sequential formation of L2-L6 and the sequential generation of the different classes of pyramids destined for a single layer, ensure a shifting environment as new cells are born and begin to migrate. Distinct expression patterns of a large array of genes coding for transcription factors and regulators, growth factors, receptors, peptidase inhibitors, acetylation regulatory factors, glycoproteins, kinases, guidance-, signal-, adhesion-, and extracellular matrix- molecules, reelin, its receptors and their downstream signaling pathways, not to mention those genes for which no function has yet been found, have been identified in sub-populations of progenitors and differentiating neurones. The milieu into which a neurone is born, those it travels through as it migrates from VZ/SVZ, through MAZ, IZ and into CP/HP and where it eventually establishes itself, are both temporally and spatially regulated. One example is the postmitotic expression of Sox5 in subcortically projecting deep layer pyramids and Satb2 in corticocortically projecting, superficial layer cells (Slomianka et al., 2011). The latter, if induced to express Sox5 ectopically, lose their corticocortical projections and instead project subcortically (Arlotta et al., 2005; Alcamo et al., 2008; Britanova et al., 2008; Fishell and Hanashima, 2008, for review).

Neocortical Layer 6 Pyramidal Cells

Like other layers, L6 contains several distinct classes of spiny, glutamatergic principal cells (Thomson, 2010 for review).

TABLE 1 | Summary of properties of pyramidal cells in cortical layers 3–6, for references, see text.

Layer 6 spiny cell type	Structural features		Excitatory inputs	Outputs	Firing characteristics
	Dendrites	Axons			
L6 Cortico-thalamic pyramidal cells	Small-medium, upright pyramidal cells. Apical dendritic tuft in L4	Axon ascending to L4 (some also to lower L3). Drumstick-like branches in L4	Reciprocal from specific thalamic nuclei. From L6 cortico-cortical pyramids	To specific thalamic nuclei and nRT. Local outputs predominantly to L6-L4 GABAergic interneurones (synapses on shafts of aspiny dendrites). Facilitating EPSPs to all targets	Modest Accommodation and Adaptation. Almost tonic discharge in response to maintained depolarization.
L6 Cortico-thalamic pyramidal cells	Short, small-medium, upright pyramidal cells. Apical dendritic tuft in L5	Ascending to L5. Some with drumstick-like branches	Thalamus. L6 cortico-cortical pyramids	To specific and non-specific thalamus and local L5/6 interneurones. Facilitating EPSPs to all targets	Modest Accommodation and Adaptation. Almost tonic discharge in response to maintained depolarization.
L6 Cortico-cortical pyramidal cells (latexin positive)	Small-medium "pyramids."Dendrites confined to L5/6. Several structural classes: short upright pyramids, bipolar, inverted and multipolar "pyramids"	Long horizontal branches confined to L5/6	Other local and distant cortical neurones	Preferentially innervate cortical pyramids with depressing EPSPs	Rapidly and powerfully adapting. Spike inactivation can be "rescued" with ramp-shaped current
L6 Claustrum-projecting pyramidal cells	Tall, upright, long thin apiical dendrite to L1-no tuft	Long horizontal branches confined to L5/6	Other local and distant cortical neurones	Claustrum, L5/6 pyramids with depressing EPSPs	Near tonic firing
Layer 5 spiny cell type	**Structural features**		**Excitatory inputs**	**Outputs**	**Electrophysiology**
	Dendrites	**Axons**			
L5 Large burst-firing pyramids, upper L5	Thick basal dendrites L5, Thick apical with tuft L3-L1	Largely confined to deep layers, short branches	Local inputs include other large and small L5 cells and a powerful focused input from deep L3 as well as distant cortical and subcortical. Most inputs accocunted for	To non-specific thalamic nuclei, superior colliculus, pons, spinal cord (targets depending on cortical region). Depressing EPSPs to most targets	Intrinsic burst-firing superimposed on a depolarizing envelope. Resting Potential *in vitro* near firing threshold.
L5 smaller cortico-thalamic pyramids	Smaller upright pyramids. Slender apical dendrites terminating in L2/3 with little/no tuft	Ascending to L2/3 and horizontal branches	No reciprocal input from thalamus	Large boutons to non-specific thalamus. Depressing EPSPs	Adapting and accommodating firing pattern
L5 smaller cortico-cortical pyramids, incl. transcallosally projecting cells	Smaller upright pyramids. Slender apical dendrites terminating in L2/3 with little/no tuft	Long horizontally oriented	Other cortical pyramidal cells, local and distant	Local and distant cortical neurones with largely depressing EPSPs	Radidly adapting and accommodating firing pattern
Layer 4 spiny cell type	**Structural features**		**Excitatory inputs**	**Outputs**	**Electrophysiology**
	Dendrites	**Axons**			
L4 pyramidal cells predominantly innervating L4 cells	Often small, simple cells. A modest number of slender dendrites, basals in L4, apical obliques in L3, with a tuft in L1	Local axonal arbor and a descending arbor with sparse branching in L5 and/or L6	From local L4 cells (28% of input), 6% from specific thalamus (large, potent *en-passant* boutons on dendritic shafts), 45% from L6 corticothalamic (small boutons, on spines). Almost none from L3. Remainder currently unaccounted for	Predominantly other L4 cells. Strength and probability falling off rapidly with separation. Proximal, basal dendritic inputs. Brief, depressing EPSPs	Rapidly adapting and accommodating

(Continued)

TABLE 1 | Continued

Layer 4 spiny cell type	Structural features		Excitatory inputs	Outputs	Electrophysiology
	Dendrites	Axons			
L4 pyramidal cells preferentially innervating L3 cells	Often small, simple cells. A modest number of slender dendrites, basals in L4, apical obliques in L3, with a tuft in L1	Strong, ascending, topographically precise input to L3 and descending projection with sparse branching in L5 and/or L6		Predominantly to L3 cells. Pyramids more than interneurones. Proximal, basal dendritic inputs. Brief, depressing EPSPs	Brief, short interspike interval spike train followed by brief afterdepolartization, slow hyperpolarization then tonic firing
L4 Spiny stellate cells	Often small, simple cells, with slender dendrites largely confined to L4. No apical dendrite	Ascending topographically precise input to L3, descending projection with sparse branching in L5			Probably similar to the above
Layer 3 spiny cell type	**Structural features**		**Excitatory inputs**	**Outputs**	**Electrophysiology**
	Dendrites	**Axons**			
L3 pyramidal cells	Well developed basal and apical oblique dendrites and a tuft in L1. Largest cells close to L4 border	Dense, fairly narrow ramifications in L3 and L5, not in L4 (but see text for mouse)	Inputs from L4 and thalamus to deep L3 proximal basal dendrites. Tall, brief, depressing EPSPs. High hit-rate inputs from other local L3 pyramids. Cortical and thalamic inputs account for most synapses. 97% of L3 pyramid-pyramid inputs onto spines of less proximal basal and apical oblique dendrites	Dense local innervation of L3 pyramids and interneurones and patchy, long distance terminal axonal arbors. Dense, very high probability innervation of large (not small) L5 pyramids sharing the same vertical axis. To interneurones in L4 that have dendrites in L3, but not to spiny L4 cells. Transcallosal projections	Very negative resting potentials −80mV *(in vitro)*. "Typical" adapting/accommodating pyramidal cells

With the exception of presynaptic L6 cortico-thalamic pyramids, all pyramidal inputs to FS, parvalbumin-immunopositive interneurones recorded were depressing and all excitatory inputs to SOM cells were facilitating.

Few studies in L4 have systematically correlated anatomy with electrophysiology and connectivity. Some characteristics, like their inputs and the descending projections may, or may not be common to 2 or more subclasses.

The birth-dates of two broad groups are distinguished by their expression of latexin (carboxypeptidase-A inhibitor). Corticortical cells, which express latexin are born after corticothalamic cells which do not: E15 *cf* E14 (Arimatsu and Ishida, 2002). (Thomson and Lamy, 2007, Figure 5, https://www.ncbi.nlm.nih.gov/pmc/articles/PMC2518047/figure/F5/).

Only earlier born, corticothalamic pyramids receive direct thalamic input. One subclass of these upright cells, with apical dendritic tufts in L4, send narrow, ascending axonal arbors to L4 (and sometimes lower L3) where it terminates with characteristic short, drumstick-like side branches. These neurones project subcortically to "specific," or primary sensory thalamic nuclei and to *nucleus reticularis thalami* (nRT, the thalamic inhibitory nucleus) (Zhang and Deschenes, 1998). All L6 corticothalamic pyramids fire with minimally accommodating/adapting, near tonic discharge and preferentially innervate GABAergic cells with consistently facilitating patterns of transmitter release (West et al., 2006). In neocortex, >90% of their synaptic boutons contact dendritic shafts of non-spiny neurones (White and Keller, 1987), including L4 (Tarczy-Hornoch et al., 1999; Beierlein et al., 2003) and L5 interneurones (Staiger et al., 1996). Despite their frequent innervation of parvalbumin (PV) interneurones (which receive depressing inputs from all other pyramidal classes), L6 corticothalamic pyramids elicited facilitating EPSPs (excitatory postsynaptic potentials) in *all* cell types studied, including ventroposterior, posterior medial thalamic and nRT neurones. This contrasts with the depressing EPSPs elicited by L5 pyramids in posterior medial thalamic nucleus (Reichova and Sherman, 2004).

The second corticothalamic subclass, more commonly found in deep L6, projects to *both* specific and non-specific thalamic regions such as PO (posterior thalamic group) The apical dendrites of these short, upright pyramids and their ascending axons typically terminate in upper L5. Neither subgroup of corticothalamic cells has long horizontal axon collaterals in the infragranular layers, all branches turn toward the pial surface.

In cats and primates, where L4 subdivisions are morphologically and functionally distinct, subclasses of

corticothalamic cells are found, each with its apical dendritic branches and axonal ramifications restricted to a specific L4 sublayer (Lund, 1987; Wiser and Callaway, 1996). Further specificity was demonstrated by a study combining *in vivo* physiology and morphology in cat V1 (Hirsch et al., 1998a,b). L6 pyramidal simple cells ("simple" implying significant direct input from lateral geniculate nucleus, LGN and resembling "specific" thalamocortical pyramids) targeted L6 and/or L4, layers rich in simple cells. L6 complex cells (receiving integrated, rather than "specific" corticothalamic inputs), targeted L2/3 and L5, layers rich in complex cells.

In striking contrast to corticothalamic pyramidal cells, are the rapidly adapting, corticocortical L6 pyramids, which preferentially innervate other pyramidal cells with "depressing" synapses and display an array of morphologies (Mercer et al., 2005), short, upright pyramids whose apical dendrites terminate in L5, bipolar cells and inverted pyramids. All have long, horizontal axons confined to L5/6 (Zhang and Deschenes, 1998; Mercer et al., 2005), some crossing areal boundaries. Their pronounced spike accommodation/adaptation cannot be overcome by injecting larger square-wave current pulses; these only result in more rapid and profound soma/initial segment Na^+ channel inactivation. However, a ramp-shaped current superimposed on the original threshold square-wave pulse, activates tonic firing of overshooting APs, probably originating at more distant axonal locations and propagated, or reflected passively, back to the soma (unpublished; Stuart et al., 1997; Colbert and Pan, 2002; Clark et al., 2005, for axonal spike-initiation).

The near tonically firing claustrum-projecting cells form the third major L6 pyramidal class, with long slender apical dendrites that reach L1 without forming a tuft there and a broad, axonal arbor confined to L5 and L6 (Katz, 1987). Like L6 corticocortical cells, claustrum-projecting pyramids preferentially innervate pyramids locally, with "depressing" synapses (Mercer et al., 2005).

L6 is often perceived as a predominantly thalamo-recipient layer, but only corticothalamic pyramids receive powerful, direct thalamic input. Nor do corticocortical cells receive powerful excitation from neighboring thalamo-recipient corticothalamic cells. Some descending inhibitory projections from L4 ramify in L6, but excitatory projections from superficial layers are often narrow and sparse. Binzegger et al. (2004, cat V1) estimated the numbers of synapses supplied to each layer by cortical and LGN relay neurones. When compared with estimates based on stereological analysis (Beaulieu and Colonnier, 1985), the estimates for excitatory synapses were within 10% for L2/3 and L5, but differed by 32% for L4 and 70% for L6. Many additional corticocortical, or subcortical inputs are required to account for the boutons in these thalamo-recipient layers. (Thomson, 2010, Figure 4; https://www.ncbi.nlm.nih.gov/pmc/articles/PMC2885865/figure/F4/).

In cats and primates most subplate (SP) neurones disappear during development; a few remaining in the underlying white matter as interstitial neurones (Kostovic and Rakic, 1980; Luskin and Shatz, 1985; Valverde et al., 1989; Naegele et al., 1991). However, in rodents, degeneration in SP is less dramatic and the SP becomes L6b (or L7) (Valverde et al., 1989; Ferrer et al., 1992).

Neocortical Layer 5 Pyramidal Cells

The principal inputs to L5 (and to L5 pyramidal dendrites in L3) are local and more distant corticocortical projections. In turn, large L5 pyramidal cells project to many subcortical targets, including "non-specific" thalamic nuclei, superior colliculus, pons and spinal cord (targets depending on cortical region). Smaller L5 pyramids project to other cortical and subcortical regions and transcallosally, to contralateral neocortex.

Upper L5 contains the largest neocortical pyramids (only these approaching the size and spine densities of CA pyramids). In cat V1, the large cells that project to the colliculi, and/or the pons (Hallman et al., 1988), have thick apical dendrites with well-developed apical tufts in L1/2 and substantial basal dendritic arbors largely contained within L5. The largest, Betz cells (Betz, 1874), are found in motor cortex and project via the corticospinal tract to the spinal cord. Large L5 cells display a stereotypical "intrinsically burst-firing" behavior (Connors et al., 1982); the burst of two or more, high frequency spikes being superimposed on a well-developed depolarizing envelope, due to activation of a dendritic Ca^{2+} spike (Purpura and Shofer, 1965; Llinas, 1975; Larkum et al., 1999). The short interspike-interval train of two or more spikes, typical of rapidly adapting/accommodating neurones (smaller L5-, L6 corticocortical-, and some L4 pyramids), should not be confused with stereotypical bursts (though it often is); it is not superimposed upon, or triggered by a stereotypical depolarizing envelope and does not occur repetitively if the cell is held near spike threshold. Quasi burst-firing can also be elicited in adapting cells electrically coupled to intrinsic bursters (Mercer et al., 2006). The local axons of large L5 pyramids arborize almost exclusively within the deep layers while the smaller pyramids also project to the superficial layers (Larsen and Callaway, 2006).

A significant input to these large, intrinsically burst-firing pyramids comes from smaller L5 pyramids. Whether these smaller pyramids project to non-specific thalamus, or to other cortical regions was not determined. In adult rat L5, small adapting pyramids were 10 times more likely to innervate large burst-firing pyramids than vice versa (unpublished data: Thomson and West, 1993; Deuchars et al., 1994). Large L5 pyramidal cells that are close neighbors are, however, relatively densely interconnected (hit rate of 1:10: Markram, 1997). Large, but not small L5 pyramids, also receive a dense, highly focussed, input from deep L3 pyramids (hit rate $>$ 1:4, Hübener et al., 1990; Thomson and Bannister, 1998, for reconstructions of cat L5 pyramids).

The apical dendrites of small-medium corticothalamic and corticocortical L5 pyramids are slender, rarely extend beyond L2/3 and have no significant apical tuft. L5 corticothalamic pyramids provide large boutons to non-specific thalamic regions from which they receive no reciprocal inputs, in contrast to L6 corticothalamic cells which are reciprocally connected with "specific" thalamic nuclei and deliver small boutons (Van Horn and Sherman, 2004). A separate population of smaller, shorter L5 pyramids projects transcallosally (Hübener et al., 1990; Kasper

et al., 1994). Transcallosal cells are found in all layers except L1 (Kasper et al., 1994).

Neocortical Layer 4 Spiny Cells: Pyramidal Cells and Spiny Stellate Cells

If we can assume that three layered cortices in some non-mammalian species do a perfectly good job, as far as the requirements of those animals are concerned, receiving e.g., sensory information in one layer (equivalent to mammalian L6) and integrating that information with signals from elsewhere, in the adjacent layer (equivalent to L5), which then sends instructions to other brain regions, we could ask why a presumed need for more complex and sophisticated organization and integration of that information could not have been achieved simply by expanding these two existing layers. Whether this was attempted in some long lost evolutionary dead-end, we may never know, we can only assume that such an attempt did not survive. Instead, a new germinal zone, SVC and three new layers (L2-L4) to which the SVC contributes spiny cells, were added. Interestingly, these new layers repeat the pattern established in deeper layers: peripheral input into L4, with integration within, and distribution from L2/3.

Layer 4 contains two broad classes of spiny excitatory cells. Typically, the basal dendrites of L4 pyramidal cells are contained within L4 with apical oblique dendrites in L2/3 (though they receive little or no input from local L3 pyramids) and an apical dendrite extending into L1, often forming a small tuft there. Spiny stellate cells lack an apical dendrite, most or all of their dendrites are confined to L4 (Lund, 1973). Perhaps the most striking distinguishing feature of L4 spiny neurones in rat and cat, especially when compared with the "chunkier" pyramids in adjacent layers, is their simple (Rojo et al., 2016) and delicate appearance (Bannister and Thomson, 2007).

Despite being a major thalamo-recipient layer, thalamocortical inputs to L4 contribute only 6% of the synapses onto spiny stellate neurones in cat V1 and up to 22.9% in mouse (Benshalom and White, 1986), terminating predominantly on dendritic spines via large *en-passant* boutons. In contrast, ascending L6 corticothalamic pyramidal axons, form synapses with small boutons, but provide 45% of the excitatory inputs onto L4 spiny cells (cat, primate, Lund et al., 1988, for review). In primate V1 axons from area MT terminate in L1, L4B, and L6. This contrasts with other so called "feedback" connections from "higher" visual areas terminating in L1; projections that might more meaningfully be termed "cognitive" or "attentional" feed-forward. In V2 they terminate primarily in L1 and L5 or L6 (Rockland and Knutson, 2000). A further 28% of the excitatory input to L4 spiny cells originates from within L4 (cat, Ahmed et al., 1994). Despite the small numbers of thalamocortical inputs, their large boutons provide secure, faithful transmission of early presynaptic spikes, albeit followed by pronounced presynaptically mediated depression. Thalamocortical synapses have three times more release sites than those of local circuit axons, with higher release probabilities, making the average thalamocortical connection several times more effective (Gil et al., 1999, mouse S1), *at the start* of a spike train.

The axons of L4 spiny neurones make dense, topographically precise ascending projections to L3 and sparse descending projections to upper L5 (rat, cat) (Valverde, 1976; Parnavelas et al., 1977; Feldman and Peters, 1978; Gilbert, 1983; Burkhalter, 1989) where they innervate pyramids and (less commonly) interneurones (Thomson et al., 2002). Pyramids and spiny stellates contribute to these projections and both provide relatively narrow, horizontal arbors within L4. In cat V1, some spiny cell axons make most of their synapses within L4, others form a larger proportion in L3 (Binzegger et al., 2004), a finding supported by morphometric analysis coupled with paired recordings in rat barrel cortex (Lübke et al., 2003) and one that correlates with distinct electrophysiological classes (below). The sparse projection, from L4 to L6, appears to originate predominantly with pyramids (unpublished).

The firing patterns of adult L4 pyramidal and/or spiny stellate cells correlated with distinct connectivity patterns. Stereotypical intrinsic bursts were rare. Around 60% displayed rapid spike accommodation and frequency adaptation (recoverable with a superimposed ramp) and innervated other L4 spiny cells. The remaining 40% produced a short train of 3–5 short interspike interval spikes, followed by a brief afterdepolarization, then a slow afterhyperpolarization upon which a spike-train of increasing interspike interval was superimposed. These cells preferentially innervated L3 pyramids (Bannister and Thomson, 2007). This raises interesting questions about patterns of synaptic input *in vivo* and how they might interact with the cells' inherent firing characteristics; tonic input to L3, phasic to neighboring L4 pyramids in reponse to maintained depolarization.

Connectivity ratios for pairs of L4 pyramids were relatively low (1:18 adult rat; 1:14 cat V1), with no selection for firing characteristics, and fell off extremely rapidly with increasing horizontal somatic separation. All identified synaptic contacts onto spiny cells (L4 and L3, rat and cat) were onto proximal primary, secondary, and tertiary, electrotonically compact basal dendrites, and all EPSPs were brief and depressing (Bannister and Thomson, 2007).

Neocortical Layer 3 Pyramidal Cells

Layer 3 pyramidal cells are "typical" pyramids, with adapting firing patterns, well developed basal and apical oblique dendrites and an apical dendrite forming a tuft in L1. The largest are close to the L4 border. More superficial L2 cells are, naturally, very short with almost no apical dendrite. L3 pyramidal axons ramify densely in L2/3 delivering depressing inputs to other L3 pyramids with a hit rate of 1:3 that falls off only gradually with distance. Their main descending axons typically pass through L4 without branching to ramify in L5, in rat (Lorente de Nó, 1922; Burkhalter, 1989), cat (O'Leary, 1941; Gilbert and Wiesel, 1983; Kisvárday et al., 1986), and primate (Spatz et al., 1970; Lund et al., 1993; Yoshioka et al., 1994; Kritzer and Goldman-Rakic, 1995; Fujita and Fujita, 1996), where they innervate large L5 pyramids;. Somewhat surprisingly some deep L3 pyramids in mice have substantial axonal arbors within L4 (Larsen and Callaway, 2006). Their targets in L4 are of interest, because although L3 pyramids innervate L4 interneurones that have dendrites projecting into

L3, they rarely, if ever excite L4 spiny cells in adult rat or cat (Bannister and Thomson, 2007).

An additional, distinctive firing pattern has been described in cat V1—chattering cells (Gray and McCormick, 1996). These neurones generate extremely fast intrinsic spike-bursts, with an intraburst firing rate up to 800 s^{-1} and a repeat rate of 20–70 s^{-1}, in response to visual stimuli or suprathreshold current injection. During visual stimulation these cells exhibit pronounced oscillations in membrane potential that are largely absent at rest. All chattering cells recovered after dye-filling were typical L2/3 pyramidal neurones.

L3 receives a substantial trans-callosal input, larger than that to L5 (Porter and White, 1986) and pyramids in both layers project trans-callosally, often to topographically related cortical areas. In L2/3 of rat barrel cortex, 97% of the connections, both local and distant, made by L3 pyramidal axons are onto dendritic spines. This is a striking target preference (seen in all layers), when only 80% of all asymmetrical synapses in L3 are onto spines (White and Czeiger, 1991) and L6 corticothalamic cells preferentially innervate aspiny dendritic shafts in L4 and L6 (Elhanany and White, 1990). In primate visual, motor and somatosensory cortex, L3 (and to a lesser extent L5) cells also provide dense innervation of patches of cortex a few 100 μ wide and up to a few millimeters from the injection site within L1–3 (Levitt et al., 1993, 1994). In prefrontal cortex, a narrow stripe-like, rather than a patchy pattern is apparent (Levitt et al., 1993).

Deep L3 pyramids can also receive thalamocortical inputs from primary sensory thalamus, again, largely to proximal basal dendrites, though the further they are from the L4 border, the weaker this input becomes (White and Hersch, 1982). A major part of the projection from the pulvinar (the most caudal thalamic group, with roles in attention and oculomotor behavior) also terminates in L3 extrastriate visual areas (Rockland et al., 1999). The dense, focussed, excitatory input from L4 spiny cells onto L3 pyramids also terminates proximally, on first, second, or third order basal dendrites (Thomson et al., 2002; Thomson and Bannister, 2003), while the many inputs from other L3 pyramids are located more distally (mean 97 μm *cf*. 69 μm: Feldmeyer et al., 2002), on both basal and apical oblique dendritic branches. Proximal basal synapses result in taller, narrower EPSPs (excitatory postsynaptic potentials) than more distal inputs.

The Relationship between Dendritic Location and EPSP Size and Shape

This relationship is partly due to the smoothing of current transfer over the length of a cable with resistance and capacitance (Rall, 1962) and partly to the activation of voltage-gated ion channels distributed with unique patterns of surface expression across somata, axons and dendrites of each class of neurone (Nusser, 2009, 2012, for reviews). Amongst the conductances whose density increases with distance from the soma, perhaps the most studied has been the rapidly inactivating K^+ current, I_A. The I_A α-subunit Kv4.3 clusters in neocortical pyramidal dendrites and dendritic spines (Burkhalter et al., 2006) and I_A density increases as I_{Na} decreases more distally in large L5 pyramidal basal dendrites (Kampa et al., 2006). In CA1 pyramidal dendrites, the density of Kv4.2 also increases along the soma-dendritic axis (Kerti et al., 2012), although the gradient was shallower than expected from dendritic recordings of I_A (e.g., Hoffman et al., 1997; Sun et al., 2011; Nestor and Hoffman, 2012); a discrepancy that might result from involvement of other I_A α-subunits, auxiliary subunits, or modulators of channel conductance.

In mouse L3 pyramids, selective blockade of Kv4.2/4.3 enhanced glu-EPSPs activated by focal glutamate-uncaging at single spines. It also promoted activation of fast, dendritic spikes by summed glu-EPSPs at proximal dendritic locations and of slower, all-or-none, stereotypical, depolarizing events at proximal-intermediate dendritic locations (A Biro, A Bremaud, A. Ruiz, unpublished). Without channel-blockers these additional events required near simultaneous activation at 7–8 closely neighboring locations. Such events would enhance responses of L3 cells to thalamocortical inputs. However, two excitatory synapses provided by any one presynaptic axon rarely, if ever innervate the same pyramidal dendrite, let alone 7 or 8. They distribute across the dendritic tree on different branches, albeit at similar electrotonic distances from the soma. How frequently 7–8 presynaptic terminals, each from 7 to 8 different presynaptic neurones, all impinging on a single dendritic compartment, are activated simultaneously in life, is difficult to predict. More distal inputs e.g., from other L3 neurones or cortical regions may lower the threshold for such events (Branco and Häusser, 2011), perhaps when attention to a behaviourally important input is required. In both mouse A1 and V1 L4, local circuit activation amplified and prolonged thalamocortical responses, without altering frequency or direction selectivity and with spectral range and tuning (auditory), or with frequency and direction selectivity (visual) preserved (Li et al., 2013a,b).

Unidirectional Flow of Excitation in Neocortex and Hippocampus

Both cellular and circuit properties appear to have developed to preserve the integrity of the signals arriving from the periphery. In L4, thalamocortical input arrives in proximal postsynaptic compartments that are near optimal for rapid, faithful transmission to soma/axon. The signals carrying this information may then be enhanced or suppressed in L3 and additional features, like direction in V1, computed there. However, the purity of salient feature representation in the direct thalamocortical signal is not compromised by excitation from other layers; from cells dealing with more highly integrated and processed information. The flow of excitatory input from the thalamus is unidirectional: from thalamus (and L6) to L4, L4 to L3, and L3 to L5 and transmitted thence to other cortical and subcortical regions. The strength of a response may be altered by coincident inputs from the recipient layer, from other layers, or regions; the response may be tuned, or suppressed by inhibition in L4 activated from elsewhere, but its fundamental integrity is preserved (Thomson et al., 2002; Thomson and Lamy, 2007, for review).

In this, the neocortical circuit is strongly reminiscent of hippocampus where dentate granule cells, activated by inputs from enthorinal cortex, send excitatory inputs to CA3, CA3 pyramids send excitatory inputs to CA2 and CA1 and CA1 pyramids project to different layers of the enthorinal cortex via the subiculum. CA1 pyramids do not project "back" to excite CA3 pyramidal cells. The CA1 neurones that innervate CA3 and dentate gyrus are not glutamatergic pyramidal cells, but GABAergic interneurones—"back projection cells" (below and Supplementary Figure 1, http://uclsop.net/interneuron-reconstruction/backprojection/). Some CA2 pyramids, as well as interneurones, do project "back" to CA3 (**Figure 1**; Mercer et al., 2007, 2012b; Mercer, 2012), but their targets there have yet to be identified.

One of the reasons such an elegant organization in neocortex has been difficult to accept, or even imagine (e.g., Binzegger et al., 2004) is the apparent chaos that results from neocortical layering, *cf* the discreet regional organization in hippocampus. In neocortical layers 2–6, there are somata, axons and apical and basal dendrites arising from many different classes of neurones whose somata reside in any of these layers. The inputs from other layers, from other cortical and subcortical areas may terminate neatly in specific layers, or sublayers, but what do they find there but a jumbled multiplicity of potential targets. To propose that these axons can seek out and connect only to specific targets amongst this confusion—not only to connect to certain subclasses of neurones, but to specific postsynaptic compartments belonging to those neurones—seemed quite preposterous.

It is, however, the case. Those of us not skilled in the art may view electron micrographs of the neocortical neuropil with a sense of horrified bewilderment, but axons and dendrites apparently know with whom they are destined to communicate and make it their business to find each other. We have come to accept that GABAergic interneuronal axons can find and innnervate very specific targets, eschewing all others in their path, so why have we assumed that excitatory axons make synaptic contacts indiscriminately, with any old neuronal element they happen to pass? (see also Markram et al., 2015). Different pyramidal classes are born on different embryonic days, express different combinations of gene products at different times during migration and differentiation, migrate through gradually changing chemical and physical environments, halt for different lengths of time *en route* and receive different incoming synapses. Neocortical pyramidal (unlike interneuronal) axons may often follow almost linear, class-specific trajectories, but their targets are more flexible—employing spines to sample the environment and twisting and bending to capture an attractive input.

We do not yet know which molecules are involved in this synaptic partner-identification; they are likely to be different at each class of synapse (defined by the subclasses of pre- and post-synaptic neurones). But we do know that each class of synapse, so defined, displays its own unique characteristics: specificity in transmitter(s) used, pre- and post-synaptic receptors inserted, frequency-dependent patterns of transmitter release, postsynaptic compartments involved and thereby the modulation of each input by cable and voltage-gated properties and by other nearby inputs.

Subplate Neurones and Afferent Axons

Neocortex

There is considerable evidence that epigenetic cues are required for the final differentiation of neocortical neurones, still somewhat multi-potent on arrival. Obvious candidates for such cues are in-growing axons, particularly, perhaps, thalamocortical axons in primary sensory regions (López-Bendito and Molnár, 2003, for review).

Connections between the neocortex and subcortical structures course through the internal capsule, a thick fiber tract lying between the caudate nucleus and thalamus. Subplate neurones, diverse in site of origin, birth date, survival and gene expression, exhibit a range of morphologies and axonal projection patterns (Hoerder-Suabedissen and Molnár, 2013), including pioneer axons to the emerging internal capsule and commissural fibers of the early hippocampus (Sarnat and Flores-Sarnat, 2002). The subplate zone becomes a "waiting compartment" in which thalamocortical-, basal forebrain cholinergic-, callosal, commissural, and ipsilateral corticocortical-afferents cease growing until an appropriate environment or signal emerges.

Early born GABAergic cells migrate tangentially from their germinal zone in the LGE (lateral ganglionic eminence) and into the MGE (medial ganglionic eminence), forming a stream of cells between the MGE and globus pallidus (E11.5 to E14). These "corridor" cells form a permissive pathway through which thalamocortical axons can grow (López-Bendito et al., 2006) (Molnár et al., 2012: Figures 1 and 2; https://www.ncbi.nlm.nih.gov/pmc/articles/PMC4370206/figure/F1/; https://www.ncbi.nlm.nih.gov/pmc/articles/PMC5040712/figure/F2/). Otherwise chemical repellents and the structure of the PSPB (pallial-subpallial boundaries): high cell-density, and a radial glial fascicle running across the trajectory of thalamocortical axons, would hinder their onward growth toward the cortex. Cortigofugal axons may also assist the forward growth of thalamocortical axons through this barrier (Molnár et al., 1998; Molnár and Butler, 2002).

Like many cortical neurones, most thalamic neurones are born between E13 and E19 (rat), the LGN, for example, between E12 and E14. By E16/E17, nuclear differentiation in thalamus has begun and both neocortex and dorsal (specific) thalamus have started to generate prospective reciprocal connections. To reach their destinations, these axons must overcome and cross several emerging barriers, or boundary zones: the diencephalic-telencephalic (DTB) and (PSPB) form transient barriers to axon growth, but interestingly, also a route for early born migrating neurones that form the permissive corridor. A largely transient population of pioneering subplate neurones sends the first projections to the internal capsule (IC) and beyond; though the axons of other cortical neurones actually invade and innervate specific thalamic nuclei first. However, without subplate projections, thalamocortical axons cannot traverse the PSPB to enter the telencephalon. Moreover, subplate ablation

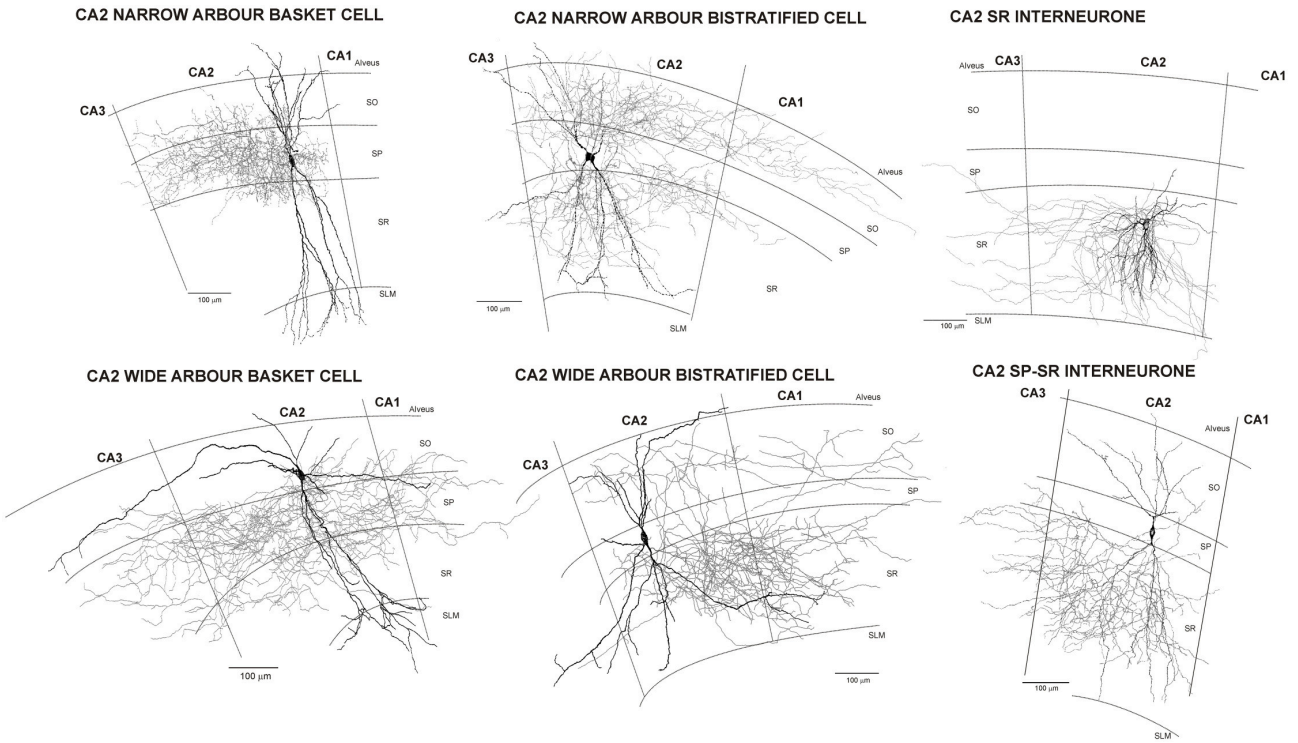

FIGURE 1 | Reconstructions of CA2 interneurones filled during intracellular recordings in adult rat hippocampus (from Mercer et al., 2007, 2012b). The largest population of interneurones recorded and filled in CA2 were basket cells. Like those in CA1, CA2 basket cells had dendrites that extended through *stratum oriens*, sometimes entering the alveus, and through *stratum radiatum* and into *stratum lacunosum moleculare*. Their axons arbourized extensively in *stratum pyramidale* and in some, also in very proximal *stratum oriens* and/or *radiatum* (wide axonal arbor basket cells). Two distinct subtypes of CA2 basket cells were identified. The first (CA2 narrow dendritic arbor basket cells) resembled those of CA1 with a narrow, aspiny dendritic arbor and axon confined to CA2. In contrast, both the axons and dendrites of the CA2 wide dendritic arbor basket cells, extended into all three CA-subfields and the horizontally oriented, distal dendritic branches were sparsely spiny. Similarly, two subtypes of CA2 bistratified cells were reported, CA2 narrow and wide dendritic arbor bistratified cells. The dendrites of both subtypes extended through *stratum oriens* and *radiatum* without entering *stratum lacunosum moleculare*, those of wide dendritic arbor cells extending further horizontally than is typical of CA1 bistratified cells and becoming sparsely spiny. Bistratified cell axons ramified in both CA2 and proximal CA1, but stopped abruptly at the CA2/CA3 border. The somata of CA2 SP-SR interneurones were found in *stratum pyramidale* and their dendrites extended to *stratum oriens*, branched extensively in *stratum radiatum*, rarely penetrated SLM, but often extended horizontally to CA1 and CA3. Their axons emerged from the soma and arbourized almost exclusively in *stratum radiatum* of CA2. The axons and dendrites of CA2 stratum radiatum, Reelin-immunopositive interneurones ramified predominantly in CA2 *stratum radiatum*, with a few axonal branches extending into neighboring regions.

at this time, prevents formation of ocular dominance columns, inhibition in L4 does not mature, barrels are disrupted and spindle activity abolished (Hoerder-Suabedissen and Molnár, 2015).

By P0, axons from L6 have reached the ventrobasal thalamic nucleus (primary somatosensory) and over the next 4 days they invade and form a barreloid pattern. Corticothalamic fibers do not, however, ramify within LGN until the eyes open and spontaneous activity begins. By E16-19 thalamocortical axons have accumulated in the subplate, but they also wait, extending horizontal collaterals that may facilitate reorganization of maps at a later date, until peripheral afferents innervate the appropriate dorsal thalamic nucleus (Molnár et al., 2012).

Here we see an important change in the forward growth of thalamocortical axons from the external route seen in lower vertebrates lacking a six layered cortex, where they run over the developing cortex, to the internal route of mammals, via the corpus callosum. The midline repellent, Slit2, redirects the migration of corridor neurones, switching thalamic axons from an external to a mammalian-specific internal path (Bielle et al., 2011). It is proposed that this switch allowed the neocortex to grow radially. Interestingly, the hippocampus is deep in the brain and bounded by dense fiber tracts. Perhaps it was not able to grow in this way.

Having accumulated in the subplate, the growth of thalamocortical axons into neocortex is prevented if SNARE-complex proteins, essential for AP-driven, Ca^{2+}-dependent transmitter release (though not spontaneous, "miniatures," Ramirez and Kavalali, 2011) are knocked out. With the arrival of thalamocortical axons, transient circuits form between thalamic axons, subplate and L4 neurones. Multiple interactions now control the growth of- and connections made by-incoming axons and the development of cortical neurones and circuits. For example, two extracellular molecules: NRN1 (Neuritin-1, a GPI-anchored neuronal protein that modulates neurite outgrowth) and VGF (a nerve growth factor), both

manufactured by thalamic cells and transported to their neocortical terminals, promote L4 spiny stellate dendritic growth—selectively (Sato et al., 2012). Lhx2 promotes activity-dependent L4 dendritic growth toward thalamic afferents, by inducing the transcription factor BBtbd3 (Wang et al., 2017), while several neurotrophins are implicated in the critical stages during which precise thalamocortical connections are made (Ma et al., 2002; Yamamoto and Hanamura, 2005). As L4 and its thalamic inputs mature postnatally, spiny stellate cells receive a transient input from SOM interneurones in L5b, which themselves receive thalamic input. Development of thalamic input to spiny stellates is delayed in the absence of this transient input (Marques-Smith et al., 2016), while thalamic afferents are misdirected to inappropriate barrels when Proteoglycan-2 (PRG-1, a phospholipid- interacting molecule) is knocked out (Cheng et al., 2016).

Hippocampus

As in neocortex, expression patterns demonstrate that pyramidal classes are predestined at E15.5 while they are still in IZ. For example, SCIP (POU domain transcription factor), is present in future CA1 pyramids (Frantz et al., 1994; Tole et al., 1997), while KA1 (GluR subunit) is expressed in future CA3 neurones (Wisden and Seeburg, 1993; Tole et al., 1997) and many regulators that control neurogenesis in neocortex also act here (Urbán and Guillemot, 2014).

From LII and LIII of the entorhinal cortex information from many subcortical structures is relayed to the hippocampus via the perforant path, providing powerful input to the molecular layer of the dentate gyrus and to distal apical dendritic tufts of CA1-3 pyramidal cells in *stratum lacunosum moleculare*. Mossy fibers project from dentate granule cells to CA3 *stratum lucidum*, innervating the most proximal apical dendrites of CA3 pyramids with huge boutons. In turn, CA3 pyramidal axons (Schaffer collaterals) project to *stratum radiatum* and *oriens* of CA1. The hippocampus also sends information to and receives inputs from subcortical regions: medial septum, cingulate gyrus, mammillary bodies, thalamus and amygdala as well as regions of association cortex.

The precise position of CA2 in this unidirectional trisynaptic pathway has been unveiled more recently (Chevaleyre and Piskorowski, 2016; Dudek et al., 2016; for reviews). LII of the entorhinal cortex provides strong, proximal excitation to CA2 pyramidal cells via dentate and mossy fiber synapses in *stratum lucidum* (Kohara et al., 2014). CA2 is also thought to receive direct input from LIII of the entorhinal cortex in *stratum radiatum* and *lacunosum moleculare* (Chevaleyre and Siegelbaum, 2010) in addition to Schaffer collaterals (Chevaleyre and Siegelbaum, 2010; Jones and McHugh, 2011). In turn, CA2 pyramids project preferentially to calbindin-negative, deep CA1 pyramids which lie adjacent to *stratum oriens* (Kohara et al., 2014). CA2 pyramids also project "back" to the supramammillary nucleus (Tamamaki et al., 1988; Cui et al., 2013) and in some cases, back to LII of the medial enthorinal cortex (Rowland et al., 2013).

During development, a projection from CA1 non-pyramidal cells to the medial septum, (hippocampo-septal pathway) (Supèr and Soriano, 1994) develops before the reverse, septo-hippocampal projection: E15 vs. E17 (mouse) (for parallel studies in rat and involvement of Cajal-Retzius cells: Ceranik et al., 1999, 2000). Chemo-repulsive semiphorins repel septal axons, promote growth cone collapse and may contribute to target selection; GABAergic septo-hippocampal fibers terminate preferentially on sema3C-expressing GABAergic interneurones, while cholinergic septo-hippocampal fibers terminate on sema3E- and sema3A-expressing CA pyramidal and dentate granule cells (Pascual et al., 2005).

By E17, LIII entorhinal axons are ramifying densely and exclusively in *stratum lacunosum moleculare*. Invasion of the dentate comes later, but by E19, the first entorhinal axons begin to ramify there, predominantly in the outer molecular layer (Supèr and Soriano, 1994). Commissural fibers first enter the contralateral hippocampus at E18 and arborize in *stratum radiatum* and *oriens*, along with the Schaffer collaterals. The earliest commissural fibers to enter the dentate gyrus are seen even later, at P2, terminating in the inner zone of the molecular layer and the hilus. Thus, as in neocortex, incoming pathways do not meander indiscriminately; they invade their ultimate target layers and regions from their earliest appearance, some following paths marked by early born, non-pyramidal neurones.

Again, a host of genes selectively expressed at different times, in different locations and in different cell classes in the developing hippocampus appear to contribute to its normal development. For examples, see Fazzari et al. (2010) for signaling with Nrg1(Neuregulin1, a ligand for ERBB3 and 4) and ErbB4 (receptor tyrosine kinase, an epidermal growth factor receptor); Silva et al. (2015), for LGI1 (Leucine-rich, glioma inactivated 1) in both neocortex and hippocampus; (Mingorance et al., 2004), for tempero-spatial patterns of Nogo expression and its debated involvement in perforant path development (Urbán and Guillemot, 2014).

A Note on Cajal-Retzius Cells (Cajal, 1891, 1899a,b, 1904; Retzius, 1893)

Large numbers of calretinin-expressing (CR), bipolar or multipolar Cajal-Retzius neurones appear in the molecular layer of the developing CP, becoming distributed through all layers. Collaterals of their thick primary axon make synaptic contact first with pyramidal cells in emerging L6, then sequentially with pyramids in L5 to L2 (del Rio et al., 1995). In hippocampus they become densely innervated by afferent axons from entorhinal cortex, whose ramification in CA *stratum lacunosum moleculare* and dentate outer molecular layer is severely reduced if Cajal-Retzius cells are ablated. Up to 90% of these cells disappear during development; the remainder form a sparse population in adult neocortical L1 (del Rio et al., 1995), hippocampal *stratum lacunosum moleculare* and the dentate gyrus outer molecular layer (Del Río et al., 1997). Cajal-Retzius neurones produce GABA, possibly ACh, calmodulin, PV(parvalbumin) and CR and neuropeptides. They express important mediators of radial neuroblast migration and lamination of the cortical plate: Reelin (a secreted extracellular matrix protein, essential for the normal "inside-out" development of neocortical layering), Lis1 (a motor protein Dynein-regulator), and Dscam (Down

syndrome cell adhesion molecule). In addition to forming the first intrinsic synaptic circuits of the cortical plate and its first afferent and efferent connections with subcortical structures, Cajal-Retzius neurones may contribute to ocular dominance column-formation, to regulation of neurogenesis, and to cortical repair (Sarnat and Flores-Sarnat, 2002, for review).

GABAERGIC INTERNEURONES

Origins of the Many Classes of GABAergic Cortical Interneurones

(Meyer and Wahle, 1988; Wonders and Anderson, 2006; Batista-Brito and Fishell, 2009; Vitalis and Rossier, 2011; Miyoshi et al., 2013; Li and Pleasure, 2014; Wamsley and Fishell, 2017, for reviews; Yavorska and Wehr, 2016, Figure 1, https://www.ncbi.nlm.nih.gov/pmc/articles/PMC5040712/figure/F1/; Batista-Brito and Fishell, 2009, Figure 3, https://www.ncbi.nlm.nih.gov/pmc/articles/PMC4465088/figure/F3/; Cauli et al., 2014, Figure 1, https://www.ncbi.nlm.nih.gov/pmc/articles/PMC4067953/figure/F1/; Jovanovic and Thomson, 2011, Figure 1, https://www.ncbi.nlm.nih.gov/pmc/articles/PMC3139172/figure/F1/; Brandão and Romcy-Pereira, 2015, Figure 1, https://www.ncbi.nlm.nih.gov/pmc/articles/PMC4412069/figure/F1/).

In humans, 65% of neocortical interneurones develop from Mash1-expressing progenitor cells of the VZ and SVC. Mash1 is a gene responsible for differentiation of GABAergic neurones and is also expressed in the subpallium (Letinic et al., 2002; Jakovcevski et al., 2011). In most mammals, however, the majority of GABAergic cortical interneurones are born in the subpallium, divisible into lateral (LGE), medial (MGE), and caudal (CGE) ganglionic eminences and preoptic area (POA). Interneurones expressing PV are born in ventral MGE (vMGE); those expressing SOM in dorsal MGE (dMGE); interneurones expressing the 5HT3 receptor (5HT3R, ionotropic serotonin receptor, Lee et al., 2010) plus cells variously expressing CR, CCK, VIP, SOM, PV, reelin and NPY (neuropeptide Y) are born in CGE (Lee et al., 2010). Finally, a mixed population of CR, CCK, VIP (vasoactive intestinal polypeptide), SOM, PV, reelin, and NPY cells are born in POA. Between E9.5 and E15.5, PV cells in vMGE, SOM cells in the dMGE and cells expressing reelin, SOM, CR, are born. 5HT3R cells are born later (E12.5–E15.5). The orphan nuclear receptor COUP-TFII is expressed in the CGE and in hippocampal interneurone-specific interneurones. It is required, with COUP-TFI, for caudal migration of cortical interneurones (Cauli et al., 2014), while activation of 5HT3AR promotes migration and appropriate positioning of CGE-derived reelin-cells (Murthy et al., 2014) (Yavorska and Wehr, Figure 2, https://www.ncbi.nlm.nih.gov/pmc/articles/PMC5040712/figure/F2/).

The interneurones then migrate tangentially toward the cortex. Corticofugal axons expressing TAG-1 (an axonal glycoprotein) provide a pathway for early-born MGE interneurones, while later-born interneurones migrate preferentially along axons lacking TAG-1 (McManus et al., 2004; Denaxa et al., 2011). Along two main migratory streams (in MZ and SVZ) they interact with soluble chemo-attractants and-repellents. For example, Cxcl12, interacting with its receptors, Cxcr4, Cxcr7, is a potent chemo-attractant for MGE-derived interneurones and required for normal positioning of these interneurones (Li et al., 2008; López-Bendito et al., 2008). Activation of GluRs and $GABA_BRs$, promotes tangential migration of interneurones into the cortex (Luhmann et al., 2015). Early born, SOMinterneurones, in receipt of strong thalamic input at this time, innervate PV interneurones and pyramids. These transient circuits promote maturation of thalamocortical input to PV interneurones (Tuncdemir et al., 2016; see above, for the influence of transient circuits involving thalamorecipient-SOM interneurones, on spiny stellate maturation). CGE-derived interneurones must insinuate themselves into the cortex even later, after many other interneurones are in place. To migrate properly and develop appropriate processes, they need network activity and, after P3, glutamate-release (De Marco García et al., 2011).

Each subpallial region expresses different combinations of transcription factors and both birth-date and -location influence the classes of interneurones generated. By P0, a large part of their fate has been defined by their own genetic programmes, but most interneurones arrive after pyramidal neurones and early interneurones have populated the cortex. Additional factors fine tune their structure and function: interactions with pyramidal cells influence their final positions, electrical activity regulates late acquisition of neurochemical identity and of soluble factors, which also influence chemical identity and thereby the relative proportions of interneuronal subtypes (Brandão and Romcy-Pereira, 2015, for review).

Ambiguity and Uncertainty in the Classification of Interneurones

Many recent studies have used rodents—young enough for many neuronal properties still to be maturing. Neonatal voltage gated channels, transporters and receptors are replaced during the first few postnatal weeks, resulting in a dramatic—up to four fold—reduction in the time course of many electrophysiological events. This "juvenile" period is also a time of synapse proliferation and pruning, and the speed and complexity of short term synaptic dynamics (Thomson, 2000a,b, 2003) increase in parallel. Some of the ambiguity encountered in attempts to classify cortical interneurones could result from cells at different stages of maturity; a day or two at these ages could make quite a difference: Kvα1 (Butler et al., 1998); SK2 (Cingolani et al., 2002); Kv3.2 (Tansey et al., 2002); Kv3.1b (Du et al., 1996); speeding of AMPA-R-EPSPs, P8 *cf* P35; shortening of synaptically released glutamate waveform, P8-P18 (Cathala et al., 2003, 2005); $GABA_A$-R α6-subunit expression, P7 *cf* P30 (Tia et al., 1996; time course of NMDA-R mediated EPSCs (Hestrin, 1992; Cathala et al., 2000); NMDA-R subunits (Farrant et al., 1994); switch from FLIP to FLOP GluR splice variants P8-14 (Monyer et al., 1991). (Batista-Brito and Fishell, 2009, Figure 5, https://www.ncbi.nlm.nih.gov/pmc/articles/PMC4465088/figure/F5/).

Moreover, reconstructions of "juvenile" cells typically demonstrate rather limited axonal ramification.

Studying a more restricted developmental stage might, therefore result in a "tidier" picture. However, cortical interneurones have to establish their own territories within

a field of already established cortical layers, sublayers and regions; environments, moreover, that continue to change throughout development and in ways not entirely prescribed genetically. Following detailed studies of the crab stomatogastric ganglion,Marder and Prinz (2002) concluded that "*...similar neuronal and network outputs can be produced by a number of different combinations of ion channels and synapse strengths. This suggests that individual neurons of the same class may each have found an acceptable solution to a genetically determined pattern of activity, and that networks of neurons in different animals may produce similar output patterns by somewhat variable underlying mechanisms....*" It is perhaps not surprising, therefore, that while many properties are common to all members, where a given clearly definable subclass exists, others may be subject to variation and modification by the existing environment. It is only necessary to study the convoluted trajectories of interneuronal axons (and pyramidal dendritic branches) to appreciate how thoroughly they explore their environment for appropriate synaptic partners.

Hippocampal Interneurones

(Klausberger et al., 2003, for review) (**Figure 1**. Supplementary Figure 1 for 3D reconstructions of CA1 interneurones). (Klausberger and Somogyi, 2008, Figures 1,2, https://www.ncbi.nlm.nih.gov/pmc/articles/PMC4487503/figure/F1/; https://www.ncbi.nlm.nih.gov/pmc/articles/PMC4487503/figure/F2/; Bezaire and Soltesz, 2013, Figure 1, https://www.ncbi.nlm.nih.gov/pmc/articles/PMC3775914/figure/F1/; Markram et al., 2004).

Hippocampal interneurones are generated in much the same way and in the same regions as neocortical interneurones, though they take a more caudal path to their destination. They must also become integrated into an existing network, but the organization of that network, with only one principal cell layer and major pathways spatially separated, is more straightforward.

Proximally Targeting Hippocampal Interneurones

Two broad classes of interneurones target somata/proximal dendrites and axon initial segments of pyramidal cells, respectively. Many of their axonal branches become significantly—if sporadically—myelinated and their synaptic boutons are large and contain mitochondria; facilitating the fast, precisely timed, proximal inhibition they provide.

Basket cells "Baskets" of axons bearing large synaptic boutons that surrround principal cell somata were first described in cerebellum (Golgi, 1883, 1906) then elsewhere (Cajal, 1888, 1906; Lorente de Nó, 1922; Kritzer and Goldman-Rakic, 1995; Buhl et al., 1997; Ali et al., 1998; Tamás et al., 1998). A hippocampal interneurone destined to inhibit pyramidal somata has little choice but to innervate *stratum pyramidale*. Similarly, to sample all excitatory inputs controlling activity in its target cells, it extends its dendrites across all layers, from *stratum oriens* to *lacunosum moleculare*—an easily identifiable, classical CA basket cell. Some basket cell axons can also extend to proximal *stratum oriens* and *stratum radiatum* (wide arbor basket cells, Supplementary Figure 1, http://uclsop.net/interneuron-reconstruction/basket).

Three types of CA1 basket cells, the majority otherwise fairly similar in their appearance, are distinguished by immunoreactivity for PV, CCK/VIP; or CCK/VGLUT3 (Katona et al., 1999; Somogyi et al., 2004) and CB1R (type-1 cannabinoid receptor: Takács et al., 2015) (Pawelzik et al., 2002, for distributions of CA1 PV and CCK interneurones). CA1 CCK basket cells receive less synaptic input than PV baskets, with proportionally more inhibition, suggesting that they do indeed subserve different rôles (Mátyás et al., 2004) and unlike PV basket cells, whose cell bodies lie predominantly in *stratum pyramidale*, CCK basket somata are also found in *stratum oriens* and *radiatum*, i.e. their sampling of incoming information also has a different bias.

For neurones with such a similar overall structure and specific target preference, it is surprising perhaps that PV and CCK basket cells originate in different subpallial regions: PV interneurones in vMGE, CCK interneurones in POA or CGE and may be born later. PV interneurones (devoid of other common markers) are typically fast spiking (FS) and deliver fast IPSPs mediated by $\alpha1\beta2/3\gamma2$-$GABA_A$Rs to pyramids, while many CCK basket cells display adapting firing patterns, have broader action potentials (Pawelzik et al., 2002) and activate $\alpha2\beta2/3\gamma2$-$GABA_A$Rs on pyramids. The different pharmacologies of these receptors (hippocampus: Pawelzik et al., 1999, 2003; Thomson et al., 2000; neocortex: Ali and Thomson, 2008) and the behavioral effects of manipulating their efficacy (Möhler et al., 2002) suggest that PV baskets mediate pharmacological sedation and contribute to anti-convulsant therapies, CCK basket cells (and possibly axo-axonic cells, Nusser et al., 1996) promote anxiolysis (Möhler et al., 2002), while certain dendrite-preferring interneurones, acting on $\alpha5\beta1\gamma2$-$GABA_A$Rs (Pawelzik et al., 1999, 2003; Ali and Thomson, 2008) influence cognition (Rudolph and Möhler, 2014).

Chandelier, or Axo-axonic cells innervate pyramidal axon initial segments in deep *stratum pyramidale* and proximal *oriens*. Their cartridge bouton arrays are only partially coincident with basket cell axonal arbors (Buhl et al., 1994b). For chandeliers with somata in *stratum pyramidale* this and the often distinctive claw-like appearance of their apical dendritic terminal branches as they extend into *stratum lacunosum moleculare* assist their identification (Pawelzik et al., 2002) (Supplementary Figure 1, http://uclsop.net/interneuron-reconstruction/axo-axonic). For *stratum oriens* axo-axonic cells with horizontal dendrites, see Ganter et al. (2004).

Dendrite-Targeting Interneurones

At least nine classes of CA1 interneurones preferentially innervate pyramidal dendrites. Their termination zones suggest that each class selectively innervates dendritic regions also receiving a particular afferent pathway, or combination thereof. The names they have acquired often reflect this preference (Klausberger et al., 2003; Klausberger and Somogyi, 2008; Bezaire and Soltesz, 2013, for reviews). As a gross generalization, dendrite-targeting interneurones have finer, unmyelinated axons and smaller, mitochondria-poor synaptic boutons than proximally targeting cells. They display a range of firing patterns, but are rarely classical FS. Those that have horizontally oriented dendrites (OLM cells being a prime example), be they in *stratum*

oriens, *radiatum*, or *lacunosum moleculare*, in CA1 or CA2, often display an adapting firing pattern and a pronounced "sag" current in responses to large hyperpolarizing current pulses, which can elicit rebound firing and many receive facilitating EPSPs from pyramids.

Perforant path associated cells Perforant path associated cells whose axons and dendrites are restricted to *stratum lacunosum moleculare* respond to perforant path input by inhibiting pyramidal apical dendritic tufts that are also in receipt of perforant path input. (CCK) (Vida et al., 1998; Pawelzik et al., 2002) (Supplementary Figure 1, http://uclsop.net/interneuron-reconstruction/ppa).

Bistratified cells have axonal arbors ramifying in *stratum oriens* and *radiatum*, but not in *stratum pyramidale or lacunosum moleculare*. Bistratified cells with somata in *stratum pyramidale*, have dendrites that span stratum oriens and radiatum. Those with cell bodies in *stratum oriens*, have horizontal dendrites confined to *stratum oriens*.The axons of both subtypes are associated with Schaffer collateral/commissural inputs to intermediate pyramidal dendrites via $\alpha5\beta1\gamma2$-$GABA_A$Rs (Pawelzik et al., 1999; Thomson et al., 2000; Thomson and Jovanovic, 2010 for review). (Supplementary Figure 1, http://uclsop.net/interneuron-reconstruction/bistratified).

(SOM, PV, CCK) (Buhl et al., 1994a, 1996; Halasy et al., 1996; Pawelzik et al., 2002; Klausberger et al., 2004; Baude et al., 2007).

Schaffer collateral-associated cells innervate the same regions as bistratified cells, but receive a different combination of inputs. Their somata lie close to the *stratum radiatum-lacunosum moleculare* border and their dendrites span both these layers and *stratum oriens*. In addition to Schaffer collateral and commissural input, therefore, these interneurones receive proximal input from perforant path, but restrict their influence to the termination regions of the Schaffer/commissural inputs (CCK: Vida et al., 1998; Pawelzik et al., 2002). (Supplementary Figure 1, http://uclsop.net/interneuron-reconstruction/sca).

Apical dendrite-innervating cells have axonal and dendritic spans similar to those of the Schaffer collateral-associated cells, but innervate the main apical dendritic trunks of pyramids, rather than their apical oblique branches (Klausberger et al., 2005; Klausberger, 2009) (CCK).

Oriens-lacunosum moleculare, or **OLM** cells (Cajal, 1911; Lacaille et al., 1987; Lacaille and Williams, 1990; Buckmaster et al., 1994; Blasco-Ibáñez and Freund, 1995), have horizontal thorny dendrites restricted to *stratum oriens* (in CA1) where they receive their most powerful drive from CA1 pyramids (Blasco-Ibáñez and Freund, 1995) with facilitating EPSPs (Ali and Thomson, 1998). In CA3, OLM dendrites also project into *stratum radiatum*, where local CA3 pyramidal axons also ramify. OLM cells do not, however, innervate *stratum oriens*, *pyramidale*, or *radiatum*. They send one or more long axons to *stratum lacunosum moleculare*, where they form a dense arbor in the perforant path termination zone and deliver fast IPSPs, almost invisible at the soma, but apparent in distal apical dendritic recordings (Hannelore Pawelzik, 1960-2004; Hannelore Pawelzik, unpublished) (Supplementary Figure 1, http://uclsop.net/interneuron-reconstruction/olm).

(SOM: Morrison et al., 1982; Kosaka et al., 1988; Kunkel and Schwartzkroin, 1988). (mGluR1α: Ferraguti et al., 2004) (up to one third express PV weakly: Ferraguti et al., 2004; Varga et al., 2012) one (metabotropic glutamate receptor 7, mGluR7, selectively expressed in excitatory boutons contacting OLM cells: Shigemoto et al., 1996).

GABAergic Projection Neurones

(Jinno, 2009, Figure 1, https://www.ncbi.nlm.nih.gov/pmc/articles/PMC2718779/figure/F1/).

These are perhaps the group most difficult to classify and one of the smallest 4% of CA1 interneurones. Since the majority of reported cells in the following four classes have horizontally oriented dendrites confined to *stratum oriens*, it is probable that, like OLM cells, they receive strong excitatory input from CA1 pyramids and relay information about activity here to other regions. In addition to long distance projections, they have local axonal arbors in *stratum oriens* and *radiatum*.

(SOM; Jinno et al., 2007; Katona et al., 2017) PV possible: Ferraguti et al., 2004).

Oriens-retrohippocampal projection cells project to the subiculum. (SOM/Cb: Jinno et al., 2007; Klausberger and Somogyi, 2008). A range of subtypes project to subiculum, including an mGluR8-decorated, M2R-expressing, SOM-negative trilaminar cell (Ferraguti et al., 2005).

Double projection cells (Klausberger and Somogyi, 2008) project to the septum and subiculum (SOM/Cb, or CR). Some also express mGluR1α and/or NPY and up to 30% express PV weakly.

Back-projection cells (Sik et al., 1994; Katona et al., 2017, for *in vivo* filled cells) project to CA3 and/or dentate gyrus, sometimes crossing the fissure, which appears to be an impenetrable barrier to other neuronal processes. (PV, SOM, Cb-negative). (Supplementary Figure 1, http://uclsop.net/interneuron-reconstruction/backprojection).

Cb-septal projection cells project to the septum (SOM, Cb) (Gulyás et al., 2003).

Amygdala-projecting interneurones project from ventral CA1 *stratum oriens*, *pyramidale* and *radiatum*, to the amygdala (Lübkemann et al., 2015). (PV, Cb, SOM, NPY and/or CCK).

The Neurogliaform Family

The neurogliaform family (Overstreet-Wadiche and McBain, 2015, for review).

Two classes have been described, which differ predominantly in the inputs they receive and the subcellular compartments they inhibit.

Neurogliaform cells are often found at the *stratum radiatum-lacunosum moleculare* border, with short, fine, often highly convoluted dendrites and a dense and spatially restricted axonal arbor, positioned to inhibit distal apical dendrites of pyramidal cells; (nNOS (neuronal nitric oxide synthase), NPY, α-actinin-2, COUP-TFII) (Price et al., 2005; Fuentealba et al., 2010).

Ivy cells are structurally similar to neurogliaform cells, but lie close to the *stratum radiatum-pyramidale* border where they inhibit proximal pyramidal compartments. Although the

$GABA_A$Rs activated by ivy cells demonstrate rapid kinetics via receptors also utilized at PV basket synapses (α1β2/3γ2, unpublished results), the proximal IPSPs elicited by ivy cells are very slow. This may be due to non-synaptic, as well as synaptic release of GABA, since what appear to be synaptic vesicles in these axons are not always apposed to postsynaptic specializations (Fuentealba et al., 2008a; see also Oláh et al., 2009; Armstrong et al., 2012, for review) (nNOS, NPY). (Supplementary Figure 1, http://uclsop.net/interneuron-reconstruction/ivy).

Interneurone-Specific Interneurones

(Acsády et al., 1996; Freund and Buzsaki, 1996; Freund and Gulyas, 1997) (CR and/or VIP and COUP-TFII: Gulyas et al., 1999).

Interneurone-specific type I somata are found in *stratum pyramidale*. Their dendrites and axons span *stratum oriens* and *radiatum*. They innervate Cb interneurones, VIP-, but not PV-basket cells and other IS-1 interneurones (CR).

Interneurone-specific type II somata lie near the *stratum lacunosum moleculare- radiatum* border. Their dendites run horizontally in *lacunosum moleculare*. They innervate distal *stratum radiatum*, making multiple contacts with Cb, but not PV-dendrites (VIP).

Interneurone-specific type III somata are found in *stratum pyramidale*, their bipolar/bitufted dendrites span *stratum oriens* through *radiatum* to *lacunosum moleculare*. Their axons innervate *stratum oriens*, where they inhibit Cb and SOM/mGluRa, interneurones including OLM cells (Acsády et al., 1996) (CR, VIP and possibly nNOS).

We cannot leave hippocampal interneurones without mentioning, however briefly, the elegant experiments in which a neurone is recorded through different e.g., states, then filled juxta-cellularly and identified; studies that demonstrate distinctive patterns of firing in relation to network rhythms such as theta and sharp wave ripples, for each class of interneurone (Klausberger et al., 2003, 2004; Fuentealba et al., 2008b, 2010; Klausberger and Somogyi, 2008; Varga et al., 2012; Katona et al., 2017).

Can We Transfer What We Know about Interneurones in CA Regions to the Neocortex?

There are around twenty, more or less distinct, classifiable classes of interneurones in CA1. Although those in CA3 remain to be explored as thoroughly, there appears to be a similar variety. In CA2, much the same profile is seen, but some unique subclass features and a *stratum pyramidale-stratum radiatum* interneuronal class, specific to this region, have been demonstrated (**Figure 1**) (Mercer et al., 2007, 2012a,b).

Some of the distinguishing features used to classify hippocampal interneurones, such as topographical relationship to specific pathways, have not been systematically applied to neocortical interneurone classification. If we look at broad classes of GABAergic neurones, those, for example that express the same markers, we find a similar picture in hippocampus and neocortex. Nearly all neocortical interneurones also belong to three broad groups, 40% expressing PV, 30% SOM and 30% 5-HT3αR, with little overlap (Rudy et al., 2011). As a broad generalization, PV interneurones (expressing neither SOM, Cb, nor CR) display fast spiking (FS) behavior, innervate proximal regions of pyramidal cells, generate fast IPSPs mediated by α1β2/3γ2 $GABA_A$Rs (Ali and Thomson, 2008) and receive depressing EPSPs from pyramids (excepting L6 corticothalamic pyramids). SOM cells including bipolar and bitufted neurones, display adapting or "burst-firing" behavior, innervate pyramidal dendrites with slower IPSPs (somatic recordings) and receive facilitating EPSPs from pyramids. 5HT3R cells displaying various non-FS behaviors are often relatively small cells with small overlapping axonal and dendritic trees (Lee et al., 2010). Expression of mRNA for certain voltage-gated ion channels clusters with three major calcium binding proteins, PV, Cb, and CR, and correlates with firing characteristics: fast I_A K^+ channel subunits in the PV cluster, that rapidly repolarize action potentials, reducing Na^+-channel inactivation, would facilitate fast spiking behavior, while a T-type Ca^{2+} current in the Cb cluster that would support burst-firing behavior (Toledo-Rodriguez et al., 2004).

Neocortical proximally targeting interneurones include subclasses of basket and chandelier or axo-axonic cells, but with a far wider range of sizes, axonal and dendritic distributions, potential inputs and targets than in hippocampus.

Basket cells in neocortex have complex choices to make. Some of the pyramids that a neocortical basket cell is destined to control will receive excitatory input in several, or even in all layers, while some spiny cells, like inverted, or bipolar L6 corticocortical cells, or L4 spiny stellate cells, may receive inputs only in one. A neocortical basket cell must also choose which spiny cells it will inhibit - any or all pyramids in a given layer, or a specific subtype, perhaps one receiving only certain inputs. Some smaller basket cells have axonal arbors restricted to a single layer, or sublayer. Large basket cells often innervate more than one layer, though this choice is not indiscriminate; the axonal arbors are often restricted to two related layers, such as the two thalamorecipient layers, L4 and L6, or the integration layers, L3 and L5, with only unbranched collaterals passing through intermediate layers (e.g., L3 and L5: Lund, 1987; Lund et al., 1988; Buhl et al., 1997; L6 and L4: Lund, 1987; Lund et al., 1988; Thomson et al., 2002; Thomson and Bannister, 2003). These larger basket cells often have dendrites that extend over several layers and some, in cat and primate primary sensory regions, also generate long horizontal axonal branches that terminate in smaller, but equally dense arbors in more distant columns (Lund, 1987; Lund et al., 1988; Kritzer and Goldman-Rakic, 1995; Lund and Wu, 1997; Thomson et al., 2002; Thomson and Bannister, 2003).

Traditionally, as in hippocampus, neocortical basket cells have been found to stain either for PV, or CCK. However, neocortical basket cells have also been classified according to axonal branch length and angle, bouton frequency etc. and these parameters correlated with their potential to generate calcium binding proteins and neuropeptides (RT-PCR). "Small basket cells," including "clutch cells" (Kisvárday et al., 1985) express mRNA for VIP and SOM or CCK and variously PV, Cb, or CR.

Large basket cells express mRNA for PV or Cb and variously NPY or CCK. "Nest basket cells" express PV or Cb mRNA and approximately equal proportions mRNA for NPY, SOM, or CCK (Wang et al., 2002).

For quality reconstructions of identified neocortical basket cells and of other GABAergic interneurones: (Jones, 1975; Jones and Peters, 1984; Lund, 1987; Lund et al., 1988; Lund and Yoshioka, 1991; Lund and Wu, 1997; DeFelipe, 2002; Thomson et al., 2002; Thomson and Bannister, 2003; West et al., 2006) and for connections with these cells: (Somogyi et al., 1983; Kritzer and Goldman-Rakic, 1995; Buhl et al., 1996; Halasy et al., 1996; Tamás et al., 1997; Dantzker and Callaway, 2000; Thomson et al., 2002; Thomson and Bannister, 2003; West et al., 2006; Ali et al., 2007).

Chandelier or Axo-axonic cells (Inan and Anderson, 2014). Since the targets of chandelier cells are highly restricted—to pyramidal axon initial segments (Somogyi, 1977; Somogyi et al., 1982) and their function - to control pyramidal firing, is well documented (if somewhat controversial), we can assign part of their function according to the distribution of their cartridge synapses. The synapses made by some neocortical axo-axonic cells are restricted to a single layer, others to two physically separated, but related layers/sublayers. Cartridge synapses, on short, radially projecting collaterals make these cells easy to identify (Szentagothai and Arbib, 1974; Lund, 1987; Lund et al., 1988; Lund and Yoshioka, 1991; Kritzer and Goldman-Rakic, 1995; Lund and Wu, 1997; Thomson and Bannister, 2003). Although most studies identify PV as a predominant marker for chandelier cells, (DeFelipe et al., 1989; Kawaguchi and Kubota, 1997; Gonchar and Burkhalter, 1999) some primate and human L5/L6 chandeliers contain Cb (del Rio and DeFelipe, 1997) and a separate population of corticotrophin-containing cells has been described in primate, although relative proportions vary between species, layer and area (Lewis and Lund, 1990).

Neocortical dendrite-targeting interneurones may, like their hippocampal equivalents, sample only certain inputs and seek only those targets that receive specific inputs. We are inclined to suspect that they most probably do, in the face of little direct evidence.

Somatostatin (SOM) dendrite-targeting interneurones (Yavorska and Wehr, 2016), often bipolar or bitufted, have fine axons forming dense, vertically oriented arbors with small boutons, spanning one, two or more adjoining layers. They are typically adapting, or burst-firing, with broader APs than FS cells and receive facilitating inputs from pyramids (Deuchars and Thomson, 1995; Thomson et al., 1995; Thomson and Bannister, 2003), stronger inhibition from VIP interneurones than PV cells receive and deliver slower IPSPs than basket cells (somatic recordings), mediated by α5-subunit-containing-$GABA_A$Rs (Ali and Thomson, 2008).

Martinotti cells from the dMGE, were first described as resident in L5, with a fine, dense axonal arbor extending to L1 and innervating pyramidal dendrites (Martinotti, 1889); leading some to claim, erroneously, any cell with a portion of axon drifting northwards as a "Martinotti." They display "low threshold spiking" behavior (Kawaguchi and Kubota, 1996, 1997; Beierlein et al., 2000, 2003; Wang et al., 2004; Ma et al., 2006). This class is now agreed to include similar, but adapting/burst-firing SOM cells in superficial layers. However, L5/6 and L2/3/4 Martinotti cells do differ; two distinct populations are identifiable in GIN and X98 mice respectively (Ma et al., 2006), both populations including SOM/Cb and SOM/NPY cells and in mouse, SOM/Cb/CR or SOM/Cb/NPY (Ma et al., 2006).

Other, probably dendrite-targeting, SOM interneurones are less distinctive.

SOM cells in L4/5 of the X94 mouse did not express Cb or NPY,

SOM cells not labeled in X94, X98 or GIN lines express NPY, nNOS and SPR (substance P receptor) (Xu and Callaway, 2009).

VIP Bipolar/bitufted interneurones, from the CGE, also containing neither PV nor SOM, often show irregular spiking behavior, supported by an I_D-like K^+ current (Porter et al., 1998). Their slender axonal tree preferentially innervates fine/medium caliber dendrites of other VIP cells as well as pyramids (rat: Peters, 1990; Acsády et al., 1996; Staiger et al., 1996, 1997; mouse: Prönneke et al., 2015), with boutons often closely associated with asymmetrical synapses (rat: Hajós et al., 1988). They receive high probability, depressing inputs from pyramidal cells mediated by AMPA-Rs with fast kinetics (GluR1/2 flop: Porter et al., 1998), particularly strong inputs from deep layers and stronger inputs from distant cortical areas: basal nucleus of Meynert and thalamus (Wall et al., 2016) and from PV cells (Staiger et al., 1997) than other interneurones.

Double bouquet cells (Cajal, 1899b; DeFelipe et al., 2006) with somata in L2/3/4 have a distinctive, narrow, axonal arbor ("horse-tail") descending to L6, in addition to a dense local arbor (often unstained in Golgi preparations). They contain VIP or CR, commonly display a "sag" in response to hyperpolazing current and a range of firing patterns including stuttering and adapting, but not classical FS (Prönneke et al., 2015).

(rat: VIP, Kawaguchi and Kubota, 1997 or CR, primate: Lund and Lewis, 1993).

Smaller VIP/CCK or **VIP/CR cells** (Kawaguchi and Kubota, 1997) probably include small basket cells, like **Arcade cells**, whose axon first ascends toward the pia, then turns south, to form a cone-shaped arbor (Jones, 1975) innervating somata and proximal dendrites.

Multipolar burst-firing dendrite-targeting cells which are strongly interconnected (electrically and chemically) and unusually express both PV and Cb, may form an additional VIP subclass (mouse, Blatow et al., 2003).

5HT3R cells include subsets of later born CCK, CR and NPY expressing neurones (Lee et al., 2010; Rudy et al., 2011), from the CGE.

Neurogliaform cells (Cajal, 1891; Lund and Yoshioka, 1991; Lund and Wu, 1997; Armstrong et al., 2012, for review) with dense, convoluted dendritic and axonal arbors display late-spiking behavior. As in hippocampus, non-synaptic, but AP-driven, vesicular release (in addition to synaptic) may account for the slow time course of the IPSPs, the presynaptic GABAergic inhibition and activation of extrasynaptic α4βxδ-$GABA_A$Rs these cells elicit (Oláh et al., 2009).

NPY (Xu and Callaway, 2009), COUP-TFII (Fuentealba et al., 2010) 5HT3aR, but not VIP (Lee et al., 2010; Rudy et al., 2011).

COUP-TFII - Interneurone-specific interneurones? In rat hippocampus, COUP-TFII is expressed in neurogliaform cells and basket cells in *stratum radiatum* and by CR- and/or VIP-interneurone-specific-interneurones (Fuentealba et al., 2010). This member of the steroid/thyroid-receptor family is expressed in the dMGE and CGE, in the SVZ in humans and by interneurones, predominantly in L1-3. They do not co-express PV, SOM, or Cb, but half express CR (80%), a quarter reelin (VIP not tested). They display irregular or adapting firing patterns, exhibit a pronounced "sag" and innervate small dendritic shafts of both interneurones and pyramids (Human temporal cortex; Varga et al., 2015). Two classes of mouse L2/3 CR cells preferentially innervate interneurones: burst-firing, bipolar VIP/CR-cells and adapting, accommodating multipolar CR-cells and may be cortical equivalents of ISI-I and III respectively (Caputi et al., 2009).

Projection neurones: A small population (6–9%) of low threshold spiking SOM cells that also express NPY, nNOS and SPR form a distinct morphological class with long distance corticocortical or corticofugal projections (Yavorska and Wehr, 2016).

CONCLUSION

The similarities between hippocampal CA regions and neocortical layers are striking: their development, the classes of neurones which result and the unidirectional flow of excitation through the regions and layers, which preserves the integrity of original signals. The prominent differences may result from a need for a far larger number of often smaller and simpler principal neurones in neocortex to perform a wider range of sophisticated computations, while avoiding the inefficiency of long, myelinated "local circuit" connections. Stacking principal cells in columns maximizes efficiency. However, this new arrangement presents new challenges, both to axons and dendrites that must make appropriate connections, to interneurones that must infiltrate this apparent chaos and to neuroscientists trying to understand the circuitry. Within these columns, myriad neuronal compartments, belonging to many neuronal classes, lie side by side. How do the axons that ramify there, or those simply passing through, choose from amongst these targets and how do postsynaptic compartments know which to accept? Understanding the mechanisms already apparent in simpler cortices, but hitherto largely unexplained; mechanisms that ensure the rejection of inappropriate and the formation of appropriate connections, each with its own unique signature, is an exciting challenge for the future.

AUTHOR CONTRIBUTIONS

AM and AT wrote the manuscript and designed the figures.

ACKNOWLEDGMENTS

The work of many years from our own laboratories and reported here was supported (in approximately chronological order) by the Wellcome Trust (1985–2000), the Medical Research Council (1984–2014), Novartis Pharma (1995–2005), the Engineering and Physical Sciences Research Council (COLAMN), EU Framework 6 (FACETS), Glaxo Smith Kline, the Biotechnology and Biological Sciences Research Council, the Physiological Society and the Human Brain Project, (European Commission FET Flagship) (2013-). Contributions made by lab-members who recorded, dye-filled and reconstructed neurones and analyzed data, are gratefully acknowledged: D. C. West, J. Deuchars, H. Pawelzik, D. I. Hughes, P. Ogun-Muyiwa, A. B Ali, J. Hahn, A. P. Bannister, O. T.Morris, S. Kirchhecker, H. McPhail K. Eastlake, H. Trigg, N. A. Botcher, J. E. Falck, S. Lange and Georgia Economides. Unpublished glutamate uncaging studies were performed by A. Biro A, Brémaud and A. Ruiz.

SUPPLEMENTARY MATERIAL

The Supplementary Material for this article can be found online at: http://journal.frontiersin.org/article/10.3389/fnana.2017.00083/full#supplementary-material

REFERENCES

Acsády, L., Arabadzisz, D., and Freund, T. F. (1996). Correlated morphological and neurochemical features identify different subsets of vasoactive intestinal polypeptide-immunoreactive interneurons in rat hippocampus. *Neuroscience* 73, 299–315. doi: 10.1016/0306-4522(95)00610-9

Ahmed, B., Anderson, J. C., Douglas, R. J., Martin, K. A. C., and Nelson, J. C. (1994). Polyneuronal innervation of spiny stellate neurons in cat visual cortex. *J. Comp. Neurol.* 341, 39–49. doi: 10.1002/cne.903410105

Alcamo, E. A., Chirivella, L., Dautzenberg, M., Dobreva, G., Fariñas, I., Grosschedl, R., et al. (2008). Satb2 regulates callosal projection neuron identity in the developing cerebral cortex. *Neuron* 57, 364–377. doi: 10.1016/j.neuron.2007.12.012

Ali, A. B., and Thomson, A. M. (1998). Facilitating pyramid to horizontal oriens-alveus interneurone inputs: dual intracellular recordings in slices of rat hippocampus. *J. Physiol.* 507 (Pt. 1), 185–199. doi: 10.1111/j.1469-7793.1998.185bu.x

Ali, A. B., and Thomson, A. M. (2008). Synaptic alpha 5 subunit-containing $GABA_A$ receptors mediate IPSPs elicited by dendrite-preferring cells in rat neocortex. *Cereb. Cortex* 18, 1260–1271 doi: 10.1093/cercor/bhm160

Ali, A. B., Bannister, A. P., and Thomson, A. M. (2007). Robust correlations between action potential duration and the properties of synaptic connections in layer 4 interneurones in neocortical slices from juvenile rats and adult rat and cat. *J. Physiol.* 580, 149–169. doi: 10.1113/jphysiol.2006.124214

Ali, A. B., Deuchars, J., Pawelzik, H., and Thomson, A. M. (1998). CA1 pyramidal to basket and bistratified cell EPSPs: dual intracellular recordings in rat hippocampal slices. *J. Physiol.* 507(Pt. 1), 201–217. doi: 10.1111/j.1469-7793.1998.201bu.x

Allen, K., Fuchs, E. C., Jaschonek, H., Bannerman, D. M., and Monyer, H. (2011). Gap junctions between interneurons are required for normal spatial coding in the hippocampus and short-term spatial memory. *J. Neurosci.* 31, 6542–6552. doi: 10.1523/JNEUROSCI.6512-10.2011

Altman, J., and Bayer, S. A. (1990a). Mosaic organization of the hippocampal neuroepithelium and the multiple germinal sources of dentate granule cells. *J. Comp. Neurol.* 301, 325–342.

Altman, J., and Bayer, S. A. (1990b). Prolonged sojourn of developing pyramidal cells in the intermediate zone of the hippocampus and their settling in the stratum pyramidale. *J. Comp. Neurol.* 301, 343–364. doi: 10.1002/cne.903010303

Amitai, Y., Gibson, J. R., Beierlein, M., Patrick, S. L., Ho, A. M., Connors, B. W., et al. (2002). The spatial dimensions of electrically coupled networks of interneurons in the neocortex. *J. Neurosci.* 22, 4142–4152.

Arimatsu, Y., and Ishida, M. (2002). Distinct neuronal populations specified to form corticocortical and corticothalamic projections from layer VI of developing cerebral cortex. *Neuroscience* 114, 1033–1045. doi: 10.1016/S0306-4522(02)00201-4

Arlotta, P., Molyneaux, B. J., Chen, J., Inoue, J., Kominami, R., and Macklis, J. D. (2005). Neuronal subtype-specific genes that control corticospinal motor neuron development *in vivo*. *Neuron* 45, 207–221. doi: 10.1016/j.neuron.2004.12.036

Armstrong, C., Krook-Magnuson, E., and Soltesz, I. (2012). Neurogliaform and Ivy cells: a major family of nNOS expressing GABAergic neurons. *Front. Neural Circuits* 6:23. doi: 10.3389/fncir.2012.00023

Baimbridge, K. G., Peet, M. J., McLennan, H., and Church, J. (1991). Bursting response to current-evoked depolarization in rat CA1 pyramidal neurons is correlated with lucifer yellow dye coupling but not with the presence of calbindin-D28k. *Synapse* 7, 269–277. doi: 10.1002/syn.890070404

Bannister, A. P., and Thomson, A. M. (2007). Dynamic properties of excitatory synaptic connections involving layer 4 pyramidal cells in adult rat and cat neocortex. *Cereb. Cortex* 17, 2190–2203. doi: 10.1093/cercor/bhl126

Batista-Brito, R., and Fishell, G. (2009). The developmental integration of cortical interneurons into a functional network. *Curr. Top. Dev. Biol.* 87, 81–118. doi: 10.1016/S0070-2153(09)01203-4

Baude, A., Bleasdale, C., Dalezios, Y., Somogyi, P., and Klausberger, T. (2007). Immunoreactivity for the $GABA_A$ receptor alpha1 subunit, somatostatin and Connexin36 distinguishes axoaxonic, basket, and bistratified interneurons of the rat hippocampus. *Cereb. Cortex* 17, 2094–2107. doi: 10.1093/cercor/bhl117

Bayer, S. A. (1980). Development of the hippocampal region in the rat. I. Neurogenesis examined with 3H-thymidine autoradiography. *J. Comp. Neurol.* 190, 87–114. doi: 10.1002/cne.901900107

Beaulieu, C., and Colonnier, M. (1985). A laminar analysis of the number of round-asymmetrical and flat-symmetrical synapses on spines, dendritic trunks, and cell bodies in area 17 of the cat. *J. Comp. Neurol.* 231, 180–189. doi: 10.1002/cne.902310206

Beierlein, M., Gibson, J. R., and Connors, B. W. (2000). A network of electrically coupled interneurons drives synchronized inhibition in neocortex. *Nat. Neurosci.* 3, 904–910. doi: 10.1038/78809

Beierlein, M., Gibson, J. R., and Connors, B. W. (2003). Two dynamically distinct inhibitory networks in layer 4 of the neocortex. *J. Neurophysiol.* 90, 2987–3000 doi: 10.1152/jn.00283.2003

Benshalom, G., and White, E. L. (1986). Quantification of thalamocortical synapses with spiny stellate neurons in layer IV of mouse somatosensory cortex. *J. Comp. Neurol.* 253, 303–314 doi: 10.1002/cne.902530303

Betz, W. (1874). Anatomischer Nachweis zweier Gehirncentra. *Centralblatt für die Medizinischen Wissenschaften* 12, 578-580, 595–599.

Bezaire, M. J., and Soltesz, I. (2013). Quantitative assessment of CA1 local circuits: knowledge base for interneuron-pyramidal cell connectivity. *Hippocampus* 23, 751–785. doi: 10.1002/hipo.22141

Bielle, F., Marcos-Mondejar, P., Keita, M., Mailhes, C., Verney, C., Nguyen Ba-Charvet, K., et al. (2011). Slit2 activity in the migration of guidepost neurons shapes thalamic projections during development and evolution. *Neuron* 69, 1085–1098. doi: 10.1016/j.neuron.2011.02.026

Binzegger, T., Douglas, R., and Martin, K. (2004). A quantitative map of the circuit of cat primary visual cortex. *J. Neurosci.* 24, 8441–8453. doi: 10.1523/JNEUROSCI.1400-04.2004

Blasco-Ibáñez, J. M., and Freund, T. F. (1995). Synaptic input of horizontal interneurons in stratum oriens of the hippocampal CA1 subfield: structural basis of feed-back activation. *Eur. J. Neurosci.* 7, 2170–2180.

Blatow, M., Rozov, A., Katona, I., Hormuzdi, S. G., Meyer, A. H., Whittington, M. A., et al. (2003). A novel network of multipolar bursting interneurons generates theta frequency oscillations in neocortex. *Neuron* 38, 805–817. doi: 10.1016/S0896-6273(03)00300-3

Bonifazi, P., Goldin, M., Picardo, M. A., Jorquera, I., Cattani, A., Bianconi, G., et al. (2009). GABAergic hub neurons orchestrate synchrony in developing hippocampal networks. *Science* 326, 1419–1424. doi: 10.1126/science.1175509

Branco, T., and Häusser, M. (2011). Synaptic integration gradients in single cortical pyramidal cell dendrites. *Neuron* 69, 885–892. doi: 10.1016/j.neuron.2011.02.006

Brandão, J. A., and Romcy-Pereira, R. N. (2015). Interplay of environmental signals and progenitor diversity on fate specification of cortical GABAergic neurons. *Front. Cell Neurosci.* 9:149. doi: 10.3389/fncel.2015.00149

Britanova, O., Akopov, S., Lukyanov, S., Gruss, P., and Tarabykin, V. (2005). Novel transcription factor Satb2 interacts with matrix attachment region DNA elements in a tissue-specific manner and demonstrates cell-type-dependent expression in the developing mouse CNS. *Eur. J. Neurosci.* 21, 658–668. doi: 10.1111/j.1460-9568.2005.03897.x

Britanova, O., De Juan Romero, C., Cheung, A., Kwan, K. Y., Schwark, M., Gyorgy, A., et al. (2008). Satb2 is a postmitotic determinant for upper-layer neuron specification in the neocortex. *Neuron* 57, 378–392. doi: 10.1016/j.neuron.2007.12.028

Buckmaster, P. S., Kunkel, D. D., Robbins, R. J., and Schwartzkroin, P. A. (1994). Somatostatin-immunoreactivity in the hippocampus of mouse, rat, guinea pig, and rabbit. *Hippocampus* 4, 167–180. doi: 10.1002/hipo.450040207

Buhl, E. H., Halasy, K., and Somogyi, P. (1994a). Diverse sources of hippocampal unitary inhibitory postsynaptic potentials and the number of synaptic release sites. *Nature* 8, 823–828. doi: 10.1038/368823a0

Buhl, E. H., Han, Z. S., Lörinczi, Z., Stezhka, V. V., Karnup, S. V., and Somogyi, P. (1994b). Physiological properties of anatomically identified axo-axonic cells in the rat hippocampus. *J. Neurophysiol.* 71, 1289–1307.

Buhl, E. H., Szilágyi, T., Halasy, K., and Somogyi, P. (1996). Physiological properties of anatomically identified basket and bistratified cells in the CA1 area of the rat hippocampus *in vitro*. *Hippocampus* 6. 294–305. doi: 10.1002/(SICI)1098-1063(1996)6:3<294::AID-HIPO7>3.0.CO;2-N

Buhl, E. H., Tamas, G., Szilagyi, T., Stricker, C., Paulsen, O., and Somogyi, P. (1997). Effect, number and location of synapses made by single pyramidal cells onto aspiny interneurones of cat visual cortex. *J. Physiol.* 500, 689–713. doi: 10.1113/jphysiol.1997.sp022053

Burkhalter, A. (1989). Intrinsic connections of rat primary visual cortex: laminar organization of axonal projections. *J. Comp. Neurol.* 279, 171–186 doi: 10.1002/cne.902790202

Burkhalter, A., Gonchar, Y., Mellor, R. L., and Nerbonne, J. M. (2006). Differential expression of I(A) channel subunits Kv4.2 and Kv4.3 in mouse visual cortical neurons and synapses. *J. Neurosci.* 26, 12274–12282. doi: 10.1523/JNEUROSCI.2599-06.2006

Butler, D. M., Ono, J. K., Chang, T., McCaman, R. E., and Barish, M. E. (1998). Mouse brain potassium channel beta1 subunit mRNA: cloning and distribution during development. *J. Neurobiol.* 34, 135–150. doi: 10.1002/(SICI)1097-4695(19980205)34:2<135::AID-NEU4>3.0.CO;2-3

Cajal, S. R. (1888). Estructura de los centros nerviosos de las ayes. *Rev. Trim. Hist. Norm. Pat.* 1, 1–10.

Cajal, S. R. (1891). "*Sur la structure de l'ecorce cérébrale de quelques mammifères*" [On the structure of the cerebral cortex in some mammals]. *La Cellule* 7, 123–176.

Cajal, S. R. (1899a). "Estudios sobre la corteza cerebral humana. I. Corteza visual" [Studies on the human cerebral cortex. I. Visual Cortex]. *Rev. Trim. Micrográf.* 4, 1–63.

Cajal, S. R. (1899b). Estudios sobre la corteza cerebral humana II: estructura de la corteza motriz del hombre y mamíferos superiores. *Rev. Trim. Micrográf. Madrid* 4, 117–200.

Cajal, S. R. (1904). *Textura del Systema Nervioso del Hombre y los Vertebrados,* Vol. 2. Madrid: Moya.

Cajal, S. R. (1906). *The Structure and Connexions of Neurons*. Nobel Lecture.

Cajal, S. R. (1911). *Histologie du Systéme Nerveux de l'Homme et des Vertébrés*, Vol. 2. Paris: Maloine.

Caputi, A., Rozov, A., Blatow, M., and Monyer, H. (2009). Two calretinin-positive GABAergic cell types in layer 2/3 of the mouse neocortex provide different forms of inhibition. *Cereb. Cortex* 19, 1345–1359. doi: 10.1093/cercor/bhn175

Cathala, L., Brickley, S., Cull-Candy, S., and Farrant, M. (2003). Maturation of EPSCs and intrinsic membrane properties enhances precision at a cerebellar synapse. *J. Neurosci.* 23, 6074–6085. Erratum in: *J. Neurosci.* 2004 24:2343.

Cathala, L., Holderith, N. B., Nusser, Z., DiGregorio, D. A., and Cull-Candy, S. G. (2005). Changes in synaptic structure underlie the developmental speeding of AMPA receptor-mediated EPSCs. *Nat. Neurosci.* 8, 1310–1318. doi: 10.1038/nn1534

Cathala, L., Misra, C., and Cull-Candy, S. (2000). Developmental profile of the changing properties of NMDA receptors at cerebellar mossy fiber-granule cell synapses. *J. Neurosci.* 20, 5899–5905.

Cauli, B., Zhou, X., Tricoire, L., Toussay, X., and Staiger, J. F. (2014). Revisiting enigmatic cortical calretinin-expressing interneurons. *Front. Neuroanat.* 8:52. doi: 10.3389/fnana.2014.00052

Ceranik, K., Deng, J., Heimrich, B., Lübke, J., Zhao, S., Förster, E., et al. (1999). Hippocampal Cajal-Retzius cells project to the entorhinal cortex: retrograde tracing and intracellular labelling studies. *Eur. J. Neurosci.* 11, 4278–4290. doi: 10.1046/j.1460-9568.1999.00860.x

Ceranik, K., Zhao, S., and Frotscher, M. (2000). Development of the entorhino-hippocampal projection: guidance by Cajal-Retzius cell axons. *Ann. N.Y. Acad. Sci.* 911, 43–54 doi: 10.1111/j.1749-6632.2000.tb06718.x

Cheng, J., Sahani, S., Hausrat, T. J., Yang, J. W., Ji, H., Schmarowski, N., et al. (2016). Precise somatotopic thalamocortical axon guidance depends on LPA-mediated PRG-2/Radixin Signaling. *Neuron* 92, 126–142. doi: 10.1016/j.neuron.2016.08.035

Cheung, A. F., Pollen, A. A., Tavare, A., DeProto, J., and Molnár, Z. (2007). Comparative aspects of cortical neurogenesis in vertebrates. *J. Anat.* 211, 164–176. doi: 10.1111/j.1469-7580.2007.00769.x

Chevaleyre, V., and Piskorowski, R. (2016). Hippocampal Area CA2: an Overlooked but Promising Therapeutic Target. *Trends Mol. Med.* 22, 645–655. doi: 10.1016/j.molmed.2016.06.007

Chevaleyre, V., and Siegelbaum, S. A. (2010). Strong CA2 pyramidal neuron synapses define a powerful disynaptic cortico-hippocampal loop. *Neuron* 66, 560–572. doi: 10.1016/j.neuron.2010.04.013

Cingolani, L. A., Gymnopoulos, M., Boccaccio, A., Stocker, M., and Pedarzani, P. (2002). Developmental regulation of small-conductance Ca^{2+}activated K^{+} channel expression and function in rat Purkinje neurons. *J. Neurosci.* 22, 4456–4467.

Clark, B. A., Monsivais, P., Branco, T., London, M., and Hausser, M. (2005). The site of action potential initiation in cerebellar Purkinje neurons. *Nat. Neurosci.* 8, 137–139. doi: 10.1038/nn1390

Colbert, C. M., and Pan, E. (2002). Ion channel properties underlying axonal action potential initiation in pyramidal neurons. *Nat. Neurosci.* 5, 533–538. doi: 10.1038/nn0602-857

Connors, B. W., Gutnick, M. J., and Prince, D. A. (1982). Electrophysiological properties of neocortical neurons *in vitro*. *J. Neurophysiol.* 48, 1302–1320.

Costa, M. R., and Hedin-Pereira, C. (2010). Does cell lineage in the developing cerebral cortex contribute to its columnar organization? *Front. Neuroanat.* 4:26. doi: 10.3389/fnana.2010.00026

Cui, Z., Gerfen, C. R., and Young, W. S. (2013). Hypothalamic and other connections with dorsal CA2 area of the mouse hippocampus. *J. Comp. Neurol.* 521, 1844–1866. doi: 10.1002/cne.23263

Dantzker, J. L., and Callaway, E. M. (2000). Laminar sources of synaptic input to cortical inhibitory interneurons and pyramidal neurons. *Nat. Neurosci.* 3, 701–707. doi: 10.1038/76656

De Marco García, N. V., Karayannis, T., and Fishell, G. (2011). Neuronal activity is required for the development of specific cortical interneuron subtypes. *Nature* 472, 351–355. doi: 10.1038/nature09865

DeFelipe, J. (2002). Cortical interneurons: from Cajal to 2001. *Prog. Brain Res.* 136, 215–238. doi: 10.1016/S0079-6123(02)36019-9

DeFelipe, J., Ballesteros-Yáñez, I., Inda, M. C., and Muñoz, A. (2006). Double-bouquet cells in the monkey and human cerebral cortex with special reference to areas 17 and 18. *Prog Brain Res.* 154, 15–32. doi: 10.1016/S0079-6123(06)54002-6

DeFelipe, J., Hendry, S. H., and Jones, E. G. (1989). Visualization of chandelier cell axons by parvalbumin immunoreactivity in monkey cerebral cortex. *Proc. Natl. Acad. Sci. U.S.A.* 86, 2093–2097. doi: 10.1073/pnas.86.6.2093

Deguchi, Y., Donato, F., Galimberti, I., Cabuy, E., and Caroni, P. (2011). Temporally matched subpopulations of selectively interconnected principal neurons in the hippocampus. *Nat. Neurosci.* 14, 495–504. doi: 10.1038/nn.2768

Del Río, J. A., Heimrich, B., Borrell, V., Förster, E., Drakew, A., Alcántara, S., et al. (1997). A role for Cajal-Retzius cells and reelin in the development of hippocampal connections. *Nature* 385, 70–74. doi: 10.1038/385070a0

del Rio, J. A., Martinez, A., Fonseca, M., Auladell, C., and Soriano, C. (1995). Glutamate-like immunoreactivity and fate of Cajal-Retzius cells in the murine cortex as identified with calretinin antibody. *Cereb. Cort.* 5, 13–21.

del Rio, J., and DeFelipe, J. (1997). Colocalization of parvalbumin and calbindin D-28k in neurons including chandelier cells of the human temporal neocortex. *J. Chem. Neuroanat.* 12, 165–173. doi: 10.1016/S0891-0618(96)00191-3

Denaxa, M., Chan, C. H., Schachner, M., Parnavelas, J. G., and Karagogeos, D. (2011). The adhesion molecule TAG-1 mediates the migration of cortical interneurons from the ganglionic eminence along the corticofugal fiber system. *Development* 128, 4635–4644.

Deuchars, J., and Thomson, A. M. (1995). Innervation of burst firing spiny interneurons by pyramidal cells in deep layers of rat somatomotor cortex: paired intracellular recordings with biocytin filling. *Neuroscience.* 69, 739–755. doi: 10.1016/0306-4522(95)00288-T

Deuchars, J., West, D. C., and Thomson, A. M. (1994). Relationships between morphology and physiology of pyramid-pyramid single axon connections in rat neocortex *in vitro*. *J. Physiol.* 478, 423–435. doi: 10.1113/jphysiol.1994.sp020262

Dobreva, G., Chahrour, M., Dautzenberg, M., Chirivella, L., Kanzler, B., Fariñas, I., et al. (2006). SATB2 is a multifunctional determinant of craniofacial patterning and osteoblast differentiation. *Cell* 125, 971–986. doi: 10.1016/j.cell.2006.05.012

Du, J., Zhang, L., Weiser, M., Rudy, B., and McBain, C. J. (1996). Developmental expression and functional characterization of the potassium-channel subunit Kv3.1b in parvalbumin-containing interneurons of the rat hippocampus. *J. Neurosci.* 16, 506–518.

Dudek, S. M., Alexander, G., and Farris, S. (2016). Rediscovering area CA2: unique properties and functions. *Nat. Rev. Neurosci.* 17, 89–102. doi: 10.1038/nrn.2015.22

Elhanany, E., and White, E. L. (1990). Intrinsic circuitry: synapses involving the local axon collaterals of corticocortical projection neurons in the mouse primary somatosensory cortex. *J. Comp. Neurol.* 291, 43–54. doi: 10.1002/cne.902910105

Evsyukova, I., Plestant, C., and Anton, E. S. (2013). Integrative mechanisms of oriented neuronal migration in the developing brain. *Annu. Rev. Cell Dev. Biol.* 29, 299–353. doi: 10.1146/annurev-cellbio-101512-122400

Farrant, M., Feldmeyer, D., Takahashi, T., and Cull-Candy, S. G. (1994). NMDA-receptor channel diversity in the developing cerebellum. *Nature* 6469, 335–339. doi: 10.1038/368335a0

Fazzari, P., Paternain, A. V., Valiente, M., Pla, R., Luján, R., Lloyd, K., et al. (2010). Control of cortical GABA circuitry development by Nrg1 and ErbB4 signalling. *Nature* 464, 1376–1380. doi: 10.1038/nature08928

Feldman, M. L., and Peters, A. (1978). The forms of non-pyramidal cells in the visual cortex of the rat. *J. Comp. Neurol.* 179, 761–794. doi: 10.1002/cne.901790406

Feldmeyer, D., Lübke, J., Silver, R. A., and Sakmann, B. (2002). Synaptic connections between layer 4 spiny neurone- layer 2/3 pyramidal cell pairs in juvenile rat barrel cortex: physiology and anatomy of interlaminar signalling within a cortical column. *J. Physiol.* 538, 803–822. doi: 10.1113/jphysiol.2001.012959

Ferraguti, F., Cobden, P., Pollard, M., Cope, D., Shigemoto, R., Watanabe, M., et al. (2004). Immunolocalization of metabotropic glutamate receptor 1alpha (mGluR1alpha) in distinct classes of interneuron in the CA1 region of the rat hippocampus. *Hippocampus* 14, 193–215. doi: 10.1002/hipo.10163

Ferraguti, F., Klausberger, T., Cobden, P., Baude, A., Roberts, J. D. B., Szucs, P., et al. (2005). Metabotropic glutamate receptor 8-expressing nerve terminals target subsets of GABAergic neurons in the hippocampus. *J. Neurosci.* 25, 10520–10536. doi: 10.1523/JNEUROSCI.2547-05.2005

Ferrer, I., Soriano, E., del Rio, J. A., Alcántara, S., and Auladell, C. (1992). Cell death and removal in the cerebral cortex during development. *Prog. Neurobiol.* 39, 1–43. doi: 10.1016/0301-0082(92)90029-E

Fishell, G., and Hanashima, C. (2008). Pyramidal neurons grow up and change their mind. *Neuron* 57, 333–338. doi: 10.1016/j.neuron.2008.01.018

Frantz, G., Bohner, A. P., Akers, R. M., and McConnell, S. K. (1994). Regulation of the POU domain gene SCIP during cerebral cortical development. *J. Neurosci.* 14, 472–485.

Freund, T., and Buzsaki, G. (1996). Interneurons of the hippocampus. *Hippocampus* 6, 347–470. doi: 10.1002/(SICI)1098-1063(1996)6:4<347::AID-HIPO1>3.0.CO;2-I

Freund, T., and Gulyas, A. (1997). Inhibitory control of GABAergic interneurons in the hippocampus. *Can. J. Physiol. Pharmacol.* 75, 479–487. doi: 10.1139/y97-033

Fuentealba, P., Begum, R., Capogna, M., Jinno, S., Marton, L., Csicsvari, J., et al. (2008a). Ivy cells: a population of nitric-oxide-producing, slow-spiking GABAergic neurons and their involvement in hippocampal network activity. *Neuron* 57, 917–929. doi: 10.1016/j.neuron.2008.01.034

Fuentealba, P., Klausberger, T., Karayannis, T., Suen, W. Y., Huck, J., Tomioka, R., et al. (2010). Expression of COUP-TFII nuclear receptor in restricted GABAergic neuronal populations in the adult rat hippocampus. *J. Neurosci.* 30, 1595–1609. doi: 10.1523/JNEUROSCI.4199-09.2010

Fuentealba, P., Tomioka, R., Dalezios, Y., Márton, L. F., Studer, M., Rockland, K., et al. (2008b). Rhythmically active enkephalin-expressing GABAergic cells in the CA1 area of the hippocampus project to the subiculum and preferentially innervate interneurons. *J Neurosci.* 28, 10017–10022. doi: 10.1523/JNEUROSCI.2052-08.2008

Fujita, I., and Fujita, T. (1996). Intrinsic connections in the macaque inferior temporal cortex. *J. Comp. Neurol.* 368, 467–486. doi: 10.1002/(SICI)1096-9861(19960513)368:4<467::AID-CNE1>3.0.CO;2-2

Fukuda, T., and Kosaka, T. (2000). Gap junctions linking the dendritic network of GABAergic interneurons in the hippocampus. *J. Neurosci.* 20, 1519–1528.

Ganter, P., Szücs, P., Paulsen, O., and Somogyi, P. (2004). Properties of horizontal axo-axonic cells in stratum oriens of the hippocampal CA1 area of rats *in vitro*. *Hippocampus* 14, 232–243. doi: 10.1002/hipo.10170

Geiller, T., Royer, S., and Choi, J. S. (2017). Segregated Cell Populations Enable Distinct Parallel Encoding within the Radial Axis of the CA1 Pyramidal Layer. *Exp. Neurobiol.* 26, 1–10. doi: 10.5607/en.2017.26.1.1

Gibson, J. R., Beierlein, M., and Connors, B. W. (1999). Two networks of electrically coupled inhibitory neurons in neocortex. *Nature* 402, 75–79. doi: 10.1038/47035

Gil, Z., Connors, B. W., and Amitai, Y. (1999). Efficacy of thalamocortical and intracortical synaptic connections: quanta, innervation, and reliability. *Neuron.* 23, 385–397. doi: 10.1016/S0896-6273(00)80788-6

Gilbert, C. D. (1983). Microcircuitry of the visual cortex. *Annu. Rev. Neurosci.* 6, 217–247. doi: 10.1146/annurev.ne.06.030183.001245

Gilbert, C. D., and Wiesel, T. N. (1983). Clustered intrinsic connections in cat visual cortex. *J. Neurosci.* 3, 1116–1133.

Golgi, C. (1883). Sulla fina anatomia degli organi centrali del sistema nervoso IV. Sulla fina anatomia delle circonvoluzioni cerebellari. *Rivista Sperimentale di Freniatria* 9, 1–17.

Golgi, C. (1906). *The Neuron Doctrine - Theory and Facts.* Nobel Lecture. Amsterdam: Elsevier Publishing Company.

Gonchar, Y., and Burkhalter, A. (1999). Differential subcellular localization of forward and feedback interareal inputs to parvalbumin expressing GABAergic neurons in rat visual cortex. *J. Comp. Neurol.* 406, 346–360. doi: 10.1002/(SICI)1096-9861(19990412)406:3<346::AID-CNE4>3.0.CO;2-E

Gray, C. M., and McCormick, D. A. (1996). Chattering cells: superficial pyramidal neurons contributing to the generation of synchronous oscillations in the visual cortex. *Science* 274:5284. doi: 10.1126/science.274.5284.109

Gulyás, A. I., Hájos, N., Katona, I., and Freund, T. F. (2003). Interneurons are the local targets of hippocampal inhibitory cells which project to the medial septum. *Eur. J. Neurosci.* 17, 1861–1872. doi: 10.1046/j.1460-9568.2003.02630.x

Gulyas, A. I., Megias, M., Emri, Z., and Freund, T. F. (1999). Total number and ratio of excitatory and inhibitory synapses converging onto single interneurons of different types in the CA1 area of the rat hippocampus. *J. Neurosci.* 19, 10082–10097.

Hajós, F., Zillesm, K., Schleicher, A., and Kálmán, M. (1988). Types and spatial distribution of vasoactive intestinal polypeptide (VIP)-containing synapses in the rat visual cortex. *Anat. Embryol.* 178, 207–217. doi: 10.1007/BF00318224

Halasy, K., Buhl, E. H., Lörinczi, Z., Tamás, G., and Somogyi, P. (1996). Synaptic target selectivity and input of GABAergic basket and bistratified interneurons in the CA1 area of the rat hippocampus. *Hippocampus* 6, 306–329. doi: 10.1002/(SICI)1098-1063(1996)6:3<306::AID-HIPO8>3.0.CO;2-K

Hallman, L. E., Schofield, B. R., and Lin, C. S. (1988). Dendritic morphology and axon collaterals of corticotectal, corticopontine, and callosal neurons in layer V of primary visual cortex of the hooded rat. *J. Comp. Neurol.* 272, 149–160. doi: 10.1002/cne.902720111

Hayashi, K., Kubo, K., Kitazawa, A., and Nakajima, K. (2015). Cellular dynamics of neuronal migration in the hippocampus. *Front Neurosci. Rev.* 9:135. doi: 10.3389/fnins.2015.00135

Hestrin, S. (1992). Developmental regulation of NMDA receptor-mediated synaptic currents at a central synapse. *Nature* 357, 686–689. doi: 10.1038/357686a0

Hirsch, J. A., Alonso, J. M., Reid, R. C., and Martinez, L. M. (1998b). Synaptic integration in striate cortical simple cells. *J. Neurosci.* 18, 9517–9528.

Hirsch, J. A., Gallagher, C. A., Alonso, J. M., and Martinez, L. M. (1998a). Ascending projections of simple and complex cells in layer 6 of the cat striate cortex. *J. Neurosci.* 18, 8086–8094.

Hoerder-Suabedissen, A., and Molnár, Z. (2012). Morphology of mouse subplate cells with identified projection targets changes with age. *J. Comp. Neurol.* 520, 174–185. doi: 10.1002/cne.22725

Hoerder-Suabedissen, A., and Molnár, Z. (2013). Molecular diversity of early-born subplate neurons. *Cereb. Cortex* 23, 1473–1483. doi: 10.1093/cercor/bhs137

Hoerder-Suabedissen, A., and Molnár, Z. (2015). Development, evolution and pathology of neocortical subplate neurons. *Nat. Rev. Neurosci.* 16, 133–146. doi: 10.1038/nrn3915

Hoffman, D. A., Magee, J. C., Colbert, C. M., and Johnston, D. (1997). K+ channel regulation of signal propagation in dendrites of hippocampal pyramidal neurons. *Nature* 387, 869–875. doi: 10.1038/43119

Hübener, M., Schwarz, C., and Bolz, J. (1990). Morphological types of projection neurons in layer 5 of cat visual cortex. *J. Comp. Neurol.* 301, 655–674. doi: 10.1002/cne.903010412

Inan, M., and Anderson, S. A. (2014). The chandelier cell, form and function. *Curr. Opin. Neurobiol.* 26, 142–148. doi: 10.1016/j.conb.2014.01.009

Jakovcevski, I., Mayer, N., and Zecevic, N. (2011). Multiple origins of human neocortical interneurons are supported by distinct expression of transcription factors. *Cereb. Cortex* 8, 1771–1782. doi: 10.1093/cercor/bhq245

Jinno, S. (2009). Structural organization of long-range GABAergic projection system of the hippocampus. *Front. Neuroanat.* 3:13. doi: 10.3389/neuro.05.013.2009

Jinno, S., Klausberger, T., Marton, L. F., Dalezios, Y., Roberts, J. D., Fuentealba, P., et al. (2007). Neuronal diversity in GABAergic long-range projections from the hippocampus. *J. Neurosci.* 27, 8790–8804. doi: 10.1523/JNEUROSCI.1847-07.2007

Jones, E. G. (1975). Varieties and distribution of non-pyramidal cells in the somatic sensory cortex of the squirrel monkey. *J. Comp. Neurol.* 160, 205–267. doi: 10.1002/cne.901600204

Jones, E. G., and Peters, A. (1984). *Cerebral Cortex v2.* New York, NY: Plenum Press.

Jones, M. W., and McHugh, T. J. (2011). Updating hippocampal representations: CA2 joins the circuit. *Trends Neurosci.* 34, 526–553. doi: 10.1016/j.tins.2011.07.007

Jovanovic, J. N., and Thomson, A. M. (2011). Development of cortical GABAergic innervation. *Front. Cell. Neurosci.* 5:14. doi: 10.3389/fncel.2011.00014

Kampa, B. M., Letzkus, J. J., and Stuart, G. J. (2006). Cortical feed-forward networks for binding different streams of sensory information. *Nat. Neurosci.* 9, 1472–1473. doi: 10.1038/nn1798

Kasper, E. M., Larkman, A. U., Lübke, J., and Blakemore, C. (1994). Pyramidal neurons in layer 5 of the rat visual cortex. I. Correlation among cell morphology, intrinsic electrophysiological properties, and axon targets. *J. Comp. Neurol.* 339, 459–474 doi: 10.1002/cne.903390402

Katona, I., Sperlágh, B., Sík, A., Käfalvi, A., Vizi, E. S., Mackie, K., et al. (1999). Presynaptically located CB1 cannabinoid receptors regulate GABA release from axon terminals of specific hippocampal interneurons. *J. Neurosci.* 19, 4544–4558.

Katona, L., Micklem, B., Borhegyi, Z., Swiejkowski, D. A., Valenti, O., Viney, T., et al. (2017). Behavior-dependent activity patterns of GABAergic long-range projecting neurons in the rat hippocampus. *Hippocampus* 27, 359–377. doi: 10.1002/hipo.22696

Katz, L. C. (1987). Local circuitry of identified projection neurons in cat visual cortex brain slices. *J. Neurosci.* 7, 1223–1249.

Kawaguchi, Y., and Kubota, Y. (1996). Physiological and morphological identification of somatostatin- or vasoactive intestinal polypeptide-containing cells among GABAergic cell subtypes in rat frontal cortex. *J. Neurosci.* 16, 2701–2715.

Kawaguchi, Y., and Kubota, Y. (1997). GABAergic cell subtypes and their synaptic connections in rat frontal cortex. *Cereb. Cortex* 7, 476–486. doi: 10.1093/cercor/7.6.476

Kawauchi, T. (2015). Cellullar insights into cerebral cortical development: focusing on the locomotion mode of neuronal migration. *Front. Cell. Neurosci.* 9:394. doi: 10.3389/fncel.2015.00394

Kerti, K., Lorincz, A., and Nusser, Z. (2012). Unique somato-dendritic distribution pattern of Kv4.2 channels on hippocampal CA1 pyramidal cells. *Eur. J. Neurosci.* 35, 66–75. doi: 10.1111/j.1460-9568.2011.07907.x

Kisvárday, Z. F., Martin, K. A. C., Freund, T. F., Maglóczky, Z. S., W.hitteridge, D., and Somogyi, P. (1986). Synaptic targets of HRP-filled layer III pyramidal cells in the cat striate cortex. *Expl. Brain Res.* 64, 541–552. doi: 10.1007/BF00340492

Kisvárday, Z. F., Martin, K. A., Whitteridge, D., and Somogyi, P. (1985). Synaptic connections of intracellularly filled clutch cells: a type of small basket cell in the visual cortex of the cat. *J. Comp. Neurol.* 241, 111–137. doi: 10.1002/cne.902410202

Kitazawa, A., Kubo, K., Hayashi, K., Matsunaga, Y., Ishii, K., and Nakajima, K. (2014). Hippocampal pyramidal neurons switch from a multipolar migration mode to a novel "climbing" migration mode during development. *J. Neurosci.* 34, 1115–1126. doi: 10.1523/JNEUROSCI.2254-13.2014

Klausberger, T. (2009). GABAergic interneurons targeting dendrites of pyramidal cells in the CA1 area of the hippocampus. *Eur. J. Neurosci.* 30, 947–957. doi: 10.1111/j.1460-9568.2009.06913.x

Klausberger, T., and Somogyi, P. (2008). Neuronal diversity and temporal dynamics: the unity of hippocampal circuit operations. *Science* 321, 53–57. doi: 10.1126/science.1149381

Klausberger, T., Magill, P., Marton, L., Roberts, J., Cobden, P., Buzsáki, G., et al. (2003). Brain-state- and cell-type-specific firing of hippocampal interneurons *in vivo*. *Nature* 421: 844–848. doi: 10.1038/nature01374

Klausberger, T., Márton, L. F., Baude, A., Roberts, J. D., Magill, P. J., and Somogyi, P. (2004). Spike timing of dendrite-targeting bistratified cells during hippocampal network oscillations *in vivo*. *Nat. Neurosci.* 7, 41–47. doi: 10.1038/nn1159

Klausberger, T., Marton, L. F., O'Neill, J., Huck, J. H., Dalezios, Y., Fuentealba, P., et al. (2005). Complementary roles of cholecystokinin- and parvalbumin-expressing GABAergic neurons in hippocampal network oscillations. *Neuroscience* 25, 9782–9793. doi: 10.1523/JNEUROSCI.3269-05.2005

Kohara, K., Pignatelli, M., Rivest, A. J., Jung, H. Y., Kitamura, T., Suh, J., et al. (2014). Cell type-specific genetic and optogenetic tools reveal novel hippocampal CA2 circuits. *Nat. Neurosci.* 17, 269–279. doi: 10.1038/nn.3614

Kosaka, T., Wu, J. Y., and Benoit, R. (1988). GABAergic neurons containing somatostatin-like immunoreactivity in the rat hippocampus and dentate gyrus. *Exp Brain Res.* 71, 388–398. doi: 10.1007/BF00247498

Kostovic, I., and Rakic, P. (1980). Cytology and time of origin of interstitial neurons in the white matter in infant and adult human and monkey telencephalon. *J. Neurocytol.* 9, 219–242. doi: 10.1007/BF01205159

Kritzer, M. F., and Goldman-Rakic, P. S. (1995). Intrinsic circuit organization of the major layers and sublayers of the dorsolateral prefontal cortex in the rhesus monkey. *J. Comp. Neurol.* 359, 131–143. doi: 10.1002/cne.903590109

Kunkel, D. D., and Schwartzkroin, P. A. (1988). Ultrastructural characterization and GAD co-localization of somatostatin-like immunoreactive neurons in CA1 of rabbit hippocampus. *Synapse* 2, 371–381. doi: 10.1002/syn.890020404

Lacaille, J. C., and Williams, S. (1990). Membrane properties of interneurons in stratum oriens-alveus of the CA1 region of rat hippocampus *in vitro*. *Neuroscience* 36, 349–359. doi: 10.1016/0306-4522(90)90431-3

Lacaille, J. C., Mueller, A. L., Kunkel, D. D., and Schwartzkroin, P. A. (1987). Local circuit interactions between oriens/alveus interneurones and CA1 pyramidal cells in hippocampal slices: electrophysiology and morphology. *J. Neurosci.* 7, 1979–1993.

Larkum, M. E., Zhu, J. J., and Sakmann, B. (1999). A new cellular mechanism for coupling inputs arriving at different cortical layers. *Nature* 398, 338–341. doi: 10.1038/18686

Larsen, D. D., and Callaway, E. M. (2006). Development of layer-specific axonal arborizations in mouse primary somatosensory cortex. *J. Comp. Neurol.* 494, 398–414. doi: 10.1002/cne.20754

Lee, S., Hjerling-Leffler, J., Zagha, E., Fishell, G., and Rudy, B. (2010). The largest group of superficial neocortical GABAergic interneurons expresses ionotropic serotonin receptors. *J. Neurosci.* 30, 16796–16808. doi: 10.1523/JNEUROSCI.1869-10.2010

Leone, D. P., Srinivasan, K., Chen, B., Alcamo, E., and McConnell, S. K. (2008). The determination of projection neuron identity in the developing cerebral cortex. *Curr. Opin. Neurobiol.* 18, 28–35. doi: 10.1016/j.conb.2008.05.006

Letinic, K., Zoncu, R., and Rakic, P. (2002). Origin of GABAergic neurons in the human neocortex. *Nature* 417, 645–649. doi: 10.1038/nature00779

Levitt, J. B., Lewis, D. A., Yoshioka, T., and Lund, J. S. (1993). Topography of pyramidal neuron intrinsic connections in macaque monkey prefrontal cortex (areas 9 and 46). *J. Comp. Neurol.* 338, 360–376. doi: 10.1002/cne.903380304

Levitt, J. B., Yoshioka, T., and Lund, J. S. (1994). Intrinsic cortical connections in macaque visual area V2: evidence for interaction between different functional streams. *J. Comp. Neurol.* 342, 551–570. doi: 10.1002/cne.903420405

Lewis, D. A., and Lund, J. S. (1990). Heterogeneity of chandelier neurons in monkey neocortex: corticotropin-releasing factor- and parvalbumin-immunoreactive populations. *J. Comp. Neurol.* 293, 599–615. doi: 10.1002/cne.902930406

Li, G., and Pleasure, S. J. (2014). The development of hippocampal cellular assemblies. *Wiley Interdiscip. Rev. Dev. Biol.* 3, 165–177. doi: 10.1002/wdev.127

Li, H., Han, Y. R., Bi, C., Davila, J., Goff, L. A., Thompson, K., et al. (2008). Functional differentiation of a clone resembling embryonic cortical interneuron progenitors. *Dev. Neurobiol.* 68, 1549–1564. doi: 10.1002/dneu.20679

Li, L. Y., Li, Y. T., Zhou, M., Tao, H. W., and Zhang, L. I. (2013a). Intracortical multiplication of thalamocortical signals in mouse auditory cortex. *Nat. Neurosci.* 16, 1179–1181. doi: 10.1038/nn.3493

Li, Y. T., Ibrahim, L. A., Liu, B. H., Zhang, L. I., and Tao, H. W. (2013b). Linear transformation of thalamocortical input by intracortical excitation. *Nat. Neurosci.* 16, 1324–1330. doi: 10.1038/nn.3494

Li, Y., Lu, H., Cheng, P. L., Ge, S., Xu, H., Shi, S. H., et al. (2012). Clonally related visual cortical neurons show similar stimulus feature selectivity. *Nature* 486, 118–121. doi: 10.1038/nature11110

Llinas, R. (1975). "Electroresponsive properties of dendrites in central neurons," in *Advances in Neurology, Vol. 12*, *Physiology and Pathology of Dendrites,* ed G. W. Kreutzberg (New York, NY: Raven Press), 1–13.

López-Bendito, G., and Molnár, Z. (2003). Thalamocortical development: how are we going to get there? *Nat. Rev. Neurosci.* 4, 276–289. doi: 10.1038/nrn1075

López-Bendito, G., Cautinat, A., Sánchez, J. A., Bielle, F., Flames, N., Garratt, A. N., et al. (2006). Tangential neuronal migration controls axon guidance: a role for neuregulin-1 in thalamocortical axon navigation. *Cell* 125, 127–142. doi: 10.1016/j.cell.2006.01.042

López-Bendito, G., Sánchez-Alcañiz, J. A., Pla, R., Borrell, V., Pic,ó, E., Valdeolmillos, M., et al. (2008). Chemokine signaling controls intracortical migration and final distribution of GABAergic interneurons. *J. Neurosci.* 28, 1613–1624. doi: 10.1523/JNEUROSCI.4651-07.2008

Lorente de Nó, R. (1922). La corteza cerebral del ratón. *Trab. Lab. Invest. Biol. Madrid* 20, 41–78.

Lorente de Nò, R. (1934). Studies on the structure of the cerebral cortex II. Continuation of the study of the ammonic system. *J. Psychol. Neurol.* 46, 113–177.

Lübke, J., Roth, A., Feldmeyer, D., and Sakmann, B. (2003). Morphometric analysis of the columnar innervation domain of neurons connecting layer 4 and layer 2/3 of juvenile rat barrel cortex. *Cereb. Cortex* 13, 1051–1063. doi: 10.1093/cercor/13.10.1051

Lübkemann, R., Eberhardt, J., Röhl, F. W., Janitzky, K., Nullmeier, S., Stork, O., et al. (2015). Identification and characterization of GABAergic projection neurons from ventral hippocampus to amygdala. *Brain Sci.* 5, 299–317. doi: 10.3390/brainsci5030299

Luhmann, H. J., Fukuda, A., and Kilb, W. (2015). Control of cortical neuronal migration by glutamate and GABA. *Front. Cell. Neurosci.* 94:4. doi: 10.3389/fncel.2015.00004

Lukaszewicz, A., Savatier, P., Cortay, V., Giroud, P., Huissoud, C., Berland, M., et al. (2005). G1 phase regulation, area-specific cell cycle control,

and cytoarchitectonics in the primate cortex. *Neuron* 47, 353–364. doi: 10.1016/j.neuron.2005.06.032

Lund, J. S. (1973). Organization of neurons in the visual cortex area 17, of the monkey (*Macaca mulatta*). *J. Comp. Neurol.* 147, 455–496 doi: 10.1002/cne.901470404

Lund, J. S. (1987). Local circuit neurons of macaque monkey striate cortex: I. Neurons of laminae 4C and 5A. *J. Comp. Neurol.* 257, 60–92. doi: 10.1002/cne.902570106

Lund, J. S., and Lewis, D. A. (1993). Local circuit neurons of developing and mature macaque prefrontal cortex: golgi and immunocytochemical characteristics. *J. Comp. Neurol.* 328, 282–312. doi: 10.1002/cne.903280209

Lund, J. S., Hawken, M. J., and Parker, A. J. (1988). Local circuit neurons of macaque monkey striate cortex: II. Neurons of laminae 5B and 6. *J. Comp. Neurol.* 276, 1–29. doi: 10.1002/cne.902760102

Lund, J. S., and Wu, C. Q. (1997). Local Circuit Neurons of Macaque Monkey Striate Cortex: IV. Neurons of Laminae 1–3A. *J. Comp. Neurol.* 384, 109–126. doi: 10.1002/(SICI)1096-9861(19970721)384:1<109::AID-CNE7>3.0.CO;2-5

Lund, J. S., and Yoshioka, T. (1991). Local circuit neurons of macaque monkey striate cortex: III. Neurons of laminae 4B, 4A, and 3B. *J. Comp. Neurol.* 311, 234–258. doi: 10.1002/cne.903110206

Lund, J. S., Yoshioka, T., and Levitt, J. B. (1993). Comparison of intrinsic connectivity in different areas of macaque monkey cerebral cortex. *Cereb. Cortex* 3, 148–162. doi: 10.1093/cercor/3.2.148

Luskin, M. B., and Shatz, C. J. (1985). Neurogenesis of the cat's primary visual cortex. *J. Comp. Neurol.* 242, 611–631. doi: 10.1002/cne.902420409

Ma, L., Harada, T., Harada, C., Romero, M., Hebert, J. M., McConnell, S. K., et al. (2002). Neurotrophin-3 is required for appropriate establishment of thalamocortical connections. *Neuron* 36, 623–634. doi: 10.1016/S0896-6273(02)01021-8

Ma, Y., Hu, H., Berrebi, A. S., Mathers, P. H., and Agmon, A. (2006). Distinct subtypes of somatostatin-containing neocortical interneurons revealed in transgenic mice. *J. Neurosci.* 26, 5069–5082. doi: 10.1523/JNEUROSCI.0661-06.2006

Marder, E., and Prinz, A. A. (2002). Modeling stability in neuron and network function: the role of activity in homeostasis. *Bioessays* 24, 1145–1154. doi: 10.1002/bies.10185

Markram, H. (1997). A network of tufted layer 5 pyramidal neurons. *Cereb. Cortex* 7, 523–533. doi: 10.1093/cercor/7.6.523

Markram, H., Muller, E., Ramaswamy, S., Reimann, M. W., Abdellah, M., Sanchez, C. A., et al. (2015). Reconstruction and Simulation of Neocortical Microcircuitry. *Cell* 163, 456–492. doi: 10.1016/j.cell.2015.09.029

Markram, H., Toledo-Rodriguez, M., Wang, Y., Gupta, A., Silberberg, G., and Wu, C. (2004). Interneurons of the neocortical inhibitory system. *Nat. Rev. Neurosci.* 5, 793–807. doi: 10.1038/nrn1519

Marques-Smith, A., Lyngholm, D., Kaufmann, A. K., Stacey, J. A., Hoerder-Suabedissen, A., Becker, E. B., et al. (2016). A transient translaminar GABAergic interneuron circuit connects thalamocortical recipient layers in neonatal somatosensory cortex. *Neuron* 89, 536–549. doi: 10.1016/j.neuron.2016.01.015

Martinotti, C. (1889). Contributo allo studio della corteccia cerebrale, ed all'origine centrale dei nervi. *Ann. Freniatr. Sci. Affini.* 1, 14–381.

Mátyás, F., Freund, T. F., and Gulyás, A. I. (2004). Convergence of excitatory and inhibitory inputs onto CCK-containing basket cells in the CA1 area of the rat hippocampus. *Eur. J. Neurosci.* 19, 1243–1256. doi: 10.1111/j.1460-9568.2004.03225.x

McManus, M. F., Nasrallah, I. M., Gopal, P. P., Baek, W. S., and Golden, J. A. (2004). Axon mediated interneuron migration. *J. Neuropathol. Exp. Neurol.* 63, 932–941. doi: 10.1093/jnen/63.9.932

Mercer, A. (2012). Electrically coupled excitatory neurones in cortical regions. *Brain Res.* 1487, 192–197. doi: 10.1016/j.brainres.2012.03.069

Mercer, A., Bannister, A. P., and Thomson, A. M. (2006). Electrical coupling between pyramidal cells in adult cortical regions. *Brain Cell. Biol.* 35, 13–27. doi: 10.1007/s11068-006-9005-9

Mercer, A., Botcher, N. A., Eastlake, K., and Thomson, A. M. (2012a). SP-SR interneurones: a novel class of neurones of the CA2 region of the hippocampus. *Hippocampus* 22 , 1758–1769. doi: 10.1002/hipo.22010

Mercer, A., Eastlake, K., Trigg, H. L., and Thomson, A. M. (2012b). Local circuitry involving parvalbumin-positive basket cells in the CA2 region of the hippocampus. *Hippocampus* 22, 43–56. doi: 10.1002/hipo.20841

Mercer, A., Trigg, H. L., and Thomson, A. M. (2007). Characterization of neurons in the CA2 subfield of the adult rat hippocampus. *J. Neurosci.* 27, 7329–7338. doi: 10.1523/JNEUROSCI.1829-07.2007

Mercer, A., West, D. C., Morris, O. T., Kirchhecker, S., Kerkhoff, J. E., and Thomson, A. M. (2005). Excitatory connections made by presynaptic cortico-cortical pyramidal cells in layer 6 of the neocortex. *Cereb. Cortex* 15, 1485–1496. doi: 10.1093/cercor/bhi027

Meyer, A. H., Katona, I., Blatow, M., Rozov, A., and Monyer, H. (2002). *In vivo* labeling of parvalbumin-positive interneurons and analysis of electrical coupling in identified neurons. *J. Neurosci.* 22, 7055–7064.

Meyer, G., and Wahle, P. (1988). Early postnatal development of cholecystokinin-immunoreactive structures in the visual cortex of the cat. *J. Comp. Neurol.* 276, 360–386. doi: 10.1002/cne.902760304

Mingorance, A., Fontana, X., Solé, M., Burgaya, F., Ureña, J. M., Teng, F. Y., et al. (2004). Regulation of Nogo and Nogo receptor during the development of the entorhino-hippocampal pathway and after adult hippocampal lesions. *Mol. Cell. Neurosci.* 26, 34–49. doi: 10.1016/j.mcn.2004.01.001

Miyata, T., Kawaguchi, A., Okano, H., and Ogawa, M. (2001). Asymmetric inheritance of radial glial fibers by cortical neurons. *Neuron.* 31, 727–741. doi: 10.1016/S0896-6273(01)00420-2

Miyoshi, G., Machold, R. P., and Fishell, G. (2013). "Specification of GABAergic neocortical interneurons," in *Cortical Development: Neural Diversity and Neocortical Organization,* eds R. Kageyama and T. Yamamori (Tokyo: Springer), 89–126. doi: 10.1007/978-4-431-54496-8_5

Möhler, H., Fritschy, J. M., and Rudolph, U. (2002). A new benzodiazepine pharmacology. *J. Pharmacol. Exp. Ther.* 300, 2–8. doi: 10.1124/jpet.300.1.2

Molnár, Z., Métin, C., Stoykova, A., Tarabykin, V., Price, D. J., Francis, F., et al. (2006). Comparative aspects of cerebral cortical development. *Eur. J. Neurosci.* 23, 921–934. doi: 10.1111/j.1460-9568.2006.04611.x

Molnár, Z., Adams, R., Goffinet, A. M., and Blakemore, C. (1998). The role of the first postmitotic cortical cells in the development of thalamocortical innervation in the reeler mouse. *J. Neurosci.* 18, 5746–5765.

Molnár, Z., and Butler, A. B. (2002). The corticostriatal junction: a crucial region for forebrain development and evolution. *Bioessays* 24, 530–541. doi: 10.1002/bies.10100

Molnár, Z., and Hoerder-Suabedissen, A. (2016). Regional scattering of primate subplate. *Proc. Natl.Acad. Sci. U.S.A.* 113, 9676–9678. doi: 10.1073/pnas.1611194113

Molnár, Z., Garel, S., López-Bendito, G., Maness, P., and Price, D. J. (2012). Mechanisms controlling the guidance of thalamocortical axons through the embryonic forebrain. *Eur. J. Neurosci.* 35, 1573–1585. doi: 10.1111/j.1460-9568.2012.08119.x

Montiel, J. F., Vasistha, N. A., Garcia-Moreno, F., and Molnár, Z. (2016). From sauropsids to mammals and back: new approaches to comparative cortical development. *J. Comp. Neurol.* 524, 630–645. doi: 10.1002/cne.23871

Monyer, H., Seeburg, P. H., and Wisden, W. (1991). Glutamate-operated channels: developmentally early and mature forms arise by alternative splicing. *Neuron* 6, 799–810.

Morrison, J. H., Benoit, R., Magistretti, P. J., Ling, N., and Bloom, F. E. (1982). Immunohistochemical distribution of pro-somatostatin-related peptides in hippocampus. *Neurosci. Lett.* 34, 137–142. doi: 10.1016/0304-3940(82)90165-3

Mountcastle, V. B. (1957). Modality and topographic properties of single neurons of cat's somatic sensory cortex. *J. Neurophysiol.* 20, 408–434.

Murthy, S., Niquille, M., Hurni, N., Limoni, G., Frazer, S., Chameau, P., et al. (2014). Serotonin receptor 3A controls interneuron migration into the neocortex. *Nat Commun.* 5:5524. doi: 10.1038/ncomms6524

Nadarajah, B., and Parnavelas, J. G. (2002). Modes of neuronal migration in the developing cerebral cortex. *Nat. Rev. Neurosci.* 3, 423–432. doi: 10.1038/nrn845

Nadarajah, B., Brunstrom, J. E., Grutzendler, J., Wong, R. O., and Pearlman, A. L. (2001). Two modes of radial migration in early development of the cerebral cortex. *Nat. Neurosci.* 4, 143–150. doi: 10.1038/83967

Naegele, J. R., Barnstable, C. J., and Wahle, P. R. (1991). Expression of a unique 56-kDa polypeptide by neurons in the subplate of the developing cerebral cortex. *Proc. Natl. Acad. Sci. U.S.A.* 88, 330–334. doi: 10.1073/pnas.88.2.330

Nakahira, E., and Yuasa, S. (2005). Neuronal generation, migration, and differentiation in the mouse hippocampal primoridium as revealed by enhanced green fluorescent protein gene transfer by means of in utero electroporation. *J. Comp. Neurol.* 483, 329–340. doi: 10.1002/cne.20441

Nestor, M. W., and Hoffman, D. A. (2012). Differential cycling rates of Kv4.2 channels in proximal and distal dendrites of hippocampal CA1 pyramidal neurons. *Hippocampus* 22, 969–980. doi: 10.1002/hipo.20899

Nielsen, J. V., Blom, J. B., Noraberg, J., and Jensen, N. A. (2010). Zbtb20-induced CA1 pyramidal neuron development and area enlargement in the cerebral midline cortex of mice. *Cereb. Cortex* 20, 1904–1914. doi: 10.1093/cercor/bhp261

Noctor, S. C., Flint, A. C., Weissman, T. A., Dammerman, R. S., and Kriegstein, A. R. (2001). Neurons derived from radial glial cells establish radial units in neocortex. *Nature* 409, 714–720. doi: 10.1038/35055553

Noctor, S. C., Martínez-Cerdeño, V., Ivic, L., and Kriegstein, A. R. (2004). Cortical neurons arise in symmetric and asymmetric division zones and migrate through specific phases. *Nat. Neurosci.* 7, 136–144. doi: 10.1038/nn1172

Nowakowski, R. S., and Rakic, P. (1979). The mode of migration of neurons to the hippocampus: a Golgi and electron microscopic analysis in foetal rhesus monkey. *J. Neurocytol.* 8, 697–718. doi: 10.1007/BF01206671

Nusser, Z. (2009). Variability in the subcellular distribution of ion channels increases neuronal diversity. *Trends Neurosci.* 32, 267–274. doi: 10.1016/j.tins.2009.01.003

Nusser, Z. (2012). Differential subcellular distribution of ion channels and the diversity of neuronal function. *Curr. Opin. Neurobiol.* 22, 366–371. doi: 10.1016/j.conb.2011.10.006

Nusser, Z., Sieghart, W., Benke, D., Fritschy, J. M., and Somogyi, P. (1996). Differential synaptic localization of two major gamma-aminobutyric acid type A receptor alpha subunits on hippocampal pyramidal cells. *Proc. Natl. Acad. Sci. U.S.A.* 93, 11939–11944. doi: 10.1073/pnas.93.21.11939

O'Leary, J. L. (1941). Structure of the area striate in the cat. *J. Comp. Neurol.* 75, 131–164.

Oláh, S., Füle, M., Komlósi, G., Varga, C., Báldi, R., Barzo, P., et al. (2009). Regulation of cortical microcircuits by unitary GABA-mediated volume transmission. *Nature* 461, 1278–1281. doi: 10.1038/nature08503

Overstreet-Wadiche, L., and McBain, C. J. (2015). Neurogliaform cells in cortical circuits. *Nat. Rev. Neurosci.* 16, 458–468. doi: 10.1038/nrn3969

Parnavelas, J. G., Lieberman, A. R., and Webster, K. E. (1977). Organization of neurons in the visual cortex, area 17, of the rat. *J. Anat.* 124, 305–322.

Pascual, M., Pozas, E., and Soriano, E. (2005). Role of class 3 semaphorins in the development and maturation of the septohippocampal pathway. *Hippocampus* 15, 184–202. doi: 10.1002/hipo.20040

Pawelzik, H., Bannister, A. P., Deuchars, J., Ilia, M., and Thomson, A. M. (1999). Modulation of bistratified cell IPSPs and basket cell IPSPs by pentobarbitone sodium, diazepam and Zn^{2+}: dual recordings in slices of adult rat hippocampus. *Eur. J. Neurosci.* 11, 3552–3564. doi: 10.1046/j.1460-9568.1999.00772.x

Pawelzik, H., Hughes, D. I., and Thomson, A. M. (2002). Physiological and morphological diversity of immunocytochemically defined parvalbumin-and cholecystokinin-positive interneurones in CA1 of the adult rathippocampus. *J. Comp. Neurol.* 443, 346–367. doi: 10.1002/cne.10118

Pawelzik, H., Hughes, D. I., and Thomson, A. M. (2003). Modulation of inhibitory autapses and synapses on rat CA1 interneurones by $GABA_A$ receptor ligands. *J. Physiol.* 546, 701–716. doi: 10.1113/jphysiol.2002.035121

Peters, A. (1990). The axon terminals of vasoactive intestinal polypeptide (VIP)-containing bipolar cells in rat visual cortex. *J. Neurocytol.* 19, 672–685. doi: 10.1007/BF01188036

Picardo, M. A., Guigue, P., Bonifazi, P., Batista-Brito, R., Allene, C., Ribas, A., et al. (2011). Pioneer GABA cells comprise a subpopulation of hub neurons in the developing hippocampus. *Neuron* 71, 695–709. doi: 10.1016/j.neuron.2011.06.018

Porter, J. T., Cauli, B., Staiger, J. F., Lambolez, B., Rossier, J., and Audinat, E. (1998). Properties of bipolar VIPergic interneurons and their excitation by pyramidal neurons in the rat neocortex. *Eur. J. Neurosci.* 10, 3617–3628. doi: 10.1046/j.1460-9568.1998.00367.x

Porter, L. L., and White, E. L. (1986). Synaptic connections of callosal projection neurons in the vibrissal region of mouse primary motor cortex: an electron microscopic/horseradish peroxidase study. *J. Comp. Neurol.* 248, 573–587. doi: 10.1002/cne.902480409

Price, C. J., Cauli, B., Kovacs, E. R., Kulik, A., Lambolez, B., Shigemoto, R., et al. (2005). Neurogliaform neurons form a novel inhibitory network in the hippocampal CA1 area. *J. Neurosci.* 25, 6775–6786. doi: 10.1523/JNEUROSCI.1135-05.2005

Prönneke, A., Scheuer, B., Wagener, R. J., Möck, M., Witte, M., and Staiger, J. F. (2015). Characterizing VIP Neurons in the Barrel Cortex of VIPcre/tdTomato Mice Reveals Layer-Specific Differences. *Cereb, Cortex* 25, 4854–4868. doi: 10.1093/cercor/bhv202

Purpura, D. P., and Shofer, R. J. (1965). Spike-generation in dendrites and synaptic inhibition in immature cerebral cortex. *Nature* 206, 833–834. doi: 10.1038/206833a0

Rakic, P. (1972). Mode of cell migration to the superficial layers of fetal monkey neocortex. *J. Comp. Neurol.* 145, 61–83. doi: 10.1002/cne.901450105

Rakic, P. (1988). Specification of cerebral cortical areas. *Science* 241, 170–176. doi: 10.1126/science.3291116

Rall, W. (1962). Electrophysiology of a dendritic neuron model. *Biophys. J.* 2(2 Pt. 2), 145–167. doi: 10.1016/S0006-3495(62)86953-7

Ramirez, D. M., and Kavalali, E. T. (2011). Differential regulation of spontaneous and evoked neurotransmitter release at central synapses. *Curr. Opin. Neurobiol.* 21, 275–282. doi: 10.1016/j.conb.2011.01.007

Reichova, I., and Sherman, S. M. (2004). Somatosensory corticothalamic projections: distinguishing drivers from modulators. *J. Neurophysiol.* 92, 2185–2197. doi: 10.1152/jn.00322.2004

Retzius, G. (1893). The Cajal'schen cells of the cerebral cortex in humans and mammals. *Biol. Unter.* 5, 1–8.

Rockland, K. S., and Knutson, T. (2000). Feedback connections from area MT of the squirrel monkey to areas V1 and V2. *J. Comp. Neurol.* 425, 345–368. doi: 10.1002/1096-9861(20000925)425:3<345::AID-CNE2>3.0.CO;2-O

Rockland, K. S., Andresen, J., Cowie, R. J., and Robinson, D. L. (1999). Single axon analysis of pulvinocortical connections to several visual areas in the macaque. *J. Comp. Neurol.* 406, 221–250. doi: 10.1002/(SICI)1096-9861(19990405)406:2<221::AID-CNE7>3.0.CO;2-K

Rojo, C., Leguey, I., Kastanauskaite, A., Bielza, C., Larrañaga, P., DeFelipe, J., et al. (2016). Laminar Differences in Dendritic Structure of Pyramidal Neurons in the Juvenile Rat Somatosensory Cortex. *Cereb. Cortex* 26, 2811–2822. doi: 10.1093/cercor/bhv316

Rowland, D. C., Weible, A. P., Wickersham, I. R., Wu, H., Mayford, M., Witter, M. P., et al. (2013). Transgenically targeted rabies virus demonstrates a major monosynaptic projection from hippocampal area CA2 to medial entorhinal layer II neurons. *J. Neurosci.* 33, 14889–14898. doi: 10.1523/JNEUROSCI.1046-13.2013

Rudolph, U., and Möhler, H. (2014). $GABA_A$ receptor subtypes: therapeutic potential in Down syndrome, affective disorders, schizophrenia, and autism. *Annu. Rev. Pharmacol. Toxicol.* 54, 483–507. doi: 10.1146/annurev-pharmtox-011613-135947

Rudy, B., Fishell, G., Lee, S., and Hjerling-Leffler, J. (2011). Three groups of interneurons account for nearly 100% of neocortical GABAergic neurons. *Dev. Neurobiol.* 71, 45–61. doi: 10.1002/dneu.20853

San Antonio, A., Liban, K., Ikrar, T., Tsyganovskiy, E., and Xu, X. (2014). Distinct physiological and developmental properties of hippocampal CA2 subfield revealed by using anti-Purkinje cell protein 4 (PCP4) immunostaining. *J. Comp. Neurol.* 522, 1333–1354. doi: 10.1002/cne.23486

Sarnat, H. B., and Flores-Sarnat, L. (2002). Role of Cajal-Retzius and subplate neurons in cerebral cortical development. *Semin. Pediatr. Neurol.* 9, 302–308. doi: 10.1053/spen.2002.32506

Sato, H., Fukutani, Y., Yamamoto, Y., Tatara, E., Takemoto, M., Shimamura, K., et al. (2012). Thalamus-derived molecules promote survival and dendritic growth of developing cortical neurons. *J. Neurosci.* 32, 15388–15402. doi: 10.1523/JNEUROSCI.0293-12.2012

Schmitz, D., Schuchmann, S., Fisahn, A., Draguhn, A., Buhl, E.,H., Petrasch-Parwez, E., et al. (2001). Axo-axonal coupling. A novel mechanism for ultrafast neuronal communication. *Neuron* 31, 831–840. doi: 10.1016/S0896-6273(01)00410-X

Sekine, K., Honda, T., Kawauchi, T., Kubo, K., and Nakajima, K. (2011). The outermost region of the developing cortical plate is crucial for both the switch of the radial migration mode and the Dab1-dependent "inside-out" lamination in the neocortex. *J. Neurosci.* 31, 9426–9439. doi: 10.1523/JNEUROSCI.0650-11.2011

Sekine, K., Kubo, K., and Nakajima, K. (2014). How does Reelin control neuronal migration and layer formation in the developing mammalian neocortex? *Neurosci. Res.* 86, 50–58. doi: 10.1016/j.neures.2014.06.004

Shigemoto, R., Kulik, A., Roberts, J. D., Ohishi, H., Nusser, Z., Kaneko, T., et al. (1996). Target-cell-specific concentration of a metabotropic glutamate receptor in the presynaptic active zone. *Nature* 381, 523–525. doi: 10.1038/381523a0

Shitamukai, A., Konno, D., and Matsuzaki, F. (2011). Oblique radial glial divisions in the developing mouse neocortex induce self-renewing progenitors outside the germinal zone that resemble primate outer subventricular zone progenitors. *J. Neurosci.* 31, 3683–3695. doi: 10.1523/JNEUROSCI.4773-10.2011

Sik, A., Penttonen, M., Ylinen, A., and Buszáki, G. (1994). Inhibitory CAI-CA3-hilar region feedback in the hippocampus. *Science* 265, 1722–1724. doi: 10.1126/science.8085161

Silva, J., Sharma, S., and Cowell, J. K. (2015). Homozygous Deletion of the LGI1 Gene in Mice Leads to Developmental Abnormalities Resulting in Cortical Dysplasia. *Brain Pathol.* 25, 587–597. doi: 10.1111/bpa.12225

Simon, A., Oláh, S., Molnár, G., Szabadics, J., and Tamás, G. (2005). Gap-junctional coupling between neurogliaform cells and various interneuron types in the neocortex. *J. Neurosci.* 25, 6278–6285. doi: 10.1523/JNEUROSCI.1431-05.2005

Slomianka, L., Amrein, I., Knuesel, I., Sørensen, J. C., and Wolfer, D. P. (2011). Hippocampal pyramidal cells: the reemergence of cortical lamination. *Brain Struct. Funct.* 216, 301–317. doi: 10.1007/s00429-011-0322-0

Slomianka, L., and Geneser, F. A. (1997). Postnatal development of zinc-containing cells and neuropil in the hippocampal region of the mouse. *Hippocampus* 7, 321–340.

Somogyi, J., Baude, A., Omori, Y., Shimizu, H. E., Mestikawy, S., Fukaya, M., et al. (2004). GABAergic basket cells expressing cholecystokinin contain vesicular glutamate transporter type 3 (VGLUT3) in their synaptic terminals in hippocampus and isocortex of the rat. *Eur. J. Neurosci.* 19, 552–569. doi: 10.1111/j.0953-816X.2003.03091.x

Somogyi, P. (1977). A specific 'axo-axonal' interneuron in the visual cortex of the rat. *Brain Res.* 136, 345–350. doi: 10.1016/0006-8993(77)90808-3

Somogyi, P., Freund, T. F., and Cowey, A. (1982). The axo-axonic interneuron in the cerebral cortex of the rat, cat and monkey. *Neuroscience* 7, 2577–2607. doi: 10.1016/0306-4522(82)90086-0

Somogyi, P., Kisvárday, Z. F., Martin, K. A., and Whitteridge, D. (1983). Synaptic connections of morphologically identified and physiologically characterized large basket cells in the striate cortex of cat. *Neuroscience* 10, 261–294. doi: 10.1016/0306-4522(83)90133-1

Song, S., Sjostrom, P. J., Reigl, M., Nelson, S., and Chklovskii, D. B. (2005). Highly nonrandom features of synaptic connectivity in local cortical circuits. *PLoS Biol.* 3:e68. doi: 10.1371/journal.pbio.0030068

Spatz, W. B., Tigges, J., and Tigges, M. (1970). Subcortical projections, cortical associations and some intrinsic interlaminar connections of the striate cortex in the squirrel monkey. *J. Comp. Neurol.* 140, 155–174. doi: 10.1002/cne.901400203

Staiger, J. F., Freund, T. F., and Zilles, K. (1997). Interneurons immunoreactive for vasoactive intestinal polypeptide (VIP) are extensively innervated by parvalbumin-containing boutons in rat primary somatosensory cortex. *Eur. J. Neurosci.* 9, 2259–2268. doi: 10.1111/j.1460-9568.1997.tb01644.x

Staiger, J. F., Zilles, K., and Freund, T. F. (1996). Distribution of GABAergic elements postsynaptic to ventroposteromedial thalamic projections in layer IV of rat barrel cortex. *Eur. J. Neurosci.* 8, 2273–2285. doi: 10.1111/j.1460-9568.1996.tb01191.x

Stuart, G., Schiller, J., and Sakmann, B. (1997). Action potential initiation and propagation in rat neocortical pyramidal neurons. *J. Physiol.* 505, 617–632. doi: 10.1111/j.1469-7793.1997.617ba.x

Sugiyama, T., Osumi, N., and Katsuyama, Y. (2014). A novel cell migratory zone in the developing hippocampal formation. *J. Comp. Neurol.* 522, 3520–3538. doi: 10.1002/cne.23621

Sun, W., Maffie, J. K., Lin, L., Petralia, R. S., Rudy, B., and Hoffman, D. A. (2011). DPP6 establishes the A-type K(+) current gradient critical for the regulation of dendritic excitability in CA1 hippocampal neurons. *Neuron* 71, 1102–1115. doi: 10.1016/j.neuron.2011.08.008

Supèr, H., and Soriano, E. (1994). The organization of the embryonic and early postnatal murine hippocampus. II. Development of entorhinal, commissural, and septal connections studied with the lipophilic tracer DiI. *J. Comp. Neurol.* 344, 101–120. doi: 10.1002/cne.903440108

Szentagothai, J., and Arbib, M. A. (1974). Conceptual models of neural organization. *Neurosci. Res. Program Bull.* 12, 305–510.

Tabata, H., and Nakajima, K. (2003). Multipolar migration: the third mode of radial neuronal migration in the developing cerebral cortex. *J. Neurosci.* 23, 9996–10001.

Tabata, H., Kanatani, S., and Nakajima, K. (2009). Differences of migratory behavior between direct progeny of apical progenitors and basal progenitors in the developing cerebral cortex. *Cereb. Cortex* 19, 2092–2105. doi: 10.1093/cercor/bhn227

Tabata, H., Yoshinaga, S., and Nakajima, K. (2012). Cytoarchitecture of mouse and human subventricular zone in developing cerebral neocortex. *Exp Brain Res.* 216, 161–168. doi: 10.1007/s00221-011-2933-3

Takács, V. T., Szőnyi, A., Freund, T. F., Nyiri, G., and Gulyás, A. I. (2015). Quantitative ultrastructural analysis of basket and axo-axonic cell terminals in the mouse hippocampus. *Brain Struct. Funct.* 220, 919–940. doi: 10.1007/s00429-013-0692-6

Tamamaki, N., Abe, K., and Nojyo, Y. (1988). Three-dimensional analysis of the whole axonal arbors originating from single CA2 pyramidal neurons in the rat hippocampus with the aid of a computer graphic technique. *Brain Res.* 452, 255–272. doi: 10.1016/0006-8993(88)90030-3

Tamás, G., Buhl, E. H., Lörincz, A., and Somogyi, P. (2000). Proximally targeted GABAergic synapses and gap junctions synchronize cortical interneurons. *Nat. Neurosci.* 3, 366–371. doi: 10.1038/73936

Tamás, G., Buhl, E. H., and Somogyi, P. (1997). Fast IPSPs elicited via multiple synaptic release sites by different types of GABAergic neurone in the cat visual cortex. *J. Physiol.* 500, 715–738.

Tamás, G., Somogyi, P., and Buhl, E. H. (1998). Differentially interconnected networks of GABAergic interneurons in the visual cortex of the cat. *J. Neurosci.* 18, 4255–4270.

Tan, X., and Shi, S. H. (2013). Neocortical neurogenesis and neuronal migration. *Wiley Interdiscip. Rev. Dev. Biol.* 2, 443–459. doi: 10.1002/wdev.88

Tansey, E. P., Chow, A., Rudy, B., and McBain, C. J. (2002). Developmental expression of potassium-channel subunit Kv3.2 within subpopulations of mouse hippocampal inhibitory interneurons. *Hippocampus* 12, 137–148. doi: 10.1002/hipo.1104

Tarczy-Hornoch, K., Martin, A., Stratford, J., and Jack, J. J. (1999). Intracortical excitation of spiny neurons in layer 4 of cat striate cortex *in vitro*. *Cereb. Cortex* 9, 833–843. doi: 10.1093/cercor/9.8.833

Thomson, A. M. (2000a). Facilitation, augmentation and potentiation at central synapses. *Trends Neurosci.* 23, 305–312. doi: 10.1016/S0166-2236(00)01580-0

Thomson, A. M. (2000b). Molecular frequency filters at central synapses. *Prog Neurobiol.* 62, 159–196. doi: 10.1016/S0301-0082(00)00008-3

Thomson, A. M. (2003). Presynaptic frequency- and pattern-dependent filtering. *J. Comput. Neurosci.* 15, 159–202. doi: 10.1023/A:1025812808362

Thomson, A. M. (2010). Neocortical layer 6, a review. *Front. Neuroanat.* 4:13. doi: 10.3389/fnana.2010.00013

Thomson, A. M., and Bannister, A. P. (1998). Postsynaptic pyramidal target selection by descending layer III pyramidal axons: dual intracellular recordings and biocytin filling in slices of rat neocortex. *Neuroscience* 84, 669–683 doi: 10.1016/S0306-4522(97)00557-5

Thomson, A. M., and Bannister, A. P. (2003). Interlaminar Connections in the Neocortex. *Cereb. Cortex* 13 , 5–14. doi: 10.1093/cercor/13.1.5

Thomson, A. M., and Jovanovic, J. N. (2010). Mechanisms underlying synapse-specific clustering of GABA(A) receptors. *Eur. J. Neurosci.* 31, 2193–2203. doi: 10.1111/j.1460-9568.2010.07252.x

Thomson, A. M., and Lamy, C. (2007). Functional maps of neocortical local circuitry. *Front. Neurosci.* 1, 19–42. doi: 10.3389/neuro.01.1.1.002.2007

Thomson, A. M., and West, D. C. (1993). Fluctuations in pyramid-pyramid EPSPs modified by presynaptic firing pattern and postsynaptic membrane potential using paired intracellular recordings in rat neocortex. *Neuroscience* 54, 329–346. doi: 10.1016/0306-4522(93)90256-F

Thomson, A. M., West, D. C., and Deuchars, J. (1995). Properties of single axon excitatory postsynaptic potentials elicited in spiny interneurons by action potentials in pyramidal neurons in slices of rat neocortex. *Neuroscience* 69, 727–738. doi: 10.1016/0306-4522(95)00287-S

Thomson, A. M., Bannister, A. P., Hughes, D. I., and Pawelzik, H. (2000). Differential sensitivity to Zolpidem of IPSPs activated by morphologically identified CA1 interneurons in slices of rat hippocampus. *Eur. J. Neurosci.* 12, 425–436. doi: 10.1046/j.1460-9568.2000.00915.x

Thomson, A. M., West, D. C., Wang, Y., and Bannister, A. P. (2002). Synaptic connections and small circuits involving excitatory and inhibitory neurons in layers 2–5 of adult rat and cat neocortex: triple intracellular recordings and biocytin labeling *in vitro*. *Cereb. Cortex* 12, 936–953. doi: 10.1093/cercor/12.9.936

Tia, S., Wang, J. F., Kotchabhakdi, N., and Vicini, S. (1996). Developmental changes of inhibitory synaptic currents in cerebellar granule neurons: role of $GABA_A$ receptor alpha 6 subunit. *J. Neurosci.* 16, 3630–3640.

Tole, S., Christian, C., and Grove, E. A. (1997). Early specification and autonomous development of cortical fields in the mouse hippocampus. *Development* 124, 4959–4970.

Toledo-Rodriguez, M., Blumenfeld, B., Wu, C., Luo, J., Attali, B., Goodman, P., et al. (2004). Correlation maps allow neuronal electrical properties to be predicted from single-cell gene expression profiles in rat neocortex. *Cereb. Cortex* 14, 1310–1327. doi: 10.1093/cercor/bhh092

Tuncdemir, S. N., Wamsley, B., Stam, F. J., Osakada, F., Goulding, M., Callaway, E. M., et al. (2016). Early somatostatin interneuron connectivity mediates the maturation of deep layer cortical circuits. *Neuron* 89, 521–535. doi: 10.1016/j.neuron.2015.11.020

Urbán, N., and Guillemot, F. (2014). Neurogenesis in the embryonic and adult brain: same regulators, different roles. *Front. Cell. Neurosci.* 8:396. doi: 10.3389/fncel.2014.00396

Valverde, F. (1976). Aspects of cortical organization related to the geometry of neurons with intra-cortical axons. *J. Neurocytol.* 5, 509–529 doi: 10.1007/BF01175566

Valverde, F., Facal-Valverde, M. V., Santacana, M., and Heredia, M. (1989). Development and differentiation of early generated cells of sublayer VIb in the somatosensory cortex of the rat: a correlated Golgi and autoradiographic study. *J. Comp. Neurol.* 290, 118–140. doi: 10.1002/cne.902900108

Van Horn, S. C., and Sherman, S. M. (2004). Differences in projection patterns between large and small corticothalamic terminals. *J. Comp. Neurol.* 475, 406–415 doi: 10.1002/cne.20187

Varga, C., Golshani, P., and Soltesz, I. (2012). Frequency-invariant temporal ordering of interneuronal discharges during hippocampal oscillations in awake mice. *Proc. Natl. Acad. Sci. U.S.A.* 109, 2726–2734. doi: 10.1073/pnas.1210929109

Varga, C., Tamas, G., Barzo, P., Olah, S., and Somogyi, P. (2015). Molecular and electrophysiological characterization of GABAergic interneurons expressing the transcription factor COUP-TFII in the adult human temporal cortex. *Cereb. Cortex* 25, 4430–4449. doi: 10.1093/cercor/bhv045

Vida, I., Halasy, K., Szinyei, C., Somogyi, P., and Buhl, E. H. (1998). Unitary IPSPs evoked by interneurons at the stratum radiatum-stratum lacunosum-moleculare border in the CA1 area of the rat hippocampus *in vitro*. *J. Physiol.* 506, 755–773. doi: 10.1111/j.1469-7793.1998.755bv.x

Villette, V., Guigue, P., Picardo, M. A., Sousa, V. H., Leprince, E., Lachamp, P., et al. (2016). Development of early-born γ-Aminobutyric acid hub neurons in mouse hippocampus from embryogenesis to adulthood. *J. Comp. Neurol.* 524, 2440–2461. doi: 10.1002/cne.23961

Vitalis, T., and Rossier, J. (2011). New insights into cortical interneurons development and classification: contribution of developmental studies. *Dev. Neurobiol.* 71, 34–44. doi: 10.1002/dneu.20810

Wall, N. R., De La Parra, M., Sorokin, J. M., Taniguchi, H., Huang, Z. J., and Callaway, E. M. (2016). Brain-wide maps of synaptic input to cortical interneurons. *J. Neurosci.* 36, 4000–4009. doi: 10.1523/JNEUROSCI.3967-15.2016

Wamsley, B., and Fishell, G. (2017). Genetic and activity-dependent mechanisms underlying interneuron diversity. *Nat. Rev. Neurosci.* 18, 299–309. doi: 10.1038/nrn.2017.30

Wang, C. F., Hsing, H. W., Zhuang, Z. H., Wen, M. H., Chang, W. J., Briz, C. G., et al. (2017). Lhx2 Expression in postmitotic cortical neurons. *Cell Rep.* 4, 849–856. doi: 10.1016/j.celrep.2017.01.001

Wang, X., Tsai, J. W., LaMonica, B., and Kriegstein, A. R. (2011). A new subtype of progenitor cell in the mouse embryonic neocortex. *Nat. Neurosci.* 14, 555–561. doi: 10.1038/nn.2807

Wang, Y., Barakat, A., and Zhou, H. (2010). Electrotonic coupling between pyramidal neurons in the neocortex. *PLoS ONE* 5:e10253. doi: 10.1371/journal.pone.0010253

Wang, Y., Gupta, A., Toledo-Rodriguez, M., Wu, C. Z., and Markram, H. (2002). Anatomical, physiological, molecular and circuit properties of nest basket cells in the developing somatosensory cortex. *Cereb. Cortex* 12, 395–410. doi: 10.1093/cercor/12.4.395

Wang, Y., Toledo-Rodriguez, M., Gupta, A., Wu, C., Silberberg, G., Luo, J., et al. (2004). Anatomical, physiological and molecular properties of Martinotti cells in the somatosensory cortex of the juvenile rat. *J. Physiol.* 561, 65–90. doi: 10.1113/jphysiol.2004.073353

West, D. C., Mercer, A., Kirchhecker, S., Morris, O. T., and Thomson, A. M. (2006). Layer 6 cortico-thalamic pyramidal cells preferentially innervate interneurons and generate facilitating EPSPs. *Cereb. Cortex* 16, 200–211. doi: 10.1093/cercor/bhi098

White, E. L., and Czeiger, D. (1991). Synapses made by axons of callosal projection neurons in mouse somatosensory cortex: emphasis on intrinsic vonnections. *J. Comp. Neurol.* 303, 233–244. doi: 10.1002/cne.903030206

White, E. L., and Hersch, S. M. (1982). A quantitative study of thalamocortical and other synapses involving the apical dendrites of corticothalamic projection cells in mouse SmI cortex. *J. Neurocytol.* 11, 137–157. doi: 10.1007/BF01258009

White, E. L., and Keller, A. (1987). Intrinsic circuitry involving the local axon collaterals of corticothalamic projection cells in mouse SmI cortex. *J. Comp. Neurol.* 262, 13–26. doi: 10.1002/cne.902620103

Wisden, W., and Seeburg, P. H. (1993). A complex mosaic of high-affinity kainate receptors in rat brain. *J. Neurosci.* 13, 3582–3598.

Wiser, A. K., and Callaway, E. M. (1996). Contributions of individual layer 6 pyramidal neurons to local circuitry in the macaque primary visual cortex. *J. Neurosci.* 16, 2724–2739.

Wonders, C. P., and Anderson, S. A. (2006). The origin and specification of cortical interneurons. *Nat. Rev. Neurosci.* 7, 687–696. doi: 10.1038/nrn1954

Wu, S. X., Goebbels, S., Nakamura, K., Nakamura, K., Kometani, K., Minato, N., et al. (2005). Pyramidal neurons of upper cortical layers generated by NEX-positive progenitor cells in the subventricular zone. *Proc. Natl. Acad. Sci. U.S.A.* 102, 17172–17177. doi: 10.1073/pnas.0508560102

Xie, Z., Ma, X., Ji, W., Zhou, G., Lu, Y., Xiang, Z., et al. (2010). Zbtb20 is essential for the specification of CA1 field identity in the developing hippocampus. *Proc. Natl. Acad. Sci. U.S.A.* 107, 6510–6515. doi: 10.1073/pnas.0912315107

Xu, H. T., Han, Z., Gao, P., He, S., Li, Z., Shi, W., et al. (2014). Distinct lineage-dependent structural and functional organization of the hippocampus. *Cell* 157, 1552–1564. doi: 10.1016/j.cell.2014.03.067

Xu, X., and Callaway, E. M. (2009). Laminar specificity of functional input to distinct types of inhibitory cortical neurons. *J. Neurosci.* 29, 70–85. doi: 10.1523/JNEUROSCI.4104-08.2009

Yamamoto, N., and Hanamura, K. (2005). Formation of the thalamocortical projection regulated differentially by BDNF- and NT-3-mediated signaling. *Rev. Neurosci.* 16, 223–231. doi: 10.1515/REVNEURO.2005.16.3.223

Yavorska, I., and Wehr, M. (2016). Somatostatin-expressing inhibitory interneurons in cortical circuits. *Front. Neural Circuits* 10:76. doi: 10.3389/fncir.2016.00076

Yoshimura, Y., and Callaway, E. M. (2005). Fine-scale specificity of cortical networks depends on inhibitory cell type and connectivity. *Nat. Neurosci.* 8, 1552–1559. doi: 10.1038/nn1565

Yoshioka, T., Levitt, J. B., and Lund, J. S. (1994). Independence and merger of thalamocortical channels within macaque monkey primary visual cortex: anatomy of interlaminar projections. *Vis. Neurosci.* 11, 1–23. doi: 10.1017/S0952523800002406

Yu, Y. C., Bultje, R. S., Wang, X., and Shi, S. H. (2009). Specific synapses develop preferentially among sister excitatory neurons in the neocortex. *Nature* 458, 501–504. doi: 10.1038/nature07722

Zhang, Z. W., and Deschenes, M. (1998). Projections to layer VI of the posteromedial barrel field in the rat: a reappraisal of the role of corticothalamic pathways. *Cereb. Cortex* 8, 428–436. doi: 10.1093/cercor/8.5.428

Conflict of Interest Statement: The authors declare that the research was conducted in the absence of any commercial or financial relationships that could be construed as a potential conflict of interest.

frontiers in Neuroanatomy

REVIEW
published: 04 October 2017
doi: 10.3389/fnana.2017.00084

The Human Periallocortex: Layer Pattern in Presubiculum, Parasubiculum and Entorhinal Cortex. A Review

Ricardo Insausti[1], Mónica Muñoz-López[1], Ana M. Insausti[2] and Emilio Artacho-Pérula[1]*

[1]Human Neuroanatomy Laboratory, School of Medicine, University of Castilla-La Mancha, Albacete, Spain, [2]Department of Health Sciences, Physical Therapy School, Public University of Navarra, Tudela, Spain

The cortical mantle is not homogeneous, so that three types of cortex can be distinguished: allocortex, periallocortex and isocortex. The main distinction among those three types is based on morphological differences, in particular the number of layers, overall organization, appearance, etc., as well as its connectivity. Additionally, in the phylogenetic scale, this classification is conserved among different mammals. The most primitive and simple cortex is the allocortex, which is characterized by the presence of three layers, with one cellular main layer; it is continued by the periallocortex, which presents six layers, although with enough differences in the layer pattern to separate three different fields: presubiculum (PrS), parasubiculum (PaS), and entorhinal cortex (EC). The closest part to the allocortex (represented by the subiculum) is the PrS, which shows outer (layers I–III) and inner (V–VI) principal layers (*lamina principalis externa* and *lamina principalis interna*), both separated by a cell poor band, parallel to the pial surface (layer IV or *lamina dissecans*). This layer organization is present throughout the anterior-posterior axis. The PaS continues the PrS, but its rostrocaudal extent is shorter than the PrS. The organization of the PaS shows the layer pattern more clearly than in the PrS. Up to six layers are recognizable in the PaS, with layer IV as *lamina dissecans* between superficial (layers I–III) and deep (V–VI) layers, as in the PrS. The EC presents even more clearly the layer pattern along both mediolateral and rostrocaudal extent. The layer pattern is a thick layer I, layer II in islands, layer III medium pyramids, layer IV as *lamina dissecans* (not present throughout the EC extent), layer V with dark and big pyramids and a multiform layer VI. The EC borders laterally the proisocortex (incomplete type of isocortex). Variations in the appearance of its layers justify the distinction of subfields in the EC, in particular in human and nonhuman primates. EC layers are not similar to those in the neocortex. The transition between the periallocortical EC and isocortex is not sharp, so that the proisocortex forms an intervening cortex, which fills the gap between the periallocortex and the isocortex.

Keywords: human, entorhinal cortex, presubiculum, parasubiculum, layer pattern

OPEN ACCESS

Edited by:
Javier DeFelipe,
Cajal Institute (CSIC), Spain

Reviewed by:
James C. Vickers,
University of Tasmania, Australia
Fiorenzo Conti,
Università Politecnica delle Marche, Italy

****Correspondence:***
Ricardo Insausti
ricardo.insausti@uclm.es

Received: *28 July 2017*
Accepted: *08 September 2017*
Published: *04 October 2017*

Citation:
Insausti R, Muñoz-López M, Insausti AM and Artacho-Pérula E (2017) The Human Periallocortex: Layer Pattern in Presubiculum, Parasubiculum and Entorhinal Cortex. A Review. Front. Neuroanat. 11:84. doi: 10.3389/fnana.2017.00084

INTRODUCTION AND HISTORICAL ACCOUNT

The great anatomists of the early 20th century (Vogt, 1903, cited in Triarhou, 2009) recognized that the human cerebral cortex was not homogeneous. Vogt (1903) named the six-layered cortex, isocortex (homogeneous cortex), which made much of the cortex in the brain. In contrast, "allocortex" (inhomogeneous, other, or strange cortex) lacked multiple neuron lamination.

Ariëns-Kappers (1909) defined archicortex and paleocortex, which are "roughly identical" to the allocortex. The archicortex included the hippocampus and related structures, while paleocortex included what was called "*rhinencephalon*" (meaning olfactory brain). In this term both olfactory and hippocampal structures were considered together. Interestingly, while in other mammals the allocortical structures make up a great proportion of the cortical mantle, in humans that proportion is considerably reduced.

The concept of periallocortex (Pall) can be defined in classical neuroanatomy literature, dating back to the late nineteen and early twentieth centuries. Brodmann (1909) gave the first account of all Pall regions in man: Presubiculum (PrS), Parasubiculum (PaS) and entorhinal cortex (EC), and identified the main features of all of them.

The anatomical terms of "isocortex" and "allocortex" were introduced by Oskar Vogt in 1910 (cited in Stephan and Andy, 1970) and the purpose was to differentiate between the more common six-layered type of cortex vs. the uncommon, restricted to the rhinencephalon in broad sense, which one single neuron layer organization. For this reason, it was considered a more primitive-type of cortex. Filimonoff (1947) introduced the term periallocortex because it surrounded the allocortex, which was interposed between the isocortex and the allocortex. The allocortex itself was also divided into paleocortex, which corresponds to secondary olfactory centers, and archicortex, which is the hippocampus. Both, paleocortex and archicortex, present a peripheral region named peripaleocortex (i.e., periamygdaloid cortex and anterior insular related structures) and periallocortex which comprises the PrS, PaS and EC (**Table 1**). From the classification of the cerebral cortex in allocortex and isocortex derived the commonly used concepts of neocortex (new cortex, opposite to archicortex or old cortex). Another type of cortex interposes in between the periallocortex and the isocortex, which is known as proisocortex. The term proisocortex defines a type of cortex that does not fulfill all the layering features of isocortex, although is close (Bailey and von Bonin, 1951).

The layer organization of the three separated fields belonging to the periallocortex will be addressed in this review for its structural relevance and functional meaning in spatial navigation and memory. The connectional relationship of the different layers with other brain centers will be briefly addressed in this review (for more details see Insausti et al., 2017).

A common feature of all components of the periallocortex is the presence of a cell free zone, parallel to the pial surface, which receives the name of *lamina dissecans*. The presence of this cell free layer "splits" the thickness of the cortex into approximately equal halves. For this reason, Rose (1927) denominated these fields as *"schizocortex"*. This proposal is substantiated by the fact that the PrS, PaS and EC are present in all mammals, and all are principal components of the hippocampal formation.

COMMON FEATURES OF THE PERIALLOCORTEX

Figure 1 shows a general representation of the typical appearance of the PrS (A), PaS (B) and EC (C), the three periallocortical fields. The main and distinctive characteristic of the periallocortex is the presence of higher number of layers than the allocortex. The periallocortex boundaries are with the allocortex represented by the subiculum, and with the proisocortex, present in the cortex lining the collateral sulcus. Here, the lateral boundary of the periallocortex forms an interface with either the perirhinal cortex[1] or the posterior parahippocampal cortex (areas TH and TF of von Economo and Koskinas, 1925). A similar organization is present in a number of species (Ramón y Cajal, 1893; Brodmann, 1909; Lorente de Nó, 1933, 1934; Bakst and Amaral, 1984; Amaral et al., 1987; Insausti et al., 1995).

Probably the most common feature of the periallocortical cortex is the presence of a cell free band, halfway in the thickness of the cortex, which is named *lamina dissecans* (from latin, *dissecare*, to dissect), which dissects (splits) the cortex into two main layers, an external between the piamater, and the *lamina dissecans*, and an internal one, between *lamina dissecans* and the white matter. Although *lamina dissecans* is far from homogeneous, it is nonetheless present in all three fields of the periallocortex. The laminar structure and nomenclature of the periallocortex has been subject of debate, in particular the EC, which is the most laminated of all the Pall structures (for more details see Amaral et al., 1987).

FIELDS OF THE PERIALLOCORTEX

The distinction among the three fields of the periallocortex is based on morphological differences (number of layers, overall appearance), and connectional-functional significance. As mentioned above, Brodmann (1909) gave the first account of all the periallocortical regions in man: PrS, PaS and EC.

While the common feature of the allocortex is the presence of one neuron layer (i.e., dentate gyrus, hippocampal fields), the

[1]The term perirhinal cortex is used in a generic way, to denote the band of cortex that mainly borders laterally the entorhinal cortex, and encompasses both area 35 (true perirhinal cortex) and area 36, or ectorhinal cortex (Brodmann, 1909).

TABLE 1 | Classification of the types of cortex.

3 layers	Oflactory Dentate gyrus, Hippocampus & Subiculum	Allocortex (archicortex)
6 layers (with LD)	Presubiculum & Parasubiculum Entorhinal cortex	Periallocortex
6 layers (without LD)	Proisocortex, i.e. perirhinal cortext	
6 layers (with granular layer)	Isocortex (neocortex), i.e. association cortex	

The number of layers is indicated in each type: 3 layers for allocortex; 6 layers for periallocortex (including lamina dissecans); 6 layers for proisocortex (without lamina dissecans); 6 layers for isocortex (internal granular layer without lamina dissecans).

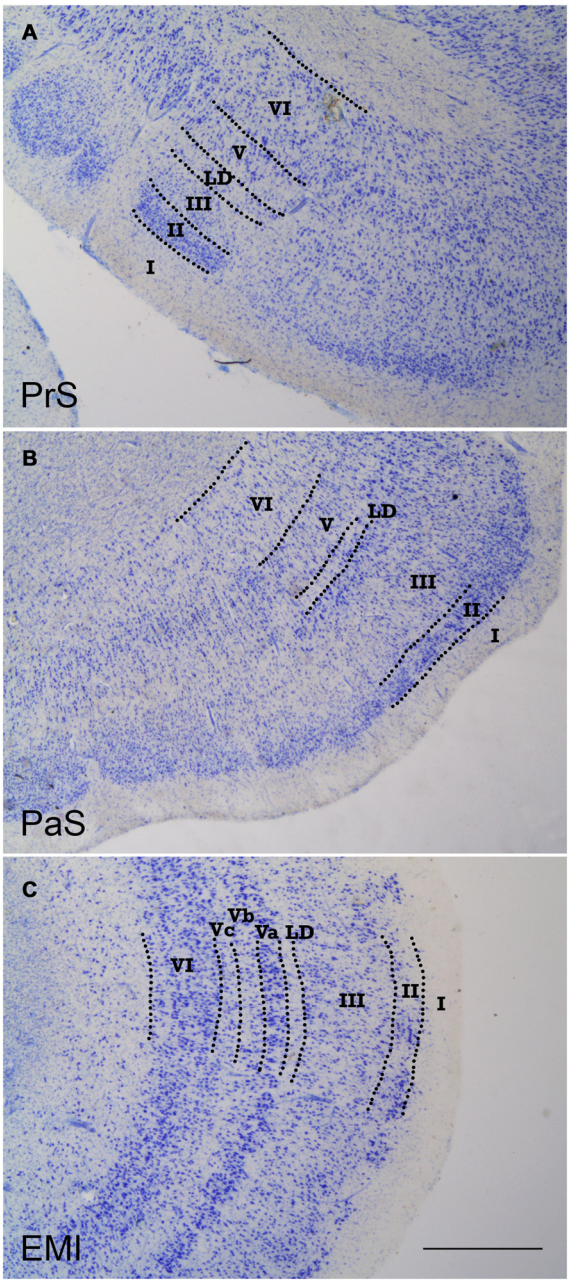

FIGURE 1 | Low-power photomicrographs of coronal sections that show the three components of the periallocortex. **(A)** shows a coronal section of the presubiculum (PrS). The layer pattern is indicated in roman numerals. **(B)** is the parasubiculum (PaS), equally depicting the morphological features and layer pattern. **(C)** shows a representative section of subfield E_{MI} of the entorhinal cortex (EC). The layer pattern is equally demarcated by the broken lines. The similitudes and differences of the progressive differentiation of the layer pattern can be appreciated, from the more rudimentary in the PrS, to more developed in the PaS, to the maximal differentiation of layers in the EC. Note the constant presence of *lamina dissecans* in all three components of the periallocortex. Scale bar 500 μm.

periallocortex shows several more layers. Of note, those layers are not similar to the layers in the neocortex, although we will use a similar sequence of roman numerals, meaning merely the order in which they appear, counting them from the pial surface to the underlying white matter.

The subtle transition of layers is most noticeable at the junction of the EC (periallocortex) and the proisocortex. The proisocortex marks the transition between periallocortex and the isocortex. The proisocortex shows six layers, as in the isocortex, but retain some of the periallocortical features such as prominent layers II and V, the lack or a thin layer IV, and an overall lesser columnarity than the isocortex. The proisocortex is largely coincident with the paralimbic cortex.

PERIALLOCORTICAL FIELDS

Presubiculum

The PrS has been clearly identified since the second half of the nineteenth century. However, its detailed structure in human and nonhuman primates has been rather fragmentary (Insausti and Amaral, 2012; Ding, 2013). Brodmann (1909) assigned, the number 27 to the PrS among the numbers he labeled the cortical areas. In his depiction of the medial surface of the human brain, this area runs in parallel to the hippocampus as far as the splenium of the corpus callosum, where it borders the retrosplenial cortex. He also noted the presence of the PrS in a number of nonhuman primates. Unfortunately, the description of the field and layers is almost nonexistent. von Economo and Koskinas (1925) provided a much more detailed account of the structure of the PrS[2]. According to their classic report, the PrS is characterized as a granular type of cortex (koniocortex). The layers that can be recognized in the human PrS, as well as in other mammals are:

1. Layer I or molecular layer. Thick and containing a great amount of fibers, whose origin is, in part, the EC through the perforant path.
2. Layers II and III, made up of rounded cells, which Ding (2013) calls pyramidal neurons, is subdivided into layers II and layer III. Both layers fuse together, with no clear boundary between both of them. Both layers II and III, are referred to by Braak (1980) as *lamina cellularis superficialis*, which is the nomenclature followed in this report.
3. Layer III, fused to the deep part of layer II. Layer III neurons are larger than its layer II counterpart.
4. Layer IV or *lamina dissecans*, which is one of the most characteristic features of the PrS, it separates the *lamina cellularis superficialis* from the *lamina cellularis profunda*, and divides the PrS into external and internal layers, approximately equal in thickness (0.61 mm outer, vs. 0.70 mm inner, excluding layer I, von Economo, 2009).
5. Layer V, is better identified at lateral portions of the PrS.
6. Layer VI, which has indistinct borders with layer V continues it as far as the limit with the white matter of the angular bundle.

A further layer (layer 7) has been identified in the monkey (Ding and Rockland, 2001), although it could be also a local

[2]The translated edition of Triarhou (2009) is used in this review.

extension of horizontal neurons of the internal part of the pyramidal cell layer of the subiculum.

There are almost no specific studies on the neurochemical phenotype of the human PrS; notwithstanding, partial information can be collected from different studies. In this sense, the immunoreactivuty for the calcium binding protein parvalbumin stands as the most remarkable, since the densely aggregated small neurons in the outer layers of the PrS are densely labeled (i.e., Figure 5 in Thangavel et al., 2008). The immunoreactivity of the PrS contrasts with the much lower immunoreactivity in the subiculum medially, and the PaS laterally.

Figure 2 shows representative levels of the PrS at three different levels along the rostrocaudal axis. One of the most prominent and conspicuous features of the PrS layer II is the presence of clumps of small, rounded neurons, or aggregates of cells, amidst the white matter of layer I. Layer I is thicker in between clumps, in particular at the medial portion (closest to the subiculum). At this location, the PrS forms two or three conspicuous groups[3] of small, densely packed and rounded neurons (granular appearance). Although the granular neurons are in layer II, it cannot be ruled out that some layer III neurons might be present. Seen from the surface, the PrS offers a lattice-like pattern, the *substantia reticulata alba* (Arnold, 1851), which can also be seen in the EC. Interestingly, the nonhuman primate PrS does not form islands throughout its extent, therefore this feature is exclusively present in the human brain. It is interesting to note that this organization of cell aggregates in layer II is also present at the caudal portions of the PaS and the EC, at precisely the same levels at which grid cells and head directions neurons have been described (Glasgow and Chapman, 2007; Miller et al., 2015; Suthana et al., 2015).

Rostrocaudal Variation of the PrS

According to Braak (1978, 1980) the small cells of layer II are "endogenous" to the PrS, while the deep layers mimic the adjacent fields, either subiculum proximally or EC distally. The latter is further caudally replaced by the posterior parahippocampal cortex (proisocortex).

Layers II–III appearance varies along the rostrocaudal axis of the PrS. Anteriorly, it breaks up into densely packed clumps of granular cells, while progressively the number of clumps decreases at posterior levels, where the PrS takes a more continuous appearance.

Of note, the PrS islands of small cells lie on top of the subiculum, and therefore the deep layers are limited to a small layer adjacent to the white matter. This portion of the PrS has also been considered as part of the subiculum (Braak, 1980), although laminar differences between both areas are obvious. However, the subiculum extends medially under these clumps and forms a termination of pyramidal neurons which form a rounded distal end of the subiculum (**Figures 2A,B**).

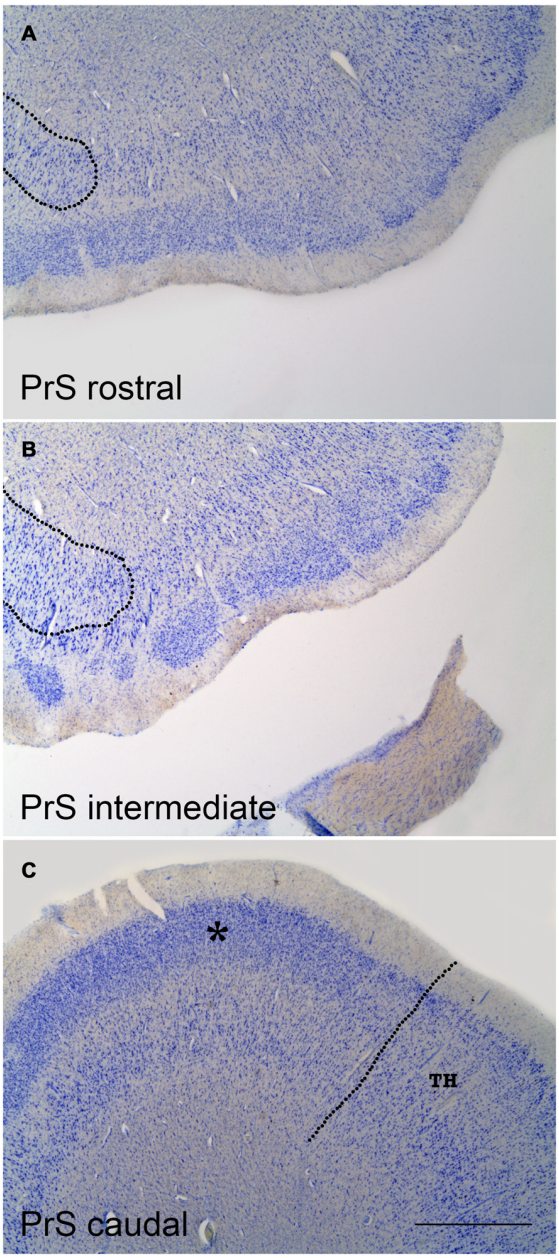

FIGURE 2 | Coronal sections at three levels of the PrS as shown in low-power photomicrographs. **(A)** is at a very rostral level of the PrS; the rounded border with the distal subiculum is indicated by the broken line to the left. **(B)** is at midlevel of the PrS. Again, the border with the subiculum is indicated at the left; the overlap of the clumps of the PrS with the subiculum is evident. **(C)** is a coronal section through the caudal level of the PrS. The continuous band of layer II–III neurons (asterisk) is noticeable, as well as the border with area TH (von Economo and Koskinas, 1925) of the posterior parahippocampal cortex, which is indicated by the broken line. The layer pattern of PrS is not indicated for clarity, but it is similar to that indicated in **Figure 1**. Scale bar is 500 μm.

On tangential sections of the PrS, the arrangement of these clumps forms a lattice-like structure, not much different to the EC. The functional significance of this particular arrangement of layer II neurons of the PrS is unknown, although the possibility

[3]We denominate clump the conspicuous aggregates of layer II neurons in the PrS, while we reserve the term "island" to the formation of layer II neurons in the EC. Other names have been used in the past such as "clouds" (Braak, 1980)

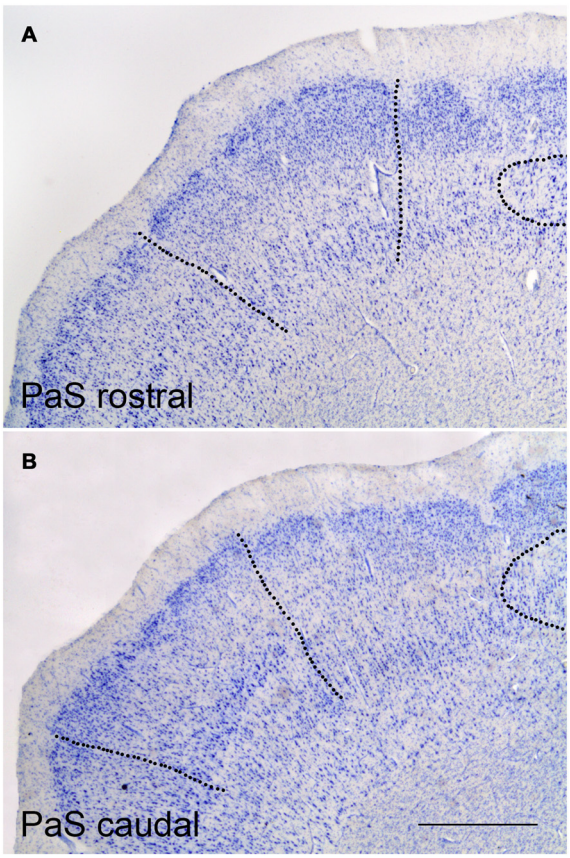

FIGURE 3 | Representative low-power photomicrographs at two PaS levels. **(A)** shows a rostral coronal section where the borders with the PrS (right side) and caudal EC (left side) are indicated as broken lines Likewise, the rounded termination of the subiculum under the clumps of the PrS can be appreciated. **(B)** shows the PaS at a caudal level. The border of PaS with the PrS and the distal end of the subiculum (to the right side), and with area TH (to the left side), are indicated by broken lines. Scale bar is 500 μm.

of interaction between presubicular layers on top and subicular layers underneath is intriguing.

Although the layering pattern of the PrS may be obscure at some levels, the layer organization is maintained throughout the anterior-posterior axis. A more complete account of the longitudinal variation of the PrS has been reported (Figure 1 in Braak, 1978).

The caudal extreme of the PrS continues with the granular portion of the retrosplenial cortex (BA 29) at the level of the *istmus* of the parahippocampal gyrus, which is also in the near vicinity of the rostralmost extreme of the calcarine fissure (Frankó et al., 2014). Here, layers II–III of the PrS form a more homogeneous association as a unique clump, and takes a continuous, elongated shape. The boundary with the granular part of the retrosplenial cortex (BA 29) is rather indistinct. The PrS extends as far as the end of the hippocampus.

No functional data on the specific activity of the PrS exist, although nonhuman primate studies show that the PrS is the main source of commissural, contralateral afferents to the EC (Demeter et al., 1985; Amaral et al., 1987; reviewed

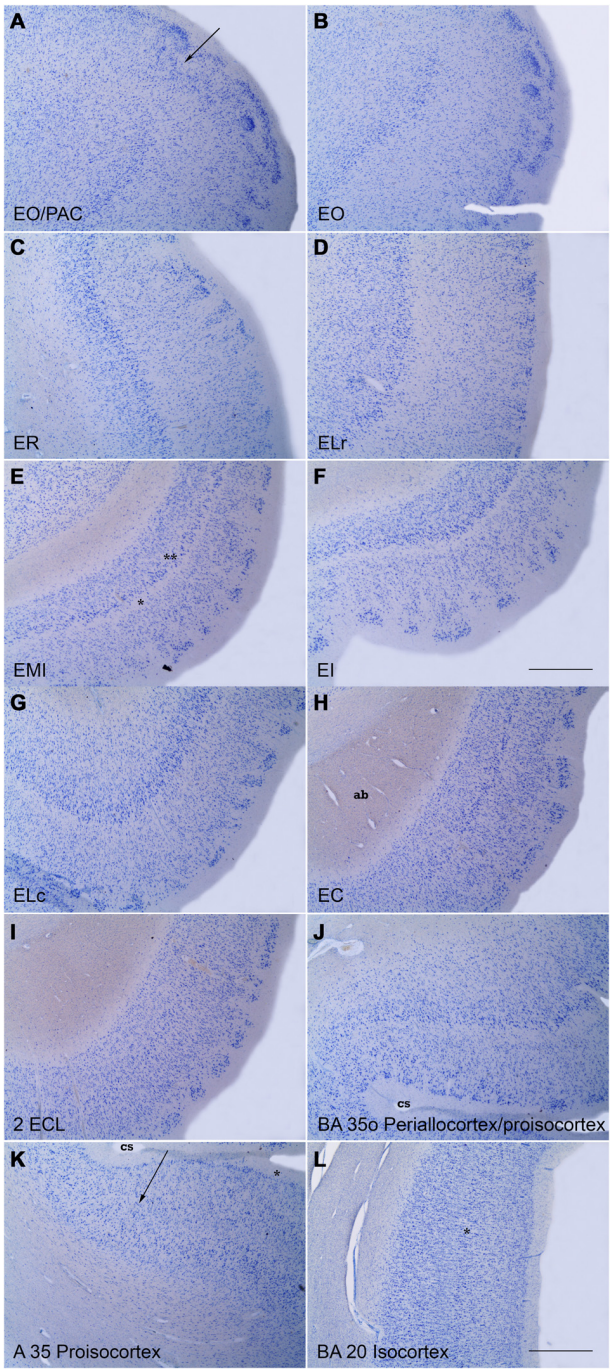

FIGURE 4 | Series of low power photomicrographs of coronal sections throughout the different subfields of the EC and adjacent proisocortical and isocortical cortices. **(A)** is at the transition between the rostral part of the EC (subfield E_O) and the amygdaloid complex (periamygdaloid cortex) The arrow indicates the border between the two. **(B)** is a representative section of subfield E_O. Note the absence of *lamina dissecans* and the characteristic *lamina cellularis profunda*. **(C)** shows subfield ER. Note the organization of layer III neurons in clusters. The bottom of the panel shows the transition with subfield E_{LR}. **(D)** is a representative section of subfield E_{LR}. Note the wide space (III–V interval), characteristic of this subfield. **(E)** is subfield E_{MI}. Note the sharpness of *lamina dissecans* (asterisk) and sublayer Vc (double asterisk).
(*Continued*)

FIGURE 4 | Continued
(F) is subfield E_I. Note the clear layer pattern of layer II islands, and a clear *lamina dissecans*. **(G)** is subfield E_{LC}, which occupies the shoulder of the lateral bank of the collateral sulcus (cs). Note the likeness with subfield E_{LR}. **(H)** is a representative level of subfield E_C. Note the absence of *lamina cellularis profunda* as a neat border with the white matter of the angular bundle (ag). **(I)** shows subfield E_{CL}. Note layer II islands surrounded by white matter, the columnarity of layers III to VI, and the neat border with the white matter. **(J)** shows the oblique transition between the lateral part of EC (subfield E_{LC}) and the proisicortex of BA 35 (transentorhinal cortex of Braak and Braak, 1985). **(K)** shows respectively the transition between BA 35 and 36 (arrow) at the lateral bank of the collateral sulcus (asterisk). **(L)** is an example of isocortex with an evident inner granular layer IV (asterisk). No delimitation of the layers is indicated for clarity. Scale bar in all layers is 500 μm.

in Insausti et al., 2017). As direct commissural connections of the dentate gyrus and other hippocampal fields are scarce in human as well as in nonhuman primates, this feature becomes a clear species difference in the structural organization of the commissural hippocampal system relative i.e., to rodents. Connectional studies have also revealed that the PrS is one of the main non-entorhinal hippocampal output systems; connections with temporal cortices (in particular perirhinal cortex), frontal and parietal cortices have also been demonstrated (Barbas and Blatt, 1995; Blatt and Rosene, 1998; Ding et al., 2000; Insausti and Muñoz, 2001).

Comparison with the Nonhuman Primate

The demonstration of acetylcholinesterase (AChE) in the nonhuman primate brain gives further support for a layering pattern of the PrS very similar to humans. Bakst and Amaral (1984) study describe in the *Macaca fascicularis* monkey an outer layer I, the molecular layer, followed by the external principal layer made up of a dense, continuous band of small neurons. The lamina dissecans stands clearly, deeper to which the lamina principalis interna lies. This layer is much less stained than the lamina principalis externa, and contains a population of polymorphic neurons, without any specific orientation. While the outer layers of the PrS are easily identified, the deep layers present blurred boundaries with the adjacent subiculum and PaS.

Parasubiculum (Figure 3)

The PaS continues the PrS towards the midline; it occupies the ventral shoulder of the hippocampal fissure. The PaS parallels the PrS for most of its course, although its rostrocaudal extent is shorter than PrS. The PaS starts a little caudal to the beginning of the PrS, and borders laterally the medial part of the EC. At caudal levels to the EC, area TH of von Economo and Koskinas (1925) forms the lateral boundary.

While the overall laminar organization of the PaS keeps some similarities with the PrS, the laminar organization of the PaS is more complex than in the PrS. The number of layers present increases to up to five layers; a *lamina dissecans* extends between the superficial and deep layers, similar to the PrS. The layers than can be distinguished are:

1. Layer I or molecular layer. It is smooth, and presents no specific feature.
2. Layer II is made up of more widely spaced pyramids and larger than the granular neurons in layer II of the PrS.
3. Layer III is made up of rounded medium or small neurons, some pyramids and other neurons with variable shape, whose boundary with layer II is rather indistinct.
4. *Lamina dissecans* is ill defined and discontinuous at some points.
5. Layer V lies beneath *lamina dissecans* and intermingle with layer VI of the EC, caudal to the start of the hippocampal fissure, (see below), although the large, deeply stained large pyramids in layer V of the EC are missing in the PaS.
6. Layer VI has no clear boundary, neither with layer V nor with the white matter. Laterally, at the transition with the EC, layers V and VI of EC seem to be in continuation with the PaS, although the latter shows more variety in the morphology and orientation.

The PaS extends behind the EC caudally, although the boundary is far from being smooth. Instead, in series of coronal sections through the end of the EC clumps of small layer II neurons intermingle with the PaS. In nonhuman primates, however, the PaS forms a continuous band that surrounds caudally the extent of the EC (Amaral et al., 1987). In humans, the PaS does not form a continuous band at the transition between the caudal end of the EC and the field TH of von Economo and Koskinas (1925), but an intermingling of layer II islands of the caudal pole of the EC and layer II PaS neurons, a feature that brings complexity to this part of the PaS. Eventually, the PaS recedes and continues approximately as far as the beginning of the caudal part of the PrS.

The information related to the neurochemical phenotype of the human PaS specifically is almost non-existent, although scattered data can be gathered in the literature (Thangavel et al., 2008).

In the nonhuman primate, the laminar structure of the PaS is basically similar to the PrS (Bakst and Amaral, 1984). The outer part of the PaS contains a molecular layer and an outer layer, which can be subdivided into a more densely packed outer band that covers approximately 25% of its depth, while the deep portion contains rounded or pyramidal neurons, more evenly spaced and less dense than the outer 25% (Bakst and Amaral, 1984). The lamina dissecans is present, although it is much less conspicuous than in the EC or the PrS. The deep portion contains larger neurons, which show little staining density in Nissl stain. Acetylcholinesterase staining preparations reveal a high density of the reaction product in the outer cell band of the PaS.

Entorhinal Cortex (Figure 4)

The human EC extends for a sizeable surface on the anterior part of the medial temporal lobe, in the anterior part of the macroscopically defined parahippocampal gyrus *(Gyrus parahippocampalis)*. In this location the EC borders rostrally the perirhinal cortex BA 35 (PRC, proisocortex) and amygdaloid complex. The PRC continues back laterally to the EC, in the medial bank of the collateral sulcus. In this location related to the collateral sulcus, PRC accompanies the whole rostrocaudal extent of the EC (Insausti et al., 1998; Ding and van Hoesen, 2015).

Medially, the limits of the EC are clear, first, with the amygdaloid complex by the *sulcus semiannularis*, and, once the hippocampal fissure is present, the caudal boundary is with the PaS for about the caudal one-half of the EC (Insausti et al., 1995).

Along its extent the EC presents a clear six -layered pattern. The number and names of the layers have been changing along the years, but the common notion of six (or seven) layers predominates. (for more details see Amaral et al., 1987). Layering in the EC has been best observed with aldehyde fuchsin stain in thick sections (800 μm), as reported by Braak (1972, 1980).

Despite this common pattern, substantial differences exist along its mediolateral and rostrocaudal extents of the EC. Those differences have been taken into account, and historically, different terminology and number of subfields have been described (Sgonina, 1938; Macchi, 1951; Braak, 1980; De Lacalle et al., 1994; Insausti et al., 1995; Krimer et al., 1997). Based on the peculiarities in the mediolateral and rostrocaudal extent of the EC, we proposed up to eight subfields, which are architectonically very similar to the subfields proposed in the nonhuman primate (Amaral et al., 1987).

The specific features of the different EC subfields have been reported previously in detail (Insausti et al., 1995). However, we present here the general organization and laminar particularities of each subfield. It needs to be taken into account that although the layers of the EC have been named layers I to VI, they are not homologous to neocortical layers I to VI. For instance, layer IV in the cortex does not correspond to layer IV in the EC (inner granular layer vs. a cell-free band).

Olfactory Subfield (E_O)

This subfield is located at the rostral-most portion of the EC. In nonhuman primates receives direct olfactory afferents from the olfactory bulb. The layer organization can be described as follows:

1. Layer I, or molecular layer is wide.
2. Layer II is thin, and broken up into two or three narrow islands
3. Layer III contains medium size, pale neurons homogeneously distributed
4. No *lamina dissecans* present
5. Layer V is indistinct and fuses with layer VI
6. Layer VI is wide and extends deep into the white matter. For this reason, it receives the name of *lamina cellularis profunda* (Braak, 1980)

Rostral Subfield (E_R)

E_R subfield borders medially subfield E_O. E_R makes up much of the anterior portion of the EC. Laterally it continues with subfield EL_R. The pattern of layers in subfield E_R is:

1. Layer I, wide, but without specific features. Some little prominences called *verrucae hippocampi* or warts, make the surface uneven (Klingler and Gloor, 1960; Simic et al., 2005).
2. Layer II is discontinuous, and forms small, rounded islands of neurons.
3. Layer III is typically organized into clusters of small or medium pyramids, which are separated by cell-poor spaces. The inner part of the layer shows a more continuous appearance.
4. No *lamina dissecans* is present at rostral levels; at a more caudal level, a thin band of low cellularity separates layers III and V.
5. Layer V is distinguished by the presence of a continuous band of larger, deeply stained neurons.
6. Layer VI contains neurons of various sizes and shapes. There is no distinct border with the white matter, and the inner part of layer VI enters for some distance into the white matter. This feature has been named by Braak (1980) *lamina cellularis profunda*, which interestingly is not present at more caudal subfields of the EC.

Lateral Rostral Subfield (E_{LR})

This subfield occupies much of the lateral surface of the anterior one-half of the EC. E_{LR} borders medially E_R, and laterally its boundary is marked by the transentorhinal cortex (Braak and Braak, 1985), which is a subdivision of BA35 or (PRC, proisocortex). The laminar features of subfield EL_R are:

1. Layer I, shows a smooth appearance (much fewer *verrucae hippocampi*).
2. Layer II is thick and broken into wide islands.
3. Layer III presents homogeneous appearance of medium sized pyramids.
4. Layer IV is wide and makes a clear separation between layers III and V. Myelin stain reveals a dense mesh of fibers that occupies the space. This feature is maintained all along the subfield and it is distinct to, and present at levels where the *lamina dissecans* has not appeared yet. This layer has been named "III–V interval" (Insausti et al., 1995).
5. Layer V is thick and prominent and invested with large pyramids, densely stained in Nissl preparations.
6. Layer VI contains neurons of various sizes and shapes and lacks a *lamina cellularis profunda*.

Intermediate Subfield (E_I)

This subfield is situated midway in the EC. It is usually presented as the most typical level of the EC in which all layers of the EC are clearly shown (Braak, 1972, 1980). E_I borders medially subfield E_{MI}, while laterally it limits with E_{LC}. The layer features of this subfield are as follows:

1. Layer I, is wide and the surface presents a bumpy appearance due to the presence of the *verrucae hippocampi*, which can be appreciated to the naked eye (Simic et al., 2005; Insausti and Amaral, 2012).
2. Layer II is discontinuous by the presence of a neat layer II islands of dark stellate neurons.
3. Layer III is irregular at the limit with layer II, but more homogeneous at the inner part, and forms a neat line with layer IV.
4. Layer IV has the appearance of typical *lamina dissecans*, which shows an almost complete absence of neurons, forming a neat line with both layer III and layer V.
5. Layer V is made up of large pyramids which are organized into three sublayers. The outer part (sublayer Va) borders *lamina*

dissecans, and it displays dense concentration of pyramids. Sublayer Vb lies underneath, and contains a lesser density of pyramids. Finally, the innermost is sublayer Vc, which contains a low density of neurons that forms a cell-poor band at the boundary with layer VI.
6. Layer VI is formed by homogeneous pyramids, which are densely packed. In contrast with more rostral levels, layer VI lacks *lamina cellularis profunda*, and shows a clear boundary with the white matter.

Medial Intermediate Subfield (E_{MI})

This subfield is coincident with the *Gyrus ambiens*, and is located at the dorsomedial part of the EC, immediately behind the olfactory subfield (E_O). This subfield is very noticeable as it lies between the *sulcus semiannularis* dorsally, and the *sulcus intrarhinalis* (Insausti and Amaral, 2012) which ends at the rostral tip of the hippocampal fissure. The laminar organization of the subfield E_{MI} shows the representative layer organization of the periallocortex even more clearly than subfield E_I. The medial part of E_{MI} shows all the layers with a compact appearance, while the lateral part resembles subfield E_I. The *sulcus intrarhinalis* ends at the caudal part of the subfield E_{MI}, at the point where the hippocampal fissure first appears. Then, the *Gyrus ambiens* (E_{MI} subfield) is replaced caudally by the *Gyrus uncinatus*, which is the transitional zone between the amygdaloid complex and the hippocampus. The layer organization of the subfield E_{MI} is:

1. Layer I is thinner relative to the adjacent subfield E_I and smooth (few or no *verrucae hippocampi*).
2. Layer II is thin and more continuous than the adjacent subfield E_I. In this respect, it resembles more layer II of subfield E_O.
3. Layer III is compact and homogeneous with medium pyramids evenly distributed.
4. Layer IV is *lamina dissecans*, and it presents a neat appearance.
5. Layer V is narrow. Sublayer Va is made up of big and dark pyramids. Sublayer Vb is indistinct. Sublayer Vc is very prominent and appears as a cell-free band that clearly separates sublayers Va and Vb from layer VI, and parallels *lamina dissecans*. This is a unique feature in all subfields of the EC, and an unmistakable feature of the subfield E_{MI}.
6. Layer VI is narrow and compact. At the medial extreme of the layer, it fuses with the overlying hippocampo-amygdalar transitional area (HATA) area (Rosene and van Hoesen, 1987).

Lateral Caudal Subfield (E_{Lc})

This subfield continues caudally the subfield E_{LR}. The posterior end of E_{LC} subfield takes place approximately at the level at which the hippocampal fissure is present. The layer organization of this subfield E_{LC} is:

1. Layer I, is wide with little indication of the presence of *verrucae hippocampi*.
2. Layer II has fewer, thick islands of stellate neurons.
3. Layer III presents medium-size pyramids, skewed towards the adjacent transentorhinal cortex.
4. Layer IV is made up of a thick mesh of fibers, which is narrower than layer III-V interval in subfield E_{LR}.
5. Layer V is thick and shows loosely arranged pyramids.
6. Layer VI is indistinct and continues with layer VI of the transentorhinal cortex without any clear border.

Caudal Subfield (E_C)

This subfield is in direct continuation with subfield E_I. While the transition between E_I and E_C is gradual, the presence of the hippocampal fissure is an indication of the boundary between these adjacent subfields. Therefore, E_C subfield occupies the part of EC immediately caudal to the opening of the hippocampal fissure. E_C subfield spans from the PaS (or PrS very rostrally) to the transentorhinal area, at the medial bank of the *sulcus collateralis*. The main layer features of subfield EC are:

1. Layer I, is thick and presents numerous *verrucae hippocampi*.
2. Layer II is invested with clearly separated cell islands made up of big, stellate neurons, which show a rounded or polygonal appearance. The upper limit of layer II islands corresponds to the *verrucae hippocampi* present on the surface of the subfield. The inner part of layer II is isolated from the underlying layer III by a dense stratum of fibers.
3. Layer III is a homogeneous stratum of medium-to-big pyramidal neurons, which organize in a radial, columnar fashion.
4. Layer IV is *lamina dissecans*, although much less prominent than in subfields E_{MI} and E_I.
5. Layer V is formed by big pyramids, homogeneously distributed. Sublayers can be recognized although sublayers Va and Vb tend to fuse; in contrast, sublayer Vc is increasingly wider and more evident; this is a feature that may confound with *lamina dissecans*, although the location of this sublayer is under the pyramidal neurons of layer Vc-b, and not above them, under layer III.
6. Layer VI is thick and presents a sharp boundary with the underlying white matter.

Caudal Limiting Subfield (E_{CL})

This subfield forms the caudal-most portion of EC. Subfield E_{CL} spans from the indistinct boundary with subfield EC as far as the transition with the PaS and its caudal continuation with the medialmost part of area TH (posterior parahippocampal cortex, von Economo and Koskinas, 1925). This subfield is as wide as subfield EC anteriorly, but progressively decreases in breadth. The medial border is coincident with the lower lip of the hippocampal fissure, while the lateral boundary is the posterior part of the transentorhinal cortex. The layer organization is:

1. Layer I, is thick and progressively presents fewer *verrucae hippocampi*. This surrounds completely layer Layer II islands.
2. Layer II is made up of neat cell islands with no significant difference with layer II islands of subfield E_C.
3. Layer III presents a very columnar appearance, as neat and radial columns of medium pyramids. The outer part of the layer is adjacent to the mesh of fibers which surrounds layer

II, thereby, in Nissl preparations, a cell free band interposes between layers II and III.
4. Layer IV, *lamina dissecans*, is absent so that layers III and V fuse together.
5. Layer V is made up of large pyramids, also radially oriented. The upper limit of the layer is fused with layer III, the only difference being the size and staining density of the pyramids, more pronounced in layer V, although they become progressively more similar. Sublayers Va and Vb cannot be distinguished, and make a single sublayer. However, sublayer Vc increases in width, and it is often mistaken with *lamina dissecans*.
6. Layer VI is also homogeneous, and presents a sharp border with the white matter of the angular bundle.

There are more data on the neurochemical phenotype or receptor layer distribution of different populations of the EC, although they are usually restricted to a sample or specific subfield as detailed above (Solodkin and van Hoesen, 1996, and Palomero-Gallagher and Zilles, 2017). From the structural point of view different techniques ranging from histochemical stains to receptor ligand demonstration demonstrate differences in the density of staining across different layers.

In this regard, it is important to note that histochemical staining for the demonstration of acetylcholinesterase reveals that the staining density is higher in the upper layers (Solodkin and van Hoesen, 1996). Likewise, the density of the enzyme cytochrome oxidase, which is related to energy demand of neurons, also shows stain in the upper layers II and III, while the layers V and VI present much lower staining density (Hevner and Wong-Riley, 1992; Solodkin and van Hoesen, 1996). Immunohistochemical demonstration of peptides have also been reported (i.e., somatostatin$_{28}$, Friederich-Ecsy et al., 1988; Solodkin and van Hoesen, 1996), its distribution being denser in layer II stellate cells and pyramids of layers III and V. Likewise the distribution of neuropeptide Y (NPY) was mainly located in layers III and V. It is worth noting that the distribution of different staining methods yield an arrangement as "modules" pattern (Solodkin and van Hoesen, 1996).

An interesting approach, although seldom used, is the analysis of receptor distribution in the EC, of which there is a very recent report (Palomero-Gallagher and Zilles, 2017). In this report, the distribution of several receptors is reported in a very small portion of subfield γ15 of Sgonina (1938), which corresponds to a sample of subfield E_{LR} in more recent studies on the subfields of the EC (Insausti et al., 1995). Regardless of the nomenclature and laminar terminology (it is used the layer terminology of Braak, 1980), it is interesting to note that it is mostly the upper layers (layers II and III of the present report, layers Preβ, Preγ, Preγ_1, Preγ_2, and Preγ_3), the layers which show a higher density of several receptors (subunits of GABA receptor, AMPA, A1, mGLUR 2/3, A1 M1, and β1). The deep layers (V and VI of the present report, layers Priβ and Priγ) show high density in kainate receptors, while the muscarinic receptor M_2 is present in the deep portion of layer III (Preγ_2 and Preδ). Interestingly, NMDA receptors do not show any particular layer distribution, and other receptors (nic β4γ_2, D_1, and 5-HT_2), show little density.

Functional Implication

At the present, it is difficult to ascribe any given function to periallocortex layers (PrS, PaS, EC) as such. However, there is experimental and clinical evidence of the involvement of the periallocortex in memory (Suthana et al., 2015) and spatial navigation (Glasgow and Chapman, 2007; Miller et al., 2015).

The concept of periallocortex is a type of cortex which presents more layers than in the allocortex. This fact could be used as a guide for the separation of the subiculum (allocortex) from the periallocortex (PrS, PaS and EC), and at the same time, to suggest dropping the term "subicular cortex", which includes both the PrS and PaS as incorrect, as it combines allocortical (subiculum) and periallocortica (PrS, PaS) fields. The information available on the structure of the periallocortex in the human brain is very limited in terms of neurochemical phenotype or presence of different receptors. However, the increasing number of studies about functional activity in the hippocampal formation and the medial temporal lobe in general, precise a clarification and substantiation of the anatomical terminology used in the ascription of a name to any particular activated brain region in the hippocampal formation. Therefore, a renewed interest is arising on the location, boundaries and extension of periallocortical cortices in the human brain in different physiological and pathological situations, singularly human memory and, on the pathological side, Alzheimer's disease.

AUTHOR CONTRIBUTIONS

RI designed the format and wrote the manuscript. MM-L and AMI extended and revised the original manuscript. EA-P chose and prepared the photomicrographs of the manuscript.

REFERENCES

Amaral, D. G., Insausti, R., and Cowan, W. M. (1987). The entorhinal cortex of the monkey: I. Cytoarchitectonic organization. *J. Comp. Neurol.* 264, 326–355. doi: 10.1002/cne.902640305

Ariëns-Kappers, C. U. (1909). The phylogenesis of the paleocortex and archicortex compared with the evolution of the visual neocortex. *Arch. Neurol. Psychiatry* 4, 161–173.

Arnold, F. (1851). *Handbuch der Anatomie des Menschen, mit Besonderer Rück-sicht auf Physiologie und Praktische Medicin.* Freiburg im Breisgau: A. Emmerling and Herder.

Bailey, P., and von Bonin, G. V. (1951). *The Isocortex of Man.* Urbana: University of Illinois Press.

Bakst, I., and Amaral, D. G. (1984). The distribution of acetylcholinesterase in the hippocampal formation of the monkey. *J. Comp. Neurol.* 225, 344–371. doi: 10.1002/cne.902250304

Barbas, H., and Blatt, G. J. (1995). Topographically specific hippocampal projections target functionally distinct prefrontal areas in the rhesus monkey. *Hippocampus* 5, 511–533. doi: 10.1002/hipo.450050604

Blatt, G. J., and Rosene, D. L. (1998). Organization of direct hippocampal efferent projections to the cerebral cortex of the rhesus monkey: projections from CA1, prosubiculum, and subiculum to the temporal lobe. *J. Comp. Neurol.* 392,

92–114. doi: 10.1002/(SICI)1096-9861(19980302)392:1<92::AID-CNE7>3.0.CO;2-K

Braak, H. (1972). Pigmentarchitecture of the human cortex cerebri. I. Regio entorhinalis. *Z Zellforsch. Mikrosk. Anat.* 127, 407–438. doi: 10.1007/BF00306883

Braak, H. (1978). Pigment architecture of the human telencephalic cortex. III. Regio presubicularis. *Cell Tissue Res.* 190, 509–523. doi: 10.1007/BF00219561

Braak, H. (1980). *Architectonics of the Human Telencephalic Cortex*. 4th Edn. Berlin: Springer-Verlag.

Braak, H., and Braak, E. (1985). On areas of transition between entorhinal allocortex and temporal isocortex in the human brain. Normal morphology and lamina-specific pathology in Alzheimer's disease. *Acta Neuropathol.* 68, 325–332. doi: 10.1007/bf00690836

Brodmann, K. (1909). *Vergleichende Lokalisationslehre der Groshirnrinde*. Leipzig: Verlag von Johann Ambrosius Barth.

De Lacalle, S., Lim, C., Sobreviela, T., Mufson, E. J., Hersh, L. B., and Saper, C. B. (1994). Cholinergic innervation in the human hippocampal formation including the entorhinal cortex. *J. Comp. Neurol.* 345, 321–344. doi: 10.1002/cne.903450302

Demeter, S., Rosene, D. L., and van Hoesen, G. W. (1985). Interhemispheric pathways of the hippocampal formation, presubiculum, and entorhinal and posterior parahippocampal cortices in the rhesus monkey: the structure and organization of the hippocampal commissures. *J. Comp. Neurol.* 233, 30–47. doi: 10.1002/cne.902330104

Ding, S. L. (2013). Comparative anatomy of the prosubiculum, subiculum, presubiculum, postsubiculum, and parasubiculum in human, monkey, and rodent. *J. Comp. Neurol.* 521, 4145–4162. doi: 10.1002/cne.23416

Ding, S. L., and Rockland, K. S. (2001). Modular organization of the monkey presubiculum. *Exp. Brain Res.* 139, 255–265. doi: 10.1007/s002210100778

Ding, S. L., and van Hoesen, G. W. (2015). Organization and detailed parcellation of human hippocampal head and body regions based on a combined analysis of cyto- and chemoarchitecture. *J. Comp. Neurol.* 523, 2233–2253. doi: 10.1002/cne.23786

Ding, S. L., van Hoesen, G., and Rockland, K. S. (2000). Inferior parietal lobule projections to the presubiculum and neighboring ventromedial temporal cortical areas. *J. Comp. Neurol.* 425, 510–530. doi: 10.1002/1096-9861(20001002)425:4<510::aid-cne4>3.0.co;2-r

Frankó, E., Insausti, A. M., Artacho-Pérula, E., Insausti, R., and Chavoix, C. (2014). Identification of the human medial temporal lobe regions on magnetic resonance images. *Hum. Brain Mapp.* 35, 248–256. doi: 10.1002/hbm.22170

Filimonoff, I. N. (1947). A rational subdivision of the cerebral cortex. *Arch. Neurol. Psychiatry* 58, 296–311. doi: 10.1001/archneurpsyc.1947.02300320047002

Friederich-Ecsy, B., Braak, E., Braak, H., and Probst, A. (1988). Somatostatin-like immunoreactivity in non-pyramidal neurons of the human entorhinal region. *Cell Tissue Res.* 254, 361–367. doi: 10.1007/bf00225808

Glasgow, S. D., and Chapman, C. A. (2007). Local generation of theta-frequency EEG activity in the parasubiculum. *J. Neurophysiol.* 97, 3868–3879. doi: 10.1152/jn.01306.2006

Hevner, R. F., and Wong-Riley, M. T. (1992). Entorhinal cortex of the human, monkey, and rat: metabolic map as revealed by cytochrome oxidase. *J. Comp. Neurol.* 326, 451–469. doi: 10.1002/cne.903260310

Insausti, R., and Amaral, D. G. (2012). "Hippocampal formation," in *The Human Nervous System*, 3rd Edn. eds J. K. Mai and G. Paxinos (San Diego, CA: Elsevier), 896–942.

Insausti, R., Juottonen, K., Soininen, H., Insausti, A. M., Partanen, K., Vainio, P., et al. (1998). MR volumetric analysis of the human entorhinal, perirhinal, and temporopolar cortices. *Am. J. Neuroradiol.* 19, 659–671.

Insausti, R. M., Marcos, P., Mohedano-Moriano, A., Arroyo-Jiménez, M. M., Córcoles-Parada, M., Artacho-Pérula, E., et al. (2017). "The nonhuman primate hippocampus: neuroanatomy and patterns of cortical connectivity," in *The Hippocampus from Cells to Systems*, eds D. E. Hannula and M. C. Du (Cham, Switzerland: Springer), 3–36.

Insausti, R., and Muñoz, M. (2001). Cortical projections of the non-entorhinal hippocampal formation in the cynomolgus monkey *(Macaca fascicularis)*. *Eur. J. Neurosci.* 14, 435–451. doi: 10.1046/j.0953-816x.2001.01662.x

Insausti, R., Tuñón, T., Sobreviela, T., Insausti, A. M., and Gonzalo, L. M. (1995). The human entorhinal cortex: a cytoarchitectonic analysis. *J. Comp. Neurol.* 355, 171–198. doi: 10.1002/cne.903550203

Klingler, J. G., and Gloor, P. (1960). The connections of the amygdala and of the anterior temporal cortex in the human brain. *J. Comp. Neurol.* 115, 333–369. doi: 10.1002/cne.901150305

Krimer, L. S., Hyde, T. M., Herman, M. M., and Saunders, R. C. (1997). The entorhinal cortex: an examination of cyto- and myeloarchitectonic organization in humans. *Cereb. Cortex* 7, 722–731. doi: 10.1093/cercor/7.8.722

Lorente de Nó, R. (1933). Studies on the structure of the cerebral cortex. I. The area entorhinalis. *J. Psychol. Neurol.* 45, 381–438.

Lorente de Nó, R. (1934). Studies on the structure of the cerbral cortex. II. Continuation of the study of the Ammonic system. *J. Psychol. Neurol.* 46, 113–177.

Macchi, G. (1951). The ontogenetic development of the olfactory telencephalon in man. *J. Comp. Neurol.* 95, 245–305. doi: 10.1002/cne.900950203

Miller, J. F., Fried, I., Suthana, N., and Jacobs, J. (2015). Repeating spatial activations in human entorhinal cortex. *Curr. Biol.* 25, 1080–1085. doi: 10.1016/j.cub.2015.02.045

Palomero-Gallagher, N., and Zilles, K. (2017). Cortical layers: Cyto-, myelo-, receptor- and synaptic architecture in human cortical areas. *Neuroimage* doi: 10.1016/j.neuroimage.2017.08.035 [Epub ahead of print].

Ramón y Cajal, S. (1893). Estructura de asta de Ammon. *Anal. Soc. Esp. Hist. Nat. Madrid* 22.

Rose, M. (1927). Die sog. Riechrinde beim Menschen und beim Affen. *J. Psychol. Neurol.* 34, 261–401.

Rosene, D. L., and van Hoesen, G. W. (1987). "The hippocampal formation of the primate brain: a review of some comparative aspects of cytoarchitecture and connections," in *Cerebral Cortex*, (Vol. 6) eds E. Jones and A. Peters (New York, NY: Plenum Press), 345–456.

Sgonina, K. (1938). Zur vergleichenden anatomie der entorhinal und prasubikularregion. *J. Psychol. Neurol.* 48, 56–163.

Simic, G., Bexheti, S., Kelovic, Z., Kos, M., Grbic, K., Hof, P. R., et al. (2005). Hemispheric asymmetry, modular variability and age-related changes in the human entorhinal cortex. *Neuroscience* 130, 911–925. doi: 10.1016/j.neuroscience.2004.09.040

Solodkin, A., and van Hoesen, G. W. (1996). Entorhinal cortex modules of the human brain. *J. Comp. Neurol.* 365, 610–627. doi: 10.1002/(SICI)1096-9861(19960219)365:4<610::AID-CNE8>3.3.CO;2-X

Stephan, H., and Andy, O. J. (1970). "The allocortex in primates," in *The Primate Brain*, eds C. R. Noback and W. Montagna (New York, NY: Appleton-Century-Crofts), 109–135.

Suthana, N. A., Donix, M., Wozny, D. R., Bazih, A., Jones, M., Heidemann, R. M., et al. (2015). High-resolution 7T fMRI of human hippocampal subfields during associative learning. *J. Cogn. Neurosci.* 27, 1194–1206. doi: 10.1162/jocn_a_00772

Thangavel, R., van Hoesen, G. W., and Zaheer, A. (2008). Posterior parahippocampal gyrus pathology in Alzheimer's disease. *Neuroscience* 154, 667–676. doi: 10.1016/j.neuroscience.2008.03.077

Triarhou, L. C. (2009). Alfons Maria Jakob (1884–1931), neuropathologist par excellence. Scientific endeavors in Europe and the Americas. *Eur. Neurol.* 61, 52–58. doi: 10.1159/000175123

Vogt, O. (1903). Zur anatomischen gliedwrung des cortex cerebri. *J. Psychol. Neurol.* 2, 160–180.

von Economo, C. (2009). *Cellular Structure of the Human Cerebral Cortex*. ed. L. C. Triarhou (Basel, Switzerland: Karger).

von Economo, C., and Koskinas, G. N. (1925). *Atlas of Cytoarchitectoncs of the Adult Human Cerebral Cortex*. Basel: Karger.

Conflict of Interest Statement: The authors declare that the research was conducted in the absence of any commercial or financial relationships that could be construed as a potential conflict of interest.

frontiers in Neuroanatomy

PERSPECTIVE
published: 07 November 2017
doi: 10.3389/fnana.2017.00100

Neocortical Lamination: Insights from Neuron Types and Evolutionary Precursors

Gordon M. Shepherd[1]* *and Timothy B. Rowe*[2]

[1]Department of Neuroscience, Yale University School of Medicine, New Haven, CT, United States, [2]Jackson School of Geosciences, University of Texas at Austin, Austin, TX, United States

The neocortex is characterized by lamination of its neuron cell bodies in six layers, but there are few clues as to how this comes about and what is its function. Recent studies provide evidence that evolution from simple three-layer cortex may give insight into this problem. Three-layer cortex arose in the olfactory, hippocampal and dorsal cortex of the early amniote forebrain based on a cortical module of excitatory and inhibitory inputs to an intratelencephalic (IT) type of pyramidal neuron with feedback excitation and inhibition and related interneurons. We summarize recent evidence suggesting the hypothesis that the developmental program of three-layer olfactory cortex was co-opted to form six-layer mammalian neocortex, elaborating IT cortical units in layers 2–6 while adding layer 4 stellate cells, layer 5B pyramidal tract (PT) cells and layer 6 corticothalamic (CT) cells.

Keywords: amniote, intratelencephalic, serial homology, cortical hierarchy, olfactory cortex, feedback excitation, feedback inhibition, gene expression

OPEN ACCESS

Edited by:
Kathleen S. Rockland, Boston University School of Medicine, United States

Reviewed by:
Stewart Shipp, University College London, United Kingdom
Andre Goffinet, Université catholique de Louvain, Belgium

***Correspondence:**
Gordon M. Shepherd
gordon.shepherd@yale.edu

Received: *12 September 2017*
Accepted: *20 October 2017*
Published: *07 November 2017*

Citation:
Shepherd GM and Rowe TB (2017) Neocortical Lamination: Insights from Neuron Types and Evolutionary Precursors. Front. Neuroanat. 11:100. doi: 10.3389/fnana.2017.00100

Initial evidence for cortical function at the cellular level came from stained cell bodies in mammals, which were found to be arranged in six layers that varied in different cortical areas. Similarity of the layers in different areas suggested a similarity of functions, whereas differences suggested different properties related to different cortical systems. A century of research on lamination produced a useful guide to cell location and function. However, cortical layering is variable among amniotes (Mammalia plus Reptilia, including Aves), and is absent in birds (Streidter, 2005). Both six-layer mammalian cortex and the absence of cortical layering in birds are now understood to have evolved from a common ancestor inferred to possess three cortical layers (Ulinski, 1983; ten Donkelaar, 1998; Rowe and Shepherd, 2016; Rowe, 2017). This variation raises the question of a more general cortical organization, one based not on lamination but on fundamental neuron functions, dependent on dendrites, axons, synapses and their physiological properties, connections and actions. Can a more general cortical organization be inferred in amniotes ancestrally, one which underlies both layering and its loss in descendent lineages?

Methods from gene targeting to physiological and pharmacological analysis are emerging to decipher neuron functions across different cortical areas. A synthesis of this work (Harris and Shepherd, 2015) identified a rich domain of inquiry in patterns of connectivity, the hodology, between genetically defined cell types as a primary organizing principle of the neocortex. Parallel work sets the functional organization of cortical neurons within an explicit evolutionary context. These suggest the existence of a basic cortical circuit that had its origin in three-layer forebrain cortex of the ancestral amniote, that was conserved in non-avian reptiles, and that became elaborated in mammalian six-layer neocortex (Shepherd, 2011; Rowe and Shepherd, 2016).

We summarize these approaches to suggest a new synthesis of the evolution of neocortical neuron types. It offers insights into the ancestral amniote three-layer cortex as an associative network of higher level functions. It presents the mammalian neocortex as a further elaboration

of this network that came to directly influence the entire neuraxis as it further elaborated higher functions including multidimensional perception, memory, planning and execution. This emphasis on fundamental neuron functions and general cortical organization adds new insight into the roles of gene duplications, olfaction, somatosensation and motor control in driving neocortical evolution.

NEOCORTICAL CELL TYPES AND THEIR LAMINAR LOCATION

Connectivity of pyramidal cells (PCs) in different neocortical laminae is summarized in **Figure 1**. Complementary to classifying cells in terms of their layers or morphology, pyramidal neurons carrying cortical output can be divided into four main types based on their output targets (Reiner et al.'s, 1998; Oberlaender et al., 2012; Harris and Shepherd, 2015).

A key type is the intratelencephalic (IT) pyramidal neuron, located in all layers from L2-L6, whose axon projects within the telencephalon and to other cortical areas or to the striatum. There are different combinations of inputs in each layer; the outputs are also diverse and exceed what can be covered here (for a summary, see Table 1, Harris and Shepherd, 2015). IT cells are excitatory, as are all cortical PCs. IT neurons are highly diverse, yet their connectivity patterns appear to be similar in different cortical areas. We will see that this is evidence of their evolutionary origin.

The outcome of physiological activity in IT cells must be carried to the rest of the nervous system. In basal amniotes (inferred from comparing living turtles, lizards and amphibians), this depended on connections from basal ganglia to neurons in the midbrain and brainstem which relayed the outcome to the rest of the neuraxis. By contrast, the mammalian neocortex evolved its own output neuron in the form of a cell that sends its long axon from the cortex through the pyramidal tract (PT) to the brain stem and spinal cord, carrying cortical output to many centers and nuclei. This PT cell is found in a specific sublayer, L5B. The long apical dendrite of PT cells extends toward L1, receiving inputs from every intervening layer; on the output side, subsets of PT neurons innervate different combinations of targets within the brainstem and spinal cord. These complex combinations of targets mirror the complex combinations of cortical neurons and their inputs for which PT cells are the final common path.

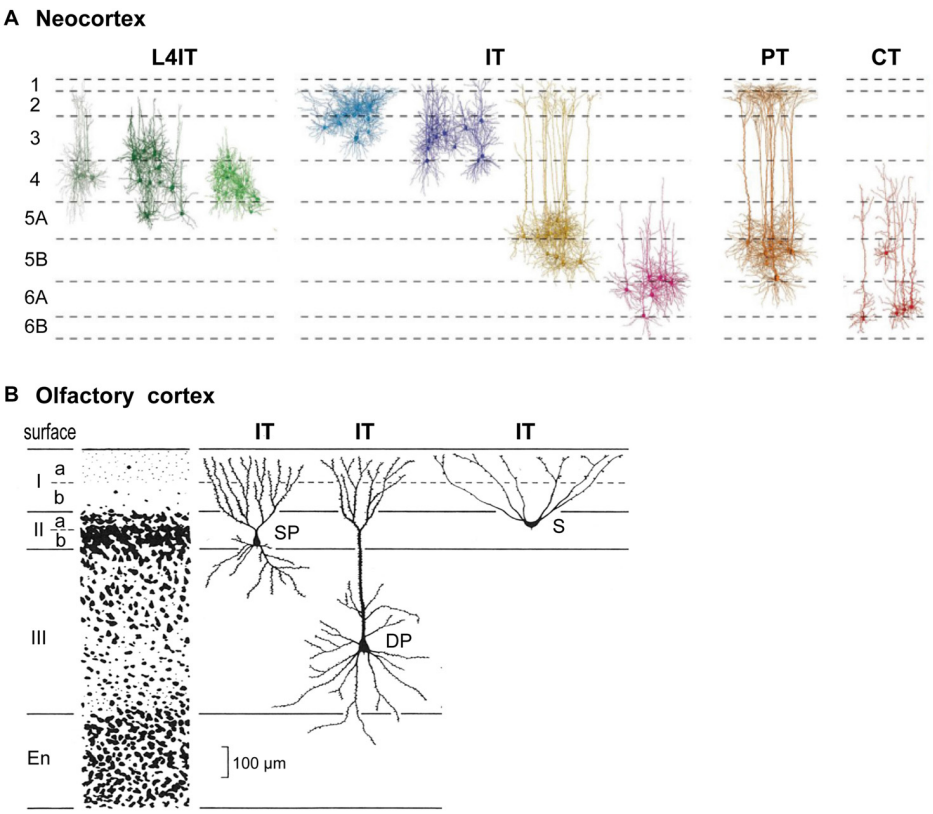

FIGURE 1 | Basic cortical neuron types and laminae. **(A)** Neocortex (S1 barrel cortex). Intratelencephalic (IT) cells are found in layers 2–6; they connect only within the neocortex and basal ganglia. Pyramidal tract (PT) cells are restricted to L5B; they connect through the PT to the entire neuraxis. Corticothalamic (CT) cells are restricted to L6; they connect to the thalamus. L4IT: found mostly in L4, connect locally. See text. Adapted from Oberlaender et al. (2012) and Harris and Shepherd (2015). **(B)** Olfactory cortex IT pyramidal neurons are found in layers IIa, IIb and III. S, semilunar cells (lack basal dendrites); SP, small pyramids; DP, deep pyramids. Adapted from Neville and Haberly (2004).

The third main type with a long axon is the corticothalamic (CT) cell. Its cell body is found in a single sublayer, L6, distinct from IT cells also found there. Its axon projects to the thalamic nucleus related to the area in which it is located. In primary sensory areas this goes to the specific sensory relay nucleus and associated reticular nucleus. In motor and association areas the thalamic relations are less clear. Traditionally it has been recognized that CT cells are part of a loop with thalamocortical (TC) cells binding the cortex and thalamus.

A final cortical cell type is the short-axon IT cell (**Figure 1**), localized mostly in layer 4 (L4); it receives thalamic inputs and sends its axon only locally. In sensory areas the L4IT cell usually lacks an apical dendrite, appearing as a stellate cell; elsewhere it is often a pyramidal or other type. Its axon usually targets only nearby cells in L2/3 or L5.

Thus, the main interaction between cortical areas is through the IT cells, and can be subsumed as "serial homology" (Harris and Shepherd, 2015), the idea that cell types and connections did not evolve independently in each area, but rather that a general, repeated organization was adapted for different functions in different locales. Another principle is the concept of "cortical hierarchy", for example, between primary and secondary sensory areas. In some cases this involves outputs and inputs involving different layers, but this is not a universal rule. There may be a limited number of IT subclasses that are homologous in the sense that they arose at more general levels of the hierarchy and connect different cortical areas.

Three main types of cortical interneurons have emerged: parvalbumin (Pvalb), somatostatin (Sst) and vasoactive intestinal peptide (Vip), all inhibitory, but with specific connections with the PCs and with each other. Serial homologous principles appear to apply to their interactions in different areas, but are beyond the focus of this review.

EVOLUTIONARY ORIGINS OF NEOCORTICAL NEURONS AND LAMINATION

Cortical lamination is not unique to neocortex. From an evolutionary perspective it began with simple three-layer cortex. The basic circuit organization within a three-layered cortical structure was established by Haberly's classic study of olfactory cortex (summarized in Neville and Haberly, 2004), and later extended to general circuit organization in dorsal cortex and hippocampus in all non-avian reptiles (Güntürkün et al., 2017; Naumann and Laurent, 2017). Olfactory cortex in the ancestral amniote is inferred to have contained three subtypes of pyramidal neuron—semilunar, superficial and deep pyramidal—with distinct morphologies, located at successive depths that define specific cell sublayers (**Figure 1B**). This may indicate an underlying potential for three-layer cortex to evolve sublayers related to different pyramidal neurons at different depths, as eventually expressed most highly in neocortex. The three subtypes develop in an inside-out sequence, the same sequence expressed in neocortex (Luzzati, 2015; Klingler, 2017).

Our focus on a physiological approach to neocortex began with the synaptic organization of the mammalian olfactory cortex as a simple system for elucidating organizational principles. This suggested a basic circuit of PC with feedforward and feedback excitation and inhibition as a foundation for all cortical structures (Haberly and Shepherd, 1973; Shepherd, 1974). This was followed by the proposal that olfactory cortex is not a low level processing station, but rather is a high level association cortex that implements content addressable memory (Haberly, 1985). This critical insight underlies a growing consensus that higher association functions were already built into simple three layer cortex.

The functional organization of turtle dorsal cortex put these common features in a comparative evolutionary context (Smith et al., 1980; Kriegstein and Connors, 1986) in which six-layer mammalian neocortex evolved from a three-layer cortex in the ancestral amniote (Shepherd, 1988, 2011; Rowe and Shepherd, 2016). This has become an active field, with many current studies testing these ideas (Aboitiz and Montiel, 2015; Brunjes and Osterberg, 2015; Fournier et al., 2015; Luzzati, 2015; Naumann et al., 2015; Diodato et al., 2016; Klingler, 2017).

The core of the amniote cortex is a layer of PCs with long apical dendrites (**Figure 2A**). Inputs enter the superficial layer where they are excitatory to dendrites and, in parallel, to feedforward inhibitory interneurons to the dendrites. PC axon branches give rise to internal feedback circuits that are widespread and excitatory to themselves and other PCs, and to interneurons that spread feedback and lateral inhibition. Output axons go to other parts of cortex or basal ganglia, and to the hypothalamus. These are IT cells. The only exception is a small projection from dorsal cortex to the superior colliculus, which may reflect dominance of the dorsal cortex by visual input (Fournier et al., 2015). These features are built into the simple circuit for all three types of three-layer cortex (**Figure 2A**). We term this PC with its feedforward and feedback excitatory and inhibitory circuits a basic circuit module for the cerebral cortex.

Olfactory cortex is expanded from this basic circuit module into sublayers related to each of the three PC subtypes (**Figure 2B**). Each subtype projects within the cortex, qualifying it as an IT cell, processing inputs (the multidimensional encoding of olfactory molecules) for further projection to higher processing (in orbitofrontal cortex) and eventually to motor output via entorhinal cortex. Association fibers are major constituents defining the laminae, and are subjects of current investigation.

How might the neocortex have evolved based on the basic circuit module? A simplified representation of the modules of multi-layer neocortex (**Figure 2C**) shows the IT cell. This appears to be the same type as in the three-layer cortex, interacting primarily with other forebrain regions at higher levels of associative function. In early amniotes, IT cells performed these higher functions almost entirely "offline" from the main flow of sensory input and motor outflow in subcortical

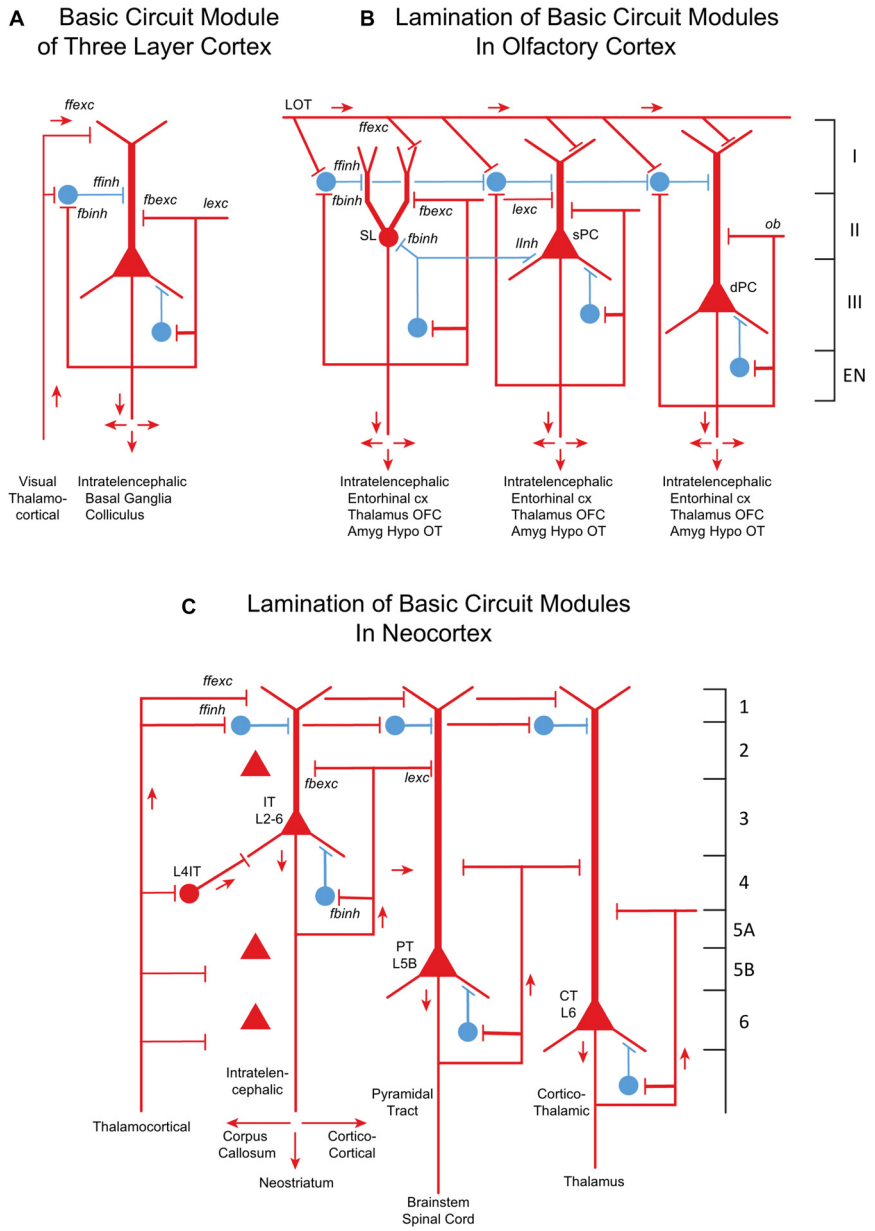

FIGURE 2 | From three-layer to six-layer cortical microcircuits. **(A)** Simplified basic cortical module of ancestral three-layer olfactory cortex, hippocampus and reptilian dorsal cortex. Based on Kriegstein and Connors (1986) and Shepherd (2011). PC, pyramidal cell. Abbreviations of functional actions: ffexc, feedforward excitation; ffinh, feedforward inhibition; fbexc, feedback excitation; fbinh, feedback inhibition; lexc, lateral excitation; linh, lateral inhibition. **(B)** Olfactory cortex: lamination of basic circuit modules. **(C)** Mammalian neocortex: lamination of basic circuit modules. Abbreviations as in **(A)**. Laminae for the cell types are indicated. Presumed excitatory cells shown in red, inhibitory cells shown in blue. Based on Shepherd (1988) and Rowe and Shepherd (2016).

brain regions. As with olfactory cortex, the higher associative functions of IT cells were inherited from their three-layer antecedents.

A major innovation in neocortex is the PT cell. Through this cell in layer 5b, its axon potentially connects to virtually all levels of the central nervous system. Kita and Kita (2012) have shown labeling of PT branches to other parts of ipsilateral cortex and basal ganglia, and to the thalamus and especially on down through the midbrain and hindbrain to the spinal cord. Individual neurons do not branch to all possible targets, but rather to subsets, which vary from neuron to neuron. The complexities of these multiple subcerebral connections may be as profound as complexities of the interactions within the expanded IT network of the neocortex itself.

The new principle of the neocortex is therefore not the associative network of IT cells *per se*, but two things: first, elaboration of the associative networks inherited from three layer cortex to give higher functions that include not only

multidimensional perception and memory but also planning and execution; and second, connections through PT cells to give the cortex direct influence on the entire neuraxis. Far from being a level of higher associative function "offline" from the lower centers, the neocortex makes its higher functions available for direct insertion at all levels into the ongoing interactions of the neuraxis with the environment. Increased layering of IT cells, and increased elaboration of many cortical areas based on different sensory and motor connectivity, give neocortex its immense power in representing the world and acting upon it.

The CT PC in layer 6 connects specifically to the thalamic nuclei and thalamic reticular nucleus. It plays several roles in modulating vastly increased sensory input that occurs in the neocortex depending on motor output in the context of the behavioral state (Thomson, 2010). The fact that the CT and PT cells are found in specific layers suggests that they are inserted into the main multilayer framework of the IT cells. We speculate that CT cells evolved in their positions to direct output from IT cells to the thalamus, and that PT cells were placed to collect IT outputs to distribute throughout the neuraxis.

All three neocortical cell types have basic circuit modules of a principle neuron and its interneurons similar to their three layer counterparts, showing the conservation of principle. Given this basic module format, in each area are specific adaptations of cell morphology, subtypes and connectivities.

Other changes in mammals involved increases in information from somatosensation, motor control and in certain clades from audition and vision. This multidimensional inflow evidently required staging to put the information into a common form readily processed by the different cortical circuits by excitatory TC inputs. There are several types of TC projections (Clascá et al., 2012); two important types are "core" and "matrix". Prominent in sensory systems is the "core" type of thalamic nuclei, with axons that target layer 4, where they activate pyramidal, stellate and other specialized IT cells (**Figure 2B**). The TC → layer 4 connection is present in specialized sensory systems such as rodent barrel cortex, and in "agranular" areas such as motor cortex, albeit in a diminutive, prototypical form (Yamawaki et al., 2014). The other major type of TC projection is the "matrix" type that targets layer 1 and layer 5A; this is probably the most prevalent type in the neocortex and evolutionarily the oldest. Layers may thus provide separation of targets for intralaminar interactions.

Not shown in **Figure 2** is the evolution in neocortex of interneurons, especially the three types expressing Sst, Vip, and Pvalb, each with its specific morphology, local hodology and control of different integrated modules of principal neurons.

OLFACTION AS A DRIVER OF NEOCORTICAL EVOLUTION

We can now see neocortex as a complex microcircuit based on four excitatory cell classes distributed across multiple layers. The superficial layers receiving major inputs to layer 1, the presence of IT neurons in multiple layers, and wide cortico-cortical projections of IT cells resemble the organization of three-layer cortex (Luzzati, 2015). It is a reasonable hypothesis that IT pyramidal neurons of the neocortex originated from amniote three-layer cortex, but what factors drove this transformation?

Duplication of the olfactory receptor genome in the antecedents of mammals may have been a dominant driver of neocortical evolution (Rowe et al., 2011; Rowe and Shepherd, 2016; Rowe, 2017). Peripheral sensory arrays are known to influence central organization and, through epigenetic population matching, cortical re-organization and increased neuron numbers may have been driven by connectional invasions from peripheral sensory cell populations (Katz and Lasek, 1978; Krubitzer and Kaas, 2005). Fossils documenting mammalian antecedents record initial pulses of encephalization tied to expansion of olfactory cortex, and only later is there evidence suggesting neocortical differentiation. Increased input from teeth, hair and other peripheral systems were influential, but to a lesser degree.

Gene expression offers clues to developmental programs that may be specific for the cells in the regions involved. Luzzati (2015) found localization of Doublecortin (DCX+/Tbr+) in olfactory cortex and in regions of neocortex believed to be derived from the dorsal cortex, but not in dorsal cortex itself. This supported Reiner et al.'s (1998) proposition that the superficial layers are a mammalian novelty. However, sharing the same gene expressed in olfactory three-layer cortex and upper layer neocortex supported the possibility that the superficial layers of dorsal cortex were produced by co-option of the generation program for cell types in olfactory cortex (Luzzati, 2015; Klingler, 2017). Similarities between olfactory cortex and layers 2 and 3 also include *in situ* hybridization data from the Allen Mouse Brain Atlas of many shared expressed genes between these regions. Both regions have interhemispheric projections, olfactory cortex through the anterior commissure, which also carries neocortical projections in monotremes and marsupials (in placentals via the corpus callosum), and both olfactory cortex and neocortex project to the lateral entorhinal cortex to reach the hippocampus.

These similarities further support "a potential role for the olfactory system as a driver for the evolution of the neocortex" (Luzzati, 2015).

As Aboitiz and Montiel (2015) comment: "our hypothesis has common ground with those proposed by Lynch (1986), Rowe et al. (2011) and Rowe and Shepherd (2016) that olfactory systems were key in early mammalian evolution. Here we add to these hypotheses the role of the emergent isocortex as a multimodal interface in the olfactory-hippocampal axis for behavioral navigation".

Layering in olfactory cortex may reflect expansion of the olfactory repertoire that evolved in early mammalian history. The long fibers of semilunar cells have remained within their layer (Wilson and Barkai, 2010; Susuki and Bekkers, 2012; Brunjes and Osterberg, 2015), implying that specific associational fiber systems in layers may be required by increased odor object processing with expanded odor input. As noted above, pyramidal

neuron types at different depths develop in an inside-out sequence in olfactory cortex and in mammalian neocortex. The olfactory system thus appeared to play a key role in neocortical evolution, via epigenetic effects of odorant receptor gene duplication and possibly by co-opting a genetic module originally expressed in three-layer olfactory cortex to produce the six IT layers of the neocortex.

In summary, an evolutionary context for hodologically-defined cell types provides a new framework for understanding neocortical lamination. IT cells of dorsal and olfactory three-layer cortex appear to have higher associative functions that provided the basis for IT cells with greatly increased interconnectivity in mammalian neocortex. The six-layer neocortex manifests evolution of increased IT connectivity, increased cell populations, and expanded interlaminar integration underlying columnar organization. Current studies now aim to elucidate specific thalamic inputs into L4IT cells for preprocessing, specific integration with thalamus through CT cells, and the final common path through PT cells to allow higher associative functions generated by IT cells to have direct control over much of the neuraxis.

AUTHOR CONTRIBUTIONS

GMS originated the manuscript based on an ongoing collaboration with TBR, wrote the first draft, combined the comments from TBR, and finalized it for submission. TBR read the first draft, contributed critical input on the evolutionary context for the perspective, and reviewed for submission.

FUNDING

This work was funded by National Institute for Deafness and Other Communicative Disorders (NIDCD 5R01DC009977-08) to GMS; and by National Science Foundation (NSF, EAR 1258878) Division of Earth Sciences to TBR.

ACKNOWLEDGMENTS

We thank Nenad Sestan, Zoltan Molnar, and Gordon MG Shepherd for valuable discussions.

REFERENCES

Aboitiz, F., and Montiel, J. F. (2015). Olfaction, navigation, and the origin of isocortex. *Front. Neurosci.* 9:402. doi: 10.3389/fnins.2015.00402

Brunjes, P. C., and Osterberg, S. K. (2015). Developmental markers expressed in neocortical layers are differentially exhibited in olfactory cortex. *PLoS One* 10:e0138541. doi: 10.1371/journal.pone.0138541

Clascá, F., Rubio-Garrido, P., and Jabaudon, D. (2012). Unveiling the diversity of thalamocortical neuron subtypes. *Eur. J. Neurosci.* 35, 1524–1532. doi: 10.1111/j.1460-9568.2012.08033.x

Diodato, A., Ruinart de Brimont, M., Yim, Y. S., Derian, N., Perrin, S., Pouch, J., et al. (2016). Molecular signatures of neural connectivity in the olfactory cortex. *Nat. Commun.* 7:12238. doi: 10.1038/ncomms12238

Fournier, J., Müller, C. M., and Laurent, G. (2015). Looking for the roots of cortical sensory computation in three-layer cortices. *Curr. Opin. Neurobiol.* 31, 119–126. doi: 10.1016/j.conb.2014.09.006

Güntürkün, O., Stacho, M., and Ströckens, F. (2017). "The brains of reptiles and birds," in *Evolution of Nervous Systems 2*, (Vol. 1) ed. J. Kaas (Elsevier: Academic Press), 171–221.

Haberly, L. B. (1985). Neuronal circuitry in olfactory cortex: anatomy and functional implications. *Chem. Senses.* 10, 219–238. doi: 10.1093/chemse/10.2.219

Haberly, L. B., and Shepherd, G. M. (1973). Current-density analysis of summed evoked potentials in opossum prepyriform cortex. *J. Neurophysiol.* 36, 789–802.

Harris, K. D., and Shepherd, G. M. G. (2015). The neocortical circuit: themes and variations. *Nat. Neurosci.* 18, 170–181. doi: 10.1038/nn.3917

Katz, M. J., and Lasek, R. J. (1978). Evolution of the nervous system: role of ontogenetic mechanisms in the evolution of matching populations. *Proc. Natl. Acad. Sci. U S A* 75, 1349–1352. doi: 10.1073/pnas.75.3.1349

Kita, T., and Kita, H. (2012). The subthalamic nucleus is one of multiple innervation sites for long-range corticofugal axons: a sigle-axon tracing study in the rat. *J. Neurosci.* 32, 5990–5999. doi: 10.1523/JNEUROSCI.5717-11.2012

Klingler, E. (2017). Development and organization of the evolutionarily conserved three-layered olfactory cortex. *eNeuro* 4:ENEURO.0193-16.2016. doi: 10.1523/ENEURO.0193-16.2016

Kriegstein, A. R., and Connors, B. W. (1986). Cellular physiology of the turtle visual cortex: synaptic properties and intrinsic circuitry. *J. Neurosci.* 6, 178–191.

Krubitzer, L., and Kaas, J. (2005). The evolution of the neocortex in mammals: how is phenotypic diversity generated? *Curr. Opin. Neurobiol.* 15, 444–453. doi: 10.1016/j.conb.2005.07.003

Luzzati, F. (2015). A hypothesis for the evolution of the upper layers of the neocortex through co-option of the olfactory cortex developmental program. *Front. Neurosci.* 9:162. doi: 10.3389/fnins.2015.00162

Lynch, G. (1986). *Synapses, Circuits, and the Beginnings of Memory*. Cambridge, MA: MIT Press.

Naumann, R. K., and Laurent, G. (2017). "Function and evolution of the reptilian cerebral cortex," in *Evolution of Nervous Systems 2*, (Vol. 1) ed. J. Kaas (Elsevier: Academic Press), 491–518.

Naumann, R. K., Ondracek, J. M., Reiter, S., Shein-Idelson, M., Tosches, M. A., Yamawaki, T. M., et al. (2015). The reptilian brain. *Curr. Biol.* 25, R317–R321. doi: 10.1016/j.cub.2015.02.049

Neville, K. R., and Haberly, L. B. (2004). "Olfactory cortex," in *The synaptic Organization of the Brain*, ed. G. M. Shepherd (New York, NY: Oxford University Press), 415–454.

Oberlaender, M., de Kock, D. P. J., Bruno, R. M., Ramirez, A., Meyer, H. S., Dercksen, V. J., et al. (2012). Cell type-specific three-dimensional structure of thalamocortical circuits in a column of rat vibrissal cortex. *Cereb. Cortex* 22, 2375–2391. doi: 10.1093/cercor/bhr317

Reiner, A., Medina, L., and Veenman, C. L. (1998). Structural and functional evolution of the basal ganglia in vertebrates. *Brain Res. Rev.* 28, 235–285. doi: 10.1016/s0165-0173(98)00016-2

Rowe, T. B., Macrini, T. E., and Luo, Z.-X. (2011). Fossil evidence on origin of the mammalian brain. *Science* 332, 955–957. doi: 10.1126/science.1203117

Rowe, T. B. (2017). "The emergence of mammals," in *Evolution of Nervous Systems 2*, (Vol. 2) ed. J. Kaas (Oxford: Elsevier), 1–52.

Rowe, T. B., and Shepherd, G. M. (2016). The role of ortho-retronasal olfaction in mammalian cortical evolution. *J. Comp. Neurol.* 524, 471–495. doi: 10.1002/cne.23802

Shepherd, G. M. (1974). *The Synaptic Organization of the Brain*. New York, NY: Oxford University Press.

Shepherd, G. M. (1988). *Neurobiology*. 2nd Edn. New York, NY: Oxford University Press.

Shepherd, G. M. (2011). The microcircuit concept applied to cortical evolution: from three-layer to six-layer cortex. *Front. Neuroanat.* 5:30. doi: 10.3389/fnana.2011.00030

Smith, L. M., Ebner, F. F., and Colonnier, M. (1980). The thalamocortical projection in Pseudemys turtles: a quantitative electron microscopic study. *J. Comp. Neurol.* 190, 445–461. doi: 10.1002/cne.901900304

Streidter, G. F. (2005). *Principles of Brain Evolution.* Sunderland, MA: Sinauer Associates Inc.

Susuki, N., and Bekkers, J. M. (2012). Two layers of synaptic processing by principal neurons in piriform cortex. *J. Neurosci.* 31, 2156–2166. doi: 10.1523/JNEUROSCI.5430-10.2011

ten Donkelaar, H. J. (1998). "Reptiles," in *The Central Nervous System of Vertebrates*, (Vol. 2) eds R. Nieuwenhuys, H. J. ten Donkelaar, and C. Nicholson (Berlin: Springer), 1315–1524.

Thomson, A. (2010). Neocortical layer 6, a review. *Front. Neuroanat.* 4:13. doi: 10.3389/fnana.2010.00013

Ulinski, P. S. (1983). *Dorsal Ventricular Ridge; A Treatise on Forebrain Organization in Reptiles and Birds.* New York, NY: John Wiley and Sons.

Wilson, D. A., and Barkai, E. (2010). "Olfactory cortex," in *Handbook of Brain Microcircuits*, 2nd Edn. eds G. M. Shepherd and S. Grillner (New York, NY: Oxford University Press), 263–276.

Yamawaki, N., Borges, K., Suter, B. A., Harris, K. D., and Shepherd, G. M. G. (2014). A genuine layer 4 in motor cortex with prototypical synaptic circuit connectivity. *Elife* 3:e05422. doi: 10.7554/eLife.05422

Conflict of Interest Statement: The authors declare that the research was conducted in the absence of any commercial or financial relationships that could be construed as a potential conflict of interest.

frontiers in Neuroanatomy

REVIEW
published: 09 November 2017
doi: 10.3389/fnana.2017.00102

Transcriptional and Post-Transcriptional Mechanisms of the Development of Neocortical Lamination

*Tatiana Popovitchenko and Mladen-Roko Rasin**

Neuroscience and Cell Biology, Robert Wood Johnson Medical School, New Brunswick, NJ, United States

The neocortex is a laminated brain structure that is the seat of higher cognitive capacity and responses, long-term memory, sensory and emotional functions, and voluntary motor behavior. Proper lamination requires that progenitor cells give rise to a neuron, that the immature neuron can migrate away from its mother cell and past other cells, and finally that the immature neuron can take its place and adopt a mature identity characterized by connectivity and gene expression; thus lamination proceeds through three steps: genesis, migration, and maturation. Each neocortical layer contains pyramidal neurons that share specific morphological and molecular characteristics that stem from their prenatal birth date. Transcription factors are dynamic proteins because of the cohort of downstream factors that they regulate. RNA-binding proteins are no less dynamic, and play important roles in every step of mRNA processing. Indeed, recent screens have uncovered post-transcriptional mechanisms as being integral regulatory mechanisms to neocortical development. Here, we summarize major aspects of neocortical laminar development, emphasizing transcriptional and post-transcriptional mechanisms, with the aim of spurring increased understanding and study of its intricacies.

Keywords: neocortical lamination, mouse neocortex, transcription factors, RNA-binding proteins, post-transcriptional regulation, neurogenesis, pyramidal neuron, alternative splicing

OPEN ACCESS

Edited by:
Javier DeFelipe,
Cajal Institute (CSIC), Spain

Reviewed by:
Jochen Ferdinand Staiger,
University of Göttingen, Germany
Kazue Hashimoto-Torii,
Children's National Health System,
United States

****Correspondence:***
Mladen-Roko Rasin
roko.rasin@rutgers.edu

Received: *05 June 2017*
Accepted: *25 October 2017*
Published: *09 November 2017*

Citation:
Popovitchenko T and Rasin MR (2017) Transcriptional and Post-Transcriptional Mechanisms of the Development of Neocortical Lamination. Front. Neuroanat. 11:102. doi: 10.3389/fnana.2017.00102

INTRODUCTION

The neocortex is laminated brain structure that coordinates our cognitive capacities and responses, long-term memory, sensory and emotional functions, and voluntary motor behavior (Rakic, 2009; **Figure 1**). More than a century has passed since the organization of the neocortex was identified through by classic neuroscientists including Cajal, Brodmann, Economo, Kskinas, Sarkissov, Bailey, Boning, and others (Douglas and Martin, 2007). The six neocortical layers were first characterized using traditional neuroanatomical techniques, relying on the morphological features of the layers such as thickness, cell density, myelination, and the size of cell perikarya. Modern classification has utilized updated approaches, such as transcriptional profiling and receptor mapping, to identify the layers as unique compartments based on their molecular expression patterns that correspond to classic anatomical boundaries (Molyneaux et al., 2007; Leone et al., 2008; Zilles and Amunts, 2009; Kang et al., 2011; Kwan et al., 2012; DeBoer et al., 2013, 2014; He et al., 2017). The maturation of a stereotyped neocortical structure continues to be an indication of appropriate neuroanatomical development and brain function. Aberrations in neocortical anatomy have been correlated with

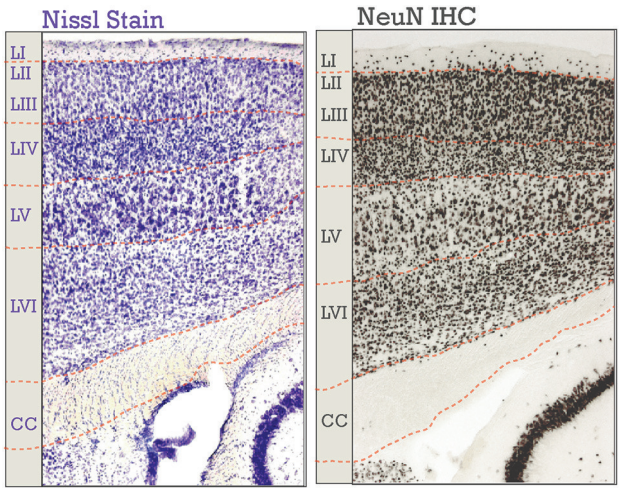

FIGURE 1 | Neocortical six-layered lamination in adult mice. A Nissl stained section is on the left; on the right is an immunohistochemical (IHC) labeling of NeuN. Corresponding boundaries between each layer and the corpus callosum (CC) were drawn in. Layers I-VI are labeled, "LI-LVI."

disease manifestation in autism case studies (DiCicco-Bloom et al., 2006; Amaral et al., 2008; Stoner et al., 2014) as well as in studies of schizophrenia patients (Jones, 1995; Lewis and Levitt, 2002; Wagstyl et al., 2016).

Six-layered lamination of the neocortex can be viewed through several different aspects of the neurons contained within. For example, there are the neurons themselves as well as the patterns the projections form. There are two major classes of neurons in the adult neocortex: inhibitory, or Gamma-aminobutyric acid (GABA) utilizing, and excitatory, or glutamate-utilizing. Both classes shows a specific laminar distribution in the neocortex (Jones, 1986; Pla et al., 2006; Molyneaux et al., 2007; Leone et al., 2008; Zilles and Amunts, 2009; Kwan et al., 2012; DeBoer et al., 2013; Tasic et al., 2016), though inhibitory subtypes do not have laminar preference to the same extent as do excitatory neuronal subtypes (He et al., 2017). Pyramidal neurons are glutamate-utilizing projection neurons, represent the majority of neurons (70–85%) in the neocortex (Jones, 1986; Kasthuri et al., 2015), and will be the primary focus of this review (**Figure 2**). Also of note is that laminar organization is seen in the axonal connectivity of the neocortex, the so-called "myelinated thicket" of projections that traverse the cortex (Jones, 2009). New studies have re-emphasized the importance of myelin organization to brain function (Tomassy et al., 2014; Micheva et al., 2016).

The layered organization of the adult neocortex stems from the unique placement of its pyramidal neurons, which arise from diverse progenitors during intricate prenatal developmental processes (**Figures 2A**, **3**). Pyramidal neurons are named after the three-dimensional pyramid-like shape of their somata. Pyramidal neurons also have characteristic neurite structure: an apical dendritic tree bearing oblique branches and ending in a terminal tuft, a basal dendritc tree, and a single axon (Jones, 1986; Ramaswamy and Markram, 2015; **Figure 2B**).

The steps that each pyramidal neuron goes through to form the appropriate layers are **genesis**, **migration**, and **maturation**. While each of these three steps individually has been reviewed extensively (Molyneaux et al., 2007; Kriegstein and Alvarez-Buylla, 2009; Kwan et al., 2012; Shim et al., 2012; Cooper, 2013; Custo Greig et al., 2013; Malatesta and Gotz, 2013; D'Arcangelo, 2014), we will highlight the roles that post-transcriptional regulation plays in these steps (Zilles and Amunts, 2009; Kwan et al., 2012; DeBoer et al., 2013; Pilaz and Silver, 2015; Silver, 2016; Lennox et al., 2017), with a focus on recent literature. Interference at any of these steps can lead to debilitating disorders, such as microcephaly, epilepsy, and cognitive/behavioral impairments (Abdel Razek et al., 2008; Staley, 2015; Willsey and State, 2015; Silbereis et al., 2016; Oaks et al., 2017). For example, recent evidence has uncovered that an epidemic of microcephaly in South America is due to an attack by the Zika virus on neocortical progenitors that give rise to pyramidal neurons (Cugola et al., 2016; Garcez et al., 2016; Tang et al., 2016), affecting the genesis phase of lamination.

Each of the three steps to achieve a laminar six-layered neocortex is guided by transcriptional, post-transcriptional, and epigenetic mechanisms (Leone et al., 2008; Shim et al., 2012; DeBoer et al., 2013; Tuoc et al., 2013b; Pilaz and Silver, 2015; Nguyen et al., 2016). Transcription factors regulate cohorts of genes and as such have been associated with certain subpopulations of cells in the neocortex (Molyneaux et al., 2007; Tasic et al., 2016). Post-transcriptional factors include: RNA-binding proteins (**RBPs**), ribosomal proteins (**RPs**), micro-RNAs (**miRNAs**), and long non-coding RNAs (**lncRNAs**). Recent evidence that will be presented here suggests that these factors also play a crucial role in the generation of the neocortical layers. RBPs are of immense importance. RBPs are not only active in translation promotion and repressing post-transcriptional processing, but also in alternative splicing (AS) and transport/localization of many kinds of RNAs, including the mRNAs encoding transcription factors themselves as well as non-coding regulatory RNAs (Boutz et al., 2007; Chawla et al., 2009; DeBoer et al., 2013; Pilaz and Silver, 2015; Hart and Goff, 2016; Kraushar et al., 2016; Yano et al., 2016; Zheng, 2016). As such, their capacity for intervention in post-transcriptional processing, and consequently all developmental processes, endows cells with an additional layer of regulatory control (Keene, 2007; **Figure 5**).

A thorough understanding of events and molecular mechanisms underlying the development of neocortical lamination will contribute insight to neuronal differentiation and neurodevelopmental/cognitive disorders as varied as microcephaly, autism, and schizophrenia. Here, we review the three stages of neocortical laminar development through exploration of transcriptional and post-transcriptional mechanisms with the aim of spurring increased understanding and future studies.

GENESIS OF PYRAMIDAL NEURONS

The laminar destiny of pyramidal neurons is largely established during the embryonic period. Ultimately, each

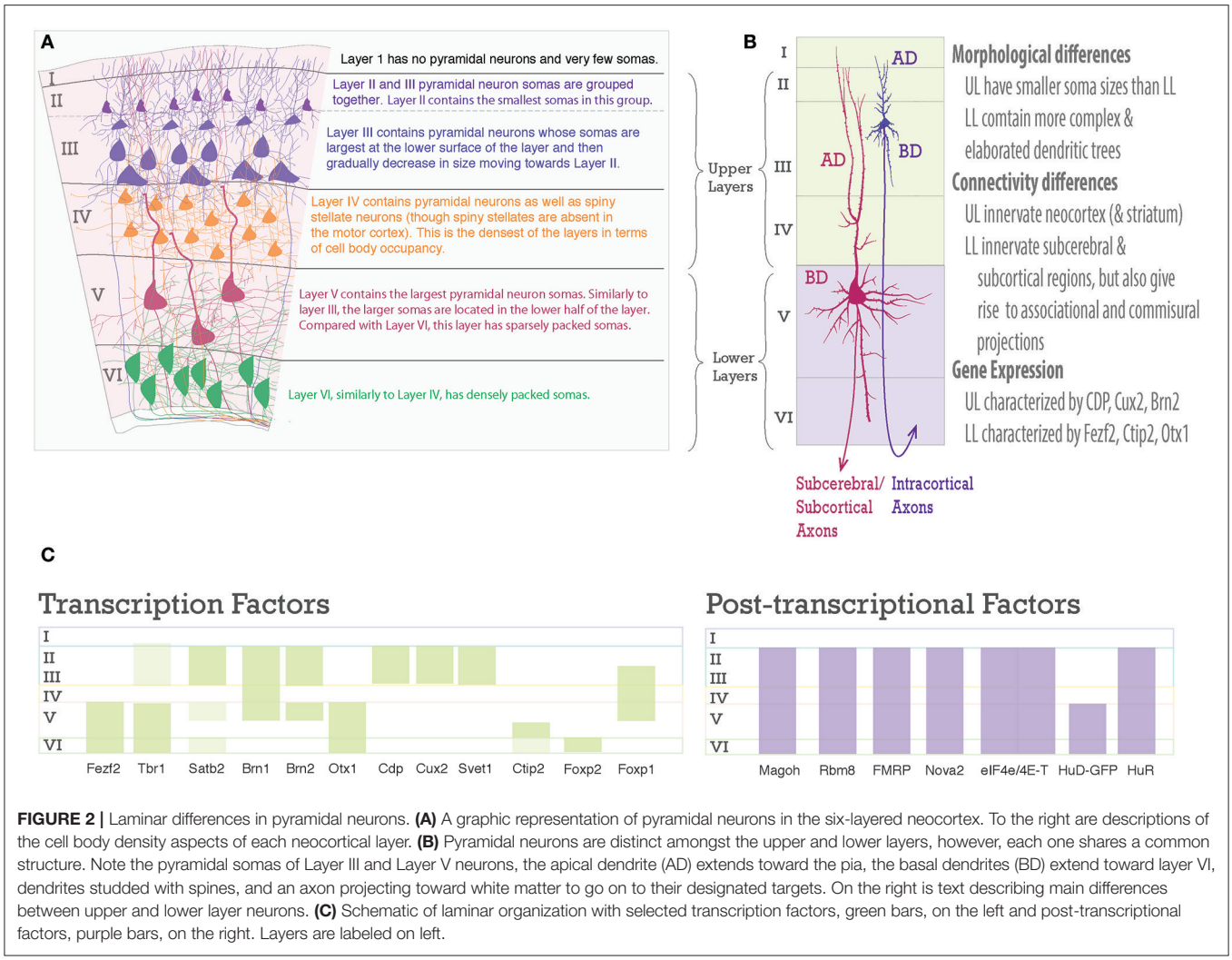

FIGURE 2 | Laminar differences in pyramidal neurons. **(A)** A graphic representation of pyramidal neurons in the six-layered neocortex. To the right are descriptions of the cell body density aspects of each neocortical layer. **(B)** Pyramidal neurons are distinct amongst the upper and lower layers, however, each one shares a common structure. Note the pyramidal somas of Layer III and Layer V neurons, the apical dendrite (AD) extends toward the pia, the basal dendrites (BD) extend toward layer VI, dendrites studded with spines, and an axon projecting toward white matter to go on to their designated targets. On the right is text describing main differences between upper and lower layer neurons. **(C)** Schematic of laminar organization with selected transcription factors, green bars, on the left and post-transcriptional factors, purple bars, on the right. Layers are labeled on left.

neocortical layer contains neurons that share specific projection patterns, morphological, electrophysiological, and molecular characteristics. These differences are largely genetically programmed according to their prenatal birth date (Molyneaux et al., 2007; Leone et al., 2008; Kwan et al., 2012; Shim et al., 2012; Custo Greig et al., 2013; DeBoer et al., 2013; Harris and Shepherd, 2015; Tasic et al., 2016; He et al., 2017; **Figure 2**). However, layered subpopulations are often not completely homogenous groups (Arlotta et al., 2005; Molyneaux et al., 2007, 2015; Custo Greig et al., 2013; DeBoer et al., 2014; Sorensen et al., 2015). For example, while lower layer neurons tend to project corticofugally, neurons in layer V have diverse corticocortical and corticofugal axonal projection patterns, including: corticospinal, corticocortical, corticostriatal, and non-specific corticothalamic nuclei in mouse motor cortex (Arlotta et al., 2005; DeBoer et al., 2013; Oswald et al., 2013). Evidence from genetic profiling is in agreement with this characterization: excitatory neurons within a layer are generally more similar to each other than to those in another layer, but still can be grouped into distinct transcriptomic subpopulations. Notably, this is more-so true for lower layers than for upper layers (Tasic et al., 2016). Some studies have gone further and combined retrograde tracing with molecular profiling and found that diverse axonal projections trace back to neurons with distinct transcriptomic patterns (Arlotta et al., 2005; Molyneaux et al., 2007; Custo Greig et al., 2013; Sorensen et al., 2015).

Differences in subpopulations arguably begin to arise from the three main progenitor types present during development: neuroepithelial progenitor cells (NECs), radial glia progenitors (RG), and intermediate progenitors (IPs) (**Figure 3A**; Gal, 2006; Stancik et al., 2010; Johnson et al., 2015; Pollen et al., 2015; Tyler et al., 2015). These progenitor types overlap in their occurrence; NECs have been prepopulating the nascent ventricular zone when RG first begin to proliferate, RG continue proliferating throughout neurogenesis, and IPs begin to appear after RG and will also continue proliferating throughout neurogenesis. Thus, proportions of progenitors change during the course of development (Noctor et al., 2001, 2004; Götz and Huttner, 2005; Kowalczyk et al., 2009; Pollen et al., 2015;

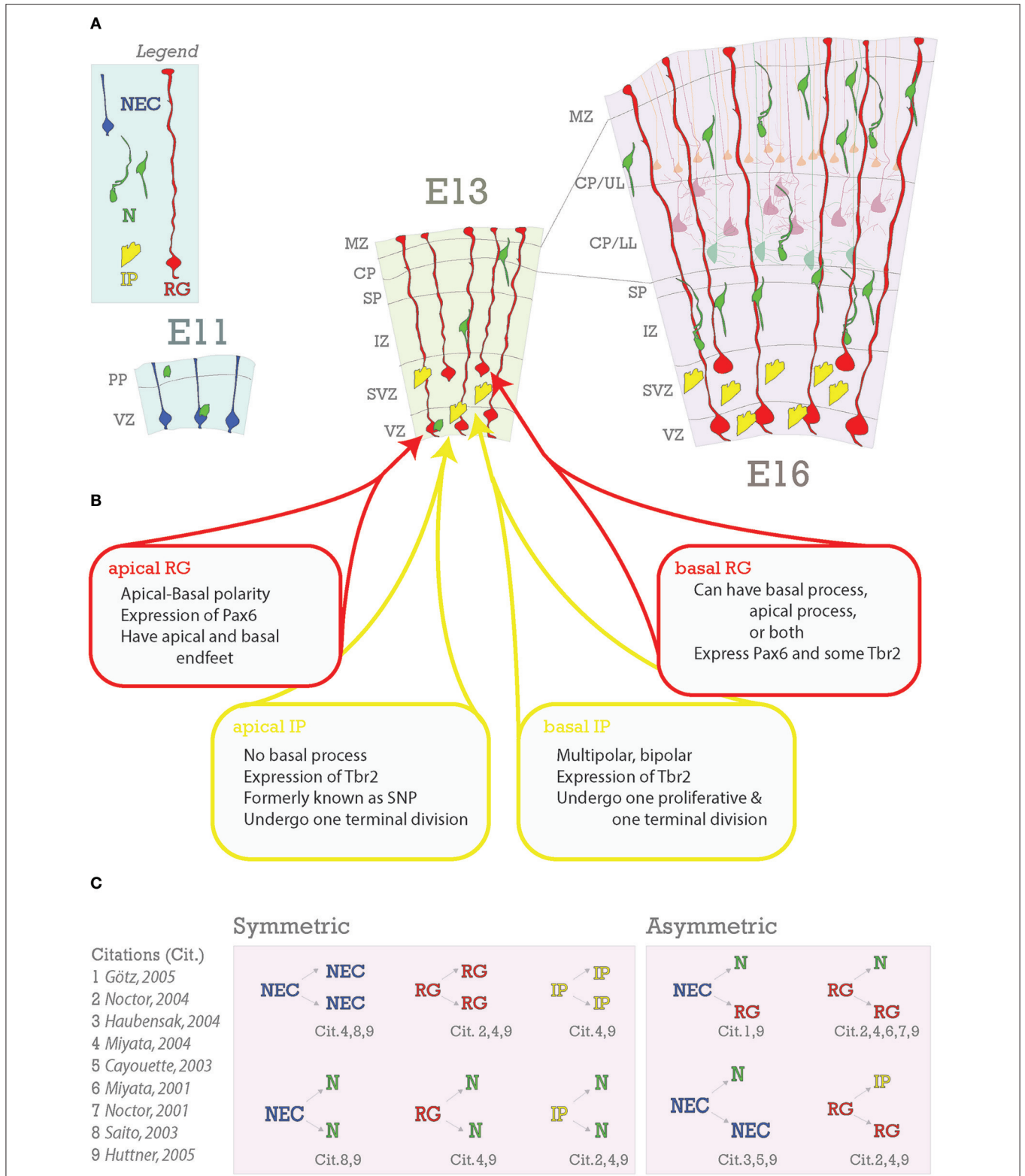

FIGURE 3 | Embryonic foundations of lamination. **(A)** Schematic representation of the progression of neocortical development during prenatal neurogenesis. Legend is in the top left with the main cell types depicted: neuroepithelial cells (NEC), radial glia (RG), intermediate progenitors (IP), and neurons (N). The ages depicted are key stages during prenatal neurogenesis: E11 (onset), E13 (deep layer production), and E16 (transition from deep layer to upper layer and upper layer production). At E11, some neurons have already been generated from NECs and some have arrived from subpallial origins. At E13, pyramidal neurons and progenitors are generated in the

(Continued)

FIGURE 3 | Continued
VZ from apical RG (aRG) and apical intermediate progenitors (aIPs). In addition, pyramidal neurons are generated in the subventricular zone (SVZ) from basal RG (bRG) and basal IPs (bIPs). Migrating pyramidal neurons pass through the intermediate zone (IZ) and SP to the CP. Later born pyramidal neurons will migrate past the earlier born ones successively to generate the neocortical layers in an inside-out fashion. Nascent layers are seen at E16. Lower layers (LL) have immature neurons and mature neurons already in place (lighter cells in background), extending apical dendrites towards Layer I. **(B)** Heterogeneity of RG and IP progenitors. **(C)** Neurons are generated from both symmetric and asymmetric divisions. References for these events are indicated below each event and detailed to the right.

Telley et al., 2016). One tantalizing hypothesis that arises from recent studies is that the diversity of the progenitor pool, changing through the course of development, allows for acquisition of diverse subpopulations in the developed neocortex. The extent to which post-transcriptional regulation plays a role in this process is only recently becoming elucidated.

Pyramidal neurons are born from their progenitors in the dorsal pallium within the proliferative layers named the ventricular zone (VZ) and subventricular zone (SVZ). It is in these zones that neural stem cells divide and begin to generate the cellular diversity of the neocortex. During the first stage of neocorticogenesis, the developing neocortex is composed of just one of these layers- the ventricular zone (VZ) **(Figure 3A)**, which will remain a major proliferative site throughout neocortical development.

Neuroepithelial Progenitor Cells (NECs)

The first lineage of neocortical neural progenitor cells, also called neural stem cells and/or neural precursor cells, is composed of NECs. They are identified by Nestin and Sox1 expression (Nestin+ and Sox1+) (Tohyama et al., 1992). Sox1 maintains NECs in their progenitor state (Suter et al., 2009). In the murine neocortex, the earliest neurons will be born between E9 and E10 from NECs and form the preplate (PP) (Bystron et al., 2006); PP cells thus form the first band of neurons above the VZ (**RG are red cells in Figure 3A**; Angevine et al., 1970; Marin-Padilla, 1978; De Carlos and O'Leary, 1992).

NECs divide symmetrically to produce more NECs (Rakic, 1995; Götz and Huttner, 2005) **(Figure 3C)**, and asymmetrically to generate neurons and RG (Cayouette and Raff, 2003; Haubensak et al., 2004). Symmetric divisions lead either to the expansion of the proliferative pool, resulting in two new stem cells as it is the case with NECs, or to the termination of proliferation with two new neurons or glia (Saito et al., 2003)-frequently seen in later stages of neocorticogenesis (Huttner and Kosodo, 2005). Early divisions of stem cells are important for amplification of the progenitor pool while later divisions tend to be neurogenic (Gao et al., 2014). A depletion of progenitors and increase in neurogenic output during neocorticogenesis has results in decreased cortical thicknesses (Caviness et al., 2003). As a further proof of principle, the *reeler* mutant (discussed in depth in the Migration section of this review), shows disruption in normal balance of proliferative divisions with reduced neuronal production in early stages and increased neuronal production at later stages (Polleux et al., 1998), with the final effect being a severely disorganized neocortex (Guy et al., 2015; Wagener et al., 2016; Guy and Staiger, 2017). As we will demonstrate with the following examples, deficiencies in early neocortical progenitor populations compromise cell fate and localization (**Figure 4**).

NECs are polarized with apical and basal processes extending over the entire developing neocortex and as such begin to form the structure of the cortex (Kadowaki et al., 2007). They are highly dependent on a stable interaction with the ventricular surface. Apical end-feet, which attach NECs as well as RG to the VZ surface, are regions of cadherin localization and form adherens junctions with the VZ surface to stably attach NECs and RGs there (Kadowaki et al., 2007; Miyamoto et al., 2015). Downregulation of cadherin leads to detachment of these polarized progenitors from the ventricular surface, premature neuronal differentiation, and increased cell cycle exit (Zhang et al., 2010), all leading to a disorganized neocortical structure (Kadowaki et al., 2007). Cadherin localization to apical end feet was found to be dependent on the endocytic adaptor proteins NUMB/NUMBL. NUMB, through N-Cadherin binding, maintains the integrity of the VZ surface and subsequent neocortical organization (Rasin et al., 2007).

The RBP Musashi1 (Msi1) was found to bind mammalian *Numb* (Imai et al., 2001; Yano et al., 2016), and to compete with the translation initiation factor eIF4G to bind poly-A binding protein (PABP). Binding of PABP by Msi1 acts as a translational brake and thereby represses translation of Msi1-bound transcripts, such as *Numb*. Msi1 was found, in retinal Müller glia, to localize to the cytoplasm in mitotic cells and to the nucleus during post-mitotic stages (Nickerson et al., 2011). Thus, in the cytoplasm during mitosis, Msi1 is available to repress translation of Numb and thereby inhibit stable cadherin localization. Numb is decreased in mitotic cells, evidenced by the lack of co-localization with PH3 and P-Vimentin and immunogold electron microscopy (markers of mitosis) (Rasin et al., 2007). It would be fruitful to confirm that this pattern of Msi1 subcellular localization holds true in cortical NECs/RG. This would further demonstrate that Msi1 indeed can act in a cell-cycle-locked manner to promote neocortical stem-cell proliferation through regulation of Numb.

Notably, this is just one mechanism by which Msi1 maintains stem-cell fate. The most prominent example, regulation of Notch through Numb, has been thoroughly elucidated by Okano and others (Imai et al., 2001; Kohyama et al., 2005). Recent evidence has also implicated Msi1 as necessary for ZIKV replication (Chavali et al., 2017), paradoxically leading to the death of the very cells Msi1 normally maintains. Dependence on the RBP Msi1 further demonstrates why ZIKV is so efficient in its targeting of

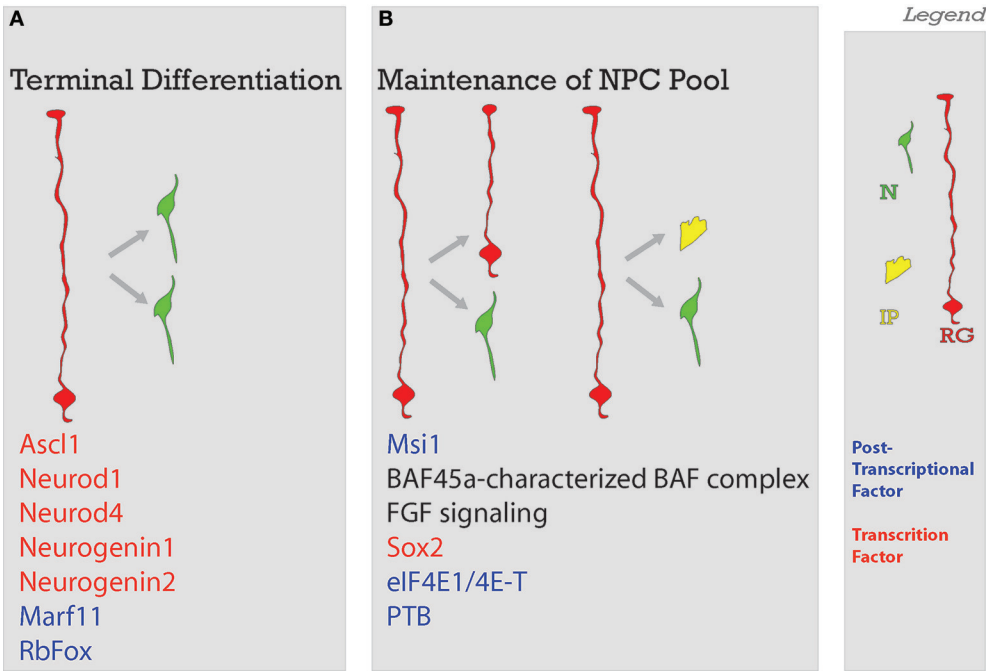

FIGURE 4 | Balance of differentiation and proliferation. This process ensures that an adequate amount of neurons will be produced. Neurons will be produced through **(A)** terminal symmetrical division or in a way that the **(B)** maintenance of the neural progenitor cell pool is ensured with the self-renewal of enough progenitors. Factors guiding each process are listed below. Legend to the right. NSC, neural stem cell; N, neuron; IP, intermediate progenitor; RG, radial glia; Post-transcriptional factors in blue in A and B; TF, transcription factors in red in A and B.

neural progenitor cells and subsequent formation of the tragic microcephaly phenotype.

Interestingly, knockouts (KO) of a nuclear protein Akirin2 show a phenotype that is similar to, but more drastic than, cadherin disruption. Akirin2 KOs show increased cell cycle exit, disorganized neocortex, and down regulation of N-cadherin and Connexin-42 protein. Downregulation of these genes leads to a loss of adherens junctions and a "spilling" of progenitor cells into the lateral ventricle (Bosch et al., 2016). Akirin2 acts as a bridge between transcription factors and BAF complexes, which are epigenetic chromatin remodeling complexes (Bosch et al., 2016). Called SWI/SNF in yeast and BAP in *Drosophila*, the BAF complex is composed of ten proteins which have been shown to differentially associate in specific cell types. The BAF45a/53a subunits are highly expressed in progenitors and BAF45a is sufficient to keep progenitors in their proliferative state. When a cell becomes post-mitotic, there is a repression of BAF45a/53b and a switch to expression of BAF45b/45c/53b (Lessard et al., 2007). While loss of individual BAF subunits results in expression changes in specific genes, total loss of these complexes leads to global effects on gene expression. This was demonstrated with the generation of the BAF155/170 double conditional KO- in these mutants no BAF complexes form. Researchers determined that there was a concomitant increase in heterochromatin formation due to increased H2K27Me2/3 methylation in the telencephalon (Narayanan et al., 2015; Nguyen et al., 2016). Together, these experiments demonstrate the local and global roles that tight epigenetic control can have over cell fate.

Another RBP, Hu antigen R (HuR), could play a role in maintaining the appropriate balance of NECs to neurons. HuR was found to be expressed in a NEC-like cell line (H2-b2T) at high levels during mitosis (M-phase), during growth (G1 and G2), and at low levels during synthesis (S-phase) (Garcia-Dominguez et al., 2011). HuR stabilizes mRNA transcripts through binding of AU-rich elements (AREs); though notably AREs were initially identified to lead of instability of transcripts (Fan and Steitz, 1998; Peng et al., 1998; Brennan and Steitz, 2001). During M-phase, HuR stabilizes *Delta-like 1* (*Dll1*) mRNA via interaction with ARE-elements in *Dll1*. Stabilization likely allows for high levels of *Dll1* to be obtained, which in turn allows the NEC expressing *Dll1* to differentiate while laterally inhibiting its neighbors from differentiating (Louvi and Artavanis-Tsakonas, 2006). Briefly, neighbors of the *Dll1*-high cell are expressing Notch and upon interaction with the ligand, transcription of neuronal-fate repressors (bHLH genes *Hes1* and *Hes4*) is enacted (Ohtsuka et al., 2001; Liao and Oates, 2017). Either decreased DLL1 or decreased Notch means that pro-neuronal genes will be transcribed (Appel et al., 2001; Homem et al., 2015). HuR heterozygotes in this study were shown to have a decreased expression of *Dll1* at E10.5 (Garcia-Dominguez et al., 2011). By postnatal day 0 (P0), *HuR* conditional knockout, with deletions at the NEC stage (*Foxg1-Cre*) and the RG stage (*Emx1-Cre*), have significantly reduced cortical thicknesses (Kraushar et al., 2014).

Radial Glia

The first pyramidal neurons are born about a day later around E11.5 and migrate toward the pial/basal surface to form the cortical plate (CP). These CP neurons split the PP into the superficial marginal zone (MZ) and the deeper subplate (SP) (Molliver et al., 1973; Kostovic and Rakic, 1990; Allendoerfer, 1994). From there, each successive group of neurons will migrate past those already present to form nascent layers. As neurogenesis progresses, there is an increase in the expression of Tbr2, a marker of intermediate progenitors (IPs) in the SVZ (IPs are yellow cells in **Figure 3A;** Englund, 2005). Once the bulk of embryonic neurogenesis ends at E18, RG will give rise to glial lineages. In the adult brain, neurons are accompanied by astrocytes, microglia, oligodendrocyte precursor cells, oligodendrocytes, and endothelial cells (Rakic, 1995, 2009; Molyneaux et al., 2007; Leone et al., 2008; Kwan et al., 2012; DeBoer et al., 2013; Tasic et al., 2016).

The genesis of pyramidal neurons is characterized by the switch from NEC-characteristic symmetric divisions to RG-characteristic asymmetric ones (Götz and Huttner, 2005). RG are a more specialized lineage of neural stem cells and have both basal and apical processes spanning the extent of the length of the nascent neocortex, similar to NECs. However, in contrast to NECs, RG asymmetric divisions result in two different kinds of daughter cells: one self-renewing RG and one either terminal neuron, IP, or RG (Noctor et al., 2004, 2008).

This important switch from NECs to RG is regulated by both extrinsic and intrinsic factors. The extracellular factor Fgf10 in the rostral, but not caudal, part of the neocortex favors a rapid transition to RG fate (Sahara and O'Leary, 2009). Experiments involving the deletion of cortically-expressed FGF receptors (*−1*, *−2*, and *−3*), demonstrates that FGF signaling maintains RG in a proliferative state (Kang et al., 2009). Intrinsically, Pax6 expression drives NECs to RG fate (Suter et al., 2009). Sox2 has been identified as a maker of RG (Hutton and Pevny, 2011), but is also expressed at low levels in IPs (Pollen et al., 2015). Unlike NECs, RG are not restricted to the VZ; those that stay at the VZ are called **aRG** and those that are found in the SVZ are called **bRG**, also called outer RG (oRG) (Miyata et al., 2004; Noctor et al., 2004, 2008; Götz and Huttner, 2005; Huttner and Kosodo, 2005; Kowalczyk et al., 2009; Kriegstein and Alvarez-Buylla, 2009; Hansen et al., 2010; Wang et al., 2011).

aRG express PAX6, several astroglial markers (e.g., GLAST and BLBP), and maintain apical-basal polarity (Hutton and Pevny, 2011). bRG were recently split into three subtypes: unipolar with a basal process attached to basal lamina, unipolar with an apical process attached to the pial surface, and bipolar. bRG all express PAX6, but many also express Tbr2 (Betizeau et al., 2013). Recently, a screen aiming to transcriptionally profile the outer SVZ (OSVZ), found that while cells that expressed *Tbr2* indeed had diverse morphological characteristics, they had transcriptomes distinct from classic RG molecular profiles (Pollen et al., 2015). *In vitro* experiments have demonstrated that all TBR2-expressing cells have once had RG markers, but progressively go through "transcriptional waves" rather than drastically shift in their expression patterns (Telley et al., 2016). With the plethora of new molecules that can be used for subtype identification in these screens, enhanced identification and distinction amongst progenitors is on the horizon (**Figure 4B**).

There is a proven dependence of early-born progenitors on cell-cycle stage in their fate decision (McConnell and Kaznowski, 1991). Using auto-radiographic tracing with [^{3}H] thymidine, ferret RG from E29 (when deep layers are being generated in ferret) were heterochronically ("different time") transplanted into postnatal ferrets. 24 h after transplantation, >85% of migrating cells were found in layer VI. If cells were transplanted immediately after being labeled (still in S-phase and thus able to incorporate the label), ∼85% of them migrated to layers II/III. Proliferative cells in the murine VZ have also been found to stay clustered with their "sisters" (Cai et al., 1997). Finally, of the cells that continued to divide in the ferret host cortex (Identified by a diluted [^{3}H]thymidine), 98.3% migrated to layer II/III. These results suggest that the environment in which the RG cycles can provoke the RG to acquire a certain fate. Yet, if the RG it has gone through its final S-phase, it seems to have made its decision and its terminal daughter cell will follow this instruction (McConnell and Kaznowski, 1991).

Recent evidence demonstrates that progenitor cells going through a self-renewing cell-cycle will have longer S-phases than those producing a neuron (Arai et al., 2011), suggesting that the window of opportunity to make a fate decision is increased. Indeed, this was likely observed with clonal analysis on clusters of proliferative cells (Cai et al., 1997) as well as demonstrated by manipulating a cell-cycle inhibitor (p27) to increase cell cycle exit (Caviness et al., 2003). This is further reflected in KOs of Dmrta2, a pro-neuroepithelial gene, where more cells in the knockout are in G0/1 (Young et al., 2017) and fewer in S compared to controls (Konno et al., 2012; Young et al., 2017). This suggests increased cell cycle exit; indeed, forced expressed of the pro-neuroepithelium factor *Dmrta2* leads to an increase in Ki67+ cells (Young et al., 2017).

Acting through post-transcriptional means, specific translational partners have been found to directly contribute to neurogenesis. Yang et al. identified eIF4E, eukaryotic initiation factor 4E, and 4E-T are interacting protein partners. Using immunohistochemistry, they found that 4E-T colocalized with eIF4E1 70% of the time; though eIF4E1 colocalized with 4E-T only 2.7% of the time (Yang et al., 2014)- possibly pointing to other interacting partners like 4E-T for translation of specific transcripts. The sites of colocalization were in Processing-bodies (P-bodies) (Yang et al., 2014). P-bodies are a kind of ribonucleoprotein (RNP) complex, similar to, but distinct from stress granules (Kedersha et al., 2005; Decker and Parker, 2012). These are hypothesized to be packages of inactive translational machinery which are important for local translation (Decker and Parker, 2012; **Figure 5,** step 5). In an elegant series of experiments, the authors demonstrated that when protein of Neurogenin1 or Neurogenin2 was present, the mRNA transcripts of either were not colocalized with 4E-T+ RNPs. Both eIF4E1 and 4E-T were found to maintain cells in a progenitor state and repress neuronal fate by directly repressing neuron-fate promoting transcripts *ascl1*, *neurod1*, *neurod4*, *neurogenin1*, and *neurogenin2* from translation (Yang et al., 2014). It should be noted that a direct interaction between

4E-T and mRNA has been demonstrated, suggesting that 4E-T requires a capable partner to enact this translational repression. Importantly, eIF4E1 knockdown experiments resulted in precocious differentiation, not increased cell death. This demonstrates that the phenotype seen here is not simply a consequence of wide-spread translational deficiency, but rather the result of interference in a fate-determining pathway.

More subtly, experiments with eIF4E1/4E-T demonstrated that the mere presence of mRNA (i.e., *neurod4*) should not be correlated with protein expression- as active repressive mechanisms operate post-transcriptionally to control transcript translation. This pattern is seen repeatedly in RBP-control of mRNAs (DeBoer et al., 2013, 2014; Kraushar et al., 2014, 2016; Popovitchenko et al., 2016). Normal mRNA expression and absent protein is a hallmark of post-transcriptional regulation.

Recent studies have shown an expansion in the types of neuronal progenitors through evolution (Florio et al., 2015; Johnson et al., 2015; Pollen et al., 2015). Specifically, an expansion of the SVZ has been found in primates such that the SVZ is divided into outer (oSVZ) and inner (iSVZ) portions. Johnson et al. used fluorescence-activated cell sorting (FACS) to separate cell types in the developing human brain in order to understand transcriptional programs in human neural progenitors (Johnson et al., 2015). Three groups were isolated based on expression of cell-surface markers LeX, GLAST, and high/low/negative Prominin: (1) aRG (similar to typical rodent RG), (2) IPs and neurons, and (3) non-aRG called outer radial glia (oRG, an expanded cell type in primates present in very few numbers in rodent (Wang et al., 2011). Relying on combinations of cell-surface markers in sorting ensures an enrichment of a desired subpopulation, which can be advantageous of the population of interest is scarce. As with all methods, there are drawbacks, as it should be noted that the use of LeX (also called CD15) and Prominin (also called CD133) as markers of NPCs has been shown to be exclusive of at least one highly-proliferative population of cells (Sun et al., 2009; Hutton and Pevny, 2011). Despite this, the combined power of the single-cell sorting achieved with FACs and the unbiased profiling with RNA-seq allowed for novel discovery, specifically of post-transcriptional mechanisms responsible for isoform differences and non-protein coding elements- aspects of the transcriptome that other methods like a microarray would not allow for.

Johnson et al. uncovered that long non-coding RNAs (lncRNAs) (Hart and Goff, 2016) account for at least a part of the diversity of progenitors between higher-order mammals and rodents (Johnson et al., 2015). Specifically, 253 unannotated human-specific loci were identified; 2.4% specific to ORG and thus, given that they were unannotated, were postulated to be lncRNAs (Johnson et al., 2015). This is particularly intriguing as lncRNAs were found to be expressed at relatively low levels in the brain, and hypothesized to have high cell-type specificity (Cabili et al., 2011)- possibly in different progenitor types. That lncRNAs have lower levels of gene expression than protein-coding genes was confirmed in another RNAseq screen of mouse cortical excitatory neurons at all developmental ages examined (Molyneaux et al., 2015). During development, Molyneaux, Goff et al. found that ∼56% of lncRNAs are associated with "cell-type specific clusters" of neurons, while ∼32% of transcripts associate with "cell-type independent" clusters, i.e., not defined by high individual levels of *Bcl11b*, *Satb2*, or *Tle4* expression (Molyneaux et al., 2015).

Another study mapped seventy-six cortical lncRNAs (specifically: *intergenic* non-coding RNAs, "lincRNA," long, > 200 basepairs), and found them to be layer-specific (Belgard et al., 2011). These findings suggest that non-protein coding transcripts like lncRNAs can substantially impact lamination and vice-versa. Furthermore, a specific lncRNA, lncND, has been associated with intellectual disability (ID), and was found to be a part of an ID-associated microdeletion in six affected individuals (Rani et al., 2016). To further explore the extent of the contribution of lncRNAs to neurodevelopment, D'Haene et al. carried out a transcriptomic screen enriched for lncRNAs in human models. Researchers found 53 lncRNAs with high correlation to intellectual disability and that contained a disease-associated SNP (D'Haene et al., 2016). Further confirmation of these results in murine models would aid in the development of tractable models of ID.

Overall, we can see that there is a diverse regulatory machinery which we may be able to tap for more specific distinction amongst progenitor types, and that post-transcriptional processing plays a large role in establishing this diversity and ultimately a high-functioning cortex.

Intermediate Progenitors

Appropriate production of progenitors is the result of the balance between proliferation and neurogenesis during development. IPs are posited as the major intermediary neurogenic source. Several transcriptional and post-transcriptional mechanisms are involved in the adoption of IP identity.

IPs arise as a result of *Pax6* downregulation and *Tbr2* upregulation in these cells (Martynoga et al., 2012). Seemingly paradoxically, the onset of Tbr2 expression is in fact positively regulated by Pax6 binding (Sansom et al., 2009). Though the *Tbr2* transcript is produced, *miR-92a* has been found to maintain the RG pool by targeting *Tbr2* for translational repression (**Figure 5,** step 4); co-electroporation with a Tb2-protector that blocks binding of the miRNA to the Tbr2-3′ untranslated region (UTR) allowed for accumulation of Tbr2 protein and transition to IP fate. *miR-17-92* conditional knockout experiments show a decrease in RG and a concomitant increase in IPs (Bian et al., 2013). Authors demonstrated expression of the miRNA cluster in the proliferative zones, but did not identify the specific progenitors expressing it. Studies examining *miR-92b* showed similar results, though did additionally localize higher expression of the miRNA in the VZ and lower expression in the SVZ, with varying levels amongst cells (Nowakowski et al., 2013). Though another group has shown that expression of *miR-92b* decreases as Tbr2 increases (Nielsen et al., 2009), it remains unclear what mechanism allows for increased Tbr2 expression in IPs. Three possibilities (of many) are that the miRNA itself is targeted, it is no longer transcribed, or that some factor protects *Tbr2* from the miRNAs. This protector could very well be an RBP as competition between RBPs and miRNAs is a common

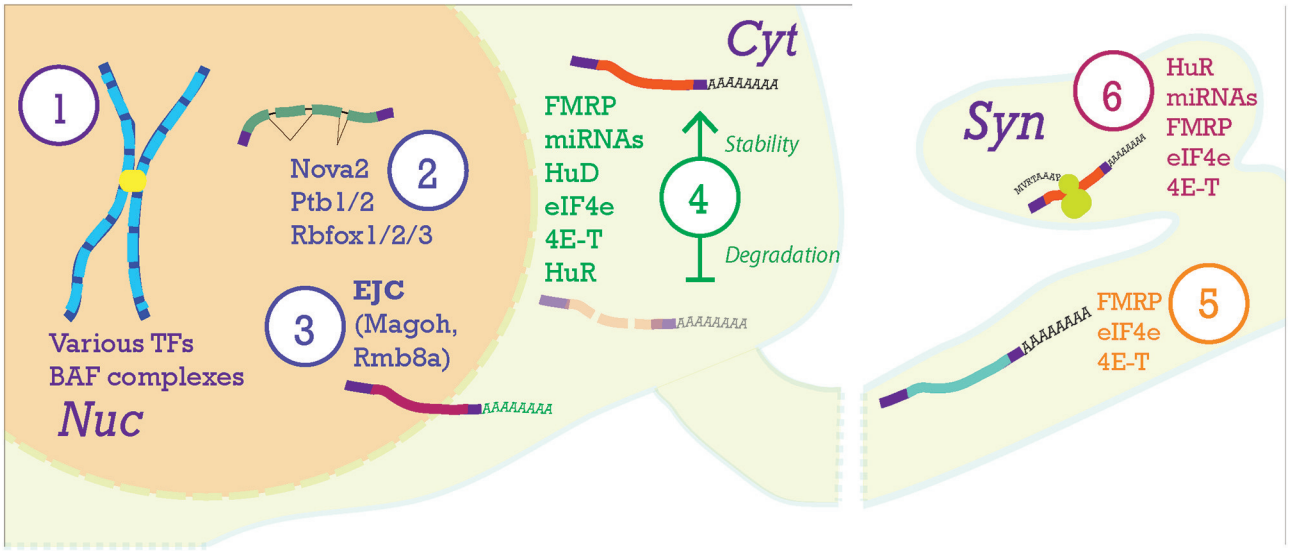

FIGURE 5 | Post-transcriptional processing steps in the neocortex. At the top of the figure, the progression of mRNA post-transcriptional processing is shown. **Transcription** begins in the nucleus (Nuc) from chromosomes producing pre-mRNA. Pre-mRNA is processed in the nucleus where the Exon-Junction Complex (EJC) will label the mRNA after **splicing** and help with nucleo-cytoplasmic **transport**. Once the transcript is moving to and throughout the cytoplasm (Cyt), **stability** of the mRNA becomes paramount. Here, transcripts will be stabilized (top transcript) or degraded (lower transcript). Then, transcripts will be **localized** to their final compartments of **translation**, in this case the synapse (Syn).

theme in stable mRNA expression (Gardiner et al., 2015). As an aside, specific interaction between lncRNAs and miRNAs has also been demonstrated (Rani et al., 2016), further expanding the competitive dynamics of the post-transcriptional regulatory framework.

Epigenetic factors also contribute to the switch from RG to IP. Two BAF complex members, BAF170 and BAF155, switch in different fates and compete to interact with Pax6. BAF170, normally expressed at higher levels in more differentiated cells, is an intrinsic factor of RG and the conditional knockouts shows enhanced production of Tbr2+ IPs. This is due to increased incorporation of BAF155, normally expressed at higher levels in less-differentiated cells (Tuoc et al., 2013a,b). Considering the neurogenesis-specific genes that Pax6 regulates (Cux1, Tle4, Tbr2), timely access to its targets through "loose" euchromatin ensures appropriate laminar development (**Figure 5,** step 1).

Similarly to RG, IPs come in two varieties in the neocortex: apical and basal **(Figure 3A)**. Apical intermediate progenitors (aIPs) were identified along with aRG in the VZ during neurogenesis (Englund, 2005; Tyler and Haydar, 2013). Unlike RG, IPs do not have a basal process and downregulate expression of astroglial markers. Additionally, instead of self-renewal stages of division, aIPs undergo terminal symmetric division to produce two neurons, amplifying the neuronal output. bIPs completely lose astroglial markers and Pax6 expression, but they gain Tbr2 expression in the SVZ (Englund, 2005). bIPs first divide symmetrically to produce two more bIPs and then once again symmetrically, the result of which is four neurons. Therefore, these bIPs are also called "transient amplifying cells" (Noctor et al., 2004; Stenzel et al., 2014) or "transient amplifying progenitors" (Betizeau et al., 2013).

Tbr2 was first identified as an important factor in the generation of upper layers and, is expressed in all bIPs and to an extent in bRG. In a conditional Tbr2 knockout, lower layers form normally and the majority of cells in upper layers are also distributed normally (Sessa et al., 2008). However, the subpopulations expressing the transcription factors Satb2 and Brn2 are reduced, implicating Tbr2 as a crucial upstream transcriptional step in subpopulation-specific neuronal development. Though upper layers in Tbr2 conditional knockouts are present and several examined subpopulations are unaffected, mice display increased aggressiveness and participate in infanticide (Arnold et al., 2008). This demonstrates that imbalances in Tbr2-derived subpopulations can yield severe cognitive deficits, while having no gross effects on lamination.

Several lines of evidence demonstrate that lower layers are also populated by neurons from the Tbr2+ lineage (Englund, 2005; Sessa et al., 2008; Kowalczyk et al., 2009; Mihalas et al., 2016). In a recent study, Tbr2+ cell fate on a given day was found to be similar to overall cell fate that day; i.e., neurons born early from IPs will be found in lowers layers (Ctip2+) and neurons born later from IPs will occupy upper layers. A portion of early-born Tbr2+ cells continue proliferating, as ∼14% of cells generated at E13.5 and ∼68% at E16.5 ended up in upper layers (Mihalas et al., 2016). It would be interesting to further evaluate if Tbr2 is sufficient to maintain the proliferative ability of a cell. Conditional knockout of Tbr2 resulted in an increase of

early-born lower layer neurons (Mihalas et al., 2016), suggesting an exit from the cell-cycle and early termination of the stem-cell program. Authors conclude that Tbr2 is necessary for proper neuronal differentiation as opposed to the genesis of IPs (Mihalas et al., 2016).

Tbr2 has been useful in distinguishing progenitor types and more importantly in understanding how different progenitors can build the myriad of subpopulations in the laminar neocortex. One study in particular has elegantly demonstrated how progenitor heterogeneity directly leads to diverse laminar subpopulations. Tyler et al. found that they could identify two distinct post-mitotic populations in the same cortical layer based on the presence (Tbr2+) or absence (Tbr2-) of Tbr2. These cells were shown to be born at the same time, but had unique identities. The populations arising from the SVZ, Tbr2+ cells, had less complex branching than cells originating from progenitors in the VZ, mostly Tbr2-, and a higher input resistance corresponding to higher excitability (Tyler et al., 2015). These results demonstrate that Tbr2 expression in a progenitor will lead to a different downstream neuronal identity and transcriptional program than those cells which do not express Tbr2 (Stancik et al., 2010).

A recent screen also isolated NPCs based on their gene expression of Tbr2. Tbr2- cells were confirmed as being Sox2+, and were thus called the RG-NPC population. Tbr2+ cells are IPs and early postmitotic neurons (Englund, 2005; Hutton and Pevny, 2011). Cells were processed with FACS and RNA-seq. The screen revealed that alternative splicing regulated 622 exons differentially between Tbr2- NPCs and Tbr2+ cells (Zhang et al., 2016). The most common regulatory event (accounting for ∼37% of alternative splicing events) was a skipped exon. 61% of skipped exons contained regulatory motifs of two prominent splicing factors, Ptb1/2 and/or Rbfox1/2/3 (**Figure 5,** step 2). This further highlights the immense regulatory potential and role of RBPs in both maintaining progenitor populations and transitioning to neurogenesis (Zhang et al., 2016). Ptb1 was previously implicated in actively repressing neuronal differentiation and conversely Rbfox was previously implicated promoting neuronal identity (Boutz et al., 2007; Gehman et al., 2011; Xue et al., 2013). The Zhang et al. screen of NPCs corroborates both of these roles and provides further mechanistic information. Authors of the screen showed that Ptb1 is a potential target of Sox2 in NPCs and that Rbfox overexpression resulted in fewer progenitors suggesting a premature switch to neuronal fate (Zhang et al., 2016). Alternative splicing thus emerges as one of the post-transcriptional mechanisms responsible for generating a heterogeneous progenitor pool (**Figure 3B**).

Efficient alternative splicing requires the actions of the spliceosome. After splicing, the spliceosome labels mRNA transcripts with a group of proteins called the exon-exon junction complex (EJC) (**Figure 5,** step 3). The EJC is usually located 20–24 nucleotides upstream of an exon-exon junction. It has been found to be required for the efficient splicing of some introns, but not all (Fukumura et al., 2016). Its presence has also been found to promote transport out of the nucleus as well as provide an anchoring point for NMD-proteins Upf2 and Upf3 (Le Hir, 2001; Hir et al., 2015). A mutagenesis screen identified one of the members of the EJC complex, Magoh, as responsible for a microcephaly phenotype. Upon investigation of the small brains from Magoh haploinsufficient mutants ($Magoh^{Mos2/+}$), the group found a depletion of Tbr2+ IPs, but not Pax6+ RG, from E13.5-E16.5 with a concomitant decrease in dividing IPs. Interestingly, Cux1+ upper layers were reduced and disorganized in the Magoh mutant (Silver et al., 2010). Another member of the EJC, Rbm8a, was also found to cause defects in lamination and microcephaly. In addition to a decrease in Tbr2+ IPs, Rbm8a haploinsufficient mutants also had a decrease in Pax6+ RG by E13.5. Concommitant with a decrease in progenitors, an increase in neurons was seen at early stages. By postnatal day 0, Cux1 (layer II/III) and Foxp1 (layers III-V) subpopulations, but not Tbr1 (layer VI), were essentially depleted (Mao et al., 2015).

The mechanism behind progenitor deficiencies in Magoh haploinsufficient mutants was further explored and found to be related to the cell cycle length. Using live imaging, authors found that the prometaphase and mitosis stages of the cell cycle in mutant RGs was increased by 2.4-fold. Magoh mutant progenitors also underwent more neurogenic divisions at E12.5 and had more apoptotic neurons. Finally, using pharmacological inhibitors of mitosis, authors recapitulated the phenotypes seen with live-imaging; namely, that more neurons were produced and 25% fewer IPs were produced when the cell cycle was lengthened (Pilaz et al., 2016b).

The RNA-binding protein (RBP) Marf1 was found to contribute to the generation of Tbr2+ cells and the reduction of Pax6+ cells. Overexpression of the somatic form of Marf1 at E13.5 resulted in increased Satb2+ neurons (corticocortical projection neurons) at postnatal day 2, though did not impact overall lamination, suggesting premature terminal differentiation. Marf1 was found to function through a somewhat unique mechanism: repression of transcripts through its RNAse activity (Kanemitsu et al., 2017), further demonstrating the wide range of activity that RBPs can have.

The RBP Fragile-X Mental Retardation Protein (FMRP) has also been implicated in regulating the RG to IP transition in neurons. It was first posited that FMRP interacts with cytoskeleton proteins in RG (Saffary and Xie, 2011). One mechanism that supports this hypothesis was recently proposed by Debra Silver's group. In RG, FMRP acts as an active transport vehicle for endfoot-localized mRNA and authors effectively used live-imaging to demonstrate this. By following EGFP-FMRP in organotypic slice cultures, they found that the protein moves to localize in RG basal endfeet. Using RIP-chip, the FMRP-associated basal endfoot transcriptome was identified. Importantly, 31% of transcripts isolated from RG basal endfeet were associated with neurological disease. With the use of the photoconvertible molecule Dendra2 and the translation inhibitor anisomycin, the authors determined that these transcripts were being actively transported into basal endfeet (Pilaz et al., 2016a).

MIGRATION

The day of birth of a pyramidal neuron from progenitors determines its location, and ultimately its identity and function (Pollen et al., 2015; Tasic et al., 2016; Telley et al., 2016; He et al., 2017). The earliest-born neurons take their place in layer VI and the next wave of neurons will form layer V; both groups project subcortically. Later-born neurons will give rise to intracortically projecting neurons mainly occupying layers II-IV, but can also be found in deep layers at lower numbers. In this way, the neocortex is formed in an "inside-out" fashion, with the deepest neurons born first and the most superficial ones born last.

The generation of neocortical layers has been faithfully reproduced using several methods in mice and higher mammals. The landmark study by Angevine and Sidman in laminar cortical development first demonstrated that progenitors labeled at a certain stage are destined for a certain population by postnatal day 10 (P10, late in development) in mice. This is most apparent when progenitors and their progeny were observed at E17; only neurons close to the pial surface are labeled by thymidine showing that active progenitors at this time point will give rise to progeny in upper layers (Angevine and Sidman, 1961).

In another series of classic experiments, McConnell et al. demonstrated that the fate of progenitors is, again, mostly predictable based on their birthdate. Isochronic transplantation (isochonronic: "same time") experiments were conducted in ferrets during P1 and P2, when upper layers were being generated in this animal (this neurogenic period corresponds to ∼E14.5-E18 in rodents). VZ tissue, which contains RG, from donor ferrets that were previously injected with tritiated-thymidine ([^{3}H]thymidine) was dissected out, cells dissociated, labeled, and injected into the ventricular zone of a same-age host ferret. Hosts were sacrificed at several timepoints after transplantation in order to observe long-term and immediate cell migration. By two months, the long-term period, ∼90% of injected cells had taken their positions in layers II/III (McConnell, 1985).

Modern approaches have further confirmed these classic experiments. Observing sparse labeling in mosaic mice, investigators have been able to begin to determine the relative contributions of progenitors in Mosaic Analysis with Double Markers (MADM) mice (Tasic et al., 2012; Hippenmeyer et al., 2013). NECs/RG labeled at an early age (E10) will give rise, eventually, to neurons spanning the upper layers II-IV (∼55%) and lower layers V-VI (∼45%). In keeping with the birthday being predictive of laminar location, progenitors actively dividing later in neurogenesis (E15) overwhelmingly give rise to neurons that will occupy layers II-IV (98%) (Gao et al., 2014). More recently, using a FlashTag (FT) approach, similar results were demonstrated. FT, similarly to [^{3}H]thymidine, dilutes upon division so progeny are easy to trace. Laminar fate was tightly locked to birthday so authors were able to trace cells born at E14.5 that would eventually take their place in layer IV; authors also demonstrated that cells generated at E14.5 could remarkably be distinguished from cells generated at E14.0. Using this precise temporal pattern to their advantage, authors dissected and sorted cells at 6, 12, 24, and 48 h post-mitosis using FACS. Transcriptomes of cells demonstrated distinct "waves" of gene expression that correlated with the biology occurring at those time points. For example, at the 6 and 12 h time points, proliferation-associated genes were downregulated and translational factors were increased (Telley et al., 2016).

The *reeler* mouse has a null version of the Reelin protein and disorganized cortical layers. It is necessary for the proper migration of cortical neurons. It has also been observed to affect radial glia scaffolds (D'Arcangelo, 2014), which immature cortical neurons utilize in migration, as well as glia-independent somal translocation (Miyata et al., 2001; Franco et al., 2011). Reelin, a factor secreted by Cajal-Retzius cells, acts through the receptors ApoER2 and Vldlr. These receptors bind a central fragment of cleaved reelin, but not the N- or C- termini. Both phosphorylate Dab1, the downstream effector of reelin signaling. Mutations in all of these reelin-associated proteins result in laminar disorganization, though the reelin mutation itself is the most severe suggesting undiscovered redundancy in the pathway (D'Arcangelo, 2014). The extent of laminar disorganization seems to be dependent upon cortical area (Polleux et al., 1998). Paradoxically, in studies of mutant reeler mice connectivity and postnatal functionality are largely preserved (Polleux et al., 1998; Guy et al., 2015).

Notch turns out to be involved not only in genesis of neurons, but also in control of their lamination through Reelin signaling. When examining *reeler* mice, researchers observed that while full-length Notch1 was not different between *reeler* and control mice, the intracellular domain (NICD) of Notch1 was not present in nuclei of *reeler* mice (Hashimoto-Torii et al., 2008). The NICD is the enactor of the Notch transcriptional pathway such that its absence predicts precocious neuronal entry. To test the significance of a mislocalized NICD, Cre recombinase was electroporated along with a fluorescent reporter into an E14.5 floxed double mutant cortex. Over 50% of cells ended up beneath Layer VI, while electroporation in control heterozygous cortices resulted in ∼90% of neurons being localized to layers II-IV; interestingly suggesting a failure to migrate in the Notch mutants. This mechanism was found to be dependent on Dab1-Notch1 interaction and specific to post-mitotic neurons (Hashimoto-Torii et al., 2008).

The Nova2 RBP knockout mouse has a disorganized laminar phenotype reminiscent of the *reeler* mouse (Yano et al., 2010). Some, but not all, neurons expressing upper layer markers were incapable of migrating past layer V. It was found that divisions at E14, but not E12, were responsible for mislocalized neurons; consistent with the observation that some upper layer cells were unable to migrate but lower layer neurons were relatively normally-positioned. It was demonstrated that Nova2 regulates Dab1 through inhibition of exon inclusion and seems to be important for late-born neuronal migration (Yano et al., 2010). Thus, Nova2 is an example of a post-transcriptional regulator, and specifically of an RBP, that can affect migration. Its regulation of the reelin pathway is through exon exclusion, a kind of AS (Matera and Wang, 2014).

The odyssey of neurons from the VZ to the CP have been grouped into four stages: (1) cells in the VZ take on a bipolar morphology and migrate toward the SVZ, (2) migratory arrest and assumption of a multipolar morphology, (3) migration *back*

toward the VZ and again a bipolar morphology is observed, and (4) final phase in which cells migrate from the VZ to the CP and also reverse their polarity (Noctor et al., 2004; Tan and Shi, 2013). Phases of migration are thus found to correlate with morphology. In the knockout of Fmr1, neurons do not always migrate to their appropriate layers; though major aspects of cytoarchitectonics are retained. The multipolar to bipolar morphology transition during the migration steps was found to be defective in this mutant, suggesting that adoption of bipolar morphology is important for laminar positioning. N-Cadherin2 (*Cdh2*) regulation by FMRP was found to be responsible for this transition (La Fata et al., 2014). A separate study identified the gap junction proteins Connexin-26 and Connexin-43 as necessary for RG-guided migration of neurons (Elias et al., 2007). Molecules such as Notch and gap-junction proteins function differently during genesis and migration because of the different cell types they are acting in and consequent to what regulatory factors are active at the time.

POSTMITOTIC POSTMIGRATORY MATURATION

Once a neuron has migrated past older cohorts of neurons and reached its target destination in the cortical plate, it begins to transition to final maturity. This process begins in the prenatal period and continues well into the postnatal period. The period of extended maturation is most dramatic in primates, where laminar signatures begin to show signs of maturation at around 1 year old (Lein et al., 2017). Intriguingly, *in vitro* preparations of cortical neurons recapitulate aspects of development, such as gene progression (Telley et al., 2016) and laminar markers (Handel et al., 2016). While a neuronal stem cell can feasibly make a mature group of neurons (Gaspard et al., 2008), it will ultimately be a confluence of both extrinsic effectors (Kraushar et al., 2015) as well as continued intrinsic maturation driven by transcriptional as well as post-transcriptional mechanisms that generate a functional neocortex as characterized by **gene expression** and **circuit integration**.

There are several classifications of cortical pyramidal neurons based on their connectivity, otherwise known as hodological classification. Neocortical pyramidal neurons have been grouped into callosal projection neurons, layer IV granular neurons, forward and backward projection neurons, corticostriatal, corticothalamic, subcerebral, and corticospinal motor neurons (Custo Greig et al., 2013). Another classification more succinctly divides pyramidal neurons into three main categories based on these diverse projection types: **intratelecephalic (IT)** with axons projecting to neocortex, striatum, amygdala, claustrum; **pyramidal tract (PT)** with axons projecting to subcerebral targets, i.e., brainstem, spinal cord, and midbrain; and **corticothalamic (CT)** with axons projecting to the ipsilateral thalamus (Harris and Shepherd, 2015). It should be noted that like excitatory neurons, inhibitory neurons also establish circuits with non-cortical brain regions as well as within the cortex (Tamamaki and Tomioka, 2010; Lee et al., 2014; Tomioka et al., 2015). Broadly, we can understand the framework of the neocortex by dividing it into its upper and lower layers **(Figure 2B)**. Neurons in the upper layers project to their own cortical hemisphere (associative neurons) and/or to neurons to the neighboring hemisphere (commissural neurons). In addition to some commissural and associative neurons, lower layers have more diverse targets located subcortically (thalamus, amygdala, claustrum- IT and CT neurons) and subcerebrally (midbrain, spinal cord- PT neurons (Molyneaux et al., 2007; Feldmeyer, 2012). Thus, the three categories mentioned- IT, PT, and CT- comingle in the lower layers but not in the upper layers, which are primarily IT neurons (Harris and Shepherd, 2015).

Development of appropriate axonal and dendritic projections is a key event in neuronal maturation. In a classic transcriptomic screen for cortico-spinal motor neuron (CSMN)-specific genes, Arlotta et al. confirmed that the transcription factor Ctip2 is expressed in all subcerebrally-projecting neurons and is required for CSMN axon extension to the spinal cord and postnatal maintenance of these axons (Arlotta et al., 2005). Satb2, another transcription factor, is an important marker of corticocortical connectivity. Satb2 mutant brains have a thinner cortex (∼15% in CP and ∼20% in intermediate zone) than found in wild-type brains, as a consequence Satb2 null mice die at birth (Alcamo et al., 2008; Britanova et al., 2008). Reduced cortical thickness is due to defects in migration, proven with BrdU-labeling. Satb2 null mouse axons do not cross to the other hemisphere via the corpus callosum, but rather join CSMN in projecting subcerebrally. In mutant brains, ectopic Ctip2 expression was seen in upper layer neurons based on BrdU-tracing at E15.5; WT neurons cycling at this time do not express Ctip2, but Satb2-/- neurons cycling at this time do express Ctip2 (Alcamo et al., 2008). This resulted in ∼27% more cells projecting subcerebrally to the cerebral peduncle (a fascicle containing axons projecting corticopontine, corticobulbar, and corticospinal) (Britanova et al., 2008). Satb2 is likely a transcriptional repressor of Ctip2 via histone acetylation (Alcamo et al., 2008), by assembling the NURD chromatin complex (Britanova et al., 2008).

In order to better understand callosal projections, further study of cortical transcription factor Lmo4 would be informative as, unlike Satb2, it is expressed in all callosal neurons (Arlotta et al., 2005). In the Satb2 knockout, Lmo4 expression is reduced in layers V and VI mediodorsally and elevated in the intermediate zone (expression patterns were analyzed at E18.5 due to Satb2 -/- lethality) (Alcamo et al., 2008). This could imply that Lmo4 helps to define a subpopulation of corticocortical neurons in a majority corticofugal environment.

Post-transcriptional regulation was described in a previous section of this review as partly responsible for the genesis of a heterogeneous progenitor pool. This further extends into the maturation phase. A recent screen of post-natal cells in the mouse visual cortex found that 320 genes, and specifically 567 exons, were subject to differential mRNA processing (i.e., polyadenylation, alternative splicing) between diverse subpopulations (Tasic et al., 2016). Within the somatosensory cortex, ∼16% (1,646) of genes were subject to differential patterns of alternative splicing (Belgard et al., 2011). These results

suggest that post-transcriptional processing remains abundant throughout and beyond the progenitor period- possibly as a mechanism for fate maintenance.

Lmo4 mRNA is a target of a lower-layer specific RBP, HuD (Chen et al., 2007; DeBoer et al., 2014). HuD, one of the Hu antigens, is a neuronal lineage-specific RBP (Okano and Darnell, 1997). In addition to being expressed in a subpopulation of lower layer neurons in the adult murine neocortex (DeBoer et al., 2014), it has been found in human IPs as well (Pollen et al., 2015). Constitutive knockout of this protein results in a specific loss of Tle4+ lower layer populations (∼12% reduction compared to WT), but does not significantly affect upper layer populations (DeBoer et al., 2014). HuD is known to be important for post-mitotic maturation of neurons, and specifically for formation of dendritic trees. miR-375 has been found to inhibit dendritic differentiation by targeting *HuD* mRNA (Abdelmohsen et al., 2010). Accordingly, *in vivo*, HuD depletion resulted in decreased dendritic complexity (DeBoer et al., 2014). Considering that HuD is widely expressed in lower layers of the cortex, including neurons which project axons along the corticospinal tract, it is not surprising that HuD loss affects motor performance on the rotorod (Akamatsu et al., 2005).

One of the most striking abnormalities in HuD mutants is their propensity for sound-induced seizures: when confronted with a metallic stimulus (i.e., rapid jingling of a metal object), ∼63% of mutants convulsed and of these, ∼38% of these events resulted in death. A battery of behavioral testing also revealed that HuD mutants spent more time in the open arms of the elevated plus maze. Mutants also spent more time engaging in low-energy activities such as standing still and less time engaging in high-energy activities such as running (DeBoer et al., 2014). Overall, the phenotypes seen in HuD mutants demonstrate that interfering in an RBP will have salient disruption of specific aspects of neuronal development such as dendritic maturation and circuit integration.

HuR is a ubiquitously-expressed RBP and another of the ELAVL proteins. It has been found to be expressed in NEC, RG, IPs, and neurons (Garcia-Dominguez et al., 2011; Kraushar et al., 2014). In order to study the role of HuR in neocortical development, HuR conditional knockout (*Emx1-Cre* driven knockout) neocortex was dissected at E13 and postnatal day 0 and compared to wildtype cortices in a recent study (Kraushar et al., 2014). The neocortex was processed through polysome-fractionation, mRNA isolation from the fractions, and finally RNAseq of fraction-specific mRNA. Kraushar et al. found that transcripts expressed in layers II/III and V were disproportionately impacted by HuR deletion at both ages and both in mono- and polysomes. Strikingly, by age P0, layer II/III transcripts were enriched in HuR conditional knockout cortices while layer V transcripts were decreased in the HuR conditional knockout cortices (Kraushar et al., 2014). Transcriptomic profiling has identified significant gene expression overlap between layers II/III and V (Hoerder-Suabedissen et al., 2013). In this context, results obtained with HuR conditional knockout are tantalizing because of HuR's widespread expression across all the neocortical layers, suggesting differential actions between upper and lower layers. An extended comparison across layers in this mutant for AS variants could be revealing.

In order to investigate a specific example of the upper/lower layer bias of HuR, two of its regulated transcripts were examined: *Foxp1* and *Foxp2*. Both are members of the Forkhead box family of transcription factors; these are distinct from RBFOX-1/2, RBFOX-3 is also known as NeuN (**Figure 1**), which are the mammalian homologs of the *C. elegans* RBP Fox-1. Mammalian FOXP2 is a transcription factor expressed in a subpopulation of cells in layer VI (Ferland et al., 2003) that project corticothalmaically (Sorensen et al., 2015). It is expressed in post-mitotic cells and has been implicated in Autism Spectrum Disorders (ASDs) (Vernes et al., 2011). It has been shown that *Foxp2* mRNA translation requires the RBP HuR during prenatal cortical development (Popovitchenko et al., 2016). *Foxp2* was identified alongside *Foxp1* as bound targets of HuR in a RIP-ChIP (RNA immunoprecipitation coupled with a microarray) screen. In the HuR conditional knockout, FOXP2 protein was absent when it normally should have been present in the neonatal brain (P0), however, *Foxp2* mRNA levels in HuR conditional knockout were comparable to levels in wildtype, demonstrating the reliance of the *Foxp2* transcript on post-transcriptional processes to enact its translation. Interestingly, the related protein FOXP1 was precociously expressed in the appropriate subpopulation of cells (Layers III-V), suggesting that HuR is important for translational-repression of this transcription factor (**Figure 5,** step 6). Differential phosphorylation was proposed as a likely mechanism for HuR's differential treatment of these two transcripts, and demonstrated with an *in vitro* translational assay (Popovitchenko et al., 2016), though no specific kinase was identified. It would be informative to further investigate HuR's control of neuronal maturation and layer formation; specifically as to whether dysregulation of Foxp2 translation confers an anatomical, i.e., cortico-thalamic connectivity, or behavioral, i.e., murine ultra-sonic vocalizations, phenotype.

CONCLUSIONS

Proper lamination requires that progenitor cells give rise to a neuron at a certain time point during development, that the immature neuron can migrate away from its birth place and past other cells on its way, and finally that the immature neuron can stop to take its proper place and adopt a mature identity as characterized by dendritic and axonal patterns, electrophysiology, and gene expression. It is becoming clear that both transcriptional and post-transcriptional mechanisms guide the progression of each of these steps, crucial to neocortical laminar identity.

Fate is often exquisitely linked to functional gene expression. For example, we can confidently identify a RG because it expresses Pax6. However, relying on one molecule for identification leaves the possibility open that co-expressing subpopulations (i.e., Pax6 and Tbr2) will be improperly identified at the progenitor (Telley et al., 2016) and the post-mitotic levels (Handel et al., 2016). Furthermore, a recent single-cell RNA seq screen of iPSCs found that *Bcl11b/Ctip2* was co-expressed with

Brn2 in a subpopulation of cells; and that this is recapitulated in neurons from human fetal and adult brains (Handel et al., 2016). Therefore, the use of several overlapping factors will lead to better understanding of the progenitor and post-mitotic subpopulation heterogeneity.

Characterization of transcription factors in specific subpopulations of neurons was analyzed at depth and several important determinants of cell fate have been identified. In particular, the onset of studies using RNAseq, which allows for unbiased sequencing of transcripts and subsequently the discovery of processes occurring post-transcriptionally, such as alternative splicing or unanticipated identification of novel non-coding transcripts, is beginning to reveal the importance of mRNA processing across cell types. Alternative splicing and translational repression, such as that enacted by lncRNAs, are emerging as two distinct mechanisms by which regulation occurs in addition to the localization of transcripts by RBPs and translational suppression/repression through binding. Also of note is the heavy involvement and dependence of posttranscriptional regulation with cell-cycle control (Abdelmohsen et al., 2008; Filippova et al., 2012; Boulay et al., 2014; Duggimpudi et al., 2015), regulation of which is repeatedly found to correspond to state-transitions.

Unlike TFs, post-transcriptional regulators often have ubiquitous expression patterns and are not bound by the neat compartments of gene expression that characterize the layers (**Figure 2C**). Thus, how can they fit into our understanding of laminar development? Differential phosphorylation states that are controlled by distinct kinases may play a role in translational specificity of bound mRNAs (Popovitchenko et al., 2016). In addition, competitive roles of distinct RBPs, miRNAs and their targets may further contribute to the diversity (Gardiner et al., 2015). Interestingly, genes that did not have laminar specificity were more likely to be important in development in an RNA-seq screen of post-natal brains (Belgard et al., 2011). Though largely speculative at this point, this observation could be a clue to the over-arching importance of RNA processing during development.

Further exploration into post-transcriptional determinants of cell fate is demonstrably needed. With every step of mRNA processing open to spatiotemporally specific post-transcriptional intervention, the full contribution of post-transcriptional processes to laminar characterization remains to be discovered.

AUTHOR CONTRIBUTIONS

TP and MRR conducted literature searches, designed figures, and completed writing of the manuscript.

ACKNOWLEDGMENTS

We would like to thank our funding agencies, the National Institute of Neurological Disease and Stroke/NIH (NS075367) and the New Jersey Commission of Spinal Cord Research (CSCR14IRG001), for supporting our investigations. We also thank several people for their insights during discussions, including Drs. Xioabing Luo, Hui Wang, Matthew Kraushar, and Huaye Zhang. We thank all of the researchers who strive to elucidate the mechanisms behind development of the neocortex. While we sought to provide a general review of laminar mechanisms, we extend our apology to those who we do not cite due to space limitations.

REFERENCES

Abdel Razek, A. A., Kandell, A. Y., Elsorogy, L. G., Elmongy, A., and Basett, A. A. (2008). Disorders of cortical formation: MR imaging features. *Am. J. Neuroradiol.* 30, 4–11. doi: 10.3174/ajnr.A1223

Abdelmohsen, K., Hutchison, E. R., Lee, E. K., Kuwano, Y., Kim, M. M., Masuda, K., et al. (2010). miR-375 inhibits differentiation of neurites by lowering HuD levels. *Mol. Cell. Biol.* 30, 4197–4210. doi: 10.1128/MCB.00316-10

Abdelmohsen, K., Srikantan, S., Kuwano, Y., and Gorospe, M. (2008). miR-519 reduces cell proliferation by lowering RNA-binding protein HuR levels. *Proc. Natl. Acad. Sci. U.S.A.* 105, 20297–20302. doi: 10.1073/pnas.0809376106

Akamatsu, W., Fujihara, H., Mitsuhashi, T., Yano, M., Shibata, S., Hayakawa, Y., et al. (2005). The RNA-binding protein HuD regulates neuronal cell identity and maturation. *Proc. Natl. Acad. Sci. U.S.A.* 102, 4625–4630. doi: 10.1073/pnas.0407523102

Alcamo, E. A., Chirivella, L., Dautzenberg, M., Dobreva, G., Fariñas, I., Grosschedl, R., et al. (2008). Satb2 regulates callosal projection neuron identity in the developing cerebral cortex. *Neuron* 57, 364–377. doi: 10.1016/j.neuron.2007.12.012

Allendoerfer, K. (1994). The subplate, a transient neocortical structure: its role in the development of connections between thalamus and cortex. *Annu. Rev. Neurosci.* 17, 185–218. doi: 10.1146/annurev.ne.17.030194.001153

Amaral, D. G., Schumann, C. M., and Nordahl, C. W. (2008). Neuroanatomy of autism. *Trends Neurosci.* 31, 137–145. doi: 10.1016/j.tins.2007.12.005

Angevine, J. B., and Sidman, R. L. (1961). Autoradiographic study of cell migration during histogenesis of cerebral cortex in the mouse. *Nature* 192, 766–768. doi: 10.1038/192766b0

Angevine, J. B., Bodian, D., Coulombre, A. J., Edds, M. V., Hamburger, V., Jacobson, M., et al. (1970). Embryonic vertebrate central nervous system: revised terminology. *Anat. Rec.* 166, 257–261. doi: 10.1002/ar.1091660214

Appel, B., Givan, L. A., and Eisen, J. S. (2001). Delta-Notch signaling and lateral inhibition in zebrafish spinal cord development. *BMC Dev. Biol.* 1:13. doi: 10.1186/1471-213X-1-13

Arai, Y., Pulvers, J. N., Haffner, C., Schilling, B., Nüsslein, I., Calegari, F., et al. (2011) Neural stem and progenitor cells shorten S-phase on commitment to neuron production. *Nat. Commun.* 2, 154. doi: 10.1038/ncomms1155

Arlotta, P., Molyneaux, B. J., Chen, J., Inoue, J., Kominami, R., and Macklis, J. D. (2005). Neuronal subtype-specific genes that control corticospinal motor neuron development *in vivo*. *Neuron* 45, 207–221. doi: 10.1016/j.neuron.2004.12.036

Arnold, S. J., Huang, G. J., Cheung, A. F. P., Era, T., Nishikawa, S. I., Bikoff, E. K., et al. (2008). The T-box transcription factor Eomes/Tbr2 regulates neurogenesis in the cortical subventricular zone. *Genes Dev.* 22, 2479–2484. doi: 10.1101/gad.475408

Belgard, T. G., Marques, A. C., Oliver, P. L., Abaan, H. O., Sirey, T. M., Hoerder-Suabedissen, A., et al. (2011). A transcriptomic atlas of mouse neocortical layers. *Neuron* 71, 605–616. doi: 10.1016/j.neuron.2011.06.039

Betizeau, M., Cortay, V., Patti, D., Pfister, S., Gautier, E., Bellemin-Ménard, A., et al. (2013). Precursor diversity and complexity of lineage relationships in the outer subventricular zone of the primate. *Neuron* 80, 442–457. doi: 10.1016/j.neuron.2013.09.032

Bian, S., Hong, J., Li, Q., Schebelle, L., Pollock, A., Knauss, J. L., et al. (2013). MicroRNA cluster miR-17-92 regulates neural stem cell expansion and

transition to intermediate progenitors in the developing mouse neocortex. *Cell Rep.* 3, 1398–1406. doi: 10.1016/j.celrep.2013.03.037

Bosch, P. J., Fuller, L. C., Sleeth, C. M., and Weiner, J. A. (2016). Akirin2 is essential for the formation of the cerebral cortex. *Neural. Dev.* 11, 21. doi: 10.1186/s13064-016-0076-8

Boulay, K., Ghram, M., Viranaicken, W., Trepanier, V., Mollet, S., Frechina, C., et al. (2014). Cell cycle-dependent regulation of the RNA-binding protein Staufen1. *Nucleic Acids Res.* 42, 7867–7883. doi: 10.1093/nar/gku506

Boutz, P. L., Stoilov, P., Li, Q., Lin, C. H., Chawla, G., Ostrow, K., et al. (2007). A post-transcriptional regulatory switch in polypyrimidine tract-binding proteins reprograms alternative splicing in developing neurons. *Genes Dev.* 21, 1636–1652. doi: 10.1101/gad.1558107

Brennan, C. M., and Steitz, J. A. (2001). HuR and mRNA stability. *Cell Mol. Life Sci.* 58, 266–277. doi: 10.1007/PL00000854

Britanova, O., de Juan Romero, C., Cheung, A., Kwan, K. Y., Schwark, M., Gyorgy, A., et al., (2008). Satb2 Is a postmitotic determinant for upper-layer neuron specification in the neocortex. *Neuron* 57, 378–392. doi: 10.1016/j.neuron.2007.12.028

Bystron, I., Rakic, P., Molnar, Z., and Blakemore, C. (2006). The first neurons of the human cerebral cortex. *Nat. Neurosci.* 9, 880–886. doi: 10.1038/nn1726

Cabili, M. N., Trapnell, C., Goff, L., Koziol, M., Tazon-Vega, B., Regev, A., et al. (2011). Integrative annotation of human large intergenic noncoding RNAs reveals global properties and specific subclasses. *Genes Dev.* 25, 1915–1927. doi: 10.1101/gad.17446611

Cai, L., Hayes, N. L., and Nowakowski, R. S. (1997). Synchrony of clonal cell proliferation and contiguity of clonally related cells: production of mosaicism in the ventricular zone of developing mouse neocortex. *J. Neurosci.* 17, 2088–2100.

Caviness, V. S. Jr., Goto, T., Tarui, T., Takahashi, T., Bhide, P. G., and Nowakowski, R. S. (2003). Cell output, cell cycle duration and neuronal specification: a model of integrated mechanisms of the neocortical proliferative process. *Cereb. Cortex* 13, 592–598. doi: 10.1093/cercor/13.6.592

Cayouette, M., and Raff, M. (2003). The orientation of cell division influences cell-fate choice in the developing mammalian retina. *Development* 130, 2329–2339. doi: 10.1242/dev.00446

Chavali, P. L., Stojic, L., Meredith, L. W., Joseph, N., Nahorski, M. S., Sanford, T. J., et al. (2017). Neurodevelopmental protein Musashi-1 interacts with the Zika genome and promotes viral replication. *Science* 357, 83–88. doi: 10.1126/science.aam9243

Chawla, G., Lin, C. H., Han, A., Shiue, L., Ares, M. Jr., and Black, D. L. (2009). Sam68 regulates a set of alternatively spliced exons during neurogenesis. *Mol. Cell Biol.* 29, 201–213. doi: 10.1128/MCB.01349-08

Chen, H.-H., Xu, J., Safarpour, F., and Stewart, A. F. R. (2007). LMO4 mRNA stability is regulated by extracellular ATP in F11 cells. *Biochem. Biophys. Res. Commun.* 357, 56–61. doi: 10.1016/j.bbrc.2007.03.113

Cooper, J. A. (2013). Cell biology in neuroscience: mechanisms of cell migration in the nervous system. *J. Cell Biol.* 202, 725–734. doi: 10.1083/jcb.201305021

Cugola, F. R., Fernandes, I. R., Russo, F. B., Freitas, B. C., Dias, J. L., Guimaraes, K. P., et al. (2016). The Brazilian Zika virus strain causes birth defects in experimental models. *Nature* 534, 267–271. doi: 10.1038/nature18296

Custo Greig, L. F., Woodworth, M. B., Galazo, M. J., Padmanabhan, H., and Macklis, J. D. (2013). Molecular logic of neocortical projection neuron specification, development and diversity. *Nat. Rev. Neurosci.* 14, 755–769. doi: 10.1038/nrn3586

D'Arcangelo, G. (2014). Reelin in the years: controlling neuronal migration and maturation in the mammalian brain. *Adv. Neurosci.* 2014, 1–19. doi: 10.1155/2014/597395

De Carlos, J. A., and O'Leary, D. D. (1992). Growth and targeting of subplate axons and establishment of major cortical pathways. *J. Neurosci.* 12, 1194–211.

DeBoer, E. M., Azevedo, R., Vega, T. A., Brodkin, J., Akamatsu, W., Okano, H., et al. (2014). Prenatal deletion of the RNA-binding protein HuD disrupts postnatal cortical circuit maturation and behavior. *J. Neurosci.* 34, 3674–3686. doi: 10.1523/JNEUROSCI.3703-13.2014

DeBoer, E. M., Kraushar, M. L., Hart, R. P., and Rasin, M. R. (2013). Post-transcriptional regulatory elements and spatiotemporal specification of neocortical stem cells and projection neurons. *Neuroscience* 248, 499–528. doi: 10.1016/j.neuroscience.2013.05.042

Decker, C. J., and Parker, R. (2012). P-bodies and stress granules: possible roles in the control of translation and mRNA degradation. *Cold Spring Harb. Perspect. Biol.* 4:*a*012286. doi: 10.1101/cshperspect.a012286

D'Haene, E., Jacobs, E. Z., Volders, P. J., De Meyer, T., Menten, B., and Vergult, S. (2016). Identification of long non-coding RNAs involved in neuronal development and intellectual disability. *Sci. Rep.* 6:28396. doi: 10.1038/srep28396

DiCicco-Bloom, E., Lord, C., Zwaigenbaum, L., Courchesne, E., Dager, S. R., Schmitz, C., et al. (2006). The developmental neurobiology of autism spectrum disorder. *J. Neurosci.* 26, 6897–6906. doi: 10.1523/JNEUROSCI.1712-06.2006

Douglas, R. J., and Martin, K. A. (2007). Mapping the matrix: the ways of neocortex. *Neuron* 56, 226–238. doi: 10.1016/j.neuron.2007.10.017

Duggimpudi, S., Larsson, E., Nabhani, S., Borkhardt, A., and Hoell, J. I. (2015). The cell cycle regulator CCDC6 is a key target of RNA-binding protein EWS. *PLoS ONE* 10:e0119066. doi: 10.1371/journal.pone.0119066

Elias, L. A., Wang, D. D., and Kriegstein, A. R. (2007). Gap junction adhesion is necessary for radial migration in the neocortex. *Nature* 448, 901–917. doi: 10.1038/nature06063

Englund, C. (2005). Pax6, Tbr2, and Tbr1 are expressed sequentially by radial glia, intermediate progenitor cells, and postmitotic neurons in developing neocortex. *J. Neurosci.* 25, 247–251. doi: 10.1523/JNEUROSCI.2899-04.2005

Fan, X. C., and Steitz, J. A. (1998). Overexpression of HuR, a nuclear-cytoplasmic shuttling protein, increases the *in vivo* stability of ARE-containing mRNAs. *EMBO J.* 17, 3448–3460. doi: 10.1093/emboj/17.12.3448

Feldmeyer, D. (2012). Excitatory neuronal connectivity in the barrel cortex. *Front. Neuroanat.* 6:24. doi: 10.3389/fnana.2012.00024

Ferland, R. J., Cherry, T. J., Preware, P. O., Morrisey, E. E., and Walsh, C. A. (2003). Characterization of Foxp2 and Foxp1 mRNA and protein in the developing and mature brain. *J. Comp. Neurol.* 460, 266–279. doi: 10.1002/cne.10654

Filippova, N., Yang, X., King, P., and Nabors, L. B. (2012). Phosphoregulation of the RNA-binding protein Hu antigen R (HuR) by Cdk5 affects centrosome function. *J. Biol. Chem.* 287, 32277–32287. doi: 10.1074/jbc.M112.353912

Florio, M., Albert, M., Taverna, E., Namba, T., Brandl, H., Lewitus, E., et al. (2015). Human-specific gene *ARHGAP11B* promotes basal progenitor amplification and neocortex expansion. *Science* 347, 1465–1470. doi: 10.1126/science.aaa1975

Franco, S. J., Martinez-Garay, I., Gil-Sanz, C., Harkins-Perry, S. R., and Müller, U. (2011). Reelin regulates cadherin function via Dab1/Rap1 to Control neuronal migration and lamination in the neocortex. *Neuron* 69, 482–497. doi: 10.1016/j.neuron.2011.01.003

Fukumura, K., Wakabayashi, S., Kataoka, N., Sakamoto, H., Suzuki, Y., Nakai, K., et al. (2016). The exon junction complex controls the efficient and faithful splicing of a subset of transcripts involved in mitotic cell-cycle progression. *Int. J. Mol. Sci.* 17:E1153. doi: 10.3390/ijms17081153

Gal, J. S. (2006). Molecular and morphological heterogeneity of neural precursors in the mouse neocortical proliferative zones. *J. Neurosci.* 26, 1045–1056. doi: 10.1523/JNEUROSCI.4499-05.2006

Gao, P., Postiglione, M. P., Krieger, T. G., Hernandez, L., Wang, C., Han, Z., et al. (2014). Deterministic progenitor behavior and unitary production of neurons in the neocortex. *Cell* 159, 775–788. doi: 10.1016/j.cell.2014.10.027

Garcez, P. P., Loiola, E. C., Madeiro da Costa, R., Higa, L. M., Trindade, P., Delvecchio, R., et al. (2016). Zika virus impairs growth in human neurospheres and brain organoids. *Science* 352, 816–818. doi: 10.1126/science.aaf6116

Garcia-Dominguez, D. J., Morello, D., Cisneros, E., Kontoyiannis, D. L., and Frade, J. M. (2011). Stabilization of Dll1 mRNA by Elavl1/HuR in neuroepithelial cells undergoing mitosis. *Mol. Biol. Cell* 22, 1227–1239. doi: 10.1091/mbc.E10-10-0808

Gardiner, A. S., Twiss, J. L., and Perrone-Bizzozero, N. I. (2015). Competing Interactions of RNA-Binding Proteins, MicroRNAs, and their targets control neuronal development and function. *Biomolecules* 5, 2903–2918. doi: 10.3390/biom5042903

Gaspard, N., Bouschet, T., Hourez, R., Dimidschstein, J., Naeije, G., van den Ameele, J., et al. (2008). An intrinsic mechanism of corticogenesis from embryonic stem cells. *Nature* 455, 351–357. doi: 10.1038/nature07287

Gehman, L. T., Stoilov, P., Maguire, J., Damianov, A., Lin, C.-H., Shiue, L., et al. (2011). The splicing regulator Rbfox1 (A2BP1) controls neuronal excitation in the mammalian brain. *Nat. Genet.* 43, 706–711. doi: 10.1038/ng.841

Götz, M., and Huttner, W. B. (2005). The cell biology of neurogenesis. *Nat. Rev. Mol. Cell Biol.* 6, 777–788. doi: 10.1038/nrm1739

Guy, J., and Staiger, J. F. (2017). The functioning of a cortex without layers. *Front. Neuroanat.* 11:54. doi: 10.3389/fnana.2017.00054

Guy, J., Wagener, R. J., Mock, M., and Staiger, J. F. (2015). Persistence of functional sensory maps in the absence of cortical layers in the somsatosensory cortex of reeler mice. *Cereb. Cortex* 25, 2517–2528. doi: 10.1093/cercor/bhu052

Handel, A. E., Chintawar, S., Lalic, T., Whiteley, E., Vowles, J., Giustacchini, A., et al. (2016). Assessing similarity to primary tissue and cortical layer identity in induced pluripotent stem cell-derived cortical neurons through single-cell transcriptomics. *Hum. Mol. Genet.* 25, 989–1000. doi: 10.1093/hmg/ddv637

Hansen, D. V., Lui, J. H., Parker, P. R., and Kriegstein, A. R. (2010). Neurogenic radial glia in the outer subventricular zone of human neocortex. *Nature* 464, 554–561. doi: 10.1038/nature08845

Harris, K. D., and Shepherd, G. M. G. (2015). The neocortical circuit: themes and variations. *Nat. Neurosci.* 18, 170–181. doi: 10.1038/nn.3917

Hart, R. P., and Goff, L. A. (2016). Long noncoding RNAs: central to nervous system development. *Int. J. Dev. Neurosci.* 55, 109–116. doi: 10.1016/j.ijdevneu.2016.06.001

Hashimoto-Torii, K., Torii, M., Sarkisian, M. R., Bartley, C. M., Shen, J., Radtke, F., et al. (2008). Interaction between reelin and notch signaling regulates neuronal migration in the cerebral cortex. *Neuron* 60, 273–284. doi: 10.1016/j.neuron.2008.09.026

Haubensak, W., Attardo, A., Denk, W., and Huttner, W. B. (2004). Neurons arise in the basal neuroepithelium of the early mammalian telencephalon: a major site of neurogenesis. *Proc. Natl. Acad. Sci. U.S.A.* 101, 3196–3201. doi: 10.1073/pnas.0308600100

He, Z., Han, D., Efimova, O., Guijarro, P., Yu, Q., Oleksiak, A., et al. (2017). Comprehensive transcriptome analysis of neocortical layers in humans, chimpanzees and macaques. *Nat. Neurosci.* 20, 886–895. doi: 10.1038/nn.4548

Hippenmeyer, S., Johnson, R. L., and Luo, L. (2013). Mosaic analysis with double markers reveals cell-type-specific paternal growth dominance. *Cell Rep.* 3, 960–967. doi: 10.1016/j.celrep.2013.02.002

Hir, H. L., Saulière, J., and Wang, Z. (2015). The exon junction complex as a node of post-transcriptional networks. *Nat. Rev. Mol. Cell Biol.* 17, 41–54. doi: 10.1038/nrm.2015.7

Hoerder-Suabedissen, A., Oeschger, F. M., Krishnan, M. L., Belgard, T. G., Wang, W. Z., Lee, S., et al. (2013). Expression profiling of mouse subplate reveals a dynamic gene network and disease association with autism and schizophrenia. *Proc. Natl. Acad. Sci. U.S.A.* 110, 3555–3560. doi: 10.1073/pnas.1218510110

Homem, C. C., Repic, M., and Knoblich, J. A. (2015). Proliferation control in neural stem and progenitor cells. *Nat. Rev. Neurosci.* 16, 647–659. doi: 10.1038/nrn4021

Huttner, W. B., and Kosodo, Y. (2005). Symmetric versus asymmetric cell division during neurogenesis in the developing vertebrate central nervous system. *Curr. Opin. Cell Biol.* 17, 648–657. doi: 10.1016/j.ceb.2005.10.005

Hutton, S. R., and Pevny, L. H. (2011). SOX2 expression levels distinguish between neural progenitor populations of the developing dorsal telencephalon. *Dev. Biol.* 352, 40–47. doi: 10.1016/j.ydbio.2011.01.015

Imai, T., Tokunaga, A., Yoshida, T., Hashimoto, M., Mikoshiba, K., Weinmaster, G., et al. (2001). The neural RNA-binding protein Musashi1 translationally regulates mammalian numb gene expression by interacting with its mRNA. *Mol. Cell Biol.* 21, 3888–3900. doi: 10.1128/MCB.21.12.3888-3900.2001

Johnson, M. B., Wang, P. P., Atabay, K. D., Murphy, E. A., Doan, R. N., Hecht, J. L., et al. (2015). Single-cell analysis reveals transcriptional heterogeneity of neural progenitors in human cortex. *Nat. Neurosci.* 18, 637–646. doi: 10.1038/nn.3980

Jones, E. G. (1986). Neurotransmitters in the cerebral cortex. *J. Neurosurg.* 65, 135–153. doi: 10.3171/jns.1986.65.2.0135

Jones, E. G. (1995). Cortical development and neuropathology in schizophrenia. *Ciba Found. Symp.* 193, 277–295.

Jones, E. G. (2009). "Cerebral cortex," in *Encyclopedia of Neuroscience*, Vol. 1, ed L. R. Squire (San Diego, CA: Academic Press), 769–773.

Kadowaki, M., Nakamura, S., Machon, O., Krauss, S., Radice, G. L., and Takeichi, M. (2007). N-cadherin mediates cortical organization in the mouse brain. *Dev. Biol.* 304, 22–33. doi: 10.1016/j.ydbio.2006.12.014

Kanemitsu, Y., Fujitani, M., Fujita, Y., Zhang, S., Su, Y. Q., Kawahara, Y., et al. (2017). The RNA-binding protein MARF1 promotes cortical neurogenesis through its RNase activity domain. *Sci. Rep.* 7, 1155. doi: 10.1038/s41598-017-01317-y

Kang, H. J., Kawasawa, Y. I., Cheng, F., Zhu, Y., Xu, X., Li, M., et al.. (2011). Spatio-temporal transcriptome of the human brain. *Nature* 478, 483–489. doi: 10.1038/nature10523

Kang, W., Wong, L. C., Shi, S. H., and Hebert, J. M. (2009). The transition from radial glial to intermediate progenitor cell is inhibited by FGF signaling during corticogenesis. *J. Neurosci.* 29, 14571–14580. doi: 10.1523/JNEUROSCI.3844-09.2009

Kasthuri, N., Hayworth, K. J., Berger, D. R., Schalek, R. L., Conchello, J. A., Knowles-Barley, S., et al. (2015). Saturated reconstruction of a volume of neocortex. *Cell* 162, 648–661. doi: 10.1016/j.cell.2015.06.054

Kedersha, N., Stoecklin, G., Ayodele, M., Yacono, P., Lykke-Andersen, J., Fritzler, M. J., et al. (2005). Stress granules and processing bodies are dynamically linked sites of mRNP remodeling. *J. Cell Biol.* 169, 871–884. doi: 10.1083/jcb.200502088

Keene, J. D. (2007). RNA regulons: coordination of post-transcriptional events. *Nat. Rev. Genet.* 8, 533–543. doi: 10.1038/nrg2111

Kohyama, J., Tokunaga, A., Fujita, Y., Miyoshi, H., Nagai, T., Miyawaki, A., et al. (2005). Visualization of spatiotemporal activation of Notch signaling: live monitoring and significance in neural development. *Dev. Biol.* 286, 311–325. doi: 10.1016/j.ydbio.2005.08.003

Konno, D., Iwashita, M., Satoh, Y., Momiyama, A., Abe, T., Kiyonari, H., et al. (2012). The mammalian DM domain transcription factor Dmrta2 is required for early embryonic development of the cerebral cortex. *PLoS ONE* 7:e46577. doi: 10.1371/journal.pone.0046577

Kostovic, I., and Rakic, P. (1990). Developmental history of the transient subplate zone in the visual and somatosensory cortex of the macaque monkey and human brain. *J. Comp. Neurol.* 297, 441–470. doi: 10.1002/cne.902970309

Kowalczyk, T., Pontious, A., Englund, C., Daza, R. A., Bedogni, F., Hodge, R., et al. (2009). Intermediate neuronal progenitors (basal progenitors) produce pyramidal-projection neurons for all layers of cerebral cortex. *Cereb. Cortex* 19, 2439–2450. doi: 10.1093/cercor/bhn260

Kraushar, M. L., Popovitchenko, T., Volk, N. L., and Rasin, M.-R. (2016). The frontier of RNA metamorphosis and ribosome signature in neocortical development. *Int. J. Dev. Neurosci.* 55, 131–139. doi: 10.1016/j.ijdevneu.2016.02.003

Kraushar, M. L., Thompson, K., Wijeratne, H. R. S., Viljetic, B., Sakers, K., Marson, J. W., et al. (2014). Temporally defined neocortical translation and polysome assembly are determined by the RNA-binding protein Hu antigen R. *Proc. Natl. Acad. Sci.* 111, *E*3815–E3824. doi: 10.1073/pnas.1408305111

Kraushar, M. L., Viljetic, B., Wijeratne, H. R., Thompson, K., Jiao, X., Pike, J. W., et al. (2015). Thalamic WNT3 secretion spatiotemporally regulates the neocortical ribosome signature and mRNA translation to specify neocortical cell subtypes. *J. Neurosci.* 35, 10911–10926. doi: 10.1523/JNEUROSCI.0601-15.2015

Kriegstein, A., and Alvarez-Buylla, A. (2009). The glial nature of embryonic and adult neural stem cells. *Annu. Rev. Neurosci.* 32, 149–184. doi: 10.1146/annurev.neuro.051508.135600

Kwan, K. Y., Sestan, N., and Anton, E. S. (2012). Transcriptional co-regulation of neuronal migration and laminar identity in the neocortex. *Development* 139, 1535–1546. doi: 10.1242/dev.069963

La Fata, G., Gartner, A., Dominguez-Iturza, N., Dresselaers, T., Dawitz, J., Poorthuis, R. B., et al. (2014). FMRP regulates multipolar to bipolar transition affecting neuronal migration and cortical circuitry. *Nat. Neurosci.* 17, 1693–1700. doi: 10.1038/nn.3870

Le Hir, H. (2001). The exon-exon junction complex provides a binding platform for factors involved in mRNA export and nonsense-mediated mRNA decay. *EMBO J.* 20, 4987–4997. doi: 10.1093/emboj/20.17.4987

Lee, A. T., Vogt, D., Rubenstein, J. L., and Sohal, V. S. (2014). A class of GABAergic neurons in the prefrontal cortex sends long-range projections to the nucleus accumbens and elicits acute avoidance behavior. *J. Neurosci.* 34, 11519–11525. doi: 10.1523/JNEUROSCI.1157-14.2014

Lein, E. S., Belgard, T. G., Hawrylycz, M., and Molnar, Z. (2017). Transcriptomic perspectives on neocortical structure, development, evolution, and disease. *Annu. Rev. Neurosci.* 40, 629–652. doi: 10.1146/annurev-neuro-070815-013858

Lennox, A. L., Mao, H., and Silver, D. L. (2017). RNA on the brain: emerging layers of post-transcriptional regulation in cerebral cortex development. *Wiley Interdiscip. Rev. Dev. Biol.* doi: 10.1002/wdev.290. [Epub ahead of print].

Leone, D. P., Srinivasan, K., Chen, B., Alcamo, E., and McConnell, S. K. (2008). The determination of projection neuron identity in the developing cerebral cortex. *Curr. Opin. Neurobiol.* 18, 28–35. doi: 10.1016/j.conb.2008.05.006

Lessard, J., Wu, J. I., Ranish, J. A., Wan, M., Winslow, M. M., Staahl, B. T., et al. (2007). An essential switch in subunit composition of a chromatin remodeling complex during neural development. *Neuron* 55, 201–215. doi: 10.1016/j.neuron.2007.06.019

Lewis, D. A., and Levitt, P. (2002). Schizophrenia as a disorder of neurodevelopment. *Annu. Rev. Neurosci.* 25, 409–32. doi: 10.1146/annurev.neuro.25.112701.142754

Liao, B. K., and Oates, A. C. (2017). Delta-Notch signalling in segmentation. *Arthropod. Struct. Dev.* 46, 429–447. doi: 10.1016/j.asd.2016.11.007

Louvi, A., and Artavanis-Tsakonas, S. (2006). Notch signalling in vertebrate neural development. *Nat. Rev. Neurosci.* 7, 93–102. doi: 10.1038/nrn1847

Malatesta, P., and Gotz, M. (2013). Radial glia - from boring cables to stem cell stars. *Development* 140, 483–486. doi: 10.1242/dev.085852

Mao, H., Pilaz, L. J., McMahon, J. J., Golzio, C., Wu, D., Shi, L., et al. (2015). *Rbm8a* haploinsufficiency disrupts embryonic cortical development resulting in microcephaly. *J. Neurosci.* 35, 7003–7018. doi: 10.1523/JNEUROSCI.0018-15.2015

Marin-Padilla, M. (1978). Dual origin of the mammalian neocortex and evolution of the cortical plate. *Anatomy Embryol.* 152, 109–126. doi: 10.1007/BF00315920

Martynoga, B., Drechsel, D., and Guillemot, F. (2012). Molecular control of neurogenesis: a view from the mammalian cerebral cortex. *Cold Spring Harb. Perspect. Biol.* 4:a008359. doi: 10.1101/cshperspect.a008359

Matera, A. G., and Wang, Z. (2014). A day in the life of the spliceosome. *Nat. Rev. Mol. Cell Biol.* 15, 108–121. doi: 10.1038/nrm3742

McConnell, S. (1985). Migration and differentiation of cerebral cortical neurons after transplantation into the brains of ferrets. *Science* 229, 1268–1271. doi: 10.1126/science.4035355

McConnell, S., and Kaznowski, C. (1991). Cell cycle dependence of laminar determination in developing neocortex. *Science* 254, 282–285. doi: 10.1126/science.1925583

Micheva, K. D., Wolman, D., Mensh, B. D., Pax, E., Buchanan, J., Smith, S. J., et al. (2016). A large fraction of neocortical myelin ensheathes axons of local inhibitory neurons. *Elife* 5:e15784. doi: 10.7554/eLife.15784

Mihalas, A. B., Elsen, G. E., Bedogni, F., Daza, R. A., Ramos-Laguna, K. A., Arnold, S. J., et al. (2016). Intermediate progenitor cohorts differentially generate cortical layers and require Tbr2 for timely acquisition of neuronal subtype identity. *Cell Rep.* 16, 92–105. doi: 10.1016/j.celrep.2016.05.072

Miyamoto, Y., Sakane, F., and Hashimoto, K. (2015). N-cadherin-based adherens junction regulates the maintenance, proliferation, and differentiation of neural progenitor cells during development. *Cell Adh. Migr.* 9, 183–192. doi: 10.1080/19336918.2015.1005466

Miyata, T., Kawaguchi, A., Okano, H., and Ogawa, M. (2001). Asymmetric inheritance of radial glial fibers by cortical neurons. *Neuron* 31, 727–741. doi: 10.1016/S0896-6273(01)00420-2

Miyata, T., Kawaguchi, A., Saito, K., Kawano, M., Muto, T., and Ogawa, M. (2004). Asymmetric production of surface-dividing and non-surface-dividing cortical progenitor cells. *Development* 131, 3133–3145. doi: 10.1242/dev.01173

Molliver, M. E., Kostovic, I., and Van Der Loos, H. (1973). The development of synapses in cerebral cortex of the human fetus. *Brain Res.* 50, 403–407. doi: 10.1016/0006-8993(73)90741-5

Molyneaux, B. J., Arlotta, P., Menezes, J. R. L., and Macklis, J. D. (2007). Neuronal subtype specification in the cerebral cortex. *Nat. Rev. Neurosci.* 8, 427–437. doi: 10.1038/nrn2151

Molyneaux, B. J., Goff, L. A., Brettler, A. C., Chen, H. H., Hrvatin, S., Rinn, J. L., et al. (2015). DeCoN: genome-wide analysis of *in vivo* transcriptional dynamics during pyramidal neuron fate selection in neocortex. *Neuron* 85, 275–288. doi: 10.1016/j.neuron.2014.12.024

Narayanan, R., Pirouz, M., Kerimoglu, C., Pham, L., Wagener, R. J., Kiszka, K. A., et al. (2015). Loss of BAF (mSWI/SNF) complexes causes global transcriptional and chromatin state changes in forebrain development. *Cell Rep.* 13, 1842–1854. doi: 10.1016/j.celrep.2015.10.046

Nguyen, H., Sokpor, G., Pham, L., Rosenbusch, J., Stoykova, A., Staiger, J. F., et al. (2016). Epigenetic regulation by BAF (mSWI/SNF) chromatin remodeling complexes is indispensable for embryonic development. *Cell Cycle* 15, 1317–1324. doi: 10.1080/15384101.2016.1160984

Nickerson, P. E., Myers, T., Clarke, D. B., and Chow, R. L. (2011). Changes in Musashi-1 subcellular localization correlate with cell cycle exit during postnatal retinal development. *Exp. Eye Res.* 92, 344–352. doi: 10.1016/j.exer.2011.02.002

Nielsen, J. A., Lau, P., Maric, D., Barker, J. L., and Hudson, L. D. (2009). Integrating microRNA and mRNA expression profiles of neuronal progenitors to identify regulatory networks underlying the onset of cortical neurogenesis. *BMC Neurosci.* 10:98. doi: 10.1186/1471-2202-10-98

Noctor, S. C., Flint, A. C., Weissman, T. A., Dammerman, R. S., and Kriegstein, A. R. (2001). Neurons derived from radial glial cells establish radial units in neocortex. *Nature* 409, 714–720. doi: 10.1038/35055553

Noctor, S. C., Martinez-Cerdeno, V., and Kriegstein, A. R. (2008). Distinct behaviors of neural stem and progenitor cells underlie cortical neurogenesis. *J. Comp. Neurol.* 508, 28–44. doi: 10.1002/cne.21669

Noctor, S. C., Martínez-Cerdeño, V., Ivic, L., and Kriegstein, A. R. (2004). Cortical neurons arise in symmetric and asymmetric division zones and migrate through specific phases. *Nat. Neurosci.* 7, 136–144. doi: 10.1038/nn1172

Nowakowski, T. J., Fotaki, V., Pollock, A., Sun, T., Pratt, T., and Price, D. J. (2013). MicroRNA-92b regulates the development of intermediate cortical progenitors in embryonic mouse brain. *Proc. Natl. Acad. Sci. U.S.A.* 110, 7056–7061. doi: 10.1073/pnas.1219385110

Oaks, A. W., Zamarbide, M., Tambunan, D. E., Santini, E., Di Costanzo, S., Pond, H. L., et al. (2017). Cc2d1a loss of function disrupts functional and morphological development in forebrain neurons leading to cognitive and social deficits. *Cereb. Cortex* 27, 1670–1685. doi: 10.1093/cercor/bhw009

Ohtsuka, T., Sakamoto, M., Guillemot, F., and Kageyama, R. (2001). Roles of the basic helix-loop-helix genes Hes1 and Hes5 in expansion of neural stem cells of the developing brain. *J. Biol. Chem.* 276, 30467–30474. doi: 10.1074/jbc.M102420200

Okano, H. J., and Darnell, R. B. (1997). A hierarchy of Hu RNA binding proteins in developing and adult neurons. *J. Neurosci.* 17, 3024–3037.

Oswald, M. J., Tantirigama, M. L. S., Sonntag, I., Hughes, S. M., and Empson, R. M. (2013). Diversity of layer 5 projection neurons in the mouse motor cortex. *Front. Cell. Neurosci.* 7:174. doi: 10.3389/fncel.2013.00174

Peng, S. S., Chen, C. Y., Xu, N., and Shyu, A. B. (1998). RNA stabilization by the AU-rich element binding protein, HuR, an ELAV protein. *EMBO J.* 17, 3461–3470. doi: 10.1093/emboj/17.12.3461

Pilaz, L.-J., and Silver, D. L. (2015). Post-transcriptional regulation in corticogenesis: how RNA-binding proteins help build the brain. *Wiley Interdiscip. Rev.* 6, 501–515. doi: 10.1002/wrna.1289

Pilaz, L.-J., Lennox, A. L., Rouanet, J. P., and Silver, D. L. (2016a). Dynamic mRNA transport and local translation in radial glial progenitors of the developing brain. *Curr. Biol.* 26, 3383–3392. doi: 10.1016/j.cub.2016.10.040

Pilaz, L.-J., McMahon, J. J., Miller, E. E., Lennox, A. L., Suzuki, A., Salmon, E., et al. (2016b). Prolonged mitosis of neural progenitors alters cell fate in the developing brain. *Neuron* 89, 83–99. doi: 10.1016/j.neuron.2015.12.007

Pla, R., Borrell, V., Flames, N., and Marin, O. (2006). Layer acquisition by cortical GABAergic interneurons is independent of reelin signaling. *J. Neurosci.* 26, 6924–6934. doi: 10.1523/JNEUROSCI.0245-06.2006

Pollen, A. A., Nowakowski, T. J., Chen, J., Retallack, H., Sandoval-Espinosa, C., Nicholas, C. R., et al. (2015). Molecular identity of human outer radial glia during cortical development. *Cell* 163, 55–67. doi: 10.1016/j.cell.2015.09.004

Polleux, F., Dehay, C., and Kennedy, H. (1998). Neurogenesis and commitment of corticospinal neurons in reeler. *J. Neurosci.* 18, 9910–9923.

Popovitchenko, T., Thompson, K., Viljetic, B., Jiao, X., Kontonyiannis, D. L., Kiledjian, M., et al. (2016). The RNA binding protein HuR determines the differential translation of autism-associated FoxP subfamily members in the developing neocortex. *Sci. Rep.* 6:28998. doi: 10.1038/srep28998

Rakic, P. (1995). A small step for the cell, a giant leap for mankind: a hypothesis of neocortical expansion during evolution. *Trends Neurosci.* 18, 383–388. doi: 10.1016/0166-2236(95)93934-P

Rakic, P. (2009). Evolution of the neocortex: a perspective from developmental biology. *Nat. Rev. Neurosci.* 10, 724–735. doi: 10.1038/nrn2719

Ramaswamy, S., and Markram, H. (2015). Anatomy and physiology of the thick-tufted layer 5 pyramidal neuron. *Front. Cell Neurosci.* 9:233. doi: 10.3389/fncel.2015.00233

Rani, N., Nowakowski, T. J., Zhou, H., Godshalk, S. E., Lisi, V., Kriegstein, A. R., et al. (2016). A Primate lncRNA mediates notch signaling during

neuronal development by sequestering miRNA. *Neuron* 90, 1174–1188. doi: 10.1016/j.neuron.2016.05.005

Rasin, M. R., Gazula, V. R., Breunig, J. J., Kwan, K. Y., Johnson, M. B., Liu-Chen, S., et al. (2007). Numb and Numbl are required for maintenance of cadherin-based adhesion and polarity of neural progenitors. *Nat. Neurosci.* 10, 819–827. doi: 10.1038/nn1924

Saffary, R., and Xie, Z. (2011). FMRP regulates the transition from radial glial cells to intermediate progenitor cells during neocortical development. *J. Neurosci.* 31, 1427–1439. doi: 10.1523/JNEUROSCI.4854-10.2011

Sahara, S., and O'Leary, D. D. M. (2009). Fgf10 regulates transition period of cortical stem cell differentiation to radial glia controlling generation of neurons and basal progenitors. *Neuron* 63, 48–62. doi: 10.1016/j.neuron.2009.06.006

Saito, K., Kawaguchi, A., Kashiwagi, S., Yasugi, S., Ogawa, M., and Miyata, T. (2003). Morphological asymmetry in dividing retinal progenitor cells. *Dev. Growth Differ.* 45, 219–229. doi: 10.1046/j.1524-4725.2003.690.x

Sansom, S. N., Griffiths, D. S., Faedo, A., Kleinjan, D. J., Ruan, Y., Smith, J., et al. (2009). The level of the transcription factor Pax6 is essential for controlling the balance between neural stem cell self-renewal and neurogenesis. *PLoS Genet.* 5:*E*1000511. doi: 10.1371/journal.pgen.1000511

Sessa, A., Mao, C.-A. A., Hadjantonakis, A.-K. K., Klein, W. H., and Broccoli, V. (2008). Tbr2 directs conversion of radial glia into basal precursors and guides neuronal amplification by indirect neurogenesis in the developing neocortex. *Neuron* 60, 56–69. doi: 10.1016/j.neuron.2008.09.028

Shim, S., Kwan, K. Y., Li, M., Lefebvre, V., and Šestan, N. (2012). Cis-regulatory control of corticospinal system development and evolution. *Nature* 486, 74–79. doi: 10.1038/nature11094

Silbereis, J. C., Pochareddy, S., Zhu, Y., Li, M., and Sestan, N. (2016). The cellular and molecular landscapes of the developing human central nervous system. *Neuron* 89, 248–268. doi: 10.1016/j.neuron.2015.12.008

Silver, D. L. (2016). Genomic divergence and brain evolution: how regulatory DNA influences development of the cerebral cortex. *Bioessays* 38, 162–171. doi: 10.1002/bies.201500108

Silver, D. L., Watkins-Chow, D. E., Schreck, K. C., Pierfelice, T. J., Larson, D. M., Burnetti, A. J., et al. (2010). The exon junction complex component Magoh controls brain size by regulating neural stem cell division. *Nat. Neurosci.* 13, 551–558. doi: 10.1038/nn.2527

Sorensen, S. A., Bernard, A., Menon, V., Royall, J. J., Glattfelder, K. J., Desta, T., et al. (2015). Correlated gene expression and target specificity demonstrate excitatory projection neuron diversity. *Cereb. Cortex* 25, 433–449. doi: 10.1093/cercor/bht243

Staley, K. (2015). Molecular mechanisms of epilepsy. *Nat. Neurosci.* 18, 367–372. doi: 10.1038/nn.3947

Stancik, E. K., Navarro-Quiroga, I., Sellke, R., and Haydar, T. F. (2010). Heterogeneity in ventricular zone neural precursors contributes to neuronal fate diversity in the postnatal neocortex. *J. Neurosci.* 30, 7028–7036. doi: 10.1523/JNEUROSCI.6131-09.2010

Stenzel, D., Wilsch-Brauninger, M., Wong, F. K., Heuer, H., and Huttner, W. B. (2014). Integrin $\alpha_v\beta_3$ and thyroid hormones promote expansion of progenitors in embryonic neocortex. *Development* 141, 795–806. doi: 10.1242/dev.101907

Stoner, R., Chow, M. L., Boyle, M. P., Sunkin, S. M., Mouton, P. R., Roy, S., et al. (2014). Patches of disorganization in the neocortex of children with autism. *N. Engl. J. Med.* 370, 1209–1219. doi: 10.1056/NEJMoa1307491

Sun, Y., Kong, W., Falk, A., Hu, J., Zhou, L., Pollard, S., et al. (2009). CD133 (Prominin) negative human neural stem cells are clonogenic and tripotent. *PLoS ONE* 4:e5498. doi: 10.1371/journal.pone.0005498

Suter, D. M., Tirefort, D., Julien, S., and Krause, K.-H. (2009). A Sox1 to Pax6 switch drives neuroectoderm to radial glia progression during differentiation of mouse embryonic stem cells. *Stem Cells* 27, 49–58. doi: 10.1634/stemcells.2008-0319

Tamamaki, N., and Tomioka, R. (2010). Long-range GABAergic connections distributed throughout the neocortex and their possible function. *Front. Neurosci.* 4:202. doi: 10.3389/fnins.2010.00202

Tan, X., and Shi, S. H. (2013). Neocortical neurogenesis and neuronal migration. *Wiley Interdiscip. Rev. Dev. Biol.* 2, 443–459. doi: 10.1002/wdev.88

Tang, H., Hammack, C., Ogden, S. C., Wen, Z., Qian, X., Li, Y., et al. (2016). Zika virus infects human cortical neural progenitors and attenuates their growth. *Cell Stem Cell* 18, 587–590. doi: 10.1016/j.stem.2016.02.016

Tasic, B., Menon, V., Nguyen, T. N., Kim, T. K., Jarsky, T., Yao, Z., et al. (2016). Adult mouse cortical cell taxonomy revealed by single cell transcriptomics. *Nat. Neurosci.* 19, 335–46. doi: 10.1038/nn.4216

Tasic, B., Miyamichi, K., Hippenmeyer, S., Dani, V. S., Zeng, H., Joo, W., et al. (2012). Extensions of MADM (mosaic analysis with double markers) in mice. *PLoS ONE* 7:e33332. doi: 10.1371/journal.pone.0033332

Telley, L., Govindan, S., Prados, J., Stevant, I., Nef, S., Dermitzakis, E., et al. (2016). Sequential transcriptional waves direct the differentiation of newborn neurons in the mouse neocortex. *Science* 351, 1443–1446. doi: 10.1126/science.aad8361

Tohyama, T., Lee, V. M., Rorke, L. B., Marvin, M., McKay, R. D., and Trojanowski, J. Q. (1992). Nestin expression in embryonic human neuroepithelium and in human neuroepithelial tumor cells. *Lab Invest.* 66, 303–313.

Tomassy, G. S., Berger, D. R., Chen, H. H., Kasthuri, N., Hayworth, K. J., Vercelli, A., et al. (2014). Distinct profiles of myelin distribution along single axons of pyramidal neurons in the neocortex. *Science* 344, 319–324. doi: 10.1126/science.1249766

Tomioka, R., Sakimura, K., and Yanagawa, Y. (2015). Corticofugal GABAergic projection neurons in the mouse frontal cortex. *Front. Neuroanat.* 9:133. doi: 10.3389/fnana.2015.00133

Tuoc, T. C., Boretius, S., Sansom, S. N., Pitulescu, M. E., Frahm, J., Livesey, F. J., et al. (2013a). Chromatin regulation by BAF170 controls cerebral cortical size and thickness. *Dev. Cell* 25, 256–69. doi: 10.1016/j.devcel.2013.04.005

Tuoc, T. C., Narayanan, R., and Stoykova, A. (2013b). BAF chromatin remodeling complex: cortical size regulation and beyond. *Cell Cycle* 12, 2953–2959. doi: 10.4161/cc.25999

Tyler, W. A., and Haydar, T. F. (2013). Multiplex genetic fate mapping reveals a novel route of neocortical neurogenesis, which is altered in the Ts65Dn mouse model of down syndrome. *J. Neurosci.* 33, 5106–5119. doi: 10.1523/JNEUROSCI.5380-12.2013

Tyler, W. A., Medalla, M., Guillamon-Vivancos, T., Luebke, J. I., and Haydar, T. F. (2015). Neural precursor lineages specify distinct neocortical pyramidal neuron types. *J. Neurosci.* 35, 6142–6152. doi: 10.1523/JNEUROSCI.0335-15.2015

Vernes, S. C., Oliver, P. L., Spiteri, E., Lockstone, H. E., Puliyadi, R., Taylor, J. M., et al. (2011). Foxp2 regulates gene networks implicated in neurite outgrowth in the developing brain. *PLoS Genet.* 7:e1002145. doi: 10.1371/journal.pgen.1002145

Wagener, R. J., Witte, M., Guy, J., Mingo-Moreno, N., Kugler, S., and Staiger, J. F. (2016). Thalamocortical connections drive intracortical activation of functional columns in the mislaminated reeler somatosensory cortex. *Cereb Cortex* 26, 820–837. doi: 10.1093/cercor/bhv257

Wagstyl, K., Ronan, L., Whitaker, K. J., Goodyer, I. M., Roberts, N., Crow, T. J., et al. (2016). Multiple markers of cortical morphology reveal evidence of supragranular thinning in schizophrenia. *Transl. Psychiatry* 6:e780. doi: 10.1038/tp.2016.43

Wang, X., Tsai, J. W., LaMonica, B., and Kriegstein, A. R. (2011). A new subtype of progenitor cell in the mouse embryonic neocortex. *Nat. Neurosci.* 14, 555–561. doi: 10.1038/nn.2807

Willsey, A. J., and State, M. W. (2015). Autism spectrum disorders: from genes to neurobiology. *Curr. Opin. Neurobiol.* 30, 92–99. doi: 10.1016/j.conb.2014.10.015

Xue, Y., Ouyang, K., Huang, J., Zhou, Y., Ouyang, H., Li, H., et al. (2013). Direct Conversion of fibroblasts to neurons by reprogramming PTB-regulated MicroRNA Circuits. *Cell* 152, 82–96. doi: 10.1016/j.cell.2012.11.045

Yang, G., Smibert, C. A., Kaplan, D. R., and Miller, F. D. (2014). An eIF4E1/4E-T complex determines the genesis of neurons from precursors by translationally repressing a proneurogenic transcription program. *Neuron* 84, 723–739. doi: 10.1016/j.neuron.2014.10.022

Yano, M., Hayakawa-Yano, Y., and Okano, H. (2016). RNA regulation went wrong in neurodevelopmental disorders: the example of Msi/Elavl RNA binding proteins. *Int. J. Dev. Neurosci.* 55, 124–130. doi: 10.1016/j.ijdevneu.2016.01.002

Yano, M., Hayakawa-Yano, Y., Mele, A., and Darnell, R. B. (2010). Nova2 Regulates Neuronal Migration through an RNA Switch in Disabled-1 Signaling. *Neuron* 66, 848–858. doi: 10.1016/j.neuron.2010.05.007

Young, F. I., Keruzore, M., Nan, X., Gennet, N., Bellefroid, E. J., and Li, M. (2017). The doublesex-related Dmrta2 safeguards neural progenitor maintenance

involving transcriptional regulation of Hes1. *Proc. Natl. Acad. Sci. U.S.A.* 114, *E*5599–E5607. doi: 10.1073/pnas.1705186114

Zhang, J., Woodhead, G. J., Swaminathan, S. K., Noles, S. R., McQuinn, E. R., Pisarek, A. J., et al. (2010). Cortical neural precursors inhibit their own differentiation via N-cadherin maintenance of beta-catenin signaling. *Dev. Cell* 18, 472–429. doi: 10.1016/j.devcel.2009.12.025

Zhang, X., Chen, M. H., Wu, X., Kodani, A., Fan, J., Doan, R., et al. (2016). Cell-type-specific alternative splicing governs cell fate in the developing cerebral cortex. *Cell* 166, 1147–1162. doi: 10.1016/j.cell.2016.07.025

Zheng, S. (2016). Alternative splicing and nonsense-mediated mRNA decay enforce neural specific gene expression. *Int. J. Dev. Neurosci.* 55, 102–108. doi: 10.1016/j.ijdevneu.2016.03.003

Zilles, K., and Amunts, K. (2009). Receptor mapping: architecture of the human cerebral cortex. *Curr. Opin. Neurol.* 22, 331–339. doi: 10.1097/WCO.0b013e32832d95db

Conflict of Interest Statement: The authors declare that the research was conducted in the absence of any commercial or financial relationships that could be construed as a potential conflict of interest.

frontiers in Neuroanatomy

ORIGINAL RESEARCH
published: 05 December 2017
doi: 10.3389/fnana.2017.00111

A Radial Glia Fascicle Leads Principal Neurons from the Pallial-Subpallial Boundary into the Developing Human Insula

*Emilio González-Arnay[1], Miriam González-Gómez[2] and Gundela Meyer[3]**

[1] Unit of Pathology, Department of Basic Medical Science, Faculty of Medicine, University of La Laguna, San Cristóbal de La Laguna, Spain, [2] Unit of Anatomy, Department of Basic Medical Science, Faculty of Medicine, University of La Laguna, San Cristóbal de La Laguna, Spain, [3] Unit of Histology, Department of Basic Medical Science, Faculty of Medicine, University of La Laguna, San Cristóbal de La Laguna, Spain

The human insular lobe, in the depth of the Sylvian fissure, displays three main cytoarchitectonic divisions defined by the differentiation of granular layers II and IV. These comprise a rostro-ventral agranular area, an intermediate dysgranular area, and a dorso-caudal granular area. Immunohistochemistry in human embryos and fetuses using antibodies against PCNA, Vimentin, Nestin, Tbr1, and Tb2 reveals that the insular cortex is unique in that it develops far away from the ventricular zone (VZ), with most of its principal neurons deriving from the subventricular zone (SVZ) of the pallial-subpallial boundary (PSB). In human embryos (Carnegie stage 16/17), the rostro-ventral insula is the first cortical region to develop; its Tbr1+ neurons migrate from the PSB along the lateral cortical stream. From 10 gestational weeks (GW) onward, lateral ventricle, ganglionic eminences, and PSB grow forming a C-shaped curvature. The SVZ of the PSB gives rise to a distinct radial glia fiber fascicle (RGF), which courses lateral to the putamen in the external capsule. In the RGF, four components can be established: PF, descending from the prefrontal PSB to the anterior insula; FP, descending from the fronto-parietal PSB toward the intermediate insula; PT, coursing from the PSB near the parieto-temporal junction to the posterior insula, and T, ascending from the temporal PSB and merging with components FP and PT. The RGF fans out at different dorso-ventral and rostro-caudal levels of the insula, with descending fibers predominating over ascending ones. The RGF guides migrating principal neurons toward the future agranular, dysgranular, and granular insular areas, which show an adult-like definition at 32 GW. Despite the narrow subplate, and the absence of an intermediate zone except in the caudal insula, most insular subdivisions develop into a 6-layered isocortex, possibly due to the well developed outer SVZ at the PSB, which is particularly prominent at the level of the dorso-caudal insula. The small size of the initial PSB sector may, however, determine the limited surface expansion of the insula, which is in contrast to the exuberant growth of the opercula deriving from the adjacent frontal-parietal and temporal VZ/SVZ.

Keywords: cytoarchitecture, inner granular layer, pallial-subpallial boundary, lateral cortical stream, migration, radial glia

OPEN ACCESS

Edited by:
Javier DeFelipe,
Cajal Institute (CSIC), Spain

Reviewed by:
Gonzalo Alvarez-Bolado,
Universität Heidelberg, Germany
Zoltan Molnar,
University of Oxford, United Kingdom

***Correspondence:**
Gundela Meyer
gundelam@aol.com

Received: *04 July 2017*
Accepted: *17 November 2017*
Published: *05 December 2017*

Citation:
González-Arnay E, González-Gómez M and Meyer G (2017) A Radial Glia Fascicle Leads Principal Neurons from the Pallial-Subpallial Boundary into the Developing Human Insula. Front. Neuroanat. 11:111. doi: 10.3389/fnana.2017.00111

INTRODUCTION

The human insular lobe lies in the depth of the Sylvian fissure and is hidden by the opercula of the adjacent cortical areas. The dorsal operculum is formed successively by prefrontal (PF), frontal cortex (FC) and parietal cortex (PC), the ventral operculum by the temporal cortex (TC). The limen insulae represents its boundary with the primary olfactory cortex (POC), as well as the junction of the temporal lobe with the ventral insular cortex (Mesulam and Mufson, 1985). The circular or limiting sulcus forms the border between the opercula and the insula. The macroscopic anatomy of the insular lobe has been described in detail (Türe et al., 1999; Naidich et al., 2004; Tanriover et al., 2004). Similarly, the microscopic structure of the human (and non-human primate) insula has been the subject of numerous cytoarchitectonic studies, which distinguish a variable number of cytoarchitectonic subdivisions, ranging from the subdivision into an anterior and a posterior insula by Brodmann (1909) to the 31 areas identified by Rose (1928) [for review, see Nieuwenhuys (2012)]. We followed the widely accepted organization of the insula into concentric belts of increasing granularity (degree of prominence of the granular layers IV and II) around the POC (Mesulam and Mufson, 1985), established in the monkey but also valid in human. This concept is similar to the areas established by Von Economo and Koskinas (1925; **Figure 1A**). The insula is continuous with the allocortical POC through a periallocortical agranular field I*A*, which predominates in the anterior insula, an isocortical granular field I*B*, that occupies the caudal insula, and a large intermediate dysgranular region termed I*AB*. More recent cytoarchitectonic studies (Morel et al., 2013) confirmed the tripartite classification of Mesulam and Mufson (1985).

The connectivity of the insula with thalamus, other cortical areas, ventral striatum, hypothalamus and amygdala, has also been studied extensively (reviewed by Augustine, 1996, and Nieuwenhuys, 2012). Through the thalamus, gustatory, vestibular, viscerocceptive, nociceptive, and thermoceptive information reach different parts of the insula, where they converge with information from limbic centers and the brain stem. Functional neuroimaging revealed that the insula forms part of distributed neuronal networks involved in complex cognitive functions. (For reviews and meta-analyses, see Kurth et al., 2010; Cauda et al., 2011; Deen et al., 2011; Fan et al., 2011; Nieuwenhuys, 2012). Craig (2009, 2010, 2011) proposed a concept of insular function where salient information is conveyed stepwise from posterior to anterior insular levels, converging at each step with polymodal information and cortico-cortical afferents, and with the anterior insula representing the neural substrate of awareness. Electrical disruption of the left anterior-dorsal insula/claustrum selectively impaired conscious awareness (Koubeissi et al., 2014). A brain network between the left rostral dorsolateral pontine tegmentum and the left anterior insula and anterior cingulate cortex is involved in wakefulness and awareness; brain stem lesions disconnecting this network lead to coma or disorders of consciousness (Fischer et al., 2016). Interestingly, both anterior insula and anterior cingulate cortex are populated by the von Economo neurons (VEN), spindle shaped projection neurons in layer V (Allman et al., 2011). Anterior insula and anterior cingulate cortex have a close functional relationship and may belong to a neural system engaged in multiple cognitive, affective, and behavioral contexts (Medford and Critchley, 2010).

Anatomical and functional alterations of the insula have been related to important human pathologies. According to Bonthius et al. (2005), the insular subdivisions are differently affected by neurofibrillary tangles in Alzheimer's disease; the agranular region is more affected than the dysgranular region, whereas the granular insula is the less affected. Schizophrenic patients have a volume reduction of the insular cortex, with larger reductions of the anterior insula (Shepherd et al., 2012), which is particularly severe in patients with childhood-onset schizophrenia (Moran et al., 2014). Atypical patterns of insula activation, in particular hypoactivity of the right anterior insula, and dysfunctional insular connectivity was also observed in autism spectrum disorder (ASD) (Di Martino et al., 2009; Uddin and Menon, 2009; Odriozola et al., 2016).

In view of the impressive amount of data on the structure and function of the adult human insula, the almost absence of developmental studies is surprising. In the early literature, the insula was considered the first cortex to differentiate (Streeter, 1912; Kodam, 1926), which is in line with a more recent report showing that sulcation, gyration, and vascularization of the human cortex start in the insular region (Afif et al., 2007). We describe here the development of the human insula from early embryonic stages to term by using immunohistochemistry for radial glia markers vimentin (Ulfig et al., 1999; Zecevic, 2004) and nestin (Zecevic et al., 2005), PCNA and Tbr2 (Englund et al., 2005) for cell proliferation and pallial progenitors, respectively, and Tbr1 as a marker of pallial neurons (Hevner et al., 2003).

Our main questions were: Where do the progenitor cells of the insula come from? How can migrating neurons reach the insula, which is so far away from the proliferating zones of the cortex? Which mechanisms can possibly explain the distinct lamination patterns of the insular subdivisions? Our analysis of the radial glia architecture in the developing telencephalon suggests that the principal neurons of the insula derive from the pallial-subpallial boundary (PSB) and migrate along a radial glia fascicle (RGF) connecting the PSB with the insula. The RGF follows the curvature of the PSB, and serves as a migration substrate for migratory neurons from the PF, frontal, parietal, and temporal PSB into the insula, with descending radial glia fibers partially merging with ascending ones. The diversity of radial glia fiber origins and trajectories might underlie the cytoarchitectonic diversity of the human insula.

MATERIALS AND METHODS

The fetal human brains, between 9 and 25 gestational weeks (GW): 9 GW (2), 10 GW (3), 11GW (4), 12 GW (3), 13 GW (2), 14 GW (2), 15 GW (3), 16 GW (4), 17 GW (2), 18 GW (1), 19 GW(1), 20 GW (2), 21 GW(6), 22 GW (3),

23GW (2), 24 (1), and 25 GW (1) were from our collection used in previous studies (e.g., Meyer et al., 2000; González-Gómez and Meyer, 2014; Meyer and González-Gómez, 2017). The embryonic cases, 5.5–8.5 GW, are the same described in Meyer et al. (2000). They were obtained after legal abortions following national guidelines in Spain, under the supervision of the Ethical Committee of the University of La Laguna, in accordance with the Declaration of Helsinki, 1964. Written informed consent was obtained from the parents for the use of embryonic and fetal brains. The embryos were staged according to Carnegie stages (CS) defined by O'Rahilly and Müller (1994). The perinatal brains, 32 GW (1 case) and 40 GW (3 cases) were from children without known neurological pathologies that died during or shortly after birth. The embryonic and fetal brains were fixed in Bouin or Carnoy, embedded in paraffin, and cut in a coronal or, in four cases, in a horizontal plane into 10 μ-thick serial sections.

Due to their large size, the perinatal brains were cut into blocks, most of which were cut coronally. In the 32 GW case and one 40 GW case, the insula was dissected out (**Figures 1B,C**) and cut in a plane considered almost perpendicular to the main axis of most insular gyri (**Figure 1C**), as recommended by Von Economo and Koskinas (1925) for an optimal visualization of cytoarchitecture.

Immunohistochemistry

Sections were deparaffinized, hydrated, and boiled in 10 mM citrate buffer (pH 6) for 20 min for antigen retrieval, rinsed in Tris-buffered saline (TBS, pH 7.6, 0.05 M), and incubated in the primary antibodies overnight in a humid chamber. After rinsing, they were incubated in the corresponding biotinylated secondary antibodies (rabbit anti-mouse IgG or goat anti-rabbit IgG; Dako, Glostrup, Denmark), diluted at 1:200 in TBS, followed by incubation with avidin-biotin complex (ABC, DAKO) in TBS. Bound peroxidase was revealed using 0.04% 3,3-diaminobenzidine (Sigma, United States), 0.05% ammonium nickel (II) sulfate, and 0.03% hydrogen peroxide in TBS, pH 7.6. Sections were dehydrated, cleared, and coverslipped using Eukitt (O. Kindler, Freiburg, Germany). Negative controls omitted the primary antibodies.

The following primary antibodies were used: Mouse monoclonal anti-reelin antibody 142 [IgG1, 1:500, (gift of A. Goffinet), 1/500; Rabbit polyclonal anti-Calretinin, Swant, 7699/4, 1/3000; Mouse monoclonal antibody anti-PCNA, Thermo Scientific, Ab-1 (clone PC10) 1/1000; Rabbit polyclonal anti-Tbr1, Abcam, ab31940, 1/300; synthetic peptide within human Vimentin aa 400 to the C-terminus (acetyl), 1/200, Abcam]; Rabbit polyclonal anti-nestin, Abcam, ab 93666, 1/100; Rabbit polyclonal anti-MAP2, Sigma, HPA 012828, 1/100; Rabbit polyclonal anti-Eomes (Tbr2) Sigma, HPA028896, 1/100.

Sequential Two Color Immunostaining

Antigens were immunolabeled sequentially by using primary antibodies (Tbr1 and CR; CR and PCNA) generated in rabbit. The first antibody was developed using DAB/nickel as chromogen. Thereafter, sections were rinsed in TBS and incubated overnight with the second antibody. After incubation with the biotinylated secondary antibodies and ABC as described above, sections were developed by using DAB alone as chromogen. Sections were dehydrated, cleared in xylene, and cover-slipped with Eukitt (Freiburg, Germany). Photographs were taken with a Zeiss Axio microscope equipped with an AxioCam MRc5 digital camera and AxioVision LE 4.6 software. Images were processed using Adobe Photoshop CS2 for adjustment of brightness and contrast.

RESULTS

Gyration and Cytoarchitecture of the Perinatal Insula

The insula of perinatal (32–40 GW) brains displayed an adult-like gyration pattern (**Figures 1B,C**), although the case in **Figures 1B,C**, 40 GW) presented only two short anterior gyri with one accessory anterior gyrus, and two long posterior gyri on each side. Another 40 GW brain and the 32 GW case showed the more common configuration of three short anterior and two long posterior gyri. As in the adult (Mesulam and Mufson, 1985), three main modalities of insular cytoarchitecture were recognizable at term, following a gradient from rostro-ventral to caudo-dorsal, independently of the sulcal pattern: The antero-basal sector of the insula near the limen (Field I*C* of Von Economo and Koskinas, 1925; **Figure 1A**) was agranular, showing a prominent layer V but absence of the inner granular layer IV (**Figure 1D**). At levels rostral to the limen, the insular cortex was continuous with the POC via a small transition area where the neurons lacked any recognizable lamination, with superficial medium-sized pyramidal cells and deeper smaller pyramidal and non-pyramidal cells distributed apparently at random. The anterior gyri had a variable prominence of layer IV and were thus considered dysgranular (**Figure 1E**), whereas in the posterior and dorsal insula layer IV was wider, more cell-dense, and radially organized (**Figure 1F**), features characteristic of a granular isocortex. Nonetheless, the width of layer IV was variable, even along the same gyrus. The local heterogeneities of layer IV may reflect the immaturity of the perinatal brain, but may also be due to laminar distortions when a gyrus changes orientation or undergoes additional folding.

At 32 GW, the insula showed the same basic folding and lamination pattern as at 40 GW, even though neurons appeared slightly less mature, with a higher cell density than at term. Transitional (**Figure 1G**), dysgranular (**Figure 1H**) and granular (**Figure 1I**) regions were clearly established. At both 32 and 40 GW, the outer granular layer II (**Figures 1E,F**) was more cell-dense than in the adult, due to the inside-out migration gradient of the cortex, according to which layer II is the last layer to develop (Angevine and Sidman, 1961; Rakic, 1974).

We conclude that the insula acquires an adult-like gyration and architectonic pattern during the last trimester of gestation. We did not detect the VEN (Allman et al., 2011), possibly because our material did not include the fronto-insular transition area where they are more numerous, and because they mature at later stages (Allman et al., 2005).

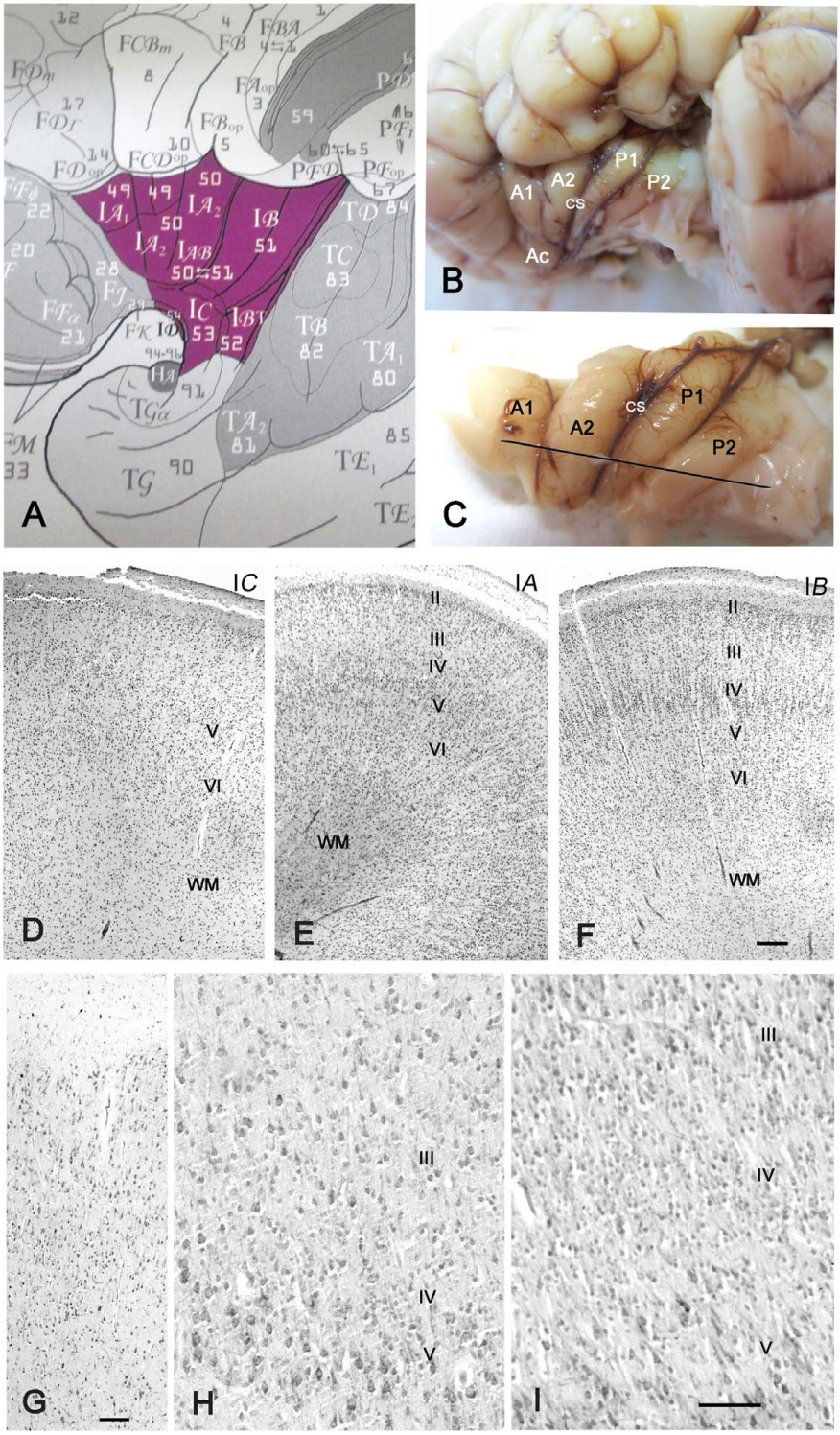

FIGURE 1 | Cytoarchitecture of the perinatal human insula. **(A)** Classification of the insular areas of Von Economo and Koskinas (1925). *IA*, anterior agranular, *IB*: posterior granular, *IAB* intermediate dysgranular areas. **(B)** Left insular lobe of a newborn infant (40 GW) after removing the anterior temporal pole. A1, A2, anterior short gyri; Ac: accessory short gyrus; P1, P2, posterior long gyri; CS: central sulcus of the insula. **(C)** Dissection of the insula in **B**. The line indicates the plane of section. **(D–F)** Nissl-stained sections from the brain in **B**,**C**. **(D)** *IC*, the agranular transition area between the POC and the isocortical insula; **(E)** Area *IA*, representing the dysgranular area, with an irregular layer IV; **(F)** area *IB*, the granular posterior insula. Notice that layer II is still cell-dense and not yet fully mature. **(G–I)** 32 GW. **(G)** Transition between POC and isocortical insula showing ill-defined layering. **(H)** A poorly developed layer IV in the dysgranular insula; **(I)** A wide, cell-rich layer IV in the granular insula. Bars: in **F**, for **D–F**: 160 μm; in **G**: 50 μm; in **I**, for **H** and **I**: 55 μm.

Early Stages of Insular Development Prior to the Appearance of the Sylvian Fissure

The Lateral Cortical Stream

Since classical studies (Streeter, 1912; Kodam, 1926) proposed that the insula is the first cortical area to appear, we examined the early stages of telencephalic development from 5.5 GW onward. While in the later stages the insular lobe is defined by the presence of the Sylvian fissure, in the embryonic and early fetal stages the future insular territory was more difficult to identify, recognizable only as the transition area between the POC and the prospective isocortex, and by its position external to the developing putamen.

A key structure at this stage is the lateral cortical stream (LCS) (Bayer and Altman, 1991), a migration pathway that originates at the PSB and leads toward the olfactory forebrain, running in a position lateral to the putamen. The LCS appeared as early as CS 16/17 (5.5 GW) (**Figures 2A,B**) at the PSB, situated slightly medial to the cortico-striatal sulcus, and represented the first Tbr1+ migration stream of the developing pallium, while the cortical anlage was still in the preplate stage, and the ganglionic eminences (GE) visible only as small elevations in the lateral ventricle. The pallial LCS migration was more massive than the subpallial one, which appeared as a small patch of calretinin+ cells in the subventricular zone (SVZ) of the lateral ganglionic eminence (LGE). Both components of the LCS were segregated and not overlapping. In this initial stage, the Tbr1+ stream extended ventrally toward the pial surface of the prospective insula and POC, whereas the calretinin+ stream had not yet left the SVZ of the LGE.

The further development of the LCS is illustrated in **Figures 2C,D** and **3A–C**. At CS 18/19 (6.5 GW), the cells forming the LCS had increased in number, concurrent with a generalized growth of the SVZ of GE and cortex anlage. The calretinin+ stream now extended ventrally and formed cell aggregates in the developing POC/endopiriform complex (**Figure 3C**). The more lateral Tbr1+ stream reached the same ventral level, but occupied the entire SVZ and ventral cortical territories (in early human corticogenesis, Tbr1 marks both SVZ progenitor cells and postmitotic migratory neurons). Concurrently, the first representatives of the calretinin+ pioneer plate (Meyer et al., 2000) had appeared in the lateral cortex (**Figure 2C**), and became more evident at CS 20 (7 GW) (**Figure 3C**). In most embryonic brains from this period, a conspicuous hole may mark the site of the future internal capsule (IC) (**Figures 3A–C**) (see also plates 190 A and B in Bayer and Altman, 2007). Mitotic figures were numerous in the striatal anlage, but absent from the LCS, which was thus a non-proliferating structure (**Figure 3A**). In the embryonic stages, the RGF [see below section Migration from the PSB to the Insula along the Radial Glia Fascicle (RGF)] had not yet formed; after its appearance around 11 GW neurons migrating into the insula used the RGF as a migration substrate, and the LCS might thus be considered as its forerunner.

At 8–10 GW, a highly complex neuronal configuration characterized the insula and adjacent POC/endopiriform area,

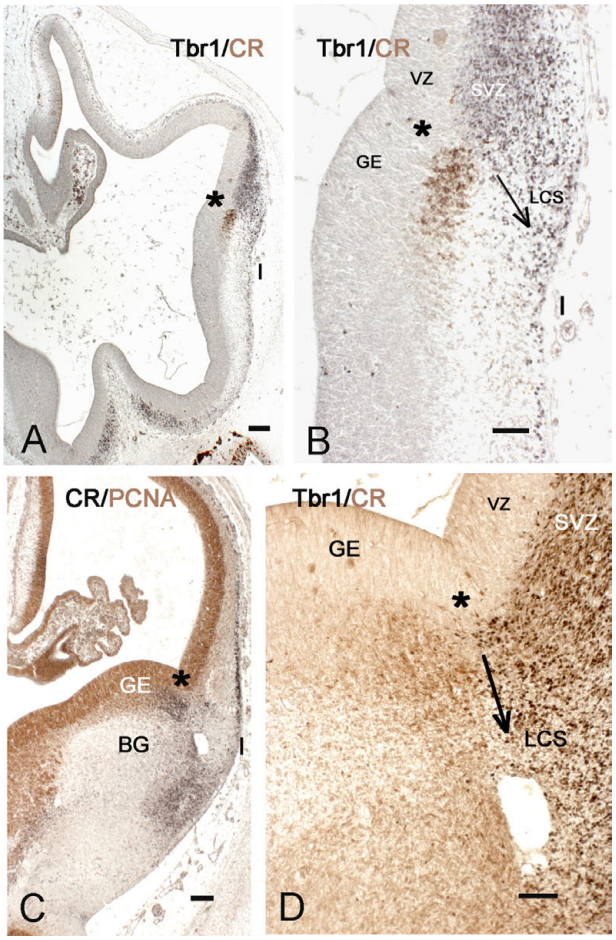

FIGURE 2 | The early appearance of the insula and the lateral cortical stream (LCS). **(A,B)** Telencephalon of a 5.5 GW embryo, double-stained with Tbr1 (black) and calretinin (brown). Tbr1+ pallial cells descend from the PSB (asterisk) to the future POC and insula (I), representing the pallial part of the LCS. The cortex is still in the early preplate stage. Calretinin+ cells in the subventricular zone (SVZ) of the lateral ganglionic eminence (LGE) form the subpallial component of the LCS. **(C,D)** PSB and LCS at Carnegie stage (CS) 19, double-stained for PCNA (brown) and calretinin (black) in **C**, and for Tbr1 (black) and calretinin (brown) in **D**. The calretinin+ cells at the PSB and in the POC are mainly post-mitotic; both the pallial, Tbr1+, and the subpallial, calretinin+ components of the LCS have largely increased in size, along with the growth of the SVZ at the PSB. The arrows in **B**,**D** indicate the proposed direction of the LCS. BG, basal ganglia; GE, ganglionic eminences. Bars: in **A**,**C**: 100 μm; in **B**,**D**: 50 μm.

determined following Bayer and Altman (2007). In the POC, aggregates of Tbr1+ cells were intermixed with CR+/Tbr1− neurons forming complex nuclear structures (**Figures 3D–F**). We considered the loosening of the compact Tbr1+ lateral cortical plate (CP), together with a narrowing of the marginal zone compared to the POC, as landmarks defining the territory of the insular cortex. Calretinin marked neurons with a pyramidal shape, which corresponded to the deep pioneer cells representing the presubplate (Meyer et al., 2000), in what we propose as the ventralmost extension of the prospective insula (**Figure 3F**). They were separated from the

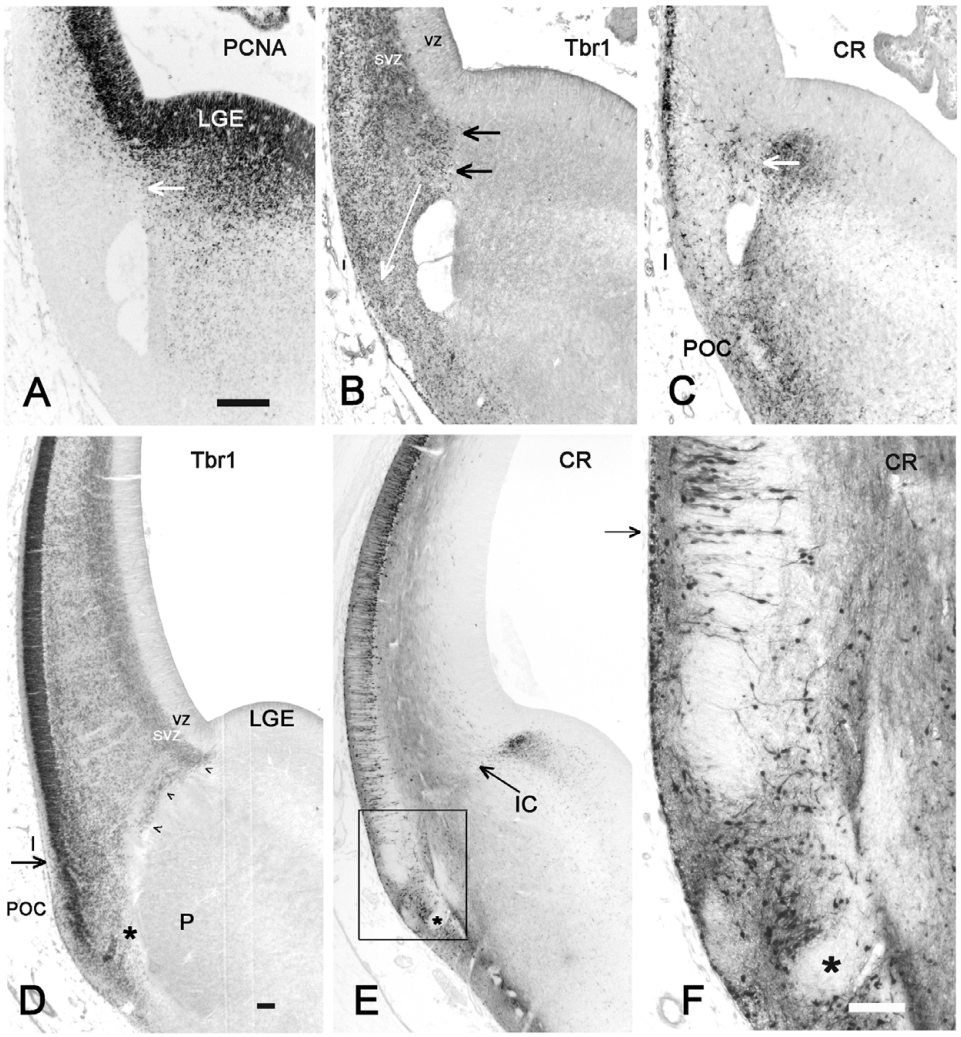

FIGURE 3 | Insula and POC derive from the PSB. **(A–C)**: 7 GW, **(D–F)**: 9 GW. **(A)** PCNA shows dividing cells in the new appeared SVZ of the lateral cortex and in the putamen, while LCS and Insula do not contain mitotic cells. The white arrow points to the PSB. The hole in **A,C,D** is probably not an artifact since it is present in almost all brains of this age group; it may represent an early blood vessel that precedes the appearance of the IC. **(B)** Tbr1, and **(C)** calretinin are expressed on the pallial and subpallial sides, respectively, of the PSB, indicated by horizontal arrows. The white arrow in **B** shows the proposed direction of the LCS into Insula and POC. The calretinin+ cells in the lateral cortex represent the first pioneer cells of the advanced preplate and are probably unrelated to the PSB. **(D)** Tbr1, **(E)** calretinin and **F** (the inset in **E**) show the further differentiation of the PSB derivatives, and the complex cell arrangement at the POC-insula transition (arrows in **D** and **F**). We suggest that the less compact arrangement of the Tbr1+ cortical plate (CP), compared to more dorsal levels, is the anlage of the rostro-ventral insula **E** and **F** show the intermixture of pallial, Tbr1+ cells and non-pallial, Tbr1-negative cells (asterisks points to the same Tbr1+, calretinin-negative in **D–F**), in the POC/endopiriform complex. In **F**, pyramidal-like deep pioneer cells may indicate the ventral boundary of the insula. Bars: **A**, for **A–C**: 100 μm; **D,E**: 100 μm; **F**: 300 μm.

superficial pioneer neurons by calretinin-negative CP neurons. Regarding the distribution of CR+ deep pioneer neurons, the transition between insula and POC appeared as a gradual one. Importantly, at this early age of 8 GW, the anteroventral insula had already a laminated organization, indicating that its deep layers were already formed as derivatives of the PSB via the LCS.

The Developing Internal Capsule Crosses the PSB and Delimits the Rostro-Caudal Extent of the Insula

The IC is an important landmark in the early fetal brain; at 8 GW it was recognizable at the PSB at the level of the prospective frontal cortex (FC) as a CR-negative fiber bundle (**Figure 3E**), but not at intermediate and caudal levels, where the IC had not yet approached the PSB. At 8 GW, the caudal PSB, prior to the crossing of the IC, consisted of a proliferating SVZ positive for PCNA, Tbr1, and Tbr2 (**Figures 4A–C**). Around 9/10 GW, the IC also crossed a more caudal, midinsular level of the PSB (**Figure 4D**), while its posterior limb had just entered the GE but still not reached the PSB near the parieto-temporal (PT) junction (**Figure 4E**). Concurrently, the lateral ventricle adopted a C-shaped curvature, growing in both a rostral (frontal lobe) and ventral (temporal lobe) direction. As a consequence of the ventricular curvature, in coronal sections

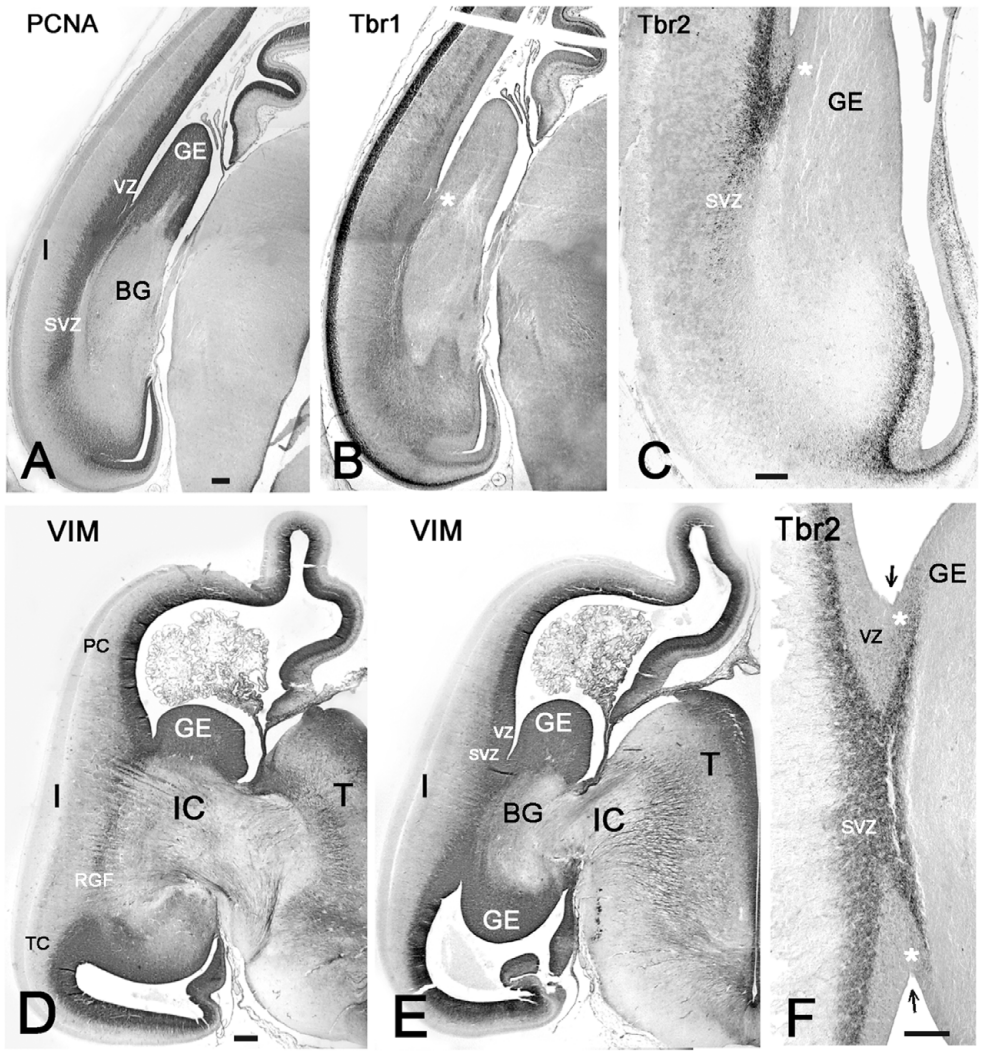

FIGURE 4 | The PSB and the growth of the internal capsule (IC). **(A–C)** Coronal sections through a caudal telencephalic level at 9 GW, and in **D–F**, through two different levels at 10 GW, show the growing curvature of the lateral ventricle and the opening of the temporal horn at 10 GW. The IC enters the cortex crossing the PSB following a rostral to caudal sequence. While the IC has crossed the PSB at rostral levels (**Figure 3E**), it has not yet appeared at caudal levels, where PCNA **(A)** and Tbr2 **(C)** show mitotic cells at the PSB (indicated by white asterisks), whereas Tbr1 marks the pallial territory **(B)**. **(D)** At 10 GW, the SVZ of the fronto-parietal PSB and the temporal PSB are connected by a vimentin+ radial glia fascicle (RGF), which is traversed by the IC and delimits the insula. At this time point, the IC has not yet reached the caudal PSB **(E)**, where the SVZ is particularly wide. In **F** (same level as **E**), the PSB extends medial to the cortico-striatal sulcus (arrows). GE, ganglionic eminence; I, insula; IC, internal capsule; PC, parietal cortex; SVZ, subventricular zone; T, thalamus; TC, temporal cortex; VZ, ventricular zone. Bars: **A–F**: 100 μm.

the ventral half of the telencephalon appeared almost like a mirror image of the dorsal half (**Figures 4D–F**). The PSB followed the curvature of the lateral ventricle; its posterior limit with the caudal part of the GE was recognizable by its SVZ, which was positive for Tbr2 and vimentin (**Figures 4E,F**). At 10 GW, the SVZ of the caudal PSB prior to the crossing of the IC was particularly broad, (**Figure 4E**) and was even wider than the SVZ of its neighboring parietal and temporal areas.

The sylvian fossa appeared at 11–12 GW, before the formation of the circular sulcus and the opercula. The insula was medially delimited by putamen and external capsule (EC), and separated from the proliferating ventricular zone (VZ) and SVZ by the growing basal ganglia (BG) and the IC, so that migrating excitatory neurons could reach the insula only indirectly via radial glia fibers crossing the IC and circumventing the putamen. To identify the insular cortex before the formation of a distinctive Sylvian fissure, we had to rely on its topographical relationships with deep structures and fiber tracts, which remain constant during development and persist into adulthood. Rostrally, the insula began at the intersection of EC and IC at the level of the PF cortex (**Figure 5A**), while caudally it was delimited by the posterior limb of the IC and the PT junction (**Figure 5C**). At this time point, the insular cortex

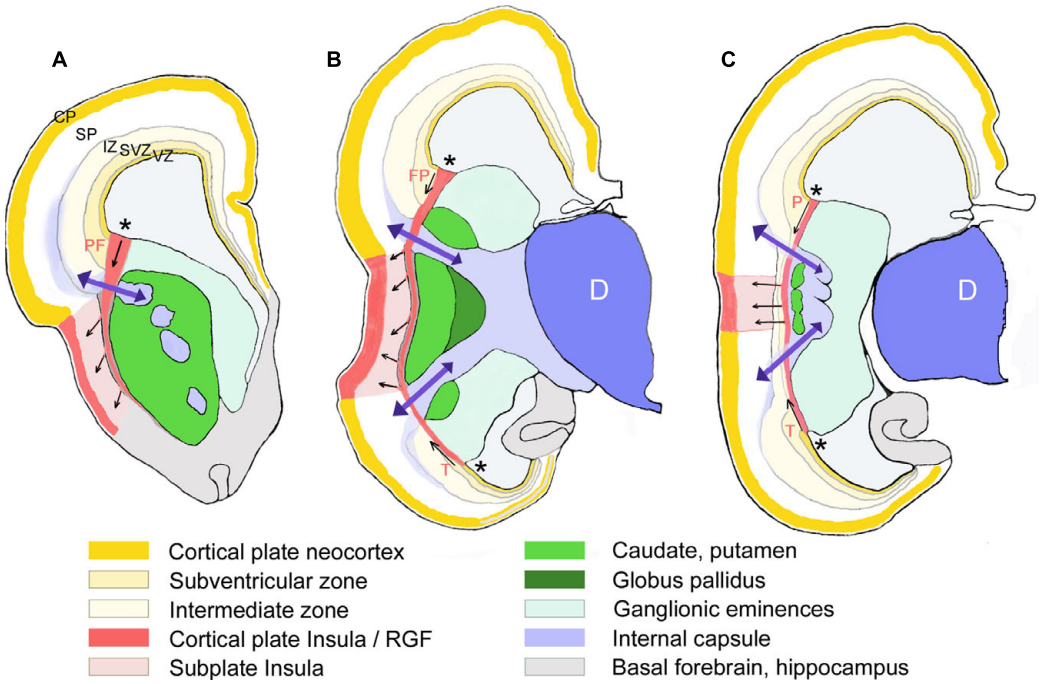

FIGURE 5 | Schematic representation of the RGF leading from the PSB into the insula. Drawn from Nissl-stained sections of a 16 GW-old fetus at three different rostral to caudal levels **(A–C)**. The proposed direction of the prefrontal (PF), frontoparietal (FP), (parietal in **C**), and temporal (T) components of the RGF from the PSB (asterisks) is indicated by arrows. Only those structures mentioned in the text are represented. D, diencephalon; SP, cortical subplate (in white).

had no distinctive features that would allow a cytoarchitectonic definition.

Migration from the PSB to the Insula along the Radial Glia Fascicle (RGF)

We tried to identify the possible proliferative sources and their migratory routes into the insula through analysis of radial glia architecture. At 11–12 GW, basal or outer radial glia (oRG) appeared in the SVZ at the PSB, which now occupied a PCNA+ and Tbr2+ wedge-shaped area at the intersection of IC and EC. This SVZ was wider than the SVZ in the adjacent cortex (**Figures 6A,B**). Radial glia processes originating in the SVZ at the PSB were positive for vimentin and nestin, and assembled in a distinct RGF coursing along the prospective EC. Following the curvature of the PSB, the RGF originating from its SVZ formed a continuous band of radial glia fibers. According to their origin, four subdivisions of the RGF could be established, which remained constant during the first half of gestation: PF, fronto-parietal (FP), PT, and T, temporal radial glia fibers, which took different directions to reach their destination in the insula. Descending RGF component FP merged with ascending RGF component T (**Figures 5B**, **6D,E**), whereas component PF descended without an ascending counterpart (**Figure 5A**). Component PT at the caudal end of the BG (putamen islands interspersed between the posterior limb of the IC) (**Figure 5C**) coursed straight to the caudal insula, where also an intermediate zone was recognizable. Along its course, the RGF fanned out and entered the insula at different dorso-ventral levels, maintaining an initially parallel orientation up to the point where descending and ascending components met (**Figure 5B**).

At 13/14 GW, migrating neurons, still positive for Tbr1, followed the direction of the RGF into the insula, populating its subplate and CP, clearly delimiting cortical and subcortical territories (**Figures 6C,G**). After this age, migrating neurons were Tbr1-negative. The wedge-shaped SVZ, marked with vimentin (**Figures 6D–F**), nestin, PCNA (**Figures 6A,D**), and Tbr2 (**Figures 6B,F**), progressively increased in width, partially entering the IC, and expanded in parallel with the proliferation of the outer SVZ (oSVZ) in the adjacent opercula. We reconstructed the course and orientation of the RGF components into the insula in a horizontal section at 21 GW (**Figure 7**). As expected, the RGF arose from both the dorsal and ventral oSVZ at the PSB, although the dorsal RGF predominated. The orientation of the fibers leaving the fascicle and entering the insular subplate is shown for different levels (**Figure 7**, from 1–4). At levels 1 and 2, fibers emerging from the RGF component FP took a descending course, while at level 3 (component T) they ascended. Level 4 shows radial glia fibers in the intermediate zone of the temporal operculum, which seemed to bend and course toward subplate and CP of the superior TC rather than into the insula. The RGF was compressed in the EC and contained also vimentin+ cells. However, PCNA+ mitoses were rare, and we did not observe Tbr2+ progenitor cells in this location; this indicates that the territory of the RGF was not an extension of the proliferative oSVZ.

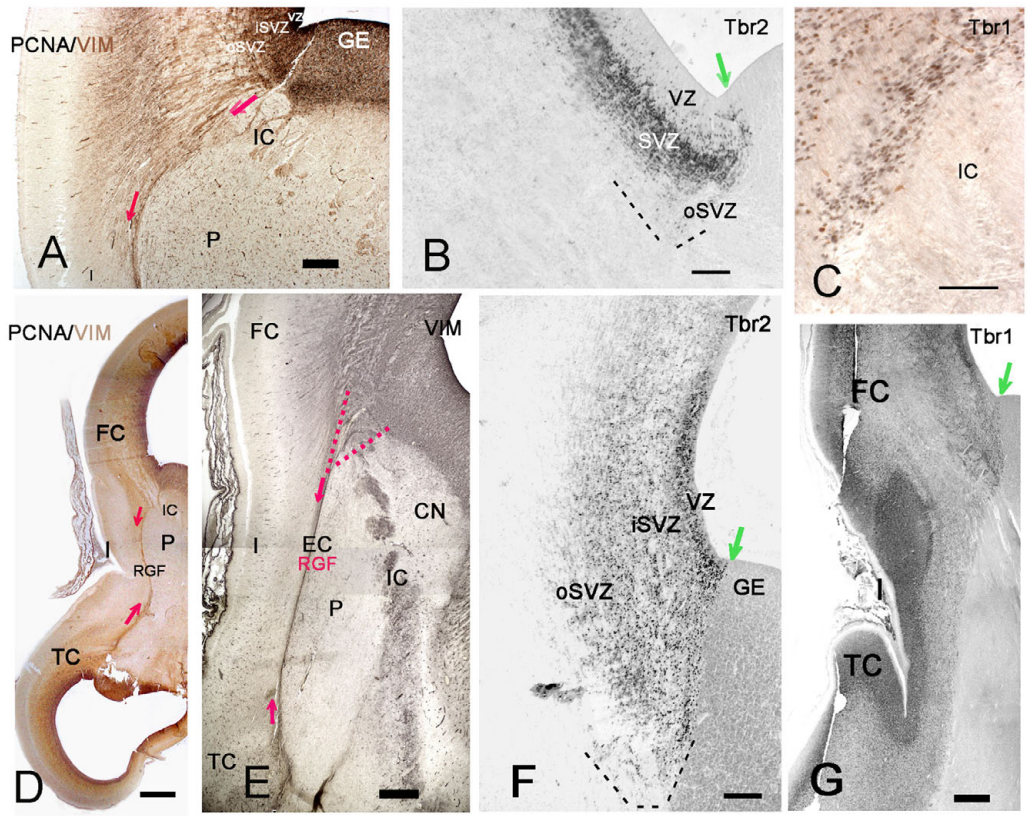

FIGURE 6 | The RGF on its route to the insula. **(A,D,E)** Development of the RGF, which is co-extensive with the external capsule (EC). **(A)** At 11GW, the RGF arises from the PSB, crosses the IC and courses lateral to the putamen (P) (red arrows). PCNA (black) is expressed in the ventricular zone (VZ) and SVZ, but not in the RGF (brown). **(B)** At 11 GW, the Tbr2+ SVZ at the PSB (green arrow) extends into the IC. The dashed line indicates the outer SVZ (oSVZ) at the PSB. **(C)** Tbr1+ neurons (black) course along the RGF into the insula. Calretinin+ neurons (yellow) do not form part of this migration. **(D)** At 12 GW, the sylvian fossa indicates the position of the insula. Two-color staining (PCNA in black, vimentin in brown) shows that the RGF is not a proliferating zone. **(E)** At 15 GW, the origin of the RGF can be traced back to the intersection of IC and EC (red dotted lines), while the oSVZ has increased in width. **(F)** At 15 GW, an inner (i) and outer (o) SVZ is particularly wide at the PSB (green arrow). **G**: 14 GW, Tbr1. At this age, of incipient opercularization, Tbr1 is still expressed by cells in all cortical compartments, and clearly visualizes the separation of pallial and subpallial regions. FC, frontal cortex, TC, temporal cortex. Bars: In **A**: 270 μm; in **B**: 160 μm; in **C**: 50 μm; in **D**: 700 μm; in **E**: 350 μm; in **F**: 150 μm; in **G**: 450 μm.

Importantly, the PF PSB (RGF component PF) extended farther rostrally than the temporal one (RGF component T) (**Figure 5A**); in consequence, the most anterior region of the insula received radial glia fibers only from the PF PSB. The middle and posterior insular regions, in turn, received radial fiber-mediated migrations from the dorsal (FP) and ventral (temporal) PSB (**Figure 5B**). Even more caudally, the posterior end of the insula was close to the PT junction, and was also populated by large numbers of oRG cells and processes. At this level, an intermediate zone was recognizable as a fiber-rich layer continuous with the intermediate zone of the adjacent cortices (**Figure 5C**).

The distinct subregions of the insular lobe were thus connected more or less abundantly via the RGF with the proliferative SVZ along the PSB. The differential availability of progenitor cells may be the basis for the differential layering of the subareas of the insular lobe. It is remarkable that the insular lobe, despite its rather distant relationship with the proliferating oSVZ, and the limited progenitor pool at the PSB, is able to fold once migration is finished (**Figure 1B**).

Fronto-Parietal and Temporal PSB at Midgestation

Vimentin, a marker of radial glia, does not define the PSB. To determine the origin of the RGF at the PSB at midgestation (21GW), we compared adjacent sections stained for vimentin and Tbr2 (**Figure 8**). When reconstructing the photomosaics for both markers from high magnification microphotographs, we noticed that the periventricular layers, inner and outer SVZ, were quite different in the various lobes. Similarly, the fiber tracts also differed, and widely varied in thickness. Particularly in the frontal and parietal lobes, the intermediate zone (future white matter) was at this time point much wider than in the temporal lobe. In parallel, Tbr2+ and PCNA+ cells extended much farther into the IZ in FP areas than in the TC. In the TC, the anterior commissure seemed to represent an obstacle

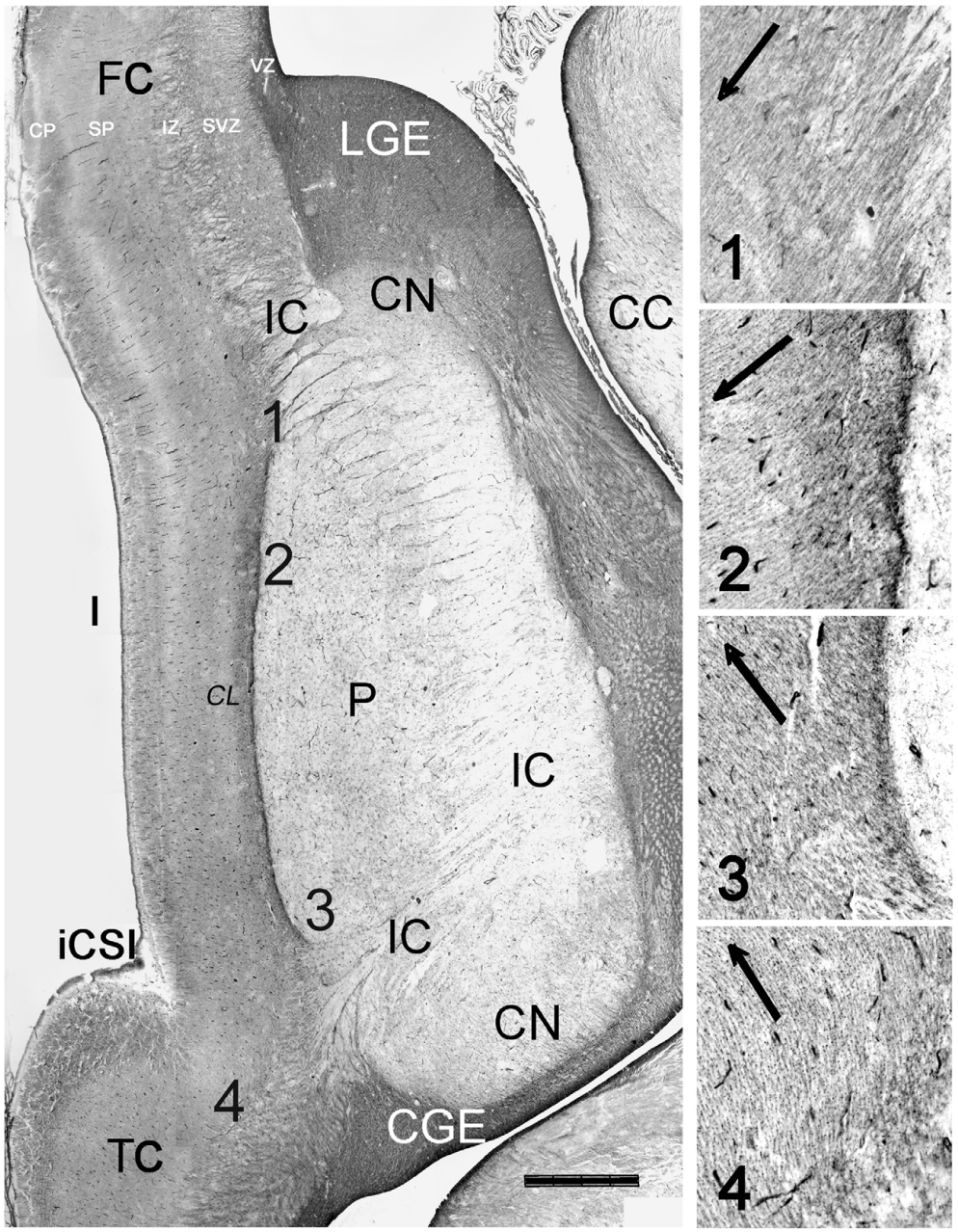

FIGURE 7 | Orientation of radial glia fibers in the RGF. Reconstruction of a horizontal section at 21 GW, immunostained for vimentin. The numbers 1–4 indicate the levels represented at higher magnification, showing the dominant orientation of radial glia fibers fanning out from the RGF. Descending radial glia fibers from the fronto-parietal PSB dominate over ascending fibers from the temporal PSB. In level 4, near the temporal operculum, radial glia fibers appear to lead into the supratemporal plane rather than into the insula. The claustrum (CL) appears as a pale zone lateral to the RGF/EC. CC, corpus callosum, CGE, caudal ganglionic eminence; CN, caudate nucleus; FC, frontal cortex; CSI, circular sulcus of the insula; LGE, lateral ganglionic eminence, TC, temporal cortex. Bar: 1400 μm.

for the RGF, since it was traversed neither by the RGF nor did it contain Tbr2+ cells. We limited our study to the PSB and the adjacent regions, where the Tbr2+ progenitor cells became less and less numerous toward the IC (**Figures 8B,D**), and were basically absent at the level of the insula. The RGF was more difficult to discern than in earlier stages, but still very thick, prominent radial glia fibers emerged at the PSB and crossed the inner fibrous layer and adjacent IC (**Figures 8A,C**).

While at early fetal stages the PSB extended medially beyond the cortico-striatal sulcus, at midgestation it had shifted laterally in the temporal lobe, but not in the frontal lobe. Future studies will show how the PSB in different lobes behaves toward the end of cortical neurogenesis.

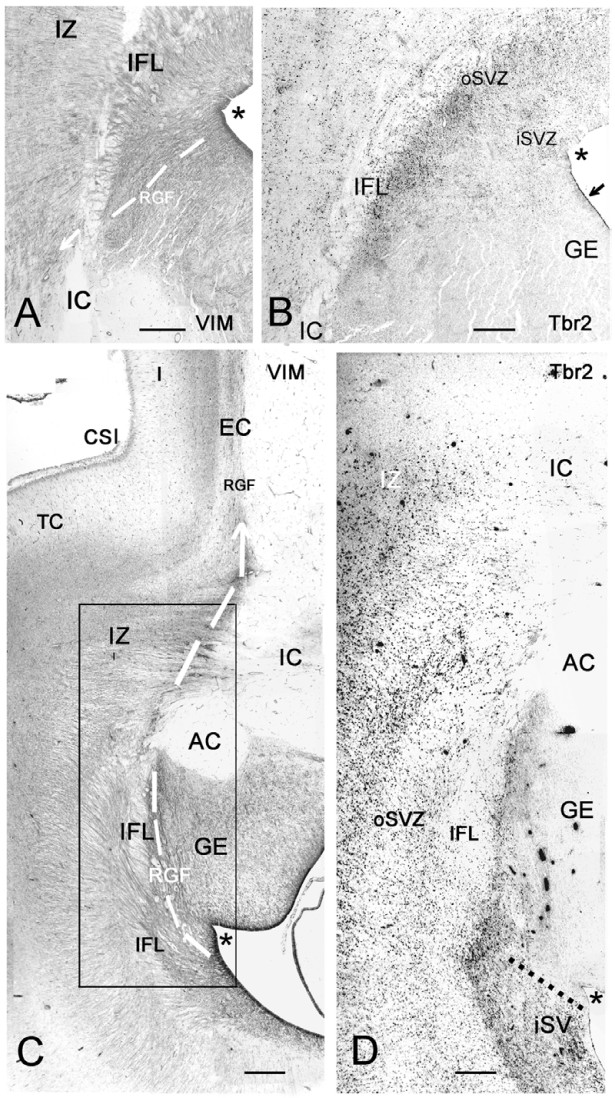

FIGURE 8 | Photographic reconstructions of the PSB in coronal sections at 21 GW. Vimentin **(A,C)** shows the distribution and orientation of radial glia cells and fibers in the frontal **(A)** and temporal **(C)** periventricular zones and the RGF route into the Insula (white arrows). Tbr2 **(B,D)** marks the PSB (arrow in **B**), which at this age is less well defined than at earlier fetal stages, and in the temporal lobe does not extend medially beyond the striato-cortical sulcus (asterisks in all panels; in **D**, the PSB is indicated by a dotted line). Tbr2+ and vimentin+ progenitor cells cross the periventricular fiber layers (Inner fibrous layer, IFL) and extend far into the oSVZ and even the intermediate zone (IZ). Note the complexity of fiber tracts in the temporal lobe, due to the presence of the anterior commissure (AC). The large black dots in the inner (i) SVZ in **D** are stained blood vessels. Bars: in **A**: 240 μm, in **B**: 140 μm, in **C**: 250 μm, in **D**: 190 μm.

Prenatal Development of Lamination in the Insula

During the first half of gestation, the insular cortex had a uniform structure, with a CP formed by densely aggregated immature neurons. On the whole, the insular CP was narrower than that of the adjacent opercular areas. The first clear appearance of layering was at midgestation (20/21 GW) (**Figures 9A–F**), when MAP2 (**Figure 9D**) and Tbr1 (**Figures 9C,F**) immunostaining (in maturing human cortical neurons, Tbr1 is cytoplasmic) indicated the presence of a distinct layer V, or inner pyramidal layer, which was particular prominent in the anterior agranular insula (**Figure 9C**). However, compared with the Betz cells in the adjacent primary motor cortex (**Figure 9E**), the dimensions and proportions of layer V pyramids in the anterior insula were rather reduced, as well as their positivity for MAP2. The deep layer VI and subplate were also Tbr1+, although in this case staining was nuclear (**Figure 9F**). The subplate was directly continuous with the subplate of the adjacent opercular cortices, but considerably reduced in width. Remarkably, the rostral and intermediate insula lacked an intermediate zone, characterized by horizontal fibers traversed by clusters of migrating neurons (Bystron et al., 2008; **Figures 6E,G**, **8C**). In the posterior insula, the intermediate zone was present, traversed by calretinin+ fibers from the posterior limb of the IC (not shown).

Also at midgestation, we observed a difference in the distribution of the Reelin+ axonal plexus of the Cajal–Retzius cells in the lower marginal zone (Meyer and González-Gómez, 2017): The plexus, characteristic of isocortex and important for laminar arrangement of neurons, was absent in the periallocortical transition area (**Figure 9B**), but appeared in the more dorsal, isocortical insula. Cajal–Retzius cells were, however, abundant in the upper marginal zone all over the insula.

In the ages examined after midgestation, 24 and 25 GW, the overall immaturity of the insular CP persisted, and there was no evidence for a future differentiation into an agranular, dysgranular and granular cortex. Since at 32 GW the insula presented an adult-like morphology, cytoarchitectonic maturation would take place during the interval between 25 and 32 GW. Similarly, in our coronal sections at 24 and 25 GW, we were unable to distinguish incipient insular sulcation and gyration.

DISCUSSION

The insula derives from the PSB of all cortical areas adjacent to the Sylvian fissure: PF, frontal, parietal, and temporal, and thus constitutes a central node of the human cortex. Radial migrations from the PSB to the insula have to cross the growing IC, and circumvent the BG, and reach the insula via a RGF that course in the EC. According to its origins, the RGF has four main components, parts of which merge, and may determine the granular, dysgranular and granular character of the insular sectors.

The Anatomy of the Developing Insula

The human insular lobe is shaped by the curvature of the lateral ventricle, and lies embedded between PF, frontal, and parietal areas dorsally, and temporal areas ventrally, from which it is separated by the Sylvian fissure and the circular sulcus. Its position external to putamen and IC prevents direct contacts with the periventricular proliferative zones, and radial migrations to the insula have to take indirect, unusual routes to reach

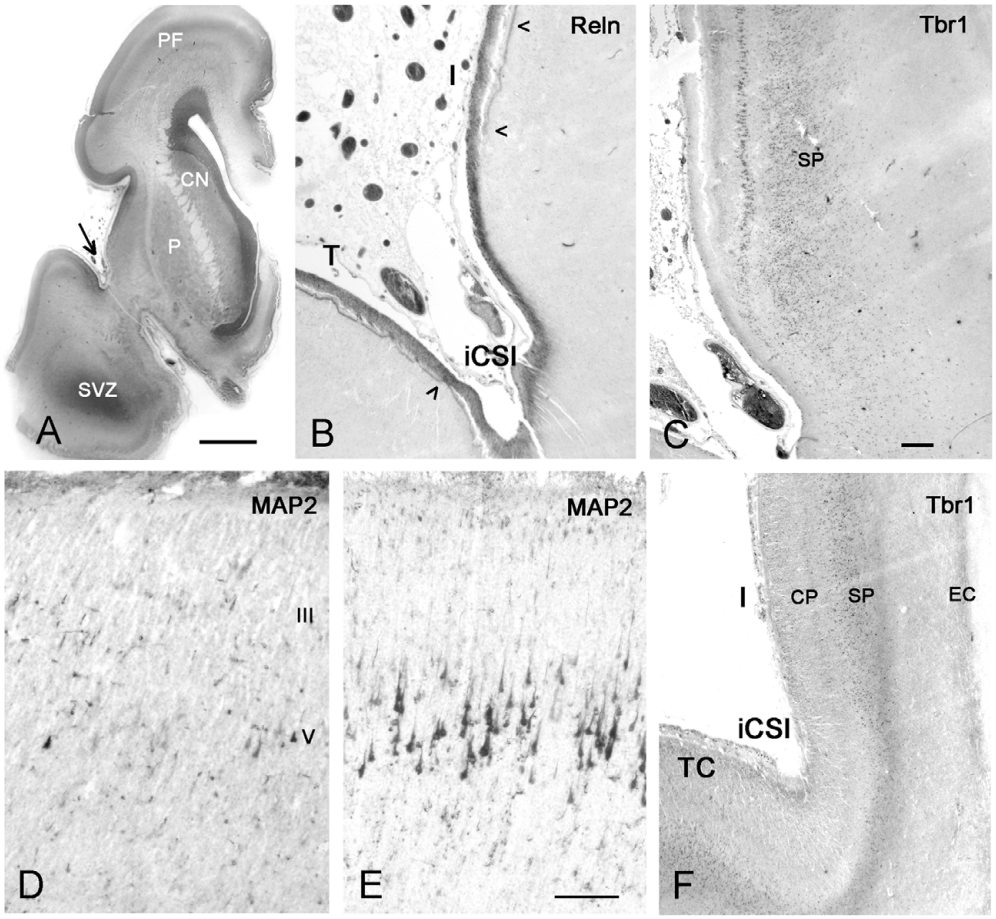

FIGURE 9 | First appearance of lamination in the insula at midgestation (21GW). **(A)** The anatomy of a Nissl-stained hemisphere near the limen insulae. The arrow points to the inferior circular sulcus (iCSI) between the rostro-ventral insula and the temporal lobe. This region, shown in **B** (Reelin) and **C** (Tbr1), represents the transition between the ventral periallocortical insula and the dorsal isocortical insula. **(B)** The periallocortical insula lacks the Reelin+ plexus of the Cajal–Retzius cells in the lower marginal zone (arrowheads), characteristic of isocortex, although Cajal–Retzius cells are present all over the outer marginal zone. **(C)** A prominent layer V shows cytoplasmic Tbr1 staining, while the subplate has nuclear staining. At a more caudal level, MAP2 reveals a few pyramidal cells in layers V and III in the anterior insula **(D)**, which are much smaller and less numerous compared to the Betz cells in layer V of the primary motor cortex **(E)**. In **F**, Tbr1 marks the subplate (SP), which is continuous with the subplate of the adjacent temporal cortex (TC), although narrower and more compressed than the latter. CN, caudate nucleus; P, putamen; SVZ, SVZ of the temporal horn which opens at more caudal levels. Bars: in **A**: 400 μm; in **C**, for **B,C,F**: 160 μm; in **D**, for **D** and **E**: 75 μm.

and populate the distant lobe. Using radial glia architectonics and the pallial markers Tbr1 and Tbr2 (Hevner et al., 2003; Englund et al., 2005), we identified the PSB as the origin of the neurons destined to form the insular cortex. During early fetal development, the PSB follows the curvature of the ventricle, and thus extends from PF to temporal levels. We suggest that local differences of the PSB along its extent through the various lobes contribute to the multifaceted lamination pattern of the insular cortex. The different timing of the entrance of the IC into the cortex traversing the PSB (Krsnik et al., 2017), with rostral parts preceding more caudal parts, is an additional influencing factor, which will require further studies.

The finding that the architecture of the insula is contingent on size and orientation of the lateral ventricle and the curved shape of the PSB, explains the differences in insular structure reported in a variety of mammals. Even though comparative studies tend to emphasize common principles of brain structure in order to establish homologies (Cat: Clascá et al., 1997; monkey: Gallay et al., 2012; Evrard et al., 2014), anatomical studies in a wide variety of mammalian species usually not studied in the laboratory, including the dolphin (Jacobs et al., 1984; Casanova et al., 2010), demonstrated an extremely variable shape, general organization, lamination and cellular specialization of the insula, to the point that there is no recognizable common model of organization of the mammalian insular cortex (Butti and Hof, 2010). The relationship between insula and claustrum is similarly controversial. We neglected the claustrum, because we did not detect migratory mechanisms similar to those of the insula (Mufson and Mesulam, 1982; Nieuwenhuys, 2012). Developmental gene expression studies postulated that insula and insular claustrum are formed from the lateral pallium (Watson and Puelles, 2017). It may be argued that the mouse is not the

best model for the human cortex, taking into account recent studies suggesting that the ancestor of mammals was probably a gyrencephalic animal (O'Leary et al., 2013; Lewitus et al., 2014). The magnitude of species differences suggests that the development of the insula is best understood when examined together with the anatomical landmarks that define this lobule in a given species.

In any case, the human insula should be considered in the context of its complex cognitive, social and emotional functions, including empathy, altruistic behavior, self-awareness, interoception, mindfulness, and consciousness (Craig, 2009; Fan et al., 2011; Fischer et al., 2016; Tusche et al., 2016; Laneri et al., 2017), or, as expressed by Craig (2010), the "sentient-self." In keeping with these human-specific functions, a volumetric comparison of the insula of human and non-human primates revealed that in terms of absolute volumes the left and right agranular insula are among the most enlarged cortical areas relative to the chimpanzee (Bauernfeind et al., 2013). The degree of "granularity" of a cytoarchitectonic area is thus unrelated to its involvement in networks engaged in human cognitive functions such as those attributed to the anterior insula.

The PSB Is the Origin of the Insula

The PSB has been extensively studied in terms of comparative anatomy, establishing homologies with the anterior dorsal ventricular ridge (ADVR) of sauropsids, and the fate of the cells in the LCS in sauropsids and mammals (Molnár and Butler, 2002), as well as in terms of developmental gene expression. Gene expression studies in the PSB of mice showed that the PSB is the main source of POC, claustrum, olfactory bulb, olfactory tubercle, and amygdala, and that the cells destined to these centers migrate ventrally via the LCS (Medina et al., 2004; Carney et al., 2006; Cocas et al., 2011). The insula as a PSB derivative has received less attention, probably because it is so unconspicuous in the rodent. The PSB is certainly an important landmark in the rodent brain, where it represents the boundary between pallium and subpallium, and is implicated in dorsoventral patterning of the telencephalon (Stoykova et al., 2000; Yun et al., 2001), but to what extent is it relevant for the human brain? Molnár and Butler (2002) recognized the evolutionary potential of the PSB, and also its function as an initial barrier zone for crossing cortico-thalamic and thalamo-cortical axons in the IC. However, the rodent studies did not take into account the enormous regression of olfactory structures in the microsmatic human, which rests importance from this aspect of the LCS. Instead, we show that the early descending migrations from the human PSB are mostly destined to the insula, although they also contribute Tbr1+ and calretinin+ cells to the POC. Furthermore, the rostro-caudal extension of the PSB is hugely increased due to the size increase of both, cortical progenitor zones and GE. Another important factor is the IC, which crosses the PSB (Molnár et al., 2012), and thus represents an additional obstacle for radial migration from the PSB to the insula. We suggest that the prominence of the PSB in human is an important factor for the development of the insular lobe. Furthermore, in the human brain, the insula does not represent the most lateral part of the cortex as in the rodent, but rather emerges as the core cortical region that makes possible the mirror arrangement of dorsal (FP) and ventral (temporal) cortical lobes. The central anatomical position of the insula in the human telencephalon is also paralleled by a similar central functional relevance, since especially the dorsal anterior insula can be considered a critical hub in connectivity networks of the human brain (Uddin et al., 2014).

Radial Glia Architectonics Reveal a Migration Route from the PSB to the Insula

Radial glia has important roles in cortex development: It serves as a guidance substrate for radially migrating neurons (Rakic, 1971), and is also the principal progenitor cell type of the developing telencephalon (Malatesta et al., 2000; Miyata et al., 2001; Noctor et al., 2001; Tamamaki et al., 2001). In early embryonic stages, radial glia somata are confined to the VZ as apical radial glia, while in later stages, basal or oRG forms the proliferating cell population in the SVZ (Fietz et al., 2010; Hansen et al., 2010; Reillo et al., 2011). An oSVZ (Smart et al., 2002) is more prominent in gyrencephalic brains than in the lissencephalic rodent, and has been suggested to play key roles in the folding of the neocortex in gyrencephalic species because of its abundance in oRG that promote cortical expansion (Fietz et al., 2010; Hansen et al., 2010; Lewitus et al., 2013; Martínez-Martínez et al., 2016). On the other hand, comparisons of lissencephalic primates, gyrencephalic rodents, and carnivores suggested that the cytoarchitectonic subdivisions of the SVZ are an evolutionary trend and not a primate-specific feature, and that a substantial population of oRG exists unrelated to the degree of cortical folding (García-Moreno et al., 2012; Kelava et al., 2012; Martínez-Cerdeño et al., 2012, 2016). The expression of transcription factors Pax6 and Tbr2 varies between the various types of progenitor cells and species (Hansen et al., 2010; Kelava et al., 2012; Betizeau et al., 2013; Cunningham et al., 2013), although the expression of Tbr2 in neural precursor cells can be used for defining the boundaries of the SVZ both developmentally and evolutionarily (Martínez-Cerdeño et al., 2016). It is not clear whether also the intermediate progenitor cells, which lack a polarized process, express the pan-radial glia marker vimentin. In any case, the vimentin-expressing radial glia cells in the SVZ of our human material displayed the various morphotypes described in the monkey (Betizeau et al., 2013), where they indicate differential mitotic potentials and cell-cycle parameters. Radial glia-guided locomotion is the migration mode of excitatory cortical neurons on their route through intermediate zone, subplate and CP, until they reach the marginal zone, detach from the radial glia fiber, and change to a somatic translocation mode (Tissir and Goffinet, 2003; Sekine et al., 2011). The critical question is the degree of horizontal dispersion along the radial glia route. Radially migrating neurons may change from one radial glia fiber to an adjacent one, so that the strictly radial orientation of a radial glia fiber does not necessarily imply a similar radial course of the migrating neurons (Reillo et al., 2011; Gertz and Kriegstein, 2015). It is thus possible that the origin of neurons in the insula might be more extensive than

described here, and that the SVZ of the adjacent opercula contribute neuroblasts dispersing tangentially into the insula. We suggest, however, that it is precisely the absence of tangential dispersion between adjacent lobes that leads to the enormous growth of the opercula, versus the restricted expansion of the insula. The distinct RGF into the insula is another argument for an origin from a specific sector of the oSVZ at the PSB. The RGF represents the main radial migration substrate from the PSB to the insula, and is set apart from the non-fasciculated oRG fibers originating from the oSVZ of the opercula. It is possible though that tangential dispersion within the spatially compressed RGF contributes to the inhomogeneities of layer IV. An important feature of the human RGF is that it is composed of descending and ascending fibers and thus connects the derivatives of the FP and temporal SVZ, which act in concert in the formation of the insula. It appeared, however, in our material that the dominant source of insular neurons is the dorsal PSB, whereas the temporal PSB contribution is less substantial. Future studies using region-specific markers might solve this question.

The Variability of the Inner Granular Layer of the Human Insula

The human neocortex displays a large diversity of size and density of neurons, which are arranged in six horizontal layers of variable width. This diversity is the foundation of the cytoarchitectonic areas described by Brodmann (1909) and Von Economo and Koskinas (1925).

A major criterion in these classifications is the differentiation of the granular layers II and IV, which define the degree of granularity of a given area. Primary sensory areas have a particularly prominent layer IV, which is the main target of thalamo-cortical fibers, and populated by its principal neurons: spiny stellate cells, star pyramids, and small to very small "dwarf pyramids" (Von Economo and Koskinas, 1925). Spiny stellate cells are glutamatergic excitatory neurons (Conti et al., 1989; Feldmeyer et al., 1999), which establish asymmetric synapses mainly with dendritic spines (Saint Marie and Peters, 1985), give rise to interlaminar projections (Qi and Feldmeyer, 2016), and even connect adjacent areas (Meyer and Albus, 1981). In human auditory cortex, layer IV is populated by transitional forms between spiny stellate and small pyramidal cells (Meyer et al., 1989). However, layer IV is also prominent in many other cortical areas, such as the posterior insula, where anatomical and functional studies stressed its afferent sensory (gustatory, auditory, and vestibular) input (Augustine, 1996; Kurth et al., 2010).

There is a general agreement in the basic classification of the insula into agranular, dysgranular and granular parts (Mesulam and Mufson, 1985), even though the number of subareas varies between authors (reviewed by Nieuwenhuys, 2012). In our perinatal material we tried, following Von Economo and Koskinas (1925), to section the insula in a plane perpendicular to the main axis of most insular gyri. However, the insular gyri undergo subtle changes in orientation, have multiple dimples and small subsulci, which altogether distort the naturally vertical columnar arrangement of all layers including layer IV, and may give the impression of a distinct cytoarchitectonic subdivision.

As described here, the insula derives from the PSB, which in turn is continuous with the VZ and SVZ of the adjacent lobes. In this sense, the agranular character of the anterior insula reflects the trend of the agranular PF and frontal areas, whereas the granular caudal insula resembles the hypergranular character of the adjacent parietal and temporal sensory areas. The dysgranular character of the intermediate areas of the insula may be attributed to the contribution and possible intermixture of RGF compartments FP and T, as well as to the possibility of tangential dispersion within the RGF.

In the literature on the oSVZ, it is often emphasized that the subgranular layers V and VI derive from the VZ and inner SVZ, whereas the supragranular layers III and II originate from the oSVZ (e.g., Smart et al., 2002; Lukaszewicz et al., 2005; Nowakowski et al., 2016), leaving open the question of the origin of layer IV. Species differences may account for this apparent neglect. As shown by Martínez-Cerdeño et al. (2012), the peak in number of Tbr2+ progenitors and mitotic divisions in the oSVZ of the macaque somatosensory cortex occurs during the generation of layer IV, whereas in rat and ferret this peak is at the end of cortical neurogenesis, when the supragranular layers are born. It is thus tempting to propose that layer IV of the human insula derives predominantly from the oSVZ. The degree of granularity of a given cytoarchitectonic area may thus depend on the availability of oSVZ progenitors characterized by high-output cycling parameters during a precise time window (Betizeau et al., 2013), along with the presence of an adequate migration substrate. The generation of a cell-rich layer IV is an important issue particularly in the primate and human brain, where the classification into anatomical and cytoarchitectonic areas is largely based on the granularity of the inner granular layer. Interestingly, the "highest" cognitive functions within the insular lobe are attributed to the agranular anterior insula, which demonstrates that the agranular character of a cortical area is not an indication of less complex functions. It would be desirable that future ontogenetic and phylogenetic studies of the cerebral cortex become more focused on the peculiarities of the human brain (Clowry et al., 2010).

AUTHOR CONTRIBUTIONS

All authors listed have made a substantial, direct and intellectual contribution to the work, and approved it for publication.

REFERENCES

Afif, A., Bouvier, R., Buenerd, A., Trouillas, J., and Mertens, P. (2007). Development of the human fetal insular cortex: study of the gyration from 13 to 28 gestational weeks. *Brain Struct. Funct.* 212, 335–346. doi: 10.1007/s00429-007-0161-1

Allman, J. M., Tetreault, N. A., Hakeem, A. Y., Manaye, K. F., Semendeferi, K., Erwin, J. M., et al. (2011). The von Economo neurons in the frontoinsular and

anterior cingulate cortex. *Ann. N. Y. Acad. Sci.* 1225, 59–71. doi: 10.1111/j.1749-6632.2011.06011.x

Allman, J. M., Watson, K. K., Tetreault, N. A., and Hakeem, A. Y. (2005). Intuition and autism: a possible role for Von Economo neurons. *Trends Cogn. Sci.* 9, 367–373. doi: 10.1016/j.tics.2005.06.008

Angevine, J. B., and Sidman, R. L. (1961). Autoradiographic study of cell migration during histogenesis of cerebral cortex in the mouse. *Nature* 192, 766–768. doi: 10.1038/192766b0

Augustine, J. R. (1996). Circuitry and functional aspects of the insular lobe in primates including humans. *Brain Res. Brain Res. Rev.* 22, 229–244. doi: 10.1016/S0165-0173(96)00011-2

Bauernfeind, A. L., de Sousa, A. A., Avasthi, T., Dobson, S. D., Raghanti, M. A., Lewandowski, A. H., et al. (2013). A volumetric comparison of the insular cortex and its subregions in primates. *J. Hum. Evol.* 64, 263–279. doi: 10.1016/j.jhevol.2012.12.003

Bayer, S. A., and Altman, J. (1991). *Neocortical Development*. New York, NY: Raven Press.

Bayer, S. A., and Altman, J. (2007). *The Human Brain during the Early First Trimester*. Boca Raton, FL: CRC Press.

Betizeau, M., Cortay, V., Patti, D., Pfister, S., Gautier, E., Bellemin-Ménard, A., et al. (2013). Precursor diversity and complexity of lineage relationships in the outer subventricular zone of the primate. *Neuron* 80, 442–457. doi: 10.1016/j.neuron.2013.09.032

Bonthius, D. J., Solodkin, A., and Van Hoesen, G. W. (2005). Pathology of the insular cortex in Alzheimer disease depends on cortical architecture. *J. Neuropathol. Exp. Neurol.* 64, 910–922. doi: 10.1097/01.jnen.0000182983.87106.d1

Brodmann, K. (1909). *Vergleichende Lokalisationslehre der Grosshirnrinde: in ihren Prinzipien dargestellt auf Grund des Zellenbaues*. Barth: Leipzig.

Butti, C., and Hof, P. R. (2010). The insular cortex: a comparative perspective. *Brain Struct. Funct.* 214, 477–493. doi: 10.1007/s00429-010-0264-y

Bystron, I., Blakemore, C., and Rakic, P. (2008). Development of the human cerebral cortex: Boulder Committee revisited. *Nat. Rev. Neurosci.* 9, 110–122. doi: 10.1038/nrn2252

Carney, R. S., Alfonso, T. B., Cohen, D., Dai, H., Nery, S., Stoica, B., et al. (2006). Cell migration along the lateral cortical stream to the developing basal telencephalic limbic system. *J. Neurosci.* 26, 11562–11574. doi: 10.1523/JNEUROSCI.3092-06.2006

Casanova, M. F., Trippe, J., Tillquist, C. R., and Switala, A. E. (2010). Dolphin insula reflects minicolumnar organization of mammalian isocortex. *Transl. Neurosci.* 1, 37–42.

Cauda, F., D'Agata, F., Sacco, K., Duca, S., Geminiani, G., and Vercelli, A. (2011). Functional connectivity of the insula in the resting brain. *Neuroimage* 55, 8–23. doi: 10.1016/j.neuroimage.2010.11.049

Clascá, F., Llamas, A., and Reinoso-Suárez, F. (1997). Insular cortex and neighboring fields in the cat: a redefinition based on cortical microarchitecture and connections with the thalamus. *J. Comp. Neurol.* 384, 456–482. doi: 10.1002/(SICI)1096-9861(19970804)384:3<456::AID-CNE10>3.0.CO;2-H

Clowry, G., Molnár, Z., and Rakic, P. (2010). Renewed focus on the developing human neocortex. *J. Anat.* 217, 276–288. doi: 10.1111/j.1469-7580.2010.01281.x

Cocas, L. A., Georgala, P. A., Mangin, J. M., Clegg, J. M., Kessaris, N., Haydar, T. F., et al. (2011). Pax6 is required at the telencephalic pallial-subpallial boundary for the generation of neuronal diversity in the postnatal limbic system. *J. Neurosci.* 31, 5313–5324. doi: 10.1523/JNEUROSCI.3867-10.2011

Conti, F., De Felipe, J., Farinas, I., and Manzoni, T. (1989). Glutamate-positive neurons and axon terminals in cat sensory cortex: a correlative light and electron microscopic study. *J. Comp. Neurol.* 290, 141–153. doi: 10.1002/cne.902900109

Craig, A. D. (2009). How do you feel—now? The anterior insula and human awareness. *Nat. Rev. Neurosci.* 10, 59–70. doi: 10.1038/nrn2555

Craig, A. D. (2010). The sentient self. *Brain Struct. Funct.* 214, 563–577. doi: 10.1007/s00429-010-0248-y

Craig, A. D. (2011). Significance of the insula for the evolution of human awareness of feelings from the body. *Ann. N. Y. Acad. Sci.* 1225, 72–82. doi: 10.1111/j.1749-6632.2011.05990.x

Cunningham, C. L., Martínez-Cerdeño, V., and Noctor, S. C. (2013). Diversity of neural precursor cell types in the prenatal macaque cerebral cortex exists largely within the astroglial cell lineage. *PLOS ONE* 28:e63848. doi: 10.1371/journal.pone.0063848

Deen, B., Pitskel, N. B., and Pelphrey, K. A. (2011). Three systems of insular functional connectivity identified with cluster analysis. *Cereb. Cortex* 21, 1498–1506. doi: 10.1093/cercor/bhq186

Di Martino, A., Ross, K., Uddin, L. Q., Sklar, A. B., Castellanos, F. X., and Milham, M. P. (2009). Functional brain correlates of social and non-social processes in autism spectrum disorders: an ALE meta-analysis. *Biol. Psychiatry* 65, 63–74. doi: 10.1016/j.biopsych.2008.09.022

Englund, C., Fink, A., Lau, C., Pham, D., Daza, R. A., Bulfone, A., et al. (2005). Pax6, Tbr2, and Tbr1 are expressed sequentially by radial glia, intermediate progenitor cells, and postmitotic neurons in developing neocortex. *J. Neurosci.* 25, 247–251. doi: 10.1523/JNEUROSCI.2899-04.2005

Evrard, H. C., Logothetis, N. K., and Craig, A. D. (2014). Modular architectonic organization of the insula in the macaque monkey. *J. Comp. Neurol.* 522, 64–97. doi: 10.1002/cne.23436

Fan, Y., Duncan, N. W., de Greck, M., and Northoff, G. (2011). Is there a core neural network in empathy? An fMRI based quantitative meta-analysis. *Neurosci. Biobehav. Rev.* 35, 903–911. doi: 10.1016/j.neubiorev.2010.10.009

Feldmeyer, D., Egger, V., Lubke, J., and Sakmann, B. (1999). Reliable synaptic connections between pairs of excitatory layer 4 neurones within a single 'barrel' of developing rat somatosensory cortex. *J. Physiol.* 521, 169–190. doi: 10.1111/j.1469-7793.1999.00169.x

Fietz, S. A., Kelava, I., Vogt, J., Wilsch-Bräuninger, M., Stenzel, D., Fish, J. L., et al. (2010). OSVZ progenitors of human and ferret neocortex are epithelial-like and expand by integrin signaling. *Nat. Neurosci.* 13, 690–699. doi: 10.1038/nn.2553

Fischer, D. B., Boes, A. D., Demertzi, A., Evrard, H. C., Laureys, S., Edlow, B. L., et al. (2016). A human brain network derived from coma-causing brainstem lesions. *Neurology* 87, 2427–2434. doi: 10.1212/WNL.0000000000003404

Gallay, D. S., Gallay, M. N., Jeanmonod, D., Rouiller, E. M., and Morel, A. (2012). The insula of Reil revisited: multiarchitectonic organization in macaque monkeys. *Cereb. Cortex* 22, 175–190. doi: 10.1093/cercor/bhr104

García-Moreno, F., Vasistha, N. A., Trevia, N., Bourne, J. A., and Molnár, Z. (2012). Compartmentalization of cerebral cortical germinal zones in a lissencephalic primate and gyrencephalic rodent. *Cereb. Cortex* 22, 482–492. doi: 10.1093/cercor/bhr312

Gertz, C. C., and Kriegstein, A. R. (2015). Neuronal migration dynamics in the developing ferret cortex. *J. Neurosci.* 35, 14307–14315. doi: 10.1523/JNEUROSCI.2198-15.2015

González-Gómez, M., and Meyer, G. (2014). Dynamic expression of calretinin in embryonic and early fetal human cortex. *Front. Neuroanat.* 8:41. doi: 10.3389/fnana.2014.00041

Hansen, D. V., Lui, J. H., Parker, P. R. L., and Kriegstein, A. R. (2010). Neurogenic radial glia in the outer subventricular zone of human neocortex. *Nature* 464, 554–561. doi: 10.1038/nature08845

Hevner, R. F., Daza, R. A., Rubenstein, J. L., Stunnenberg, H., Olavarria, J. F., and Englund, C. (2003). Beyond laminar fate: toward a molecular classification of cortical projection/pyramidal neurons. *Dev. Neurosci.* 25, 139–151. doi: 10.1159/000072263

Jacobs, M. S., Galaburda, A. M., McFarland, W. L., and Morgane, P. J. (1984). The insular formations of the dolphin brain: quantitative cytoarchitectonic studies of the insular component of the limbic lobe. *J. Comp. Neurol.* 225, 396–432. doi: 10.1002/cne.902250307

Kelava, I., Reillo, I., Murayama, A. Y., Kalinka, A. T., Stenzel, D., Tomancak, P., et al. (2012). Abundant occurrence of basal radial glia in the subventricular zone of embryonic neocortex of a lissencephalic primate, the common marmoset *Callithrix jacchus*. *Cereb. Cortex* 22, 469–481. doi: 10.1093/cercor/bhr301

Kodam, S. (1926). Über die sogenannten basalganglien, morphogenetische und pathologisch-anatomische untersuchunger. *Schweiz. Arch. Neurol. Psychiatr.* 18, 179–246.

Koubeissi, M. Z., Bartolomei, F., Beltagy, A., and Picard, F. (2014). Electrical stimulation of a small brain area reversibly disrupts consciousness. *Epilepsy Behav.* 37, 32–35. doi: 10.1016/j.yebeh.2014.05.027

Krsnik, Z., Majić, V., Vasung, L., Huang, H., and Kostovic, I. (2017). Growth of thalamocortical fibers to the somatosensory cortex in the human fetal brain. *Front. Neurosci.* 11:233. doi: 10.3389/fnins.2017.00233

Kurth, F., Zilles, K., Fox, P. T., Laird, A. R., and Eickhoff, S. B. (2010). A link between the systems: functional differentiation and integration within the human insula revealed by meta-analysis. *Brain Struct. Funct.* 214, 519–534. doi: 10.1007/s00429-010-0255-z

Laneri, D., Krach, S., Paulus, F. M., Kanske, P., Schuster, V., Sommer, J., et al. (2017). Mindfulness meditation regulates anterior insula activity during empathy for social pain. *Hum. Brain Mapp.* 38, 4034–4046. doi: 10.1002/hbm.23646

Lewitus, E., Kelava, I., and Huttner, W. B. (2013). Conical expansion of the outer subventricular zone and the role of neocortical folding in evolution and development. *Front. Hum. Neurosci.* 7:424. doi: 10.3389/fnhum.2013.00424

Lewitus, E., Kelava, I., Kalinka, A. T., Tomancak, P., and Huttner, W. B. (2014). An adaptive threshold in mammalian neocortical evolution. *PLOS Biol.* 12:e1002000. doi: 10.1371/journal.pbio.1002000

Lukaszewicz, A., Savatier, P., Cortay, V., Giroud, P., Huissoud, C., Berland, M., et al. (2005). G1 phase regulation, area-specific cell cycle control, and cytoarchitectonics in the primate cortex. *Neuron* 47, 353–364. doi: 10.1016/j.neuron.2005.06.032

Malatesta, P., Hartfuss, E., and Götz, M. (2000). Isolation of radial glial cells by fluorescent-activated cell sorting reveals a neuronal lineage. *Development* 127, 5253–5263.

Martínez-Cerdeño, V., Cunningham, C. L., Camacho, J., Antczak, J. L., Prakash, A. N., Cziep, M. E., et al. (2012). Comparative analysis of the subventricular zone in rat, ferret and macaque: evidence for an outer subventricular zone in rodents. *PLOS ONE* 7:e30178. doi: 10.1371/journal.pone.0030178

Martínez-Cerdeño, V., Cunningham, C. L., Camacho, J., Keiter, J. A., Ariza, J., Lovern, M., et al. (2016). Evolutionary origin of Tbr2-expressing precursor cells and the subventricular zone in the developing cortex. *J. Comp. Neurol.* 524, 433–447. doi: 10.1002/cne.23879

Martínez-Martínez, M. Á., De Juan Romero, C., Fernández, V., Cárdenas, A., Götz, M., and Borrell, V. (2016). A restricted period for formation of outer subventricular zone defined by Cdh1 and Trnp1 levels. *Nat. Commun.* 7:11812. doi: 10.1038/ncomms11812

Medford, N., and Critchley, H. D. (2010) Conjoint activity of anterior insular and anterior cingulate cortex: awareness and response. *Brain Struct. Funct.* 214, 535–549. doi: 10.1007/s00429-010-0265-x

Medina, L., Legaz, I., González, G., De Castro, F., Rubenstein, J. L., and Puelles, L. (2004). Expression of Dbx1, Neurogenin 2, Semaphorin 5A, Cadherin 8, and Emx1 distinguish ventral and lateral pallial histogenetic divisions in the developing mouse claustroamygdaloid complex. *J. Comp. Neurol.* 474, 504–523. doi: 10.1002/cne.20141

Mesulam, M. M., and Mufson, E. J. (1985). "The insula of Reil in man and monkey. Architectonics, connectivity, and function," in *Cerebral Cortex*, eds A. Peters and E. Jones (London: Plenum Publishing Corporation), 179–224.

Meyer, G., and Albus, K. (1981). Spiny stellates as cells of origin of association fibres from area 17 to area 18 in the cat's neocortex. *Brain Res.* 210, 335–341. doi: 10.1016/0006-8993(81)90906-9

Meyer, G., and González-Gómez, M. (2017). The subpial granular layer and transient versus persisting Cajal-Retzius neurons of the fetal human cortex. *Cereb. Cortex* doi: 10.1093/cercor/bhx110 [Epub ahead of print]

Meyer, G., González-Hernández, T. H., and Ferres-Torres, R. (1989). The spiny stellate neurons in layer IV of the human auditory cortex. A Golgi study. *Neuroscience* 33, 489–498.

Meyer, G., Schaaps, J. P., Moreau, L., and Goffinet, A. M. (2000). Embryonic and early fetal development of the human neocortex. *J. Neurosci.* 20, 1858–1868.

Miyata, T., Kawaguchi, A., Okano, H., and Ogawa, M. (2001). Asymmetric inheritance of radial glial fibers by cortical neurons. *Neuron* 31, 727–741. doi: 10.1016/S0896-6273(01)00420-2

Molnár, Z., and Butler, A. B. (2002). The corticostriatal junction: a crucial region for forebrain development and evolution. *Bioessays* 24, 530–541. doi: 10.1002/bies.10100

Molnár, Z., Garel, S., López-Bendito, G., Maness, P., and Price, D. J. (2012). Mechanisms controlling the guidance of thalamocortical axons through the embryonic forebrain. *Eur. J. Neurosci.* 35, 1573–1585. doi: 10.1111/j.1460-9568.2012.08119.x

Moran, M. E., Weisinger, B., Ludovici, K., McAdams, H., Greenstein, D., Gochman, P., et al. (2014). At the boundary of the self: the insular cortex in patients with childhood-onset schizophrenia, their healthy siblings, and normal volunteers. *Int. J. Dev. Neurosci.* 32, 58–63. doi: 10.1016/j.ijdevneu.2013.05.010

Morel, A., Gallay, M. N., Baechler, A., Wyss, M., and Gallay, D. S. (2013). The human insula: architectonic organization and postmortem MRI registration. *Neuroscience* 236, 117–135. doi: 10.1016/j.neuroscience.2012.12.076

Mufson, E. J., and Mesulam, M. M. (1982). Insula of the old world monkey. II: afferent cortical input and comments on the claustrum. *J. Comp. Neurol.* 212, 23–37. doi: 10.1002/cne.902120103

Naidich, T. P., Kang, E., Fatterpekar, G. M., Delman, B. N., Gultekin, S. H., Wolfe, D., et al. (2004). The insula: anatomic study and MR imaging display at 1.5 T. *Am. J. Neuroradiol.* 25, 222–232.

Nieuwenhuys, R. (2012). The insular cortex: a review. *Prog. Brain Res.* 195, 123–163. doi: 10.1016/B978-0-444-53860-4.00007-6

Noctor, S. C., Flint, A. C., Weissman, T. A., Dammerman, R. S., and Kriegstein, A. R. (2001). Neurons derived from radial glial cells establish radial units in neocortex. *Nature* 409, 714–720. doi: 10.1038/35055553

Nowakowski, T. J., Pollen, A. A., Sandoval-Espinosa, C., and Kriegstein, A. R. (2016). Transformation of the radial glia scaffold demarcates two stages of human cerebral cortex development. *Neuron* 91, 1219–1227. doi: 10.1016/j.neuron.2016.09.005

Odriozola, P., Uddin, L. Q., Lynch, C. J., Kochalka, J., Chen, T., and Menon, V. (2016). Insula response and connectivity during social and non-social attention in children with autism. *Soc. Cogn. Affect. Neurosci.* 11, 433–444. doi: 10.1093/scan/nsv126

O'Leary, M. A., Bloch, J. I., Flynn, J. J., Gaudin, T. J., Giallombardo, A., Giannini, N. P., et al. (2013). The placental mammal ancestor and the post-K-Pg radiation of placentals. *Science* 339, 662–667. doi: 10.1126/science.1229237

O'Rahilly, R., and Müller, F. (1994). *The Embryonic Human Brain: An Atlas of Developmental Stages*. Hoboken, NJ: Wiley-Liss Inc.

Qi, G., and Feldmeyer, D. (2016). Dendritic target region-specific formation of synapses between excitatory layer 4 neurons and layer 6 pyramidal cells. *Cereb. Cortex* 26, 1569–1579. doi: 10.1093/cercor/bhu334

Rakic, P. (1971) Guidance of neurons migrating to the fetal monkey neocortex. *Brain Res.* 33, 471–476. doi: 10.1016/0006-8993(71)90119-3

Rakic, P. (1974). Neurons in rhesus monkey visual cortex: systematic relation between time of origin and eventual disposition. *Science* 183, 425–427. doi: 10.1126/science.183.4123.425

Reillo, I., de Juan Romero, C., García-Cabezas, M. Á., and Borrell, V. (2011). A role for intermediate radial glia in the tangential expansion of the mammalian cerebral cortex. *Cereb. Cortex* 7, 1674–1694. doi: 10.1093/cercor/bhq238

Rose, M. (1928). Die Inselrinde des menschen und der tiere. *J. Psychol. Neurol.* 37, 467–624.

Saint Marie, R. L., and Peters, A. (1985). The morphology and synaptic connections of spiny stellate neurons in monkey visual cortex (area 17): a Golgi-electron microscopic study. *J. Comp. Neurol.* 233, 213–235. doi: 10.1002/cne.902330205

Sekine, K., Honda, T., Kawauchi, T., Kubo, K., and Nakajima, K. (2011). The outermost region of the developing cortical plate is crucial for both the switch of the radial migration mode and the Dab1-dependent "inside-out" lamination in the neocortex. *J. Neurosci.* 31, 9426–9439. doi: 10.1523/JNEUROSCI.0650-11.2011

Shepherd, A. M., Matheson, S. L., Laurens, K. R., Carr, V. J., and Green, M. J. (2012). Systematic meta-analysis of insula volume in schizophrenia. *Biol. Psychiatry* 72, 775–784. doi: 10.1016/j.biopsych.2012.04.020

Smart, I. H., Dehay, C., Giroud, P., Berland, M., and Kennedy, H. (2002). Unique morphological features of the proliferative zones and postmitotic compartments of the neural epithelium giving rise to striate and extrastriate cortex in the monkey. *Cereb. Cortex* 1, 37–53. doi: 10.1093/cercor/12.1.37

Stoykova, A., Treichel, D., Hallonet, M., and Gruss, P. (2000). Pax6 modulates the dorsoventral patterning of the mammalian telencephalon. *J. Neurosci.* 20, 8042–8050.

Streeter, G. L. (1912). "Chapter XIV-The development of the nervous system," in *Manual of Human Embryology*, Vol. II, eds F. Keibel and F. P. Mall (Philadelphia, PA: Lippincott).

Tamamaki, N., Nakamura, K., Okamoto, K., and Kaneko, T. (2001). Radial glia is a progenitor of neocortical neurons in the developing cerebral cortex. *Neurosci. Res.* 41, 51–60. doi: 10.1016/S0168-0102(01)00259-0

Tanriover, N., Rhoton, A. L. Jr., Kawashima, M., Ulm, A. J., and Yasuda, A. (2004). Microsurgical anatomy of the insula and the sylvian fissure. *J. Neurosurg.* 100, 891–922. doi: 10.3171/jns.2004.100.5.0891

Tissir, F., and Goffinet, A. M. (2003). Reelin and brain development. *Nat. Rev. Neurosci.* 4, 496–505. doi: 10.1038/nrn1113

Türe, U., Yaşargil, D. C., Al-Mefty, O., and Yaşargil, M. G. (1999). Topographic anatomy of the insular region. *J. Neurosurg.* 90, 720–733. doi: 10.3171/jns.1999.90.4.0720

Tusche, A., Böckler, A., Kanske, P., Trautwein, F. M., and Singer, T. (2016). Decoding the charitable brain: empathy, perspective taking, and attention shifts differentially predict altruistic giving. *J. Neurosci.* 36, 4719–4732. doi: 10.1523/JNEUROSCI.3392-15.2016

Uddin, L. Q., Kinnison, J., Pessoa, L., and Anderson, M. L. (2014). Beyond the tripartite cognition-emotion-interoception model of the human insular cortex. *J. Cogn. Neurosci.* 26, 16–27. doi: 10.1162/jocn_a_00462

Uddin, L. Q., and Menon, V. (2009). The anterior insula in autism: under-connected and under-examined. *Neurosci. Biobehav. Rev.* 33, 1198–1203. doi: 10.1016/j.neubiorev.2009.06.002

Ulfig, N., Neudörfer, F., and Bohl, J. (1999). Distribution patterns of vimentin-immunoreactive structures in the human prosencephalon during the second half of gestation. *J. Anat.* 195, 87–100. doi: 10.1046/j.1469-7580.1999.19510087.x

Von Economo, C., and Koskinas, G. N. (1925). *Die Cytoarchitektonik der Hirnrinde des Erwachsenen Menschen*. Berlin: J. Springer.

Watson, C., and Puelles, L. (2017). Developmental gene expression in the mouse clarifies the organization of the claustrum and related endopiriform nuclei. *J. Comp. Neurol.* 525, 1499–1508. doi: 10.1002/cne.24034

Yun, K., Potter, S., and Rubenstein, J. L. (2001). Gsh2 and Pax6 play complementary roles in dorsoventral patterning of the mammalian telencephalon. *Development* 128, 193–205.

Zecevic, N. (2004). Specific characteristic of radial glia in the human fetal telencephalon. *Glia* 48, 27–35. doi: 10.1002/glia.20044

Zecevic, N., Chen, Y., and Filipovic, R. (2005). Contributions of cortical subventricular zone to the development of the human cerebral cortex. *J. Comp. Neurol.* 491, 109–122. doi: 10.1002/cne.20714

Conflict of Interest Statement: The authors declare that the research was conducted in the absence of any commercial or financial relationships that could be construed as a potential conflict of interest.

frontiers in Neuroanatomy

REVIEW
published: 13 October 2017
doi: 10.3389/fnana.2017.00091

Cell Type-Specific Structural Organization of the Six Layers in Rat Barrel Cortex

*Rajeevan T. Narayanan, Daniel Udvary and Marcel Oberlaender**

Max Planck Group: In Silico Brain Sciences, Center of Advanced European Studies and Research, Bonn, Germany

The cytoarchitectonic subdivision of the neocortex into six layers is often used to describe the organization of the cortical circuitry, sensory-evoked signal flow or cortical functions. However, each layer comprises neuronal cell types that have different genetic, functional and/or structural properties. Here, we reanalyze structural data from some of our recent work in the posterior-medial barrel-subfield of the vibrissal part of rat primary somatosensory cortex (vS1). We quantify the degree to which somata, dendrites and axons of the 10 major excitatory cell types of the cortex are distributed with respect to the cytoarchitectonic organization of vS1. We show that within each layer, somata of multiple cell types intermingle, but that each cell type displays dendrite and axon distributions that are aligned to specific cytoarchitectonic landmarks. The resultant quantification of the structural composition of each layer in terms of the cell type-specific number of somata, dendritic and axonal path lengths will aid future studies to bridge between layer- and cell type-specific analyses.

Keywords: barrel cortex, whisker touch, soma, dendrite, axon

OPEN ACCESS

Edited by:
Kathleen S. Rockland, Boston University School of Medicine, United States

Reviewed by:
Dirk Feldmeyer, RWTH Aachen University, Germany
Guy Elston, Centre for Cognitive Neuroscience, Australia

****Correspondence:***
Marcel Oberlaender
marcel.oberlaender@caesar.de

Received: *29 June 2017*
Accepted: *28 September 2017*
Published: *13 October 2017*

Citation:
Narayanan RT, Udvary D and Oberlaender M (2017) Cell Type-Specific Structural Organization of the Six Layers in Rat Barrel Cortex. Front. Neuroanat. 11:91. doi: 10.3389/fnana.2017.00091

More than a century ago, Brodmann (Brodmann, 1909) described that the shapes and diameters of neuron somata vary as a function of cortical depth (see Garey, 1994 for an English translation of Brodmann's original work). These differences correlate with systematic changes in neuron densities along the vertical cortex axis (i.e., from the pial surface toward the white matter), which gave rise to the concept of cytoarchitectonic layers (Brodmann, 1909). The neocortex is typically subdivided into six layers, i.e., layers 1-6 (L1-6). Even though cortical layers are purely defined by vertical gradients in soma size, shape or density, and there are many exceptions to the division into six layers across cortical areas and species (see Elston, 2002, 2003; Spruston, 2008; DeFelipe, 2011; Elston et al., 2011; Kaas, 2013; Rockland, 2017, for comparative studies and reviews on some aspects of structural cortical heterogeneity), this concept has been widely accepted to provide a first order criterion to discriminate between neuronal cell types. Countless studies have thus grouped neurons by their laminar soma locations and provided layer-specific analyses.

Moreover, layers are often used as a synonym for elementary computational units when describing the organization of cortical circuits. For example, in primary sensory cortices, a general motif, referred to as a "canonical circuit" has been proposed (reviewed in Douglas and Martin, 2004). According to this theory, L4 is regarded as the major thalamorecipient layer and thus as the starting point of cortical information processing. Information from L4 is then thought to propagate through the cortical column, first to L2/3 from where it is then relayed to L5/6, the primary output layers of the cortex. However, each layer is populated by genetically (e.g., Zeisel et al., 2015; Tasic et al., 2016), biophysically (e.g., Ferrante et al., 2017), physiologically (e.g., de Kock et al., 2007) and morphologically (e.g., Narayanan et al., 2015) diverse neuron populations. This heterogeneity of

each layer—as well as the general structural heterogeneity across cortical areas and species—raises the question to what extent grouping of neurons by their laminar soma locations is an appropriate simplification to study and describe the structural and functional organization of cortical circuits.

In this review article, we reanalyze some of our recent work about the structural and functional organization of the posterior-medial barrel-subfield in the vibrissal part of rat primary somatosensory cortex (vS1, i.e., barrel cortex). On the example of this well-studied, yet—when compared to other cortical areas and species—uniquely organized primary sensory area (e.g., the rodent barrel cortex is characterized by neuron-dense aggregates in L4 (i.e., barrels) that form a somatotopic map of the facial whiskers), we seek to address the following general questions: *How layer-specific are physiological and morphological properties of individual excitatory neurons, and how homogeneous are cortical layers with respect to the resultant structure-function neuronal cell types?*

First, we define the borders between the six layers of rat vS1 by precise measurements of the 3D distributions of all excitatory and inhibitory neuron somata (Meyer et al., 2013). Second, we group *in vivo* recorded excitatory neurons, whose dendrite and axon morphologies have been reconstructed, into 10 structure-function cell types (Oberlaender et al., 2012; Narayanan et al., 2015). Third, these datasets are combined by registration into a precise anatomical reference frame of rat vS1 (Egger et al., 2012), which allows quantifying cell type-specific soma, dendrite and axon distributions with respect to the six layers of vS1. Finally, we determine the number of somata, as well as the amounts of dendrites and axons that each of the ten cell types contributes to each of the six layers within the volume of an average cortical barrel column. The present review article thus provides a quantitative account of the structural heterogeneity of cortical layers, which will help relating layer-specific to cell type-specific studies of cortex organization.

DEFINING CORTICAL LAYERS IN RAT vS1

To define layer borders, we had previously reported the number and 3D distribution of all excitatory and inhibitory somata in entire rat vS1 (Meyer et al., 2013). We had sliced the brains of four animals (28–29 day old, male Wistar rats) into consecutive 50 μm thick vibratome sections, at an angle that is approximately tangential to vS1. The sections were stained with NeuN (Mullen et al., 1992) and GAD67 (Kaufman et al., 1986), to label the somata of all neurons and to discriminate between excitatory and inhibitory somata, respectively. The tangential cutting plane allowed identification of the L4 barrels, which were extrapolated to barrel columns (**Figures 1A–D**). Thus, we were able to determine the number and vertical distributions of all excitatory and inhibitory somata for each individual barrel column (**Figures 1E–G**). The resultant soma density profiles along the respective vertical column axes were then used to define and calculate layer borders (see also Meyer et al., 2010), which are represented by the following distances from the pial surface: L1-L2/3: 157 ± 16 μm, L2/3-L4: 575 ± 57 μm, L4-L5: 900 ± 50 μm, L5-L6: 1,411 ± 28 μm; L6-white matter (WM): 1,973 ± 44 μm (Meyer et al., 2013).

Two caveats about these layer border values should, however, be noted. First, it was not possible to define the border between L2 and L3 based on the overall soma density distribution. This is in line with several previous attempts that failed to identify specific anatomical features that distinguish L2 from L3 (e.g., Lund, 1973; Somogyi et al., 1981; Fitzpatrick et al., 1983; Hendry et al., 1987; Lund and Wu, 1997). L2 and L3 are thus often grouped as one layer (i.e., L2/3), even though evidence for functional differences between neurons in L2 and L3 has accumulated from different cortical areas (e.g., Shepherd and Svoboda, 2005; Bureau et al., 2006; Gur and Snodderly, 2008). In our data, the vertical distribution of inhibitory somata was, in general, different compared to the layer-defining distribution of excitatory neuron somata (**Figure 1F**). Inhibitory somata were densest in upper L2/3 and at the border between L4 and L5 (Meyer et al., 2011). The distribution of inhibitory somata thus provided a quantitative basis for an anatomical separation between L2 and L3. The average border between L2 and L3 was hence calculated as 296 ± 30 μm. Potentially reflecting the different developmental origins of excitatory (Gorski et al., 2002) and inhibitory neurons (Anderson et al., 1997), the different vertical soma distributions question whether grouping inhibitory neurons by their soma locations within cortical layers is an appropriate strategy to describe the organizational principles of inhibitory circuits. For example, the densest distributions of inhibitory neurons in upper L2/3 and at the L4/5 border could underlie the observation that sensory-evoked firing rates of excitatory neurons that are located at these depths are typically much lower than those in deeper parts of L2/3 and L5 (e.g., de Kock et al., 2007). For the remainder of this review article, we will thus restrict our analyses of layer-specific structure and function to excitatory cell types.

The second caveat is that layer borders deviate between barrel columns. The differences do not reflect a linear scaling with cortical thickness. Instead, we found that the diameter of cortical barrel columns compensates for differences in cortical thickness across vS1, resulting in largely the same volume for barrel columns that represent whiskers of the same row along the animals' snout (Egger et al., 2012). More specifically, barrel columns representing whiskers at the bottom of the snout, the so-called E-row, have a volume that is more than three times larger compared to those barrel columns that represent whiskers at the top of the snout (i.e., A-row). The cortical depth changes substantially within and across whisker rows (e.g., by 303 μm from A2 to E2), whereas the location and thickness of L4 is largely preserved across barrel columns (e.g. the depth of L4 changes only by 116 μm from A2 to E2) (**Figure 1G**). Consequently, the depths and extents of the cortical layers change in a whisker-specific manner. Assigning functional data to a particular cortical layer by measuring the recording or imaging depth, may hence result in mixing neurons from different layers. For the remainder of this review article, we will thus restrict our analyses to the column representing the D2 whisker.

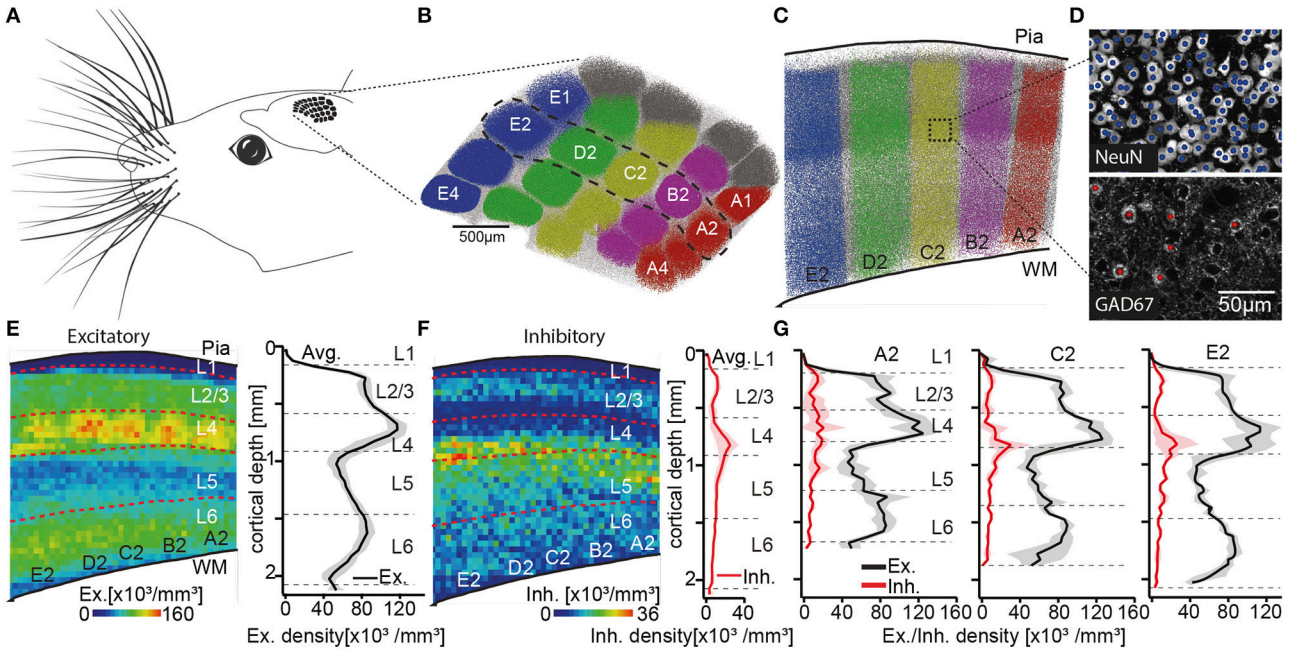

FIGURE 1 | Defining the cortical layers of rat vS1. **(A)** Schematic illustration of the somatotopic organization of vS1 into whisker related barrel columns. **(B)** Top view onto vS1 shows the center locations of all NeuN positive somata with respect to barrel columns. Somata in columns representing whiskers in the A-to-E row (i.e., top-to-bottom of the snout) are colored in red, pink, yellow, green, and blue, respectively. Somata in columns representing the greek whiskers (i.e., α-δ) and those between columns (i.e., septa) are colored in gray and white, respectively. **(C)** Semi-coronal view of cross-section through vS1, showing barrel columns representing arc-2 whiskers (dashed region in **B**). **(D)** Maximum-z projections of image stacks with center locations of all somata (top: NeuN) and the subset of inhibitory somata (bottom: GAD67) for example volume in vS1. **(E)** Left: Average distribution of excitatory somata in 2D projection view. Dashed lines represent layer borders. Right: 1D vertical density profile of excitatory somata averaged across entire vS1. Shaded regions reflect SD. **(F)** Corresponding to panel E: distribution of inhibitory somata (left), 1D vertical density profile of inhibitory somata (right panel). **(G)** 1D vertical density profiles of excitatory and inhibitory somata averaged across columns representing A2, C2, and E2 whiskers, respectively. Note the shift in depth of layer borders across barrel columns. **(B–G)** are adapted and modified from Meyer et al. (2013) with permission.

DEFINING STRUCTURE-FUNCTION CELL TYPES IN RAT vS1

To define cell types of excitatory neurons, we had previously reported a dataset that comprised the *in vivo* activity and 3D morphology of individual neurons (Oberlaender et al., 2012), whose somata were located across the entire cortical depth (**Figure 2A**). We had performed cell-attached recordings in anesthetized animals (28–35 day old, male Wistar rats) and measured spiking patterns during periods of ongoing activity (i.e., without stimulation) and during passive deflections of the somatotopically aligned whisker (de Kock et al., 2007). Following the functional measurements, the recorded neurons were labeled with biocytin (Pinault, 1996; Narayanan et al., 2014), which allowed for *post hoc* reconstructions of their soma, dendrite and intracortical (IC) axon morphologies (Narayanan et al., 2015). The neuron tracings were augmented with reconstructions of the pial surface, WM tract and barrel field in L4, which allowed for precise registration into an average geometrical reference frame of rat vS1 (Egger et al., 2012). Registration compensated for variability in cutting angle and tissue shrinkage across animals, allowing to determine the 3D position of the recorded neuron with ∼50 µm accuracy. Combining this dataset with the layer borders described above, we were able to investigate how neuronal morphology and *in vivo* spiking correlate with the neurons' locations in L2-6 (Oberlaender et al., 2012).

In line with several studies that investigated activity patterns across layers—in different sensory systems, species and during different behavioral states (e.g., Vinje and Gallant, 2000; Deweese et al., 2003; Brecht et al., 2004; Olshausen and Field, 2004)—our dataset showed that spiking activity during periods of ongoing activity is sparse (1.09 ± 1.32 Hz, $n = 57$), with neurons in L5 representing, on average, the most active population (1.72 ± 1.56 Hz, $n = 29$). During whisker stimulation, spiking activity increased primarily within L4 and L5 (**Figure 2A**). However, whisker-evoked (and ongoing) spike rates deviated substantially within each layer, ranging from neurons that did not respond to the stimulus (or decreased spiking compared to ongoing periods) to neurons that increased spike rates by more than 20 Hz within the first 50 ms after stimulation. Both observations, first that sensory stimulation evokes spiking activity most prominently within L4 and L5, and second that responses are highly variable within layers, are generalizable to other stimuli, sensory systems and species (Harris and Shepherd, 2015).

Figure 2B shows the dendrite morphologies of three example neurons that were located approximately at the same

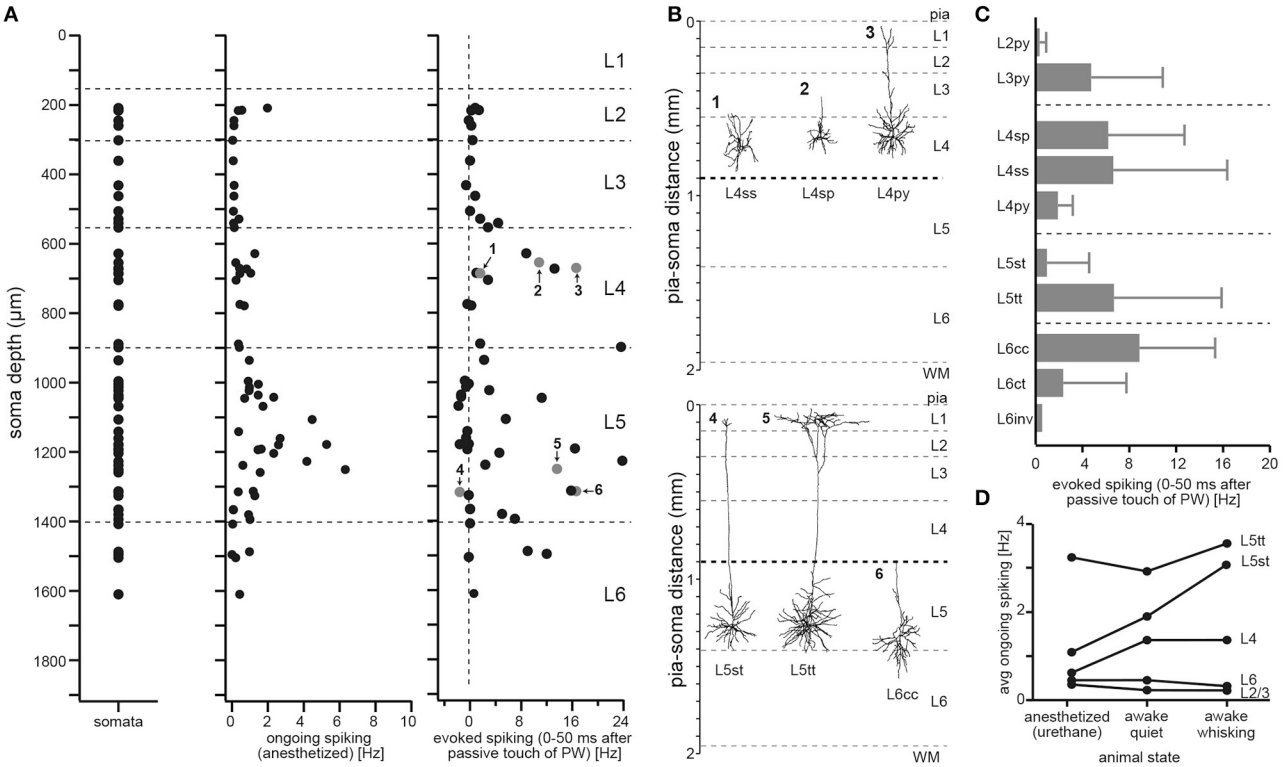

FIGURE 2 | Defining the 10 major excitatory cell types of rat vS1. **(A)** Soma depth locations of *in vivo* recorded/reconstructed excitatory neurons (left). Neuron morphologies were registered to geometrical reference frame of vS1 with ~50 µm precision. Action potentials elicited in anesthetized rats by each of the reconstructed excitatory neurons during periods of ongoing activity (center) and during passive deflection of the somatotopically aligned, so-called principal whisker (PW; right). Evoked spiking rates represent activity after PW stimulation minus ongoing spike rates (panels were modified from (Oberlaender et al., 2012)). **(B)** Example neuron morphologies located at the same depth within L4 (top) and L5 (bottom) illustrate heterogeneity of structural and functional properties within layers. **(C)** Cell type-specific evoked spiking during PW passive deflections. **(D)** Cell type-specific spiking during different behavioral states (adapted and modified from de Kock and Sakmann, 2009 with permission).

cortical depths within L4 and L5, respectively. The neurons differed in their whisker-evoked spike rates and had different dendrite morphologies. We therefore investigated whether the morphological differences of neurons within and across layers can account for the functional variability. We extracted morphological and topological dendrite parameters (see Oberlaender et al., 2012; Narayanan et al., 2015, for a list and definition of the parameters) for 153 *in vivo* recorded/labeled neurons and applied an objective clustering algorithm (Ankerst et al., 1999) to subdivide our sample into dendritic cell types. The classification determined 10 dendritic cell types, which resembled those previously reported in several studies that performed *in vitro* recording/labeling experiments in acute brain slices (see Feldmeyer et al., 2013 for a review). We adopted the cell type naming conventions from the *in vitro* studies and refer to excitatory neurons in vS1 as: L2 pyramidal neurons (L2py), L3py (Petersen and Crochet, 2013), L4py, spiny stellates and star pyramids in L4 (L4ss and L4sp) (Staiger et al., 2004), slender- and thick-tufted pyramids in L5 (L5st and L5tt) (Wise and Jones, 1977), and corticocortical and corticothalamic pyramids in L6 (L6cc and L6ct) (Zhang and Deschenes, 1997; Kumar and Ohana, 2008). The group of L6cc is subdivided into "typical" and "atypical" neurons (DeFelipe and Farinas, 1992), and we refer to the subtypes as L6cc and L6inv, respectively. Typical L6cc are characterized by the lack of apical tuft dendrites (Zhang and Deschenes, 1997; Kumar and Ohana, 2008). The group of L6inv comprises a variety of rare dendritic morphologies, e.g., neurons whose apical dendrite projects toward the white matter (i.e., inverted pyramids).

Grouping the neurons by their respective dendritic cell type could account for some of the functional variability within layers (e.g., whisker-evoked spiking of L4ss/sp vs. L4py: 6.53 vs. 1.90 Hz, or L5st vs. L5tt: 0.97 vs. 6.69 Hz, **Figure 2C**). The relationship between dendritic cell type and *in vivo* function is likely to extend to other experimental conditions (**Figure 2D**). For example, in contrast to L5tt, L5st increase spiking activity during the rhythmic back-and-forth movements of whiskers (i.e., whisking), with spike times being correlated to specific whisker positions (i.e., phase) of the whisking cycle (de Kock and Sakmann, 2009).

LAYER-SPECIFIC ORGANIZATION OF EXCITATORY CELL TYPES IN RAT vS1

Previous *in vitro* studies had revealed several relationships between the dendritic cell type and genetic/molecular profiles

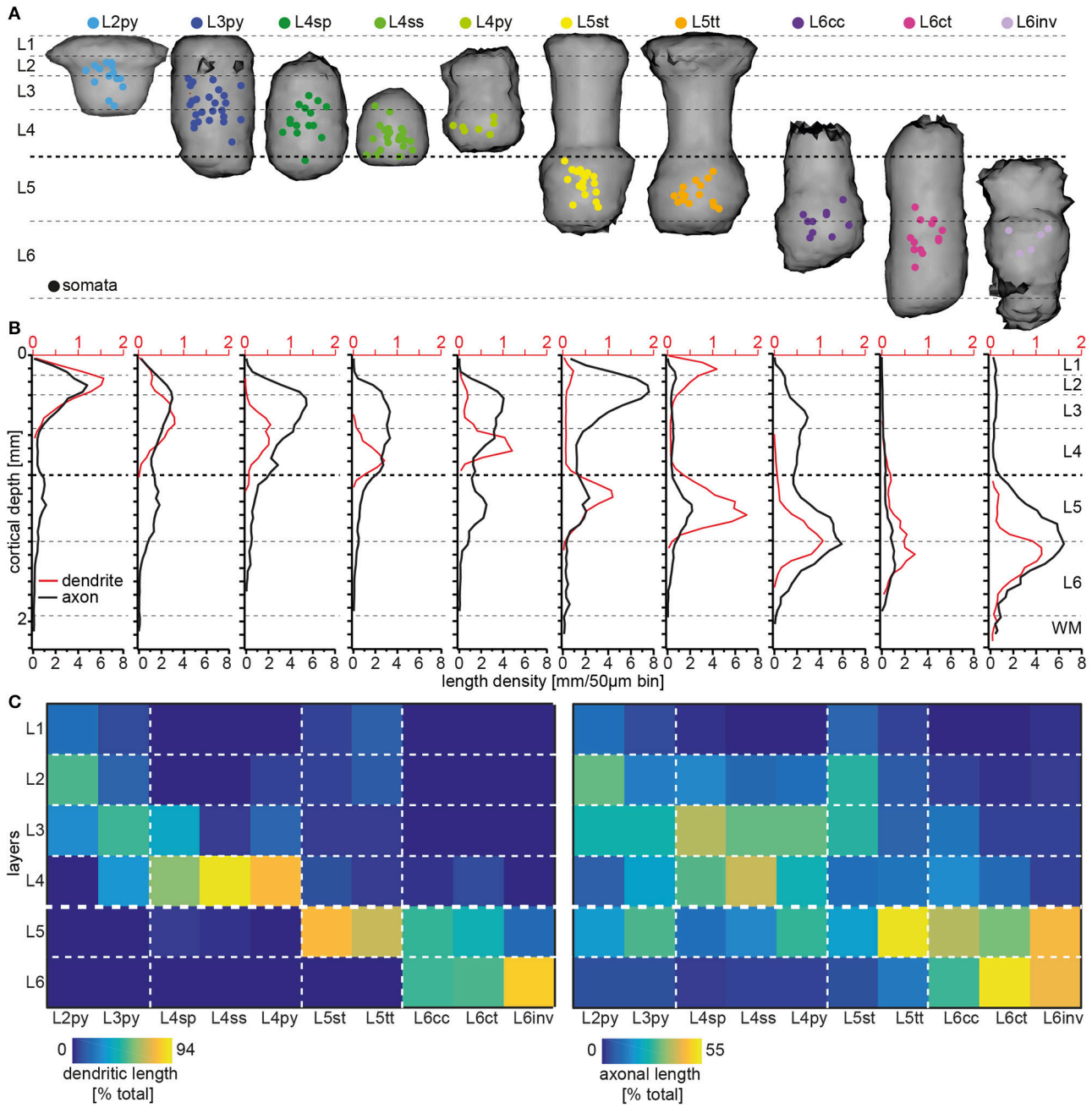

FIGURE 3 | Layer-specific organization of excitatory cell types in rat vS1. **(A)** 3D volumes spanned by registered dendrite morphologies from the 10 major excitatory cell types, respectively. Colored dots denote the soma locations of the *in vivo* recorded/reconstructed neurons (modified from Oberlaender et al., 2012; Narayanan et al., 2015 with permission). **(B)** 1D length density profile of dendrites (red) and axons (black) averaged across all neurons assigned to one of the 10 excitatory cell types (adapted from Narayanan et al., 2015 with permission). **(C)** Quantification of cell type-specific and layer-related dendrite (left panel) and axon (right panel) distributions. The colors denote the relative amount of dendrite/axon per cell type within each layer, normalized to the total dendritic/axonal length of the respective type.

(e.g., in L5 Groh et al., 2010), intrinsic physiological properties (e.g., in L5 Hattox and Nelson, 2007), local connectivity patterns (e.g., in L5 Brown and Hestrin, 2009) or brain-wide input populations (e.g., in L5 Kim et al., 2015). Not entirely surprising, we found that the cell type-specific structure-function-relationships extend to *in vivo* activity patterns. The ten classes described above may thus represent the major excitatory cell types of rat vS1, and potentially of all sensory

TABLE 1 | Number of somata, and length of dendrites and axon that each of the 10 major excitatory cell types contributes to each of the six layers of the modeled barrel column.

	L2py	L3py	L4sp	L4ss	L4py	L5st	L5tt	L6cc	L6ct	L6inv
SOMATA										
L1	34									
L2	1,074	52								
L3	725	1,501	413	113						
L4		1,028	1,024	2,336	517					
L5		67	248	4		1,446	1,106	719	260	12
L6								648	3,711	778
DENDRITE [m]										
L1	7.9	2.7				0.9	3.4			
L2	15.4	5.7	0.1		0.5	0.8	2.1			
L3	8.9	20.3	2.2	0.3	1.3	0.7	0.9			
L4	0.1	21.3	5.0	8.1	6.2	2.0	1.5	0.4	2.3	
L5		1.7	0.9	0.3		16.6	21.9	10.4	13.0	2.6
L6						0.1	0.2	8.7	37.2	11.1
AXON [m]										
L1	16.1	15.3	2.1	0.3	0.3	14.0	1.1	1.2	0.1	0.7
L2	46.5	45.7	19.4	12.3	8.8	45.0	3.0	5.7	0.7	1.5
L3	38.6	84.0	48.6	43.6	22.6	47.5	3.7	24.7	2.2	2.9
L4	12.2	73.4	43.5	59.5	19.9	22.5	5.5	35.0	9.6	3.8
L5	38.3	117.5	17.2	24.7	26.1	42.9	31.2	90.5	38.0	45.7
L6	6.8	20.3	4.9	3.6	3.3	9.6	12.1	96.0	59.3	67.7

cortices (reviewed in Harris and Shepherd, 2015). Therefore, we quantified the degree to which the structural properties of each (dendritic) cell type are organized with respect to the six (somatic) layers of the cortex.

Somata of the respective cell types are not restricted to the layer that is suggested by their naming convention (**Figure 3A**). Specifically, somata of neurons with the dendritic morphology of L2py are found throughout L2 and L3, but are more frequent within L2 (see **Table 1** for the fraction of neurons per cell type per layer). Similarly, somata of L3py are distributed throughout L3 and L4, but are not found in L2. In contrast, somata of L4ss and L4py are largely restricted to L4, whereas those of L4sp are also found in lower L3. L5st and L5tt are restricted to L5, with L5st being more abundant in upper L5 (i.e., L5A: ∼80/20% L5st/L5tt) compared to L5tt that are more abundant in deep L5 (i.e., L5B: ∼40/60% L5st/L5tt) (Oberlaender et al., 2011). Somata of L6ct and L6inv are largely restricted to L6. In contrast, L6cc are distributed around the L5/6 border (i.e. in deep L5, see also Kasper et al., 1994 and upper L6). Thus, within each layer, somata from multiple excitatory cell types intermingle. The only layer border that separated between somata of different excitatory cell types was the L4/5 border (Narayanan et al., 2015).

Next, we calculated a convex hull around the dendrites from all cells that had been assigned to a respective cell type (**Figure 3A**). Remarkably, these dendritic "innervation volumes" showed several relationships with layers (see also Elston et al., 1997, 1999). Specifically, dendrites of L2py are restricted to L1-3 and those of L3py are restricted to L1-4. In contrast, dendrites of L4py and L4sp do not innervate L1 and are restricted to L2-4. Dendrites of L4ss are largely confined to L4. Dendrites of L5st and L5tt extend across L1 to L5 and terminate at the L5/6 border. Dendrites of L6cc and L6ct range from L4-6, whereas those of L6inv remain within L5 and L6. Thus, even though soma distributions of the 10 cell types are only loosely related to layers and the borders between them, and dendrites of each cell type extend across multiple layers, the dendrite distributions display cell type-specific relationships with cytoarchitectonic landmarks (**Figure 3B**).

Finally, we investigated whether IC axon distributions of each cell type are also organized with respect to layers. In a previous study, we had shown that the IC axon projections of individual excitatory neurons are correlated with their respective dendritic cell type (Narayanan et al., 2015). The cell type-specific axon differences were only partly reflected by parameters such as overall path lengths or topology, but originated primarily from different vertical (i.e., laminar, **Figure 3B**) and horizontal (i.e., trans-columnar) projection patterns (Narayanan et al., 2015). Specifically, axons of L2py densely innervate L1-3 and less densely L5, with the two innervation peaks coinciding with the centers of L3 and L5, respectively. Axons of L3py have similar axon projection patterns compared to L2py, but innervation of L5 is as dense as innervation of L3, where the peak coincides with the L2/3 border. Axons of the three L4 cell types deviate from most other cell types, as they do not innervate L1. Apart from this difference, the vertical axon profile of L4py resembles the one of the L3py. Axons of L4sp and L4ss are restricted to L2-4. However, axons of L4sp are most dense within L2/3 (the innervation peak coincides with the L2/3 border), whereas axons of L4ss are equally dense in L2/3 and L4. Axons of both, L5st and L5tt, innervate L1-5, but in contrast to L5tt, L5st project densely to L2 and L3 (the innervation peak coincides with the L2/3 border). Axons of L6cc and L6inv innervate the entire cortical depth from the pial surface to the WM tract, whereas L6ct axons are sparse and restricted to L4-6. Axons of L6inv are sparse in L1-4, but dense in L5 and L6 (the innervation peak coincides with the L5/6 border). In contrast, axons of L6cc are most elaborate within L5-6, but also abundant in L3-4, and sparsely innervate L1-2.

We conclude that IC axon morphologies are cell type-specific and layer-related, because the peaks, minima and/or vertical extents of their respective axon density profiles coincide with layer borders and/or centers in a cell type-specific manner. Moreover, we had shown previously that the layer-related distributions of cell type-specific IC axon projection patterns are linked to multiple horizontal (i.e., trans-columnar) organizational principles (Narayanan et al., 2015). With the exception of L4ss and L6ct, the majority of axon from neurons of each cell type is located outside the barrel column containing the soma. These trans-columnar, horizontal patterns are subdivided into three principles: (1) axons that extend widest along barrel columns that represent whiskers of the same row (i.e., "rowish" axons), (2) axons that extend widest orthogonal to the row [i.e., along barrel columns that represent whiskers of the same arc ("arcish")], or (3) axons that extend unspecifically to all neighboring columns and even beyond (Narayanan et al., 2015). Interestingly, and independent of the cell type, arcish axons are primarily confined to L1-4, rowish axon projections to L5-6.

In summary, dendrite and axon distributions of the 10 excitatory cell types in rat vS1 are organized with respect to

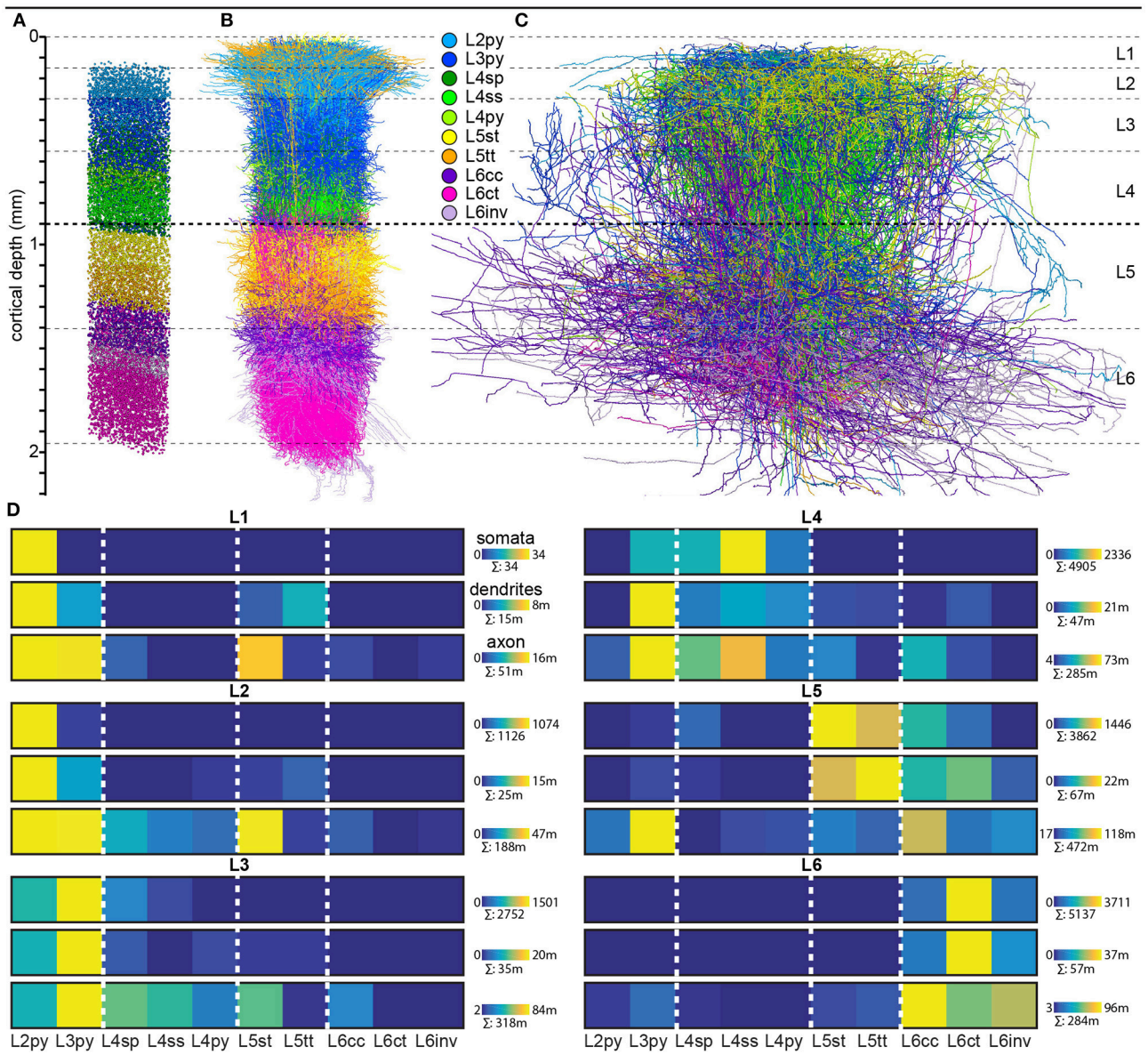

FIGURE 4 | Cell type-specific organization of cortical layers in rat vS1**. (A)** Semi-coronal view of the cell type-specific soma distribution in a dense model of an average cortical barrel column. **(B)** Corresponding to panel A: model of the cell type-specific distribution of dendrites. **(C)** Corresponding to **A**: model of the cell type-specific distribution of axons. **(D)** Quantification of cell type-specific structural composition of each layer with respect to somata (top rows), dendrites (center rows), and axons (bottom rows). Dendritic and axonal length represent all neurons in vS1 whose respective dendrites and/or axons extend into the volume of the modeled barrel column. **(A–C)** were adapted and modified from Oberlaender et al., 2012; Meyer et al., 2013; Egger et al., 2014; Narayanan et al., 2015 with permission.

cytoarchitectonic layers. However, the laminar landmarks that coincide with the respective dendrite or axon distributions are different and specific for each cell type. For example, even though somata of L2py and L3py intermingle within L3, the vertical extents of their dendrite distributions coincide with the vertical extents of L1-3 and L1-4, respectively. The vertical axon distributions of these two cell types delineate the center and extent of L5, whereas their peak axon densities in the superficial layers coincide with the center of L2 and the L2/3 border, respectively. To provide a comprehensive overview of the degrees to which dendrite and axon distributions of the different cell types are organized with respect to layers, we calculated the relative amount of dendrite and axon path length within each layer for each cell type (**Figure 3C**).

CELL TYPE-SPECIFIC ORGANIZATION OF CORTICAL LAYERS IN RAT vS1

Finally, we quantified the cell type-specific structural composition of each layer. We had previously reported an

approach to generate a dense model of the 3D distributions of cell type-specific somata, dendrites and axons within an average cortical barrel column (Egger et al., 2014). Specifically, we used the 153 reconstructed and registered neuron morphologies to estimate the frequency of occurrence of somata from each cell type along the vertical cortex axis (i.e., at 50 μm resolution), as well as the relative overlaps between cell types (Egger et al., 2014). This allowed assigning each neuron from the measured and registered soma distribution to one of the ten cell types (**Figure 4A**). The resultant model of an average barrel column representing the D2 whisker comprises 17,816 excitatory somata (see **Table 2** for the number of neurons per cell type). Each soma in this model is represented by a dendrite morphology of the respective cell type (**Figure 4B**), whose registered soma depth was within 50 μm from the location in the model (Egger et al., 2014). This upscaling of the reconstructions resulted in a total dendritic path length that is found within an average barrel column of 246 m (i.e., originating from all excitatory neurons within entire vS1; see also **Table 2** for dendritic path lengths contributed by each cell type). Similarly, we upscaled the registered axon morphologies to the respective number of neurons per cell type (**Figure 4C**). The resultant total (i.e., from all excitatory neurons in vS1) axonal path length within the average barrel column model is 1,599 m (see **Table 2** for axon path lengths by each cell type).

By combining the dense structural model of an average barrel column with our quantification of the layer borders, we estimated the number of somata, as well as the dendritic and axonal path lengths that each of the 10 cell types contributes to each of the six layers (**Figure 4D**). Within the average column model, the majority of dendrites in L1 originates from L2py, followed by L5tt, L3py, and L5st. The majority of axons originates from L2py, followed by L3py and L5st (see also **Table 1**). Similar to L1, the majority of the dendrites in L2 originates from L2py, followed by L3py and L5tt. The majority of axons in L2 originates to almost equal amounts from L2py, L3py, and L5st. In L3, L3py, followed by L2py and L4sp contribute the most dendrites, whereas axons in L3 originate from L3py, followed by L5st and the three cell types in L4. The cell type contributing the most dendrites to L4 are L3py, followed by the three L4 cell types. The majority of axon in L4 originates from L3py, L4ss, L4sp, and L6cc. Layer 5 comprises dendrites primarily from L5tt, closely followed by L5st and L6ct. In turn, the majority of axon in L5 originates from L3py, followed by L6cc, followed by similar contributions from all remaining cell types. Layer 6 is more homogeneous than the other layers, with the majority of dendrites and axons originating from the three L6 cell types.

TABLE 2 | Number of somata, and length of dendrites and axon that each of the 10 major excitatory cell types contributes to the model of an average cortical barrel column.

	L2py	L3py	L4sp	L4ss	L4py	L5st	L5tt	L6cc	L6ct	L6inv
Somata	1,833	2,648	1,685	2,453	517	1,446	1,106	1,367	3,971	790
Dendrite [m]	32.2	51.7	8.2	8.7	8.0	21.1	30.0	19.5	52.5	13.7
Axon [m]	158.5	356.3	135.8	144.0	81.0	181.4	56.7	253.0	109.9	122.3

HOW CELL TYPE-SPECIFIC ARE LAYERS AND HOW LAYER-SPECIFIC ARE CELL TYPES?

In this review article, we combined several of our previous studies to quantify the degree to which soma, dendrite and axon distributions of the ten major excitatory cell types of rat vS1 are organized with respect to cytoarchitectonic layers. Even though the cell types are purely defined by dendrite morphology, intrinsic properties (Feldmeyer et al., 2013), *in vivo* function (de Kock et al., 2007; Oberlaender et al., 2012), as well as IC axon projection patterns (Narayanan et al., 2015) are cell type-specific. Defining the six layers based on precise measurements of neuron soma distributions revealed that each layer comprises somata of multiple cell types. Nonetheless, dendrite and IC axon innervation patterns of each cell type showed distributions that were related to several laminar landmarks (i.e., center/extent of layers or layer borders). The respective laminar landmarks depended on the cell type, and typically deviated between dendrites and axons within a cell type. Thus, cytoarchitectonic layers can be regarded as a structural reference frame, which gives rise to several cell type-specific dendrite and IC axon projection patterns.

The observation that dendrites and axons of excitatory cortical cell types are organized with respect to laminar landmarks—and may hence be referred to as layer-specific—does not imply that layers are organized in a cell type-specific manner. This is because somata of multiple cell types intermingle within and across layers (i.e., only the L4/5 border represents a cell type border), and the layer-specific organization of dendrites and axons is different for each of those intermingling cell types. Hence, using layers as a synonym for cell types, for example when describing cortical circuits, may yield ambiguous results. For example, the canonical pathway theory suggests that thalamocortical input to L4 is first relayed to L2/3 and then to L5. However, apart from L4ss and L4sp that primarily project their axons to L2-4, L4 comprises also L3py and L4py, which have additional dense axon projections directly to L5. The present quantifications of the layer-related morphological organization of excitatory cell types (**Figure 3**) and the cell type-specific structural composition of cortical layers (**Figure 4**) may hence aid future studies to better interpret layer-specific measurements or manipulations with respect to the underlying cell types and circuits.

The layer-related structural organization of excitatory cell types, as reviewed here, is not limited to the local cortical circuitry, but extends to long-range pathways. For example, thalamocortical axons originating in the ventral posterior medial nucleus of the thalamus (VPM) define the extent of L4 and coincide with the L5/6 border in rat vS1. In contrast, axonal projections into vS1 from neurons in the posterior medial nucleus of the thalamus (POm) delineate L1 and coincide with the L4/5 border (Wimmer et al., 2010). In addition to layer-related thalamocortical input patterns, cortical output neurons have specific vertical soma distributions that reflect their respective long-range target areas. For example, VPM-projecting L6ct are located in upper L6 (i.e., L6A), whereas

those that project additionally to POm are found in L6B (Zhang and Deschenes, 1997). Similarly, somata of intratelencephalic L5 neurons (ITs)—which are defined by long-range axons that project to the striatum and other cortical areas (Harris and Shepherd, 2015)—are more frequent in L5A, whereas those that project to subcortical targets (i.e., pyramidal tract neurons, PTs Wise and Jones, 1977) are primarily located in L5B. Moreover, we have recently shown that somata of PTs form two sublayers that reflect specific subcortical targets (e.g., POm-projectors are more superficial within L5B than those PTs that innervate the Pons, Rojas-Piloni et al., 2017). The 10 major excitatory cell types of the cortex may thus be divided into further subtypes that differ in their long-range targets, and/or additional structural and functional properties (for a review, e.g., DeFelipe and Farinas, 1992; Spruston, 2008; Harris and Shepherd, 2015) that go beyond those described here (e.g., density and distribution of spines Elston, 2002), and whose respective vertical soma distributions define sublayers within the six cytoarchitectonic layers.

AUTHOR CONTRIBUTIONS

MO designed the review. RN and DU performed data analysis. All authors wrote the paper.

ACKNOWLEDGMENTS

Funding was provided by the Bernstein Center for Computational Neuroscience, funded by German Federal Ministry of Education and Research Grant BMBF/FKZ 01GQ1002, the European Research Council (ERC) under the European Union's Horizon 2020 research and innovation program (grant agreement No 633428), and the Center of Advanced European Studies and Research (caesar).

REFERENCES

Anderson, S. A., Eisenstat, D. D., Shi, L., and Rubenstein, J. L. (1997). Interneuron migration from basal forebrain to neocortex: dependence on Dlx genes. *Science* 278, 474–476. doi: 10.1126/science.278.5337.474

Ankerst, M., Breunig, M. M., Kriegel, H.-P., and Sander, J. (1999). "OPTICS: ordering points to identify the clustering structure", in *ACM Sigmod Record* (New York, NY: ACM), 49–60.

Brecht, M., Schneider, M., Sakmann, B., and Margrie, T. W. (2004). Whisker movements evoked by stimulation of single pyramidal cells in rat motor cortex. *Nature* 427, 704–710. doi: 10.1038/nature02266

Brodmann, K. (1909). *Vergleichende Lokalisationslehre der Großhirnrinde - in ihren Prinzipien dargestellt auf Grund des Zellenbaues*. Leipzig: Barth.

Brown, S. P., and Hestrin, S. (2009). Intracortical circuits of pyramidal neurons reflect their long-range axonal targets. *Nature* 457, 1133–1136. doi: 10.1038/nature07658

Bureau, I., Von Saint Paul, F., and Svoboda, K. (2006). Interdigitated paralemniscal and lemniscal pathways in the mouse barrel cortex. *PLoS Biol.* 4:e382. doi: 10.1371/journal.pbio.0040382

de Kock, C. P., and Sakmann, B. (2009). Spiking in primary somatosensory cortex during natural whisking in awake head-restrained rats is cell-type specific. *Proc. Natl. Acad. Sci. U.S.A.* 106, 16446–16450. doi: 10.1073/pnas.0904143106

de Kock, C. P., Bruno, R. M., Spors, H., and Sakmann, B. (2007). Layer- and cell-type-specific suprathreshold stimulus representation in rat primary somatosensory cortex. *J. Physiol.* 581, 139–154. doi: 10.1113/jphysiol.2006.124321

DeFelipe, J. (2011). The evolution of the brain, the human nature of cortical circuits, and intellectual creativity. *Front. Neuroanat.* 5:29. doi: 10.3389/fnana.2011.00029

DeFelipe, J., and Fariñas, I. (1992). The pyramidal neuron of the cerebral cortex: morphological and chemical characteristics of the synaptic inputs. *Prog. Neurobiol.* 39, 563–607. doi: 10.1016/0301-0082(92)90015-7

Deweese, M. R., Wehr, M., and Zador, A. M. (2003). Binary spiking in auditory cortex. *J. Neurosci.* 23, 7940–7949.

Douglas, R. J., and Martin, K. A. (2004). Neuronal circuits of the neocortex. *Annu. Rev. Neurosci.* 27, 419–451. doi: 10.1146/annurev.neuro.27.070203.144152

Egger, R., Dercksen, V. J., Udvary, D., Hege, H. C., and Oberlaender, M. (2014). Generation of dense statistical connectomes from sparse morphological data. *Front. Neuroanat.* 8:129. doi: 10.3389/fnana.2014.00129

Egger, R., Narayanan, R. T., Helmstaedter, M., De Kock, C. P., and Oberlaender, M. (2012). 3D reconstruction and standardization of the rat vibrissal cortex for precise registration of single neuron morphology. *PLoS Comput. Biol.* 8:e1002837. doi: 10.1371/journal.pcbi.1002837

Elston, G. N. (2002). Cortical heterogeneity: implications for visual processing and polysensory integration. *J. Neurocytol.* 31, 317–335. doi: 10.1023/A:1024182228103

Elston, G. N. (2003). Cortex, cognition and the cell: new insights into the pyramidal neuron and prefrontal function. *Cereb. Cortex* 13, 1124–1138. doi: 10.1093/cercor/bhg093

Elston, G. N., Benavides-Piccione, R., Elston, A., Manger, P. R., and Defelipe, J. (2011). Pyramidal cells in prefrontal cortex of primates: marked differences in neuronal structure among species. *Front. Neuroanat.* 5:2. doi: 10.3389/fnana.2011.00002

Elston, G. N., Defelipe, J., Arellano, J. I., Gonzilez-Albo, M. C., and Rosa, M. G. (1999). Variation in the spatial relationship between parvalbumin immunoreactive interneurones and pyramidal neurones in rat somatosensory cortex. *Neuroreport* 10, 2975–2979. doi: 10.1097/00001756-199909290-00019

Elston, G. N., Pow, D. V., and Calford, M. B. (1997). Neuronal composition and morphology in layer IV of two vibrissal barrel subfields of rat cortex. *Cereb. Cortex* 7, 422–431. doi: 10.1093/cercor/7.5.422

Feldmeyer, D., Brecht, M., Helmchen, F., Petersen, C. C., Poulet, J. F., Staiger, J. F., et al. (2013). Barrel cortex function. *Prog. Neurobiol.* 103, 3–27. doi: 10.1016/j.pneurobio.2012.11.002

Ferrante, M., Tahvildari, B., Duque, A., Hadzipasic, M., Salkoff, D., Zagha, E. W., et al. (2017). Distinct functional groups emerge from the intrinsic properties of molecularly identified entorhinal interneurons and principal cells. *Cereb. Cortex* 27, 3186–3207. doi: 10.1093/cercor/bhw143

Fitzpatrick, D., Itoh, K., and Diamond, I. T. (1983). The laminar organization of the lateral geniculate body and the striate cortex in the squirrel monkey (*Saimiri sciureus*). *J. Neurosci.* 3, 673–702.

Garey, L. J. (1994). *Brodmann's 'Localisation in the Cerebral Cortex'*. Singapore: World Scientific Publishing Co Pte Ltd.

Gorski, J. A., Talley, T., Qiu, M. S., Puelles, L., Rubenstein, J. L. R., and Jones, K. R. (2002). Cortical excitatory neurons and glia, but not GABAergic neurons, are produced in the Emx1-expressing lineage. *J. Neurosci.* 22, 6309–6314.

Groh, A., Meyer, H. S., Schmidt, E. F., Heintz, N., Sakmann, B., and Krieger, P. (2010). Cell-type specific properties of pyramidal neurons in neocortex underlying a layout that is modifiable depending on the cortical area. *Cereb. Cortex* 20, 826–836. doi: 10.1093/cercor/bhp152

Gur, M., and Snodderly, D. M. (2008). Physiological differences between neurons in layer 2 and layer 3 of primary visual cortex (V1) of alert macaque monkeys. *J. Physiol.* 586, 2293–2306. doi: 10.1113/jphysiol.2008.151795

Harris, K. D., and Shepherd, G. M. (2015). The neocortical circuit: themes and variations. *Nat. Neurosci.* 18, 170–181. doi: 10.1038/nn.3917

Hattox, A. M., and Nelson, S. B. (2007). Layer V neurons in mouse cortex projecting to different targets have distinct physiological properties. *J. Neurophysiol.* 98, 3330–3340. doi: 10.1152/jn.00397.2007

Hendry, S. H., Schwark, H. D., Jones, E. G., and Yan, J. (1987). Numbers and proportions of GABA-immunoreactive neurons in different areas of monkey cerebral cortex. *J. Neurosci.* 7, 1503–1519.

Kaas, J. H. (2013). The evolution of brains from early mammals to humans. *Wiley Interdiscip. Rev.* 4, 33–45. doi: 10.1002/wcs.1206

Kasper, E. M., Larkman, A. U., Lübke, J., and Blakemore, C. (1994). Pyramidal neurons in layer 5 of the rat visual cortex. I. Correlation among cell morphology, intrinsic electrophysiological properties, and axon targets. *J. Comp. Neurol* 339, 459–474. doi: 10.1002/cne.903390402

Kaufman, D. L., Mcginnis, J. F., Krieger, N. R., and Tobin, A. J. (1986). Brain glutamate decarboxylase cloned in lambda gt-11: fusion protein produces gamma-aminobutyric acid. *Science* 232, 1138–1140. doi: 10.1126/science.3518061

Kim, E. J., Juavinett, A. L., Kyubwa, E. M., Jacobs, M. W., and Callaway, E. M. (2015). Three Types of Cortical Layer 5 Neurons That Differ in Brain-wide Connectivity and Function. *Neuron* 88, 1253–1267. doi: 10.1016/j.neuron.2015.11.002

Kumar, P., and Ohana, O. (2008). Inter- and intralaminar subcircuits of excitatory and inhibitory neurons in layer 6a of the rat barrel cortex. *J. Neurophysiol.* 100, 1909–1922. doi: 10.1152/jn.90684.2008

Lund, J. S. (1973). Organization of neurons in the visual cortex, area 17, of the monkey (*Macaca mulatta*). *J. Comp. Neurol.* 147, 455–496. doi: 10.1002/cne.901470404

Lund, J. S., and Wu, C. Q. (1997). Local circuit neurons of macaque monkey striate cortex: IV. Neurons of laminae 1-3A. *J. Comp. Neurol.* 384, 109–126. doi: 10.1002/(SICI)1096-9861(19970721)384:1<109::AID-CNE7>3.0.CO;2-5

Meyer, H. S., Egger, R., Guest, J. M., Foerster, R., Reissl, S., and Oberlaender, M. (2013). Cellular organization of cortical barrel columns is whisker-specific. *Proc. Natl. Acad. Sci. U.S.A.* 110, 19113–19118. doi: 10.1073/pnas.1312691110

Meyer, H. S., Schwarz, D., Wimmer, V. C., Schmitt, A. C., Kerr, J. N., Sakmann, B., et al. (2011). Inhibitory interneurons in a cortical column form hot zones of inhibition in layers 2 and 5A. *Proc. Natl. Acad. Sci. U.S.A.* 108, 16807–16812. doi: 10.1073/pnas.1113648108

Meyer, H. S., Wimmer, V. C., Oberlaender, M., De Kock, C. P., Sakmann, B., and Helmstaedter, M. (2010). Number and laminar distribution of neurons in a thalamocortical projection column of rat vibrissal cortex. *Cereb. Cortex* 20, 2277–2286. doi: 10.1093/cercor/bhq067

Mullen, R. J., Buck, C. R., and Smith, A. M. (1992). NeuN, a neuronal specific nuclear protein in vertebrates. *Development* 116, 201–211.

Narayanan, R. T., Egger, R., Johnson, A. S., Mansvelder, H. D., Sakmann, B., De Kock, C. P., et al. (2015). Beyond columnar organization: cell type- and target layer-specific principles of horizontal axon projection patterns in rat vibrissal cortex. *Cereb. Cortex* 25, 4450–4468. doi: 10.1093/cercor/bhv053

Narayanan, R. T., Mohan, H., Broersen, R., De Haan, R., Pieneman, A. W., and De Kock, C. P. J. (2014). Juxtasomal biocytin labeling to study the structure-function relationship of individual cortical neurons. *J. Vis. Exp.* 25:e51359. doi: 10.3791/51359

Oberlaender, M., Boudewijns, Z. S., Kleele, T., Mansvelder, H. D., Sakmann, B., and De Kock, C. P. (2011). Three-dimensional axon morphologies of individual layer 5 neurons indicate cell type-specific intracortical pathways for whisker motion and touch. *Proc. Natl. Acad. Sci. U.S.A.* 108, 4188–4193. doi: 10.1073/pnas.1100647108

Oberlaender, M., De Kock, C. P., Bruno, R. M., Ramirez, A., Meyer, H. S., Dercksen, V. J., et al. (2012). Cell type-specific three-dimensional structure of thalamocortical circuits in a column of rat vibrissal cortex. *Cereb. Cortex* 22, 2375–2391. doi: 10.1093/cercor/bhr317

Olshausen, B. A., and Field, D. J. (2004). Sparse coding of sensory inputs. *Curr. Opin. Neurobiol.* 14, 481–487. doi: 10.1016/j.conb.2004.07.007

Petersen, C. C., and Crochet, S. (2013). Synaptic computation and sensory processing in neocortical layer 2/3. *Neuron* 78, 28–48. doi: 10.1016/j.neuron.2013.03.020

Pinault, D. (1996). A novel single-cell staining procedure performed *in vivo* under electrophysiological control: morpho-functional features of juxtacellularly labeled thalamic cells and other central neurons with biocytin or Neurobiotin. *J. Neurosci. Methods* 65, 113–136. doi: 10.1016/0165-0270(95)00144-1

Rockland, K. S. (2017). What do we know about laminar connectivity? *Neuroimage.* doi: 10.1016/j.neuroimage.2017.07.032. [Epub ahead of print].

Rojas-Piloni, G., Guest, J. M., Egger, R., Johnson, A. S., Sakmann, B., and Oberlaender, M. (2017). Relationships between structure, *in vivo* function and long-range axonal target of cortical pyramidal tract neurons. *Nat. Commun.* 8:870. doi: 10.1038/s41467-017-00971-0

Shepherd, G. M., and Svoboda, K. (2005). Laminar and columnar organization of ascending excitatory projections to layer 2/3 pyramidal neurons in rat barrel cortex. *J. Neurosci.* 25, 5670–5679. doi: 10.1523/JNEUROSCI.1173-05.2005

Somogyi, P., Cowey, A., Halász, N., and Freund, T. F. (1981). Vertical organization of neurones accumulating 3H-GABA in visual cortex of rhesus monkey. *Nature* 294, 761–763. doi: 10.1038/294761a0

Spruston, N. (2008). Pyramidal neurons: dendritic structure and synaptic integration. *Nat. Rev. Neurosci.* 9, 206–221. doi: 10.1038/nrn2286

Staiger, J. F., Flagmeyer, I., Schubert, D., Zilles, K., Kotter, R., and Luhmann, H. J. (2004). Functional diversity of layer IV spiny neurons in rat somatosensory cortex: quantitative morphology of electrophysiologically characterized and biocytin labeled cells. *Cereb, Cortex* 14, 690–701. doi: 10.1093/cercor/bhh029

Tasic, B., Menon, V., Nguyen, T. N., Kim, T. K., Jarsky, T., Yao, Z., et al. (2016). Adult mouse cortical cell taxonomy revealed by single cell transcriptomics. *Nat. Neurosci.* 19, 335–346. doi: 10.1038/nn.4216

Vinje, W. E., and Gallant, J. L. (2000). Sparse coding and decorrelation in primary visual cortex during natural vision. *Science* 287, 1273–1276. doi: 10.1126/science.287.5456.1273

Wimmer, V. C., Bruno, R. M., De Kock, C. P. J., Kuner, T., and Sakmann, B. (2010). Dimensions of a projection column and architecture of VPM and POm axons in rat vibrissal cortex. *Cereb. Cortex* 20, 2265–2276. doi: 10.1093/cercor/bhq068

Wise, S. P., and Jones, E. G. (1977). Cells of origin and terminal distribution of descending projections of the rat somatic sensory cortex. *J. Comp. Neurol* 175, 129–157. doi: 10.1002/cne.901750202

Zeisel, A., Muñoz-Manchado, A. B., Codeluppi, S., Lönnerberg, P., La Manno, G., Juréus, A., et al. (2015). Brain structure. Cell types in the mouse cortex and hippocampus revealed by single-cell RNA-seq. *Science* 347, 1138–1142. doi: 10.1126/science.aaa1934

Zhang, Z. W., and Deschenes, M. (1997). Intracortical axonal projections of lamina VI cells of the primary somatosensory cortex in the rat: a single-cell labeling study. *J. Neurosci.* 17, 6365–6379.

Conflict of Interest Statement: The authors declare that the research was conducted in the absence of any commercial or financial relationships that could be construed as a potential conflict of interest.

frontiers in Neuroanatomy

REVIEW
published: 17 July 2018
doi: 10.3389/fnana.2018.00056

A Perspective on Cortical Layering and Layer-Spanning Neuronal Elements

Matthew E. Larkum[1]*, *Lucy S. Petro*[2], *Robert N. S. Sachdev*[1]* and *Lars Muckli*[2]*

[1]Neurocure Center for Excellence, Charité Universitätsmedizin Berlin & Humboldt Universität, Berlin, Germany, [2]Centre for Cognitive Neuroimaging, Institute of Neuroscience and Psychology, University of Glasgow, Glasgow, United Kingdom

This review article addresses the function of the layers of the cerebral cortex. We develop the perspective that cortical layering needs to be understood in terms of its functional anatomy, i.e., the terminations of synaptic inputs on distinct cellular compartments and their effect on cortical activity. The cortex is a hierarchical structure in which feed forward and feedback pathways have a layer-specific termination pattern. We take the view that the influence of synaptic inputs arriving at different cortical layers can only be understood in terms of their complex interaction with cellular biophysics and the subsequent computation that occurs at the cellular level. We use high-resolution fMRI, which can resolve activity across layers, as a case study for implementing this approach by describing how cognitive events arising from the laminar distribution of inputs can be interpreted by taking into account the properties of neurons that span different layers. This perspective is based on recent advances in measuring subcellular activity in distinct feed-forward and feedback axons and in dendrites as they span across layers.

Keywords: feedback, feedforward networks, top-down processing, calcium spikes, apical dendrite, ultra-highfield fMRI, layer fMRI

OPEN ACCESS

Edited by:
Kathleen S. Rockland, Boston University, United States

Reviewed by:
Stewart Shipp, University College London, United Kingdom
Andreas H. Burkhalter, Washington University in St. Louis, United States

***Correspondence:**
Matthew E. Larkum
matthew.larkum@gmail.com
Robert N. S. Sachdev
bs387ster@gmail.com
Lars Muckli
lars.muckli@glasgow.ac.uk

Received: *02 August 2017*
Accepted: *19 June 2018*
Published: *17 July 2018*

Citation:
Larkum ME, Petro LS, Sachdev RNS and Muckli L (2018) A Perspective on Cortical Layering and Layer-Spanning Neuronal Elements. Front. Neuroanat. 12:56. doi: 10.3389/fnana.2018.00056

CONCEPTUAL SHIFT

Neuroscience has seen a dramatic evolution since the early anatomical investigations of the 19th and 20th centuries. With the discovery of different ways to stain brain tissue, the original emphasis was on cataloging the components of the brain (**Figure 1A**, "Components"). This approach was enormously successful in describing the structure of the cerebral cortex as a laminar structure based on the cytoarchitecture. Reaching its zenith in the first half of the 20th century (Defelipe et al., 1988), ever more detailed descriptions of the precise configuration of cells and axons promised to explain the function of the cerebral cortex. However, with the development of techniques for recording activity directly from the neurons of the brain, the original focus on a faithful anatomical description gave way to more simplified descriptions of the functional anatomy, i.e., organization and connectivity of structures (Hubel and Wiesel, 1962; Mountcastle, 1978). Here, various models were offered for describing the organization of the cortex (**Figure 1B**, "Connectivity"). The increased emphasis on connectivity often came at the expense of the complexity of the components, mostly treated as simple point neurons. In this article, we take the view that a full description of a laminar structure like the cortex will require the successful marriage of both the components and the connectivity that captures an adequate description of both aspects and their interplay.

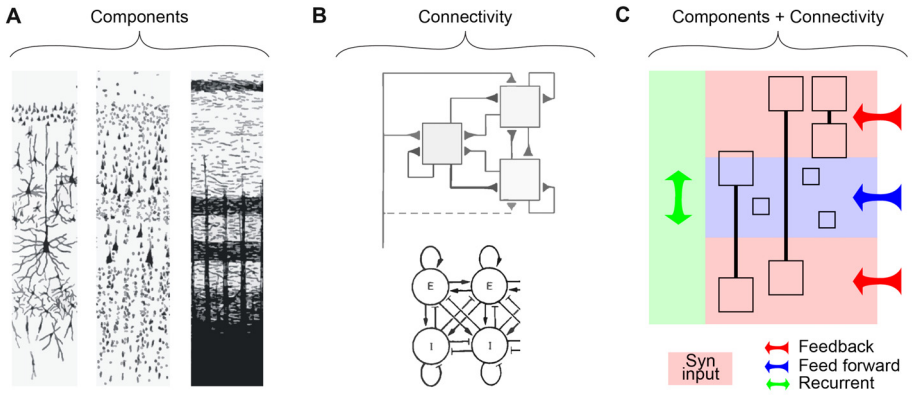

FIGURE 1 | Shifting perspectives about cortical layering. **(A)** Nineteenth century descriptions of the cortex emphasizing the components in terms of cytoarchitecture and axonal projections. Left, Golgi stain; Middle, Nissl stain; Right, Weigert stain (Heimer, 1994, adapted with permission). **(B)** Functional views emphasizing connectivity in the cortex. Top, "canonical circuit" of the neocortex (Douglas et al., 1989, adapted with permission); Bottom, balance of excitation and inhibition (Wilson and Cowan, 1972, 1973; adapted with permission). **(C)** A simplified representation of the class of description needed to describe emerging data in terms of the underlying architecture of a layered structure such as the cortex. Here, components (i.e., neurons) are described in terms of their principle dendritic compartments (boxes) and the way they span the cortical layers. Small boxes represent neurons that putatively can be still described as point neurons (although this is yet to be established). The proposed combined perspective should take into account the broad influences of long- (Feedback, red and Feed forward, blue) and short-range (Recurrent, green) connectivity and the functional components (compartmental neurons) that span multiple layers simultaneously.

WHAT DEFINES A LAYER AS A SUBUNIT OF FUNCTION?

Treating neurons as single points comes at a great price in a layered structure like the cortex. In fact, neurons have complicated morphologies and properties that typically span multiple layers. It is conventional to refer to "cells of a specific layer." The description "layer 5 neuron," for instance, conventionally refers to a neuron whose *cell body* lies in layer 5. However, the properties of this cell are distributed across multiple cortical layers throughout their dendrites and axon. The merging of components and connectivity in a description of the layered cortex needs to take into account the location and influence of synaptic inputs and the resultant electrical events that occur within layer-spanning neurons (**Figure 1**). For example, layer 5a and layer 5b pyramidal cells differ predominantly in their properties defined by the apical dendrites (Major et al., 2013).

A description of the cortex emphasizing connectivity between simple components—named after the cell body location—is seductive, particularly to computational neuroscientists, but also to physiologists who measure the "activity" of a neuron by recording from the cell body. It turns out that the neurons generate action potentials very close to the cell body, which is also the location that is most accessible for recording the neuron output. However, there is no functional consequence to this fact from the perspective of an input-output description of the cortical circuit and in particular for ascribing functionality to layers (see **Box 1**). Neither the input nor the output is actually best described as located at the cell body. Both the inputs (postsynaptic potentials) and the outputs (transmitter release) of a single neuron could literally occur in any and all of the layers of the cortex. From this perspective, there is no such thing as a "L5 pyramidal neuron." Nevertheless, there is a general correspondence between the cytoarchitecture, and between the layering apparent due to cell bodies and the layering of axonal terminations (**Figure 1A**, middle and right).

The last few decades have witnessed a huge increase in our knowledge about the properties of dendrites and how they integrate synaptic input (Spruston, 2008; Major et al., 2013; Grienberger et al., 2015). For instance, we now know that pyramidal neurons in the cortex have various types of local dendritic spikes (Na^+, Ca^{2+} and NMDA) and diverse distributions of ion channels that influence the propagation and local integration of synaptic potentials. It is now clear that these neurons are more complex than simple point neurons but a canonical description has yet to emerge. Ideally, we should be able to describe neurons in functional terms with reference to the number of compartments, the organization of input and output and their relationship to the layering of the cortex. Nevertheless, with the advent of optical methods it has become possible to directly image activity in particular axons, in dendrites and in cell bodies situated in particular layers (Svoboda et al., 1997; Petreanu et al., 2007; Jia et al., 2010; Andermann et al., 2013; Kim and Kastner, 2013) which promises to increase our understanding. Functional MRI, measuring BOLD contrast which is a combination of blood flow, blood volume and blood oxygenation, is better linked to neuronal activity by summed energy consumption than by spiking neuron output. With the increased spatial resolution of fMRI in recent years, BOLD is now measured at different cortical depths and can therefore be used to characterize the summed energy consumption in different layers of cortex. Great advances have also been made in anatomical approaches for examining brain connectivity at all scales (Bassett and Sporns, 2017). Notably missing so far

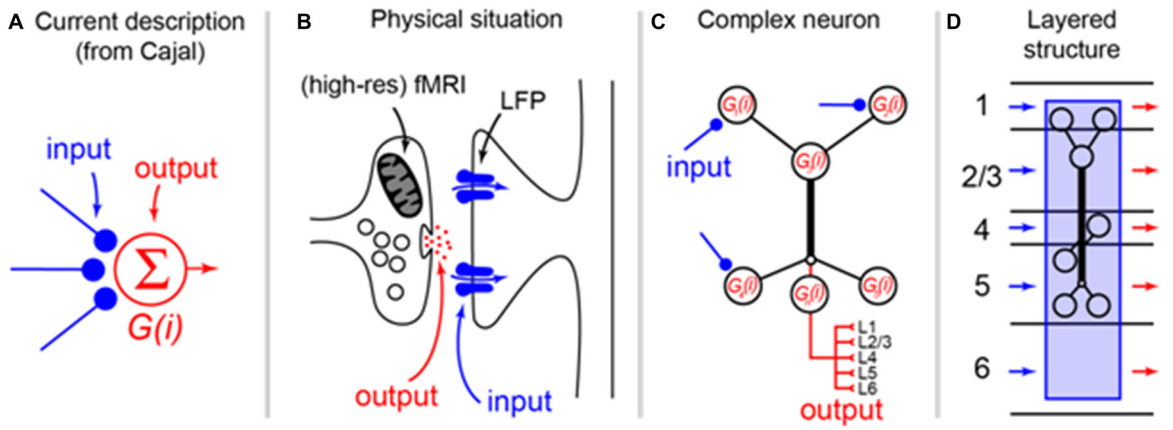

BOX 1 | Re-evaluating the somato-centric perspective in layered structures. Since Cajal (1894) proposed the Neuron Doctrine, it has been clear that information (by and large) flows uni-directionally across neurons in the nervous system. This has lead to a pervasive and reductive description of how neurons operate that is apparent both in the way most neuroscientists talk about "activity" in the brain and the way the operation of neurons is formalized **(A)**. Here, axon terminals are frequently described as the "input" to a neuron, which is usually represented only as a "conceptual cell body" that emits "output." This perspective has survived more than a century since Cajal because, we argue, it fits the intuition that cell bodies are both physically prominent and provide a convenient locus for recording action potentials. In fact, the physical situation, which is well understood but frequently overlooked, is that the output of a neuron almost always manifests as the release of transmitter *at the axon terminals* whereas the input is best described as synaptic currents located directly abutting the terminals **(B)**. From a methodological point of view, this means that methods such as fMRI are typically describing energy related to release of transmitter at axon terminals (see main text) and local field potentials describe synaptic currents located nearby. With the advent of methodologies that can more precisely resolve the layering of the cortex (e.g., high-res fMRI), it becomes necessary to shift perspectives in order to interpret the signals. Because of the close apposition of input and output, the choice of label for synapses reduces quickly to semantics and it is not the argument here that the nomenclature needs to change. However, the current "somato-centric" perspective that we owe originally to Cajal cannot be used to explain the data emerging with modern techniques. It is increasingly well understood that the "function" of a neuron (i.e., the transformation from input to output) occurs via the process of dendritic integration that in the cortex frequently occurs in active and layer-spanning dendritic trees **(C)**. Thus, the computation of a cortical neuron is actually a complex spatio-temporal phenomenon that transforms inputs arriving over various layers to output delivered to various other layers **(D)**. In this transformation process, the cell body specifies neither the location of the processing nor the output of the neuron and could in principle be collapsed to a dimensionless node in any specific layer without substantially changing the input/output function of the neuron. It is therefore not correct from a functional perspective to attribute the "activity" of a cell to the layer in which the cell body is located. The interpretation of BOLD signals from high-res fMRI recordings, for instance, cannot be attributed simply to the spiking neuronal activity occurring in the same layers as the BOLD signal, but rather to the summed mostly post synaptic membrane potential fluctuations of dendrites whose cell body is elsewhere.

is a coherent integration of these revolutionary thrusts in the neurosciences.

In summary, our perspective on cortical layering is the following:

1. The biophysical/computational input/output properties of the components of the cortex are complex and are spatiotemporal in nature often spanning several layers.
2. The cortical layer in which the cell body of a neuron is located has little or no ramifications for computing the input/output function of that neuron.
3. Understanding *any signal recorded from the cortex* needs to take these facts into account, preferably with some model or theory that accounts for the underlying structure/function.

COMBINING THE COMPONENTS AND CONNECTIVITY IN A DESCRIPTION OF THE CORTEX

To date, models of cortex that include the laminar structure are only a small proportion of the total and these models tend to ignore the dendrites or treat them only cursorily (Spratling and Johnson, 2001; Spratling, 2002; Raizada and Grossberg, 2003; Thomson and Bannister, 2003; Grossberg, 2007; George and Hawkins, 2009). By using simplified components, such models may fail to successfully account for the interactions across layers that are sometimes carried out within the neurons themselves. To achieve this, a description of the full repertoire of dendritic properties with respect to the different cortical lamina will be necessary. The final goal of such a model is a description of how the inputs between and within cortical areas are transformed into laminar-specific output throughout the system.

A simple example of such a model was proposed in a recent hypothesis of how the dendritic calcium spike in pyramidal neurons might associate feed-forward and feedback information streams arriving at different cortical layers (**Figure 2A**; Larkum, 2013). Here, the pyramidal neuron acts like a coincidence detector for simultaneous input to the upper and lower cortical layers with Ca^{2+} spikes facilitated by back-propagating action potentials (BAC firing; Larkum et al., 1999). Whether or not the cortex operates exactly in this fashion is still an open question. Evidence in favor of this particular hypothesis was recently demonstrated by showing that the threshold for perception correlates with dendritic calcium spikes in layer 5 pyramidal neurons and that down-regulating the calcium spikes suppressed perception at threshold stimulus levels (Takahashi et al., 2016).

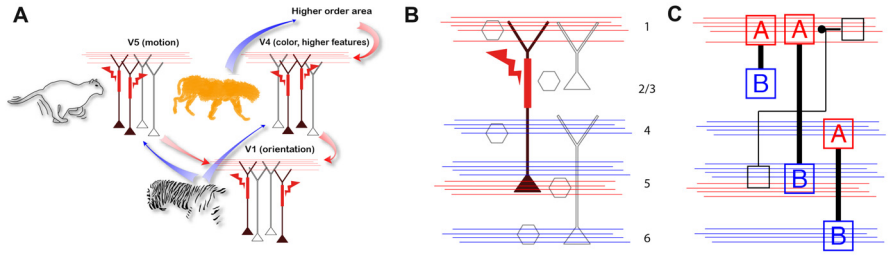

FIGURE 2 | Approaches for combining components with cortical layering. **(A)** A hypothesis for the possible ramifications of the associative properties of cortical pyramidal neurons with dendritic calcium spikes at the network level (adapted with permission from Larkum, 2013). Here, the active properties of the apical dendrites associate feed-forward and feedback information streams arriving at different layers. Here, blue arrows indicate feed forward information streams and red arrows indicate feedback. **(B)** Missing components (gray) needed for an expanded theory of the one shown in part A which should include the intrinsic properties of neurons, dendrites and synaptic inputs. Feedback and feed forward axonal input indicated with red and blue lines, respectively. **(C)** Example of abstractions of neurons needed for new theories within the new perspective. Here, A = dendrites, B = Somata.

On the other hand, alternative explanations have been offered to explain exactly which inputs lead to calcium spike firing. For instance, feedback inputs also arrive in the lower layers and possibly triggering the BAC firing mechanism on their own (Manita et al., 2015, 2017). However, the fact remains that the calcium spike apparently has an effect on the perceptual threshold that cannot be explained by models with point neurons. The main upshot is that it is necessary to have an account of how cellular processes such as local spikes and subcellular propagation (Major et al., 2013; Stuart and Spruston, 2015) interact with inputs and under what behavioral circumstances in order to interpret any given recordings and explain complex behavior.

In conclusion, we argue that it is fundamentally important first to examine all cell types of the cortex and describe and encapsulate their properties and the way they integrate synaptic inputs (**Figures 2B,C**). This task can be started *in vitro* but eventually must be validated *in vivo* under awake behaving conditions. Second, having obtained the biophysical facts about the components of the cortex, it will be necessary to develop abstractions of these components so that their functionality can be captured in a model. Third, this information has to be combined with the connectivity of the cortex so that the influence of particular inputs can be included in the model. With this information in hand, it becomes possible to interpret laminar-specific data collected from the cortex whether it comes in the form of electrical recordings from particular cells in particular layers or imaging of brain activity at various levels of resolution and various cortical depths.

A CASE STUDY—ULTRA HIGH-RESOLUTION fMRI

To elucidate this argument, we take a case study using the relatively new technique of ultra high-resolution fMRI that allows researchers to investigate brain activity non-invasively in human subjects with the ability to separate different depth layers in cortex (**Figure 3**). With this technique, blood oxygenation level-dependent signals (BOLD) can be measured for the top, middle and bottom thirds of the cortex. This, in turn, approximates to the layers known to roughly segregate according to synaptic inputs from feedback vs. feed forward connectivity (Petro and Muckli, 2016, 2017). We take this example because it highlights both the gains that can be made by demanding informed interpretations and the pitfalls of proceeding without them. It is ideal as a case study because, unlike traditional fMRI, this is a technique that can be applied to, and in our opinion calls for, an understanding of the operation of the cortex from a laminar perspective (Muckli et al., 2015; Huber et al., 2017; Lawrence et al., 2017).

But what conclusions about high-res fMRI recordings are valid? For example, suppose higher BOLD signals are detected at one depth vs. another? Signals in fMRI studies are often conflated with neuronal "activity." This is problematic on a number of levels. BOLD signals largely reflect the energy consumption of neural processing that require oxygen and glucose rather than a direct reflection of neuronal activity. Therefore, the BOLD signal most likely reflects locations of high synaptic activity (Logothetis et al., 2001; Viswanathan and Freeman, 2007; Logothetis, 2008) because the process of synaptic transmission has the largest energy requirement. Importantly, the activity of excitatory and inhibitory neurons would simply combine on this view despite their opposite affects. Nevertheless, even with this understanding, it is often implied that high synaptic activity translates to high post-synaptic activity. However, the post-synaptic effect will depend on the complexities of the post-synaptic targets. For instance, large synaptic input to the upper layers that might occur due to an increase in feedback information would have a complex relationship to the firing of neurons that have distal dendrites projecting to the upper layers and their cell bodies and proximal dendrites in deeper layers. The major effect of such activity might be to depolarize the apical dendrites of pyramidal neurons whose cell bodies are in lower layers and whose axons terminate mostly in different cortical areas. Or, the same input may activate dendrites targeting inhibitory neurons that have the opposite effect on the dendrites of pyramidal neurons. Furthermore, the relative proportion and timing of inputs to different cortical layers will lead to further complexities that are mostly determined by the biophysics of the cells themselves. Some of these predictions

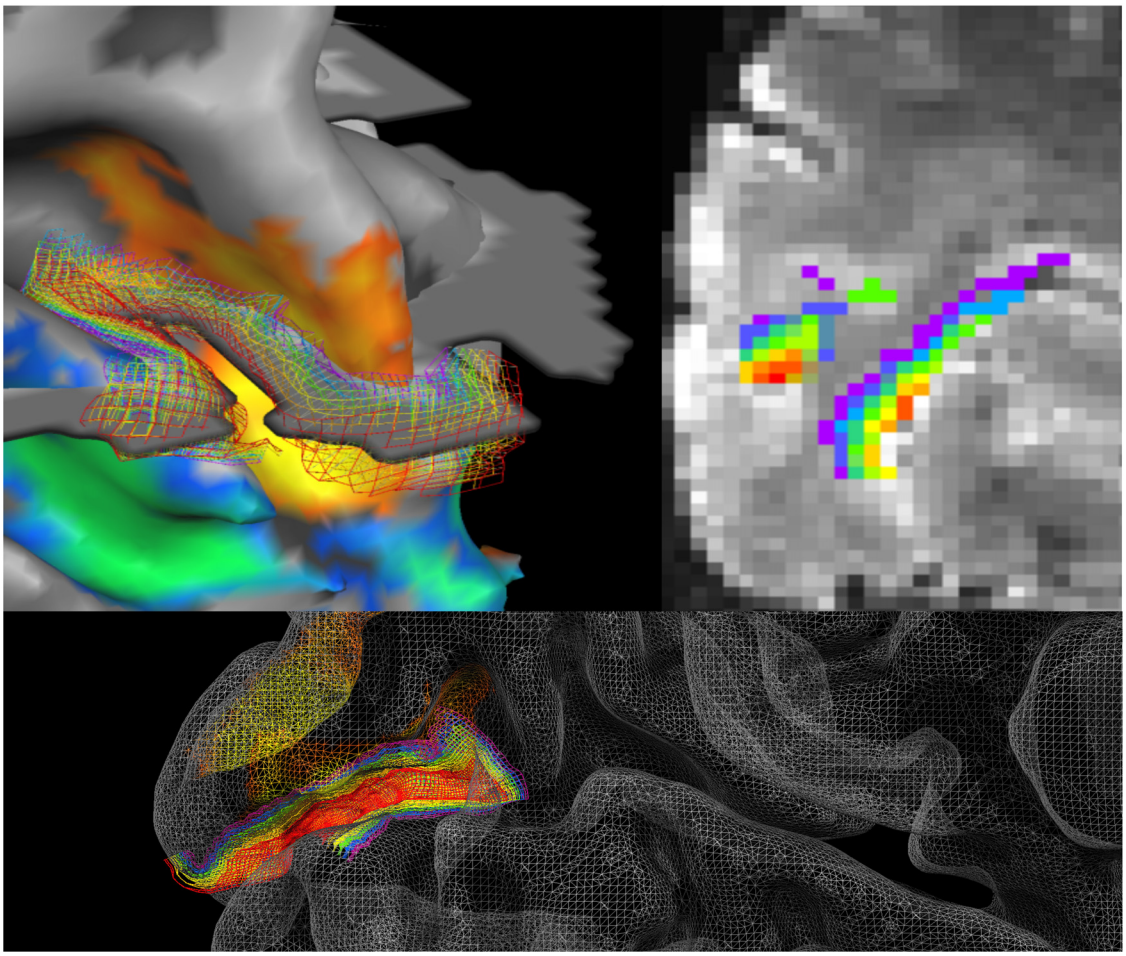

FIGURE 3 | Cortical surface reconstruction. Left hemisphere in the human acquired with high resolution 7T fMRI, overlaid with grid lines depicting cortical depths from superficial (red) to deep (purple) layers; (left upper) at the boundary of V2 and V3 right and lower indicate cortical depth levels in V1 (Muckli et al., 2015, adapted with permission). With this method, voxels in fMRI are labeled depending on their cortical depth and incorporated into depth-specific analyses. In the above example, the fMRI data is at 0.8 mm^3. Even though the bands of cortical depth level measured with fMRI are still insufficient to separate all six anatomical layers of cortex, there are important gradients that are functionally different in their processing of internal mental states, which we can capture by separating the layers into upper, middle and lower (i.e., by separating feedforward and feedback processing).

can be guessed already from our knowledge of the operation of components such as layer 5 pyramidal neurons but even for these well-studied neurons their description is probably still not complete. There is not yet a consensus description of these neurons that encapsulates their function under many simple input patterns. For other neurons of the cortex the situation is even less clear such that predictions of what happens under various different conditions remain wild guesses at best. Furthermore, most of the biophysical information we have so far about the operation of subcellular membrane potential dynamics is derived from recordings from rodent neurons under controlled conditions *in vitro*. What will happen in human neurons that are much larger (Mohan et al., 2015; Deitcher et al., 2017) and may have different properties (Eyal et al., 2016)? Good predictions about what signals should be expected using ultra high-resolution fMRI in humans during cognitive tasks will require a coherent theory of what occurs with different patterns of laminar input in different areas under different conditions.

Such a theory would be timely because layer-dependent measures using ultra high-field brain imaging are a rapidly developing field in human cognitive neuroscience (Lawrence et al., 2017; De Martino et al., 2018). At present, these high-resolution brain imaging studies have not tested the theories and tasks of their standard brain imaging counterparts at 3 Tesla. We anticipate studies of learning, memory, multisensory processing and consciousness which are surely forthcoming at laminar resolution. These studies would build on a number of successful proof-of-concept findings, measuring, for example, BOLD activation in layers of primary visual cortex in response to its preferred stimulus of contrast-reversing checkerboards (De Martino et al., 2013); cerebral blood volume and BOLD signal changes in layers of human primary motor cortex during finger tapping (Guidi et al., 2016); and layer-dependent population

receptive field sizes in human primary visual cortex (Fracasso et al., 2016). While these studies provide conceptual advances in human sensory and motor systems, they do not address the laminar influence of feedback vs. feedforward sources, or in functional terms how cognitive processing interacts with sensory processing. For example, when viewing natural scene images, cortical feedback transmits the brain's internal model of the scene back to primary visual cortex, predominantly the superficial layers (Muckli et al., 2015). In superficial layers, this feedback is detected with fMRI as changes in the activation distribution measured in multi-voxel pattern activity. Another finding relevant for the question of top-down feedback modulation of vision to cortical layers, is the demonstration that the deep layers of V1 are more active for perceptual filling-in of contours, a form of modal completion, (Kok et al., 2016). This was shown as a univariate increase of activity in deep layers. Taken together, both studies suggest how cognitive function interacts with sensory processing on a sub-neuronal level; top-down expectations are present in the dendritic tree of superficial layers of V1, and when combined with specific contextual information they can trigger activity in deeper layers and the illusory percept of visual contour filling-in. Although this interpretation of both studies has not yet been tested directly, it highlights the potential of ultra-high-field fMRI in detecting the functional properties of sub-neuronal compartments. Combined multi-method experiments are ongoing to establish this interpretation across species and scales. Another example of top-down modulation in layers of sensory cortex is provided by De Martino et al. (2015) who show that attention sharpens the representation of acoustic information mainly in the superficial layers of human primary auditory cortex. All of these studies give rise to the question of the circuit and systems level mechanisms of top-down, feedback processing. In a first demonstration of its kind, human laminar fMRI was used to derive information flow between cortical areas (Huber et al., 2017). Using BOLD and CBV (cerebral blood volume) measures, the authors revealed somatosensory and premotor input in upper layers of M1 and cortico-spinal motor output in the deeper layers. Moreover they found layer-specific functional connectivity of M1 and somatosensory and premotor areas using laminar resting-state fMRI. Technical advances in high-resolution fMRI will ensure that we can improve spatial coverage, meaning in future we can image even larger areas of cortex, that are capturing information flow between additional communicating regions.

Underpinning these functional cognitive brain imaging studies, there exists a broad field advancing laminar differences in cerebral blood flow, cerebral blood volume, neurovascular coupling, vascularity, positive and negative BOLD, blood flow regulation, and comparison to electrophysiology, not to mention laminar-specific data acquisition and analysis strategies (Goense et al., 2016; Self et al., 2017; Kashyap et al., 2018; Kemper et al., 2018). All of these topics will be bolstered by (and are essential components of) what we propose here: the necessity of interpreting layer-specific fMRI data with knowledge of the laminar distribution of inputs and layer-spanning cellular compartments. We need a theory that incorporates the complex properties of neuronal components whose dendrites and axons span multiple layers because, while these current studies already highlight the tremendous potential of this technique for the study of cognitive function in higher brain areas, it will remain difficult to fully disentangle the effects of feed forward and feedback inputs in human cortex without understanding the underlying biophysics. The interpretation of the layer specific fMRI signal therefore requires an *a priori* theory of cortical function, describing the functional consequences of the laminar distribution of synaptic inputs for a neuron. Even for studies in rodents where there is a constant evolution in the methods, and where the temporal and spatial resolution is much higher than with fMRI, the ability to collect large data sets is ultimately meaningless without a theory (Jonas and Kording, 2017).

The promise of high-resolution fMRI is in allowing a window into the neuro-computational unit of cortical layers during the most elaborate cognitive states, for example, emotion, inner speech, empathy and mental time travel. Non-invasive approaches are crucial because we are not close to being able to image activity at a cellular or subcellular resolution in human beings, or to applying experiments where one manipulates specific pathways using approaches like optogenetics. On the other hand, this situation does not mean that the underlying cellular and subcellular dynamics can therefore be ignored without influencing the interpretation. If brain imaging can reveal a functionally-relevant meso-scale abstraction of the synaptic inputs in micro-scale neuroscience, this will amount to an important breakthrough. At some point in the very near future it may then become possible to talk about consequences of activity in cortical areas during cognitive tasks in the context of feed forward and feedback inputs, and activity in the different layers.

LINKING COMPLEX COMPONENTS WITH LAMINAR CONNECTIVITY—WHAT STILL NEEDS TO BE DONE?

In our opinion it would be unwise to use oversimplified assumptions (such as point neurons) as a substitute for our ignorance. Fundamental questions remain regarding many aspects of cortical layering and how this interacts with the complexities of layer-spanning neurons with active dendrites. For instance, we lack a satisfactory account of what role "basal" dendrites play, that are largely limited to the same or adjacent layer as the cell body. It has been suggested that local dendritic NMDA spikes in these dendrites offer multiple, independent integrations of incoming signals (Mel, 1992; Polsky et al., 2009). In fact, this observation has been extended to the tuft dendrites of pyramidal neurons (Larkum et al., 2009; Palmer et al., 2014) and may be a generalization for thin dendrites of other neurons (Lavzin et al., 2012). In general, however, we still lack the specific and necessary information to accurately describe the input/output function of most neurons and their relationship to the layering of the cortex. In fact, most modern methods do not measure either input or output directly (see **Box 1**) but rather action potential activity at the cell body. In cases where

interesting processes occur in the dendrite but the cell fires no action potential, the underlying events might still be detectable with methods such as high-resolution fMRI.

Perhaps most importantly, the learning rules for synaptic connectivity are yet to be linked conclusively to the full range of intrinsic activity and laminar circuitry. There is good evidence that dendritic Na^+ and Ca^{2+} spikes influence synaptic plasticity (Kampa et al., 2006; Sjöström and Häusser, 2006; Losonczy et al., 2008) as well as NMDA spikes (Gordon et al., 2006; Brandalise et al., 2016). Nevertheless, an integrated theory of how all these isolated phenomena combine to result in network rewiring is still lacking. Recent intriguing results from the Magee group suggest that some combination of these intrinsic dendritic properties may be transformative in explaining learning in the hippocampus (Bittner et al., 2015; Grienberger et al., 2017). In the neocortex there is accumulating evidence that plasticity occurs at feedback and 2nd order thalamic synapses on to the apical tuft dendrites of L5 neurons in the upper layers of the cortex (Gambino et al., 2014; Cichon and Gan, 2015; Miyamoto et al., 2016). All these forms of plasticity depend on this activation of intrinsic dendritic activity. The exact conditions or rules that control this kind of learning are still being determined but it is clear that they cannot be understood or described without reference to both the laminar pattern of connectivity and the intrinsic properties of the neurons that process these inputs in distinct compartments lying in distinct cortical lamina.

At the present time, most laboratories still focus on recordings from cell bodies and some even still report data without reference to the cortical layer or cell type from which they are taken. Two-photon imaging approaches have opened up the possibility of collecting data from compartments other than the cell body but recording data from anything other than cell bodies is still the exception rather than the rule. In the meantime, improvements to 2-photon imaging (Ji et al., 2016; Papadopoulos et al., 2016), other methodologies such as prisms inserted into the cortex (Andermann et al., 2013) and high-resolution fMRI now make it possible to include laminar-specific information. Standard methodologies such as vertically oriented linear arrays like Michigan Probes have long been useful for probing laminar issues (BeMent et al., 1986; Cauller and Kulics, 1991) and can be used to probe the relative influence of feed forward and feedback influences in the cortex (van Kerkoerle et al., 2017). It was recently shown that intrinsic excitability of pyramidal neurons such as calcium spikes are also easily detected by these devices (Suzuki and Larkum, 2017).

In summary, it is now possible to move beyond a simple description of cortex in terms of point neurons and point-to-point connections in favor of a richer understanding that includes vertical features such as axonal termination layers and subcellular compartments spanning several layers. We have learned enough about the properties of particular neurons such as the layer 5 neuron to be able to say for certain that their active dendritic properties interact with the location of synaptic inputs in a very complex but important way. In our view, it is essential to investigate these features in all neurons and synaptic input pathways in order to understand the layering of the cortex.

AUTHOR CONTRIBUTIONS

ML, LP, RS and LM wrote the article.

FUNDING

This work was supported by the European Union's Horizon 2020 research and innovation program and Euratom research and training program 20142018 (under grant agreement No. 670118 to ML). This project has received funding from the European Union's Horizon 2020 Framework Programme for Research and Innovation under the Specific Grant Agreement No. 720270 and 785907 (Human Brain Project SGA1 and SGA2). Deutsche Forschungsgemeinschaft (Grant No. LA 3442/3-1 and Grant No. LA 3442/5-1 to ML); and European Research Council (ERC StG 2012_311751-"Brain reading of contextual feedback and predictions" to LM).

REFERENCES

Andermann, M. L., Gilfoy, N. B., Goldey, G. J., Sachdev, R. N., Wölfel, M., McCormick, D. A., et al. (2013). Chronic cellular imaging of entire cortical columns in awake mice using microprisms. *Neuron* 80, 900–913. doi: 10.1016/j.neuron.2013.07.052

Bassett, D. S., and Sporns, O. (2017). Network neuroscience. *Nat. Neurosci.* 20, 353–364. doi: 10.1038/nn.4502

BeMent, S. L., Wise, K. D., Anderson, D. J., Najafi, K., and Drake, K. L. (1986). Olid-state electrodes for multichannel multiplexed intracortical neuronal recording. *IEEE Trans. Biomed. Eng.* 33, 230–241. doi: 10.1109/tbme.1986.325895

Bittner, K. C., Grienberger, C., Vaidya, S. P., Milstein, A. D., Macklin, J. J., Suh, J., et al. (2015). Conjunctive input processing drives feature selectivity in hippocampal CA1 neurons. *Nat. Neurosci.* 18, 1133–1142. doi: 10.1038/nn.4062

Brandalise, F., Carta, S., Helmchen, F., Lisman, J., and Gerber, U. (2016). Dendritic NMDA spikes are necessary for timing-dependent associative LTP in CA3 pyramidal cells. *Nat. Commun.* 7:13480. doi: 10.1038/ncomms13480

Cajal, S. R. Y. (1894). The croonian lecture: la fine structure des centres nerveux. *Proc. R. Soc. Lond.* 55, 444–467. doi: 10.1098/rspl.1894.0063

Cauller, L. J., and Kulics, A. T. (1991). The neural basis of the behaviorally relevant N1 component of the somatosensory-evoked potential in SI cortex of awake monkeys: evidence that backward cortical projections signal conscious touch sensation. *Exp. Brain Res.* 84, 607–619. doi: 10.1007/bf00230973

Cichon, J., and Gan, W. B. (2015). Branch-specific dendritic Ca^{2+} spikes cause persistent synaptic plasticity. *Nature* 520, 180–185. doi: 10.1038/nature14251

De Martino, F., Moerel, M., Ugurbil, K., Goebel, R., Yacoub, E., and Formisano, E. (2015). Frequency preference and attention effects across cortical depths in the human primary auditory cortex. *Proc. Natl. Acad. Sci. U S A* 112, 16036–16041. doi: 10.1073/pnas.1507552112

De Martino, F., Yacoub, E., Kemper, V., Moerel, M., Uludağ, K., De Weerd, P., et al. (2018). The impact of ultra-high field MRI on cognitive and computational neuroimaging. *Neuroimage* 168, 366–382. doi: 10.1016/j.neuroimage.2017.03.060

De Martino, F., Zimmermann, J., Muckli, L., Ugurbil, K., Yacoub, E., and Goebel, R. (2013). Cortical depth dependent functional responses in

humans at 7T: improved specificity with 3D GRASE. *PLoS One* 8:e60514. doi: 10.1371/journal.pone.0060514

Defelipe, J., Cajal, S. R. Y., and Jones, E. G. (1988). *Cajal on the Cerebral Cortex. An Annotated Translation of the Complete Writings*. Oxford: Oxford University Press.

Deitcher, Y., Eyal, G., Kanari, L., Verhoog, M. B., Atenekeng Kahou, G. A., Mansvelder, H. D., et al. (2017). Comprehensive morpho-electrotonic analysis shows 2 distinct classes of L2 and L3 pyramidal neurons in human temporal cortex. *Cereb. Cortex* 27, 5398–5414. doi: 10.1093/cercor/bhx226

Douglas, R. J., Martin, K. A. C., and Witteridge, D. (1989). A canonical microcircuit for neocortex. *Neural Comput.* 1, 480–488. doi: 10.1162/neco.1989.1.4.480

Eyal, G., Verhoog, M. B., Testa-Silva, G., Deitcher, Y., Lodder, J. C., Benavides-Piccione, R., et al. (2016). Unique membrane properties and enhanced signal processing in human neocortical neurons. *Elife* 5:e16553. doi: 10.7554/eLife.16553

Fracasso, A., Petridou, N., and Dumoulin, S. O. (2016). Systematic variation of population receptive field properties across cortical depth in human visual cortex. *Neuroimage* 139, 427–438. doi: 10.1016/j.neuroimage.2016.06.048

Gambino, F., Pages, S., Kehayas, V., Baptista, D., Tatti, R., Carleton, A., et al. (2014). Sensory-evoked LTP driven by dendritic plateau potentials *in vivo*. *Nature* 515, 116–119. doi: 10.1038/nature13664

George, D., and Hawkins, J. (2009). Towards a mathematical theory of cortical micro-circuits. *PLoS Comput. Biol.* 5:e1000532. doi: 10.1371/journal.pcbi.1000532

Goense, J., Bohraus, Y., and Logothetis, N. K. (2016). fMRI at high spatial resolution: implications for BOLD-models. *Front. Comput. Neurosci.* 10:66. doi: 10.3389/fncom.2016.00066

Gordon, U., Polsky, A., and Schiller, J. (2006). Plasticity compartments in basal dendrites of neocortical pyramidal neurons. *J. Neurosci.* 26, 12717–12726. doi: 10.1523/JNEUROSCI.3502-06.2006

Grienberger, C., Chen, X., and Konnerth, A. (2015). Dendritic function *in vivo*. *Trends Neurosci.* 38, 45–54. doi: 10.1016/j.tins.2014.11.002

Grienberger, C., Milstein, A. D., Bittner, K. C., Romani, S., and Magee, J. C. (2017). Inhibitory suppression of heterogeneously tuned excitation enhances spatial coding in CA1 place cells. *Nat. Neurosci.* 20, 417–426. doi: 10.1038/nn.4486

Grossberg, S. (2007). Towards a unified theory of neocortex: laminar cortical circuits for vision and cognition. *Prog. Brain Res.* 165, 79–104. doi: 10.1016/s0079-6123(06)65006-1

Guidi, M., Huber, L., Lampe, L., Gauthier, C. J., and Möller, H. E. (2016). Lamina-dependent calibrated BOLD response in human primary motor cortex. *Neuroimage* 141, 250–261. doi: 10.1016/j.neuroimage.2016.06.030

Heimer, L. (1994). *The Human Brain and Spinal Cord: Functional Neuroanatomy and Dissection Guide*. 2nd Edn. New York, NY: Springer.

Hubel, D. H., and Wiesel, T. N. (1962). Receptive fields, binocular interaction and functional architecture in the cat's visual cortex. *J. Physiol.* 160, 106–154. doi: 10.1113/jphysiol.1962.sp006837

Huber, L., Handwerker, D. A., Jangraw, D. C., Chen, G., Hall, A., Stuber, C., et al. (2017). High-resolution CBV-fMRI allows mapping of laminar activity and connectivity of cortical input and output in human M1. *Neuron* 96, 1253.e7–1263.e7. doi: 10.1016/j.neuron.2017.11.005

Ji, N., Freeman, J., and Smith, S. L. (2016). Technologies for imaging neural activity in large volumes. *Nat. Neurosci.* 19, 1154–1164. doi: 10.1038/nn.4358

Jia, H., Rochefort, N. L., Chen, X., and Konnerth, A. (2010). Dendritic organization of sensory input to cortical neurons *in vivo*. *Nature* 464, 1307–1312. doi: 10.1038/nature08947

Jonas, E., and Kording, K. P. (2017). Could a neuroscientist understand a microprocessor? *PLoS Comput. Biol.* 13:e1005268. doi: 10.1371/journal.pcbi.1005268

Kampa, B., Letzkus, J. J., and Stuart, G. (2006). Requirement of dendritic calcium spikes for induction of spike-timing dependent synaptic plasticity. *J. Physiol.* 574, 283–290. doi: 10.1113/jphysiol.2006.111062

Kashyap, S., Ivanov, D., Havlicek, M., Poser, B. A., and Uludağ, K. (2018). Impact of acquisition and analysis strategies on cortical depth-dependent fMRI. *Neuroimage* 168, 332–344. doi: 10.1016/j.neuroimage.2017.05.022

Kemper, V. G., De Martino, F., Emmerling, T. C., Yacoub, E., and Goebel, R. (2018). High resolution data analysis strategies for mesoscale human functional MRI at 7 and 9.4T. *Neuroimage* 164, 48–58. doi: 10.1016/j.neuroimage.2017.03.058

Kim, J. G., and Kastner, S. (2013). Attention flexibly alters tuning for object categories. *Trends Cogn. Sci.* 17, 368–370. doi: 10.1016/j.tics.2013.05.006

Kok, P., Bains, L. J., van Mourik, T., Norris, D. G., and de Lange, F. P. (2016). Selective activation of the deep layers of the human primary visual cortex by top-down feedback. *Curr. Biol.* 26, 371–376. doi: 10.1016/j.cub.2015.12.038

Larkum, M. E. (2013). A cellular mechanism for cortical associations: an organizing principle for the cerebral cortex. *Trends Neurosci.* 36, 141–151. doi: 10.1016/j.tins.2012.11.006

Larkum, M. E., Nevian, T., Sandler, M., Polsky, A., and Schiller, J. (2009). Synaptic integration in tuft dendrites of layer 5 pyramidal neurons: a new unifying principle. *Science* 325, 756–760. doi: 10.1126/science.1171958

Larkum, M. E., Zhu, J. J., and Sakmann, B. (1999). A new cellular mechanism for coupling inputs arriving at different cortical layers. *Nature* 398, 338–341. doi: 10.1038/18686

Lavzin, M., Rapoport, S., Polsky, A., Garion, L., and Schiller, J. (2012). Nonlinear dendritic processing determines angular tuning of barrel cortex neurons *in vivo*. *Nature* 490, 397–401. doi: 10.1038/nature11451

Lawrence, S. J. D., Formisano, E., Muckli, L., and de Lange, F. P. (2017). Laminar fMRI: applications for cognitive neuroscience. *Neuroimage* doi: 10.1016/j.neuroimage.2017.07.004 [Epub ahead of print].

Logothetis, N. K. (2008). What we can do and what we cannot do with fMRI. *Nature* 453, 869–878. doi: 10.1038/nature06976

Logothetis, N. K., Pauls, J., Augath, M., Trinath, T., and Oeltermann, A. (2001). Neurophysiological investigation of the basis of the fMRI signal. *Nature* 412, 150–157. doi: 10.1038/35084005

Losonczy, A., Makara, J. K., and Magee, J. C. (2008). Compartmentalized dendritic plasticity and input feature storage in neurons. *Nature* 452, 436–441. doi: 10.1038/nature06725

Major, G., Larkum, M. E., and Schiller, J. (2013). Active properties of neocortical pyramidal neuron dendrites. *Annu. Rev. Neurosci.* 36, 1–24. doi: 10.1146/annurev-neuro-062111-150343

Manita, S., Miyakawa, H., Kitamura, K., and Murayama, M. (2017). Dendritic spikes in sensory perception. *Front. Cell. Neurosci.* 11:29. doi: 10.3389/fncel.2017.00029

Manita, S., Suzuki, T., Homma, C., Matsumoto, T., Odagawa, M., Yamada, K., et al. (2015). A top-down cortical circuit for accurate sensory perception. *Neuron* 86, 1304–1316. doi: 10.1016/j.neuron.2015.05.006

Mel, B. W. (1992). NMDA-based pattern discrimination in a modeled cortical neuron. *Neural Comput.* 4, 502–517. doi: 10.1162/neco.1992.4.4.502

Miyamoto, D., Hirai, D., Fung, C. C., Inutsuka, A., Odagawa, M., Suzuki, T., et al. (2016). Top-down cortical input during NREM sleep consolidates perceptual memory. *Science* 352, 1315–1318. doi: 10.1126/science.aaf0902

Mohan, H., Verhoog, M. B., Doreswamy, K. K., Eyal, G., Aardse, R., Lodder, B. N., et al. (2015). Dendritic and axonal architecture of individual pyramidal neurons across layers of adult human neocortex. *Cereb. Cortex* 25, 4839–4853. doi: 10.1093/cercor/bhv188

Mountcastle, V. B. (1978). "An organizing principle for cerebral function," in *The Mindful Brain*, eds G. M. Edelman and V. B. Mountcastle (Cambridge, MA: MIT Press), 7–50.

Muckli, L., De Martino, F., Vizioli, L., Petro, L. S., Smith, F. W., Ugurbil, K., et al. (2015). Contextual feedback to superficial layers of V1. *Curr. Biol.* 25, 2690–2695. doi: 10.1016/j.cub.2015.08.057

Palmer, L. M., Shai, A. S., Reeve, J. E., Anderson, H. L., Paulsen, O., and Larkum, M. E. (2014). NMDA spikes enhance action potential generation during sensory input. *Nat. Neurosci.* 17, 383–390. doi: 10.1038/nn.3646

Papadopoulos, I. N., Jouhanneau, J.-S., Poulet, J. F. A., and Judkewitz, B. (2016). Scattering compensation by focus scanning holographic aberration probing (F-SHARP). *Nat. Photonics* 11, 116–123. doi: 10.1038/nphoton.2016.252

Petreanu, L., Huber, D., Sobczyk, A., and Svoboda, K. (2007). Channelrhodopsin-2-assisted circuit mapping of long-range callosal projections. *Nat. Neurosci.* 10, 663–668. doi: 10.1038/nn1891

Petro, L. S., and Muckli, L. (2016). The brain's predictive prowess revealed in primary visual cortex. *Proc. Natl. Acad. Sci. U S A* 113, 1124–1125. doi: 10.1073/pnas.1523834113

Petro, L. S., and Muckli, L. (2017). The laminar integration of sensory inputs with feedback signals in human cortex. *Brain Cogn.* 112, 54–57. doi: 10.1016/j.bandc.2016.06.007

Polsky, A., Mel, B., and Schiller, J. (2009). Encoding and decoding bursts by NMDA spikes in basal dendrites of layer 5 pyramidal neurons. *J. Neurosci.* 29, 11891–11903. doi: 10.1523/JNEUROSCI.5250-08.2009

Raizada, R. D., and Grossberg, S. (2003). Towards a theory of the laminar architecture of cerebral cortex: computational clues from the visual system. *Cereb. Cortex* 13, 100–113. doi: 10.1093/cercor/13.1.100

Self, M. W., van Kerkoerle, T., Goebel, R., and Roelfsema, P. R. (2017). Benchmarking laminar fMRI: neuronal spiking and synaptic activity during top-down and bottom-up processing in the different layers of cortex. *Neuroimage* doi: 10.1016/j.neuroimage.2017.06.045 [Epub ahead of print].

Sjöström, P. J., and Häusser, M. (2006). A cooperative switch determines the sign of synaptic plasticity in distal dendrites of neocortical pyramidal neurons. *Neuron* 51, 227–238. doi: 10.1016/j.neuron.2006.06.017

Spratling, M. W. (2002). Cortical region interactions and the functional role of apical dendrites. *Behav. Cogn. Neurosci. Rev.* 1, 219–228. doi: 10.1177/1534582302001003003

Spratling, M. W., and Johnson, M. H. (2001). Dendritic inhibition enhances neural coding properties. *Cereb. Cortex* 11, 1144–1149. doi: 10.1093/cercor/11.12.1144

Spruston, N. (2008). Pyramidal neurons: dendritic structure and synaptic integration. *Nat. Rev. Neurosci.* 9, 206–221. doi: 10.1038/nrn2286

Stuart, G. J., and Spruston, N. (2015). Dendritic integration: 60 years of progress. *Nat. Neurosci.* 18, 1713–1721. doi: 10.1038/nn.4157

Suzuki, M., and Larkum, M. E. (2017). Dendritic calcium spikes are clearly detectable at the cortical surface. *Nat. Commun.* 8:276. doi: 10.1038/s41467-017-00282-4

Svoboda, K., Denk, W., Kleinfeld, D., and Tank, D. W. (1997). *In vivo* dendritic calcium dynamics in neocortical pyramidal neurons. *Nature* 385, 161–165. doi: 10.1038/385161a0

Takahashi, N., Oertner, T. G., Hegemann, P., and Larkum, M. E. (2016). Active cortical dendrites modulate perception. *Science* 354, 1587–1590. doi: 10.1126/science.aah6066

Thomson, A. M., and Bannister, A. P. (2003). Interlaminar connections in the neocortex. *Cereb. Cortex* 13, 5–14. doi: 10.1093/cercor/13.1.5

van Kerkoerle, T., Self, M. W., and Roelfsema, P. R. (2017). Layer-specificity in the effects of attention and working memory on activity in primary visual cortex. *Nat. Commun.* 8:13804. doi: 10.1038/ncomms15555

Viswanathan, A., and Freeman, R. D. (2007). Neurometabolic coupling in cerebral cortex reflects synaptic more than spiking activity. *Nat. Neurosci.* 10, 1308–1312. doi: 10.1038/nn1977

Wilson, H. R., and Cowan, J. D. (1972). Excitatory and inhibitory interactions in localized populations of model neurons. *Biophys. J.* 12, 1–24. doi: 10.1016/s0006-3495(72)86068-5

Wilson, H. R., and Cowan, J. D. (1973). A mathematical theory of the functional dynamics of cortical and thalamic nervous tissue. *Kybernetik* 13, 55–80. doi: 10.1007/bf00288786

Conflict of Interest Statement: The authors declare that the research was conducted in the absence of any commercial or financial relationships that could be construed as a potential conflict of interest.

frontiers in Neuroanatomy

PERSPECTIVE
published: 14 December 2017
doi: 10.3389/fnana.2017.00116

What Is the Evidence for Inter-laminar Integration in a Prefrontal Cortical Minicolumn?

Ioan Opris, Stephano Chang and Brian R. Noga*

The Miami Project to Cure Paralysis, Department of Neurological Surgery, University of Miami Miller School of Medicine, Miami, FL, United States

The objective of this perspective article is to examine columnar inter-laminar integration during the executive control of behavior. The integration hypothesis posits that perceptual and behavioral signals are integrated within the prefrontal cortical inter-laminar microcircuits. Inter-laminar minicolumnar activity previously recorded from the dorsolateral prefrontal cortex (dlPFC) of nonhuman primates, trained in a visual delay match-to-sample (DMS) task, was re-assessed from an integrative perspective. Biomorphic multielectrode arrays (MEAs) played a unique role in the *in vivo* recording of columnar cell firing in the dlPFC layers 2/3 and 5/6. Several integrative aspects stem from these experiments: 1. Functional integration of perceptual and behavioral signals across cortical layers during executive control. The integrative effect of dlPFC minicolumns was shown by: (i) increased correlated firing on correct vs. error trials; (ii) decreased correlated firing when the number of non-matching images increased; and (iii) similar spatial firing preference across cortical-striatal cells during spatial-trials, and less on object-trials. 2. Causal relations to integration of cognitive signals by the minicolumnar turbo-engines. The inter-laminar integration between the perceptual and executive circuits was facilitated by stimulating the infra-granular layers with firing patterns obtained from supra-granular layers that enhanced spatial preference of percent correct performance on spatial trials. 3. Integration across hierarchical levels of the brain. The integration of intention signals (visual spatial, direction) with movement preparation (timing, velocity) in striatum and with the motor command and posture in midbrain is also discussed. These findings provide evidence for inter-laminar integration of executive control signals within brain's prefrontal cortical microcircuits.

Keywords: integration, coordination, cortical layers, cortical minicolumns, microcircuits, prefrontal cortex, executive function

OPEN ACCESS

Edited by:
Javier DeFelipe,
Cajal Institute (CSIC), Spain

Reviewed by:
Srikanth Ramaswamy,
École Polytechnique Fédérale de Lausanne, Switzerland
Conrado Arturo Bosman,
University of Amsterdam, Netherlands

****Correspondence:***
Ioan Opris
ioanopris.phd@gmail.com

Received: *09 August 2017*
Accepted: *27 November 2017*
Published: *14 December 2017*

Citation:
Opris I, Chang S and Noga BR (2017) What Is the Evidence for Inter-laminar Integration in a Prefrontal Cortical Minicolumn? Front. Neuroanat. 11:116. doi: 10.3389/fnana.2017.00116

INTRODUCTION

Neural integration can be defined as the summation of excitatory and inhibitory synaptic inputs, which governs the generation of an action potential (Arnold et al., 2004). Integration of various neuronal signals within and between prefrontal cortical microcircuits plays a crucial role in cognition, perception and action (Penfield, 1958; Miller and Cohen, 2001; Opris et al., 2013; Bastos et al., 2015). Voluntary action is based on the intention to achieve a goal, and this goal determines how planning and subsequent actions lead to its achievement. However, recent studies point to evidence for neural integration of voluntary action in a prefrontal cortical minicolumn (Opris et al., 2011, 2012b, 2013; Bastos et al., 2015).

The prefrontal cortex may be regarded as an assembly of interconnected neuronal cells that sends and receives projections to/from virtually all cortical areas (sensory, motor and association), as well as to/from multiple subcortical structures (Miller and Cohen, 2001). As pointed out by Vernon Mountcastle, it is critical to identify the arrays of inputs and outputs (Mountcastle, 1997), in order to understand the integrative role of the prefrontal cortex (Miller and Cohen, 2001) and its functional organization (Kritzer and Goldman-Rakic, 1995).

Functional specialization of the brain employs cortical layers that differ from three to six layers (Shepherd, 2011). The sixth layer of cortex is, in fact, an adaptation observed exclusively in mammals, although it shares some commonalities with other species (Aboitiz, 2011; DeFelipe, 2011; Bosman and Aboitiz, 2015). A complementary role in the expression of brain function is played by the cortical minicolumns that interconnects the layers and forms functional microcircuits (Mountcastle, 1957, 1997; Shepherd and Grillner, 2010; DeFelipe et al., 2012). Just imagine if the supra-granular and infra-granular laminae would be disconnected, across the entire brain, then, one interface of the brain will be sensing without perceiving (i.e., being able to interpret their meaning) and the other interface will act/move randomly, without having a goal.

In the prefrontal cortex, the vertical "chains" of neurons called minicolumns (Mountcastle, 1957, 1997; Buxhoeveden and Casanova, 2002) are surrounded by inhibitory cells, forming a curtain of inhibition (Szentágothai and Arbib, 1975; see the **Schematic diagram**). Cortical neurons within prefrontal minicolumns are inter-connected across all layers: three upper layers (L1–L3), one granular layer (L4) and two lower layers (L5/L6). The granular layer receives the "sensory inputs" via the thalamus (Constantinople and Bruno, 2013). According to the concept of "three-stratum" functional module, lower layers execute the associative computations elaborated in upper layers (Buxhoeveden and Casanova, 2002; Casanova et al., 2011; Opris, 2013). The upper layers consist of small pyramidal cells that form vertical connections with the larger pyramidal neurons of the lower layers that generate most of the output from the cerebral cortex to other cortical/subcortical parts of the brain (Buxhoeveden and Casanova, 2002; Gabbott et al., 2003, 2005). Cortical microcircuit modules are forming topographic maps in visual and motor cortices (Mountcastle, 1997; Thomson and Lamy, 2007; Kaas, 2012), as well as in auditory (Allen et al., 2017), somatic (Mountcastle, 1997), taste (Peng et al., 2015) and smell (Qu et al., 2016) modalities of these sensory cortices. A modular network can be partitioned into nodes that are "densely interconnected internally" but only sparsely to other subsets (Chung et al., 2016).

The aim of this perspective is to examine the integration of perceptual and behavioral signals in the inter-laminar prefrontal cortical microcircuits (Opris et al., 2011, 2012a,b, 2013; Opris and Casanova, 2014). Given that the prefrontal cortex is the "seat" of the highest brain functions (Fuster, 2001), understanding the site of integration and the functional role of this computational mechanism is essential.

Cortical Layers and Functional Integration

Let's begin with few questions that address the core of modular structure and its functional role.

Why Have Cortical Layers?

Cortical layers serve multiple purposes: some serve more local microcircuits while others act as interconnecting loops (thalamo-cortical) or large-scale networks (bottom-up) that have a multifunctional role.

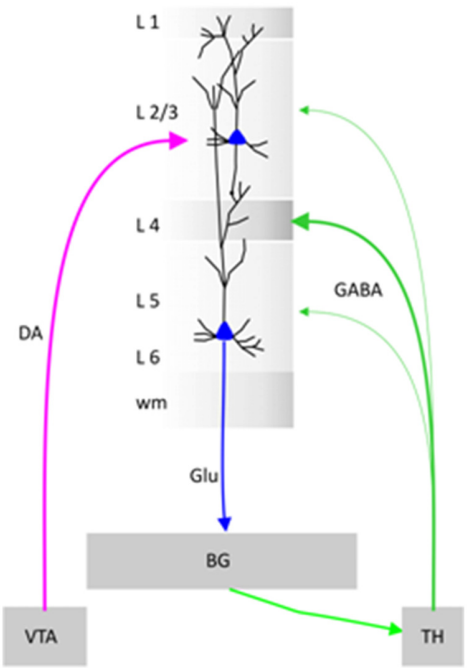

Schematic diagram. Illustration of a cortical minicolumn that integrates information from Ventral Tegmental Area (VTA) and Thalamus (TH). BG stands for Basal Ganglia, DA for Dopamine, Glu for Glutamate and GABA for gamma butyric acid.

What Is the Function of Layering?

Being part of the brain's connectome (Hilgetag et al., 2016) including the entirety of brain's connections, cortical layers serve local microcircuits processing sensory or motor information, as well as the interconnected loops (thalamo-cortical) or large-scale networks: (i) bottom-up, sensory-to-motor; (ii) top-down, cognitive-to-motor; and (iii) inter-hemispheric, for coordination of various behaviors, serving a multifunctional purpose (Miller and Phelps, 2010; Makarova et al., 2011; Georgopoulos, 2015).

Do Neurons in Cortex Integrate Information Across Different Layers or Across Columns?

Indeed, neurons from different cortical layers/columns communicate to each other via synchronized firing (Romo et al., 2003; Opris et al., 2013) across cortical layers, quantified by cross-correlation histograms (CCHs). Also, neuronal integration has been studied using "noise and signal correlations" or LFP-spike interactions (Bosman and Aboitiz, 2015).

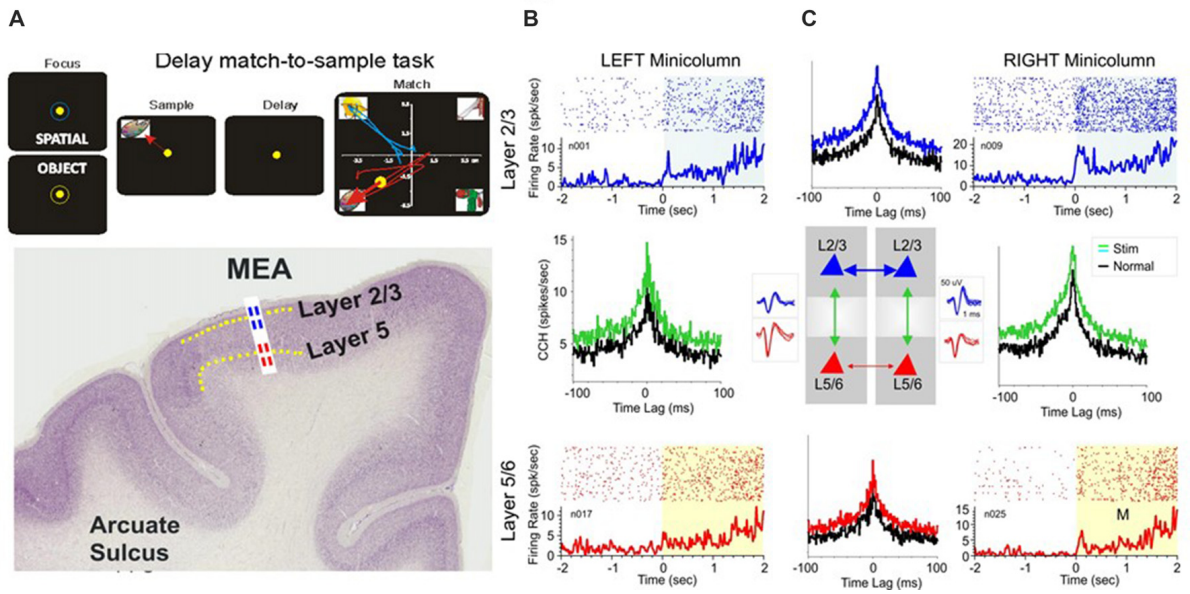

FIGURE 1 | (A) Behavioral paradigm showing the sequence of events in the rule-based delay match-to-sample (DMS) task: (1) presentation of a "focus" image (blue or yellow ring) to initiate an "object" or "spatial" trial, respectively, and prompting cursor placement to lead to (2) presentation of the "sample" image, followed by cursor movement into the image as the "sample" response followed by (3) a variable delay period of 1–60 s with a blank screen, followed by (4) the "match" phase in which the "sample" image was presented along with 1–6 other nonmatch (distractor) images on the same screen. Cursor movement into the correct (match target) image for ≥0.5 s produced a juice reward via a sipper tube mounted next to the animal's mouth. Placement of the cursor into a nonmatch image for ≥0.5 s caused the screen to blank without reward delivery. Intertrial interval: 10.0 s. **(B)** Illustrated coronal section in rhesus monkey brain showing relative location of supra-granular L2/3 (blue) and infra-granular L5 (red) with tract used for placement of conformal multielectrode array (MEA) recording probe. **(C)** Interlaminar activity recorded from adjacent prefrontal minicolumns during DMS task performance. Recording array: center insert shows the conformal MEA positioned for simultaneous interlaminar–columnar recording from adjacent mini-columns left and right with corresponding L2/3 and L5 cell pair waveforms (blue and red). Individual trial rasters and average peri-event histograms (PEHs) obtained from two cell pairs recorded simultaneously from L2/3 (blue) and L5 (red) in minicolumn format over ± 2.0 s relative to match phase (**A**) onset (0.0 s) in a single DMS session. Cross-correlation histograms (CCHs) for the same cell pairs in each minicolumn are shown (between raster-PEH displays) in left and right mini-columns for Pre (black, −2.0 s to 0.0 s) and Post (green, 0.0 s to +2.0 s) time intervals relative to match phase onset (M, 0.0 s). CCHs show increased inter-laminar synchronization (larger correlation peaks) for both cell pairs during target selection in the match phase (green, post) relative to similar correlations between the same cell pairs constructed before phase onset (pre, −2.0 s to 0.0 s). With permission from Opris et al. (2012b).

What Is the Evidence for Integration of Information Across Several Layers?

As seen in **Figure 1**, the neurons in prefrontal cortical layers L2/3 and L5 change firing patterns during the presentation of the matching target (together with the non-matching distractors), resulting in inter-laminar CCHs changes (increases the number of coincident spikes) that may represent trans-laminar integration of information (Foxworthy et al., 2013; Opris et al., 2013). Information flows through cortical layers in a feed-forward manner (Bastos et al., 2015), going from layer 4, to layers 2/3 and onwards (Bastos et al., 2012). Another view maintains that cortical layers can have distinct inputs that activate them, triggering spikes when the integration input bypasses a threshold (Opris and Casanova, 2014).

What Is the Hypothesis of Prefrontal Cortical Inter-laminar Integration?

The integrative hypothesis posits that integration of perceptual signals from supra-granular layers with the behavioral signals in the infra-granular layers takes place in the prefrontal cortical inter-laminar microcircuits (Opris et al., 2011, 2012a,b, 2013; Takeuchi et al., 2011).

What Is the Function of Each Prefrontal Cortical Layer?

Layer 1: Cross-modality modulation is achieved through layer L1 cell-mediated inhibitory and disinhibitory circuits (Ibrahim et al., 2016). Neurons in layer L1 form "canonical neuronal circuits" to control information processes in both supra- and infra-granular cortical layers (Lee et al., 2015). Projections of neurons to layer L1 from all cortical inputs has been shown to make a significant contribution to the integration process throughout the neocortex (Mitchell and Cauller, 2001).

Layer 2/3: This layer provides the integration of perceptual stimuli by inter-areal bottom up connections and the integration of perception with action by trans-laminar connections and top-down cortico-subcortical connections (Opris et al., 2011, 2012a,b, 2013).

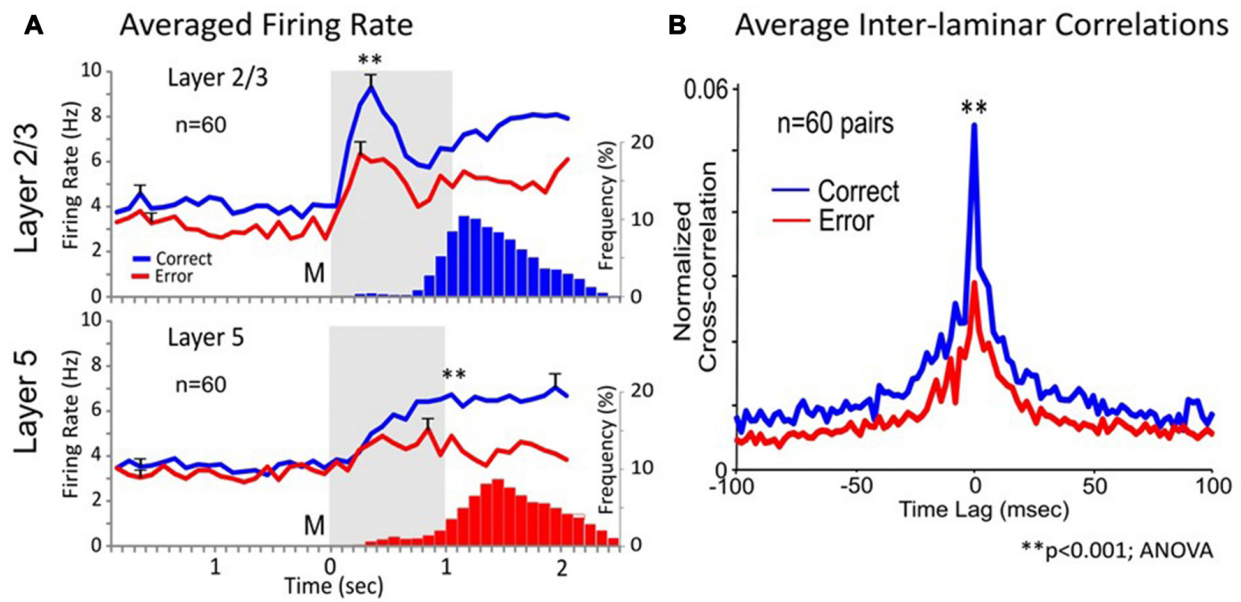

FIGURE 2 | Neural integration during correct vs. error trials. **(A)** Average Firing Rate. Mean PEHs during match phase averaged over all recorded interlaminar prefrontal cortex (PFC) cell pairs (n = 60), L2/3 (upper) and L5 (lower), on correct (blue) vs. error trials (red) summed across animals and sessions with ≥2 cell pairs recorded in same behavioral session from the same MEA. Blue and red histograms (bars) below PEHs show the associated mean frequency distributions of match response latencies (s) for correct (upper) and error (lower) trials plotted on the same time-base as the PEHs relative to match phase onset (0.0 s). **(B)** Average Inter-laminar Correlation. Mean CCHs for the same inter-laminar cell pairs (n = 60) constructed from correct (blue) and error (red) trials. ANOVA, $F_{(1,119)} = 14.18$, $^{**}p < 0.001$, difference in peak mean correlation.

Layer 3: This layer provides inter-hemispheric callosal connections (Georgopoulos, 2015).

Layer 4: The primary visual cortex receives orientation- and direction-tuned inputs from thalamus in layer 4 (Sun et al., 2016).

Layer 5: Pyramidal neurons in this layer integrate inputs from many sources and distribute outputs to cortical and subcortical structures (Kim et al., 2015). Cortical-subcortical neurons project to subcortical structures in the thalamo-cortical loop, integrate information and generate responses more relevant to movement control, while cortico-cortical neurons are more important in visual perception.

Layer 6: This layer projects to the thalamus (Opris and Casanova, 2014).

What Is the Evidence for Cortical Inter-laminar Integration?

Evidence for Functional Integration in Cortical Minicolumns

It is obvious that cortical neurons that interconnect to each other across layers play an important role in the emergence of brain function. To demonstrate this we show in **Figure 1** an ideal example that depicts simultaneously recorded cells with differential firing in adjacent minicolums and inter-laminar layers during the match epoch of the DMS task (**Figure 1A**). Functional integration may be pursued based on: (i) inter-laminar; and/or (ii) inter-columnar neuronal interactions. The cross-correlograms (**Figure 1C**) that quantify these interactions between cells provide crucial evidence for the integration process (Opris et al., 2012b).

Columnar Inter-laminar Processing in Prefrontal Cortex during "Target Selection"

Figure 1C shows an example of inter-laminar interaction between two cell pairs with individual firing rates displayed in raster/peri-event histograms (PEHs) during the epoch between matching image presentation (match phase onset) and offset of the matching "target" (0.0 s ± 2.0 s). Cell pairs in this study (Opris et al., 2012b) were recorded on "appropriate sets of adjacent pads" (corresponding to Minicolumns 1 and 2) on the biomorphic multielectrode arrays (MEAs), shown in the illustration of both trans-laminar cell pairs in L2/3 and L5/6 (**Figure 1C**). Neurons in both, upper and lower layers showed "significant increases" in mean firing rate ($p < 0.001$) in the "post"-match phase (0.0 s to 2.0 s) associated with target selection (**Figure 1A**) and the decision making phase of the task (Opris et al., 2012b), relative to the "pre"-match phase (−2.0 s to 0.0 s). An important observation

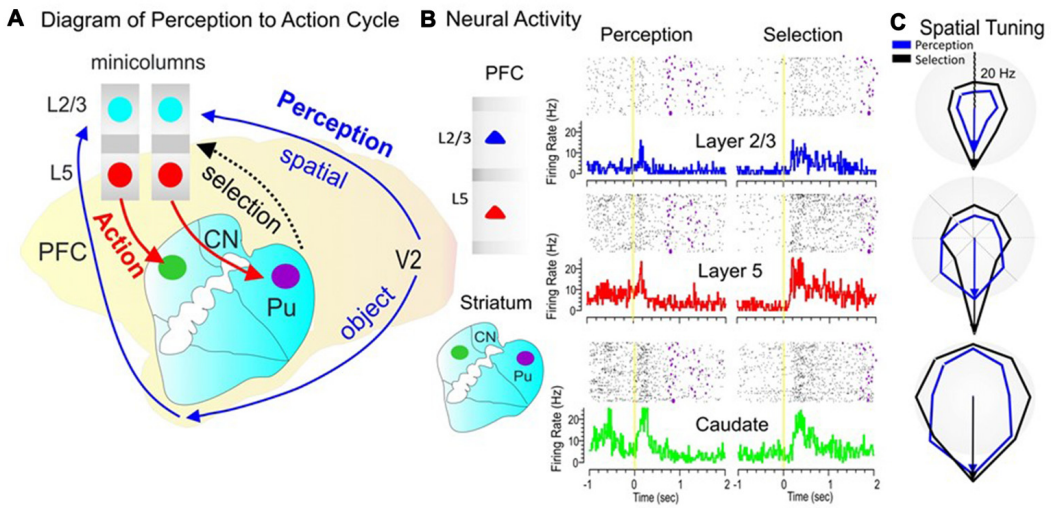

FIGURE 3 | The perception-to-action cycle with the behavioral paradigm. **(A)** The illustration of the perception-to-action cycle. The diagram depicts the flow of spatial and object signals during perceptual and executive selection of target stimuli in a rhesus macaque brain. In visual cortical area V2, visual information splits into dorsal (spatial signals) and ventral (object signals) pathways to the top of executive hierarchy in the PFC, and then top-down through the cortico-striatal-thalamo-cortical loops. Blue arrows depict the perceptual flow of information while red arrows indicate the action (executive) signal flow from prefrontal cortical layer 5 to the dorsal striatum, with the red dotted arrow indicating the thalamo-cortical projection in the cortico-striatal-thalamo-cortical loop. The two adjacent cortical minicolumns with red and blue filled circles indicate inter-laminar simultaneous recordings, while caudate-putamen recording are shown in green and pink circles. **(B)** Example of simultaneous individual activity (individual trial rasters and peri-event histograms) of single neurons recorded in prefrontal cortical layers L2/3 (blue) and L5 (red) with the conformal MEA and caudate n. (green) during "sample" (left part) and "match" target presentation (right part) on spatial trials during a single session (n = 120 trials). The purple marks in the rasters represent the time when the target was reached. **(C)** Directional tuning plots (blue for perception and black for executive selection) depict firing preference, measured by the radial eccentricity (in spikes/s or Hz) in the polygonal contour for the eight different target locations on the screen where images appear. The overlay tuning plots compare firing preferences on spatial trials for the same cells during "sample" (perception) and "match" (selection) presentation. The tuning vectors also show the magnitude of firing for preferred locations during the encoding (left panel) and selection (right panel) phases of the task on spatial trials. Spatial trials tuning vectors (black) show the same preferred directionality (i.e., 270°) during the encoding and selection phases in both PFC layers and in caudate nucleus, suggesting parallel processing streams/loops through cortical minicolumns and striatum and likely through the entire thalamo-cortical loop. The radius of polar plots is represented in Hz and tuning amplitude is measured in Hz, as well. Asterisks: $^{**}p < 0.001$, ANOVA.

highlighted with this type of recording configuration was that layer L2/3 neurons in the same minicolumn, exhibited higher firing rates in the "post"-match epoch (0.0 s to +2.0 s; **Figure 1C**, upper raster/PEHs) than neurons in L5 of the same, over the same time period (**Figure 1C**, lower raster/PEHs).

Precise "functional connections" between single units (cells) within each minicolumn were provided by cross-correlation histograms (CCHs), represented for individual L2/3 and L5 cell pairs recorded on vertically positioned electrode pads (**Figure 1B**) of the MEA (Opris et al., 2011, 2012b, 2013; Takeuchi et al., 2011). Normalized synchronized firing (shown by CCHs) for both minicolumns were shown in **Figure 1C** for cell firing in the displayed PEHs: (i) "pre"-match epoch (−2.0 s to 0.0 s, Pre, black curve); or (ii) "post"-match epoch (0.0 s to +2.0 s, Post, green) for the same cell pairs. Although both CCHs depict a "significantly correlated firing" ($p < 0.001$; t-test), the differences in max correlation for both neuron pairs suggest that inter-laminar firing was more synchronized in the "post"-match epoch (0.0–2.0 s) than in the "pre"-match epoch ($p < 0.001$; t-test).

Laminar Inter-columnar Processing in Prefrontal Cortex during "Target Selection"

The demonstration of functional connections between individual cells within same cortical layer and different minicolumns was provided by CCHs (Opris et al., 2012a) plotted for individual L2/3-vs.-L2/3 and L5-vs.-L5 cell pairs, recorded on horizontally positioned electrode pads on the MEA. Normalized correlograms for cell pairs are presented in **Figure 1C**. Although both correlograms (L2/3-vs.-L2/3 and L5-vs.-L5) show significantly correlated firing (Post vs. Pre: $p < 0.001$), the differences in peak correlation for both cell pairs indicate that intra-laminar inter-columnar firing was more synchronized in layer 2/3 than in layer 5 ($p < 0.001$). This supports the idea of laminar integration in supra-granular layers (Petro and Muckli, 2017).

Cortical-Subcortical Interaction

Cortical-subcortical integration of sensory and motor signals occurs during cortico-striatal interactions funneling signals in the cortico-thalamic loops (McFarland and Haber, 2002). Two recent results reported by Opris et al. (2013) and Santos et al. (2014) have demonstrated differential (pre)frontal cortico-

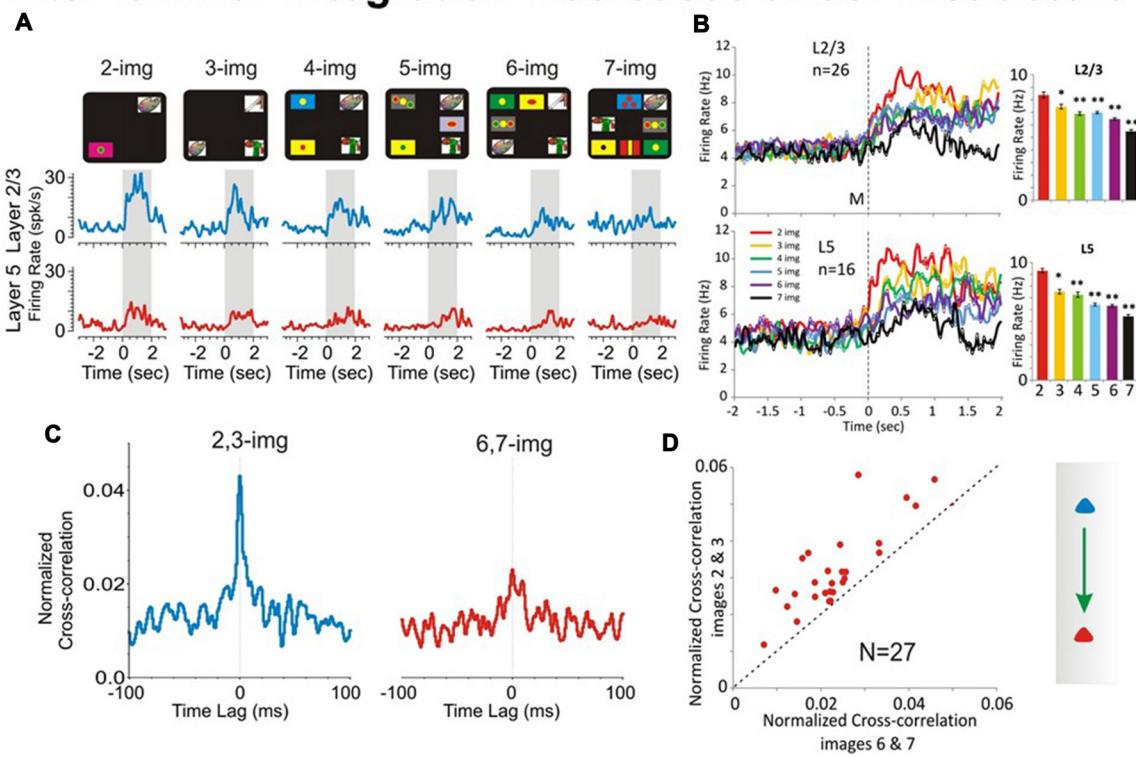

FIGURE 4 | Effect of number of images on PFC columnar firing. **(A)** Example PEHs comparing neuron firing in PFC layers L2/3 (blue) and L5 (red) as a function of the number of images presented (upper: display screens) in the match phase on Object type trials in the DMS task. **(B)** Population PEHs depicting the activity of prefrontal cells from layers L2/3 (n = 16) and L5 (n = 26) on all types of trials with different numbers of images (2, 3, 4, 5, 6 and 7) presented during match phase in the DMS task (L2/3: $F_{(6,1039)} = 8.29$, $p < 0.001$; L5: $F_{(6,639)} = 8.64$; $p < 0.001$, ANOVA). **(C)** Example inter-laminar CCHs for trials with a few (2 and 3 images) vs. many (6 and 7 images) distracter images constructed from the same interlaminar L2/3-L5 cell pair shown in **(A)**. **(D)** Normalized population CCHs for trials with low (2, 3 red) vs. high (6, 7 blue) numbers of images in the match phase consisting of the average correlation coefficients across individual CCHs from 27 different inter-laminar cell pairs. Scatter plot showing differential distributions of individual CCH peak correlation coefficients on trials with low vs. high numbers of images for the same cell pairs (n = 27) comprising the population CCH. $^{**}p < 0.001$, $^{*}p < 0.01$, ANOVA.

striatal interaction during the planning and preparation for movement in monkeys.

Laminar Inter-hemispheric Processing in Prefrontal Cortex in Layer 3

Neurons in Layer 3 of fronto-parietal cortices provide important interhemispheric callosal connections necessary for the coordination of movement (Georgopoulos, 2015). Obviously, inter-hemispheric integration is playing a key role such as coordination.

Comparison of Inter-laminar Integration in the Correct vs. Error Trials

One way to test whether trans-laminar integration takes place in cortical minicolumns is to compare the inter-laminar firing in correct vs. error trials. A trial was considered correct when the animal responded adequately to each instruction of the DMS task's event sequence (shown in **Figure 1A**), receiving a drop of juice as reward, or an error trial, when the animal failed to obey one or more instructions, and was not rewarded (Opris et al., 2012b). Experiments by Opris et al. (2012b) compared correlated firing of pairs of cells from layers L2/3 and L5 during the match epoch (dealing with target selection) under correct vs. error trials. **Figure 2A** shows that cell pairs (in layers L2/3 and L5) that exhibited increased firing during the match epoch in correct trials (left), reduced their firing on error trials, with the inappropriate target being selected (right). The trend of increased (respectively decreased) correlated firing in correct (respectively error) trials was present across entire subpopulation of prefrontal cell pairs, as shown in **Figure 2A**. Moreover, the significant increase (decrease) in the mean CCH peaks ($p < 0.001$), provides evidence for the enhanced (lack of) inter-laminar correlated firing between L2/3 and L5 in correct (error) trials, as shown in **Figure 2B**. Taken together, these unique simultaneous recordings in prefrontal cortical layers (and minicolumns) of rhesus macaques, during *in vivo* performance of a cognitive task, provide evidence for prefrontal cortical inter-laminar integration during correct trials and lack of integration during error trials.

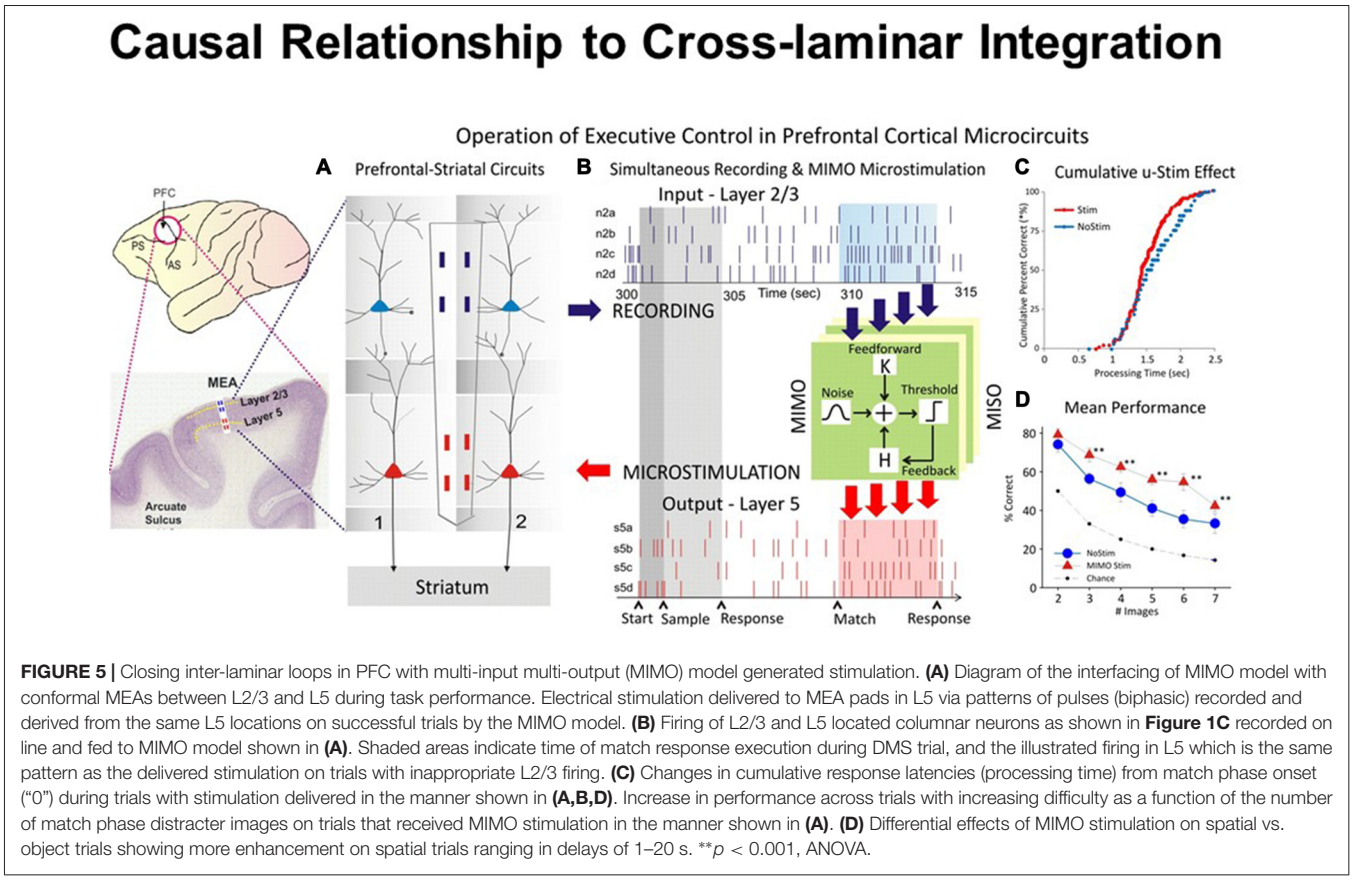

FIGURE 5 | Closing inter-laminar loops in PFC with multi-input multi-output (MIMO) model generated stimulation. **(A)** Diagram of the interfacing of MIMO model with conformal MEAs between L2/3 and L5 during task performance. Electrical stimulation delivered to MEA pads in L5 via patterns of pulses (biphasic) recorded and derived from the same L5 locations on successful trials by the MIMO model. **(B)** Firing of L2/3 and L5 located columnar neurons as shown in **Figure 1C** recorded on line and fed to MIMO model shown in **(A)**. Shaded areas indicate time of match response execution during DMS trial, and the illustrated firing in L5 which is the same pattern as the delivered stimulation on trials with inappropriate L2/3 firing. **(C)** Changes in cumulative response latencies (processing time) from match phase onset ("0") during trials with stimulation delivered in the manner shown in **(A,B,D)**. Increase in performance across trials with increasing difficulty as a function of the number of match phase distracter images on trials that received MIMO stimulation in the manner shown in **(A)**. **(D)** Differential effects of MIMO stimulation on spatial vs. object trials showing more enhancement on spatial trials ranging in delays of 1–20 s. $^{**}p < 0.001$, ANOVA.

Integration of Spatial Perception with Action

During the perception-to-action cycle, when the brain plans a movement, the executive mechanism coordinates the interactions between the environment and the perceptual/sensory-motor/executive systems (Fuster, 2000; Opris et al., 2011, 2013). On top of the executive hierarchy, the prefrontal microcircuits are assumed to "bind perceptual and executive control" functional signals to coordinate goal-driven behavior (**Figure 3A**). Here, we highlight the recorded neuronal "firing simultaneously in prefrontal cortical layers and the caudate-putamen" of rhesus monkeys (see **Figure 3B**), trained in a spatial-vs.-object version of the visual match-to-sample task (Opris et al., 2013). During the perception and executive selection epochs, cell firing in the prefrontal layers and caudate-putamen exhibited "preferences for the same location" on spatial-trials, but not on object-trials.

Transformation of Perceptual Signals into Action

When the perceptual-executive circuit is activated by the stimulation of prefrontal infra-granular-layers with electrical stimuli "patterns" obtained from supra-granular-layers, Opris et al. (2013) could replicate spatial preferences (similar to neural tuning) in percent correct performance, on spatial trials (**Figure 3C**). These results show that inter-laminar prefrontal microcircuits play causal roles in the perception-to-action cycle (Mahan and Georgopoulos, 2013; Opris et al., 2013).

Does the Number of Distractor Images Affect the Inter-laminar Integration?

In the DMS task in **Figure 1A** the distractor images are those images that represent a different object than the sample image. As shown previously (Opris et al., 2011, 2012a,b, 2013), a major factor influencing the selection of the matching target in the match phase of the DMS task was the number of distractor images presented with the "sample" image in a given trial (see **Figure 4**). The increase in task difficulty via increasing the number of distractors, allowed the animal to make a sizeable amount of error trials for comparison to the correct trials (Opris et al., 2012a). In **Figure 4A** is shown a gradual "decrease in cell pair firing in layers L2/3 and L5" as a function of the number of images presented during the matching phase. Consistent with our prior results (Opris et al., 2012a,b), neuronal population mean firing rates in layers L2/3 and L5 (**Figure 4B**) confirmed this decrease as a function of the number of distractors in the match phase ($p < 0.001$). Moreover, this decrease was also expressed in terms of "correlated firing" between L2/3-L5 cell pairs, as shown in **Figures 4C,D**, in which CCHs on trials with few (2 or 3) distracter images exhibited significantly higher correlations than on trials with more (6 or 7) distracter images ($p < 0.01$). The decrease in inter-laminar correlated firing is consistent with a decrease in integration caused by the increase in the number of distractor targets. Likely the decrease in task performance is due to an increase in the "cognitive

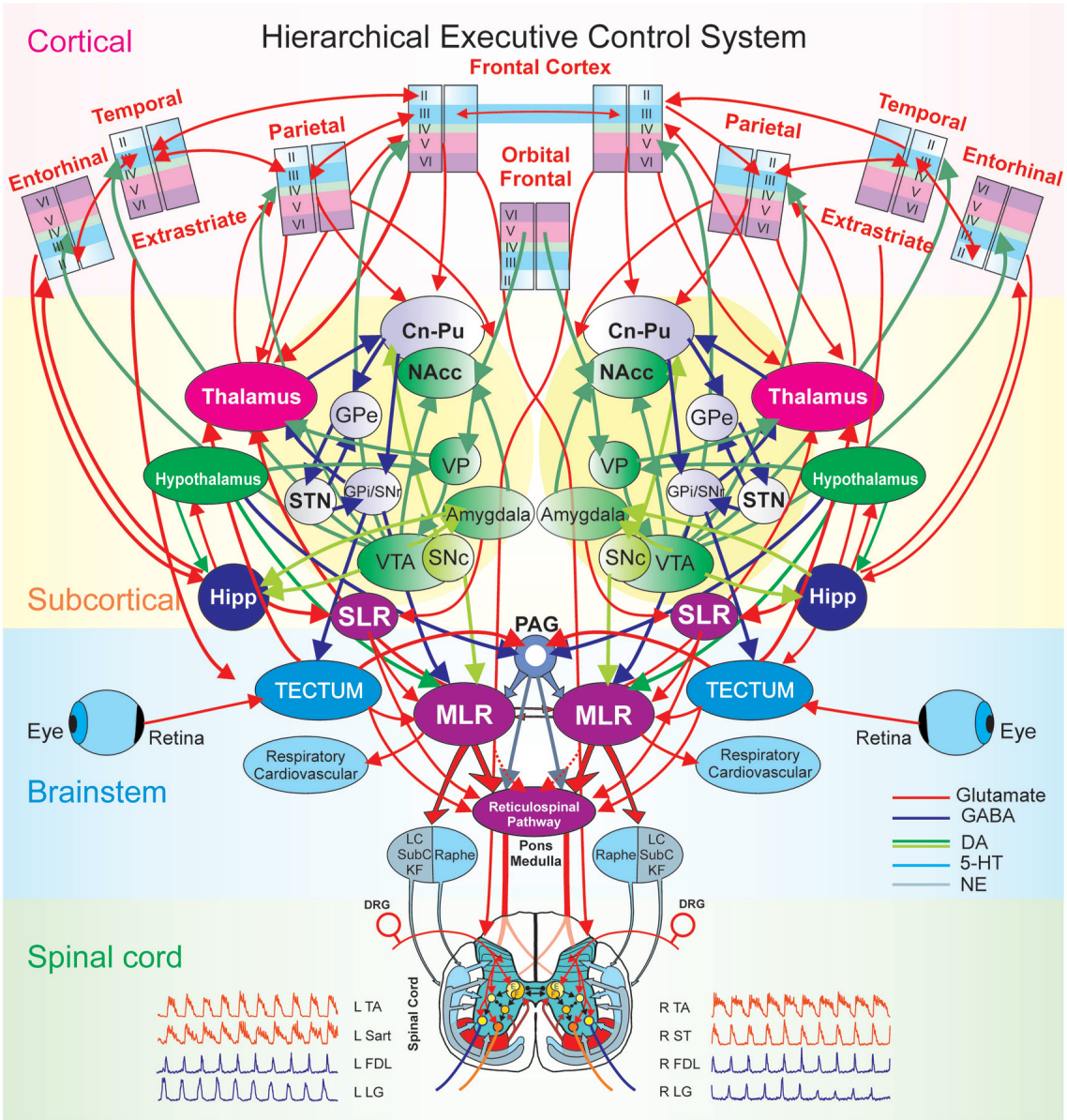

FIGURE 6 | The hierarchical executive control system for movement. The executive control system is anatomically organized via a hierarchical architecture of cortical modules (layers, minicolumns with microcircuits), subcortical nuclei (basal ganglia and thalamus with cortical-subcortical-thalamic loops; hippocampus and hypothalamus), brainstem (midbrain, pons, medulla with cortical-brainstem networks), and spinal cord (locomotor central pattern generators, CPG). At the higher level in the hierarchy are the columnar laminar modules of frontal (cognitive), parietal (motor), extrastriate (visual), temporal, orbital frontal cortices (emotion) and entorhinal (limbic), Beneath, are the subcortical structures: striatum (caudate, Cn, putamen, Pu and nucleus accumbens, NAcc), globus pallidus [GPe/GPi (external/internal segments), the dopaminergic ventral tegmental area (VTA), the ventral pallidum (VP), substantia nigra (SNc/SNr: pars compacta/pars reticulata), subthalamic nucleus (STN) and the thalamus. Motivation and emotion are processed by the hypothalamus and amygdala, respectively. The coordination of the navigation systems involves the frontal cortex and the hippocampus (Hipp). The subthalamic locomotor region (SLR) is a subcortical center for coordinating locomotion. At the level of the brain-stem and spinal cord, locomotion is initiated by the direct activation or disinhibition of the mesencephalic locomotor region (MLR) and/or the reticulospinal (RS) pathway. Stimulation of the MLR activates reticulospinal neurons which project through the ventrolateral funiculus to activate spinal locomotor central pattern generator neurons, in part, by the release of excitatory amino acids. The reticulospinal pathway is considered to comprise the primary "command pathway" for the initiation of locomotion. MLR stimulation also activates in parallel, multiple monoaminergic descending pathways during centrally-generated locomotion. The flexor (F) and extensor (E) components of the locomotor CPG are activated/modulated by descending bilateral reticulospinal and monoaminergic projections as well as by crossed excitatory (▶) and inhibitory (●) segmental projections from the CPG opposite to it. Sensory afferents from skin and muscles innervate spinal neurons in the dorsal horn, intermediate zone and ventral horn to fine-tune the locomotor step cycle. Details of the flexor and extensor components of the CPG are omitted in order to emphasize general interconnections between them and their target neurons. LC, locus ceruleus; SubC, subceruleus; KF, Kölliker-Fuse; DRG, dorsal root ganglia; L, left; R, right; TA, tibialis anterior; Sart, Sartorius; FDL, flexor digitorum longus; LG, lateral gastrocnemius; ST, semitendinosus.

work load" of the task (Kelley and Lavie, 2011; Opris et al., 2011).

Causal Relations to Columnar Integration

To test causal relationship to columnar inter-laminar integration, the recorded firing of neurons was examined via a nonlinear multi-input multi-output (MIMO) model, which extracted and characterized multi-laminar firing patterns during performance in the DMS task (Hampson et al., 2012). **Figure 5** provides causal evidence for the integration of natural signal flowing through the PFC microcircuits with the injected signal via stimulation. Minicolumnar neuronal firing of the PFC neurons was recorded from rhesus macaques trained in a DMS task, via biomorphic MEAs that provided signals from neurons in prefrontal cortical layers 2/3 and 5 (Opris et al., 2015a). The MIMO device sent patterns of electrical stimuli via *stimulation* to prefrontal cortical layer 5, during columnar "inter-laminar integration" at the time of target selection (Opris, 2013). Such stimulation improved (augmented) normal task performance significantly (**Figure 5D**). The executive control circuit was facilitated by applying stimulation patterns in the prefrontal cortical infra-granular-layers similar to the patterns coming from the supra-granular-layers that produced enhanced spatial preference in performance percentage, similar to neural tuning. Thus, inter-laminar prefrontal microcircuits may play causative roles in the cognitive perception-to-action cycle (Hampson et al., 2012; Opris, 2013). Such causal relations to integration of cognitive signals provide direct evidence that cortical minicolumns may represent the turbo-engines of the brain (Jones, 2000; Jones and Rakic, 2010; Opris et al., 2013; Chapman and Mudar, 2014).

Integration across Hierarchical Levels of Processing

Figure 6 illustrates modular integration across hierarchical levels. Executive control has been defined as the brain's ability "to control thought and action" by coordinating "multiple systems and mechanisms across multiple brain areas" to pursue a goal (Miller and Phelps, 2010). Examples of executive control functions include: attention, working memory, decision making, intention or motor plan and behavioral inhibition (Fuster and Bressler, 2012). Thus, the ability of the brain to exercise executive control over behavior relies upon the integration of the multiple microcircuitries (sensory, motor, reward), loops (thalamo-cortical) and large scale networks (bottom-up or top-down) with distributive encoding organized in a hierarchical manner.

The hierarchy of brain functions was introduced by Joaquin Fuster based on Hughlings Jackson's assumption that the neocortex is the climax of the nervous system and it controls (activates and/or inhibits) the functions of lower levels. However, cortical disease led to two sets of findings: "negative" signs and symptoms from "loss of the controlling cortex" and "positive" ones from the "emergence of the lower center" (Fuster, 1990; York and Steinberg, 2011). This implied an anatomical and physiological hierarchy of centers within the brain, with higher ones activating or suppressing the function of lower ones (Fuster, 1990; York and Steinberg, 2011).

Our focus is on the hierarchy of neural circuitry underlying the executive control of behavior (**Figure 6**) spanning from the frontal and parietal cortices, subcortical structures like the basal ganglia and thalamus, the brainstem and the spinal cord. The hierarchical integration of various stimuli (Hirabayashi et al., 2013a,b) in the executive function, may follow a bottom-up integration of visual information (Felleman and Van Essen, 1991) while the coordination of movement kinematics is performed in a top-down manner according to a prior intention/plan (Noga and Opris, 2017). At the top of the executive hierarchy are the frontal (premotor) and parietal (motor) cortical microcircuits, interconnected within thalamo-cortical loops through cortico-striatal projections and further in the brainstem to the mesencephalic locomotor region (MLR) and the central pattern generators in the spinal cord (Noga and Opris, 2017).

FUTURE DIRECTIONS

The following research topics deserve attention in the future neuroscience research. The first topic should be on the prefrontal cortical interactions with cortical (parietal, temporal and occipital) and subcortical (basal ganglia, thalamus, hypothalamus, hippocampus, amygdala) brain regions (Opris et al., 2013) during emergence of behavior and brain functions. The next topic may deal with the organization of prefrontal cortical connections within the brain's connectome from microcircuits to large scale networks (Hill et al., 2012; Markov et al., 2013; Markram et al., 2015; Reimann et al., 2017). The brain's connectome needs to be dissected at the microcircuit level. More evidence is needed for the functional organization across the prefrontal cortical areas that form a hub in the brain's connectome (Sato et al., 2016). Finally, evidence is needed for understanding brain disorders like autism, schizophrenia, Alzheimer's disease, attention deficit disorder or drug addiction (Opris and Casanova, 2014; Opris et al., 2015b).

CONCLUSION

The findings discussed here provide a unique insight into the inter-laminar integration of neural signals and illustrate the role of prefrontal cortical microcircuits in the executive control of behavior in the primate brain. This would have been impossible without the use of biomorphic multielectrode array that was tailored specifically for recording the columnar-laminar micro-architecture of the neocortex, in behaving monkeys during a cognitive task. The executive control role of prefrontal minicolumns was demonstrated by spatial preference signals, integrated and transformed into action signals which coded the intention to move to the same spatial location (Opris et al., 2013). A causal relationship using signals recorded in the upper prefrontal layers and feeding a similar pattern of electrically stimuli in the lower layers demonstrated the causal role of prefrontal mincolumn as a cognitive "turbo-engine. Prefrontal cortical integration

of perceptual signals (in supra-granular cortical layers), together with the behavioral (infra-granular layers) and reward signals (midbrain) results in the emergence of various brain functions. These cortical modules and their microcircuits represent the building blocks of these brain functions, with information passing through them in a hierarchical manner: from sensory to cognitive (bottom-up) structures in the prefrontal cortex and top-down to motor structures processing action and behavior, via thalamo-cortical loops.

AUTHOR CONTRIBUTIONS

This manuscript was written by IO together with SC and BRN.

FUNDING

This study was supported by National Institute of Neurological Disorders and Stroke (NINDS) Grant 2 R56NS-46404-061A to BRN.

REFERENCES

Aboitiz, F. (2011). Genetic and developmental homology in amniote brains. Toward conciliating radical views of brain evolution. *Brain Res. Bull.* 84, 125–136. doi: 10.1016/j.brainresbull.2010.12.003

Allen, E. J., Burton, P. C., Olman, C. A., and Oxenham, A. J. (2017). Representations of pitch and timbre variation in human auditory cortex. *J. Neurosci.* 37, 1284–1293. doi: 10.1523/JNEUROSCI.2336-16.2016

Arnold, M., Sejnowski, T., Hammerstrom, D., and Jabri, M. (2004). Neural systems integration. *Neurocomputing* 58–60, 1123–1128. doi: 10.1016/j.neucom.2004.01.176

Bastos, A. M., Usrey, W. M., Adams, R. A., Mangun, G. R., Fries, P., and Friston, K. J. (2012). Canonical microcircuits for predictive coding. *Neuron* 76, 695–711. doi: 10.1016/j.neuron.2012.10.038

Bastos, A. M., Vezoli, J., Bosman, C. A., Schoffelen, J.-M., Oostenveld, R., Dowdall, J. R., et al. (2015). Visual areas exert feedforward and feedback influences through distinct frequency channels. *Neuron* 85, 390–401. doi: 10.1016/j.neuron.2014.12.018

Bosman, C. A., and Aboitiz, F. (2015). Functional constraints in the evolution of brain circuits. *Front. Neurosci.* 9:303. doi: 10.3389/fnins.2015.00303

Buxhoeveden, D. P., and Casanova, M. F. (2002). The minicolumn hypothesis in neuroscience. *Brain* 125, 935–951. doi: 10.1093/brain/awf110

Casanova, M. F., El-Baz, A., and Switala, A. (2011). Laws of conservation as related to brain growth, aging, and evolution: symmetry of the minicolumn. *Front. Neuroanat.* 5:66. doi: 10.3389/fnana.2011.00066

Chapman, S. B., and Mudar, R. A. (2014). Enhancement of cognitive and neural functions through complex reasoning training: evidence from normal and clinical populations. *Front. Syst. Neurosci.* 8:69. doi: 10.3389/fnsys.2014.00069

Chung, A. W., Schirmer, M. D., Krishnan, M. L., Ball, G., Aljabar, P., Edwards, A. D., et al. (2016). Characterising brain network topologies: a dynamic analysis approach using heat kernels. *Neuroimage* 141, 490–501. doi: 10.1016/j.neuroimage.2016.07.006

Constantinople, C. M., and Bruno, R. M. (2013). Deep cortical layers are activated directly by thalamus. *Science* 340, 1591–1594. doi: 10.1126/science.1236425

DeFelipe, J. (2011). The evolution of the brain, the human nature of cortical circuits and intellectual creativity. *Front. Neuroanat.* 5:29. doi: 10.3389/fnana.2011.00029

DeFelipe, J., Markram, H., and Rockland, K. S. (2012). The neocortical column. *Front. Neuroanat.* 6:22. doi: 10.3389/fnana.2012.00005

Felleman, D. J., and Van Essen, D. C. (1991). Distributed hierarchical processing in the primate cerebral cortex. *Cereb. Cortex* 1, 1–47. doi: 10.1093/cercor/1.1.1

Foxworthy, W. A., Clemo, H. R., and Meredith, M. A. (2013). Laminar and connectional organization of a multisensory cortex. *J. Comp. Neurol.* 521, 1867–1890. doi: 10.1002/cne.23264

Fuster, J. M. (1990). Prefrontal cortex and the bridging of temporal gaps in the perception-action cycle. *Ann. N Y Acad. Sci.* 608, 318–329. doi: 10.1111/j.1749-6632.1990.tb48901.x

Fuster, J. M. (2000). Executive frontal functions. *Exp. Brain Res.* 133, 66–70. doi: 10.1007/s002210000401

Fuster, J. M. (2001). The prefrontal cortex-an update: time is of the essence. *Neuron* 30, 319–333. doi: 10.1016/s0896-6273(01)00285-9

Fuster, J. M., and Bressler, S. L. (2012). Cognit activation: a mechanism enabling temporal integration in working memory. *Trends Cogn. Sci.* 16, 207–218. doi: 10.1016/j.tics.2012.03.005

Gabbott, P. L., Warner, T. A., Jays, P. R. L., and Bacon, S. J. (2003). Areal and synaptic interconnectivity of prelimbic (area 32), infralimbic (area 25) and insular cortices in the rat. *Brain Res.* 993, 59–71. doi: 10.1016/j.brainres.2003.08.056

Gabbott, P. L., Warner, T. A., Jays, P. R., Salway, P., and Busby, S. J. (2005). Prefrontal cortex in the rat: projections to subcortical autonomic, motor and limbic centers. *J. Comp. Neurol.* 492, 145–177. doi: 10.1002/cne.20738

Georgopoulos, A. P. (2015). "Columnar organization of the motor cortex: direction of movement," in *Recent Advances on the Modular Organization of the Cortex*, eds M. F. Casanova and I. Opris (Amsterdam: Springer), 123–141.

Hampson, R. E., Gerhardt, G. A., Marmarelis, V., Song, D., Opris, I., Santos, L., et al. (2012). Facilitation and restoration of cognitive function in primate prefrontal cortex by a neuroprosthesis that utilizes minicolumn-specific neural firing. *J. Neural Eng.* 9:056012. doi: 10.1088/1741-2560/9/5/056012

Hilgetag, C. C., Medalla, M., Beul, S. F., and Barbas, H. (2016). The primate connectome in context: principles of connections of the cortical visual system. *Neuroimage* 134, 685–702. doi: 10.1016/j.neuroimage.2016.04.017

Hill, S. L., Wang, Y., Riachi, I., Schürmann, F., and Markram, H. (2012). Statistical connectivity provides a sufficient foundation for specific functional connectivity in neocortical neural microcircuits. *Proc. Natl. Acad. Sci. U S A* 109, E2885–E2894. doi: 10.1073/pnas.1202128109

Hirabayashi, T., Takeuchi, D., Tamura, K., and Miyashita, Y. (2013a). Functional microcircuit recruited during retrieval of object association memory in monkey perirhinal cortex. *Neuron* 77, 192–203. doi: 10.1016/j.neuron.2012.10.031

Hirabayashi, T., Takeuchi, D., Tamura, K., and Miyashita, Y. (2013b). Microcircuits for hierarchical elaboration of object coding across primate temporal areas. *Science* 341, 191–195. doi: 10.1126/science.1236927

Ibrahim, L. A., Mesik, L., Ji, X. Y., Fang, Q., Li, H. F., Li, Y. T., et al. (2016). Cross-modality sharpening of visual cortical processing through layer-1-mediated inhibition and disinhibition. *Neuron* 89, 1031–1045. doi: 10.1016/j.neuron.2016.01.027

Jones, E. G. (2000). Microcolumns in the cerebral cortex. *Proc. Natl. Acad. Sci. U S A* 97, 5019–5021. doi: 10.1073/pnas.97.10.5019

Jones, E. G., and Rakic, P. (2010). Radial columns in cortical architecture: it is the composition that counts. *Cereb. Cortex* 20, 2261–2264. doi: 10.1093/cercor/bhq127

Kaas, J. H. (2012). Evolution of columns, modules, and domains in the neocortex of primates. *Proc. Natl. Acad. Sci. U S A* 109, 10655–10660. doi: 10.1073/pnas.1201892109

Kelley, T. A., and Lavie, N. (2011). Working memory load modulates distractor competition in primary visual cortex. *Cereb. Cortex* 21, 659–665. doi: 10.1093/cercor/bhq139

Kim, E. J., Juavinett, A. L., Kyubwa, E. M., Jacobs, M. W., and Callaway, E. M. (2015). Three types of cortical layer 5 neurons that differ in brain-wide connectivity and function. *Neuron* 88, 1253–1267. doi: 10.1016/j.neuron.2015.11.002

Kritzer, M. F., and Goldman-Rakic, P. S. (1995). Intrinsic circuit organization of the major layers and sublayers of the dorsolateral prefrontal cortex in the rhesus monkey. *J. Comput. Neurol.* 359, 131–143. doi: 10.1002/cne.903590109

Lee, A. J., Wang, G., Jiang, X., Johnson, S. M., Hoang, E. T., Lanté, F., et al. (2015). Canonical organization of layer 1 neuron-led cortical inhibitory and disinhibitory interneuronal circuits. *Cereb. Cortex* 25, 2114–2126. doi: 10.1093/cercor/bhu020

Mahan, M. Y., and Georgopoulos, A. P. (2013). Motor directional tuning across brain areas: directional resonance and the role of inhibition for directional accuracy. *Front. Neural Circuits* 7:92. doi: 10.3389/fncir.2013.00092

Makarova, J., Ibarz, J. M., Makarov, V. A., Benito, N., and Herreras, O. (2011). Parallel readout of pathway-specific inputs to laminated brain structures. *Front. Syst. Neurosci.* 5:77. doi: 10.3389/fnsys.2011.00077

Markov, N. T., Ercsey-Ravasz, M., Van Essen, D. C., Knoblauch, K., Toroczkai, Z., and Kennedy, H. (2013). Cortical high-density counter stream architectures. *Science* 342:1238406. doi: 10.1126/science.1238406

Markram, H., Muller, E., Ramaswamy, S., Reimann, M. W., Abdellah, M., Sanchez, C. A., et al. (2015). Reconstruction and simulation of neocortical microcircuitry. *Cell* 163, 456–492. doi: 10.1016/j.cell.2015.09.029

McFarland, N. R., and Haber, S. N. (2002). Thalamic relay nuclei of the basal ganglia form both reciprocal and nonreciprocal cortical connections, linking multiple frontal cortical areas. *J. Neurosci.* 22, 8117–8132.

Miller, E. K., and Cohen, J. D. (2001). An integrative theory of prefrontal cortex function. *Annu. Rev. Neurosci.* 24, 167–202. doi: 10.1146/annurev.neuro.24.1.167

Miller, E. K., and Phelps, E. A. (2010). Current opinion in neurobiology—cognitive neuroscience 2010. *Curr. Opin. Neurobiol.* 20, 141–142. doi: 10.1016/j.conb.2010.03.008

Mitchell, B. D., and Cauller, L. J. (2001). Corticocortical and thalamocortical projections to layer I of the frontal neocortex in rats. *Brain Res.* 921, 68–77. doi: 10.1016/s0006-8993(01)03084-0

Mountcastle, V. B. (1957). Modality and topographic properties of single neurons of cats somatic sensory cortex. *J. Neurophysiol.* 20, 408–434.

Mountcastle, V. B. (1997). The columnar organization of the neocortex. *Brain* 120, 701–722. doi: 10.1093/brain/120.4.701

Noga, B. R., and Opris, I. (2017). "The hierarchical circuit for executive control of movement chapter 5," in *Physics of the Mind and Brain Disorders: Advances in Electrostimulation Therapies*, eds I. Opris and M. F. Casanova (Berlin: Springer), 95–127.

Opris, I. (2013). Inter-laminar microcircuits across the neocortex: repair and augmentation. *Front. Syst. Neurosci.* 7:80. doi: 10.3389/fnsys.2013.00080

Opris, I., and Casanova, M. F. (2014). Prefrontal cortical minicolumn: from executive control to disrupted cognitive processing. *Brain* 137, 1863–1875. doi: 10.1093/brain/awt359

Opris, I., Fuqua, J. L., Gerhardt, G. A., Hampson, R. E., and Deadwyler, S. A. (2015a). Prefrontal cortical recordings with biomorphic MEAs reveal complex columnar-laminar microcircuits for BCI/BMI implementation. *J. Neurosci. Methods.* 244, 104–113. doi: 10.1016/j.jneumeth.2014.05.029

Opris, I., Gerhardt, G. A., Hampson, R. E., and Deadwyler, S. A. (2015b). Disruption of columnar and laminar cognitive processing in primate prefrontal cortex following cocaine exposure. *Front. Syst. Neurosci.* 9:79. doi: 10.3389/fnsys.2015.00079

Opris, I., Fuqua, J. L., Huettl, P. F., Gerhardt, G. A., Berger, T. W., Hampson, R. E., et al. (2012a). Closing the loop in primate prefrontal cortex: inter-laminar processing. *Front. Neural Circuits* 6:88. doi: 10.3389/fncir.2012.00088

Opris, I., Hampson, R. E., Gerhardt, G. A., Berger, T. W., and Deadwyler, S. A. (2012b). Columnar processing in primate pFC: evidence for executive control microcircuits. *J. Cogn. Neurosci.* 24, 2334–2347. doi: 10.1162/jocn_a_00307

Opris, I., Hampson, R. E., Stanford, T. R., Gerhardt, G. A., and Deadwyler, S. A. (2011). Neural activity in frontal cortical cell layers: evidence for columnar sensorimotor processing. *J. Cogn. Neurosci.* 23, 1507–1521. doi: 10.1162/jocn.2010.21534

Opris, I., Santos, L., Gerhardt, G. A., Song, D., Berger, T. W., Hampson, R. E., et al. (2013). Prefrontal cortical microcircuits bind perception to executive control. *Sci. Rep.* 3:2285. doi: 10.1038/srep02285

Penfield, W. (1958). Centrencephalic integrating system. *Brain* 81, 231–234. doi: 10.1093/brain/81.2.231

Peng, Y., Gillis-Smith, S., Jin, H., Tränkner, D., Ryba, N. J., and Zuker, C. S. (2015). Sweet and bitter taste in the brain of awake behaving animals. *Nature* 527, 512–515. doi: 10.1038/nature15763

Petro, L. S., and Muckli, L. (2017). The laminar integration of sensory inputs with feedback signals in human cortex. *Brain Cogn.* 112, 54–57. doi: 10.1016/j.bandc.2016.06.007

Qu, L. P., Kahnt, T., Cole, S. M., and Gottfried, J. A. (2016). *De novo* emergence of odor category representations in the human brain. *J. Neurosci.* 36, 468–478. doi: 10.1523/JNEUROSCI.3248-15.2016

Reimann, M. W., Nolte, M., Scolamiero, M., Turner, K., Perin, R., Chindemi, G., et al. (2017). Cliques of neurons bound into cavities provide a missing link between structure and function. *Front. Comput. Neurosci.* 11:48. doi: 10.3389/fncom.2017.00048

Romo, R., Hernández, A., Zainos, A., and Salinas, E. (2003). Correlated neuronal discharges that increase coding efficiency during perceptual discrimination. *Neuron* 38, 649–657. doi: 10.1016/s0896-6273(03)00287-3

Santos, L. M., Opris, I., Hampson, R. E., Godwin, D. W., Gerhardt, G. A., and Deadwyler, S. A. (2014). Functional dynamics of primate cortico-striatal networks during volitional movements. *Front. Syst. Neurosci.* 8:27. doi: 10.3389/fnsys.2014.00027

Sato, J. R., Biazoli, C. E. Jr., Salum, G. A., Gadelha, A., Crossley, N., Vieira, G., et al. (2016). Connectome hubs at resting state in children and adolescents: reproducibility and psychopathological correlation. *Dev. Cogn. Neurosci.* 20, 2–11. doi: 10.1016/j.dcn.2016.05.002

Shepherd, G. M. (2011). The microcircuit concept applied to cortical evolution: from three-layer to six-layer cortex. *Front. Neuroanat.* 5:30. doi: 10.3389/fnana.2011.00030

Shepherd, G., and Grillner, S. (2010). *Handbook of Brain Microcircuits.* New York, NY: Oxford University Press.

Sun, W., Tan, Z., Mensh, B. D., and Ji, N. (2016). Thalamus provides layer 4 of primary visual cortex with orientation- and direction-tuned inputs. *Nat. Neurosci.* 19, 308–315. doi: 10.1038/nn.4196

Szentágothai, J., and Arbib, M. A. (1975). *Conceptual Models of Neural Organization.* Cambridge, MA: MIT Press.

Takeuchi, D., Hirabayashi, T., Tamura, K., and Miyashita, Y. (2011). Reversal of interlaminar signal between sensory and memory processing in monkey temporal cortex. *Science* 331, 1443–1447. doi: 10.1126/science.1199967

Thomson, A. M., and Lamy, C. (2007). Functional maps of neocortical local circuitry. *Front. Neurosci.* 1, 19–42. doi: 10.3389/neuro.01.1.1.002.2007

York, G. K. III, and Steinberg, D. A. (2011). Hughlings Jackson's neurological ideas. *Brain* 134, 3106–3113. doi: 10.1093/brain/awr219

Conflict of Interest Statement: The authors declare that the research was conducted in the absence of any commercial or financial relationships that could be construed as a potential conflict of interest.

frontiers in Neuroanatomy

REVIEW
published: 22 August 2017
doi: 10.3389/fnana.2017.00071

A Laminar Organization for Selective Cortico-Cortical Communication

*Rinaldo D. D'Souza * and Andreas Burkhalter*

Department of Neuroscience, Washington University School of Medicine, St. Louis, MO, United States

The neocortex is central to mammalian cognitive ability, playing critical roles in sensory perception, motor skills and executive function. This thin, layered structure comprises distinct, functionally specialized areas that communicate with each other through the axons of pyramidal neurons. For the hundreds of such cortico-cortical pathways to underlie diverse functions, their cellular and synaptic architectures must differ so that they result in distinct computations at the target projection neurons. In what ways do these pathways differ? By originating and terminating in different laminae, and by selectively targeting specific populations of excitatory and inhibitory neurons, these "interareal" pathways can differentially control the timing and strength of synaptic inputs onto individual neurons, resulting in layer-specific computations. Due to the rapid development in transgenic techniques, the mouse has emerged as a powerful mammalian model for understanding the rules by which cortical circuits organize and function. Here we review our understanding of how cortical lamination constrains long-range communication in the mammalian brain, with an emphasis on the mouse visual cortical network. We discuss the laminar architecture underlying interareal communication, the role of neocortical layers in organizing the balance of excitatory and inhibitory actions, and highlight the structure and function of layer 1 in mouse visual cortex.

Keywords: cortical hierarchy, mouse visual cortex, interareal communication, layer 1, cortical inhibition

OPEN ACCESS

Edited by:
Kathleen S. Rockland, Boston University School of Medicine, United States

Reviewed by:
Laura Busse, Ludwig-Maximilians-Universität München, Germany
Stewart Shipp, University College London, United Kingdom

****Correspondence:***
Rinaldo D. D'Souza
rinaldo.dsouza@gmail.com

Received: *30 May 2017*
Accepted: *07 August 2017*
Published: *22 August 2017*

Citation:
D'Souza RD and Burkhalter A (2017) A Laminar Organization for Selective Cortico-Cortical Communication. Front. Neuroanat. 11:71. doi: 10.3389/fnana.2017.00071

INTRODUCTION

The neocortex, arguably the pinnacle of mammalian evolution, is a layered sheet that blankets the forebrain. It is critically involved in sensory perception, guiding actions, paying attention and interpreting the world around us (Cauller, 1995; Treisman, 1996; Alfano and Studer, 2013). To perform these functions, neocortical circuits must selectively extract and amplify neuronal signals that encode various features of sensory stimuli, compare incoming signals with stored information, and route them to specialized circuits both within and outside the cortex (Douglas and Martin, 2007; Shipp, 2007; Harris and Mrsic-Flogel, 2013; Harris and Shepherd, 2015). Excitatory projection neurons and diverse local inhibitory interneurons in the neocortex form an intricate network in which synaptic connections between the neurons reveal a high level of specificity (Binzegger et al., 2004; Jiang et al., 2015). This specificity includes the genetic identity of the source and target neurons, the cortical areas the neurons reside in, and the precise locations of inputs on a neuron's dendrites (Groh et al., 2010; Sorensen et al., 2015; Zeisel et al., 2015; Tasic et al., 2016; Feldmeyer et al., 2017). The network includes local circuits composed of neurons within tens of microns of each other, as well as long-range pathways that interconnect areas that are millimeters or centimeters apart. Each cortical projection neuron consequently receives inputs from thousands of other neurons (Elston et al., 2009); the timing, strength and polarity (i.e., whether inhibitory

BOX 1 | Note that each of the words *feedforward* and *feedback* has two distinct meanings in this manuscript. When classifying pathways or axonal projections, the words describe the direction of signal flow within a hierarchy. On the other hand, feedforward and feedback *inhibition*, is a circuit motif whose definition is independent of pathway or hierarchy. For example, feedforward inhibition can be generated within both feedforward and feedback pathways.

or excitatory) of these inputs together with the intrinsic membrane properties of the postsynaptic cell (reviewed in Whitmire and Stanley, 2016) determine the projection neuron's spike output. The high specificity of connections results in a variety of functional motifs including recurrent excitation (Douglas et al., 1995; Douglas and Martin, 2007), feedforward inhibition (see **Box 1**; Pouille et al., 2009; Isaacson and Scanziani, 2011), and divisive and subtractive normalization caused by counterbalanced inhibition (Carandini and Heeger, 2011; Wilson et al., 2012), each of which plays important, specific roles in signal amplification and gain control.

Further constraining the diversity of synaptic inputs that each neuron receives is the cortex's layered architecture, commonly identified by the size and density of neurons and the arrangement of afferent inputs. As a result, a major determinant of the output of a neuron is its laminar location as well as the shape and extent of its dendritic tree (DeFelipe and Fariñas, 1992; Major et al., 2013). For instance, synaptic inputs to distal regions of a pyramidal cell's apical dendrite would be substantially more attenuated at the cell body than inputs to more proximal sites (Stuart and Spruston, 1998; Williams and Stuart, 2002). As a result, projection neurons must integrate a temporal pattern of postsynaptic currents of varying amplitudes, leading to a spike readout that is a result of nonlinear summations of synaptic inputs from different layers (Spruston, 2008). The laminar organization of neurons and their afferents, both long-range and local, is therefore central to neocortical function (Douglas and Martin, 2004). In this manuscript, we review studies that have provided important insights into the laminar structure of hierarchically organized cortico-cortical networks and discuss how the interplay between excitation and inhibition within the different laminae may differentially regulate signal transmission through intracortical and cortico-thalamo-cortical pathways.

ANATOMY OF CORTICAL HIERARCHY

The task of processing the diverse features of a sensory stimulus within the neocortex is distributed across a mosaic of many distinct, interconnected *areas* that are characterized by distinct connectivity profiles, cytoarchitecture, functions and developmental specification (Felleman and Van Essen, 1991; Andermann et al., 2011; Marshel et al., 2011; Alfano and Studer, 2013; Glasser et al., 2016). In non-human primates the areas involved in vision and visually guided actions can be described formally as being in a distributed hierarchical network with areas higher up the hierarchy underlying the representation of increasingly complex features of visual stimuli (Maunsell and van Essen, 1983; Felleman and Van Essen, 1991; Markov and Kennedy, 2013; Laramée and Boire, 2014). Visual signals are transmitted from lower to higher areas through so-called *feedforward* pathways (**Box 1**) that typically project in the rostral direction initiating from the posterior-most primary visual cortex (V1; Bastos et al., 2012; Markov and Kennedy, 2013). Concurrently, caudally-projecting sensory and motor *feedback* pathways are thought to be involved in contour integration of local stimulus features, making predictions of sensory stimuli, resulting in the context-dependent selection and modulation of relevant feedforward inputs (Bastos et al., 2012; Larkum, M. 2013; Saleem et al., 2013; Vaiceliunaite et al., 2013; Chen et al., 2014; Pafundo et al., 2016; Pakan et al., 2016; Attinger et al., 2017; Kuchibhotla et al., 2017; Nandy et al., 2017). This has led to the suggestion that ascending signals encode errors between the expected (predicted) and the actual response to sensory input, a mechanism referred to as predictive coding (Rao and Ballard, 1999; Bastos et al., 2012; Shipp, 2016).

Because of their divergent functions in bottom-up and top-down processing, it is perhaps not surprising that feedforward and feedback pathways exhibit anatomical differences across species. Felleman and Van Essen (1991) famously constructed a hierarchy of the macaque monkey visual cortex by examining termination patterns of cortico-cortical axonal projections from hundreds of prior studies and by classifying these pathways as being feedforward, feedback, or lateral (i.e., connecting areas at the same level of a hierarchy). In this classification, projections that were densest in layer 4, but which often included other layers as well, were considered feedforward; pathways preferentially terminating in superficial and deep layers were classified as being feedback; and pathways that terminated more uniformly in all layers were described as being lateral (Rockland and Pandya, 1979; Maunsell and van Essen, 1983; Felleman and Van Essen, 1991). While this meta-analysis has been extremely influential in our understanding of coding mechanisms within hierarchical networks, studies in non-primate animal models have shown that the exact laminar patterns formed by ascending and descending interareal projections differ between species. In the adult cat, for example, projections from V1 to higher cortical areas 18 and 19 terminated strongest in layers 2/3, with substantially weaker inputs to layer 4, although V1 projections to the medial bank of the suprasylvian sulcus had a more primate-like feedforward appearance with strongest terminations in layer 4 (Price and Zumbroich, 1989). This is noteworthy because Felleman and Van Essen (1991) regarded projections in the macaque cortex that were densest outside of layer 4 to be descending. Similarly in rat, axons from V1 to higher visual areas showed a multilaminar organization with roughly equally dense terminations in layers 2–5 (Coogan and Burkhalter, 1990, 1993), reminiscent of the description of lateral connections in macaque (Felleman and Van Essen, 1991). These feedforward laminar termination patterns were distinct from feedback terminations, which were densest in layers 1 and 6 (Coogan and Burkhalter, 1990, 1993).

The differences in lamination patterns of interareal connections may be expected based on the diversity of laminar architectures and mRNA expression profiles across species; for

example, V1 in primates can be divided into twelve rather than six cortical layers commonly annotated in rodents (Belgard et al., 2011; Bernard et al., 2012; Balaram and Kaas, 2014). An important contributing factor for this diversity in cortical lamination is the difference in proliferative cell cycles during corticogenesis in different species, particularly the role of the outer subventricular zone in the expansion of the superficial layers in primate cortex (Lui et al., 2011; Dehay et al., 2015). Thus the species-specificity of laminar patterns may reflect the disparate organizations of circuits required for network processing adapted to species-variant properties of cortices such as brain size, number of areas, network density and the ecological niche within which the animals evolved to survive and thrive (Kaas, 2013; Laramée and Boire, 2014). A preserved feature across mammals, however, is that feedforward connections terminate most densely in layers 3 and 4. In contrast, feedback projections are densest in layer 1, which is less strongly innervated by local, lateral and feedforward connections (Thomson and Bannister, 2003; Binzegger et al., 2004; Shipp, 2007).

With the development of powerful tools for identifying, recording and manipulating neuronal circuits with unprecedented resolution and accuracy, the mouse has emerged as an extremely useful model to examine the organization, function and synaptic architecture of the mammalian visual system (Havekes and Abel, 2009; Huberman and Niell, 2011; Katzner and Weigelt, 2013). Constructing the mouse visual cortical hierarchy is therefore an important step in the study of visual function. Based on the laminar termination patterns of interareal axonal afferents within the mouse cortical network, the density of interareal projections in layers 2–4 relative to that in layer 1 was analyzed to show a clear hierarchy between three areas, V1, LM (the lateromedial area), and PM (the posteromedial area; D'Souza et al., 2016). The relative hierarchical positions of the three areas were consistent with the increase in their respective receptive field sizes (Wang and Burkhalter, 2007). The axonal termination patterns in the higher areas suggest that layers 2–4 in mouse neocortex plays the role of the primate middle layers as the primary target of feedforward afferent connections. Supporting this idea is the observation that geniculocortical afferents to V1, while densest in layer 4, also terminate in layers 1–3 (Antonini et al., 1999; Cruz-Martín et al., 2014). The interareal connection from LM to PM also indicates that layer 1 may be an important target of feedforward projections originating in higher areas (D'Souza et al., 2016). The complete hierarchy of the approximately ten to sixteen areas that make up the mouse visual cortical network (Wang and Burkhalter, 2007; Andermann et al., 2011; Marshel et al., 2011; Garrett et al., 2014; Zhuang et al., 2017) is yet to be determined.

The anatomical hierarchy of visual cortex is observed not only in the organization of interareal axonal terminations, but also in the laminar locations of the cell bodies from which they originate (Maunsell and van Essen, 1987; Markov and Kennedy, 2013). In order to obtain a quantitative measure for hierarchical levels, the primate cortical hierarchy was constructed by measuring the proportion of neurons in layers 2 and 3 that project to a target area, to the total number of projecting neurons (Barone et al., 2000; Markov et al., 2014). The analyses were based on the observation that in primates, the fraction of supragranular neurons that project to a target area depends not only on whether the projections were feedforward or feedback, but also on the hierarchical distance between the two areas (Barone et al., 2000).

Somewhat surprisingly, given the striking organization in the primate brain, no such laminar segregation of source neurons projecting through feedforward and feedback pathways was observed in the mouse visual cortex (Berezovskii et al., 2011). By injecting retrograde tracers into V1 and the anterolateral area AL of adult mice, the authors of this study showed that LM neurons that projected to a lower area (V1) and those that projected to a higher area (AL) were both found intermingled predominantly in layers 2–4, with no obvious laminar separation. Despite the lack of laminar separation of feedforward and feedback source neurons, only a very small proportion of individual neurons in mouse V1 projected in both feedforward and feedback directions, with the vast majority projecting either only to V1 or to AL (Berezovskii et al., 2011), indicating a segregation of neurons depending on their target areas, similar to what has been observed in the macaque cortex (Sincich and Horton, 2003; Markov et al., 2014). This implies that, except for a tiny minority, individual pyramidal neurons that project to another area (these do not include the corticothalamic pyramidal cells of layer 6; Harris and Shepherd, 2015) can broadly be classified as being either feedforward- or feedback-projecting. These two putative populations of pyramidal neurons may differ in their dendritic morphologies with apical tufts in layer 1 more common in feedforward-projecting neurons (Markov et al., 2014), suggesting pathway-differences in the integration of synaptic inputs to layer 1.

THE CORTICO-THALAMIC-CORTICAL PATHWAY

In parallel with the cortical hierarchy within which areas communicate directly with each other, an additional, commonly observed mode of cortico-cortical communication is via a transthalamic route in which a higher-order thalamic nucleus relays information from one cortical area to another (reviewed in Sherman, 2017). In such a cortico-thalamic-cortical pathway, cortical layer 5 pyramidal cells from one area project their axons to the thalamus where they provide "driver" inputs (strong inputs that activate ionotropic glutamate receptors on proximal dendrites; Sherman and Guillery, 1998) to thalamic relay cells, which themselves project to another cortical area. These driver inputs are in contrast to "modulator" glutamatergic inputs, which have distinct synaptic properties and are thought to modulate the responses to driver glutamatergic inputs, much like the actions of "classic" neuromodulators such as acetylcholine and serotonin (Sherman and Guillery, 1996, 1998, 2011). In the visual system, the pulvinar is a higher-order thalamic nuclei that receives inputs from, and sends afferents to, a number of

visual cortical areas, and is therefore a key hub for visual cortico-cortical communication (Sherman and Guillery, 1996; Grieve et al., 2000; Shipp, 2003). In the mouse, the lateral posterior nucleus (LP; the rodent analog of the pulvinar), likely mediates transthalamic cortico-cortical information flow, receiving inputs from layers 5 and 6 of V1 and transmitting signals to (as well as receiving signals from) higher visual areas (Oh et al., 2014; Tohmi et al., 2014; Roth et al., 2016). LP also projects diffusely to layer 1 of V1 providing locomotion-related information (Roth et al., 2016).

Results from a number of studies indicate that the axons of cortical layer 5 neurons, in addition to providing input to the thalamus, branch out to innervate other parts of the brain including midbrain and pontine areas (Deschênes et al., 1994; Bourassa and Deschênes, 1995; Bourassa et al., 1995; Kita and Kita, 2012; Sherman, 2017). This suggests that an identical message, originating in a single axon, is transmitted to a number of different structures that underlie both sensory and motor functions. It has been proposed, therefore, that a crucial function of layer 5 pyramidal neurons that underlie visual cortico-thalamic-cortical communication, but which also branch their axons to other motor structures, is to generate the *efference copy*, a type of neuronal message that helps an animal perceive the environment as being stable even while it moves around in it (Wurtz et al., 2011; Sherman, 2017).

DISTINCT EXCITATION/INHIBITION BALANCE WITHIN LAMINAE

The importance of balanced inhibitory control of excitatory drive within and between cortical areas has been widely reported (Shadlen and Newsome, 1998; Douglas and Martin, 2009; Isaacson and Scanziani, 2011; Whitmire and Stanley, 2016). In a number of cortical areas, inhibition has been shown to scale with excitation (Okun and Lampl, 2008; Xue et al., 2014; Zhou et al., 2014), in order to sharpen receptive fields (Wehr and Zador, 2003), restrain recurrent excitation (Douglas and Martin, 1991; Sanchez-Vives and McCormick, 2000; Pinto et al., 2003), and preserve the temporal fidelity of cortical output (Pouille and Scanziani, 2001; Pouille et al., 2009). By modulating the gain of excitatory projection neurons, inhibitory neurons maintain a wide dynamic range over which brain circuits can effectively respond to sensory stimuli without saturating spike firing (Shadlen and Newsome, 1998; Pouille et al., 2009). Feedforward inhibitory (**Box 1**) control can occur by inducing pyramidal cells to act as coincidence-detectors so that only excitatory postsynaptic currents (EPSCs) resulting from spikes that arrive within a narrow time window would be permitted to summate and generate spikes in the target neuron and subsequently transmit salient information (**Figure 1A**). Such a mechanism allows for precise computations of input signals within noisy regimes wherein cortical neurons are continuously bombarded with hundreds or even thousands of inputs per second (Shadlen and Newsome, 1998; Kremkow et al., 2010; Bruno, 2011). In addition to signal transmission governed by feedforward inhibition, gain control can also be achieved by feedback inhibition (**Box 1**) within highly recurrent networks (Douglas et al., 1995; Douglas and Martin, 2007). In circuits dominated by strong recurrent, excitatory connections that amplify weak, e.g., thalamocortical, inputs (Douglas et al., 1995; Lien and Scanziani, 2013), the feedback inhibitory motif has been proposed to non-linearly modulate cortical gain by silencing individual pyramidal cells, thus transiently reconfiguring local excitatory circuits by selectively eliminating the excitatory components of a winner-take-all network (Douglas and Martin, 2009; Rutishauser et al., 2015; **Figure 1B**). Another proposed mechanism of gain control is through the balanced increase in excitatory and inhibitory background activity leading to an increase in the membrane conductance of neurons (Chance et al., 2002). Because spontaneous activity is thought to primarily be dependent on cortico-cortical connections (Sanchez-Vives and McCormick, 2000; Timofeev et al., 2000), which have a pathway-specific laminar profile (Binzegger et al., 2004), the modulation of cortical gain is likely to be layer-specific.

If an important property of cortical lamination is the segregation of functionally diverse pathways specialized for distinct spatiotemporal stimulus features (Nassi and Callaway, 2009), it would be reasonable to predict contrasting relative levels of excitation and inhibition in different layers. *In vivo* recordings from a number of studies suggest this to be true. Neurons in different layers of mouse neocortex have been shown to differentially represent sensory cues, particularly through the "sparseness" of cortical activity, in a number of areas (Barth and Poulet, 2012; Harris and Mrsic-Flogel, 2013; Petersen and Crochet, 2013). For mice performing a whisking task, recordings from barrel cortex suggested an overall sparse representation of stimuli (10% of neurons responsible for approximately 50% of all recorded spikes, and 50% of neurons contributing to less than 3% of spikes), with the largest proportion of silent neurons in layer 2/3 (O'Connor et al., 2010). The median firing rates of neurons recorded in this study were highest in layers 4 and 5, and lowest in layers 2/3 and 6. Extracellular recordings in mouse V1 showed that excitatory neurons in layers 2/3 and 4 exhibit a substantially lower rate of spontaneous spiking activity, and have smaller receptive field sizes, than neurons in layers 5 and 6 (Niell and Stryker, 2008). Similarly in auditory cortex, pyramidal neurons in layers 2/3 showed a much sparser level of activity, both evoked and spontaneous, than the deeper layer 5 cells (Sakata and Harris, 2009). A major contributor to the emergence of sparse coding, i.e., the observation that only a few active neurons underlie the representation of a sensory stimulus, is the strong inhibitory actions of local interneurons (Crochet et al., 2011; Haider et al., 2013; Harris and Mrsic-Flogel, 2013; Petersen and Crochet, 2013). These observations therefore indicate a higher level of inhibitory drive to superficial pyramidal neurons compared to those in the deep layers.

Consistent with the observed laminar differences in neuronal activity, results from synaptic and circuit-level studies further point to layer-specific differences in the relative levels of excitation and inhibition. In the mouse primary auditory cortex, for example, the balance between excitatory and inhibitory inputs showed a layer-dependence such that while the amplitudes of inhibitory postsynaptic currents (IPSCs) scaled with those of EPSCs in response to varying intensities

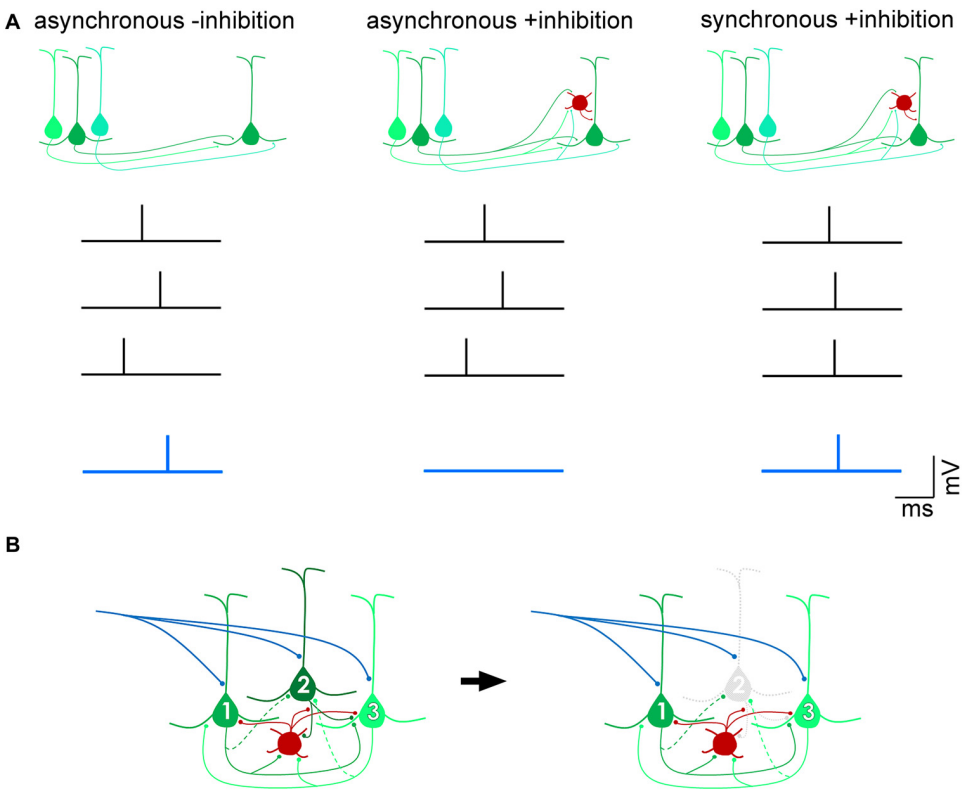

FIGURE 1 | Distinct mechanisms of gain control by feedforward and feedback inhibition. **(A)** Feedforward inhibition. In the absence of inhibition, excitatory postsynaptic potentials (EPSPs) arising from three presynaptic action potentials (black traces) that arrive within a broad time window ("asynchronous -inhibition") can summate to drive the postsynaptic pyramidal cell past threshold and fire an action potential (blue trace). In the presence of a feedforward inhibitory circuit (red, interneuron), the EPSPs are unable to successfully drive the cell past spike threshold ("asynchronous +inhibition"), unless they arrive within a narrow time window ("synchronous +inhibition"). In this way, a feedforward inhibitory mechanism allows for only coincident inputs to transmit signals, filtering out asynchronous "noise". **(B)** Feedback inhibition. Pyramidal neurons 1 and 3 are more strongly, reciprocally connected with each other than with pyramidal neuron 2 (dotted axon indicates weak input). The interneuron (red) is reciprocally connected with all three pyramidal neurons. Upon onset of an excitatory input (blue), recurrent excitation between pyramidal neurons 1 and 3 is strong enough to overcome feedback inhibition from the interneuron. Pyramidal neuron 2, however, is inhibited and does not contribute to computations performed by the circuit. Such a motif dynamically alters the components of the circuit depending on permutations of recurrent connections between pyramidal cells and inhibitory interneurons (Douglas and Martin, 2009).

of an auditory tone, the excitation/inhibition balance was scaled down in layer 2/3, but was unchanged in layer 4, during behavior (Zhou et al., 2014). In the hindlimb somatosensory cortex, interhemispheric input could evoke inhibition to the distal dendrites of layer 5 pyramidal neurons, but not to pyramidal neurons residing in layer 2/3, indicating distinct regulation of excitation/inhibition balances in the different layers by callosal projections (Palmer L. M. et al., 2012).

Similarly, laminar differences in synaptic inputs to excitatory and inhibitory neurons were also observed in the visual cortex. Within the mouse visual cortical network, the primary neuronal targets of feedforward and feedback connections between areas are pyramidal cells and the parvalbumin-expressing (PV+) GABAergic interneurons (Gonchar and Burkhalter, 1999, 2003). The strength of these interareal connections was shown to depend on pathway and on the postsynaptic cell type: interareal excitatory synaptic input to PV+ interneurons was stronger than that to pyramidal neurons in most pathways terminating in layer 2/3 but not in layer 5 (Yang et al., 2013; D'Souza et al., 2016). Further, within layer 2/3, the interareal excitation of PV+ interneurons, relative to that of pyramidal cells, showed a gradual decrease from the most feedforward to the most feedback pathway (**Figure 2**). Because PV+ interneurons are a major source of inhibition in the neocortex, inhibiting neighboring pyramidal cells with high probability (Yoshimura and Callaway, 2005; Packer and Yuste, 2011; D'Souza et al., 2016), these results suggest that the highest levels of interareal inhibition of pyramidal cells are driven by ascending pathways projecting to higher cortical areas. Notably, the hierarchical dependence of inhibition was not seen in layer 5 neurons where relative targeting of PV+ interneurons was similar across the hierarchy and was generally lower than in the upper layers (Yang et al., 2013; D'Souza et al., 2016).

Layer 2/3 consists of networks characterized by strong recurrent excitatory connections, which have been implicated in selectively amplifying salient inputs within a noisy regime that

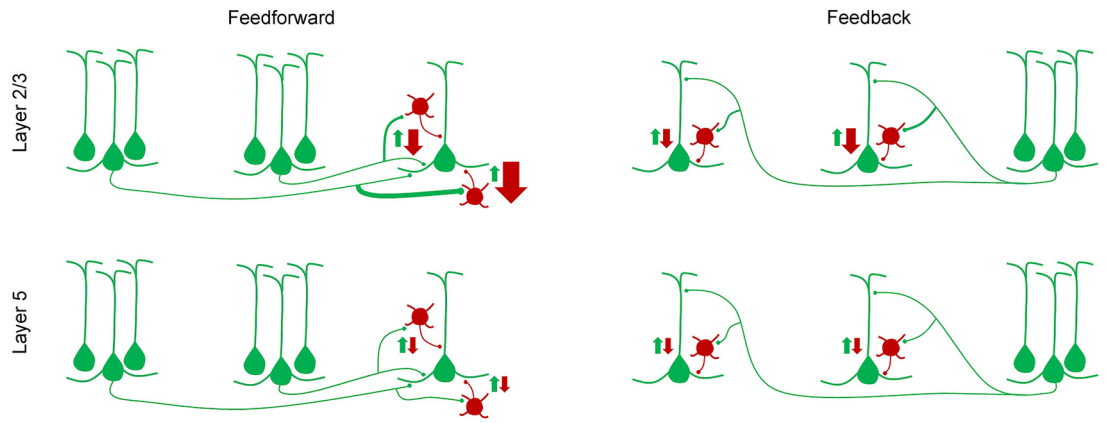

FIGURE 2 | A simplified model of how feedforward inhibition varies with hierarchical distance, pathway and laminar location of target neurons (D'Souza et al., 2016). In layer 2/3, the strength of interareal excitation of parvalbumin (PV) interneurons, relative to that of pyramidal cells, shows a gradual decline from the most feedforward to the most feedback pathway, i.e., from the pathway with the largest hierarchical distance in the feedforward direction, to the pathway with the largest hierarchical distance in the feedback direction. Hierarchical distances were quantified by measuring the ratio of the density of axonal projections in layers 2–4 to that in layer 1. In layer 5, no such gradient in the inhibition/excitation balance is observed and the overall relative excitation of PV interneurons is lower than in layer 2/3.

match information stored in the weights of excitatory synaptic connections (Douglas and Martin, 2007). Therefore, stronger inhibition in the superficial layers suggests that more effective control is required to counterbalance and dynamically regulate excitatory networks within these layers (Douglas and Martin, 2009). Because a canonical function of layer 2/3 pyramidal cells is to convey spike-encoded information to other cortical areas, the stronger targeting of PV+ interneurons may protect against signal corruption across the hierarchical cascade. This is particularly important because pyramidal cells in higher areas show an increasingly higher number and density of dendritic spines (implying a larger number and density of excitatory inputs impinging on them; Elston, 2003; Benavides-Piccione et al., 2006; Elston et al., 2006; Gilman et al., 2017), and integrate inputs over a broader time window (Murray et al., 2014; Chaudhuri et al., 2015).

Lower levels of PV+ interneuron recruitment in layer 5 supports the notion that pyramidal cells within this layer, particularly the subpopulation that projects to subcortical targets, use a "dense coding" strategy to transmit signals (Sakata and Harris, 2009; Harris and Mrsic-Flogel, 2013). These so-called pyramidal tract (PT) neurons are restricted to layer 5, are characterized by thicker apical dendrites and larger cell bodies, and project their axons outside of the telencephalon (neocortex and striatum) to targets that include the brainstem, superior colliculus, spinal cord and higher-order thalamus (Sakata and Harris, 2009; Harris and Mrsic-Flogel, 2013; Shepherd, 2013; Harris and Shepherd, 2015), putatively mediating cortico-thalamic-cortical communication and generating an efference copy (Sherman, 2017) as described in the previous section. It has been proposed that a dense coding strategy in which a relatively large number of neurons respond to a sensory stimulus, and with relatively high firing rates, allows for efficient transmission of signals to distant targets while minimizing the physical volume of neurons and their fibers (Harris and Mrsic-Flogel, 2013). This is in contrast to sparse coding, which requires a large number of neurons, only a very few of which would be active at a given time to encode a stimulus. Thus, different levels of inhibition between the superficial and deep layers may dictate the computations performed by a pyramidal cell depending on its postsynaptic targets (Apicella et al., 2012; Harris and Mrsic-Flogel, 2013).

Together, these results indicate that even though an excitation/inhibition balance is maintained within a layer (Pouille et al., 2009; Xue et al., 2014), this balance, i.e., the relative amounts of excitation and inhibition, may vary between different layers. The difference in the selectivity and sparseness of neuronal responses between the superficial and deep layers, as observed *in vivo* (Niell and Stryker, 2008; Sakata and Harris, 2009; O'Connor et al., 2010) is likely to emerge, at least partly, from the differential targeting of inhibitory and excitatory neurons in the different layers by long-range inputs (Yang et al., 2013; D'Souza et al., 2016), with both feedforward and feedback inhibitory motifs presumably playing important, distinct roles in controlling the gain and preserving the fidelity of signal transmission. In addition to the layer-specific, long-range excitation of inhibitory interneurons, inhibition to excitatory and inhibitory neurons from sources within an area also exhibits a laminar profile, with each neuron receiving inhibition from sources in multiple layers, and not just from neighboring interneurons (Xu and Callaway, 2009; Kätzel et al., 2011; Xu et al., 2016). Further, the recruitment of inhibition within the different layers depends not only on the laminar location of neuronal cell bodies, but also on the precise locations of inhibitory synaptic inputs along the dendrites of neurons that can traverse multiple layers (Kawaguchi and Kondo, 2002; Palmer L. et al., 2012; Muñoz et al., 2017).

The higher levels of inhibitory recruitment in the superficial layers may underlie the distinct frequency channels through which feedforward and feedback communication is achieved

in the human and non-human primate brains (Bastos et al., 2015; Michalareas et al., 2016). By recording local field potentials using electrocorticography in monkeys, and by using magnetoencephalography in humans, these studies showed that feedforward pathways utilize the higher frequency gamma oscillations (40–90 Hz), while feedback pathways use slower (7–17 Hz) oscillations, to mediate long-range communication. Gamma-band synchronization is largely localized in superficial layers whereas slower oscillations predominate in deeper cortical layers (Maier et al., 2010; Buffalo et al., 2011; Roberts et al., 2013), consistent with the laminar separation of feedforward and feedback afferents. These results, taken together with the crucial role that fast-spiking interneurons play in the generation of gamma rhythms (Hasenstaub et al., 2005; Cardin et al., 2009) and the previously described laminar segregation of excitation/inhibition balances, suggest a central role of local PV+ interneurons (virtually all of which show a fast-spiking, non-adapting physiology; Chattopadhyaya et al., 2004; Hu et al., 2014) in regulating long-range communication. The observations from these studies imply that the divergent functions of feedforward and feedback pathways are accomplished not only by the laminar separation of afferents, but also by the differential recruitment of interneurons in different layers, and the subsequent induction of pathway- and layer-specific oscillations.

DISINHIBITORY CIRCUITS IN NEOCORTEX

In addition to feedforward inhibition through the recruitment of PV+ interneurons, a commonly observed long-range circuit motif is the disinhibition of pyramidal cells through the excitation of GABAergic interneurons that express the vasoactive intestinal peptide (VIP). VIP+ interneurons strongly, and with high probability, inhibit somatostatin (SST)-positive interneurons, which themselves inhibit pyramidal cells (Pfeffer et al., 2013; Jiang et al., 2015). In this way, excitation of VIP+ interneurons can "release" pyramidal cells from inhibition. Such a disinhibitory mechanism was shown to be employed by the cingulate cortex in modulating the responses of V1 neurons so that the latter's responses to preferred orientations of visual stimuli were enhanced, while responses to non-preferred orientations were unchanged (Zhang et al., 2014). The disinhibitory circuit motif was also observed in the pathway connecting mouse primary vibrissal motor cortex to barrel cortex (Lee et al., 2013), and is thought to be a general mechanism for providing an additional layer of neuronal gain control by interareal connections throughout the neocortex (Pi et al., 2013; Muñoz et al., 2017).

The importance of interneurons in mediating long-range communication is further evidenced by the behavioral state-dependent modulation of visual cortex. During locomotion, the gain of V1 pyramidal cells in response to visual stimulation is enhanced (Niell and Stryker, 2010; Polack et al., 2013; Saleem et al., 2013; Reimer et al., 2014), which is accompanied by an increase in the firing frequency of local VIP+ interneurons as well (Fu et al., 2014; Reimer et al., 2014; Jackson et al., 2016). At first glance, this is consistent with the disinhibitory function of VIP+ interneurons. However, confounding this notion is the observation that during locomotion, the activity of SST+ interneurons was also enhanced during visual stimulation instead of being inhibited (Polack et al., 2013; Pakan et al., 2016). A possible explanation for this discrepancy is that the modulation of SST+ interneurons is context-dependent; their responses during locomotion depended on whether the task was performed during visual stimulation or in darkness (Pakan et al., 2016), indicating that the enhancement in the gain of V1 pyramidal cells during locomotion is not simply due to disinhibition, but may involve the actions of neuromodulators or the effects of locomotion in subcortical structures like the thalamus (Erisken et al., 2014; Saleem et al., 2017), which would contribute to increased gain by thalamocortical inputs (Pakan et al., 2016).

Together, these studies have demonstrated that the cortex employs a number of circuit motifs, including the long-range recruitment of PV+ and VIP+ interneurons to respectively inhibit and disinhibit local pyramidal cells, depending on context and the task the animal has to perform.

AN ORGANIZING ROLE OF CORTICAL LAYER 1

As the primary target of feedback pathways, particularly in primary sensory areas, neocortical layer 1 holds a unique position in understanding the hierarchical function of the laminar layout of the cortex. Characterized by a distinct paucity of neurons, this layer is a dense neuropil of axons and dendrites that lacks the cell bodies of pyramidal cells and PV+ interneurons, but contains cell bodies of other families of GABAergic interneurons, including those that can be identified by their respective expression of calretinin, SST and/or VIP (Hestrin and Armstrong, 1996; Gonchar et al., 2007; Rudy et al., 2011; Muralidhar et al., 2013). Within the layer, long-range projecting axons from other cortical areas as well as from thalamus make excitatory contacts with dendrites of neurons residing in the layers below, notably the apical dendrites of pyramidal cells (Shipp, 2007; Cruikshank et al., 2012; Yang et al., 2013; Cruz-Martín et al., 2014; D'Souza et al., 2016). The connections formed by these afferents make up the vast majority of excitatory synapses in layer 1 (>90% in cat V1; Binzegger et al., 2004), pointing to a functionally important role of this layer as a hub for selectively integrating cortico-cortical and thalamocortical inputs (Rubio-Garrido et al., 2009; Sherman and Guillery, 2011; Larkum, M. 2013; Ji et al., 2015; Roth et al., 2016). It is important to note that neocortical layer 1 is not merely a site for feedback connections but is also an explicit target of first and higher order thalamic nuclei (Jones, 1998; Rubio-Garrido et al., 2009) as well as of feedforward projections between higher (non-primary) areas of a cortical hierarchy (Coogan and Burkhalter, 1993; D'Souza et al., 2016). As touched upon earlier, layer 1 of mouse V1 receives thalamic inputs from the dorsal lateral geniculate nucleus and from LP, each of which provides distinct visual and locomotion-related

information to V1 (Cruz-Martín et al., 2014; Roth et al., 2016).

Excitatory inputs to distal regions of a pyramidal neuron's apical dendrite could be argued to have only minimal effects on spike generation at the axon because of substantial attenuation of the signal as it propagates to the cell body (Stuart and Spruston, 1998). However, stimulation of the apical dendrite, either antidromically or synaptically, can result in a spatially restricted influx of calcium and the generation of calcium-dependent regenerative potentials ("Ca^{2+} spikes") in the apical dendrite (Amitai et al., 1993; Yuste et al., 1994; Schiller et al., 1997; Larkum and Zhu, 2002). The triggering of Ca^{2+} spikes provides for a putative mechanism through which coincident or strong synaptic inputs to the apical dendrite can result in long-lasting, high frequency bursts of sodium action potentials in the soma and axon (Larkum and Zhu, 2002; Williams and Stuart, 2002), which is dependent on backpropagation of the somatic action potential into the apical dendrite (Larkum et al., 2001). This has led to the proposition that a putative cellular mechanism through which top-down influence on signal propagation can be achieved is through the coincidence of a backpropagating action potential with a Ca^{2+}-dependent plateau potential caused by feedback synaptic input to distal regions of the dendrite in layer 1, resulting in a context-dependent, behaviorally relevant amplification of feedforward input through Ca^{2+} spike generation (Larkum et al., 2004; Larkum, M. 2013; Takahashi et al., 2016).

The importance of excitatory inputs in layer 1 necessitates the regulation of their timing and efficacy by inhibition. The most likely candidates responsible for inhibitory control within layer 1 are the interneurons residing within the layer itself (Letzkus et al., 2011; Wozny and Williams, 2011; Jiang et al., 2013) as well as interneurons in the lower layers, such as the SST-expressing Martinotti cells, that project their axons into layer 1 (Kapfer et al., 2007; Silberberg and Markram, 2007; Gentet et al., 2012; Palmer L. et al., 2012). In rat sensorimotor cortex, at least two populations of layer 1 interneurons were shown to be able to differentially control the excitation of both layer 2/3 and layer 5 pyramidal cells through distinct monosynaptic and disynaptic networks (Jiang et al., 2013; Larkum, M. E. 2013; Lee et al., 2015), thus providing a multilayered regulation of cortical output.

In addition to being the site of electrically remote dendritic regions of the underlying neurons, a number of studies indicate that layer 1 itself may be anatomically partitioned into sub-regions, pointing to an additional computational strategy for modulating the responses of neurons in the deeper layers (Ichinohe and Rockland, 2002; Rubio-Garrido et al., 2009; Ji et al., 2015). In mouse V1, layer 1 and superficial regions of layer 2/3 exhibit a non-uniform pattern of repeating zones that strongly express the M2 acetylcholine receptor (Ji et al., 2015). These *patches* interdigitate with zones termed *interpatches* that have a significantly lower level of M2 expression. The patches and interpatches appear to play a spatial organizing role for neurons displaying different spatiotemporal preferences. The proportion of neurons that selectively responded to varying orientations, directions, speeds and motion coherence (measured by varying the proportion of stimulus dots moving in a particular direction) of visual stimuli was significantly different in regions lying directly below the M2-rich patches and those aligned with M2-weak interpatch zones (Ji et al., 2015). Further, the patches were a preferred target for a number of long-range pathways, including the dorsal lateral geniculate nucleus, and the higher areas LM and AL (see also Rubio-Garrido et al., 2009). This architecture is reminiscent of the honeycomb-like pattern observed at the border of layers 1 and 2 of rat visual cortex (Ichinohe et al., 2003). These "honeycombs", like the patches of mouse V1, were argued to be selectively targeted by putative thalamocortical projections, but in addition, were also shown to alternate with zinc-enriched putative cortico-cortical projections (Ichinohe et al., 2003). It is reasonable to hypothesize, therefore, that the interpatch regions of mouse V1 are also a preferred target of yet unidentified cortico-cortical projections. Such an organization of alternating, adjacent regions containing circuits with distinct functions would allow for parallel, intercommunicating representations of diverse aspects of visual stimuli while preserving the retinotopic layout within V1.

It is tempting to think of the modular organization of mouse V1 as being analogous to cortical columns of higher mammals. However, there are some important differences. Unlike V1 of primates and cats, in which neurons form orientation columns that span multiple layers (Hubel and Wiesel, 1963, 1968), neurons in mouse V1 that have similar orientation preferences are randomly organized, a pattern that has been described as "salt-and-pepper" (Ohki et al., 2005). While mouse V1 pyramidal neurons that show similar visual preferences are more likely to connect with each other (Ko et al., 2011; Cossell et al., 2015), their physical positions do not appear to be organized in any columnar fashion. Interestingly, however, the M2-based patch and interpatch system was found to also exist in monkey V1, with cytochrome oxidase-rich blobs coinciding with the interpatch regions (Ji et al., 2015). This is particularly fascinating because neurons in monkey V1 within blobs are less orientation-selective than those outside blobs (Livingstone and Hubel, 1984), consistent with the demonstration that neurons aligned with interpatches in mouse V1 are less likely to be orientation-selective than those underlying patches (Ji et al., 2015). Therefore, given the relatively small size of each M2-patch and interpatch zone, it appears that this evolutionarily conserved modular system in V1 is important for the hierarchical, distributed processing of diverse visual stimulus properties within a point image.

SUMMARY AND CONCLUDING REMARKS

The layered cortical network provides a framework to identify the fundamental connectivity rules and organizing principles by which the brain integrates internally generated cortical activity and incoming sensory stimulus-encoding signals in order to make sense of, and navigate through, the environment. In addition to stereotypic neuronal connections between layers (Thomson and Bannister, 2003; Douglas and Martin, 2004), each

layer is a selective target for a variety of long-range connections whose origins include other cortical areas, thalamus, as well as the contralateral hemisphere (Shipp, 2007; Palmer L. M. et al., 2012; Hooks et al., 2013; Harris and Shepherd, 2015). Interareal cortical connections have often broadly been classified as being feedforward, feedback, or lateral, each with distinct structural and functional properties. However, observations from several studies compel us to take a more nuanced view in understanding cortico-cortical communication. The patterned targeting of layer 1 of V1 by thalamocortical afferents (Rubio-Garrido et al., 2009; Ji et al., 2015), and the examination of feedforward connections between higher visual areas (Coogan and Burkhalter, 1993; D'Souza et al., 2016), lead to the conclusion that layer 1 is not simply a target of feedback projections but also receives input from local and feedforward-projecting pyramidal cells. Further, both feedforward and feedback pathways form circuits comprising both driver-like and modulator-like synaptic connections that originate in all layers (barring layer 1; Covic and Sherman, 2011; De Pasquale and Sherman, 2011). The brain therefore utilizes a gradient of feedforward and feedback properties, both structural and cellular, depending on the hierarchical level of the interconnecting areas. This is analogous to the gradient in the excitation/inhibition balance (D'Souza et al., 2016) as well as in the proportion of supragranular neurons that project in a particular direction (Barone et al., 2000; Markov et al., 2014) across the cortical hierarchy. The excitation of apical dendrites in layer 1 as a way to amplify excitatory inputs to proximal dendrites, through the generation of Ca^{2+} spikes, may be a general mechanism employed in the cortex, albeit most commonly by feedback projections (Phillips, 2017). A system in which feedforward and feedback afferents share their "driving" and "modulating" responsibilities has important implications for our understanding of top-down control of feedforward signals because it indicates that anatomically defined feedforward and feedback pathways can each play a role in the selection and amplification of signals from the other pathway, consistent with the notion that hierarchies do not define a strict order of areas but instead depend on sensory modality (Chaudhuri et al., 2015).

The fine-scale patchy organization of receptors and/or neurites observed not only in visual cortex but also in auditory, retrosplenial and medial entorhinal cortices (Ray et al., 2014; Ji et al., 2015) likely reflects a generalized strategy of segregating parallel pathways that process distinct sensory and motor signals while also preserving topography. In the visual system, having multiple modules within the point image (Ji et al., 2015) may enable cross-talk between neighboring pyramidal cells encoding diverse spatiotemporal information. The patchy organization of layer 1 also implies that feedback projections do not act in a diffused and generic manner across a lower area but selectively modulate the activity of individual pyramidal cells depending on the subnetwork (module) to which it belongs.

AUTHOR CONTRIBUTIONS

RDD and AB reviewed literature and wrote the manuscript.

ACKNOWLEDGMENTS

This work was supported by National Institutes of Health (NIH) Grants R01 EY016184, R01 EY022090.

REFERENCES

Alfano, C., and Studer, M. (2013). Neocortical arealization: evolution, mechanisms, and open questions. *Dev. Neurobiol.* 73, 411–447. doi: 10.1002/dneu.22067

Amitai, Y., Friedman, A., Connors, B. W., and Gutnick, M. J. (1993). Regenerative activity in apical dendrites of pyramidal cells in neocortex. *Cereb. Cortex* 3, 26–38. doi: 10.1093/cercor/3.1.26

Andermann, M. L., Kerlin, A. M., Roumis, D. K., Glickfeld, L. L., and Reid, R. C. (2011). Functional specialization of mouse higher visual cortical areas. *Neuron* 72, 1025–1039. doi: 10.1016/j.neuron.2011.11.013

Antonini, A., Fagiolini, M., and Stryker, M. P. (1999). Anatomical correlates of functional plasticity in mouse visual cortex. *J. Neurosci.* 19, 4388–4406.

Apicella, A. J., Wickersham, I. R., Seung, H. S., and Shepherd, G. M. (2012). Laminarly orthogonal excitation of fast-spiking and low-threshold-spiking interneurons in mouse motor cortex. *J. Neurosci.* 32, 7021–7033. doi: 10.1523/JNEUROSCI.0011-12.2012

Attinger, A., Wang, B., and Keller, G. B. (2017). Visuomotor coupling shapes the functional development of mouse visual cortex. *Cell* 169, 1291.e14–1302.e14. doi: 10.1016/j.cell.2017.05.023

Balaram, P., and Kaas, J. H. (2014). Towards a unified scheme of cortical lamination for primary visual cortex across primates: insights from NeuN and VGLUT2 immunoreactivity. *Front. Neuroanat.* 8:81. doi: 10.3389/fnana.2014.00081

Barone, P., Batardiere, A., Knoblauch, K., and Kennedy, H. (2000). Laminar distribution of neurons in extrastriate areas projecting to visual areas V1 and V4 correlates with the hierarchical rank and indicates the operation of a distance rule. *J. Neurosci.* 20, 3263–3281.

Barth, A. L., and Poulet, J. F. (2012). Experimental evidence for sparse firing in the neocortex. *Trends Neurosci.* 35, 345–355. doi: 10.1016/j.tins.2012.03.008

Bastos, A. M., Usrey, W. M., Adams, R. A., Mangun, G. R., Fries, P., and Friston, K. J. (2012). Canonical microcircuits for predictive coding. *Neuron* 76, 695–711. doi: 10.1016/j.neuron.2012.10.038

Bastos, A. M., Vezoli, J., Bosman, C. A., Schoffelen, J. M., Oostenveld, R., Dowdall, J. R., et al. (2015). Visual areas exert feedforward and feedback influences through distinct frequency channels. *Neuron* 85, 390–401. doi: 10.1016/j.neuron.2014.12.018

Belgard, T. G., Marques, A. C., Oliver, P. L., Abaan, H. O., Sirey, T. M., Hoerder-Suabedissen, A., et al. (2011). A transcriptomic atlas of mouse neocortical layers. *Neuron* 71, 605–616. doi: 10.1016/j.neuron.2011.06.039

Benavides-Piccione, R., Hamzei-Sichani, F., Ballesteros-Yanez, I., DeFelipe, J., and Yuste, R. (2006). Dendritic size of pyramidal neurons differs among mouse cortical regions. *Cereb. Cortex* 16, 990–1001. doi: 10.1093/cercor/bhj041

Berezovskii, V. K., Nassi, J. J., and Born, R. T. (2011). Segregation of feedforward and feedback projections in mouse visual cortex. *J. Comp. Neurol.* 519, 3672–3683. doi: 10.1002/cne.22675

Bernard, A., Lubbers, L. S., Tanis, K. Q., Luo, R., Podtelezhnikov, A. A., Finney, E. M., et al. (2012). Transcriptional architecture of the primate neocortex. *Neuron* 73, 1083–1099. doi: 10.1016/j.neuron.2012.03.002

Binzegger, T., Douglas, R. J., and Martin, K. A. (2004). A quantitative map of the circuit of cat primary visual cortex. *J. Neurosci.* 24, 8441–8453. doi: 10.1523/JNEUROSCI.1400-04.2004

Bourassa, J., and Deschênes, M. (1995). Corticothalamic projections from the primary visual cortex in rats: a single fiber study using biocytin

as an anterograde tracer. *Neuroscience* 66, 253–263. doi: 10.1016/0306-4522(95)00009-8

Bourassa, J., Pinault, D., and Deschênes, M. (1995). Corticothalamic projections from the cortical barrel field to the somatosensory thalamus in rats: a single-fibre study using biocytin as an anterograde tracer. *Eur. J. Neurosci.* 7, 19–30. doi: 10.1111/j.1460-9568.1995.tb01016.x

Bruno, R. M. (2011). Synchrony in sensation. *Curr. Opin. Neurobiol.* 21, 701–708. doi: 10.1016/j.conb.2011.06.003

Buffalo, E. A., Fries, P., Landman, R., Buschman, T. J., and Desimone, R. (2011). Laminar differences in γ and α coherence in the ventral stream. *Proc. Natl. Acad. Sci. U S A* 108, 11262–11267. doi: 10.1073/pnas.1011284108

Carandini, M., and Heeger, D. J. (2011). Normalization as a canonical neural computation. *Nat. Rev. Neurosci.* 13, 51–62. doi: 10.1038/nrn3136

Cardin, J. A., Carlén, M., Meletis, K., Knoblich, U., Zhang, F., Deisseroth, K., et al. (2009). Driving fast-spiking cells induces γ rhythm and controls sensory responses. *Nature* 459, 663–667. doi: 10.1038/nature08002

Cauller, L. (1995). Layer I of primary sensory neocortex: where top-down converges upon bottom-up. *Behav. Brain Res.* 71, 163–170. doi: 10.1016/0166-4328(95)00032-1

Chance, F. S., Abbott, L. F., and Reyes, A. D. (2002). Gain modulation from background synaptic input. *Neuron* 35, 773–782. doi: 10.1016/s0896-6273(02)00820-6

Chattopadhyaya, B., Di Cristo, G., Higashiyama, H., Knott, G. W., Kuhlman, S. J., Welker, E., et al. (2004). Experience and activity-dependent maturation of perisomatic GABAergic innervation in primary visual cortex during a postnatal critical period. *J. Neurosci.* 24, 9598–9611. doi: 10.1523/JNEUROSCI.1851-04.2004

Chaudhuri, R., Knoblauch, K., Gariel, M. A., Kennedy, H., and Wang, X. J. (2015). A large-scale circuit mechanism for hierarchical dynamical processing in the primate cortex. *Neuron* 88, 419–431. doi: 10.1016/j.neuron.2015.09.008

Chen, M., Yan, Y., Gong, X., Gilbert, C. D., Liang, H., and Li, W. (2014). Incremental integration of global contours through interplay between visual cortical areas. *Neuron* 82, 682–694. doi: 10.1016/j.neuron.2014.03.023

Coogan, T. A., and Burkhalter, A. (1990). Conserved patterns of cortico-cortical connections define areal hierarchy in rat visual cortex. *Exp. Brain Res.* 80, 49–53. doi: 10.1007/bf00228846

Coogan, T. A., and Burkhalter, A. (1993). Hierarchical organization of areas in rat visual cortex. *J. Neurosci.* 13, 3749–3772.

Cossell, L., Iacaruso, M. F., Muir, D. R., Houlton, R., Sader, E. N., Ko, H., et al. (2015). Functional organization of excitatory synaptic strength in primary visual cortex. *Nature* 518, 399–403. doi: 10.1038/nature14182

Covic, E. N., and Sherman, S. M. (2011). Synaptic properties of connections between the primary and secondary auditory cortices in mice. *Cereb. Cortex* 21, 2425–2441. doi: 10.1093/cercor/bhr029

Crochet, S., Poulet, J. F., Kremer, Y., and Petersen, C. C. (2011). Synaptic mechanisms underlying sparse coding of active touch. *Neuron* 69, 1160–1175. doi: 10.1016/j.neuron.2011.02.022

Cruikshank, S. J., Ahmed, O. J., Stevens, T. R., Patrick, S. L., Gonzalez, A. N., Elmaleh, M., et al. (2012). Thalamic control of layer 1 circuits in prefrontal cortex. *J. Neurosci.* 32, 17813–17823. doi: 10.1523/JNEUROSCI.3231-12.2012

Cruz-Martín, A., El-Danaf, R. N., Osakada, F., Sriram, B., Dhande, O. S., Nguyen, P. L., et al. (2014). A dedicated circuit links direction-selective retinal ganglion cells to the primary visual cortex. *Nature* 507, 358–361. doi: 10.1038/nature12989

DeFelipe, J., and Fariñas, I. (1992). The pyramidal neuron of the cerebral cortex: morphological and chemical characteristics of the synaptic inputs. *Prog. Neurobiol.* 39, 563–607. doi: 10.1016/0301-0082(92)90015-7

Dehay, C., Kennedy, H., and Kosik, K. S. (2015). The outer subventricular zone and primate-specific cortical complexification. *Neuron* 85, 683–694. doi: 10.1016/j.neuron.2014.12.060

De Pasquale, R., and Sherman, S. M. (2011). Synaptic properties of corticocortical connections between the primary and secondary visual cortical areas in the mouse. *J. Neurosci.* 31, 16494–16506. doi: 10.1523/JNEUROSCI.3664-11.2011

Deschênes, M., Bourassa, J., and Pinault, D. (1994). Corticothalamic projections from layer V cells in rat are collaterals of long-range corticofugal axons. *Brain Res.* 664, 215–219. doi: 10.1016/0006-8993(94)91974-7

Douglas, R. J., Koch, C., Mahowald, M., Martin, K. A., and Suarez, H. H. (1995). Recurrent excitation in neocortical circuits. *Science* 269, 981–985. doi: 10.1126/science.7638624

Douglas, R. J., and Martin, K. A. (1991). A functional microcircuit for cat visual cortex. *J. Physiol.* 440, 735–769. doi: 10.1113/jphysiol.1991.sp018733

Douglas, R. J., and Martin, K. A. (2004). Neuronal circuits of the neocortex. *Annu. Rev. Neurosci.* 27, 419–451. doi: 10.1146/annurev.neuro.27.070203.144152

Douglas, R. J., and Martin, K. A. (2007). Recurrent neuronal circuits in the neocortex. *Curr. Biol.* 17, R496–R500. doi: 10.1016/j.cub.2007.04.024

Douglas, R. J., and Martin, K. A. (2009). Inhibition in cortical circuits. *Curr. Biol.* 19, R398–R402. doi: 10.1016/j.cub.2009.03.003

D'Souza, R. D., Meier, A. M., Bista, P., Wang, Q., and Burkhalter, A. (2016). Recruitment of inhibition and excitation across mouse visual cortex depends on the hierarchy of interconnecting areas. *Elife* 5:e19332. doi: 10.7554/eLife.19332

Elston, G. N. (2003). Cortex, cognition and the cell: new insights into the pyramidal neuron and prefrontal function. *Cereb. Cortex* 13, 1124–1138. doi: 10.1093/cercor/bhg093

Elston, G. N., Elston, A., Aurelio-Freire, M., Gomes Leal, W., Dias, I. A., Pereira, A., et al. (2006). Specialization of pyramidal cell structure in the visual areas V1, V2 and V3 of the South American rodent, Dasyprocta primnolopha. *Brain Res.* 1106, 99–110. doi: 10.1016/j.brainres.2006.05.100

Elston, G. N., Oga, T., and Fujita, I. (2009). Spinogenesis and pruning scales across functional hierarchies. *J. Neurosci.* 29, 3271–3275. doi: 10.1523/JNEUROSCI.5216-08.2009

Erisken, S., Vaiceliunaite, A., Jurjut, O., Fiorini, M., Katzner, S., and Busse, L. (2014). Effects of locomotion extend throughout the mouse early visual system. *Curr. Biol.* 24, 2899–2907. doi: 10.1016/j.cub.2014.10.045

Feldmeyer, D., Qi, G., Emmenegger, V., and Staiger, J. F. (2017). Inhibitory interneurons and their circuit motifs in the many layers of the barrel cortex. *Neuroscience* doi: 10.1016/j.neuroscience.2017.05.027 [Epub ahead of print].

Felleman, D. J., and Van Essen, D. C. (1991). Distributed hierarchical processing in the primate cerebral cortex. *Cereb. Cortex* 1, 1–47. doi: 10.1093/cercor/1.1.1

Fu, Y., Tucciarone, J. M., Espinosa, J. S., Sheng, N., Darcy, D. P., Nicoll, R. A., et al. (2014). A cortical circuit for gain control by behavioral state. *Cell* 156, 1139–1152. doi: 10.1016/j.cell.2014.01.050

Garrett, M. E., Nauhaus, I., Marshel, J. H., and Callaway, E. M. (2014). Topography and areal organization of mouse visual cortex. *J. Neurosci.* 34, 12587–12600. doi: 10.1523/JNEUROSCI.1124-14.2014

Gentet, L. J., Kremer, Y., Taniguchi, H., Huang, Z. J., Staiger, J. F., and Petersen, C. C. (2012). Unique functional properties of somatostatin-expressing GABAergic neurons in mouse barrel cortex. *Nat. Neurosci.* 15, 607–612. doi: 10.1038/nn.3051

Gilman, J. P., Medalla, M., and Luebke, J. I. (2017). Area-specific features of pyramidal neurons-a comparative study in mouse and rhesus monkey. *Cereb. Cortex* 27, 2078–2094. doi: 10.1093/cercor/bhw062

Glasser, M. F., Coalson, T. S., Robinson, E. C., Hacker, C. D., Harwell, J., Yacoub, E., et al. (2016). A multi-modal parcellation of human cerebral cortex. *Nature* 536, 171–178. doi: 10.1038/nature18933

Gonchar, Y., and Burkhalter, A. (1999). Differential subcellular localization of forward and feedback interareal inputs to parvalbumin expressing GABAergic neurons in rat visual cortex. *J. Comp. Neurol.* 406, 346–360. doi: 10.1002/(sici)1096-9861(19990412)406:3<346::aid-cne4>3.0.co;2-e

Gonchar, Y., and Burkhalter, A. (2003). Distinct GABAergic targets of feedforward and feedback connections between lower and higher areas of rat visual cortex. *J. Neurosci.* 23, 10904–10912.

Gonchar, Y., Wang, Q., and Burkhalter, A. (2007). Multiple distinct subtypes of GABAergic neurons in mouse visual cortex identified by triple immunostaining. *Front. Neuroanat.* 1:3. doi: 10.3389/neuro.05.003.2007

Grieve, K. L., Acuña, C., and Cudeiro, J. (2000). The primate pulvinar nuclei: vision and action. *Trends Neurosci.* 23, 35–39. doi: 10.1016/s0166-2236(99)01482-4

Groh, A., Meyer, H. S., Schmidt, E. F., Heintz, N., Sakmann, B., and Krieger, P. (2010). Cell-type specific properties of pyramidal neurons in neocortex underlying a layout that is modifiable depending on the cortical area. *Cereb. Cortex* 20, 826–836. doi: 10.1093/cercor/bhp152

Haider, B., Häusser, M., and Carandini, M. (2013). Inhibition dominates sensory responses in the awake cortex. *Nature* 493, 97–100. doi: 10.1038/nature11665

Harris, K. D., and Mrsic-Flogel, T. D. (2013). Cortical connectivity and sensory coding. *Nature* 503, 51–58. doi: 10.1038/nature12654

Harris, K. D., and Shepherd, G. M. (2015). The neocortical circuit: themes and variations. *Nat. Neurosci.* 18, 170–181. doi: 10.1038/nn.3917

Hasenstaub, A., Shu, Y., Haider, B., Kraushaar, U., Duque, A., and McCormick, D. A. (2005). Inhibitory postsynaptic potentials carry synchronized frequency information in active cortical networks. *Neuron* 47, 423–435. doi: 10.1016/j.neuron.2005.06.016

Havekes, R., and Abel, T. (2009). Genetic dissection of neural circuits and behavior in Mus musculus. *Adv. Genet.* 65, 1–38. doi: 10.1016/s0065-2660(09)65001-x

Hestrin, S., and Armstrong, W. E. (1996). Morphology and physiology of cortical neurons in layer I. *J. Neurosci.* 16, 5290–5300.

Hooks, B. M., Mao, T., Gutnisky, D. A., Yamawaki, N., Svoboda, K., and Shepherd, G. M. (2013). Organization of cortical and thalamic input to pyramidal neurons in mouse motor cortex. *J. Neurosci.* 33, 748–760. doi: 10.1523/JNEUROSCI.4338-12.2013

Hu, H., Gan, J., and Jonas, P. (2014). Interneurons. Fast-spiking, parvalbumin^{+} GABAergic interneurons: from cellular design to microcircuit function. *Science* 345:1255263. doi: 10.1126/science.1255263

Hubel, D. H., and Wiesel, T. N. (1963). Shape and arrangement of columns in cat's striate cortex. *J. Physiol.* 165, 559–568. doi: 10.1113/jphysiol.1963.sp007079

Hubel, D. H., and Wiesel, T. N. (1968). Receptive fields and functional architecture of monkey striate cortex. *J. Physiol.* 195, 215–243. doi: 10.1113/jphysiol.1968.sp008455

Huberman, A. D., and Niell, C. M. (2011). What can mice tell us about how vision works? *Trends Neurosci.* 34, 464–473. doi: 10.1016/j.tins.2011.07.002

Ichinohe, N., Fujiyama, F., Kaneko, T., and Rockland, K. S. (2003). Honeycomb-like mosaic at the border of layers 1 and 2 in the cerebral cortex. *J. Neurosci.* 23, 1372–1382.

Ichinohe, N., and Rockland, K. S. (2002). Parvalbumin positive dendrites co-localize with apical dendritic bundles in rat retrosplenial cortex. *Neuroreport* 13, 757–761. doi: 10.1097/00001756-200205070-00005

Isaacson, J. S., and Scanziani, M. (2011). How inhibition shapes cortical activity. *Neuron* 72, 231–243. doi: 10.1016/j.neuron.2011.09.027

Jackson, J., Ayzenshtat, I., Karnani, M. M., and Yuste, R. (2016). VIP+ interneurons control neocortical activity across brain states. *J. Neurophysiol.* 115, 3008–3017. doi: 10.1152/jn.01124.2015

Ji, W., Gamanut, R., Bista, P., D'Souza, R. D., Wang, Q., and Burkhalter, A. (2015). Modularity in the organization of mouse primary visual cortex. *Neuron* 87, 632–643. doi: 10.1016/j.neuron.2015.07.004

Jiang, X., Shen, S., Cadwell, C. R., Berens, P., Sinz, F., Ecker, A. S., et al. (2015). Principles of connectivity among morphologically defined cell types in adult neocortex. *Science* 350:aac9462. doi: 10.1126/science.aac9462

Jiang, X., Wang, G., Lee, A. J., Stornetta, R. L., and Zhu, J. J. (2013). The organization of two new cortical interneuronal circuits. *Nat. Neurosci.* 16, 210–218. doi: 10.1038/nn.3305

Jones, E. G. (1998). Viewpoint: the core and matrix of thalamic organization. *Neuroscience* 85, 331–345. doi: 10.1016/s0306-4522(97)00581-2

Kaas, J. H. (2013). The evolution of brains from early mammals to humans. *Wiley Interdiscip. Rev. Cogn. Sci.* 4, 33–45. doi: 10.1002/wcs.1206

Kapfer, C., Glickfeld, L. L., Atallah, B. V., and Scanziani, M. (2007). Supralinear increase of recurrent inhibition during sparse activity in the somatosensory cortex. *Nat. Neurosci.* 10, 743–753. doi: 10.1038/nn0807-1073b

Kätzel, D., Zemelman, B. V., Buetfering, C., Wölfel, M., and Miesenböck, G. (2011). The columnar and laminar organization of inhibitory connections to neocortical excitatory cells. *Nat. Neurosci.* 14, 100–107. doi: 10.1038/nn.2687

Katzner, S., and Weigelt, S. (2013). Visual cortical networks: of mice and men. *Curr. Opin. Neurobiol.* 23, 202–206. doi: 10.1016/j.conb.2013.01.019

Kawaguchi, Y., and Kondo, S. (2002). Parvalbumin, somatostatin and cholecystokinin as chemical markers for specific GABAergic interneuron types in the rat frontal cortex. *J. Neurocytol.* 31, 277–287. doi: 10.1023/A:1024126110356

Kita, T., and Kita, H. (2012). The subthalamic nucleus is one of multiple innervation sites for long-range corticofugal axons: a single-axon tracing study in the rat. *J. Neurosci.* 32, 5990–5999. doi: 10.1523/JNEUROSCI.5717-11.2012

Ko, H., Hofer, S. B., Pichler, B., Buchanan, K. A., Sjöström, P. J., and Mrsic-Flogel, T. D. (2011). Functional specificity of local synaptic connections in neocortical networks. *Nature* 473, 87–91. doi: 10.1038/nature09880

Kremkow, J., Perrinet, L. U., Masson, G. S., and Aertsen, A. (2010). Functional consequences of correlated excitatory and inhibitory conductances in cortical networks. *J. Comput. Neurosci.* 28, 579–594. doi: 10.1007/s10827-010-0240-9

Kuchibhotla, K. V., Gill, J. V., Lindsay, G. W., Papadoyannis, E. S., Field, R. E., Sten, T. A., et al. (2017). Parallel processing by cortical inhibition enables context-dependent behavior. *Nat. Neurosci.* 20, 62–71. doi: 10.1038/nn.4436

Laramée, M.-E., and Boire, D. (2014). Visual cortical areas of the mouse: comparison of parcellation and network structure with primates. *Front. Neural Circuits* 8:149. doi: 10.3389/fncir.2014.00149

Larkum, M. (2013). A cellular mechanism for cortical associations: an organizing principle for the cerebral cortex. *Trends Neurosci.* 36, 141–151. doi: 10.1016/j.tins.2012.11.006

Larkum, M. E. (2013). The yin and yang of cortical layer 1. *Nat. Neurosci.* 16, 114–115. doi: 10.1038/nn.3317

Larkum, M. E., Senn, W., and Lüscher, H. R. (2004). Top-down dendritic input increases the gain of layer 5 pyramidal neurons. *Cereb. Cortex* 14, 1059–1070. doi: 10.1093/cercor/bhh065

Larkum, M. E., and Zhu, J. J. (2002). Signaling of layer 1 and whisker-evoked Ca^{2+} and Na^{+} action potentials in distal and terminal dendrites of rat neocortical pyramidal neurons *in vitro* and *in vivo*. *J. Neurosci.* 22, 6991–7005.

Larkum, M. E., Zhu, J. J., and Sakmann, B. (2001). Dendritic mechanisms underlying the coupling of the dendritic with the axonal action potential initiation zone of adult rat layer 5 pyramidal neurons. *J. Physiol.* 533, 447–466. doi: 10.1111/j.1469-7793.2001.0447a.x

Lee, S., Kruglikov, I., Huang, Z. J., Fishell, G., and Rudy, B. (2013). A disinhibitory circuit mediates motor integration in the somatosensory cortex. *Nat. Neurosci.* 16, 1662–1670. doi: 10.1038/nn.3544

Lee, A. J., Wang, G., Jiang, X., Johnson, S. M., Hoang, E. T., Lante, F., et al. (2015). Canonical organization of layer 1 neuron-led cortical inhibitory and disinhibitory interneuronal circuits. *Cereb. Cortex* 25, 2114–2126. doi: 10.1093/cercor/bhu020

Letzkus, J. J., Wolff, S. B., Meyer, E. M., Tovote, P., Courtin, J., Herry, C., et al. (2011). A disinhibitory microcircuit for associative fear learning in the auditory cortex. *Nature* 480, 331–335. doi: 10.1038/nature10674

Lien, A. D., and Scanziani, M. (2013). Tuned thalamic excitation is amplified by visual cortical circuits. *Nat. Neurosci.* 16, 1315–1323. doi: 10.1038/nn.3488

Livingstone, M. S., and Hubel, D. H. (1984). Anatomy and physiology of a color system in the primate visual cortex. *J. Neurosci.* 4, 309–356.

Lui, J. H., Hansen, D. V., and Kriegstein, A. R. (2011). Development and evolution of the human neocortex. *Cell* 146, 18–36. doi: 10.1016/j.cell.2011.07.005

Maier, A., Adams, G. K., Aura, C., and Leopold, D. A. (2010). Distinct superficial and deep laminar domains of activity in the visual cortex during rest and stimulation. *Front. Syst. Neurosci.* 4:31. doi: 10.3389/fnsys.2010.00031

Major, G., Larkum, M. E., and Schiller, J. (2013). Active properties of neocortical pyramidal neuron dendrites. *Annu. Rev. Neurosci.* 36, 1–24. doi: 10.1146/annurev-neuro-062111-150343

Markov, N. T., and Kennedy, H. (2013). The importance of being hierarchical. *Curr. Opin. Neurobiol.* 23, 187–194. doi: 10.1016/j.conb.2012.12.008

Markov, N. T., Vezoli, J., Chameau, P., Falchier, A., Quilodran, R., Huissoud, C., et al. (2014). Anatomy of hierarchy: feedforward and feedback pathways in macaque visual cortex. *J. Comp. Neurol.* 522, 225–259. doi: 10.1002/cne.23458

Marshel, J. H., Garrett, M. E., Nauhaus, I., and Callaway, E. M. (2011). Functional specialization of seven mouse visual cortical areas. *Neuron* 72, 1040–1054. doi: 10.1016/j.neuron.2011.12.004

Maunsell, J. H., and van Essen, D. C. (1983). The connections of the middle temporal visual area (MT) and their relationship to a cortical hierarchy in the macaque monkey. *J. Neurosci.* 3, 2563–2586.

Maunsell, J. H., and van Essen, D. C. (1987). Topographic organization of the middle temporal visual area in the macaque monkey: representational biases and the relationship to callosal connections and myeloarchitectonic boundaries. *J. Comp. Neurol.* 266, 535–555. doi: 10.1002/cne.902660407

Michalareas, G., Vezoli, J., van Pelt, S., Schoffelen, J. M., Kennedy, H., and Fries, P. (2016). Alpha-beta and gamma rhythms subserve feedback and feedforward influences among human visual cortical areas. *Neuron* 89, 384–397. doi: 10.1016/j.neuron.2015.12.018

Muñoz, W., Tremblay, R., Levenstein, D., and Rudy, B. (2017). Layer-specific modulation of neocortical dendritic inhibition during active wakefulness. *Science* 355, 954–959. doi: 10.1126/science.aag2599

Muralidhar, S., Wang, Y., and Markram, H. (2013). Synaptic and cellular organization of layer 1 of the developing rat somatosensory cortex. *Front. Neuroanat.* 7:52. doi: 10.3389/fnana.2013.00052

Murray, J. D., Bernacchia, A., Freedman, D. J., Romo, R., Wallis, J. D., Cai, X., et al. (2014). A hierarchy of intrinsic timescales across primate cortex. *Nat. Neurosci.* 17, 1661–1663. doi: 10.1038/nn.3862

Nandy, A. S., Nassi, J. J., and Reynolds, J. H. (2017). Laminar organization of attentional modulation in macaque visual area V4. *Neuron* 93, 235–246. doi: 10.1016/j.neuron.2016.11.029

Nassi, J. J., and Callaway, E. M. (2009). Parallel processing strategies of the primate visual system. *Nat. Rev. Neurosci.* 10, 360–372. doi: 10.1038/nrn2619

Niell, C. M., and Stryker, M. P. (2008). Highly selective receptive fields in mouse visual cortex. *J. Neurosci.* 28, 7520–7536. doi: 10.1523/jneurosci.0623-08.2008

Niell, C. M., and Stryker, M. P. (2010). Modulation of visual responses by behavioral state in mouse visual cortex. *Neuron* 65, 472–479. doi: 10.1016/j.neuron.2010.01.033

O'Connor, D. H., Peron, S. P., Huber, D., and Svoboda, K. (2010). Neural activity in barrel cortex underlying vibrissa-based object localization in mice. *Neuron* 67, 1048–1061. doi: 10.1016/j.neuron.2010.08.026

Oh, S. W., Harris, J. A., Ng, L., Winslow, B., Cain, N., Mihalas, S., et al. (2014). A mesoscale connectome of the mouse brain. *Nature* 508, 207–214. doi: 10.1038/nature13186

Ohki, K., Chung, S., Ch'ng, Y. H., Kara, P., and Reid, R. C. (2005). Functional imaging with cellular resolution reveals precise micro-architecture in visual cortex. *Nature* 433, 597–603. doi: 10.1038/nature03274

Okun, M., and Lampl, I. (2008). Instantaneous correlation of excitation and inhibition during ongoing and sensory-evoked activities. *Nat. Neurosci.* 11, 535–537. doi: 10.1038/nn.2105

Packer, A. M., and Yuste, R. (2011). Dense, unspecific connectivity of neocortical parvalbumin-positive interneurons: a canonical microcircuit for inhibition? *J. Neurosci.* 31, 13260–13271. doi: 10.1523/jneurosci.3131-11.2011

Pafundo, D. E., Nicholas, M. A., Zhang, R., and Kuhlman, S. J. (2016). Top-down-mediated facilitation in the visual cortex is gated by subcortical neuromodulation. *J. Neurosci.* 36, 2904–2914. doi: 10.1523/jneurosci.2909-15.2016

Pakan, J. M., Lowe, S. C., Dylda, E., Keemink, S. W., Currie, S. P., Coutts, C. A., et al. (2016). Behavioral-state modulation of inhibition is context-dependent and cell type specific in mouse visual cortex. *Elife* 5:e14985. doi: 10.7554/eLife.14985

Palmer, L., Murayama, M., and Larkum, M. (2012). Inhibitory regulation of dendritic activity *in vivo*. *Front. Neural Circuits* 6:26. doi: 10.3389/fncir.2012.00026

Palmer, L. M., Schulz, J. M., Murphy, S. C., Ledergerber, D., Murayama, M., and Larkum, M. E. (2012). The cellular basis of $GABA_B$-mediated interhemispheric inhibition. *Science* 335, 989–993. doi: 10.1126/science.1217276

Petersen, C. C., and Crochet, S. (2013). Synaptic computation and sensory processing in neocortical layer 2/3. *Neuron* 78, 28–48. doi: 10.1016/j.neuron.2013.03.020

Pfeffer, C. K., Xue, M., He, M., Huang, Z. J., and Scanziani, M. (2013). Inhibition of inhibition in visual cortex: the logic of connections between molecularly distinct interneurons. *Nat. Neurosci.* 16, 1068–1076. doi: 10.1038/nn.3446

Phillips, W. A. (2017). Cognitive functions of intracellular mechanisms for contextual amplification. *Brain Cogn.* 112, 39–53. doi: 10.1016/j.bandc.2015.09.005

Pi, H. J., Hangya, B., Kvitsiani, D., Sanders, J. I., Huang, Z. J., and Kepecs, A. (2013). Cortical interneurons that specialize in disinhibitory control. *Nature* 503, 521–524. doi: 10.1038/nature12676

Pinto, D. J., Hartings, J. A., Brumberg, J. C., and Simons, D. J. (2003). Cortical damping: analysis of thalamocortical response transformations in rodent barrel cortex. *Cereb. Cortex* 13, 33–44. doi: 10.1093/cercor/13.1.33

Polack, P. O., Friedman, J., and Golshani, P. (2013). Cellular mechanisms of brain state-dependent gain modulation in visual cortex. *Nat. Neurosci.* 16, 1331–1339. doi: 10.1038/nn.3464

Pouille, F., Marin-Burgin, A., Adesnik, H., Atallah, B. V., and Scanziani, M. (2009). Input normalization by global feedforward inhibition expands cortical dynamic range. *Nat. Neurosci.* 12, 1577–1585. doi: 10.1038/nn.2441

Pouille, F., and Scanziani, M. (2001). Enforcement of temporal fidelity in pyramidal cells by somatic feed-forward inhibition. *Science* 293, 1159–1163. doi: 10.1126/science.1060342

Price, D. J., and Zumbroich, T. J. (1989). Postnatal development of corticocortical efferents from area 17 in the cat's visual cortex. *J. Neurosci.* 9, 600–613.

Rao, R. P., and Ballard, D. H. (1999). Predictive coding in the visual cortex: a functional interpretation of some extra-classical receptive-field effects. *Nat. Neurosci.* 2, 79–87. doi: 10.1038/4580

Ray, S., Naumann, R., Burgalossi, A., Tang, Q., Schmidt, H., and Brecht, M. (2014). Grid-layout and theta-modulation of layer 2 pyramidal neurons in medial entorhinal cortex. *Science* 343, 891–896. doi: 10.1126/science.1243028

Reimer, J., Froudarakis, E., Cadwell, C. R., Yatsenko, D., Denfield, G. H., and Tolias, A. S. (2014). Pupil fluctuations track fast switching of cortical states during quiet wakefulness. *Neuron* 84, 355–362. doi: 10.1016/j.neuron.2014.09.033

Roberts, M. J., Lowet, E., Brunet, N. M., Ter Wal, M., Tiesinga, P., Fries, P., et al. (2013). Robust γ coherence between macaque V1 and V2 by dynamic frequency matching. *Neuron* 78, 523–536. doi: 10.1016/j.neuron.2013.03.003

Rockland, K. S., and Pandya, D. N. (1979). Laminar origins and terminations of cortical connections of the occipital lobe in the rhesus monkey. *Brain Res.* 179, 3–20. doi: 10.1016/0006-8993(79)90485-2

Roth, M. M., Dahmen, J. C., Muir, D. R., Imhof, F., Martini, F. J., and Hofer, S. B. (2016). Thalamic nuclei convey diverse contextual information to layer 1 of visual cortex. *Nat. Neurosci.* 19, 299–307. doi: 10.1038/nn.4197

Rubio-Garrido, P., Pérez-de-Manzo, F., Porrero, C., Galazo, M. J., and Clascá, F. (2009). Thalamic input to distal apical dendrites in neocortical layer 1 is massive and highly convergent. *Cereb. Cortex* 19, 2380–2395. doi: 10.1093/cercor/bhn259

Rudy, B., Fishell, G., Lee, S., and Hjerling-Leffler, J. (2011). Three groups of interneurons account for nearly 100% of neocortical GABAergic neurons. *Dev. Neurobiol.* 71, 45–61. doi: 10.1002/dneu.20853

Rutishauser, U., Slotine, J. J., and Douglas, R. (2015). Computation in dynamically bounded asymmetric systems. *PLoS Comput. Biol.* 11:e1004039. doi: 10.1371/journal.pcbi.1004039

Sakata, S., and Harris, K. D. (2009). Laminar structure of spontaneous and sensory-evoked population activity in auditory cortex. *Neuron* 64, 404–418. doi: 10.1016/j.neuron.2009.09.020

Saleem, A. B., Ayaz, A., Jeffery, K. J., Harris, K. D., and Carandini, M. (2013). Integration of visual motion and locomotion in mouse visual cortex. *Nat. Neurosci.* 16, 1864–1869. doi: 10.1038/nn.3567

Saleem, A. B., Lien, A. D., Krumin, M., Haider, B., Rosón, M. R., Ayaz, A., et al. (2017). Subcortical source and modulation of the narrowband γ oscillation in mouse visual cortex. *Neuron* 93, 315–322. doi: 10.1016/j.neuron.2016.12.028

Sanchez-Vives, M. V., and McCormick, D. A. (2000). Cellular and network mechanisms of rhythmic recurrent activity in neocortex. *Nat. Neurosci.* 3, 1027–1034. doi: 10.1038/79848

Schiller, J., Schiller, Y., Stuart, G., and Sakmann, B. (1997). Calcium action potentials restricted to distal apical dendrites of rat neocortical pyramidal neurons. *J. Physiol.* 505, 605–616. doi: 10.1111/j.1469-7793.1997.605ba.x

Shadlen, M. N., and Newsome, W. T. (1998). The variable discharge of cortical neurons: implications for connectivity, computation, and information coding. *J. Neurosci.* 18, 3870–3896.

Shepherd, G. M. (2013). Corticostriatal connectivity and its role in disease. *Nat. Rev. Neurosci.* 14, 278–291. doi: 10.1038/nrn3469

Sherman, S. M. (2017). Functioning of circuits connecting thalamus and cortex. *Compr. Physiol.* 7, 713–739. doi: 10.1002/cphy.c160032

Sherman, S. M., and Guillery, R. W. (1996). Functional organization of thalamocortical relays. *J. Neurophysiol.* 76, 1367–1395.

Sherman, S. M., and Guillery, R. W. (1998). On the actions that one nerve cell can have on another: distinguishing "drivers" from "modulators". *Proc. Natl. Acad. Sci. U S A* 95, 7121–7126. doi: 10.1073/pnas.95.12.7121

Sherman, S. M., and Guillery, R. W. (2011). Distinct functions for direct and transthalamic corticocortical connections. *J. Neurophysiol.* 106, 1068–1077. doi: 10.1152/jn.00429.2011

Shipp, S. (2003). The functional logic of cortico-pulvinar connections. *Philos. Trans. R. Soc. Lond. B Biol. Sci.* 358, 1605–1624. doi: 10.1098/rstb.2002.1213

Shipp, S. (2007). Structure and function of the cerebral cortex. *Curr. Biol.* 17, R443–R449. doi: 10.1016/j.cub.2007.03.044

Shipp, S. (2016). Neural elements for predictive coding. *Front. Psychol.* 7:1792. doi: 10.3389/fpsyg.2016.01792

Silberberg, G., and Markram, H. (2007). Disynaptic inhibition between neocortical pyramidal cells mediated by Martinotti cells. *Neuron* 53, 735–746. doi: 10.1016/j.neuron.2007.02.012

Sincich, L. C., and Horton, J. C. (2003). Independent projection streams from macaque striate cortex to the second visual area and middle temporal area. *J. Neurosci.* 23, 5684–5692.

Sorensen, S. A., Bernard, A., Menon, V., Royall, J. J., Glattfelder, K. J., Desta, T., et al. (2015). Correlated gene expression and target specificity demonstrate excitatory projection neuron diversity. *Cereb. Cortex* 25, 433–449. doi: 10.1093/cercor/bht243

Spruston, N. (2008). Pyramidal neurons: dendritic structure and synaptic integration. *Nat. Rev. Neurosci.* 9, 206–221. doi: 10.1038/nrn2286

Stuart, G., and Spruston, N. (1998). Determinants of voltage attenuation in neocortical pyramidal neuron dendrites. *J. Neurosci.* 18, 3501–3510.

Takahashi, N., Oertner, T. G., Hegemann, P., and Larkum, M. E. (2016). Active cortical dendrites modulate perception. *Science* 354, 1587–1590. doi: 10.1126/science.aah6066

Tasic, B., Menon, V., Nguyen, T. N., Kim, T. K., Jarsky, T., Yao, Z., et al. (2016). Adult mouse cortical cell taxonomy revealed by single cell transcriptomics. *Nat. Neurosci.* 19, 335–346. doi: 10.1038/nn.4216

Thomson, A. M., and Bannister, A. P. (2003). Interlaminar connections in the neocortex. *Cereb. Cortex* 13, 5–14. doi: 10.1093/cercor/13.1.5

Timofeev, I., Grenier, F., Bazhenov, M., Sejnowski, T. J., and Steriade, M. (2000). Origin of slow cortical oscillations in deafferented cortical slabs. *Cereb. Cortex* 10, 1185–1199. doi: 10.1093/cercor/10.12.1185

Tohmi, M., Meguro, R., Tsukano, H., Hishida, R., and Shibuki, K. (2014). The extrageniculate visual pathway generates distinct response properties in the higher visual areas of mice. *Curr. Biol.* 24, 587–597. doi: 10.1016/j.cub.2014.01.061

Treisman, A. (1996). The binding problem. *Curr. Opin. Neurobiol.* 6, 171–178. doi: 10.1016/S0959-4388(96)80070-5

Vaiceliunaite, A., Erisken, S., Franzen, F., Katzner, S., and Busse, L. (2013). Spatial integration in mouse primary visual cortex. *J. Neurophysiol.* 110, 964–972. doi: 10.1152/jn.00138.2013

Wang, Q., and Burkhalter, A. (2007). Area map of mouse visual cortex. *J. Comp. Neurol.* 502, 339–357. doi: 10.1002/cne.21286

Wehr, M., and Zador, A. M. (2003). Balanced inhibition underlies tuning and sharpens spike timing in auditory cortex. *Nature* 426, 442–446. doi: 10.1038/nature02116

Whitmire, C. J., and Stanley, G. B. (2016). Rapid sensory adaptation redux: a circuit perspective. *Neuron* 92, 298–315. doi: 10.1016/j.neuron.2016.09.046

Williams, S. R., and Stuart, G. J. (2002). Dependence of EPSP efficacy on synapse location in neocortical pyramidal neurons. *Science* 295, 1907–1910. doi: 10.1126/science.1067903

Wilson, N. R., Runyan, C. A., Wang, F. L., and Sur, M. (2012). Division and subtraction by distinct cortical inhibitory networks *in vivo*. *Nature* 488, 343–348. doi: 10.1038/nature11347

Wozny, C., and Williams, S. R. (2011). Specificity of synaptic connectivity between layer 1 inhibitory interneurons and layer 2/3 pyramidal neurons in the rat neocortex. *Cereb. Cortex* 21, 1818–1826. doi: 10.1093/cercor/bhq257

Wurtz, R. H., McAlonan, K., Cavanaugh, J., and Berman, R. A. (2011). Thalamic pathways for active vision. *Trends Cogn. Sci.* 15, 177–184. doi: 10.1016/j.tics.2011.02.004

Xu, X., and Callaway, E. M. (2009). Laminar specificity of functional input to distinct types of inhibitory cortical neurons. *J. Neurosci.* 29, 70–85. doi: 10.1523/JNEUROSCI.4104-08.2009

Xu, X., Olivas, N. D., Ikrar, T., Peng, T., Holmes, T. C., Nie, Q., et al. (2016). Primary visual cortex shows laminar-specific and balanced circuit organization of excitatory and inhibitory synaptic connectivity. *J. Physiol.* 594, 1891–1910. doi: 10.1113/jp271891

Xue, M., Atallah, B. V., and Scanziani, M. (2014). Equalizing excitation-inhibition ratios across visual cortical neurons. *Nature* 511, 596–600. doi: 10.1038/nature13321

Yang, W., Carrasquillo, Y., Hooks, B. M., Nerbonne, J. M., and Burkhalter, A. (2013). Distinct balance of excitation and inhibition in an interareal feedforward and feedback circuit of mouse visual cortex. *J. Neurosci.* 33, 17373–17384. doi: 10.1523/jneurosci.2515-13.2013

Yoshimura, Y., and Callaway, E. M. (2005). Fine-scale specificity of cortical networks depends on inhibitory cell type and connectivity. *Nat. Neurosci.* 8, 1552–1559. doi: 10.1038/nn1565

Yuste, R., Gutnick, M. J., Saar, D., Delaney, K. R., and Tank, D. W. (1994). Ca^{2+} accumulations in dendrites of neocortical pyramidal neurons: an apical band and evidence for two functional compartments. *Neuron* 13, 23–43. doi: 10.1016/0896-6273(94)90457-x

Zeisel, A., Muñoz-Manchado, A. B., Codeluppi, S., Lönnerberg, P., La Manno, G., Juréus, A., et al. (2015). Cell types in the mouse cortex and hippocampus revealed by single-cell RNA-seq. *Science* 347, 1138–1142. doi: 10.1126/science.aaa1934

Zhang, S., Xu, M., Kamigaki, T., Hoang Do, J. P., Chang, W. C., Jenvay, S., et al. (2014). Selective attention. Long-range and local circuits for top-down modulation of visual cortex processing. *Science* 345, 660–665. doi: 10.1126/science.1254126

Zhou, M., Liang, F., Xiong, X. R., Li, L., Li, H., Xiao, Z., et al. (2014). Scaling down of balanced excitation and inhibition by active behavioral states in auditory cortex. *Nat. Neurosci.* 17, 841–850. doi: 10.1038/nn.3701

Zhuang, J., Ng, L., Williams, D., Valley, M., Li, Y., Garrett, M., et al. (2017). An extended retinotopic map of mouse cortex. *Elife* 6:e18372. doi: 10.7554/eLife.18372

Conflict of Interest Statement: The authors declare that the research was conducted in the absence of any commercial or financial relationships that could be construed as a potential conflict of interest.

frontiers in Neuroanatomy

REVIEW
published: 28 September 2017
doi: 10.3389/fnana.2017.00087

Laminar and Cellular Distribution of Monoamine Receptors in Rat Medial Prefrontal Cortex

Noemí Santana[1,2] *and Francesc Artigas*[1,2,3]*

[1] *Systems Neuropharmacology, Department of Neurochemistry and Neuropharmacology, Institut d'Investigacions Biomèdiques de Barcelona, Consejo Superior de Investigaciones Científicas, Barcelona, Spain,* [2] *Centro de Investigación Biomédica en Red de Salud Mental, Madrid, Spain,* [3] *Institut d'Investigacions Biomèdiques August Pi i Sunyer, Barcelona, Spain*

The prefrontal cortex (PFC) is deeply involved in higher brain functions, many of which are altered in psychiatric conditions. The PFC exerts a top-down control of most cortical and subcortical areas through descending pathways and is densely innervated by axons emerging from the brainstem monoamine cell groups, namely, the dorsal and median raphe nuclei (DR and MnR, respectively), the ventral tegmental area and the *locus coeruleus* (LC). In turn, the activity of these cell groups is tightly controlled by afferent pathways arising from layer V PFC pyramidal neurons. The reciprocal connectivity between PFC and monoamine cell groups is of interest to study the pathophysiology and treatment of severe psychiatric disorders, such as major depression and schizophrenia, inasmuch as antidepressant and antipsychotic drugs target monoamine receptors/transporters expressed in these areas. Here we review previous reports examining the presence of monoamine receptors in pyramidal and GABAergic neurons of the PFC using double *in situ* hybridization. Additionally, we present new data on the quantitative layer distribution (layers I, II–III, V, and VI) of monoamine receptor-expressing cells in the cingulate (Cg), prelimbic (PrL) and infralimbic (IL) subfields of the medial PFC (mPFC). The receptors examined include serotonin 5-HT_{1A}, 5-HT_{2A}, 5-HT_{2C}, and 5-HT_3, dopamine D_1 and D_2 receptors, and α_{1A}-, α_{1B}-, and α_{1D}-adrenoceptors. With the exception of 5-HT_3 receptors, selectively expressed by layers I–III GABA interneurons, the rest of monoamine receptors are widely expressed by pyramidal and GABAergic neurons in intermediate and deep layers of mPFC (5-HT_{2C} receptors are also expressed in layer I). This complex distribution suggests that monoamines may modulate the communications between PFC and cortical/subcortical areas through the activation of receptors expressed by neurons in intermediate (e.g., 5-HT_{1A}, 5-HT_{2A}, α_{1D}-adrenoceptors, dopamine D_1 receptors) and deep layers (e.g., 5-HT_{1A}, 5-HT_{2A}, α_{1A}-adrenoceptors, dopamine D_2 receptors), respectively. Overall, these data provide a detailed framework to better understand the role of monoamines in the processing of cognitive and emotional signals by the PFC. Likewise, they may be helpful to characterize brain circuits relevant for the therapeutic action of antidepressant and antipsychotic drugs and to improve their therapeutic action, overcoming the limitations of current drugs.

Keywords: 5-hydroxytryptamine (serotonin) receptors, antidepressant drugs, antipsychotic drugs, cortical layers, dopamine receptors, major depressive disorder, noradrenaline receptors, schizophrenia

OPEN ACCESS

Edited by:
Kathleen S. Rockland, Boston University School of Medicine, United States

Reviewed by:
Amy F. T. Arnsten, Yale School of Medicine, United States
Trevor W. Robbins, University of Cambridge, United Kingdom

***Correspondence:**
Francesc Artigas
fapnqi@iibb.csic.es

Received: *09 June 2017*
Accepted: *15 September 2017*
Published: *28 September 2017*

Citation:
Santana N and Artigas F (2017) Laminar and Cellular Distribution of Monoamine Receptors in Rat Medial Prefrontal Cortex. Front. Neuroanat. 11:87. doi: 10.3389/fnana.2017.00087

INTRODUCTION

The prefrontal cortex (PFC) is the association cortex of the frontal lobe, located in its most rostral part. It has poorly defined anatomical boundaries although in all examined mammalian brains, it is defined by its connectivity with the mediodorsal nucleus of the thalamus. According to the original definition by Brodman, the human PFC contains areas 8–14 and 44–47, although other classifications also include ventromedial areas 14 and 25. The human PFC consists of three main regions: lateral, medial, and orbital. Orbital and ventromedial regions are mainly involved in emotional behavior whereas lateral areas (particularly the dorsolateral PFC) are involved in cognitive control. In the rat, the PFC contains four main regions, medial, lateral, ventral, and orbital, each containing several subdivisions that may vary according to different authors (Uylings et al., 2003; Dalley et al., 2004; Swanson, 2004; Paxinos and Watson, 2005; Fuster, 2008; Herculano-Houzel et al., 2013). See Fuster (2008) for extended information on PFC anatomy.

In primates, the PFC is dedicated to the representation, planning and execution of actions under a temporal pattern. It is involved in many higher brain functions, such as perception, attention, memory, language, intelligence, consciousness, affect, etc., and plays a key role in cognitive processes, such as working memory and executive functions (Miller, 2000; Fuster, 2001, 2008; Miller and Cohen, 2001). Automatic or stereotyped behaviors are bottom-up processes carried out by an innate connectivity between sensory and motor areas and do not require the engagement of the PFC (e.g., to look at a place where we hear a sudden noise). In contrast, the PFC involvement is required in situations with a large number of degrees of freedom, i.e., when flexibility is required to behave in a novel, unexpected or non-familiar environment (e.g., a EU or United States citizen driving in United Kingdom for the first time) or when behavioral rules change (Miller, 2000; Miller and Cohen, 2001; Buschman and Miller, 2007; Fuster, 2008). There is general consensus from multiple studies that the PFC reaches internally represented goals, and does this by coordinating sensory and motor processes of a lower association level. This process is thought to be influenced by the very large number of afferent and efferent connections to and from sensory and motor cortical and subcortical areas. As frequently summarized, a key feature of the PFC is a multi-layered architecture where sensory information is received from the external world, and emotional and contextual information is received and stored from limbic and temporal areas. The architecture further incorporates important intrinsic processing among the different subdivisions of the PFC itself. Projections to cortical premotor and motor areas and to the basal ganglia enable the performance of motor acts once a particular behavior has been selected (see, among other references, Bates and Goldman-Rakic, 1993; Lu et al., 1994; Jueptner et al., 1997a,b; Groenewegen and Uylings, 2000; Calzavara et al., 2007; Friedman et al., 2016). By virtue of this connectivity, the PFC can be considered at the highest level of the cortical areas, exerting a "top-down" control of behavior from a selection among multiple internally represented possible scenarios. A function specific to the PFC in cognitive control is the active maintenance of the neural activity that represents goals as well as the means to achieve these (see Miller, 2000 for further elaboration).

Working –or short-term- memory is a key function of the PFC. This capacity for sustained neuronal activity in the absence of sensory stimuli and even in the presence of distractors, allows the PFC to store and combine information for short periods of time before the execution of a given task. This property was discovered in the early 1970s by Fuster (1973) in primates and was subsequently reproduced and characterized by many groups (Funahashi et al., 1989; Miller et al., 1996; Romo et al., 1999; Arnsten, 2009). Interestingly, monoaminergic inputs to PFC (see below) play a crucial role in working memory capacity (Sawaguchi and Goldman-Rakic, 1991; Williams and Goldman-Rakic, 1995; Vijayraghavan et al., 2007). In particular, dopamine (DA) depletion in PFC induces cognitive deficits in monkeys similar to those evoked by removal of the frontal lobes (Brozoski et al., 1979).

Prefrontal Cortex Connectivity

Broadly similar to other cortical areas, the PFC is composed of ∼75–80% glutamatergic pyramidal projection neurons, and ∼20–25% GABAergic local circuit interneurons (see Beaulieu, 1993 for an early report). The functions of the PFC rely closely on its connectivity with a vast array of other cerebral structures (Fuster, 2001). Excitatory glutamatergic afferent inputs originate from parts of the amygdala and hippocampus, from other cortical areas, and from a number of thalamic nuclei, including the mediodorsal, centromedial, and several midline nuclei. Pyramidal cell excitation is sculpted by inhibitory inputs, mainly from local GABAergic inputs. The multiple interneuron subtypes have been classified by anatomical and neurochemical features, and their selective targeting of pyramidal cell postsynaptic domains (Kawaguchi and Kondo, 2002; DeFelipe et al., 2013).

The PFC also receives a dense innervation from the brainstem monoaminergic nuclei: dorsal and median raphe nuclei, *locus coeruleus* and ventral tegmental (VTA) area, which employ serotonin (5-hydroxytryptamine, 5-HT), noradrenaline (NA) and dopamine (DA) as main neurotransmitters, respectively. These neuronal groups exert an important modulatory role of the excitatory and inhibitory currents in PFC neurons (Steinbusch, 1981; Van Eden et al., 1987; Aston-Jones and Cohen, 2005; Puig et al., 2005; Celada et al., 2013; Chandler et al., 2014) which are particularly relevant for the control of executive functions of PFC (Dalley et al., 2004; Robbins and Arnsten, 2009).

In turn, brainstem monoamine groups are innervated by descending axons from layer V pyramidal neurons in the medial PFC –mPFC- (for an overall view, see Gabbott et al., 2005) which control monoamine neuron activity (Thierry et al., 1979, 1983; Sara and Hervé-Minvielle, 1995; Hajós et al., 1998; Jodo et al., 1998; Celada et al., 2001; Martin-Ruiz et al., 2001), thus establishing a reciprocal connectivity and mutual control. These PFC-brainstem loops are relevant for the pathophysiology and treatment of psychiatric disorders, since (i) many psychiatric symptoms involve alterations of PFC functions, such as cognitive and emotional control, and (ii) psychiatric medications act either on presynaptic monoamine terminals (antidepressants blocking 5HT and/or NA transporters) or on postsynaptic

monoamine receptors. Moreover, the ventral anterior cingulate cortex (vACC) has emerged as a key area in the pathophysiology and treatment of major depressive disorder (MDD), particularly in the mechanism of action of fast-acting antidepressant strategies such as deep brain stimulation (Mayberg et al., 2005; Puigdemont et al., 2011) and ketamine (Zarate et al., 2006). Hence, early neuroimaging studies reported on a reduced energy metabolism in the vACC (subgenual) of MDD patients. Further studies indicated an increased activity of the adjacent Brodmann area 25, which normalized after effective treatments, including deep brain stimulation. Likewise, optogenetic stimulation of the infralimbic cortex (IL, rodent equivalent of vACC) in rats mimicked the rapid and persistent antidepressant-like effects of systemic ketamine administration (Fuchikami et al., 2015) and the stimulation of AMPA receptors in IL (but not in the adjacent prelimbic cortex, PrL) evokes robust antidepressant-like effects, which involve an increased serotonergic activity and depend on an intact serotonergic system (Gasull-Camós et al., 2017).

Collectively, primate studies support a key role of dorsal and lateral PFC in cognition, and of ventromedial areas in the processing of emotional signals, although is still unclear whether equivalent areas in rodent PFC play similar roles. Given our interest in the pathophysiology and treatment of MDD and schizophrenia, we undertook a long-lasting effort to study the cellular and neurochemical elements involved in PFC-based circuits, in particular those existing between the PFC and brainstem monoamine nuclei. Here we summarize and review the histological data relative to the expression of the mRNAs encoding nine monoamine receptors (serotonin 5-HT_{1A}-R, 5-HT_{2A}-R, 5-HT_{2C}-R and 5-HT_3-R, dopamine D_1-R and D_2-R and α_{1A}-, α_{1B}-, and α_{1D}-adrenoceptors) in pyramidal and GABAergic neurons of the mPFC, paying special attention to their layer distribution in the different subfields of the rat mPFC. Further studies will examine the expression of other relevant monoamine receptors, such as 5-HT_4-R, 5-HT_6-R, 5-HT_7-R α_2-adrenoceptors or β-adrenoceptors.

EXPRESSION OF MONOAMINE RECEPTORS BY PFC NEURONS IN RAT BRAIN

The PFC contains a large number of pyramidal neurons and GABAergic interneurons expressing the mRNAs encoding the nine monoamine receptors examined, as reported elsewhere (Amargós-Bosch et al., 2004; Puig et al., 2004; Santana et al., 2004, 2009, 2013; Santana and Artigas, 2017). In all them we report on the cellular expression of the corresponding mRNAs in the different PFC subfields. However, in some studies we did not analyze the layer distribution of mRNAs. Therefore, in order to ensure data homogeneity and quality, we performed new cell counts on hybridized tissue sections corresponding to all previous studies (see Santana and Artigas, 2017 for analysis methodology), after checking that old and new cell counts were comparable. Remarkably, despite the long time spent since initial studies (e.g., the expression of 5-HT_{1A}-R, 5-HT_{2A}-R, and 5-HT_3-R mRNA was examined in 2003–2004) old and new data are fully coincident, which indicates an excellent preservation of radioactive (silver grains) and non-radioactive (digoxigenin) signals, as show in **Figure 1**.

Figure 2 shows the localization of the mRNAs encoding serotonergic receptors (5-HT_{1A}-R, 5-HT_{2A}-R, 5-HT_{2C}-R, and 5-HT_3-R), dopamine D_1-R and D_2-R and α_{1A}-, α_{1B}- and α_{1D}-adrenoceptors in coronal sections of rat PFC. **Table 1** shows the percentages of pyramidal neurons (vGLUT1-positive) and GABAergic interneurons (GAD-positive) expressing each of the 9 receptors in the different mPFC subfields (cingulate –Cg-, prelimbic –PrL-, and infralimbic –IL-) and PFC layers. **Figure 3** shows the same data, expressed as percentages of the *total neuronal population*, assuming a standard 80% of pyramidal neurons and 20% of GABAergic interneurons.

With the exception of 5-HT_3-R, exclusively expressed in GABAergic interneurons located mainly in superficial layers I-III, the rest of monoaminergic receptors are present in both neuronal types in varying proportions, and in middle (II–III) and deep (V–VI) layers of the Cg, PrL, and IL subfields. **Figures 4–6** show the percentages of pyramidal and GABAergic neurons expressing each receptor across layers in the three mPFC subfields (Cg, PrL, and IL, respectively).

Some receptors are highly co-localized (5-HT_{1A}-R and 5-HT_{2A}-R, Amargós-Bosch et al., 2004; 5-HT_{2A}-R and α_1-adrenoceptors, Santana et al., 2013) while others show little overlap (D_1-R and D_2-R, Santana et al., 2009). This distribution suggests a complex monoaminergic control of PFC activity, with some convergent actions on certain neuronal populations together with selective actions on other neuronal populations. In the following sections, we summarize the most important features of receptor expression in pyramidal and GABAergic neurons of the different PFC layers.

Layer I

Only two of the nine receptors examined (5-HT_{2C}-R and 5-HT_3-R) were expressed by GABA interneurons of layer I. There is a greater proportion of GABA interneurons expressing 5-HT_3-R (30–40%) than 5-HT_{2C}-R (8–14%; values in parentheses refer to the range of values in the three mPFC subfields: **Table 1**).

5-HT_{2C}-Rs are G-protein coupled metabotropic receptors that activate the phospholipase C signaling pathway. It undergoes RNA editing, which dynamically regulates its constitutive activity, unique among 5-HT receptors (Berg et al., 2008; Werry et al., 2008; Aloyo et al., 2009; O'Neil and Emeson, 2012). On the other hand, the 5-HT_3-R is the only ionotropic monoamine receptor. It is selectively expressed by a subpopulation of GABA interneurons not expressing parvalbumin or somatostatin, and displays strong actions on neuronal activity (Puig et al., 2004; Varga et al., 2009; Lee et al., 2010). **Figure 7** shows the rapid and robust excitatory action of endogenous 5-HT on layers I–III GABA neurons expressing 5-HT_3-R and its comparison with the slower and more moderate activation of layer V pyramidal neurons by metabotropic 5-HT_{2A}-R.

Despite its localization in upper cortical layers, GABA cells expressing 5-HT_3-R tightly control the activity of pyramidal

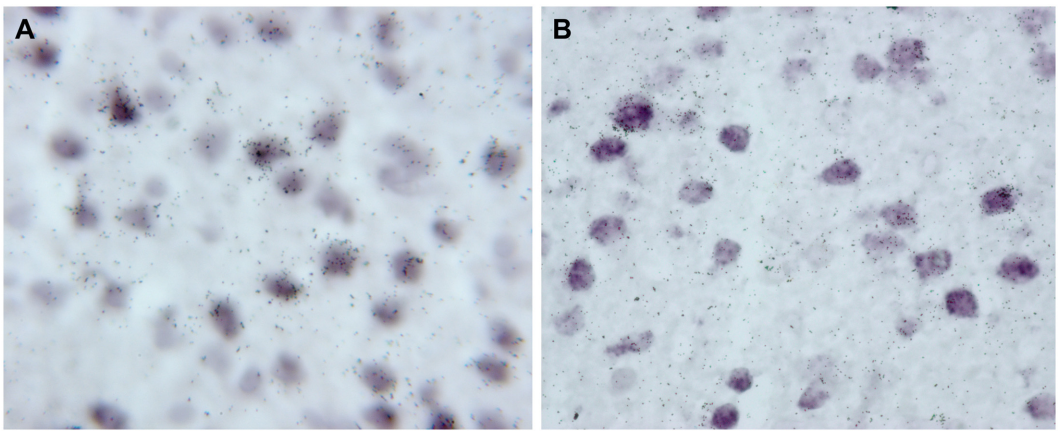

FIGURE 1 | High magnification photomicrographs showing the presence of 5-HT_{1A} receptor mRNA (^{33}P-labeled oligonucleotides) in pyramidal cells, identified by the presence of VGLUT1 mRNA (Dig-labeled oligonucleotides). Both images were acquired from the same experiment and correspond to deep layers of mPFC cingulate area. **(A)** Was captured in 2003 with a Nikon Eclipse E1000 microscope (Nikon, Tokyo, Japan) using a digital camera (DXM1200 3.0; Nikon) and analySIS Software (Soft Imaging System GmbH, Germany); **(B)** was captured in 2017 with a Zeiss Axioplan microscope equipped with a digital camera (XC50, Olympus) with Olympus CellSens Entry software.

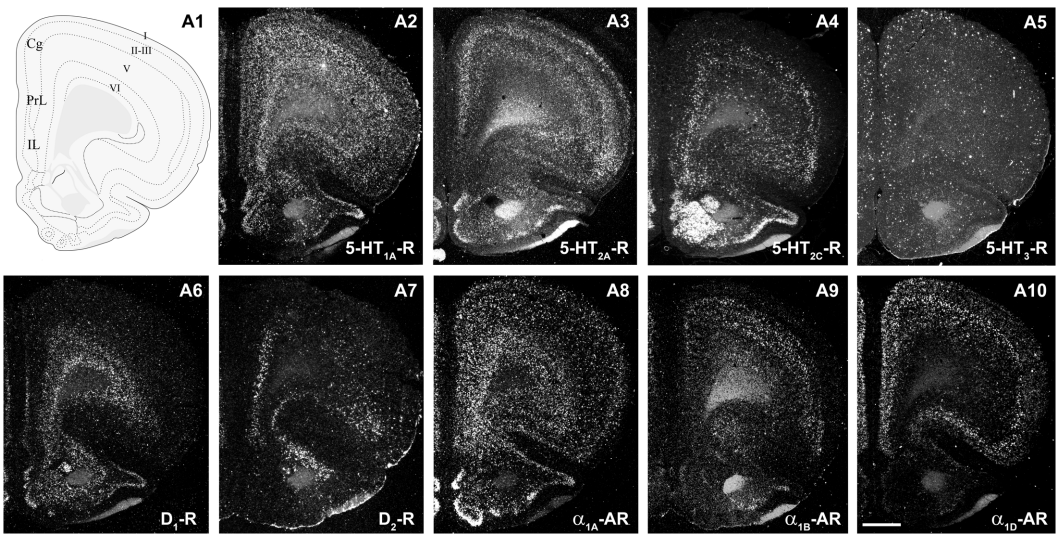

FIGURE 2 | mRNA expression of monoaminergic receptors in rat prefrontal cortex (PFC). **(A1)** Coronal diagram from the rat brain atlas Swanson (2004) (used under CC BY-NC 4.0) at the approximate AP coordinate where cell counts have been performed in the cingulate (Cg), prelimbic (PrL), and infralimbic (IL) subdivisions. **(A2–A10)** Emulsion dipped dark-field PFC coronal sections hybridized with ^{33}P-labeled oligonucleotide probes against the mRNAs encoding 5-HT_{1A}-R **(A2)**, 5-HT_{2A}-R **(A3)**, 5-HT_{2C}-R **(A4)**, 5-HT_3-R **(A5)** dopamine D_1-R **(A6)**, dopamine D_2-R **(A7)** and α_{1A}-, α_{1B}- and α_{1D}-adrenoceptors (**A8–A10**, respectively). Bar: 1 mm. See Puig et al. (2004), Santana et al. (2004, 2009, 2013), Santana and Artigas (2017) for detailed methods.

neurons located in deep layers. Hence, blockade of 5-HT_3-R in rat brain by the selective antagonist ondansetron or by the new antidepressant drug vortioxetine (combining 5-HT transporter inhibition with 5-HT_3-R blockade; Sanchez et al., 2015) markedly enhanced the discharge rate of layer V pyramidal neurons, identified by antidromic activation from midbrain (DR or VTA; Riga et al., 2016). Interestingly, ∼70% or the pyramidal neurons recorded were sensitive to 5-HT_3-R blockade, a very high percentage taking into account the relative long distance between the cell bodies of both neuronal types. This action likely involves the attenuation of tonic layers I–III GABA inputs on the tufts of layer V pyramidal neurons, thus allowing excitatory inputs (possibly thalamocortical matrix inputs reaching layer I -Jones (2001))- to enhance pyramidal neuron activity.

Much less is known on the role played by layer I 5-HT_{2C}-R on PFC neuronal activity. Unlike 5-HT_{1A}-R and 5-HT_{2A}-R, which exert a large variety of actions, including control the activity of pyramidal neurons and fast-spiking interneurons as well as cortical oscillations in rat mPFC (Araneda and Andrade, 1991; Amargós-Bosch et al., 2004;

Puig et al., 2005, 2010; Celada et al., 2013), 5-HT_{2C}-R are not involved in the latter effects. However, the relevance of 5-HT_{2C}-R for cognitive and affective processes (Heisler et al., 2007; Boulougouris and Robbins, 2010; Pennanen et al., 2013) suggests its participation in the modulation of PFC-based circuits. Yet it is unclear whether the small receptor subpopulation in layer I GABAergic cells plays a significant role given its larger abundance of 5-HT_{2C}-R in other PFC areas (**Figure 2**).

Layers II–III

Unlike in layer I, supragranular layers II and III show a large abundance of serotonergic, dopaminergic and α_1-adrenergic receptors, expressed by pyramidal and GABAergic neurons in all mPFC subfields (**Table 1** and **Figures 3–6**).

Most abundant 5-HT receptors in layers II–III are 5-HT_{1A}-R and 5-HT_{2A}-R, expressed by 45–52% of the pyramidal neurons and by 12–39% of GABA interneurons in Cg and PrL subfields, where they are abundantly co-expressed (Amargós-Bosch et al., 2004). Interestingly, the proportion of pyramidal neurons expressing 5-HT_{2A}-R is lesser than that that expressing 5-HT_{1A}-R in IL (45% vs. 22%, compared with 46–52% in PrL and 45–44% in Cg; see **Figures 4–6**). This suggests a predominance of inhibitory actions of 5-HT in the IL subfield. The differential excitation/inhibition balance in IL vs. PrL may be relevant to clarify the role of ventral cingulate areas in the pathophysiology and treatment of MDD, as summarized in the introduction. This difference is also common to layer VI, where a greater proportion of cells express 5-HT_{1A}-R vs. 5-HT_{2A}-R (**Table 1** and **Figures 4–6**), indicating a preferential inhibitory action of 5-HT on both intracortical and cortico-subcortical pathways arising from IL.

The proportion of 5-HT_3-R-expressing GABAergic cells in layers II–III is lower than in layer I, reaching 18–29% in Cg, PrL, and IL. Similarly, there is a very low percentage of pyramidal (2–7%) and GABAergic neurons (5–15%) expressing 5-HT_{2C}-R.

Dopamine modulates PFC function by multiple mechanisms, (Chen et al., 2004; Seamans and Yang, 2004) consistent with the presence of DA receptors in pyramidal neurons and GABAergic interneurons (**Table 1** and **Figures 4–6**). However, DA receptor

TABLE 1 | Percentages of pyramidal and GABAergic neurons expressing monoamine receptor mRNAs in rat mPFC.

		VGLUT1			GAD			
		Layer II–III	Layer V	Layer VI	Layer I	Layer II–III	Layer V	Layer VI
5-HT_{1A}-R	Cg	45.1 ± 2.8	60.3 ± 0.9	58.0 ± 2.7		12.5 ± 1.0	25.7 ± 2.0	25.5 ± 0.3
	PrL	46.0 ± 3.2	52.0 ± 4.5	62.9 ± 4.3		19.0 ± 2.9	33.7 ± 0.7	19.0 ± 0.6
	IL	45.1 ± 2.7	54.0 ± 6.7	59.5 ± 2.4		29.5 ± 4.3	28.2 ± 2.8	24.7 ± 1.8
5-HT_{2A}-R	Cg	43.8 ± 2.7	56.8 ± 1.2	8.5 ± 1.7		18.8 ± 3.9	44.8 ± 6.4	16.1 ± 4.7
	PrL	52.2 ± 4.4	55.3 ± 1.4	7.5 ± 0.6		39.5 ± 1.1	52.2 ± 4.8	14.0 ± 3.9
	IL	21.8 ± 4.4	22.0 ± 5.3	10.3 ± 1.6		20.4 ± 5.2	25.1 ± 7.0	17.1 ± 6.0
5-HT_{2C}-R	Cg	1.7 ± 0.4	10.3 ± 1.8	12.3 ± 1.5	7.6 ± 3.3	4.6 ± 1.5	5.7 ± 1.7	23.9 ± 2.9
	PrL	4.3 ± 2.2	13.2 ± 3.6	19.2 ± 2.2	10.3 ± 2.7	6.6 ± 1.2	12.4 ± 2.1	22.5 ± 2.7
	IL	7.3 ± 1.0	16.2 ± 1.3	18.3 ± 0.8	14.1 ± 2.4	14.8 ± 3.9	15.7 ± 3.9	26.9 ± 6.1
5-HT_3-R	Cg				29.5 ± 6.1	28.7 ± 3.6	9.1 ± 2.0	13.3 ± 3.7
	PrL				40.0 ± 2.1	18.3 ± 1.5	5.7 ± 0.9	8.0 ± 0.6
	IL				34.9 ± 7.4	23.9 ± 2.1	9.5 ± 0.8	12.4 ± 1.5
D_1-R	Cg	10.8 ± 0.1	16.9 ± 1.0	32.9 ± 5.9		24.7 ± 1.1	36.8 ± 8.0	51.9 ± 4.2
	PrL	19.2 ± 3.2	20.9 ± 1.5	37.9 ± 3.2		28.1 ± 1.0	30.5 ± 1.6	37.5 ± 3.6
	IL	21.0 ± 0.4	22.8 ± 0.8	33.8 ± 2.6		52.0 ± 3.3	55.5 ± 6.2	56.8 ± 2.0
D_2-R	Cg	4.5 ± 1.8	19.5 ± 0.4	8.3 ± 1.7		14.5 ± 5.3	36.4 ± 6.2	16.2 ± 1.4
	PrL	4.5 ± 1.0	24.9 ± 1.6	12.5 ± 0.5		4.7 ± 2.2	7.9 ± 2.3	17.2 ± 1.2
	IL	5.3 ± 1.1	21.1 ± 2.1	5.8 ± 0.4		10.9 ± 2.9	27.1 ± 2.3	17.2 ± 3.2
Alpha$_{1A}$-AR	Cg	29.6 ± 3.7	51.9 ± 10.7	59.7 ± 3.0		46.7 ± 7.2	30.4 ± 1.0	34.1 ± 10.9
	PrL	26.2 ± 3.5	60.7 ± 6.2	72.3 ± 4.6		34.4 ± 4.8	30.4 ± 1.5	28.8 ± 4.2
	IL	26.7 ± 5.7	36.6 ± 3.1	54.7 ± 2.9		47.4 ± 2.8	39.3 ± 5.5	29.4 ± 1.5
Alpha$_{1B}$-AR	Cg	7.4 ± 1.6	26.2 ± 0.0	15.5 ± 2.1		10.4 ± 3.5	13.5 ± 2.4	5.2 ± 2.9
	PrL	7.9 ± 2.1	18.7 ± 3.5	10.7 ± 1.4		23.7 ± 4.8	14.7 ± 3.5	10.3 ± 2.1
	IL	3.3 ± 0.6	7.3 ± 1.5	4.5 ± 1.0		16.8 ± 1.6	11.3 ± 5.6	12.5 ± 1.4
Alpha$_{1D}$-AR	Cg	71.6 ± 5.6	48.2 ± 2.1	4.4 ± 1.5		29.8 ± 3.8	18.4 ± 2.4	11.9 ± 3.6
	PrL	70.5 ± 3.5	42.3 ± 1.4	5.7 ± 2.6		35.6 ± 4.0	19.0 ± 9.4	2.1 ± 1.2
	IL	62.7 ± 2.6	30.8 ± 0.9	6.1 ± 1.4		19.1 ± 3.7	11.9 ± 6.1	13.8 ± 9.0

Data are means ± standard errors of the mean of 3 rats (2–3 adjacent sections per rat) and show the percentage of pyramidal (VGLUT1-positive) or GABAergic (GAD-positive) neurons expressing each monoamine receptor mRNA in layers I, II–III, V, and VI of the cingulate (Cg), prelimbic (PrL), and infralimbic (IL) subdivisions of the mPFC.

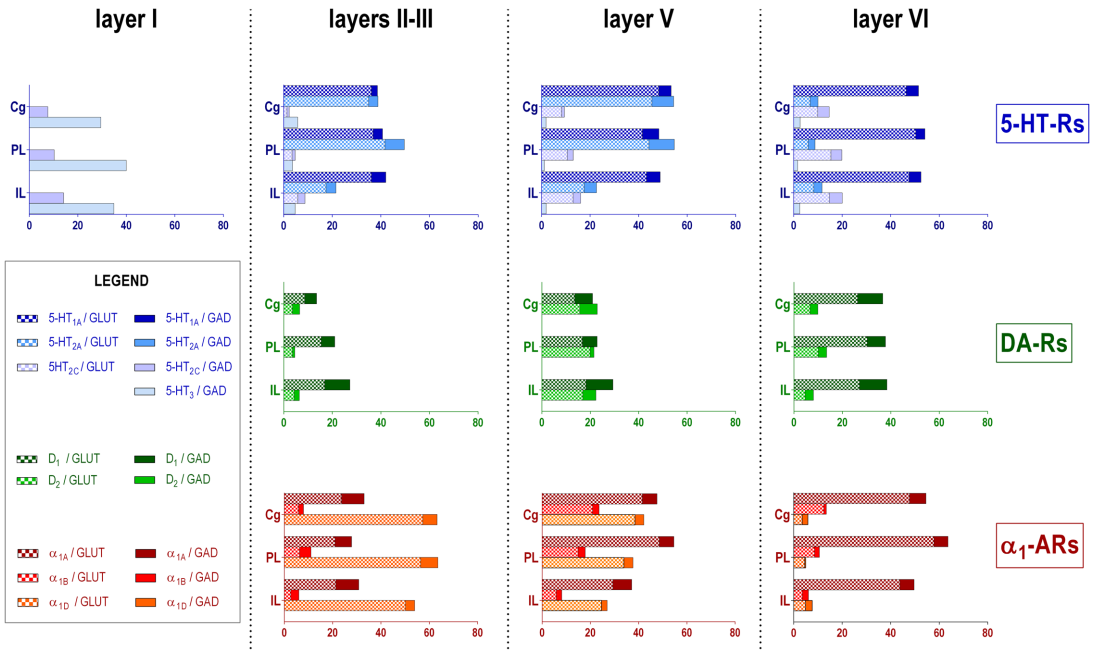

FIGURE 3 | Bar graphs showing the expression of each monoamine receptor mRNA in the different layers and PFC subfields of the mPFC. Data (mean of 3 rats, 2–3 consecutive sections per rat) are the percentages of pyramidal (VGLUT1-positive) or GABAergic (GAD-positive) neurons expressing each mRNA, expressed as percentages of the total neuronal population, assuming a standard 80% of pyramidal neurons and 20% of GABAergic interneurons. As layer I lacks glutamatergic neurons, layer I data is expressed as percentages of GAD-positive cells containing each receptor mRNA. Cg, anterior cingulate cortex; PL, prelimbic cortex; IL infralimbic cortex. Layer I, II–III, V, and VI stand for medial prefrontal cortical layers I to VI, respectively.

expression by layers II–III cells was lower than for 5-HT and NA receptors, suggesting a comparatively less relevant role of DA in the tuning of the intracortical PFC output. The proportion of pyramidal cells expressing dopamine D_1-R was lower than that expressed by GABA cells (11–21% vs. 25–52%, respectively), suggesting a predominantly inhibitory role of DA on the cortical PFC output via D_1-R activation on GABAergic interneurons. This inhibitory action may be particularly relevant in IL, with a very large contribution of D_1-R expressed in GABA interneurons. DA D_2-R were expressed by an even lesser proportion of pyramidal and GABAergic neurons (4–5% vs. 5–15%, respectively).

Unlike 5-HT and α_1-adrenoceptors, mainly expressed by a greater proportion of pyramidal neurons (except 5-HT_3-R, selectively expressed by GABA interneurons), DA D_1-R are expressed by a comparable or greater proportion of GABAergic than of pyramidal neurons. This expression pattern may be relevant to understand the inverted U relationship between D_1-R activation and working memory performance (Williams and Goldman-Rakic, 1995). Hence, the activation of D_1-R in GABAergic interneurons by an excess of endogenous DA (such as that produced by stress) may attenuate or cancel persistent neuronal activity evoked by D_1-R activation in pyramidal neurons.

In contrast to DA receptors, the three α_1-adrenoceptors were abundantly expressed in layers II–III, with α_{1D}-adrenoceptors being expressed by more than 50% of PFC neurons in all PFC subfields (>60% in Cg and PrL), and with a similar ratio of pyramidal/GABA neurons in CG and PrL (lower proportion in IL GABA interneurons). The receptor expressed in the smaller neuronal proportion was the α_{1B}-adrenoceptor (3–8% in pyramidal neurons, 10–24% in GABA interneurons).

Interestingly, α_1-adrenocptors were co-expressed with 5-HT_{2A}-R in varying proportions, depending on the receptor type and the mPFC subfield, with α_{1A}- and α_{1D}-adrenocepetors reaching a 80% co-expression in Cg (Santana et al., 2013). Although we did not perform a detailed layer analysis of co-expressing cells, the fields examined in the original study correspond mainly to layers II–III, with some contribution of deep layers in PrL and IL (Santana et al., 2013). Given the high co-expression of 5-HT_{1A}-R and 5-HT_{2A}-R mRNAs, and that of 5-HT_{2A}-R with α_1-adrenoceptors, it is likely that a substantial proportion of mPFC neurons express the three receptors. 5-HT_{1A}-R and 5-HT_{2A}-R are likely located in different cellular compartments and regulate different processes. Hence, 5-HT_{2A}-R are possibly located in dendritic spines and modulate synaptic inputs (Marek and Aghajanian, 1999) whereas 5-HT_{1A}-R in the axon hillock may regulate action potential generation, in a way similar to $GABA_A$-R (DeFelipe et al., 2001). Indeed, excitatory and inhibitory responses have been recorded in the same pyramidal neurons after DR stimulation, supporting that both receptors are functionally relevant in the control of pyramidal neuron activity (Amargós-Bosch et al., 2004). However, despite 5-HT_{2A}-R and α_1-adrenoceptors share signaling pathways ($G_{q/11}$ protein; Claro et al., 1993; Bartrup and Newberry, 1994; Berg et al.,

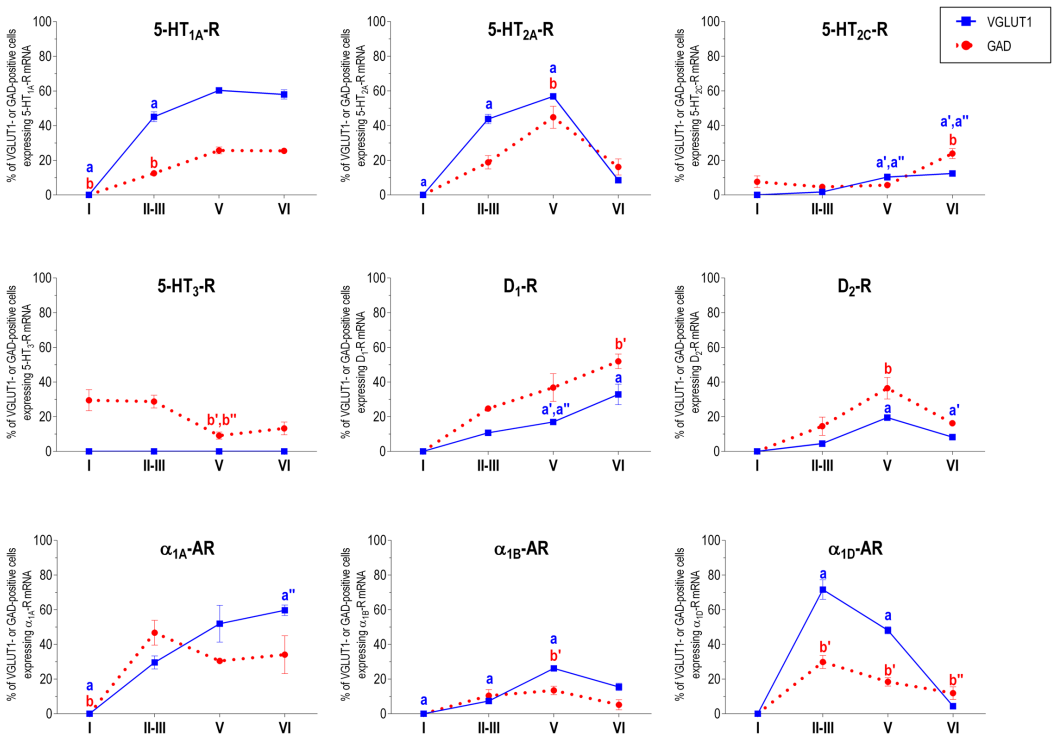

FIGURE 4 | Percentages of pyramidal (VGLUT1-positive) and GABA (GAD-positive) neurons expressing the nine monoamine receptors studied in the different layers of cingulate area of medial prefrontal cortex. $^{a}p < 0.05$ vs. rest of layers, $^{a'}p < 0.05$ vs. layer I; $^{a'''}p < 0.05$ vs. layer II–III; $^{a'''}p < 0.05$ vs. layer V (for VGLUT1 graphs). $^{b}p < 0.05$ vs. rest of layers, $^{b'}p < 0.05$ vs. layer I; $^{b''}p < 0.05$ vs. layers II–III; $^{b'''}p < 0.05$ vs. layer V (for GAD graphs), one-way ANOVA followed by Tukey's test.

1998) and there is evidence of heteromerization in artificial systems (Santana et al., unpublished observations), there is no evidence of an *in vivo* interaction between both receptors as yet.

In summary, layers II/III contain a very large proportion of pyramidal and GABAergic cells expressing 5-HT, α_1-adrenoceptors, and –to a lesser extent- DA D_1-R and D_2-R, an observation indicating a crucial role of monoamines in the modulation of the connectivity between PFC and other cortical areas, as well as with subcortical structures also innervated by layers II–III pyramidal neurons, such as the basolateral amygdala, dorsal and ventral striatum and lateral hypothalamus (Gabbott et al., 2005).

Layer V

Layer V contains the highest proportion of pyramidal and GABA neurons expressing monoamine receptors (**Table 1** and **Figures 4–6**). The proportion of pyramidal and GABA neurons expressing 5-HT receptors in layer V was very similar to that in layers II/III, yet with a greater abundance of glutamatergic cells expressing 5-HT_{2C}-R (10–16% in layer V vs. 2–7% in the different subfields of layers II–III). 5-HT_{1A}-R and 5-HT_{2A}-R were expressed by 52–60% of pyramidal neurons (except in IL, just a 22%) and 25–52% of GABA interneurons. In contrast, the 5-HT_3-R is expressed by only 6–10% of GABA neurons in this layer.

The expression of DA D_1-R was similar to that in layers II–III, whereas a substantially greater proportion of layer V pyramidal neurons express DA D_2-R (20–25% in layer V vs. 4–5% in layers II–III). The presence of both DA receptors in layer V neurons is consistent with previous electrophysiological data showing direct and GABA-mediated effects on layer V pyramidal neurons (Seamans and Yang, 2004; Tseng and O'Donnell, 2007). As discussed above for layers II/III the presence of a comparable or higher proportion of GABAergic interneurons than of pyramidal neurons may be related to the inverted U relationship between DA D_1-R occupancy and working memory performance.

With regard to α_1-adrenoceptors, there was a more balanced expression than in layers II–III, with similar or greater proportions of pyramidal neurons expressing α_{1A}- vs. α_{1D}-adrenoceptors and a greater proportion of neurons expressing α_{1B}-adrenoceptors than in layers II–III, and with a marked dorso-ventral negative gradient in mPFC (**Table 1** and **Figures 4–6**). The presence of α_1-adrenoceptors in layer V pyramidal and GABAergic neurons is consistent with previous electrophysiological reports showing that α_1-adrenoceptor stimulation can elicit excitatory or inhibitory postsynaptic currents in layer V pyramidal neurons (Marek and Aghajanian, 1999; Luo et al., 2015). Interestingly, the excitatory postsynaptic currents evoked by 5-HT through 5-HT_{2A}-R were several-fold greater than those evoked by NA and DA (Marek and

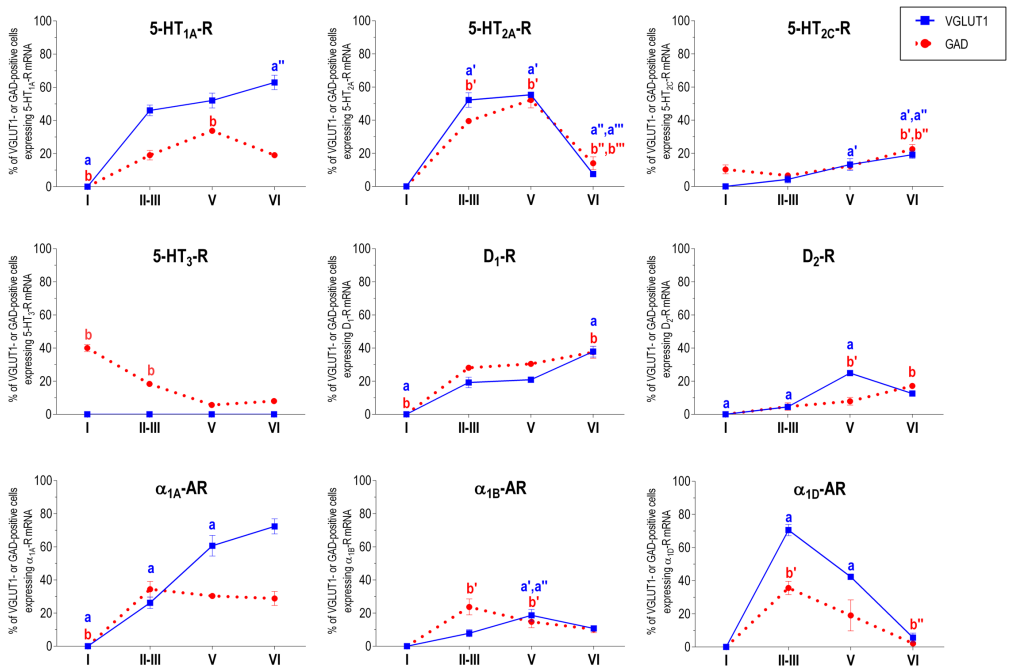

FIGURE 5 | Percentages of pyramidal (VGLUT1-positive) and GABA (GAD-positive) neurons expressing the nine monoamine receptors studied in the different layers of prelimbic area of medial prefrontal cortex. $^{a}p < 0.05$ vs. rest of layers, $^{a'}p < 0.05$ vs. layer I; $^{a''}p < 0.05$ vs. layers II–III; $^{a'''}p < 0.05$ vs. layer V (for VGLUT1 graphs). $^{b}p < 0.05$ vs. rest of layers, $^{b'}p < 0.05$ vs. layer I; $^{b''}p < 0.05$ vs. layers II–III; $^{b'''}p < 0.05$ vs. layer V (for GAD graphs), one-way ANOVA followed by Tukey's test.

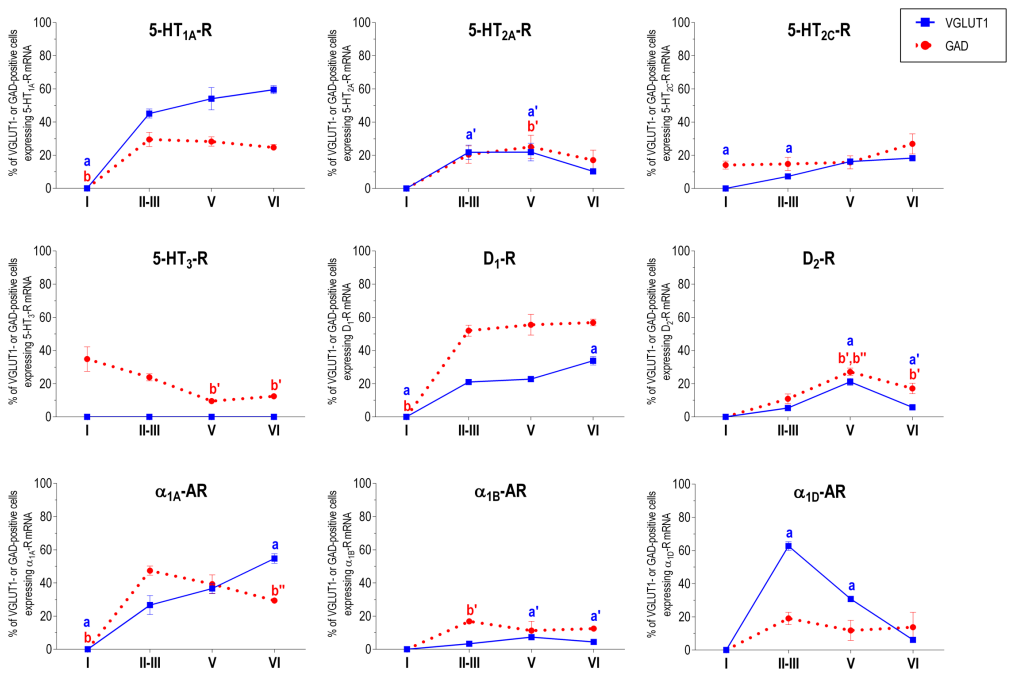

FIGURE 6 | Percentages of pyramidal (VGLUT1-positive) and GABA (GAD-positive) neurons expressing the nine monoamine receptors studied in the different layers of infralimbic area of medial prefrontal cortex. $^{a}p < 0.05$ vs. rest of layers, $^{a'}p < 0.05$ vs. layer I; $^{a''}p < 0.05$ vs. layers II–III; $^{a'''}p < 0.05$ vs. layer V (for VGLUT1 graphs). $^{b}p < 0.05$ vs. rest of layers, $^{b'}p < 0.05$ vs. layer I; $^{b''}p < 0.05$ vs. layers II–III; $^{b'''}p < 0.05$ vs. layer V (for GAD graphs), one-way ANOVA followed by Tukey's test.

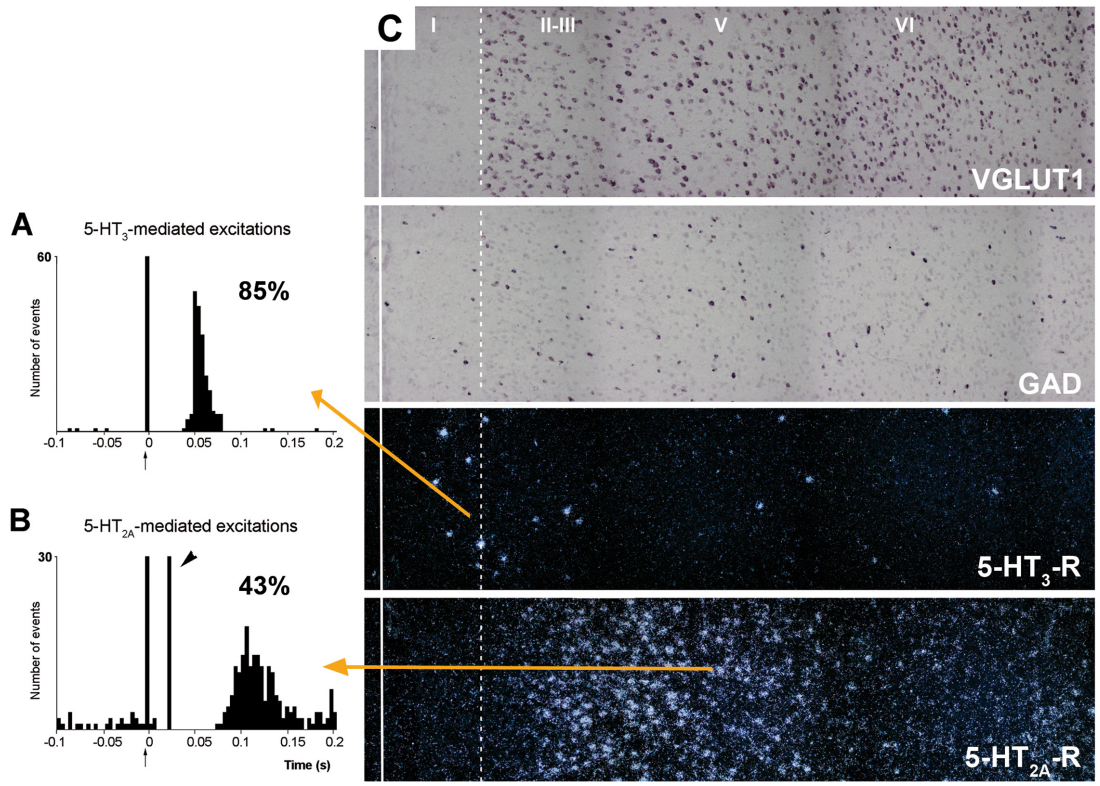

FIGURE 7 | (A,B) are peristimulus time histograms showing the orthodromic excitations elicited by the electrical stimulation of the DR at a physiological rate (0.5–1.7 mA, 0.2 ms square pulses, 0.9 Hz) on **(A)** a putatively GABAergic, 5-HT_3-R-expressing neuron and **(B)** on a layer V pyramidal neuron in the prelimbic PFC, identified by antidromic stimulation from midbrain (note the antidromic potential, arrowhead). Both responses were selectively blocked by the administration of the respective antagonists ondansetron **(A)** and M100907 **(B)** (not shown). The 5-HT_3-R-mediated responses in putative GABAergic neurons were faster and more effective than those evoked by 5-HT_{2A}-R activation in pyramidal neurons, due to the ionic nature of 5-HT_3-R. The concordance rates of the units shown are 85% **(A)** and 43% **(B)**, i.e., 100 electric stimuli delivered in the DR evoked 80 action potentials in GABAergic interneurons through 5-HT_3-R activation, compared to 45 action potentials evoked in layer V pyramidal neurons, mediated by the activation of 5-HT_{2A}-R. Each peristimulus consists of 200 triggers; bin size is 4 ms. The arrow at zero abscissa marks the stimulation artifact. **(C)** Composite photomicrographs showing the localization of cells expressing VGLUT1, GAD, 5-HT_3-R, and 5-HT_{2A}–R mRNAs through layers I–VI at the level of the prelimbic PFC. The continuous vertical line denotes the location of the midline whereas the dotted line shows the approximate border between layers I and II. Pyramidal neurons (as visualized by VGLUT1 mRNA) are present in layers II–VI whereas GAD mRNA-positive cells are present in all layers, including layer I. Note the different location of cells expressing 5-HT_3-R and 5-HT_{2A}–R. 5-HT_3-R transcript is expressed by a limited number of GABA interneurons in layers I–III, particularly in the border between layers I and II. However, they represent 40% of GABAergic neurons in layer I. Scale bar = 150 μm. Redrawn from Puig et al. (2004), by permission of Oxford University Press.

Aghajanian, 1999), an effect perhaps related to the facilitation of intrinsic PFC networks by 5-HT, acting on subpopulation of pyramidal neurons strongly excited by 5-HT_{2A}-R (Beique et al., 2007).

Given the large number of subcortical structures innervated by layer V pyramidal neurons (Gabbott et al., 2005), the wealth of monoamine receptors in this layer suggests a wide control of subcortical activity, including that of brainstem monoamine nuclei. Interestingly, layer V pyramidal neurons projecting to DR and/or VTA are highly sensitive to psychotomimetic drugs used as pharmacological models of schizophrenia, such as non-competitive NMDA-R antagonists and serotonergic hallucinogens. Remarkably, these actions on layer V pyramidal neurons are counteracted by antipsychotic drugs acting on DA and 5-HT receptors (Puig et al., 2003; Bortolozzi et al., 2005, 2007; Díaz-Mataix et al., 2006; Kargieman et al., 2007; Riga et al., 2014) suggesting a correlate of these drug actions with their therapeutic effect. Likewise, the fast antidepressant actions of ketamine are associated to an activation of layer V pyramidal neurons in the mPFC (Li et al., 2010).

Layer VI

Most pyramidal neurons in layer VI of the PFC project to the mediodorsal nucleus of the thalamus (MD), whereas a smaller proportion project to dorsal and ventral striatum and to the lateral hypothalamus (Gabbott et al., 2005). In turn, MD fibers reach layers III–V of the PFC (Kuroda et al., 1998), thus establishing a reciprocal cortico-thalamocortical connectivity and mutual control. Additionally, PFC axons projecting to MD branch to innervate fast-spiking GABA neurons in the thalamic reticular nucleus, which provides feed-forward inhibition to excitatory thalamic nuclei, including MD (Pinault, 2004). The presence of an abundant population of layer VI pyramidal and GABAergic neurons expressing monoamine receptors indicates

that the activity of thalamocortical networks is also modulated by monoamines.

Although layers V and VI are typically considered as "deep layers" and some electrophysiological studies assessing monoamine actions do not discriminate between them, there are substantial differences in the proportions of neurons expressing monoamine receptors (**Figures 4–6**), which supports different actions of the respective monoamines on both layers. Hence, while 5-HT_{1A}-R are also expressed by a large proportion of pyramidal neurons (58–63% in layer VI vs. 52–60% in layer V), 5-HT_{2A}-R were expressed by only 7–10% pyramidal neurons in layer VI, suggesting a predominantly inhibitory role of 5-HT on corticothalamic pathways. In contrast, the proportion of cells expressing 5-HT_{2C}-R was greater than in layer V and greater than that expressing 5-HT_{2A}-R.

Likewise, a remarkable difference exists in regards to catecholamine receptors, with a greater percentage of pyramidal neuros expressing DA D_1-R than in layer V (33–38% vs. 17–23% in layer V) and a much lesser percentage of those expressing α_{1D}-adrenoceptors (4–6% in layer VI vs. 31–48% in layer V) (**Figures 3–6**). Likewise, the proportion of pyramidal neurons expressing α_{1B}-adrenoceptors was lower than in layer V and exhibited a marked negative DV gradient (15% in Cg, 11% in PrL, 4% in IL).

Collectively, these data indicates that cortico-thalamic pathways are strongly modulated by 5-HT_{1A}-R, DA D_1-R and α_{1A}-adrenoceptors.

CONCLUDING REMARKS

The PFC exerts a top-down control of brain activity thanks to its ample and reciprocal connectivity with cortical and subcortical brain structures, with the exception of the basal ganglia, which are connected with the PFC via thalamic nuclei (Groenewegen and Uylings, 2000; Miller and Cohen, 2001; Gabbott et al., 2005). Monoamine receptors in the various PFC layers and subfields are located in a key position to modulate the processing of cognitive and emotional signals by the PFC in physiological conditions (Robbins and Arnsten, 2009). In addition, antidepressant and antipsychotic drugs interact with most monoamine receptors in PFC, a process likely contributing to their therapeutic effects (Artigas, 2010, 2013). These actions involve (i) direct agonist/antagonist effects, as in the case of classical antipsychotic drugs blocking DA D_2-R and D_1-R, or second generation antipsychotic drugs, also targeting 5-HT_{1A}-R, 5-HT_{2A}-R, 5-HT_{2C}-R and α_1-adrenoceptors, or (ii) indirect agonist actions, derived from the blockade of 5-HT and/or NA transporters by antidepressant drugs. Additionally, some antidepressant drugs block monoamine receptors, such as trazodone, mirtazapine, agomelatine, or vortioxetine. The presence of monoamine receptors in all cortical layers indicates that psychoactive drugs control information processing in PFC-based circuits in a complex manner, through the modulation of excitatory inputs onto PFC pyramidal neurons, the control of local microcircuits via receptors located in GABA interneurons, and finally, through the modulation of the pyramidal output to subcortical structures. As an example of this complexity, 5-HT_3-R blockade in layers I–III GABA cells (likely controlling thalamic inputs) enhances the discharge rate of layer V pyramidal neurons projecting to DR and/or VTA (Riga et al., 2016). In other words, 5-HT_3-R located in a relatively small interneuron population modulates the interplay between the thalamic matrix, the PFC and brainstem monoamine cell groups.

Important, currently missing, information for better understanding monoamine function in the PFC would be to define the projection fields of pyramidal neurons expressing one or more receptors (Vázquez-Borsetti et al., 2009; Mocci et al., 2014). This information is relevant for understanding distal actions of drugs targeting monoamine PFC receptors, since an action on PFC receptors may immediately translate into neuronal activity changes in cortical and subcortical structures receiving PFC inputs. It is hoped that novel histological and tracing technologies will help to delineate the precise role of each monoamine receptor in the control of neuronal activity in cortical and subcortical areas, thus improving our understanding of the role of monoamines in PFC function.

AUTHOR CONTRIBUTIONS

FA and NS have planned and designed experiments, analyzed data and write the manuscript. NS performed experiments.

FUNDING

This work was supported by the Spanish Ministry of Economy and Competitiveness (grant number SAF2015-68346), co-financed by European Regional Development Fund (ERDF), EU; Generalitat de Catalunya (grant number 2014-SGR798) and Instituto de Salud Carlos III, Centro de Investigación Biomédica en Red de Salud Mental (CIBERSAM).

ACKNOWLEDGMENT

We thank Verónica Paz for technical support and María Jaramillo for administrative assistance.

REFERENCES

Aloyo, V. J., Berg, K. A., Spampinato, U., Clarke, W. P., and Harvey, J. A. (2009). Current status of inverse agonism at serotonin2A (5-HT2A) and 5-HT2C receptors. *Pharmacol. Ther.* 121, 160–173. doi: 10.1016/j.pharmthera.2008.10.010

Amargós-Bosch, M., Bortolozzi, A., Puig, M. V., Serrats, J., Adell, A., Celada, P., et al. (2004). Co-expression and in vivo interaction of serotonin1A and serotonin2A receptors in pyramidal neurons of prefrontal cortex. *Cereb. Cortex* 14, 281–299. doi: 10.1093/cercor/bhg128

Araneda, R., and Andrade, R. (1991). 5-Hydroxytryptamine2 and 5-hydroxytryptamine1A receptors mediate opposing responses on

membrane excitability in rat association cortex. *Neuroscience* 40, 399–412. doi: 10.1016/0306-4522(91)90128-B

Arnsten, A. F. T. (2009). Stress signalling pathways that impair prefrontal cortex structure and function. *Nat. Rev. Neurosci.* 10, 410–422. doi: 10.1038/nrn2648

Artigas, F. (2010). The prefrontal cortex: a target for antipsychotic drugs. *Acta Psychiatr. Scand.* 121, 11–21. doi: 10.1111/j.1600-0447.2009.01455.x

Artigas, F. (2013). Serotonin receptors involved in antidepressant effects. *Pharmacol. Ther.* 137, 119–131. doi: 10.1016/j.pharmthera.2012.09.006

Aston-Jones, G., and Cohen, J. D. (2005). An integrative theory of locus coeruleus-norepinephrine function: adaptive gain and optimal performance. *Annu. Rev. Neurosci.* 28, 403–450. doi: 10.1146/annurev.neuro.28.061604.135709

Bartrup, J. T., and Newberry, N. R. (1994). 5-HT2A receptor-mediated outward current in C6 glioma cells is mimicked by intracellular IP3 release. *Neuroreport* 5, 1245–1248. doi: 10.1097/00001756-199406020-00022

Bates, J. F., and Goldman-Rakic, P. S. (1993). Prefrontal connections of medial motor areas in the rhesus monkey. *J. Comp. Neurol.* 336, 211–228. doi: 10.1002/cne.903360205

Beaulieu, C. (1993). Numerical data on neocortical neurons in adult rat, with special reference to the GABA population. *Brain Res.* 609, 284–292. doi: 10.1016/0006-8993(93)90884-P

Beique, J. C., Imad, M., Mladenovic, L., Gingrich, J. A., Andrade, R., Béïque, J.-C., et al. (2007). Mechanism of the 5-hydroxytryptamine 2A receptor-mediated facilitation of synaptic activity in prefrontal cortex. *Proc. Natl. Acad. Sci. U.S.A.* 104, 9870–9875. doi: 10.1073/pnas.0700436104

Berg, K. A., Clarke, W. P., Cunningham, K. A., and Spampinato, U. (2008). Fine-tuning serotonin2c receptor function in the brain: molecular and functional implications. *Neuropharmacology* 55, 969–976. doi: 10.1016/j.neuropharm.2008.06.014

Berg, K. A., Maayani, S., Goldfarb, J., Scaramellini, C., Leff, P., and Clarke, W. P. (1998). Effector pathway-dependent relative efficacy at serotonin type 2A and 2C receptors: evidence for agonist-directed trafficking of receptor stimulus. *Mol. Pharmacol.* 54, 94–104. doi: 10.1124/mol.54.1.94

Bortolozzi, A., Díaz-Mataix, L., Scorza, M. C., Celada, P., and Artigas, F. (2005). The activation of 5-HT2A receptors in prefrontal cortex enhances dopaminergic activity. *J. Neurochem.* 95, 1597–1607. doi: 10.1111/j.1471-4159.2005.03485.x

Bortolozzi, A., Diaz-Mataix, L., Toth, M., Celada, P., and Artigas, F. (2007). In vivo actions of aripiprazole on serotonergic and dopaminergic systems in rodent brain. *Psychopharmacology* 191, 745–758. doi: 10.1007/s00213-007-0698-y

Boulougouris, V., and Robbins, T. W. (2010). Enhancement of spatial reversal learning by 5-HT2C receptor antagonism is neuroanatomically specific. *J. Neurosci.* 30, 930–938. doi: 10.1523/JNEUROSCI.4312-09.2010

Brozoski, T., Brown, R., Rosvold, H., and Goldman, P. (1979). Cognitive deficit caused by regional depletion of dopamine in prefrontal cortex of rhesus monkey. *Science* 205, 929–932. doi: 10.1126/science.112679

Buschman, T. J., and Miller, E. K. (2007). Top-down versus bottom-up control of attention in the prefrontal and posterior parietal cortices. *Science* 315, 1860–1862. doi: 10.1126/science.1138071

Calzavara, R., Mailly, P., and Haber, S. N. (2007). Relationship between the corticostriatal terminals from areas 9 and 46, and those from area 8A, dorsal and rostral premotor cortex and area 24c: an anatomical substrate for cognition to action. *Eur. J. Neurosci.* 26, 2005–2024. doi: 10.1111/j.1460-9568.2007.05825.x

Celada, P., Puig, M. V., and Artigas, F. (2013). Serotonin modulation of cortical neurons and networks. *Front. Integr. Neurosci.* 7:25. doi: 10.3389/fnint.2013.00025

Celada, P., Puig, M. V., Casanovas, J. M., Guillazo, G., and Artigas, F. (2001). Control of dorsal raphe serotonergic neurons by the medial prefrontal cortex: involvement of serotonin-1A, GABA A, and glutamate receptors. *J. Neurosci.* 21, 9917–9929.

Chandler, D. J., Gao, W. J., and Waterhouse, B. D. (2014). Heterogeneous organization of the locus coeruleus projections to prefrontal and motor cortices. *Proc. Natl. Acad. Sci. U.S.A.* 111, 6816–6821. doi: 10.1073/pnas.1320827111

Chen, G., Greengard, P., and Yan, Z. (2004). Potentiation of NMDA receptor currents by dopamine D1 receptors in prefrontal cortex. *Proc. Natl. Acad. Sci. U.S.A.* 101, 2596–2600. doi: 10.1073/pnas.0308618100

Claro, E., Fain, J. N., and Picatoste, F. (1993). Noradrenaline stimulation unbalances the phosphoinositide cycle in rat cerebral cortical slices. *J. Neurochem.* 60, 2078–2086. doi: 10.1111/j.1471-4159.1993.tb03492.x

Dalley, J. W., Cardinal, R. N., and Robbins, T. W. (2004). Prefrontal executive and cognitive functions in rodents: neural and neurochemical substrates. *Neurosci. Biobehav. Rev.* 28, 771–784. doi: 10.1016/j.neubiorev.2004.09.006

DeFelipe, J., Arellano, J. I., Mez, A. G., Azmitia, E. C., and Oz, A. M. (2001). Pyramidal cell axons show a local specialization for GABA and 5-HT inputs in monkey and human cerebral cortex. *J. Comp. Neurol.* 433, 148–155. doi: 10.1002/cne.1132

DeFelipe, J., López-Cruz, P. L., Benavides-Piccione, R., Bielza, C., Larrañaga, P., Anderson, S., et al. (2013). New insights into the classification and nomenclature of cortical GABAergic interneurons. *Nat. Rev. Neurosci.* 14, 202–216. doi: 10.1038/nrn3444

Díaz-Mataix, L., Artigas, F., and Celada, P. (2006). Activation of pyramidal cells in rat medial prefrontal cortex projecting to ventral tegmental area by a 5-HT1A receptor agonist. *Eur. Neuropsychopharmacol.* 16, 288–296. doi: 10.1016/j.euroneuro.2005.10.003

Friedman, A., Homma, D., Gibb, L. G., Amemori, K., Rubin, S. J., Hood, A. S., et al. (2016). A corticostriatal path targeting striosomes controls decision-making under conflict. *Cell* 161, 1320–1333. doi: 10.1016/j.cell.2015.04.049.A

Fuchikami, M., Thomas, A., Liu, R., Wohleb, E. S., Land, B. B., DiLeone, R. J., et al. (2015). Optogenetic stimulation of infralimbic PFC reproduces ketamine's rapid and sustained antidepressant actions. *Proc. Natl. Acad. Sci. U.S.A.* 112, 8106–8111. doi: 10.1073/pnas.1414728112

Funahashi, S., Bruce, C. J., and Goldman-Rakic, P. S. (1989). Mnemonic coding of visual space in the monkey's dorsolateral prefrontal cortex. *J. Neurophysiol.* 61, 331–349.

Fuster, J. M. (1973). Unit activity in prefrontal cortex during delayed-response performance: neuronal correlates of transient memory. *J. Neurophysiol.* 36, 61–78.

Fuster, J. M. (2001). The prefrontal cortex - An update: time is of the essence. *Neuron* 30, 319–333. doi: 10.1016/S0896-6273(01)00285-9

Fuster, J. M. (2008). *The Prefrontal Cortex*. Amsterdam: Elsevier.

Gabbott, P. L. A., Warner, T. A., Jays, P. R. L., Salway, P., and Busby, S. J. (2005). Prefrontal cortex in the rat: projections to subcortical autonomic, motor, and limbic centers. *J. Comp. Neurol.* 492, 145–177. doi: 10.1002/cne.20738

Gasull-Camós, J., Tarrés-Gatius, M., Artigas, F., and Castañé, A. (2017). Glial GLT-1 blockade in infralimbic cortex as a new strategy to evoke rapid antidepressant-like effects in rats. *Transl. Psychiatry* 7:e1038. doi: 10.1038/tp.2017.7

Groenewegen, H. J., and Uylings, H. B. M. (2000). The prefrontal cortex and the integration of sensory, limbic and autonomic information. *Prog. Brain Res.* 126, 3–28. doi: 10.1016/S0079-6123(00)26003-2

Hajós, M., Richards, C. D., Székely, A. D., and Sharp, T. (1998). An electrophysiological and neuroanatomical study of the medial prefrontal cortical projection to the midbrain raphe nuclei in the rat. *Neuroscience* 87, 95–108. doi: 10.1016/S0306-4522(98)00157-2

Heisler, L. K., Zhou, L., Bajwa, P., Hsu, J., and Tecott, L. H. (2007). Serotonin 5-HT2C receptors regulate anxiety-like behavior. *Genes Brain Behav.* 6, 491–496. doi: 10.1111/j.1601-183X.2007.00316.x

Herculano-Houzel, S., Watson, C., and Paxinos, G. (2013). Distribution of neurons in functional areas of the mouse cerebral cortex reveals quantitatively different cortical zones. *Front. Neuroanat.* 7:35. doi: 10.3389/fnana.2013.00035

Jodo, E., Chiang, C., and Aston-Jones, G. (1998). Potent excitatory influence of prefrontal cortex activity on noradrenergic locus coeruleus neurons. *Neuroscience* 83, 63–79. doi: 10.1016/S0306-4522(97)00372-2

Jones, E. G. (2001). The thalamic matrix and thalamocortical synchrony. *Trends Neurosci.* 24, 595–601. doi: 10.1016/S0166-2236(00)01922-6

Jueptner, M., Frith, C. D., Brooks, D. J., Frackowiak, R. S. J., Passingham, R. E., Ropele, S., et al. (1997a). Anatomy of motor learning. II. Subcortical structures and learning by trial and error. *J. Neurophysiol.* 77, 1325–1337.

Jueptner, M., Stephan, K. M., Frith, C. D., Brooks, D. J., Frackowiak, R. S., and Passingham, R. E. (1997b). Anatomy of motor learning. I. Frontal cortex and attention to action. *J. Neurophysiol.* 77, 1313–1324.

Kargieman, L., Santana, N., Mengod, G., Celada, P., and Artigas, F. (2007). Antipsychotic drugs reverse the disruption in prefrontal cortex function produced by NMDA receptor blockade with phencyclidine. *Proc. Natl. Acad. Sci. U.S.A.* 104, 14843–14848. doi: 10.1073/pnas.0704848104

Kawaguchi, Y., and Kondo, S. (2002). Parvalbumin, somatostatin and cholecystokinin as chemical markers for specific GABAergic interneuron types in the rat frontal cortex. *J. Neurocytol.* 31, 277–287. doi: 10.1023/A:1024126110356

Kuroda, M., Yokofujita, J., and Murakami, K. (1998). An ultrastructural study of the neural circuit between the prefrontal cortex and the mediodorsal nucleus of the thalamus. *Prog. Neurobiol.* 54, 417–458. doi: 10.1016/S0301-0082(97)00070-1

Lee, S., Hjerling-Leffler, J., Zagha, E., Fishell, G., and Rudy, B. (2010). The largest group of superficial neocortical GABAergic interneurons expresses ionotropic serotonin receptors. *J. Neurosci.* 30, 16796–16808. doi: 10.1523/JNEUROSCI.1869-10.2010

Li, N., Lee, B., Liu, R.-J., Banasr, M., Dwyer, J. M., Iwata, M., et al. (2010). mTOR-dependent synapse formation underlies the rapid antidepressant effects of NMDA antagonists. *Science* 329, 959–964. doi: 10.1126/science.1190287

Lu, M. T., Preston, J. B., and Strick, P. L. (1994). Interconnections between the prefrontal cortex and the premotor areas in the frontal lobe. *J. Comp. Neurol.* 341, 375–392. doi: 10.1002/cne.903410308

Luo, F., Tang, H., and Cheng, Z.-Y. (2015). Stimulation of α1-adrenoceptors facilitates GABAergic transmission onto pyramidal neurons in the medial prefrontal cortex. *Neuroscience* 300, 63–74. doi: 10.1016/j.neuroscience.2015.04.070

Marek, G., and Aghajanian, G. (1999). 5-HT2A receptor or alpha1-adrenoceptor activation induces excitatory postsynaptic currents in layer V pyramidal cells of the medial prefrontal cortex. *Eur. J. Pharmacol.* 367, 197–206. doi: 10.1016/S0014-2999(98)00945-5

Martin-Ruiz, R., Ugedo, L., Honrubia, M. A., Mengod, G., and Artigas, F. (2001). Control of serotonergic neurons in rat brain by dopaminergic receptors outside the dorsal raphe nucleus. *J. Neurochem.* 77, 762–775. doi: 10.1046/j.1471-4159.2001.00275.x

Mayberg, H. S., Lozano, A. M., Voon, V., McNeely, H. E., Seminowicz, D., Hamani, C., et al. (2005). Deep brain stimulation for treatment-resistant depression. *Neuron* 45, 651–660. doi: 10.1016/j.neuron.2005.02.014

Miller, E. K. (2000). The prefrontal cortex and cognitive control. *Nat. Rev. Neurosci.* 1, 59–65. doi: 10.1038/35036228

Miller, E. K., and Cohen, J. D. (2001). An integrative theory of prefrontal cortex function. *Annu. Rev. Neurosci.* 24, 167–202. doi: 10.1146/annurev.neuro.24.1.167

Miller, E. K., Erickson, C. A., and Desimone, R. (1996). Neural mechanisms of visual working memory in prefrontal cortex of the macaque. *J. Neurosci.* 16, 5154–5167.

Mocci, G., Jiménez-Sánchez, L., Adell, A., Cortés, R., and Artigas, F. (2014). Expression of 5-HT2A receptors in prefrontal cortex pyramidal neurons projecting to nucleus accumbens. Potential relevance for atypical antipsychotic action. *Neuropharmacology* 79, 49–58. doi: 10.1016/j.neuropharm.2013.10.021

O'Neil, R. T., and Emeson, R. B. (2012). Quantitative analysis of 5HT(2C) receptor RNA editing patterns in psychiatric disorders. *Neurobiol. Dis.* 45, 8–13. doi: 10.1016/j.nbd.2011.08.026

Paxinos, G., and Watson, C. (2005). *The Rat Brain in Stereotaxic Coordinates*. San Diego, CA: Elsevier Academic Press.

Pennanen, L., van der Hart, M., Yu, L., and Tecott, L. H. (2013). Impact of serotonin (5-HT)2C receptors on executive control processes. *Neuropsychopharmacology* 38, 957–967. doi: 10.1038/npp.2012.258

Pinault, D. (2004). The thalamic reticular nucleus: structure, function and concept. *Brain Res. Brain Res. Rev.* 46, 1–31. doi: 10.1016/j.brainresrev.2004.04.008

Puig, M. V., Artigas, F., and Celada, P. (2005). Modulation of the activity of pyramidal neurons in rat prefrontal cortex by raphe stimulation in vivo: involvement of serotonin and GABA. *Cereb. Cortex* 15, 1–14. doi: 10.1093/cercor/bhh104

Puig, M. V., Celada, P., Díaz-Mataix, L., and Artigas, F. (2003). In vivo modulation of the activity of pyramidal neurons in the rat medial prefrontal cortex by 5-HT2A receptors: relationship to thalamocortical afferents. *Cereb. Cortex* 13, 870–882. doi: 10.1093/cercor/13.8.870

Puig, M. V., Santana, N., Celada, P., Mengod, G., and Artigas, F. (2004). In vivo excitation of GABA interneurons in the medial prefrontal cortex through 5-HT3 receptors. *Cereb. Cortex* 14, 1365–1375. doi: 10.1093/cercor/bhh097

Puig, M. V., Watakabe, A., Ushimaru, M., Yamamori, T., and Kawaguchi, Y. (2010). Serotonin modulates fast-spiking interneuron and synchronous activity in the rat prefrontal cortex through 5-HT1A and 5-HT2A receptors. *J. Neurosci.* 30, 2211–2222. doi: 10.1523/JNEUROSCI.3335-09.2010

Puigdemont, D., Pérez-Egea, R., Portella, M. J., Molet, J., de Diego-Adeliño, J., Gironell, A., et al. (2011). Deep brain stimulation of the subcallosal cingulate gyrus: further evidence in treatment-resistant major depression. *Int. J. Neuropsychopharmacol.* 15, 121–133. doi: 10.1017/S1461145711001088

Riga, M. S., Sánchez, C., Celada, P., and Artigas, F. (2016). Involvement of 5-HT3 receptors in the action of vortioxetine in rat brain: focus on glutamatergic and GABAergic neurotransmission. *Neuropharmacology* 108, 73–81. doi: 10.1016/j.neuropharm.2016.04.023

Riga, M. S., Soria, G., Tudela, R., Artigas, F., and Celada, P. (2014). The natural hallucinogen 5-MeO-DMT, component of Ayahuasca, disrupts cortical function in rats: reversal by antipsychotic drugs. *Int. J. Neuropsychopharmacol.* 17, 1269–1282. doi: 10.1017/S1461145714000261

Robbins, T. W., and Arnsten, A. F. (2009). The neuropsychopharmacology of fronto-executive function: monoaminergic modulation. *Annu. Rev. Neurosci.* 32, 267–287. doi: 10.1146/annurev.neuro.051508.135535

Romo, R., Brody, C. D., Hernández, A., and Lemus, L. (1999). Neuronal correlates of parametric working memory in the prefrontal cortex. *Nature* 399, 470–473. doi: 10.1038/20939

Sanchez, C., Asin, K. E., and Artigas, F. (2015). Vortioxetine, a novel antidepressant with multimodal activity: review of preclinical and clinical data. *Pharmacol. Ther.* 145, 43–47. doi: 10.1016/j.pharmthera.2014.07.001

Santana, N., and Artigas, F. (2017). Expression of serotonin2C receptors in pyramidal and GABAergic neurons of rat prefrontal cortex: a comparison with striatum. *Cereb. Cortex* 27, 3125–3139. doi: 10.1093/cercor/bhw148

Santana, N., Bortolozzi, A., Serrats, J., Mengod, G., and Artigas, F. (2004). Expression of serotonin1A and serotonin2A receptors in pyramidal and GABAergic neurons of the rat prefrontal cortex. *Cereb. Cortex* 14, 1100–1109. doi: 10.1093/cercor/bhh070

Santana, N., Mengod, G., and Artigas, F. (2009). Quantitative analysis of the expression of dopamine D1 and D2 receptors in pyramidal and GABAergic neurons of the rat prefrontal cortex. *Cereb. Cortex* 19, 849–860. doi: 10.1093/cercor/bhn134

Santana, N., Mengod, G., and Artigas, F. (2013). Expression of α1-adrenergic receptors in rat prefrontal cortex: cellular co-localization with 5-HT2A receptors. *Int. J. Neuropsychopharmacol.* 16, 1139–1151. doi: 10.1017/S1461145712001083

Sara, S. J., and Hervé-Minvielle, A. (1995). Inhibitory influence of frontal cortex on locus coeruleus neurons. *Proc. Natl. Acad. Sci. U.S.A.* 92, 6032–6036. doi: 10.1073/pnas.92.13.6032

Sawaguchi, T., and Goldman-Rakic, P. S. (1991). D1 dopamine receptors in prefrontal cortex: involvement in working memory. *Science* 251, 947–950. doi: 10.1126/science.1825731

Seamans, J. K., and Yang, C. R. (2004). The principal features and mechanisms of dopamine modulation in the prefrontal cortex. *Prog. Neurobiol.* 74, 1–58. doi: 10.1016/j.pneurobio.2004.05.006

Steinbusch, H. W. M. (1981). Distribution of serotonin-immunoreactivity in the central nervous system of the rat-Cell bodies and terminals. *Neuroscience* 6, 557–618. doi: 10.1016/0306-4522(81)90146-9

Swanson, L. (2004). *Brain Maps: Structure of the Rat Brain*, 3rd Edn. Amsterdam: Elsevier.

Thierry, A. M., Deniau, J. M., Chevalier, G., Ferron, A., and Glowinski, J. (1983). An electrophysiological analysis of some afferent and efferent pathways of the rat prefrontal cortex. *Prog. Brain Res.* 58, 257–261. doi: 10.1016/S0079-6123(08)60027-8

Thierry, A. M., Deniau, J. M., and Feger, J. (1979). Effects of stimulation of the frontal cortex on identified output VMT cells in the rat. *Neurosci. Lett.* 15, 102–107. doi: 10.1016/0304-3940(79)96097-X

Tseng, K. Y., and O'Donnell, P. (2007). D2 dopamine receptors recruit a GABA component for their attenuation of excitatory synaptic transmission in the adult rat prefrontal cortex. *Synapse* 61, 843–850. doi: 10.1002/syn.20432

Uylings, H. B. M., Groenewegen, H. J., and Kolb, B. (2003). Do rats have a prefrontal cortex? *Behav. Brain Res.* 146, 3–17. doi: 10.1016/j.bbr.2003.09.028

Van Eden, C. G., Hoorneman, E. M., Buijs, R. M., Matthijssen, M. A., Geffard, M., and Uylings, H. B. (1987). Immunocytochemical localization

of dopamine in the prefrontal cortex of the rat at the light and electron microscopical level. *Neuroscience* 22, 849–862. doi: 10.1016/0306-4522(87)92964-2

Varga, V., Losonczy, A., Zemelman, B. V., Borhegyi, Z., Nyiri, G., Domonkos, A., et al. (2009). Fast synaptic subcortical control of hippocampal circuits. *Science* 326, 449–453. doi: 10.1126/science.1178307

Vázquez-Borsetti, P., Cortés, R., and Artigas, F. (2009). Pyramidal neurons in rat prefrontal cortex projecting to ventral tegmental area and dorsal raphe nucleus express 5-HT2A receptors. *Cereb. Cortex* 19, 1678–1686. doi: 10.1093/cercor/bhn204

Vijayraghavan, S., Wang, M., Birnbaum, S. G., Williams, G. V., and Arnsten, A. F. T. (2007). Inverted-U dopamine D1 receptor actions on prefrontal neurons engaged in working memory. *Nat. Neurosci.* 10, 376–384. doi: 10.1038/nn1846

Werry, T. D., Loiacono, R., Sexton, P. M., and Christopoulos, A. (2008). RNA editing of the serotonin 5HT2C receptor and its effects on cell signalling, pharmacology and brain function. *Pharmacol. Ther.* 119, 7–23. doi: 10.1016/j.pharmthera.2008.03.012

Williams, G. V., and Goldman-Rakic, P. S. (1995). Modulation of memory fields by dopamine Dl receptors in prefrontal cortex. *Nature* 376, 572–575. doi: 10.1038/376572a0

Zarate, C. A., Singh, J. B., Carlson, P. J., Brutsche, N. E., Ameli, R., Luckenbaugh, D. A., et al. (2006). A randomized trial of an N-methyl-D-aspartate antagonist in treatment-resistant major depression. *Arch. Gen. Psychiatry* 63:856. doi: 10.1001/archpsyc.63.8.856

Conflict of Interest Statement: The authors declare that the research was conducted in the absence of any commercial or financial relationships that could be construed as a potential conflict of interest.

frontiers in Neuroanatomy

ORIGINAL RESEARCH
published: 20 September 2017
doi: 10.3389/fnana.2017.00078

Multiple Transmitter Receptors in Regions and Layers of the Human Cerebral Cortex

Karl Zilles[1,2]* *and Nicola Palomero-Gallagher*[1,2]

[1]*Research Centre Jülich, Institute of Neuroscience and Medicine (INM-1), Jülich, Germany,* [2]*Department of Psychiatry, Psychotherapy, and Psychosomatics, Medical Faculty, RWTH Aachen, and JARA—Translational Brain Medicine, Aachen, Germany*

We measured the densities (fmol/mg protein) of 15 different receptors of various transmitter systems in the supragranular, granular and infragranular strata of 44 areas of visual, somatosensory, auditory and multimodal association systems of the human cerebral cortex. Receptor densities were obtained after labeling of the receptors using quantitative *in vitro* receptor autoradiography in human postmortem brains. The mean density of each receptor type over all cortical layers and of each of the three major strata varies between cortical regions. In a *single* cortical area, the multi-receptor fingerprints of its strata (i.e., polar plots, each visualizing the densities of multiple *different* receptor types in supragranular, granular or infragranular layers of the *same* cortical area) differ in shape and size indicating regional and laminar specific balances between the receptors. Furthermore, the three strata are clearly segregated into well definable clusters by their receptor fingerprints. Fingerprints of *different* cortical areas systematically vary between functional networks, and with the hierarchical levels within sensory systems. Primary sensory areas are clearly separated from all other cortical areas particularly by their very high muscarinic M_2 and nicotinic $\alpha_4\beta_2$ receptor densities, and to a lesser degree also by noradrenergic α_2 and serotonergic 5-HT_2 receptors. Early visual areas of the dorsal and ventral streams are segregated by their multi-receptor fingerprints. The results are discussed on the background of functional segregation, cortical hierarchies, microstructural types, and the horizontal (layers) and vertical (columns) organization in the cerebral cortex. We conclude that a cortical column is composed of segments, which can be assigned to the cortical strata. The segments differ by their patterns of multi-receptor balances, indicating different layer-specific signal processing mechanisms. Additionally, *the differences between the strata-and area-specific fingerprints* of the 44 areas reflect the segregation of the cerebral cortex into functionally and topographically definable groups of cortical areas (visual, auditory, somatosensory, limbic, motor), and reveals their hierarchical position (primary and unimodal (early) sensory to higher sensory and finally to multimodal association areas).

Highlights

- Densities of transmitter receptors vary between areas of human cerebral cortex.
- Multi-receptor fingerprints segregate cortical layers.

OPEN ACCESS

Edited by:
Kathleen S. Rockland, Boston University School of Medicine, United States

Reviewed by:
Anita Disney, Vanderbilt University, United States
Floris G. Wouterlood, VU University Amsterdam, Netherlands

***Correspondence:**
Karl Zilles
k.zilles@fz-juelich.de

Received: *07 July 2017*
Accepted: *24 August 2017*
Published: *20 September 2017*

Citation:
Zilles K and Palomero-Gallagher N (2017) Multiple Transmitter Receptors in Regions and Layers of the Human Cerebral Cortex. Front. Neuroanat. 11:78. doi: 10.3389/fnana.2017.00078

- The densities of all examined receptor types together reach highest values in the supragranular stratum of all areas.
- The lowest values are found in the infragranular stratum.
- Multi-receptor fingerprints of entire areas and their layers segregate functional systems
- Cortical types (primary sensory, motor, multimodal association) differ in their receptor fingerprints.

Keywords: visual cortex, ventral stream, dorsal stream, somatosensory cortex, supragranular layers, granular layer, infragranular layers, multimodal association cortex

INTRODUCTION

Cortical layers—as defined in classical architectonic studies (Brodmann, 1909; von Economo and Koskinas, 1925)—differ by cell types (Markram et al., 2004; Xu and Callaway, 2009; DeFelipe et al., 2013; Jiang et al., 2015), number or packing density of cells (von Economo and Koskinas, 1925; Haug et al., 1984; Zilles et al., 1986; Meyer et al., 2010), density of myelinated fibers (Vogt and Vogt, 1919; Annese et al., 2004), and densities of various transmitter receptors (e.g., Cortés et al., 1986, 1987; Hoyer et al., 1986a,b; Pazos et al., 1987a,b; Jansen et al., 1989; Scheperjans et al., 2005a; Eickhoff et al., 2008; Amunts et al., 2010; Vogt et al., 2013; Zilles and Palomero-Gallagher, 2017). For recent reviews see Nieuwenhuys (2013) and Zilles et al. (2015b).

Cortical layers also differ by their input and output, as well as by the preferred direction of connections with other cortical areas (Rockland and Pandya, 1979; Felleman and Van Essen, 1991; Rockland, 1997, 2015; Markov and Kennedy, 2013; Markov et al., 2014). The feedforward connection from V1 to V2 has cells of origin mainly in layers III and IVb (Kennedy and Bullier, 1985; Sincich et al., 2010). Cells which give rise to feedback connections are typically distributed over several cortical layers and are found in the supragranular layers II to upper layer III, and the infragranular layer VI. However, the specific differentiation into layers in V1, and the organization of functionally diverse visual input (direction, color, shape) makes V1 to an example which cannot be generalized for the entire cortex. Although most of the source neurons of feedforward pathways are present in the supragranular layers and terminate in the same layers of the target region, the source neurons of feedback pathways are found in the infragranular layers, but terminate in both supra- and infragranular layers (Rockland and Van Hoesen, 1994; Markov et al., 2014). Thus, a single cortical layer does not exclusively contain feedforward or feedback neurons; instead they are found in varying proportions in both of these strata (Barone et al., 2000).

Also important for the present analysis of receptor fingerprints is the location of the terminal fields of connections which build most of the synapses, and thus must contain most of the receptors required for signal processing. Cortico-cortical neurons of the supragranular layers extend their apical dendrites up to layer I, where they form tufts, whereas not all of the infragranular neurons reach layer I with their apical dendrites, but have most of their dendritic arborizations in supragranular layers (Lund et al., 1981; Katz, 1987; Hübener et al., 1990; Mohan et al., 2015). Layer IV neurons receive most of their input from thalamo-cortical connections. Since transmitter receptors are key molecules of signal transmission, we hypothesized that the distinct regional and laminar distribution patterns of multiple transmitter receptors may also contribute to a better understanding of connectivity. It is hitherto largely unknown, whether the regional and laminar density of transmitter receptors and the locally distinct balances between the densities of multiple receptor types (regional and laminar receptor fingerprints) reflect hierarchies of cortical areas, and also may provide insight into principle rules of cortical architecture and connectivity. It is also unknown whether the receptor fingerprints of the three major cortical strata studied here are similar, or each of them exhibits distinct patterns. Therefore, densities of 15 different receptor types are studied in the supragranular, granular and infragranular layers of 44 human visual, somatosensory, auditory and multimodal association areas. The relatively large number of receptors and cortical areas enables the detection of probably general rules valid for the entire cerebral cortex.

MATERIALS AND METHODS

Brains of three donors without any record of neurological or psychiatric diseases or of long-term drug treatment (age range: 72–77 years; 2 males, 1 female) were removed at autopsy. Subjects had given written consent before death and/or had been included in the body donor program of the Department of Anatomy, University of Düsseldorf, Germany, which also requires written consent by the donor. All procedures complied with the requirements defined by the local ethical committee. Post mortem delay before deep freezing was between 8 h and 18 h. Causes of death were cardiac arrest, lung edema, and myocardial infarction. After having separated each hemisphere into approximately 3 cm thick slabs, the slabs were shock frozen in isopentane at −40°C and stored at −80°C in airtight plastic bags until further processing. Thus, brain tissue was not treated with any chemical fixation substances. The total post mortem delay, including the deep freezing step, varied between 8 h and 18 h.

The unfixed frozen slabs were serially sectioned in the coronal plane (section thickness 20 μm) with a large scale cryostat microtome. Alternating sections were processed for quantitative *in vitro* receptor autoradiography, or stained for the visualization of cell bodies (Merker, 1983) or of myelin

(Gallyas, 1979) using silver staining methods. Fifteen different receptors for glutamate (AMPA, NMDA, kainate), GABA ($GABA_A$, $GABA_A$ benzodiazepine binding sites [$GABA_A$/BZ], $GABA_B$), acetylcholine (muscarinic M_1, M_2, M_3, nicotinic $\alpha_4\beta_2$), noradrenaline (α_1, α_2), serotonin (5-HT_{1A}, 5-HT_2), and dopamine (D_1) were identified using tritium-labeled ligands according to previously published receptor protocols (Zilles et al., 2002a,b; Graebenitz et al., 2011; Palomero-Gallagher and Zilles, 2017b) which are summarized in Supplementary Table S1. In short, sections were rehydrated during the pre-incubation, and endogenous substances which could block the binding site for the tritiated receptor ligands were removed. Sections were then incubated in buffer solutions containing the receptor-specific tritiated ligand (in nM concentrations), or the tritiated ligand plus a non-labeled specific displacer (in mM concentrations). Incubation with the labeled ligand alone demonstrates total binding, whereas incubation with the tritiated ligand and the displacer reveals the non-specific binding. Specific binding can be calculated as the difference between total and non-specific binding. Since for the experimental protocols used here non-specific binding only amounted to 95% of total binding in all cases, we consider autoradiographs visualizing total binding to also be representative for the specific binding of the ligand in question.

The labeled sections were exposed against tritium-sensitive films (Hyperfilm, Amersham, Braunschweig, Germany) together with plastic (Microscales®, Amersham) or brain tissue scales (with a known protein density) containing step-wise increasing radioactivity concentrations. Protein content in the homogenate used to create the brain tissue scales had previously been determined by means of the Lowry method (Lowry et al., 1951), and radioactivity concentrations had been measured by liquid scintillation. The resulting autoradiographs were digitized by means of an image acquisition and processing system Axiovision (Zeiss, Germany) for subsequent densitometric analysis (Zilles et al., 2002b; Palomero-Gallagher and Zilles, 2017b). The relationship between the gray value of a pixel in the digitized autoradiograph and the receptor binding site density was defined in two steps: first, the gray value images of the co-exposed scales were used to compute a calibration curve by non-linear, least-squares fitting, thus defining the relationship between gray values in the autoradiographs and concentrations of radioactivity. Then, these concentrations of radioactivity were corrected to account for experimental conditions (e.g., specific activity, dissociation constant and free concentration of the ligand during incubation) by means of formula 1:

$$C_b = \frac{R}{E \cdot B \cdot W_b \cdot S_a} \cdot \frac{K_D + L}{L} \quad (1)$$

where R is the concentration of radioactivity in counts per minute (cpm), E is the efficiency of the scintillation counter (depends on the actual counter), B is a constant representing the number of decays per unit of time and radioactivity (Ci/min), W_b the protein weight of a standard (mg), S_a the specific activity of the ligand (Ci/mmol), K_D the dissociation constant of the ligand (nM), and L the free concentration of the ligand during incubation (nM). Thus, the gray value of each pixel in a digitized autoradiograph, which can be color coded for visualization purposes, codes for a receptor concentration per unit protein (B_{max}, in fmol/mg protein) at saturation of ligand-receptor complexes.

Equidistant receptor profiles oriented vertically to the cortical surface were extracted by means of a minimum length algorithm from the linearized autoradiographs (Schleicher et al., 2000). Special attention was given to collect the profiles at sites where the cortex is not obliquely or tangentially sectioned. These profiles quantify the receptor density from the pial surface to the border between layer VI and the white matter, and were obtained from cytoarchitectonically defined regions. These receptor profiles were subdivided into three strata representing the supragranular (layers I–III), granular (layer IV) and infragranular (layers V–VI) layers by overlaying the laminar borders visible in the neighboring cell body-stained sections (cytoarchitectonic definition of the laminar borders). Since the motor cortex (areas 4 and 6) does not have a clearly recognizable granular layer (layer IV, Brodmann, 1909; von Economo and Koskinas, 1925), but the typical cells of layer IV have been demonstrated at the border region between layers III and V (García-Cabezas and Barbas, 2014; Barbas and García-Cabezas, 2015), we tentatively defined layer IV of areas 4 and 6 as stripe with a thickness of 3% of the total cortical depth below the lower border of layer III. A 3% thickness for layer IV is an estimate derived from the thickness of this layer in the rostrally adjoining prefrontal cortex (von Economo and Koskinas, 1925). The surface defined beneath a receptor profile, or beneath the discrete sectors defined by the position of borders between strata, can be computed to yield the absolute binding site densities for the entire cortical depth (mean density over all layers) or for the each of the three strata in each particular area. Differential shrinkage between autoradiographs and neighboring silver-stained sections does not play a role, since we projected the cell-body (silver) stained section onto the images of the different receptor autoradiographs by means of a microscope equipped with a drawing tube. Thus, we could control the precise spatial matching of the autoradiographs and the histologically stained sections.

We examined laminar distributions of 15 different receptors in 44 iso- and periallocortical areas (**Figure 1**). Regions were defined based on the description by Brodmann (1909), or the JuBrain Atlas (Amunts and Zilles, 2015). In detail, the cortical areas were described in the following publications:

- Isocortical prefrontal areas 11, 8, 9, 10L, 10M, 46 and 47 (Brodmann, 1909),
- 4 and 6 (primary motor and premotor cortices; Brodmann, 1909),
- 3b, 1, 2, and 3a (primary somatosensory cortex; Brodmann, 1909; Jones, 1986; Geyer et al., 1999; Grefkes et al., 2001),
- V1 (primary visual cortex, cytoarchitectonical area 17; Brodmann, 1909; Amunts et al., 2000),
- Dorsal (V2d) and ventral (V2v) parts of the secondary visual cortex (cytoarchitectonical area 18; Brodmann, 1909; Amunts et al., 2000),

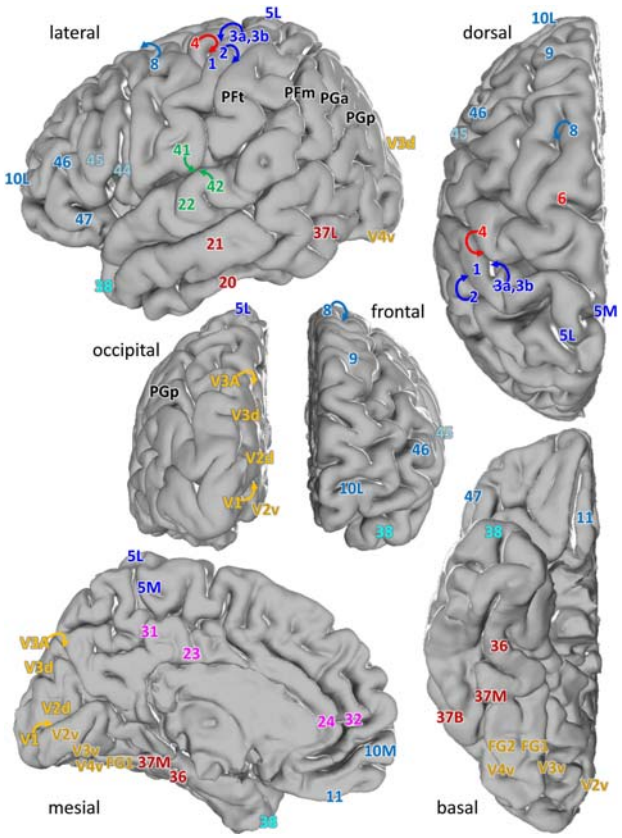

FIGURE 1 | Location of the analyzed cortical regions in the single subject template brain of the Montreal Neurological Institute. Location of areas: 10M, 10L from Bludau et al. (2014); 24, 32 from Palomero-Gallagher et al. (2009), 44 and 45 from Amunts et al. (1999), 1, 2, 3a, 3b, 4, 5L and 5M from Geyer et al. (1996,1999), Grefkes et al. (2001) and Scheperjans et al. (2008), PFm, PFt, PGa, PGp from Caspers et al. (2006), 41, 42 from Morosan et al. (2001, 2005), V1, V2 from Amunts et al. (2000), V3A, V3d, V3v, V4v from Rottschy et al. (2007) and Kujovic et al. (2013), FG1, FG2 from Caspers J. et al. (2013) and of all other areas from Brodmann (1909).

- V3d, V3A, V3v, V4v, FG1 and FG2 (higher visual areas, cyto- and receptorarchitectonically defined areas hOc3d, hOc4d, hOc3v, hOc4v, FG1 and FG2, respectively; Rottschy et al., 2007; Caspers J. et al., 2013; Kujovic et al., 2013; Caspers et al., 2015),
- 44 and 45 (receptorarchitectonically defined ventral and anterior portions of Brodmann's areas 44 (44v) and 45 (45a) in Broca's region; Amunts et al., 2010),
- superior parietal areas 5L and 5M (cyto- and receptorarchitectonically identified areas of the higher unimodal somatosensory cortex; Scheperjans et al., 2005b, 2008),
- inferior parietal areas PFt, PFm, PGa, and PGp (cyto- and receptorarchitectonically defined; Caspers et al., 2006; Caspers S. et al., 2013),
- primary and higher unimodal auditory areas 41, 42, and 22 (cytoarchitectonically defined Te1, Te2 and 22; Morosan et al., 2001, 2005),
- lateral, medial and basal portions of the parieto-temporo-occipital regtion (37L, 37M and 37B, respective parts of area 37; Brodmann, 1909),
- multimodal temporal areas 20, 21, 36 and 38 (Brodmann, 1909),
- periarchicortical cingulate area 24 and isocortical cingulate areas 23, 31 and 32 (Brodmann, 1909; Palomero-Gallagher et al., 2008).

Analysis of the region-specific balance between the densities of multiple receptors in a single cortical area prompted the introduction of the term receptor fingerprint (Zilles et al., 2002a). The size of a fingerprint is given by the area of the polar coordinate graph and the actual shape of a fingerprint depends on the contribution by the absolute density of each receptor type to the multi-receptor fingerprint. The shape reflects the balance between the different receptor types in each area. For comparison of fingerprints between different cortical areas, the sequence of receptors around the polar graph and the scaling of absolute receptor densities must be identical in each cortical area. Multivariate analyses of the multi-receptor fingerprints were conducted to visualize putative clusters of areas and strata according to the degree of (dis)similarity of their fingerprints using the Matlab Statistics Toolbox (MatLab R2009a; Mathworks Inc., Natick, MA, USA), in house R-scripts and Systat (Systat 13; Systat Software Inc., Chicago, IL, USA). In these analyses, receptor fingerprints were treated as feature vectors describing the balance between all receptors studied here in a defined cortical area or its strata. Before each analysis, densities were normalized by computing z-scores for each receptor type separately, thus ensuring an equal weighting of each receptor without eliminating relative differences in receptor densities among areas or each of their three strata. Hierarchical cluster analyses were performed as previously described (Palomero-Gallagher et al., 2009) using the Euclidean distance as a measure of (dis)similarity and the Ward linkage algorithm as the linkage method. Euclidean distances were chosen because they take both the differences in size and in shape of receptor fingerprints into account, and in combination with the Ward linkage yielded the maximum cophenetic correlation coefficient as compared to any combination of alternative dissimilarity measurement and linkage methods. The number of clusters in the dendrograms was defined using k-means clustering. A multidimensional scaling analysis was carried out as described previously (Sherwood et al., 2004) using the Kruskal stress scaling method to reduce the 15-dimensional space resulting from the analysis of 15 different receptors into two dimensions for graphical representation of the Euclidean distances between the stratum-specific fingerprints of cortical areas.

To determine whether the density (over all layers) of each receptor type separately was homogeneously or not homogeneously distributed over the 44 areas, ANOVA tests were carried out and p values were Bonferroni corrected for multiple comparisons (15 receptor types). Threshold was set at $p \leq 0.05$. Subsequently, one-sample t-tests were carried out for

each receptor type to determine whether its density in a given area differed significantly from the mean density of that receptor over all examined areas (expected value). Since these tests were only carried out for the receptor types for which the ANOVA was found to be significant, p values (threshold $p \leq 0.05$) of the one-sample t-tests must not corrected for multiple testing. The same procedure was applied to densities measured in each of the three strata.

For the question whether the 44 areas significantly differed in their receptor fingerprints, a discriminant analysis was carried with "area" as a grouping factor. This enables the determination of homogeneity or inhomogeneity of the fingerprints between areas. Since the discriminant analysis over all areas indicated a highly significant inhomogeneity of the fingerprints between the areas ($p < 0.000$), a pairwise comparison between all areas was also performed. The p values of these subsequent discriminant analyses were not corrected for multiple comparisons, because the Omnibus test was significant and the subsequent tests were performed as *post hoc* tests. This procedure was carried out for the fingerprints of the mean densities over all layers as well as for those of each of the three strata.

RESULTS

Transmitter Receptors Are Heterogeneously Distributed Over Regions and Layers in the Human Cerebral Cortex

The color coded images of receptor densities give a first impression of their heterogeneous regional and laminar receptor distribution (**Figure 2**). By comparison with neighboring cell body stained sections, the precise upper and lower limits of the cerebral cortex and the borders between layers were determined (**Figure 2**), and then used to define the borders of supragranular, granular and infragranular strata in the receptor profiles.

The regional densities (fmol/mg protein) of 15 different transmitter receptors for glutamate, GABA, acetylcholine, dopamine, noradrenaline and serotonin were measured in the three strata (supragranular, granular and infragranular strata)

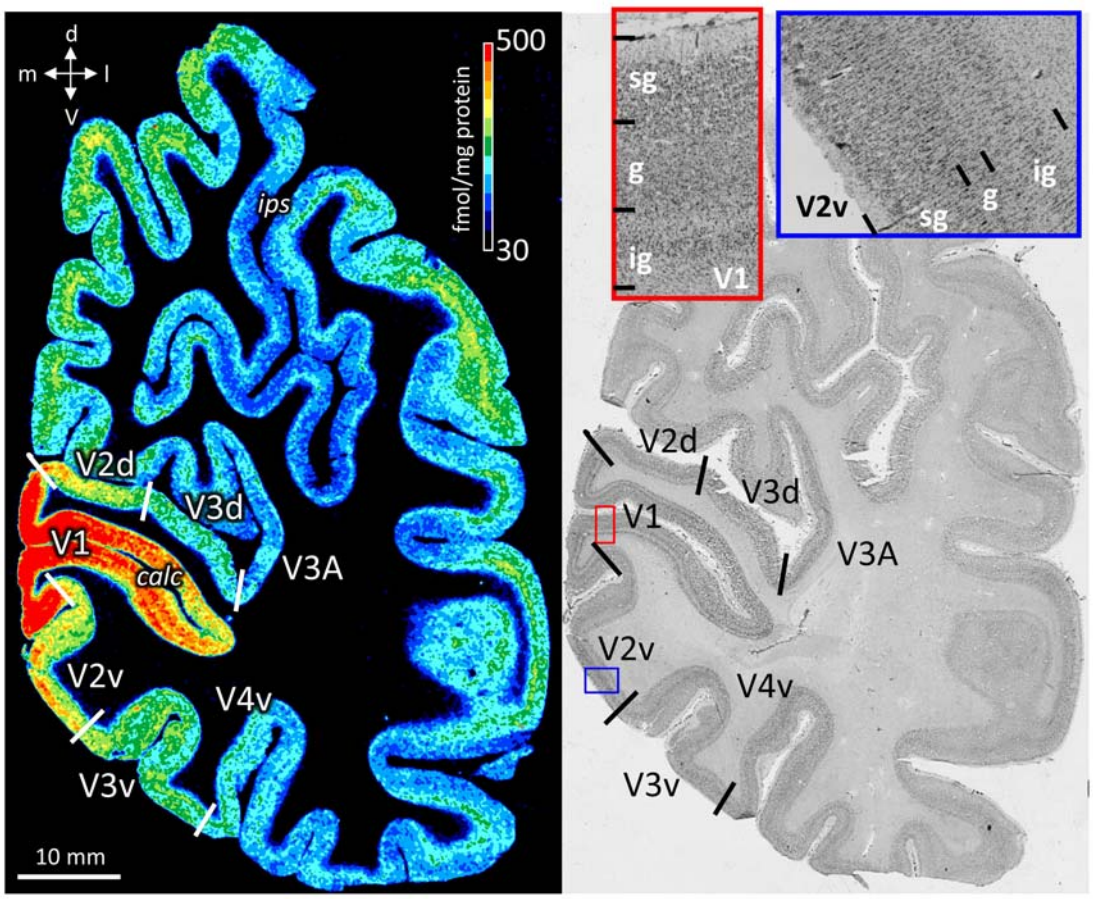

FIGURE 2 | Neighboring coronal sections through the human occipital lobe. Left: distribution of the cholinergic muscarinic M_2 receptors. Color bar codes for receptor densities in fmol/mg protein. Right: Cell body stained section. Red contoured inset from primary visual cortex (V1) and blue contoured inset from V2v. The high magnifications in cell body stained sections were used to define the borders of the supragranular (sg), granular (g), and infragranular (ig) strata, which were then manually traced in the neighboring receptor autoradiograph. calc, calcarine sulcus; d, dorsal direction; ips, intraparietal sulcus; l, lateral direction; m, medial direction; v, ventral direction.

TABLE 1 | *p* values (after Bonferroni correction) of the ANOVA tests carried out to determine the inhomogeneous distribution ($p \leq 0.05$) of 15 receptor types throughout the 44 areas in the three brains (over all layers, or in the supragranular, granular or infragranular strata).

Receptor	All layers	Supragranular	Granular	Infragranular
AMPA	7.190	7.468	1.2936	0.981
NMDA	**0.000**	**0.000**	**0.000**	**0.001**
Kainate	11.386	13.877	13.651	12.354
$GABA_A$	**0.000**	**0.003**	**0.007**	0.787
$GABA_A$/BZ	3.917	6.892	6.093	7.391
$GABA_B$	**0.014**	0.176	0.104	**0.013**
M_1	**0.043**	0.477	0.092	0.171
M_2	**0.000**	**0.000**	**0.000**	0.106
M_3	5.617	0.472	0.274	0.088
$\alpha_4\beta_2$	0.246	0.258	**0.018**	5.837
α_1	**0.000**	**0.000**	0.687	**0.000**
α_2	**0.050**	0.532	1.273	8.385
5-HT_{1A}	**0.018**	9.792	**0.000**	**0.000**
5-HT_2	12.009	4.544	8.523	12.998
D_1	1.231	2.040	0.188	5.412

Significant values highlighted in bold font.

of 44 cytoarchitectonically defined iso- and periarchicortical areas of the human brain. Additionally, the mean density of each receptor over all cortical layers (mean areal density) was calculated. All original data are provided in Supplementary Table S2.

Mean Areal Densities of Single Transmitter Receptors in the Human Cerebral Cortex

Figure 3 provides an overview of the strata-specific and mean areal receptor densities of all 44 analyzed areas. ANOVAs revealed significant differences in mean densities (averaged over all layers) as well as in those of the three strata only for the NMDA, $GABA_A$, $GABA_B$, M_1, M_2, α_1, α_2 and 5-HT_{1A} receptors (*p* values after Bonferroni correction, see **Table 1**). Interestingly, also the nicotinic $\alpha_4\beta_2$ receptors reached significance when densities of the granular stratum were analyzed. AMPA, kainate, M_3, 5-HT_2 and D_1 receptors were not significant in the ANOVA. Therefore, significance of minima and maxima was not tested in these cases. The *mean areal densities* (dotted line in **Figure 3**) demonstrate that NMDA, $GABA_A$, $GABA_A$/BZ, M_2, α_2, 5-HT_2, and D_1 receptors reach their maximal densities in V1. The absolute maxima of other receptors are found in areas 24 (NMDA), 11 (AMPA, $GABA_B$), lateral part of area 37 (M_1), PGp (M_3), 32 (nicotinic $\alpha_4\beta_2$), 6 (α_1), and 36 (5-HT_{1A}). The lowest densities of AMPA receptors are reached in the posterior cingulate area 23, NMDA receptors in area 4, kainate receptors in area V2d, GABAergic $GABA_A$ receptors and $GABA_A$/BZ binding sites in the motor cortex (areas 4 and 6, respectively), and of $GABA_B$ receptors in area 45. Muscarinic M_1 and M_2 receptors have their minima in area 4, M_3 receptors in area V4v, nicotinic $\alpha_4\beta_2$ receptors in area 2, adrenergic α_1 receptors in area 44, adrenergic α_2 receptors in area 38, serotonergic 5-HT_{1A} receptors in area V1, serotonergic 5-HT_2 receptors in area FG1, and dopaminergic D_1 receptors in premotor area 6. Despite of this considerable regional heterogeneity of the maximal and minimal mean areal densities of single receptor types, regional preferences can be detected. NMDA, $GABA_A$, $GABA_A$/BZ, M_2, α_2, 5-HT_2, and D_1 receptors all reach high densities in the primary visual cortex V1, whereas the same receptor types (except α_2 and 5-HT_2) and the M_1 receptor show very low densities over all layers in primary motor and premotor areas.

Strata Specific Densities of Transmitter Receptors in the Human Cerebral Cortex

If we focus on the *strata-specific densities* of each receptor type (Supplementary Table S2), the courses of all three strata seem to run nearly parallel to each other throughout all cortical areas (**Figure 3**). Thus, regionally coincident maxima of all three strata are found for $GABA_B$, M_2, and D_1 receptors in area V1, and for M_1 and M_3 receptors in areas 37L and PGp, respectively. Coincident maxima in the supragranular and granular strata occur in area V1 (NMDA, $GABA_A$, 5-HT_2), and in the anterior cingulate area 32 (nicotinic $\alpha_4\beta_2$). The supra- and infragranular strata reach coincident maxima in the orbitofrontal area 11 (AMPA) and the premotor area 6 (α_1, D_1), whereas such coincident maxima of granular and infragranular layers are found in areas 11 (kainate) and 3b (α_2) (**Figure 3**). Coincident minima of 5-HT_2 receptors are found in area FG1 in all three strata, whereas NMDA and kainate receptors show such minima in supragranular and granular layers of area V1, $GABA_A$/BZ binding sites in area 6, $GABA_B$ in area 45, and α_1 in area 44. Coincident minima in supra- and infragranular strata are found in area 6 for the D_1 receptor, and in granular and infragranular strata for NMDA, $GABA_A$, $GABA_A$/BZ and M_2 receptors in the primary motor or the premotor cortices 4 and 6, respectively (**Figure 3**).

Large differences between 5-HT_{1A} receptor densities of the different strata are visible throughout all regions studied (**Figure 3**). The density of the 5-HT_{1A} receptor is considerably higher in the supragranular stratum than in the other two strata, suggesting a modulatory influence preferably on cortico-cortical projection neurons and interneurons, which are more frequent in this stratum than in the other two strata, as well as on the apical dendrites of the pyramidal cells located in deeper layers. The location of exceptionally high densities of the nicotinic $\alpha_4\beta_2$ receptor only in the granular layer of all three primary sensory areas is also notable (**Figure 3**), since these three maxima considerably differ from the density of this receptor in the supra- and infragranular strata of the same areas (3b, 41 and V1). Thus, the predominant input layer of primary sensory cortices seems to be under a strong modulatory influence of this cholinergic receptor type. Three coincident maxima of $\alpha_4\beta_2$ receptors are visible in all strata of the multimodal association areas 8 and 46 of the prefrontal cortex and the anterior cingulate cortex (area 32). In all other areas the density of this receptor is low, and shows no clear-cut local preference.

In most areas a canonical sequence of receptor densities from highest values in the supragranular stratum, intermediate values in the granular layer IV, and lowest values in the infragranular stratum is found. Exceptions from this rule are seen for the kainate receptor, which shows highest densities in the infragranular stratum, the M_2 receptor, which reaches highest densities in the granular stratum of most areas, and the α_1 and 5-HT_{1A} receptors, which in some areas present

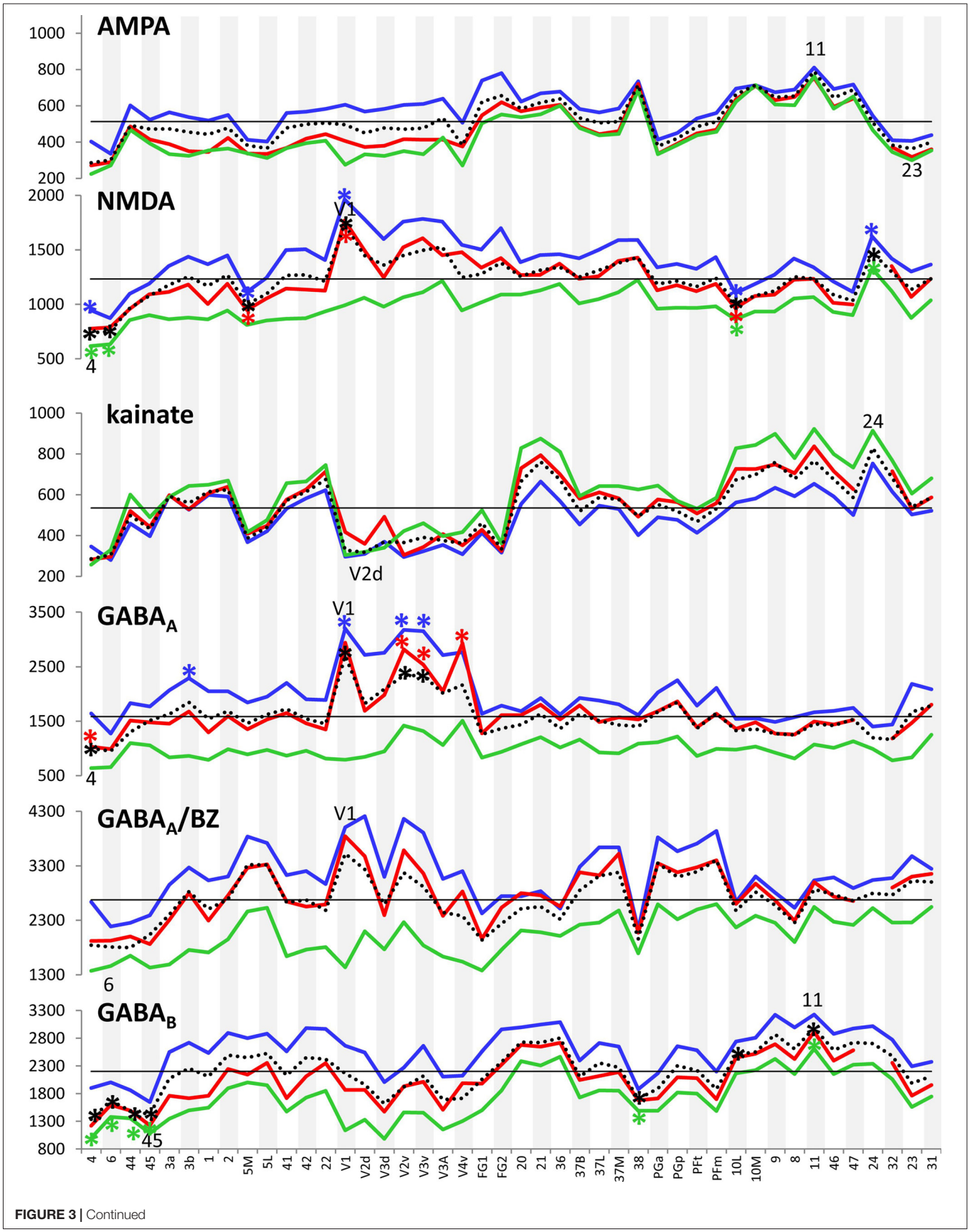

FIGURE 3 | Continued

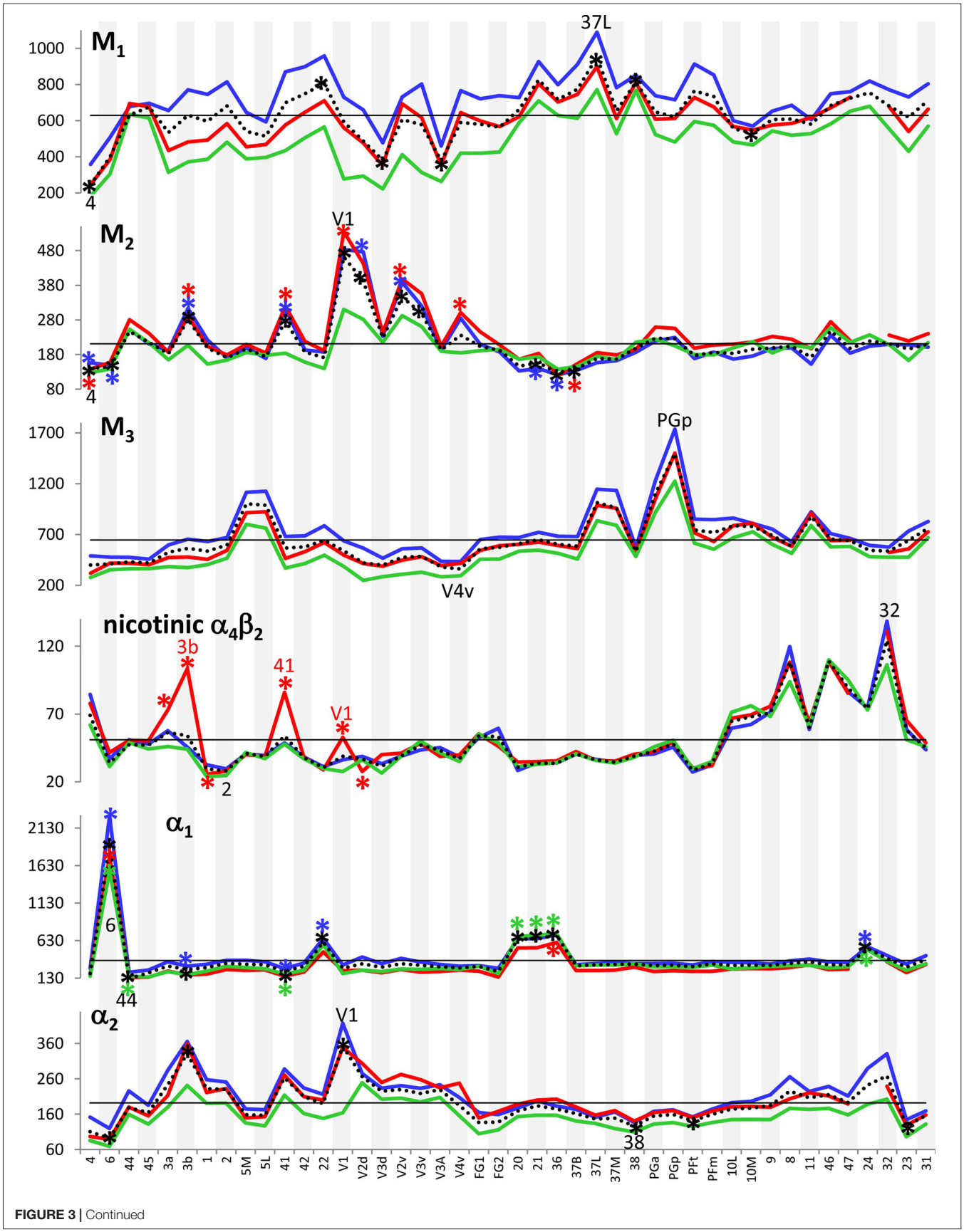

FIGURE 3 | Continued

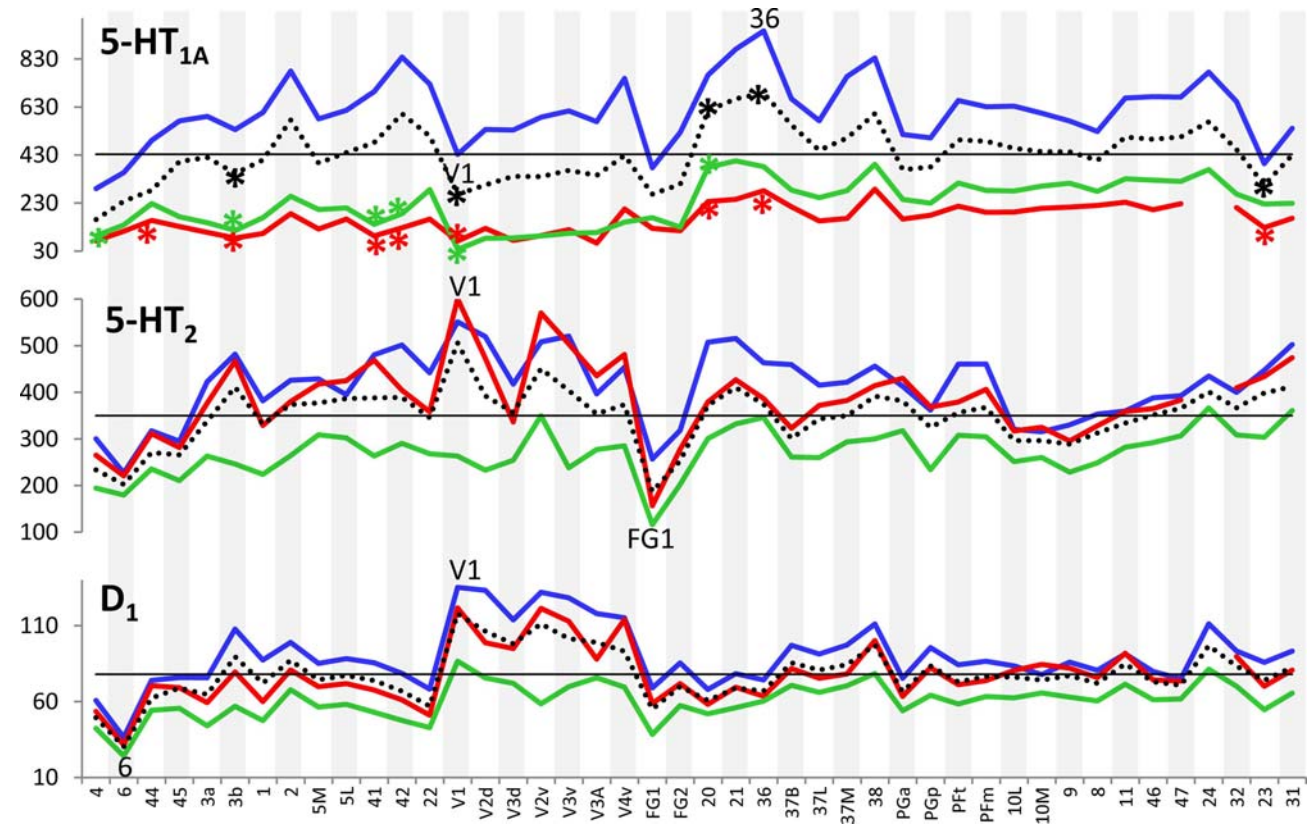

FIGURE 3 | Absolute densities (fmol/mg protein) of each of the studied receptor types in 44 cortical areas. Dotted line: mean areal receptor density; blue line: receptor density in the supragranular stratum; red line: receptor density in the granular stratum; green line: receptor density in the infragranular stratum; straight black line indicates the mean areal density of each receptor averaged over all 44 areas. Areas with maximal or minimal mean areal receptor densities are indicated by their names in the respective graphs. In the case of the nicotinic $\alpha_4\beta_2$ receptor, the absolute density of this receptor in the granular stratum of the three primary sensory areas (V1, 3b and 41) is highlighted. Asterisks indicate maxima and/or minima in the densities of supragranular (in blue), granular (in red), infragranular (in green) or all layers (in black) which differ significantly from the mean density of the given receptor averaged over all examined areas.

higher densities in the infragranular than in the granular stratum.

Multi-Receptor Fingerprints of Areas and Layers Reflect Principle Aspects of Cortical Organization

Each cortical area expressed all receptor types, but at different mean areal and laminar densities (Supplementary Table S2). The regional-specific expression of all receptors studied constitutes the receptor fingerprint of an area or a stratum. We generated four receptor fingerprints per cortical area, visualizing the mean areal density, as well as the density in its supragranular, granular and infragranular strata. This is done for both the absolute (for selected areas see **Figure 4**, for all other areas see Supplementary Figure S1), and the *z*-score normalized (for selected areas see **Figure 5**, for all areas see Supplementary Figure S2) receptor densities, which is done because the absolute densities of the various receptors differ by the order of one to two magnitudes. Specifically, the GABA and glutamate receptors reach much higher densities than those of all other receptor types in the absolute fingerprints (**Figure 4**, Supplementary Figure S1). Therefore, it is difficult to estimate the contribution of the modulatory receptors to the shape of the fingerprint because there receptors occur at much lower densities. In the normalized fingerprints, a receptor density above the mean of that receptor over all examined areas has a positive z-score, a receptor density below the mean of that receptor has a negative *z*-score (**Figure 5**, Supplementary Figure S2). The normalized fingerprint facilitates a visual comparison of the relative contribution of a single receptor to the fingerprint of each area.

Discriminant analyses of the fingerprints over all layers, and separately for the three strata shows that the fingerprints of all 44 areas are heterogeneous ($p = 0.000$ for each of the analyses). After these Omnibus tests, a pairwise comparison between all combinations of areas revealed some significant inter-areal differences, but most comparisons did not reach significance (Supplementary Tables S3–S6).

Absolute Fingerprints of Cortical Areas

Since a pure visual comparison between the different fingerprints depends on the interpretation by the observer, we quantified

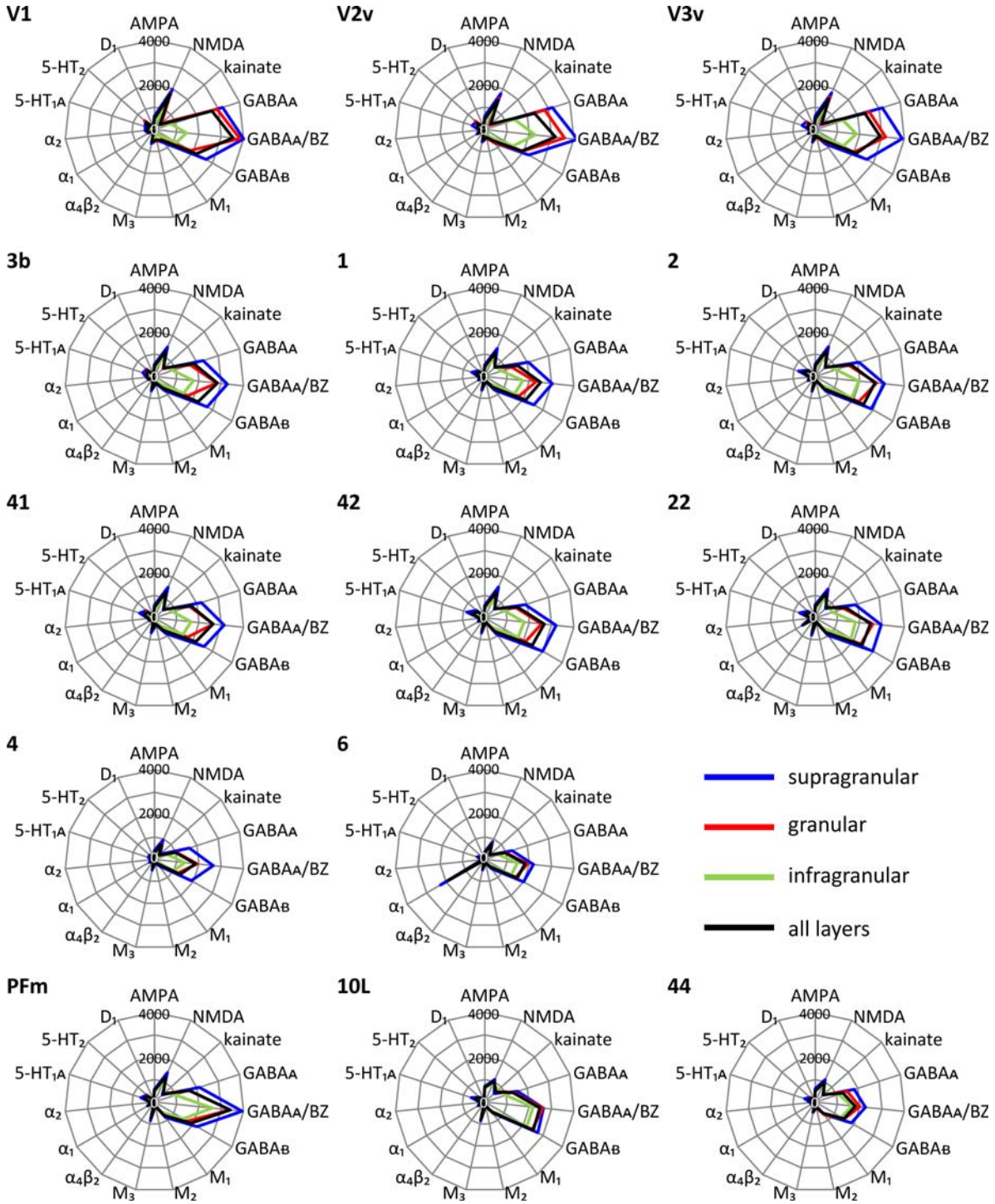

FIGURE 4 | Absolute multi-receptor fingerprints of 15 different receptor types in each of the 44 cortical areas. From these areas, V1, V2v and V3v (visual system), 3b, 1 and 2 (somatosensory system), 41, 42 and 22 (auditory system), 4 and 6 (motor cortex), PFm (inferior parietal cortex), 10L (lateral part of the frontopolar cortex) and 44 (part of Broca's region) were chosen as typical fingerprints representing different functional systems. The fingerprints of all other areas are found in Supplementary Figure S1. Scaling of the absolute fingerprints in fmol/mg protein is the same in all areas.

the size of the mean areal and strata-specific fingerprints by computing the sum of the densities of all receptors over all layers or in each of the three strata.

The ranges of the sizes overlap slightly between the strata, if the standard deviations are taken as measure (**Figure 6**). The comparison between all areas reveals a general rule: the

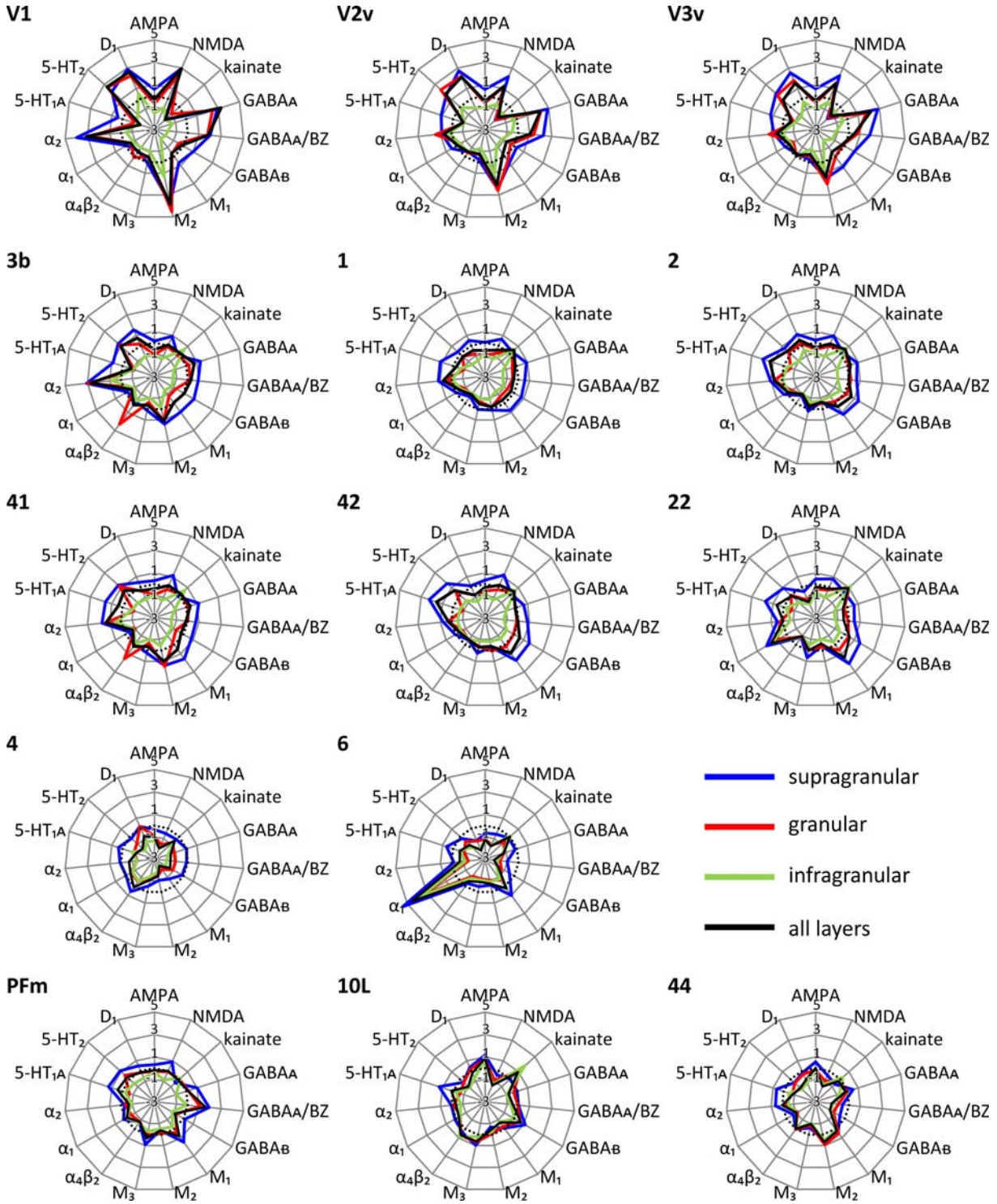

FIGURE 5 | Normalized multi-receptor fingerprints of 15 different receptor types in each of the 44 cortical areas. For further information see **Figure 4**. The fingerprints are normalized by their *z*-scores, and the dotted line indicates the average *z*-score over all areas. Positive *z*-scores indicate receptor densities above average, negative *z*-scores those below average. The normalized fingerprints of all other areas are found in Supplementary Figure S2.

areal sizes of absolute fingerprints are always larger in the supragranular stratum, followed by the granular and then the infragranular stratum (**Figure 6**). The size of the fingerprint over all layers shows values above the grand mean plus standard deviation in the primary visual cortex V1, ventral part of V2, temporo-occipital transition area 37L, temporal association area

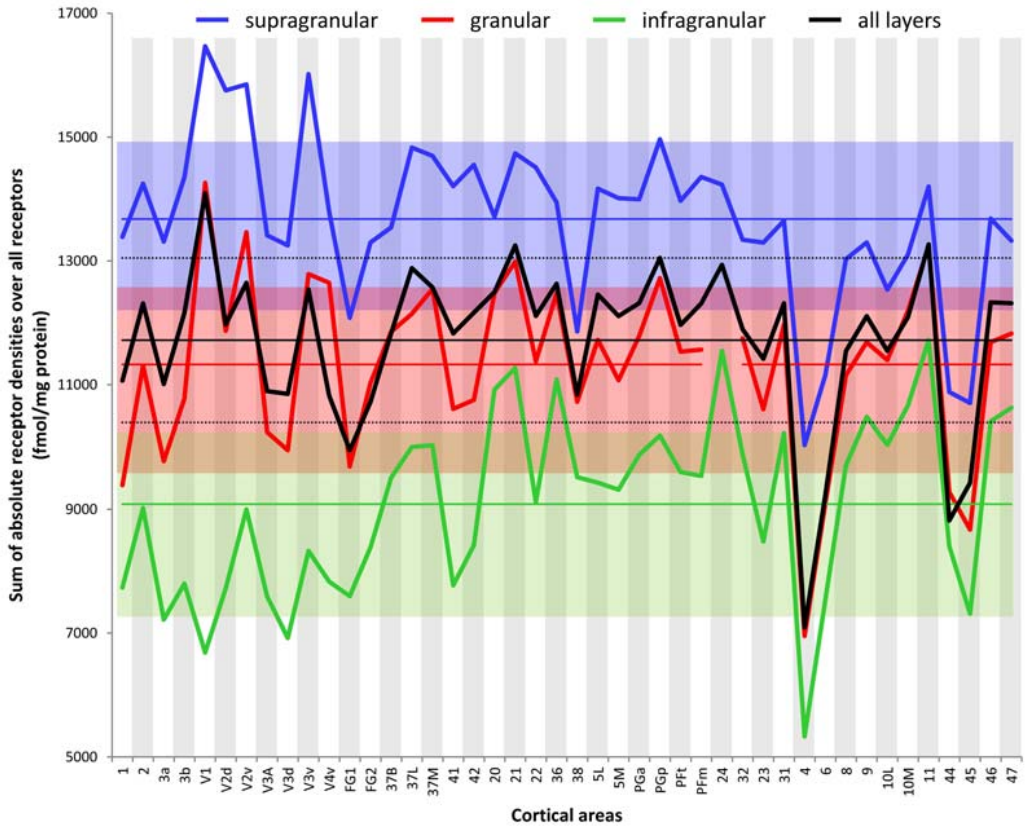

FIGURE 6 | Sum of the absolute densities of all receptors examined in each area and stratum as well as over all layers of each brain region. Mean values over all areas of the three strata and the total cortical depth and their standard deviations are indicated by straight lines and dotted lines, respectively.

21, parietal association areas 5L and PGp, as well as orbitofrontal area 11. Corresponding lowest values are found in the higher visual area FG1, the temporal association area 38, the motor cortical areas 4 and 6, as well as in the Broca areas 44 and 45. Significant higher values for the supragranular fingerprints were found only in the early visual areas V1, dorsal and ventral parts of V2 as well as in V3v. The corresponding lowest values were found in the same areas as described for the size of the mean areal fingerprints (FG1, 38, 4, 6, 44, 45). Significant higher values for the granular fingerprints were found in V1, V2v, V3v, 21 and 11. The corresponding lowest values were found in the somatosensory area 1, higher visual area FG1, motor areas 4 and 6, as well as in Broca areas 44 and 45. The highest values of the infragranular fingerprints are found in temporal association areas 20, 21, 36, anterior cingulate area 24, posterior cingulate area 31, as well as in the prefrontal areas 9, 10L, 10M, 11, 46 and 47. The corresponding lowest values were seen in the somatosensory area 3a, visual areas V1, V3A, V3d, and FG1, motor areas 4 and 6, as well as in Broca's area 45.

Although the absolute densities of the different receptors vary between the examined brains (as revealed by the SD values and the variation coefficients specified in Supplementary Table S2), the proportional changes in densities between cortical areas remain constant when comparing different brains; e.g., in all examined brains, V1 contained higher overall NMDA, $GABA_A$, or α_2, but lower α_1, or 5-HT_{1A} receptor densities than did V2. Likewise, the relationship between receptor densities in the examined strata was also constant in the different brains examined; e.g., in area V1 of all brains highest 5-HT_{1A} receptor densities were always found in the supragranular stratum, and lowest ones in the infragranular stratum.

In conclusion, the sizes of absolute fingerprints, and thus the density of all receptors together in each area or stratum, are regional-specific and show a canonical sequence (supragranular to granular to infragranular) of the strata from large to small fingerprints.

Normalized Fingerprints of Cortical Areas

Using the normalized fingerprints, differences in the *shape*, and thus in the regional balance between multiple receptors can be better visualized.

Unimodal sensory areas

The shapes of the normalized fingerprints (**Figure 5**, Supplementary Figure S2) of visual areas clearly differ from those of the somatosensory and auditory systems with a notably higher similarity between the fingerprints of the latter two functional systems. The impact of receptor density analyses

on revealing regional organizational principles of the cortex is further supported by the exceptionally high nicotinic $\alpha_4\beta_2$ receptor densities in the granular layers of the core regions of the primary somatosensory (3b) and auditory (41) cortices. Within each of the three sensory systems, the fingerprints are most similar between primary and early sensory areas (areas V1, V2d, and V2v in the visual system; areas 1, 2, 3a and 3b in the somatosensory system; areas 41 and 42 in the auditory system). Furthermore, the fingerprints of early unimodal visual areas (V3v, V3A, V3d, V4v) are more similar to V1and V2 than to the hierarchically higher visual areas (areas FG1 and FG2 of the fusiform gyrus). Notably, the fingerprints of the early visual areas of the dorsal stream (V3A, V3d) differ from those of the ventral stream (V3v, V4v). The primary visual area V1 shows considerably higher normalized densities of NMDA, $GABA_A$, $GABA_A$/BZ, M_2, α_2, 5-HT_2 and D_1 receptors in all strata than the primary somatosensory (1, 2, 3a and 3b) and auditory (41) areas (**Figure 5**, Supplementary Figure S2).

The fingerprints of areas of the primary auditory (area 41) and the secondary and multimodal auditory/temporal areas (areas 42, 20–22, 36) systematically differ. Particularly, the normalized density of the α_1 receptor is higher in the association areas 20–22 and 36 compared to the unimodal auditory areas 41 and 42. The fingerprint of the temporo-polar area 38 differs in shape from all other temporal areas studied here. Likewise, the fingerprints of the temporo-occipital transition region (areas 37B, 37L and 37M) differ from those of the areas of the temporal and occipital lobes (**Figure 5**, Supplementary Figure S2).

The normalized fingerprints of motor areas 4 and 6 completely contrast with those of all sensory areas. Additionally, the high density of α_1 receptors in the premotor cortex (area 6) contributes to the segregation of this area from the primary motor cortex (area 4).

Multimodal association areas

Multimodal association regions are located in the prefrontal, temporal and parietal lobes including the precuneus region. Areas of the inferior parietal lobule are clearly segregated by different shapes of receptor fingerprints into two different groups: the supramarginal group with areas PFm and PFt, and the angular group with areas PGa and PGp. Both groups of fingerprints are separated by the high to very high density of the muscarinic M_3 receptors in the angular group, and a lower density of this receptor in the supramarginal group which resembles only that of the average over all 44 areas. Notably, the fingerprints of PGa and the postcentral areas 5L and 5M are very similar, although the latter areas are not located in the inferior parietal lobule. Additional to their high M_3 receptor density, the supragranular and granular strata of 5L, 5M, PGa and PGp show a $GABA_A$/BZ density clearly above average. Thus, both receptors largely contribute to the similarity of the fingerprints between these four parietal areas and segregate them from PFm and PFt.

In a next step the area- and stratum-specific fingerprints were tested to answer two questions:

- Do the fingerprints of the three strata build separate, strata-specific clusters if all cortical areas are compared?

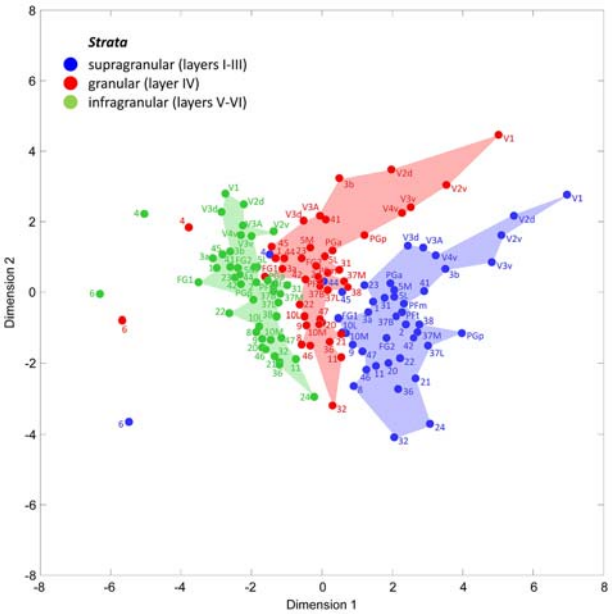

FIGURE 7 | Multidimensional scaling analysis to visualize the different clusters of receptor fingerprints extracted from the supragranular, granular and infragranular strata of all examined areas. Note the exceptional positions of both motor areas 4 and 6, and of the Broca areas 44 and 45. These are the only areas whose supragranular and granular fingerprints take positions outside the cluster of all other areas.

- Do the fingerprints over all layers and/or the stratum-specific fingerprints systematically differ by their shapes and sizes between cortical areas? Do these variations indicate principal aspects of functional and topographical segregation, as well as hierarchical organization?

Multidimensional Scaling Analysis of Receptor Fingerprints

A multidimensional scaling analysis of the stratum-specific fingerprints shows three clusters (**Figure 7**), which clearly separate the fingerprints of the supragranular from those of the granular and the infragranular strata in nearly all areas. Only exceptions are the positions of fingerprints of the granular stratum of the motor areas 4 and 6, which are shifted into the range of the infragranular cluster. Furthermore, the fingerprints of the supragranular stratum of areas 4, 44 and 45 are slightly shifted into the cluster of the fingerprints of the granular stratum. The cause of these exceptional shifts will be addressed in the "Discussion" Section. In conclusion, the laminar fingerprints of the iso- and periarchicortex completely differ between the three strata. Therefore, the multi-receptor densities are specific for each of the three groups of cortical layers (strata), and thus indicate a canonical receptor balance in each stratum.

Hierarchical Cluster Analyses of Receptor Fingerprints

The hierarchical cluster analysis of fingerprints of mean areal receptor densities separates all early visual areas from the rest of

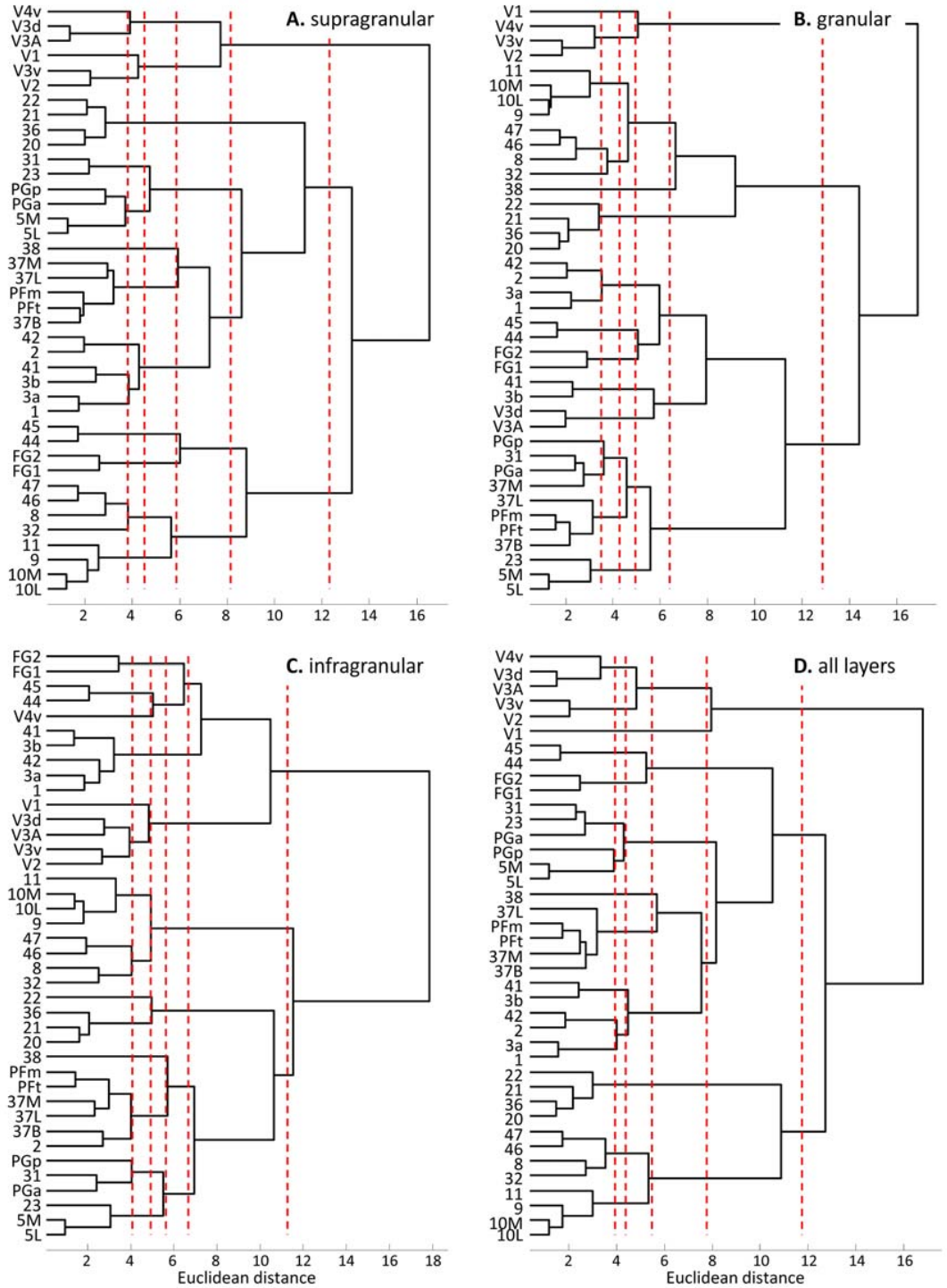

FIGURE 8 | Hierarchical clustering of all regions except the agranular cortices of areas 4, 6 and 24 based on the receptor fingerprints extracted from their supragranular **(A)**, granular **(B)**, or infragranular **(C)** strata, or based on the fingerprints of mean receptor densities over all layers **(D)**. Dashed red lines indicate the number of "main" clusters as determined by the k-means analyses.

the cortex already after the first branching in the dendrogram (**Figure 8D**). The highest acceptable number of clusters after k-means analysis shows that the fingerprint of the primary visual cortex differs from those of the early (V2, V3v, V3A, V3d, V4v) and higher (FG1, FG2) visual areas. The highest possible level of clustering is mapped in **Figure 9D** on the single subject

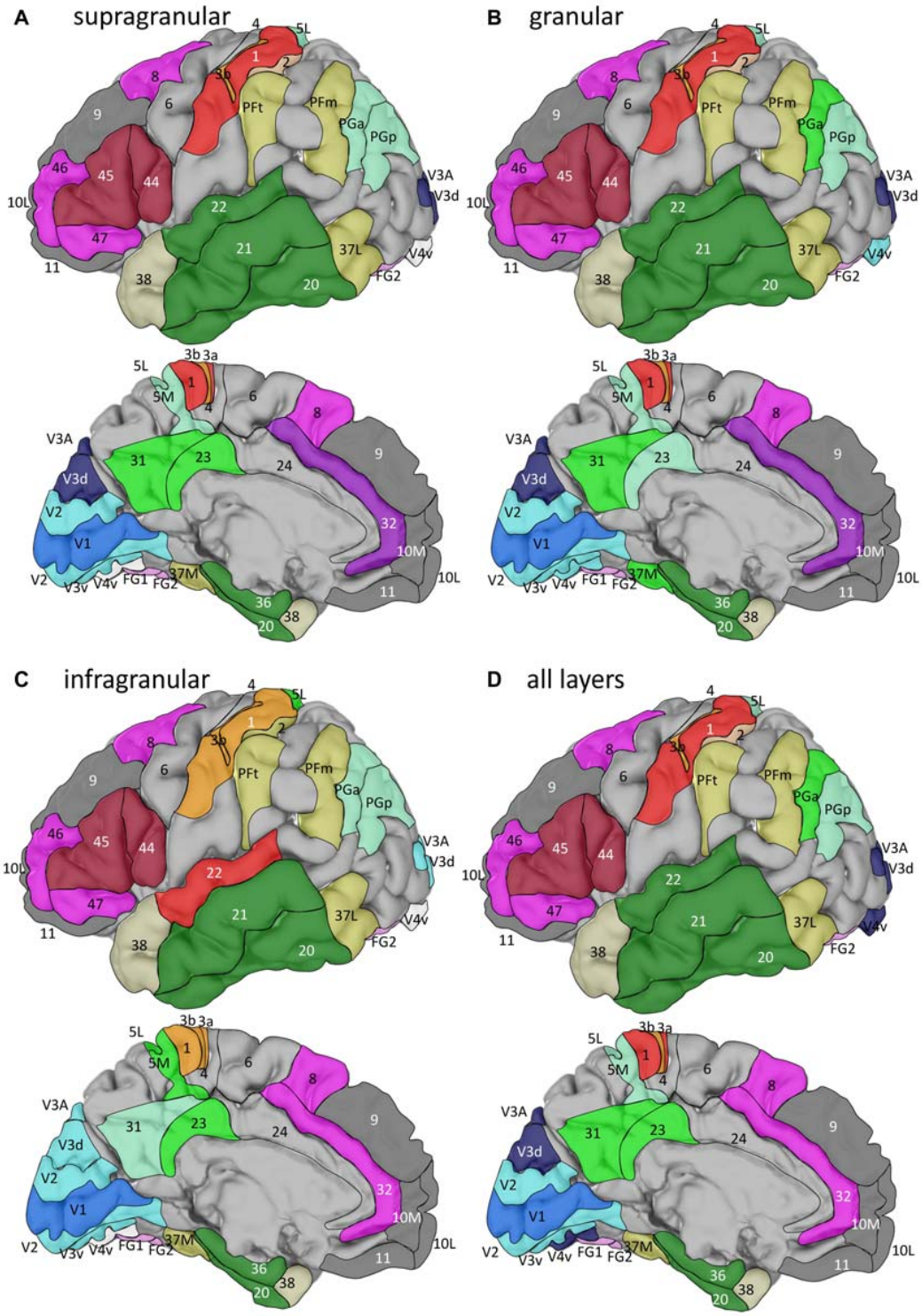

FIGURE 9 | Location of the clusters with areas of similar fingerprints in the single subject template brain of the Montreal Neurological Institute. Clusters were identified by hierarchical and k-means cluster analyses (see **Figure 8**) of fingerprints extracted from the supragranular **(A)**, granular **(B)**, or infragranular **(C)** strata, or from all layers **(D)**. For the lateral views, anterior is on the left, and for the medial views it is on the right.

MNI template brain. At this clustering level, the areas of the Broca region (44 and 45) form a separate cluster, as well as the parietal areas PGa, PGp, 5L, 5M with the cingulate areas 23 and 32. The temporo-polar area 38 forms a cluster by its own

(**Figure 9D**), but is relatively similar to the multimodal temporal and inferior parietal regions as well as the temporo-occipital transition region (**Figure 8D**). Areas of the latter regions are found in a cluster, which comprises the temporo-occipital areas 37B, 37L and 37M as well as the inferior parietal areas PFm and PFt. Notably, the fingerprints of the primary somatosensory and primary auditory cortex cluster together. Areas 3a and 1 of the somatosensory cortex form another cluster which is separated from a cluster with somatosensory area 2 and the secondary auditory area 42. Then, all temporal isocortical areas (20–22 and 36) are found in one cluster, as well as the lateral prefrontal areas 46, 47, 8 and anterior cingulate area 32 in another cluster. Finally, the most rostral prefrontal areas 9, 10L and 10M are comprised in a cluster with the orbitofrontal area 11 (**Figure 9D**).

The fingerprints of the supragranular stratum (**Figures 8A**, **9A**) again separate the visual areas from all other areas of the neo- and periarchicortex. Interestingly, V1 is again separated from the other early visual areas. Areas V3A and V3d are in one cluster, different from those of the other early visual areas. Thus, a segregation of the ventral and dorsal visual streams is supported by the multi-receptor fingerprints. All other areas show a very similar clustering as described above for the mean (all layers together) receptor fingerprints. Only PGa and PGp are found in separate clusters if the fingerprints of all layers together are analyzed, whereas both areas are in the same cluster when fingerprints from the supragranular stratum are studied.

The fingerprints of the granular stratum (**Figures 8B**, **9B**) clearly separate the visual areas of the ventral stream from those of the dorsal stream, and also from the higher visual areas FG1 and FG2. Area V4v represented a separate cluster in the analysis of the supragranular stratum, but here in the granular stratum (**Figures 8B**, **9B**) it clusters together with the early visual areas of the ventral stream. All other clusters contain the same areas as found in the analysis of the supragranular stratum with the exceptions of area 23 (which clusters together with 5L, 5M and PGp) and of area 37M (which clusters together with 31).

The fingerprints of the infragranular stratum (**Figures 8C**, **9C**) do not separate the early visual areas of the ventral and dorsal streams, as found in the analyses of the supragranular and granular strata. Moreover, V4v forms a separate cluster. Considerable differences to the clustering pattern of the supragranular and granular strata are also found in the cases of the temporal area 22, the anterior cingulate area 32 and the superior parietal areas 5M and 5L as well as area 31 on the precuneus.

The cluster analyses of stratum-specific fingerprints (**Figures 8**, **9**) highlight the special position of visual areas, particularly the early ones, since they always segregate from the remaining bulk of areas at an earlier branching level and remain separated even at the highest branching level. The fingerprints of the granular stratum most clearly support the separation of the early visual areas into dorsal and ventral streams. To a lesser extent (with the exception of V4v which forms a cluster by itself), this separation is also found in the analysis of the supragranular stratum, but not in that of the infragranular stratum.

In summary, the fingerprints of the different strata differed greatly and enabled a separation of these strata-specific fingerprints into three clusters (**Figure 7**). Only the agranular motor areas 4 and 6, as well as the agranular cingulate area 24 did not follow this principal segregation of the strata-specific fingerprints. Regarding the motor areas, we must conclude that a typical receptor pattern indicating the presence of an inner granular layer IV could not be demonstrated by the receptor density analyses. If the fingerprints of the three strata and that of all strata together are analyzed for all 41 granular areas, a clustering could be found which roughly follows the topographical segregation of the areas into prefrontal, parietal, temporal and occipital regions (**Figures 8**, **9**). It is notable that the fingerprints of prefrontal multimodal association areas always cluster together and are different from those of parietal or temporal association areas. However, a deeper analysis reveals that the topographical segregation is superposed by a functional classification of areas. Hence, a further segregation of the receptor fingerprints of early visual areas into separate clusters is found in the granular and to a lesser degree also in the supragranular stratum following the concept of dorsal and ventral visual streams. Finally, the fingerprints of the supragranular and granular strata show a similar clustering pattern, whereas those of the infragranular stratum show divergent patterns in the precuneus region, the superior temporal sulcus and the anterior cingulate cortex. The analysis of the contribution of single receptor types (**Figure 3**) highlights the distinct increased levels of the nicotinic $\alpha_4\beta_2$ receptor in the granular layers of all three primary sensory areas, and of the M_2 receptor in the same layer of V1 and early visual areas of the ventral stream, as well as in the primary auditory cortex (area 41). In these areas, the density of the nicotinic $\alpha_4\beta_2$ and the M_2 receptors in the granular layer exceeds that of the supragranular stratum, which is the stratum with the highest receptor density in most areas. The general rule of a sequence in receptor densities from highest levels in the supragranular strata and lowest in the infragranular strata of all 44 areas is only violated by the kainate, noradrenergic α_1 and serotonin 5-HT_{1A} receptors where the canonical sequence from highest to lowest levels is changed in some or most areas.

DISCUSSION

Mean Areal Densities of Single Transmitter Receptors in the Human Cerebral Cortex

The new aspect of this study is the large scale cross area comparison of stratum-specific receptor fingerprints. It has been demonstrated that the densities of various transmitter receptors vary considerably between different cytoarchitectonically defined areas in the human cerebral cortex (Cortés et al., 1986, 1987; Hoyer et al., 1986b; Pazos et al., 1987b; Jansen et al., 1989; Zilles and Palomero-Gallagher, 2001; Zilles et al., 2004, 2015a; Morosan et al., 2005; Scheperjans et al., 2005a,b; Eickhoff et al., 2007, 2008; Palomero-Gallagher et al., 2008, 2009, 2015; Zilles and Amunts, 2009; Caspers S. et al., 2013; Vogt et al., 2013;

Caspers et al., 2015; Palomero-Gallagher and Zilles, 2017a). Frequently, the densities show distinct changes at the borders between cytoarchitectonic areas, or reveal a finer parcellation of the cortex than found in cytoarchitectonic studies (Geyer et al., 1996; Amunts et al., 2010). As stated in the articles from our group, this obvious regional heterogeneity is not random, but shows systematic changes depending on the participation of cortical areas in different functional networks and their subdivisions. In the present observations, we included numerous areas for interareal comparison which were not previously studied. More importantly, the previous comparisons by cluster analyses were focussed on some specific functional networks (e.g., language-related areas, cingulate areas), thus neglecting the impact on the results of a cluster analysis caused by a greater number of cortical areas included and by a brain-wide balanced analysis. Most importantly, previous studies concentrated on mean areal densities, i.e., regional distribution patterns of receptors averaged over all cortical layers. The present study hypothesizes, that layers show different receptor balances and their fingerprints reflect the different contribution of layers to the regional fingerprints described in previous articles from our group.

As previously stated (Mash et al., 1988; Zilles et al., 2002a; Zilles, 2005), the cholinergic muscarinic M_2 receptor consistently reaches higher densities in human and non-human primate primary visual, auditory and somatosensory areas than in hierarchically higher isocortical sensory areas or in areas of the motor cortex. This could be confirmed for V1 in the present study by new measurements at different sites in the cortical areas and by a partly new sample of brains (**Figure 2**). A similar outcome for previously reported noradrenergic α_2 and serotonergic 5-HT_2 receptors in primary sensory areas (Zilles and Palomero-Gallagher, 2017) was also observed in the present study, again using a partly new sample of brains. Accordingly, the previously mentioned principal classifications of cortical areas as primary visual, unimodal visual or higher visual cortices (Caspers et al., 2015) is confirmed by the detection of characteristic levels of densities of single or several (fingerprints) receptor types in a brain-wide analysis. Using that analysis, we could now show that NMDA, $GABA_A$, $GABA_A$/BZ, M_2, α_2, 5-HT_2, and D_1 receptors all reach absolute maxima in the primary visual cortex V1, whereas the same receptor types (except α_2 and 5-HT_2) and the M_1 receptor reach very low densities in primary motor and premotor areas. Furthermore, the mean areal densities of $GABA_A$, $GABA_A$/BZ, M_2, 5-HT_2 and D_1 receptors are higher in the early visual areas than in other isocortical regions. This latter finding is in sharp contrast to the regional distribution of kainate receptors, which are present at exceptionally low densities in all areas of the visual system. The multimodal association areas of the prefrontal and temporal cortices are characterized by high $GABA_B$ densities above the mean of all areas. The higest AMPA and kainate receptor densities are found in areas of the prefrontal association cortex or in this region and in the temporal association cortex, respectively. Low densities of the M_2 receptor were found in the temporal and prefrontal association cortices, whereas the nicotinic receptor reached highest mean areal densites in the prefrontal and lowest densities in the temporal association cortex. Very high α_1 and 5-HT_{1A} receptor densities are found in the entire temporal cortex, particularly in the multimodal temporal association areas. In conclusion, primary sensory and multimodal association areas frequently showed a segregation by receptor densities. In some cases even prefrontal and temporal association areas can be separated by the distinct levels of their receptor expression. Thus, densities of single receptors are not randomly distributed over the entire cortex, but vary according to a general classification scheme into sensory, motor and multimodal areas.

Strata Specific Densities of Transmitter Receptors in the Human Cerebral Cortex

One main focus of the present study was on the layer specificity of single receptor densities. We found a canonical sequence from high to low receptor densities when moving from the supragranular, to the granular and finally the infragranular stratum in nearly all regions. This general rule is only violated by the kainate, muscarinic M_2, noradrenergic α_1 and serotonin 5-HT_{1A} receptors. Kainate receptors reach their highest densities in the infragranular stratum. However, also in this case a regional segregation into visual, multimodal temporal, parietal and prefrontal association areas can be confirmed by the variable kainate receptor densities in the different cortical areas. The M_2 receptor shows the highest and the α_1 receptor the lowest densities in the granular stratum of numerous areas. The most extreme situation was found for the 5-HT_{1A} receptor, which reached by far highest densities in the supragranular stratum and lowest densities in the granular stratum. Very high absolute densities of this receptor were found in the supragranular stratum of temporal association areas 36 and 38 as well as of unimodal somatosensory area 2, auditory area 42 and anterior cingulate area 24.

In accordance with previous reports (e.g., Rakic et al., 1988; Young et al., 1990), NMDA receptor binding was found to be most dense in the supra- and granular strata of cerebral cortex. AMPA receptor densities were highest in layers II and III of primary visual cortex and relatively low in layer IV (see also Rakic et al., 1988; Carlson et al., 1993). Although many AMPA and NMDA receptors are localized at thalamo-cortical and cortico-cortical synapses, the co-localization of these receptors with interneurons is of special importance for the analysis of local signal processing within cortical microcircuits and layers. The co-localization of AMPA and NMDA receptor subunits with calcium binding protein expressing inhibitory interneurons was immunohistochemically studied in macaque primary visual cortex (Kooijmans et al., 2014; Kooijmans, 2016). The co-localizations of parvalbumin with GluA1 or GluA4 AMPA receptor subunits in the fast spiking chandelier and basket cells was found to be minor, in contrast to a higher co-localization of parvalbumin and GluA2 or GluA3. Calbindin and GluA2 or GluA3 AMPA receptor subunits are co-localized to a minor degree, but calbindin and GluA1 or GluA4 show a higher degree in the intermediate spiking neurogliaform and Martinotti cells. Co-localization of calretinin

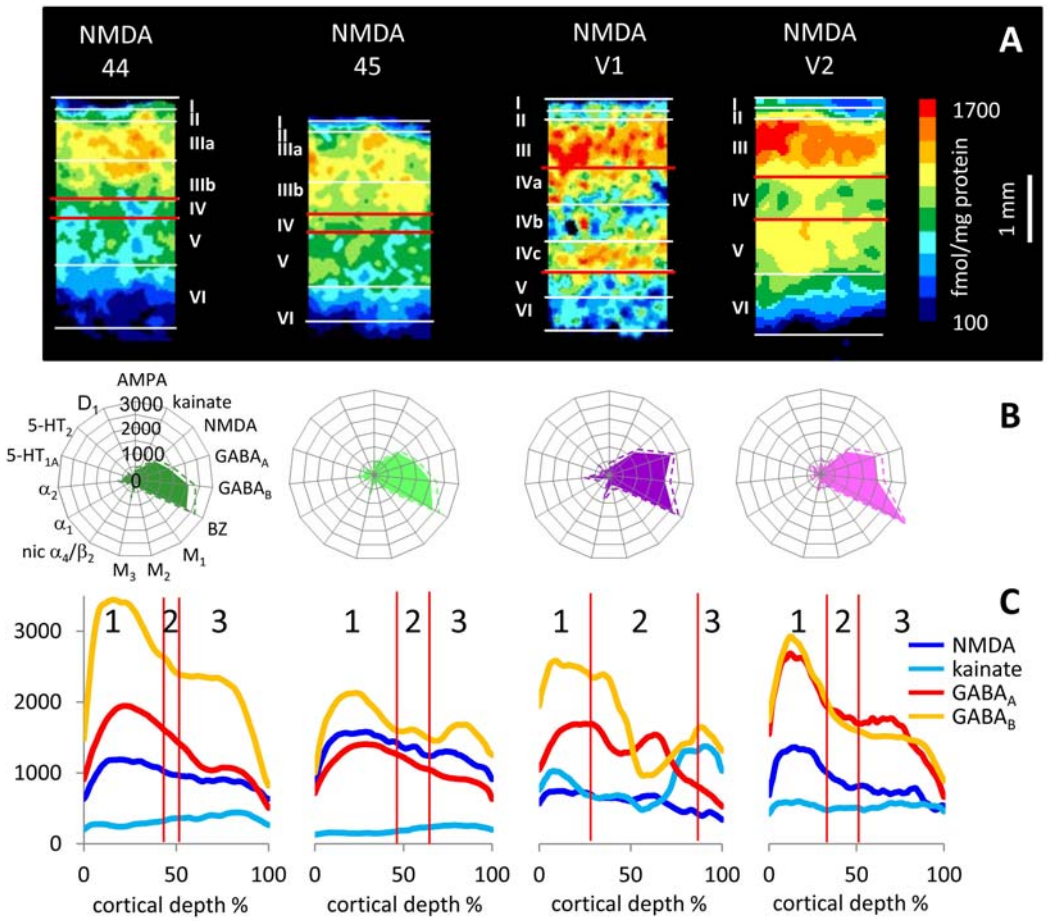

FIGURE 10 | Laminar distribution of the NMDA receptor in human primary (V1) and secondary (V2) visual cortex as well as in areas 44 and 45 of the Broca region. **(A)** Color coded autoradiographs. Scale bar codes for receptor densities in fmol/mg protein. **(B)** Multi-receptor fingerprints. **(C)** Receptor density profiles. 1 supragranular stratum, 2 granular stratum, 3 infragranular stratum. The laminar borders have been defined by comparison with neighboring cell-body stained (cytoarchitecture) sections. Cortical depths of the different areas are normalized to 100%. *Y* axis codes for receptor densities in fmol/mg protein.

with GluA2 or GluA3 is minor, but more was found between calretinin and GluA1 or GluA4 AMPA receptor subunits in the intermediate spiking double bouquet cells. Calcium binding protein expressing interneurons also synthesize NMDA receptors, which consist of two GluN1 and two GluN2 subunits in most cases (Kooijmans, 2016). Therefore, a co-localization analysis of the four isoforms of the GluN2 receptor with the three classes of calcium binding protein containing interneurons provides insight into the cellular localization of the NMDA receptor both on its interneuron-type specific and laminar-specific distribution. Parvalbumin neurons preferentially express only a few NMDA receptors, whereas the calbindin and calretinin neurons show a much higher co-localization with GluN2 NMDA receptor subunits (Kooijmans, 2016). If we compare the laminar patterns of the GluN2 receptor in the neuropil with the present autoradiographic observations of the NMDA receptors, a conspicuous similar laminar pattern can be seen. Summarizing the NMDA and AMPA receptors, our data (for NMDA receptors see **Figure 10**; Supplementary Table S2) show that the laminar patterns of NMDA and AMPA receptors in the human cortex are comparable to that previously reported in both primary sensory and motor cortices of Old World macaques (Young et al., 1990; Geyer et al., 1998; Garraghty et al., 2006).

The present findings on the laminar distribution of $GABA_A$ receptors labeled with [^{3}H] muscimol in human area V1 displayed a high density of this receptor in layer IVC that stood out due to the considerably lower densities in layers IVB and V. Notable is the patchy appearance of layer IVC with distributed $GABA_A$ receptor maxima along this layer. This is visible both in human and macaque V1 (**Figure 11**), and may be indicating the modular organization of this layer (Hubel and Wiesel, 1968, 1969; Wiesel et al., 1974). Supragranular layer II has a moderate density and layers III–IVA a high density of $GABA_A$ receptors. The infragranular layers V–VI show densities comparable or even lower than in layer I. This pattern of human V1 is well comparable with that in the macaque (**Figure 11** and Rakic et al., 1988).

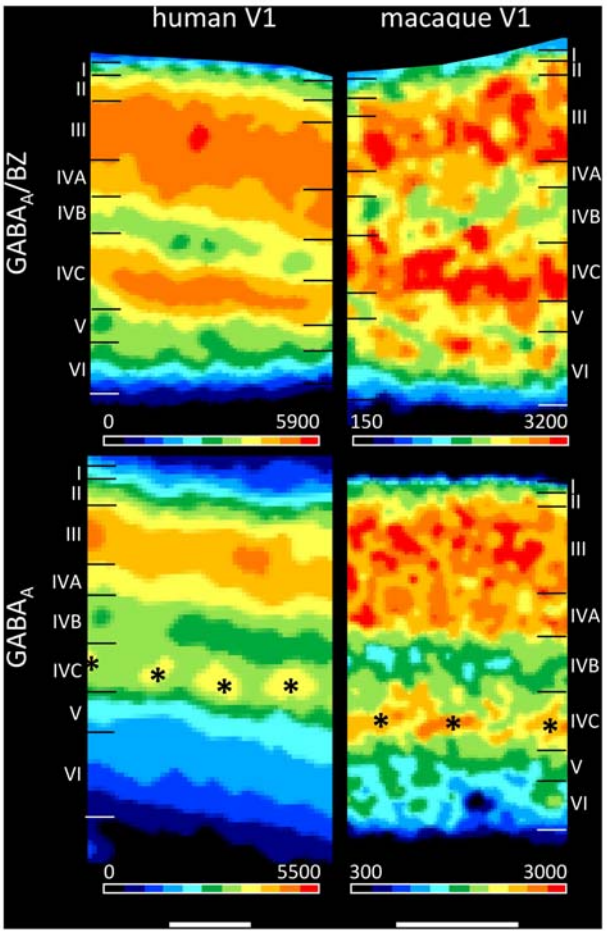

FIGURE 11 | Laminar distribution of the $GABA_A$/BZ binding sites and the $GABA_A$ receptor in human and macaque primary visual cortex V1. Color bars code for receptor densities in fmol/mg protein. Scale bars 1 mm. Asterisks highlight the portion of layer IV with higher $GABA_A$ receptor densities in macaque than in human V1.

We found a bilaminar distribution pattern of the $GABA_A$/BZ binding sites in human area V1 with the highest density in layer IVC, somewhat lower but still high densities in layers III–IVA, and the lowest densities in layers IVB and V–VI (**Figure 11**). This is comparable with autoradiographic measurements in V1 of macaque monkeys (Rakic et al., 1988), with the exception of the intermediate to high density in the upper part of macaque layer VI. To resolve the divergent finding of this layer VI band in macaque in contrast to human V1, where it is not visible, we labeled the $GABA_A$/BZ binding sites in V1 of both species. **Figure 11** shows that indeed the thin band with high binding site density in layer VI as described by Rakic et al. (1988) is caused by a species difference, since it is present in macaque but not in human V1.

The calcium-binding proteins parvalbumin, calbindin and calretinin label almost exclusively inhibitory GABAergic interneurons in the macaque visual cortex (Van Brederode et al., 1990; DeFelipe et al., 1999a; Disney and Aoki, 2008; Kooijmans et al., 2014). These interneurons with their rich axonal arborization account for more than 90% of the inhibitory cells in the primate cerebral cortex (DeFelipe et al., 1999a; Disney and Aoki, 2008), and are layer-specifically distributed (Van Brederode et al., 1990; Shaw et al., 1991; Lund and Wu, 1997; Disney and Aoki, 2008; Kooijmans et al., 2014). Since GABAergic signal processing requires GABA receptors, and GABAergic interneurons often synapse in their near surrounding (Lund and Wu, 1997), the preferential localization of GABAergic interneurons in the supragranular and granular strata (Fitzpatrick et al., 1987; Lund, 1987; Lund et al., 1988; Lund and Yoshioka, 1991; Lund and Wu, 1997) may be correlated with that of GABA receptors. The present laminar-specific data on $GABA_A$ and $GABA_A$/BZ binding sites in the supragranular and granular strata clearly supports this hypothesis (**Figures 10C**, **11**). The particularly large divergence of the laminar densities of these receptor types between the supragranular and granular strata of V1 (high densities) on the one hand, and its infragranular stratum (low densities) on the other sites demonstrates the preferential laminar localization of these inhibitory receptor types in the primate cortex (also see **Figure 3**).

The inhibitory $GABA_A$ receptors are activated by the agonist muscimol. [^{3}H]muscimol binds at the orthosteric α1/β2 subunit interface and interacts with the receptor via a high-affinity binding site. The α1 subunit has a strong influence on all binding properties, including desensitization, while the β2 subunit has minor impact (Baur and Sigel, 2003). The subunit composition of the functional $GABA_A$ receptor in the cerebral cortex is almost unknown, but it has been shown that probably all $GABA_A$ receptors contain α1, β and γ subunits (Huntsman et al., 1994). The α1 subunit of the $GABA_A$ receptor is the most frequent subunit. The highest density of this subunit was found in layer IVC of the primary visual cortex, while layers II–III and IVA show a homogeneous somewhat lower density than layer IVC. The distribution of the β2 subunit is similar to that of the α1 subunit. Layers I and IVB have low, layers II–III moderate, and layers IVA and IVC high densities of the β2 subunit. Sublayer IVCβ shows a very high density in its upper part and lower density in its deeper part. Layers V and VI have very low densities, with only slightly higher values in layer V (Huntsman et al., 1994). The laminar distribution of α1 and β2 subunits is therefore comparable to the strata-specific distribution of the [^{3}H] muscimol binding to the $GABA_A$ receptor as found in the present observations. In area 3b of the primary somatosensory cortex, the present findings of the laminar distribution of $GABA_A$ and $GABA_B$ receptors (highest in superficial layers) are also consistent with previous reports in the macaque monkey (Rakic et al., 1988; Shaw et al., 1991).

The α_1 receptor reaches highest densities in layers I–II of human V1, moderate values in upper layer III. Lowest receptor densities are found in layers IVA–IVC and VI. Layer V shows a density intermediate between layers III and VI. The macaque V1 shows a very similar laminar distribution pattern (Rakic et al., 1988). The 5-HT_2 receptors reach relatively high densities in layers III and IVa of human V1, followed by a slightly lower but still high density in layer IVC. Thus, two bands of high receptor densities are present in human V1. Lowest values are found in layers V–VI, whereas layers I–II and IVB have moderate

densities. These findings are comparable to the laminar pattern in macaque V1 (Rakic et al., 1988).

Whereas most receptors show a parallel course of the mean areal densities and the layer-specific densities, the nicotinic $\alpha_4\beta_2$ receptor is a notable exception. In all three primary sensory areas, this receptor displayed distinctly higher maxima in the granular stratum exceeding those of other strata and of mean areal densities (**Figure 3**). Thus, the predominant input layer of primary sensory cortices seems to be under a strong modulatory influence of this cholinergic receptor type. The granular strata of some visual areas also had higher M_2, α_2 and 5-HT_2 receptor densities than the supragranular strata. This complements from a molecular point of view the exceptional cytoarchitectonic differentiation and thickness of the granular layer in the visual cortical areas of the human cortex, particularly in V1. Furthermore, our present finding of generally higher receptor densities in the supragranular than in the infragranular layers of most cortical areas is supported by a comparable laminar relation of synapse numbers (Huttenlocher and Dabholkar, 1997; DeFelipe et al., 1999b), if the density of all receptors in a cortical area and layer are correlated with the number of synapses (for further details see "Discussion" in "Sizes of Absolute Receptor Fingerprints Reveal Regional and Laminar Heterogeneity of Receptor Densities" Sections, and Rakic et al., 1986, 1994).

Multi-Receptor Fingerprints of Cortical Areas and Layers Reflect Principle Aspects of Functional Organization

Since all cortical layers expressed all receptor types studied here, we analyzed the aspect of multi-receptor expression by calculating receptor fingerprints, a major tool for characterizing the balance between receptor expressions in the different strata. Here, the densities of 15 different receptor types in each of the 44 areas with a brain-wide distribution were visualized separately for each stratum. The discriminant analyses demonstrated the regional inhomogeneity of the fingerprints averaged over all layers and separately for each of the three strata. The results of the subsequent pairwise comparisons between areas, which resulted in significant differences only for a subsample of pairs, is not surprising because only three brains could be included in the present study of 15 different receptors in 44 cortical areas and their three strata. An enlargement of the sample of brains is currently not possible due to practical limitations (shortage of adequate human brain tissue with short post mortem delay, technical difficulties associated with the serial sectioning of entire deep frozen and unfixed human hemispheres and the financial requirements for autoradiographical processing of thousands of sections). The size of the fingerprints, scaled by absolute mean areal or stratum-specific densities, reflects the sum of the densities of all receptors, and shows considerable regional variations. Since the absolute densities of AMPA, NMDA, $GABA_A$, $GABA_A$/BZ and $GABA_B$ receptors are much higher than those of all other receptor types, we additionally calculated normalized fingerprints. These normalized fingerprints also show a regional heterogeneity of multi-receptor expression both for the mean areal densities and the stratum-specific densities.

Sizes of Absolute Receptor Fingerprints Reveal Regional and Laminar Heterogeneity of Receptor Densities

The size of the absolute fingerprint of a cortical area is defined by the sum of the densities of all receptors measured in that area. Since we measured all receptor types in all areas, and the absolute fingerprints are identically scaled, the sizes of fingerprints enable a comparison of the densities (fmol mg/protein) between all 44 areas, and reveal area- as well as strata-specific differences, thus demonstrating the regional heterogeneity of receptor expression (**Figure 4**). In the supragranular stratum, the sum of the densities of all receptors is consistently larger throughout all areas than that of the granular stratum. The infragranular stratum reaches the lowest value. The largest fingerprints are found in the primary, secondary, and early visual areas, as well as in temporal and parietal multimodal association areas and area 11 of the orbitofrontal cortex, particularly in the supragranular stratum. The size of the fingerprints of the infragranular stratum is very low in the primary visual cortex, which stands out by an extremely large size of the fingerprint in its supragranular stratum. This is in contrast to the supra- vs. infragranular relation of the fingerprint sizes in the areas of the motor cortex and the Broca region, since these regions have very small sized supragranular fingerprints. In conclusion, the relation of the densities of all receptors can vary between supragranular and infragranular strata in a regionally and functionally dependent manner. The independent variation of receptor expression between both strata is further supported by the shape of the fingerprints, which addresses the balance between receptor types in a given area (see below).

The smallest fingerprints are found in the primary motor cortex area 4 (as previously described in Zilles et al., 2015a) and motor area 6. Accordingly, by also studying the premotor cortex, our previous conclusion based on a multi-receptor fingerprint analysis in the primary motor cortex of a partly different brain sample can now be generalized for all motor areas, which show the lowest level of the sum of *all* receptor densities studied in the 44 cortical regions. The motor areas are followed by areas 44 and 45 of the Broca region. These results of a multi-receptor fingerprint analysis emphasize a special position of these language-related areas between language and motor function.

Interestingly, the motor and Broca areas are both highly myelinated in the adult brain (Hopf, 1956), thus potentially causing a higher quenching of the tritium-based β-radiation (Rakic et al., 1988; Zilles et al., 1990), which may lead to an underestimation of actual receptor densities in these areas. However, highest myelination levels were reported for area 41 and 42 and the fusiform gyrus, and much lower levels for area 38 and 20 (Hopf, 1955), but the size of fingerprints of these areas shows a sequence from large to small sizes of fingerprint which does not reflect the myelination degree; e.g., area 38 has small areal and laminar fingerprint sizes, but a low myelination level. Furthermore, the sparsely myelinated area 20 has a fingerprint size above the average. Moreover, the fingerprint size of area 20 is well comparable to that of the highly myelinated areas 41 and 42. Therefore, the regional myelination levels vary independently from those of receptor densities. Since

myelinated fibers do not have synaptic contacts on the surface of the myelin sheaths, and therefore do not express transmitter receptors along their course through a cortical area, a higher portion of cortical tissue in these areas is free of receptors compared to areas with lower content of myelinated fibers. This may better explain the regional and laminar heterogeneity of the sizes of absolute fingerprints and the low levels total sum of the densities of all receptors in these particular regions than a general quenching effect. The density in the granular stratum of V1 is averaged over the sublayers IVa–IVc, including the heavily myelinated layer IVb. Thus, the issue of quenching is also relevant for all data from the granular stratum of V1, and may be underestimated. However, the potential quenching effect apparently did not severely influence the clustering of the granular stratum of V1 as a whole, because layer IVb contributes by only about a third of the size of the granular stratum, and it is found in the same cluster as other granular stratum-specific data in all other cortical areas with a distinct layer IV.

In general, unimodal sensory areas show a higher inter-laminar divergence of total receptor densities than multimodal association areas. This suggests a greater difference of receptor-mediated processing mechanisms between the cortical layers in the unimodal sensory areas, particularly in the primary visual cortex, compared to multimodal association areas.

The principal differences in the total densities of all receptors in a cortical area may be associated with the different prevailing connections of cortical layers. Whereas the supragranular strata are preferred by cortical-cortical connections, the granular stratum is that of thalamo-cortical and lateral connections, and the infragranular stratum gives raise mainly to subcortical projections (Rockland and Pandya, 1979; Kennedy and Bullier, 1985; Felleman and Van Essen, 1991; Rockland and Van Hoesen, 1994; Rockland, 1997, 2015; Hupé et al., 1998; Barone et al., 2000; Ekstrom et al., 2008; Sincich et al., 2010; Markov and Kennedy, 2013; Markov et al., 2014). Thus, these different connectivity patterns may be paralleled by different receptor expression levels in the cortical strata. Furthermore, the branching of the apical dendrites is maximal in the supragranular stratum compared to the other strata (Lund et al., 1981; Katz, 1987; Hübener et al., 1990). The number of synapses shows a comparable trend (Rakic et al., 1986, 1994). The similar laminar distribution of the number of synapses and the density of receptors is further supported by reports which demonstrated their parallel development during brain maturation (Rakic et al., 1986, 1994). Thus, the stratum-specific proportion between the sizes of receptor fingerprints may also indicate a comparable laminar distribution of the total number of synapses in a given cortical area.

Shape of Receptor Fingerprints

In contrast to the absolute size of fingerprints, which is caused by the total density of all receptors in a given area, the shape of a fingerprint reflects the balance between the different receptors in an area. Since the absolute fingerprints are based on the same scaling of the densities of all receptors, the peculiarities of modulatory receptors are difficult to recognize by visual inspection, because their absolute densities are lower than those of the GABAergic receptors, sometimes by two orders of magnitude. Therefore, we additionally calculated normalized fingerprints.

E.g., the high M_2 receptor density compared to those of all other receptors in the visual cortex, particularly in V1, is reflected by the shapes of their normalized fingerprints. i.e., V1 contains the highest M_2 receptor density of all areas examined here. Thus, the impact of the M_2 receptor on the specific shape of a fingerprint, and possibly on the balance between all receptors, is relatively the highest in V1. Also the contribution of α_2 receptors on the shape of the fingerprint clearly stands out in all primary sensory areas when compared to the other receptors in these areas. Additionally, the above mentioned high absolute density of the nicotinic $\alpha_4\beta_2$ receptor in the granular stratum of the primary somatosensory and auditory areas is well recognizable in the normalized fingerprint. Another example is also the high relative density of α_1 receptors in all three strata of the premotor cortex. This suggests that the influence of this receptor is the highest in this area compared to the other areas examined here. A further exceptional position is observed for the M_3 receptor in the inferior parietal area PGp (Supplementary Figure S2). In conclusion, the normalized fingerprints clearly demonstrate locally specific roles of certain receptor types which lead to different balances between the receptors in the here studied areas and possibly to such different balances in all other regions of the cerebral cortex. That is a hint to a regional specificity of the receptor-mediated mechanisms of information processing.

Since both the different sizes and shapes of fingerprints reflect the regional and stratum-specific balances between receptors, a multidimensional scaling analysis of the fingerprints was performed. It shows that each stratum and each area have a characteristic fingerprint and thus, specific levels of total receptor densities and balances between the receptors (**Figure 5**). This analysis shows that the fingerprints of the three strata of all areas form three different clusters. This result supports our interpretation above that the stratum-specific information processing is based on different balances between the receptors. The separation between the clusters of the three strata is nearly perfect, and their fingerprints do not overlap in the multidimensional scaling analysis.

Only exceptions from this general finding are the positions of the fingerprints of the granular stratum in motor areas 4 and 6, which are shifted into the range of the infragranular cluster, and the concomitant shift of the supragranular fingerprints into the granular cluster. This shift of stratum-specific fingerprints of areas 4 and 6 to the "wrong" clusters may be caused by the method with which we defined the position of their layer IV (see "Materials and Methods" Section). In the vast majority of the literature, areas 4 and 6 are described as being agranular, i.e., lacking a layer IV (Brodmann, 1909). However, recent observations using Nissl and immunohistochemical stainings demonstrated the occurrence of layer IV cells in the primary motor cortex of rhesus monkeys (García-Cabezas and Barbas, 2014; Barbas and García-Cabezas, 2015), and led to the statement that motor areas do not lack a layer IV. Since we could not identify by visual inspection a clearly recognizable layer IV

in either area, we tried to define such a layer at the border between layers III and V by its topography as a band occupying 3% of the total cortical depth. This width was derived from data of von Economo and Koskinas (1925), who described the width of layer IV as being approximately this size in the rostrally adjacent frontal areas. This formal definition of a layer IV in the motor areas is, however, different from the identification of such a layer in all other areas (except for area 24) examined here, where we can clearly detect a thinner or broader (granular cortex) layer of small round cells ("granular" cells) not, or only to a minor degree, intermingled with pyramidal cells (dysgranular cortex). Since the fingerprints of supragranular and granular strata of areas 4 and 6 are shifted to the clusters of the granular and infragranular strata, respectively, our multidimensional scaling analysis is thus a hint to a receptor expression pattern of the granular stratum in these areas completely different from the patterns in other cortical regions. Thus, the question remains whether this is a specificity of the motor areas, or these areas do not have a granular stratum comparable to those of all other isocortical regions. The supragranular fingerprints of areas 44 and 45 are also shifted into the cluster of the fingerprints of the granular stratum, though only slightly.

The separation of the layer-specific fingerprints further supports the existence of the above discussed divergence of receptor supported processing mechanisms between the three strata. The principal separation of the layers by their receptor fingerprints does not exclude a vertically organized interaction between the layers according to the concept of functional columns. Rather, it emphasizes that the stratum-specific receptor balances occurring at the different levels of a column are embedded in a vertically organized interaction which enables the area-specific functions.

The degree of similarity between the fingerprints of the three strata and of all layers together was analyzed by hierarchical cluster analyses which revealed a considerable regional heterogeneity, but also some notable general rules. Early visual areas were clearly separated from the rest of the cortex if we focus on the supragranular stratum and on all layers together, thus emphasizing similar receptor balances in this stratum over all these areas. The analysis of the fingerprints of the granular stratum emphasizes the exceptional organization of layer IV in V1 and the similaritiy of these fingerprints in the ventral visual stream in contrast to the dorsal visual stream, since areas V3d and V3A are clearly separated from the cluster of the ventral stream areas. The infragranular stratum does not separate dorsal and ventral stream areas from each other. Therefore, we can conclude, that organizational principles of the visual cortex (primary vs. higher unimodal sensory areas; ventral vs. dorsal stream areas) are recognizable by the fingerprints, but to different degrees in the different strata. A further general finding was the close similarity of the receptor fingeprints of the primary and secondary somatosensory and auditory areas. This is most clearly seen in the supra- and infragranular strata, as well as in the fingerprints of all layers together. This leads again to the conclusion that primary and secondary sensory areas are clearly different from higher unimodal or multimodal cortices by their receptor balances. As discussed above, specific receptor types (M_2, nicotinic $\alpha_4\beta_2$, noradrenergic α_2, and serotonergic 5-HT_2) play an important role here for the special position of particularly primary secondary areas. Although the function of the single receptor types has been intensely studied, the here important aspect of the role of the different receptor types within the cortical microcircuitry is, however, presently largely unknown. Our results on strata- and area-specific fingerprints and their relationships to general classification schemes of the cortex may be seen as a stimulus to study the specific functional role of these recepotr types in a systemic environment. Beside the distinct position of primary and early sensory unimodal areas, it must be emphasized that also the separation of the cluster of all prefrontal areas (analyses of all strata and all layers together) from other multimodal association areas with separate clusters for the infraparietal and temporal regions is a strong hint to the analytical potential of the hierarchical receptor fingerprint analysis as a tool to understand principal rules of cortical segregation also in higher functional and multimodal systems.

It is remarkable that the receptor fingerprints of the primary somatosensory area 3b and the primary auditory cortex (area 41) are very similar and cluster together, while both fingerprints largely differ from that of the primary visual cortex V1. Therefore, fingerprints seem to reflect differences in modalities of sensory systems. The similarity of the fingerprints of areas 41 and 3b may be explained by their similar functional properties, i.e., mechanoreception, whereas the input in V1 is clearly different. Thus, V1 has to comply with different functional requirements compared to the auditory and somatosensory systems. Comparable differences can also be found for the unimodal sensory areas and their fingerprints. The fingerprint of area 2 (somatosensory cortex) is very similar to that of area 42 (secondary auditory cortex), and both clearly differ from the fingerprint of the secondary visual cortex V2. Finally, the fingerprints of areas 44 and 45, which are subdivisions of Broca's language region, consistently cluster together in all strata and in the entire cortical width. All these findings suggest a modality-specific component of the shape of receptor fingerprints.

The different levels of branching are indicated in the hierarchical cluster analyses. The highest possible number of clusters after k-means analysis was determined. All areas belonging to the same cluster in the supragranular, granular or infragranular strata, as well as to a cluster defined at the level of the mean over all layers are then labeled with the identical color. The resulting map indicates a subdivision of the cortex based on the similarity or dissimilarity of the regional-specific fingerprints in the different strata or entire areas. These maps are remarkable similar, since they assign in most cases the same areas to one cluster irrespective of the stratum in which the fingerprints have been yielded. Notably, the clusters comprise neighboring areas in many cases, but it must be emphasized, that the criterion of topographical neighborhood expresses at the same time a grouping of the areas according to different modalities or

principal classifications into primary sensory, motor or higher multimodal association areas. Interestingly, area 38 does not cluster with the other multimodal temporal areas, but with areas on the supramarginal gyrus (PFm, PFt) and with the temporo-occipital transition zone (areas 37B, 37L, 37M). The latter areas have been attributed to the language network of Wernicke's region (Mesulam et al., 2015). Therefore, the clustering of the fingerprint of area 38 with other language regions may be explained by the special position of this area within the larger language system based on its role in object naming (Mesulam et al., 2013). Also areas 44 and 45 of the Broca region are consistently found in an own cluster, and segregate from neighboring areas of the premotor, lateral prefrontal, orbitofrontal and frontopolar cortices. A clear segregation is also found between anterior cingulate areas 32 and 24, which are often merged in functional imaging studies. The fingerprints clearly argue against this merging, this is corroborated by more detailed cyto- and receptorarchitectonic studies (Palomero-Gallagher et al., 2008). Finally, the higher visual areas FG1 and FG2 are found in separate clusters compared to the early visual areas. This supports the results of an early study focused on these two areas of the fusiform gyrus (Caspers et al., 2015) at the level of single strata.

In conclusion, the present results provide evidence for the fact that the regional and laminar heterogeneity of multi-receptor expression patterns in the cerebral cortex is not random. Rather, transmitter receptor densities vary sytematically between cortical areas depending on the functional networks, or subdivisions thereof, to which they can be assigned. Furthermore, a general canonical sequence of densities from highest values in the supragranular stratum, intermediate values in the granular layer IV, and lowest values in the infragranular stratum is found in most areas, and for most receptor types. The stratum-specific differences in the patterns of multi-receptor balances, point at divergent receptor supported processing mechanisms between the three strata. Finally, area- and stratum-specific multi-receptor expression patterns (i.e., receptor fingerprints) reflect the segregation of the cerebral cortex into functionally and topographically definable groups of cortical areas (visual, auditory, somatosensory, limbic, motor), and reveal their hierarchical position (primary and unimodal (early) sensory to higher sensory and finally to multimodal association areas) within sensory systems.

ETHICS STATEMENT

This study was carried out in accordance with the recommendations of "Experimentelle wissenschaftliche Studien an Gewebeproben von Gehirnen und Organen von Körperspendern, Ethics Committee of the Medical Faculty of the Heinrich-Heine University Düsseldorf" with written informed consent from all subjects. All subjects gave written informed consent in accordance with the Declaration of Helsinki. The protocol was approved by the "Ethics Committee of the Medical Faculty of the Heinrich-Heine University Düsseldorf."

AUTHOR CONTRIBUTIONS

KZ and NP-G conceived of and designed the study, analyzed data, drafted the manuscript and figures. NP-G acquired data. KZ obtained funding.

ACKNOWLEDGMENTS

This project has received funding from the European Union's Horizon 2020 Framework Programme for Research and Innovation under Grant Agreement No. 720270 (Human Brain Project SGA1).

SUPPLEMENTARY MATERIAL

The Supplementary Material for this article can be found online at: http://journal.frontiersin.org/article/10.3389/fnana.2017.00078/full#supplementary-material

REFERENCES

Amunts, K., Lenzen, M., Friederici, A. D., Schleicher, A., Morosan, P., Palomero-Gallagher, N., et al. (2010). Broca's region: novel organizational principles and multiple receptor mapping. *PLoS Biol.* 8:e1000489. doi: 10.1371/journal.pbio.1000489

Amunts, K., Malikovic, A., Mohlberg, H., Schormann, T., and Zilles, K. (2000). Brodmann's areas 17 and 18 brought into stereotaxic space—where and how variable? *Neuroimage* 11, 66–84. doi: 10.1006/nimg.1999.0516

Amunts, K., Schleicher, A., Bürgel, U., Mohlberg, H., Uylings, H. B. M., and Zilles, K. (1999). Broca's region revisited: cytoarchitecture and intersubject variability. *J. Comp. Neurol.* 412, 319–341. doi: 10.1002/(sici)1096-9861(19990920)412:2<319::aid-cne10>3.0.co;2-7

Amunts, K., and Zilles, K. (2015). Architectonic mapping of the human brain beyond brodmann. *Neuron* 88, 1086–1107. doi: 10.1016/j.neuron.2015.12.001

Annese, J., Pitiot, A., Dinov, I. D., and Toga, A. W. (2004). A myelo-architectonic method for the structural classification of cortical areas. *Neuroimage* 21, 15–26. doi: 10.1016/j.neuroimage.2003.08.024

Barbas, H., and García-Cabezas, M. Á. (2015). Motor cortex layer 4: less is more. *Trends Neurosci.* 38, 259–261. doi: 10.1016/j.tins.2015.03.005

Barone, P., Batardiere, A., Knoblauch, K., and Kennedy, H. (2000). Laminar distribution of neurons in extrastriate areas projecting to visual areas V1 and V4 correlates with the hierarchical rank and indicates the operation of a distance rule. *J. Neurosci.* 20, 3263–3281.

Baur, R., and Sigel, E. (2003). On high- and low-affinity agonist sites in $GABA_A$ receptors. *J. Neurochem.* 87, 325–332. doi: 10.1046/j.1471-4159.2003.01982.x

Bludau, S., Eickhoff, S. B., Mohlberg, H., Caspers, S., Laird, A. R., Fox, P. T., et al. (2014). Cytoarchitecture, probability maps and functions of the human frontal pole. *Neuroimage* 93, 260–275. doi: 10.1016/j.neuroimage.2013.05.052

Brodmann, K. (1909). *Vergleichende Lokalisationslehre der Großhirnrinde in ihren Prinzipien dargestellt auf Grund des Zellbaues.* Leipzig: Johann Ambrosius Barth.

Carlson, M. D., Penney, J. B. Jr., and Young, A. B. (1993). NMDA, AMPA, and benzodiazepine binding site changes in Alzheimer's disease visual cortex. *Neurobiol. Aging* 14, 343–352. doi: 10.1016/0197-4580(93)90120-z

Caspers, S., Geyer, S., Schleicher, A., Mohlberg, H., Amunts, K., and Zilles, K. (2006). The human inferior parietal cortex: cytoarchitectonic parcellation and interindividual variability. *Neuroimage* 33, 430–448. doi: 10.1016/j.neuroimage.2006.06.054

Caspers, J., Palomero-Gallagher, N., Caspers, S., Schleicher, A., Amunts, K., and Zilles, K. (2015). Receptor architecture of visual areas in the face and word-form recognition region of the posterior fusiform gyrus. *Brain Struct. Funct.* 220, 205–219. doi: 10.1007/s00429-013-0646-z

Caspers, S., Schleicher, A., Bacha-Trams, M., Palomero-Gallagher, N., Amunts, K., and Zilles, K. (2013). Organization of the human inferior parietal lobule based on receptor architectonics. *Cereb. Cortex* 23, 615–628. doi: 10.1093/cercor/bhs048

Caspers, J., Zilles, K., Eickhoff, S. B., Schleicher, A., Mohlberg, H., and Amunts, K. (2013). Cytoarchitectonical analysis and probabilistic mapping of two extrastriate areas of the human posterior fusiform gyrus. *Brain Struct. Funct.* 218, 511–526. doi: 10.1007/s00429-012-0411-8

Cortés, R., Probst, A., and Palacios, J. M. (1987). Quantitative light microscopic autoradiographic localization of cholinergic muscarinic receptors in the human brain: forebrain. *Neuroscience* 20, 65–107. doi: 10.1016/0306-4522(87)90006-6

Cortés, R., Probst, A., Tobler, H. J., and Palacios, J. M. (1986). Muscarinic cholinergic receptor subtypes in the human brain. II. Quantitative autoradiographic studies. *Brain Res.* 362, 239–253. doi: 10.1016/0006-8993(86)90449-x

DeFelipe, J., González-Albo, M. C., Del Río, M. R., and Elston, G. N. (1999a). Distribution and patterns of connectivity of interneurons containing calbindin, calretinin, and parvalbumin in visual areas of the occipital and temporal lobes of the macaque monkey. *J. Comp. Neurol.* 412, 515–526. doi: 10.1002/(sici)1096-9861(19990927)412:3<515::aid-cne10>3.0.co;2-1

DeFelipe, J., Marco, P., Busturia, I., and Merchan-Perez, A. (1999b). Estimation of the number of synapses in the cerebral cortex: methodological considerations. *Cereb. Cortex* 9, 722–732. doi: 10.1093/cercor/9.7.722

DeFelipe, J., López-Cruz, P. L., Benavides-Piccione, R., Bielza, C., Larrañaga, P., Anderson, S., et al. (2013). New insights into the classification and nomenclature of cortical GABAergic interneurons. *Nat. Rev. Neurosci.* 14, 202–216. doi: 10.1038/nrn3444

Disney, A. A., and Aoki, C. (2008). Muscarinic acetylcholine receptors in macaque V1 are most frequently expressed by parvalbumin-immunoreactive neurons. *J. Comp. Neurol.* 507, 1748–1762. doi: 10.1002/cne.21616

Eickhoff, S. B., Rottschy, C., Kujovic, M., Palomero-Gallagher, N., and Zilles, K. (2008). Organizational principles of human visual cortex revealed by receptor mapping. *Cereb. Cortex* 18, 2637–2645. doi: 10.1093/cercor/bhn024

Eickhoff, S. B., Schleicher, A., Scheperjans, F., Palomero-Gallagher, N., and Zilles, K. (2007). Analysis of neurotransmitter receptor distribution patterns in the cerebral cortex. *Neuroimage* 34, 1317–1330. doi: 10.1016/j.neuroimage.2006.11.016

Ekstrom, L. B., Roelfsema, P. R., Arsenault, J. T., Bonmassar, G., and Vanduffel, W. (2008). Bottom-up dependent gating of frontal signals in early visual cortex. *Science* 321, 414–417. doi: 10.1126/science.1153276

Felleman, D. J., and Van Essen, D. C. (1991). Distributed hierarchical processing in the primate cerebral cortex. *Cereb. Cortex* 1, 1–47. doi: 10.1093/cercor/1.1.1

Fitzpatrick, D., Lund, J. S., Schmechel, D. E., and Towles, A. C. (1987). Distribution of GABAergic neurons and axon terminals in the macaque striate cortex. *J. Comp. Neurol.* 264, 73–91. doi: 10.1002/cne.902640107

Gallyas, F. (1979). Silver staining of myelin by means of physical development. *Neurol. Res.* 1, 203–209. doi: 10.1080/01616412.1979.11739553

García-Cabezas, M. Á., and Barbas, H. (2014). Area 4 has layer IV in adult primates. *Eur. J. Neurosci.* 39, 1824–1834. doi: 10.1111/ejn.12585

Garraghty, P. E., Arnold, L. L., Wellman, C. L., and Mowery, T. M. (2006). Receptor autoradiographic correlates of deafferentation-induced reorganization in adult primate somatosensory cortex. *J. Comp. Neurol.* 497, 636–645. doi: 10.1002/cne.21018

Geyer, S., Ledberg, A., Schleicher, A., Kinomura, S., Schormann, T., Bürgel, U., et al. (1996). Two different areas within the primary motor cortex of man. *Nature* 382, 805–807. doi: 10.1038/382805a0

Geyer, S., Matelli, M., Luppino, G., Schleicher, A., Jansen, Y., Palomero-Gallagher, N., et al. (1998). Receptor autoradiographic mapping of the mesial motor and premotor cortex of the macaque monkey. *J. Comp. Neurol.* 397, 231–250. doi: 10.1002/(sici)1096-9861(19980727)397:2<231::aid-cne6>3.0.co;2-1

Geyer, S., Schleicher, A., and Zilles, K. (1999). Areas 3a, 3b, and 1 of human primary somatosensory cortex. 1. Microstructural organization and interindividual variability. *Neuroimage* 10, 63–83.

Graebenitz, S., Kedo, O., Speckmann, E.-J., Gorji, A., Panneck, H., Hans, V., et al. (2011). Interictal-like network activity and receptor expression in the epileptic human lateral amygdala. *Brain* 134, 2929–2947. doi: 10.1093/brain/awr202

Grefkes, C., Geyer, S., Schormann, T., Roland, P., and Zilles, K. (2001). Human somatosensory area 2: observer-independent cytoarchitectonic mapping, interindividual variability, and population map. *Neuroimage* 14, 617–631. doi: 10.1006/nimg.2001.0858

Haug, H., Kuhl, S., Mecke, E., Sass, N. L., and Wasner, K. (1984). The significance of morphometric procedures in the investigation of age changes in cytoarchitectonic structures of human brain. *J. Hirnforsch* 25, 353–374.

Hopf, A. (1955). Über die verteilung myeloarchitektonischer merkmale in der isokortikalen schläfenlappenrinde beim menschen. *J. Hirnforsch* 2, 36–54.

Hopf, A. (1956). Über die verteilung myeloarchitektonischer merkmale in der stirnhirnrinde beim menschen. *J. Hirnforsch* 2, 311–333.

Hoyer, D., Pazos, A., Probst, A., and Palacios, J. M. (1986a). Seroronin receptors in the human brain: II. Characterization and autoradiographic localization of 5-HT_{1C} and 5-HT_2 recognition sites. *Brain Res.* 376, 97–107. doi: 10.1016/0006-8993(86)90903-0

Hoyer, D., Pazos, A., Probst, A., and Palacios, J. M. (1986b). Serotonin receptors in the human brain: I. Characterization and autoradiographic localization of 5-HT_{1A} recognition sites. Apparent absence of 5-HT_{1B} recognition sites. *Brain Res.* 376, 85–86. doi: 10.1016/0006-8993(86)90902-9

Hubel, D. H., and Wiesel, T. N. (1968). Receptive fields and functional architecture of monkey striate cortex. *J. Physiol.* 195, 215–243. doi: 10.1113/jphysiol.1968.sp008455

Hubel, D. H., and Wiesel, T. N. (1969). Anatomical demonstration of columns in the monkey striate cortex. *Nature* 221, 747–750. doi: 10.1038/221747a0

Hübener, M., Schwarz, C., and Bolz, J. (1990). Morphological types of projection neurons in layer 5 of cat visual cortex. *J. Comp. Neurol.* 301, 655–674. doi: 10.1002/cne.903010412

Huntsman, M. M., Isackson, P. J., and Jones, E. G. (1994). Lamina-specific expression and activity-dependent regulation of seven $GABA_A$ receptor subunit mRNAs in monkey visual cortex. *J. Neurosci.* 14, 2236–2259.

Hupé, J. M., James, A. C., Payne, B. R., Lomber, S. G., Girard, P., and Bullier, J. (1998). Cortical feedback improves discrimination between figure and background by V1, V2 and V3 neurons. *Nature* 394, 784–787. doi: 10.1038/29537

Huttenlocher, P. R., and Dabholkar, A. S. (1997). Regional differences in synaptogenesis in human cerebral cortex. *J. Comp. Neurol.* 387, 167–178. doi: 10.1002/(sici)1096-9861(19971020)387:2<167::aid-cne1>3.0.co;2-z

Jansen, K. L., Faull, R. L. M., and Dragunow, M. (1989). Excitatory amino acid receptors in the human cerebral cortex: a quantitative autoradiographic study comparing the distributions of TCP, [^{3}H]glycine, L-[^{3}H]-glutamate, [^{3}H]AMPA and [^{3}H]kainic acid binding sites. *Neuroscience* 32, 587–607. doi: 10.1016/0306-4522(89)90282-0

Jiang, X., Shen, S., Cadwell, C. R., Berens, P., Sinz, F., Ecker, A. S., et al. (2015). Principles of connectivity among morphologically defined cell types in adult neocortex. *Science* 350:aac9462. doi: 10.1126/science.aac9462

Jones, E. G. (1986). "Connectivity of the primate sensory-motor cortex," in *Cerebral Cortex*, eds E. G. Jones and A. Peters (New York, NY: Plenum), 113–183.

Katz, L. C. (1987). Local circuitry of identified projection neurons in cat visual cortex brain slices. *J. Neurosci.* 7, 1223–1249.

Kennedy, H., and Bullier, J. (1985). A double-labeling investigation of the afferent connectivity to cortical areas V1 and V2 of the macaque monkey. *J. Neurosci.* 5, 2815–2830.

Kooijmans, R. N. (2016). *Inhibitory Interneurons of Macaque Primary Visual Cortex [dissertation]*. Amsterdam, AN: Vrije Universiteit Amsterdam.

Kooijmans, R. N., Self, M. W., Wouterlood, F. G., Beliën, J. A., and Roelfsema, P. R. (2014). Inhibitory interneuron classes express complementary AMPA-receptor

patterns in macaque primary visual cortex. *J. Neurosci.* 34, 6303–6315. doi: 10.1523/JNEUROSCI.3188-13.2014

Kujovic, M., Zilles, K., Malikovic, A., Schleicher, A., Mohlberg, H., Rottschy, C., et al. (2013). Cytoarchitectonic mapping of the human dorsal extrastriate cortex. *Brain Struct. Funct.* 218, 157–172. doi: 10.1007/s00429-012-0390-9

Lowry, O. H., Rosebrough, N. J., Farr, A. L., and Randall, R. J. (1951). Protein measurement with the folin phenol reagent. *J. Biol. Chem.* 193, 265–275.

Lund, J. S. (1987). Local circuit neurons of macaque monkey striate cortex: I. Neurons of laminae 4C and 5A. *J. Comp. Neurol.* 257, 60–92. doi: 10.1002/cne.902570106

Lund, J. S., Hawken, M. J., and Parker, A. J. (1988). Local circuit neurons of macaque monkey striate cortex: II. Neurons of laminae 5B and 6. *J. Comp. Neurol.* 276, 1–29. doi: 10.1002/cne.902760102

Lund, J. S., Hendrickson, A. E., Ogren, M. P., and Tobin, E. A. (1981). Anatomical organization of primate visual cortex area VII. *J. Comp. Neurol.* 202, 19–45. doi: 10.1002/cne.902020104

Lund, J. S., and Wu, C. Q. (1997). Local circuit neurons of macaque monkey striate cortex: IV. Neurons of laminae 1-3A. *J. Comp. Neurol.* 384, 109–126. doi: 10.1002/(sici)1096-9861(19970721)384:1<109::aid-cne7>3.0.co;2-5

Lund, J. S., and Yoshioka, T. (1991). Local circuit neurons of macaque monkey striate cortex: III. Neurons of laminae 4B, 4A, and 3B. *J. Comp. Neurol.* 311, 234–258. doi: 10.1002/cne.903110206

Markov, N. T., and Kennedy, H. (2013). The importance of being hierarchical. *Curr. Opin. Neurobiol.* 23, 187–194. doi: 10.1016/j.conb.2012.12.008

Markov, N. T., Vezoli, J., Chameau, P., Falchier, A., Quilodran, R., Huissoud, C., et al. (2014). Anatomy of hierarchy: feedforward and feedback pathways in macaque visual cortex. *J. Comp. Neurol.* 522, 225–259. doi: 10.1002/cne.23458

Markram, H., Toledo-Rodriguez, M., Wang, Y., Gupta, A., Silberberg, G., and Wu, C. (2004). Interneurons of the neocortical inhibitory system. *Nat. Rev. Neurosci.* 5, 793–807. doi: 10.1038/nrn1519

Mash, D. C., White, W. F., and Mesulam, M. M. (1988). Distribution of muscarinic receptor subtypes within architectonic subregions of the primate cerebral cortex. *J. Comp. Neurol.* 278, 265–274. doi: 10.1002/cne.902780209

Merker, B. (1983). Silver staining of cell bodies by means of physical development. *J. Neurosci. Methods* 9, 235–241. doi: 10.1016/0165-0270(83)90086-9

Mesulam, M. M., Thompson, C. K., Weintraub, S., and Rogalski, E. J. (2015). The Wernicke conundrum and the anatomy of language comprehension in primary progressive aphasia. *Brain* 138, 2423–2437. doi: 10.1093/brain/awv154

Mesulam, M. M., Wieneke, C., Hurley, R., Rademaker, A., Thompson, C. K., Weintraub, S., et al. (2013). Words and objects at the tip of the left temporal lobe in primary progressive aphasia. *Brain* 136, 601–618. doi: 10.1093/brain/aws336

Meyer, H. S., Wimmer, V. C., Oberlaender, M., de Kock, C. P., Sakmann, B., and Helmstaedter, M. (2010). Number and laminar distribution of neurons in a thalamocortical projection column of rat vibrissal cortex. *Cereb. Cortex* 20, 2277–2286. doi: 10.1093/cercor/bhq067

Mohan, H., Verhoog, M. B., Doreswamy, K. K., Eyal, G., Aardse, R., Lodder, B. N., et al. (2015). Dendritic and axonal architecture of individual pyramidal neurons across layers of adult human neocortex. *Cereb. Cortex* 25, 4839–4853. doi: 10.1093/cercor/bhv188

Morosan, P., Rademacher, J., Palomero-Gallagher, N., and Zilles, K. (2005). "Anatomical organization of the human auditory cortex: cytoarchitecture and transmitter receptors," in *Auditory Cortex—Towards a Synthesis of Human and Animal Research*, eds P. Heil, E. König and E. Budinger (New Jersey, NJ: Lawrence Erlbaum, Mahwah), 27–50.

Morosan, P., Rademacher, J., Schleicher, A., Amunts, K., Schormann, T., and Zilles, K. (2001). Human primary auditory cortex: cytoarchitectonic subdivisions and mapping into a spatial reference system. *Neuroimage* 13, 684–701. doi: 10.1006/nimg.2000.0715

Nieuwenhuys, R. (2013). The myeloarchitectonic studies on the human cerebral cortex of the Vogt-Vogt school and their significance for the interpretation of functional neuroimaging data. *Brain Struct. Funct.* 218, 303–352. doi: 10.1007/s00429-012-0460-z

Palomero-Gallagher, N., Amunts, K., and Zilles, K. (2015). "Transmitter receptor distribution in the human brain," in *Brain Mapping: An Encyclopedic Reference*, ed. A. W. Toga (San Diego, CA: Academic Press, Elsevier), 261–275.

Palomero-Gallagher, N., Mohlberg, H., Zilles, K., and Vogt, B. A. (2008). Cytology and receptor architecture of human anterior cingulate cortex. *J. Comp. Neurol.* 508, 906–926. doi: 10.1002/cne.21684

Palomero-Gallagher, N., Vogt, B. A., Schleicher, A., Mayberg, H. S., and Zilles, K. (2009). Receptor architecture of human cingulate cortex: evaluation of the four-region neurobiological model. *Hum. Brain Mapp.* 30, 2336–2355. doi: 10.1002/hbm.20667

Palomero-Gallagher, N., and Zilles, K. (2017a). Cortical layers: Cyto-, myelo-, receptor- and synaptic architecture in human cortical areas. *Neuroimage* doi: 10.1016/j.neuroimage.2017.08.035 [Epub ahead of print].

Palomero-Gallagher, N., and Zilles, K. (2017b). "Cyto- and receptorarchitectonic mapping of the human brain," in *Brain Banking Neurological and Psychiatric Disorders*, eds I. Huitinga and M. Webster (Elsevier),

Pazos, A., Probst, A., and Palacios, J. M. (1987a). Serotonin receptors in the human brain. III. Autoradiographic mapping of serotonin-1 receptors. *Neuroscience* 21, 97–122. doi: 10.1016/0306-4522(87)90326-5

Pazos, A., Probst, A., and Palacios, J. M. (1987b). Serotonin receptors in the human brain. IV. Autoradiographic mapping of serotonin-2 receptors. *Neuroscience* 21, 123–139. doi: 10.1016/0306-4522(87)90327-7

Rakic, P., Bourgeois, J. P., Eckenhoff, M. F., Zecevic, N., and Goldman-Rakic, P. S. (1986). Concurrent overproduction of synapses in diverse regions of the primate cerebral cortex. *Science* 232, 232–235. doi: 10.1126/science.3952506

Rakic, P., Bourgeois, J. P., and Goldman-Rakic, P. S. (1994). Synaptic development of the cerebral cortex: implications for learning, memory, and mental illness. *Prog. Brain Res.* 102, 227–243. doi: 10.1016/s0079-6123(08)60543-9

Rakic, P., Goldman-Rakic, P. S., and Gallager, D. (1988). Quantitative autoradiography of major neurotransmitter receptors in the monkey striate and extrastriate cortex. *J. Neurosci.* 8, 3670–3690.

Rockland, K. S. (1997). "Elements of cortical architecture," in *Extrastriate Cortex in Primates*, eds K. S. Rockland, J. H. Kaas and A. Peters (New York, NY: Plenum Press), 243–293.

Rockland, K. S. (2015). About connections. *Front. Neuroanat.* 9:61. doi: 10.3389/fnana.2015.00061

Rockland, K. S., and Pandya, D. N. (1979). Laminar origins and terminations of cortical connections of the occipital lobe in the rhesus monkey. *Brain Res.* 179, 3–20. doi: 10.1016/0006-8993(79)90485-2

Rockland, K. S., and Van Hoesen, G. W. (1994). Direct temporal-occipital feedback connections to striate cortex (V1) in the macaque monkey. *Cereb. Cortex* 4, 300–313. doi: 10.1093/cercor/4.3.300

Rottschy, C., Eickhoff, S. B., Schleicher, A., Mohlberg, H., Kujovic, M., Zilles, K., et al. (2007). Ventral visual cortex in humans: cytoarchitectonic mapping of two extrastriate areas. *Hum. Brain Mapp.* 28, 1045–1059. doi: 10.1002/hbm.20348

Scheperjans, F., Grefkes, C., Palomero-Gallagher, N., Schleicher, A., and Zilles, K. (2005a). Subdivisions of human parietal area 5 revealed by quantitative receptor autoradiography: a parietal region between motor, somatosensory, and cingulate cortical areas. *Neuroimage* 25, 975–992. doi: 10.1016/j.neuroimage.2004.12.017

Scheperjans, F., Palomero-Gallagher, N., Grefkes, C., Schleicher, A., and Zilles, K. (2005b). Transmitter receptors reveal segregation of cortical areas in the human superior parietal cortex: relations to visual and somatosensory regions. *Neuroimage* 28, 362–379. doi: 10.1016/j.neuroimage.2005.06.028

Scheperjans, F., Hermann, K., Eickhoff, S. B., Amunts, K., Schleicher, A., and Zilles, K. (2008). Observer-independent cytoarchitectonic mapping of the human superior parietal cortex. *Cereb. Cortex* 18, 846–867. doi: 10.1093/cercor/bhm116

Schleicher, A., Amunts, K., Geyer, S., Kowalski, T., Schormann, T., Palomero-Gallagher, N., et al. (2000). A stereological approach to human cortical architecture: identification and delineation of cortical areas. *J. Chem. Neuroanat.* 20, 31–47. doi: 10.1016/s0891-0618(00)00076-4

Shaw, C., Cameron, L., March, D., Cynader, M., Zielinski, B., and Hendrickson, A. (1991). Pre- and postnatal development of GABA receptors in *Macaca* monkey visual cortex. *J. Neurosci.* 11, 3943–3959.

Sherwood, C. C., Holloway, R. L., Erwin, J. M., Schleicher, A., Zilles, K., and Hof, P. R. (2004). Cortical orofacial motor representation in Old World monkeys, great, apes, and humans. I. Quantitative analysis of cytoarchitecture. *Brain Behav. Evol.* 63, 61–81. doi: 10.1159/000075672

Sincich, L. C., Jocson, C. M., and Horton, J. C. (2010). V1 interpatch projections to v2 thick stripes and pale stripes. *J. Neurosci.* 30, 6963–6974. doi: 10.1523/JNEUROSCI.5506-09.2010

Van Brederode, J. F., Mulligan, K. A., and Hendrickson, A. E. (1990). Calcium-binding proteins as markers for subpopulations of GABAergic neurons in monkey striate cortex. *J. Comp. Neurol.* 298, 1–22. doi: 10.1002/cne.902980102

Vogt, B. A., Hof, P. R., Zilles, K., Vogt, L. J., Herold, C., and Palomero-Gallagher, N. (2013). Cingulate area 32 homologies in mouse, rat, macaque and human: cytoarchitecture and receptor architecture. *J. Comp. Neurol.* 521, 4189–4204. doi: 10.1002/cne.23409

Vogt, C., and Vogt, O. (1919). Allgemeinere ergebnisse unserer hirnforschung. *J. Psychol. Neurol.* 25, 279–462.

von Economo, C., and Koskinas, G. N. (1925). *Die Cytoarchitektonik der Hirnrinde des Erwachsenen Menschen.* Wien, Berlin: Springer.

Wiesel, T. N., Hubel, D. H., and Lam, D. M. (1974). Autoradiographic demonstration of ocular-dominance columns in the monkey striate cortex by means of transneuronal transport. *Brain Res.* 79, 273–279. doi: 10.1016/0006-8993(74)90416-8

Xu, X., and Callaway, E. M. (2009). Laminar specificity of functional input to distinct types of inhibitory cortical neurons. *J. Neurosci.* 29, 70–85. doi: 10.1523/JNEUROSCI.4104-08.2009

Young, A. B., Dauth, G. W., Hollingsworth, Z., Penney, J. B., Kaatz, K., and Gilman, S. (1990). Quisqualate- and NMDA-sensitive [^{3}H]glutamate binding in primate brain. *J. Neurosci. Res.* 27, 512–521. doi: 10.1002/jnr.490270412

Zilles, K. (2005). "Evolution of the human brain and comparative cyto- and receptor architecture," in *From Monkey Brain to Human Brain*, eds S. Dehaene, J. R. Duhamel, M. D. Hauser and G. Rizzolatti (Cambridge, MA: MIT Press), 41–56.

Zilles, K., and Amunts, K. (2009). Receptor mapping: architecture of the human cerebral cortex. *Curr. Opin. Neurol.* 22, 331–339. doi: 10.1097/WCO.0b013e32832d95db

Zilles, K., Bacha-Trams, M., Palomero-Gallagher, N., Amunts, K., and Friederici, A. D. (2015a). Common molecular basis of the sentence comprehension network revealed by neurotransmitter receptor fingerprints. *Cortex* 63, 79–89. doi: 10.1016/j.cortex.2014.07.007

Zilles, K., Palomero-Gallagher, N., Bludau, S., Mohlberg, H., and Amunts, K. (2015b). "Cytoarchitecture and maps of the human cerebral cortex," in *Brain Mapping: An Encyclopedic Reference*, ed. A. W. Toga (Elsevier: Academic Press), 115–135.

Zilles, K., and Palomero-Gallagher, N. (2001). Cyto-, myelo-, and receptor architectonics of the human parietal cortex. *Neuroimage* 14, S8–S20. doi: 10.1006/nimg.2001.0823

Zilles, K., and Palomero-Gallagher, N. (2017). "Comparative analysis of receptor types that identify primary cortical sensory areas," in *Evolution of Nervous Systems*, ed. J. H. Kaas (Oxford: Elsevier), 225–245.

Zilles, K., Palomero-Gallagher, N., Grefkes, C., Scheperjans, F., Boy, C., Amunts, K., et al. (2002a). Architectonics of the human cerebral cortex and transmitter receptor fingerprints: reconciling functional neuroanatomy and neurochemistry. *Eur. Neuropsychopharmacol.* 12, 587–599. doi: 10.1016/s0924-977x(02)00108-6

Zilles, K., Schleicher, A., Palomero-Gallagher, N., and Amunts, K. (2002b). "Quantitative analysis of cyto- and receptorarchitecture of the human brain," in *Brain Mapping. The Methods*, eds A. W. Toga and J. C. Mazziotta (Elsevier: Amsterdam), 573–602.

Zilles, K., Palomero-Gallagher, N., and Schleicher, A. (2004). Transmitter receptors and functional anatomy of the cerebral cortex. *J. Anat.* 205, 417–432. doi: 10.1111/j.0021-8782.2004.00357.x

Zilles, K., Werners, R., Büsching, U., and Schleicher, A. (1986). Ontogenesis of the laminar structure in areas 17 and 18 of the human visual cortex. A quantitative study. *Anat. Embryol.* 174, 339–353. doi: 10.1007/bf00698784

Zilles, K., zur Nieden, K., Schleicher, A., and Traber, J. (1990). A new method for quenching correction leads to revisions of data in receptor autoradiography. *Histochemistry* 94, 569–578. doi: 10.1007/bf00271983

Conflict of Interest Statement: The authors declare that the research was conducted in the absence of any commercial or financial relationships that could be construed as a potential conflict of interest.

frontiers in Neuroanatomy

REVIEW
published: 30 January 2018
doi: 10.3389/fnana.2018.00001

Layer- and Cell Type-Specific Modulation of Excitatory Neuronal Activity in the Neocortex

Gabriele Radnikow[1] *and Dirk Feldmeyer*[1,2,3]*

[1] Research Centre Jülich, Institute of Neuroscience and Medicine, INM-10, Jülich, Germany, [2] Department of Psychiatry, Psychotherapy and Psychosomatics, Medical School, RWTH Aachen University, Aachen, Germany, [3] Jülich-Aachen Research Alliance – Translational Brain Medicine, Jülich, Germany

From an anatomical point of view the neocortex is subdivided into up to six layers depending on the cortical area. This subdivision has been described already by Meynert and Brodmann in the late 19/early 20. century and is mainly based on cytoarchitectonic features such as the size and location of the pyramidal cell bodies. Hence, cortical lamination is originally an anatomical concept based on the distribution of excitatory neuron. However, it has become apparent in recent years that apart from the layer-specific differences in morphological features, many functional properties of neurons are also dependent on cortical layer or cell type. Such functional differences include changes in neuronal excitability and synaptic activity by neuromodulatory transmitters. Many of these neuromodulators are released from axonal afferents from subcortical brain regions while others are released intrinsically. In this review we aim to describe layer- and cell-type specific differences in the effects of neuromodulator receptors in excitatory neurons in layers 2–6 of different cortical areas. We will focus on the neuromodulator systems using adenosine, acetylcholine, dopamine, and orexin/hypocretin as examples because these neuromodulator systems show important differences in receptor type and distribution, mode of release and functional mechanisms and effects. We try to summarize how layer- and cell type-specific neuromodulation may affect synaptic signaling in cortical microcircuits.

Keywords: barrel cortex, cortical layers, neuromodulation, acetylcholine, adenosine, dopamine, orexin

OPEN ACCESS

Edited by:
Kathleen S. Rockland, School of Medicine, Boston University, United States

Reviewed by:
Patricia Gaspar, Institut National de la Santé et de la Recherche Médicale, France
Bertrand Lambolez, Université Pierre et Marie Curie, France

***Correspondence:**
Dirk Feldmeyer
d.feldmeyer@fz-juelich.de

Received: *24 August 2017*
Accepted: *04 January 2018*
Published: *30 January 2018*

Citation:
Radnikow G and Feldmeyer D (2018) Layer- and Cell Type-Specific Modulation of Excitatory Neuronal Activity in the Neocortex. Front. Neuroanat. 12:1. doi: 10.3389/fnana.2018.00001

INTRODUCTION

The notion that the neocortex is subdivided into six different laminae was first introduced around the middle of the 19th century and primarily based on its cytoarchitecture, i.e., the distribution and size of pyramidal cell bodies (Meynert, 1867; Brodmann, 1909) and myeloarchitecture, i.e., the projection pattern of long range, intracortical axon (Baillarger, 1840; Vogt, 1906; see also von Economo, 1929). **Figure 1** gives an overview of neocortical excitatory neuron types in the different layers of two cortical areas, the medial prefrontal and the primary somatosensory cortex (for an in-depth review of cortical lamination and excitatory neuron types see also Narayanan et al., 2017).

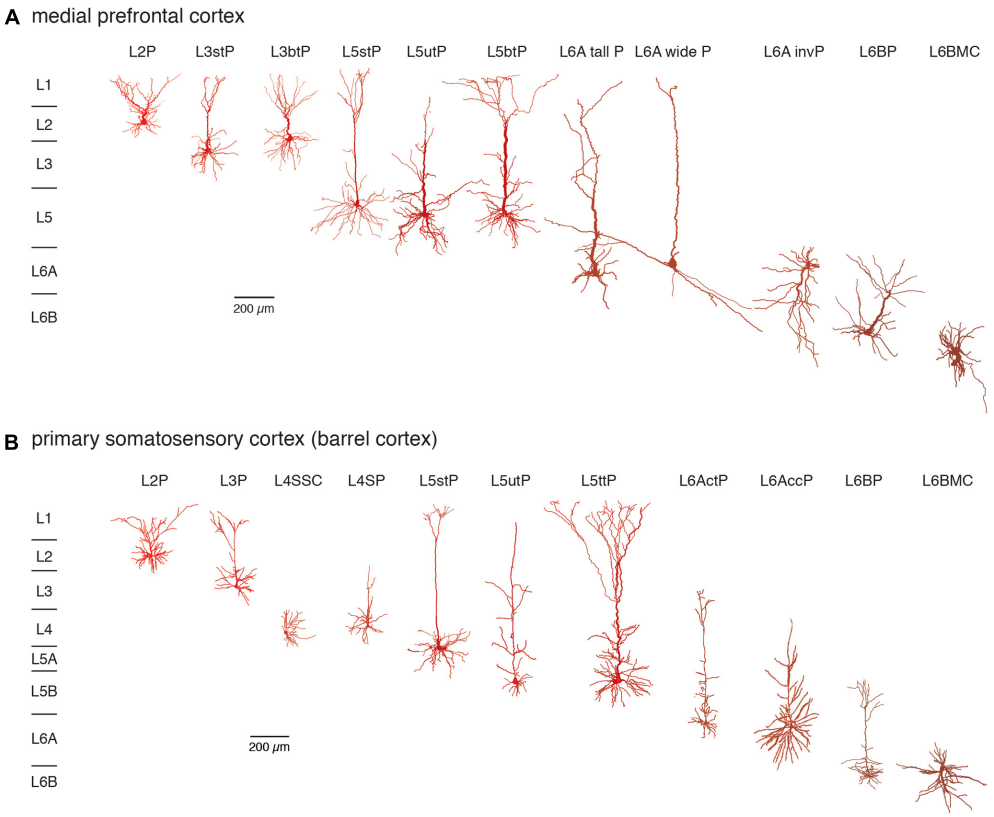

FIGURE 1 | Excitatory neuron types in layers 2–6 of the **(A)** medial prefrontal and **(B)** primary somatosensory (barrel) cortex. Different excitatory neuron types in cortical layers 2–6 (L2–L6) of rat mPFC and S1 barrel cortex are shown. Most neuron types are pyramidal cells with apical dendrites of different shape and length with the exception of spiny stellate cells in layer 4 and multipolar neurons in layer 6B. Somatodendritic domains are shown in different shades of red, with bright red indicating superficial and dark red deep layers. Note that the diversity of excitatory neurons is much higher than that shown here and that even between e.g., sensory cortices different pyramidal cell types can be found. L2P: L2 pyramidal cell; L3stP: L3 slender-tufted pyramidal cell, L3btP: L3 broad-tufted pyramidal cell; L3P: L3 pyramidal cell; L4SSC: L4 spiny stellate cell; L4SP: L4 star pyramidal cell; L5stP: L5 slender-tufted pyramidal cell (with strong axonal projections to layer 2 and 3); L5utP: L5 untufted pyramidal cell; L5btP: L5 broad-tufted pyramidal cell and L5ttP: L5 thick-tufted pyramidal cell (both of which project mainly to subcortical targets); L6A tall P: L6A tall pyramidal cell; L6A wide P: L6A wide pyramidal cell; L6A invP: L6A inverted pyramidal cell; L6AccP: L6A corticocortical pyramidal cell; L6ActP: L6A corticothalamic pyramidal cellL6AP: L6BP L6B pyramidal cell; L6BMC: L6B multipolar cell. This terminology will be used throughout the remainder of the text.

It is apparent that excitatory neuron size and shape varies markedly within and between layers but also between different brain regions. We will use the terminology presented in this figure throughout the remainder of this review.

Thus, originally cortical layers were defined by anatomical features. However, it has been demonstrated that a number of genes (in particular those that encode transcription factors or proteins involved in synaptic signaling) exhibit a clear patterned expression delineating cortical layers. Furthermore, neuronal cell types with different axonal projection patterns showed a differential gene expression suggesting that cortical lamination is not a just an anatomical concept but reflects the segregation of different neuron types into different cortical layers. Of the large number of layer- and neuron-specific genetic markers found in rodents a many have also been identified in primates (Hattox and Nelson, 2007; Belgard et al., 2011; Bernard et al., 2012; Hawrylycz et al., 2012; Lodato and Arlotta, 2015; Molyneaux et al., 2015; Zeisel et al., 2015; Tasic et al., 2016; Lein et al., 2017; Luo et al., 2017).

At a functional level, cell type-specific properties of excitatory neurons including intrinsic properties such as the passive electrical properties, their action potential (AP) firing pattern, their synaptic properties and protein/gene expression pattern have not been comprehensively studied. Only in recent years high-resolution descriptions of the different, in particular long-range axonal projection patterns of excitatory neocortical neurons have become available (Morishima et al., 2011; Oberlaender et al., 2012; Narayanan et al., 2015). A correlation of the morphological, electrophysiological and expression data to unequivocally identify excitatory neocortical neuron types has not been attempted so far and a comprehensive picture of the synaptic properties of the different identified neuronal cell types has not yet emerged.

The function of the neuronal cell types in the different cortical layers is also affected by neuromodulatory transmitters. These neuromodulators regulate the excitability of a neuron (i.e., the probability and efficacy of AP generation and propagation) by affecting ion channels (mostly different K^+ channels types) and

the efficacy and reliability of synaptic transmission via changes in the presynaptic Ca^{2+} channel activity. Most neuromodulator receptors are coupled to different types of G-proteins and act therefore on a significantly slower time scale than ligand-gated ion channels; however, the affinity of G-protein coupled neuromodulator receptors is several orders of magnitude higher than that of ligand-gated channels. While direct synaptic transmission is 'wired,' i.e., occurs only at synaptic contacts, the release of neuromodulators is less directed and is often mediated by so-calledd 'volume transmission', i.e., by diffusion of the neuromodulator over a larger distance, which will affect not only one neuron but rather neuron ensembles in the vicinity of the neuromodulator release site (Zoli et al., 1999; Taber and Hurley, 2014; Badin et al., 2016). There are many different neuromodulator types which are either released from small groups of subcortical neurons that send their axon into the neocortex (such as cholinergic afferents form the basal forebrain) or are produced intracortically (such as adenosine). While it has been shown that differences in neuromodulator receptor expression exist, studies addressing a layer- and neuronal cell-type their layer-specific action are just beginning to emerge.

In this review we will focus on four different types of neuromodulators that differ in many aspects, including their mode of release, mechanism of action and target structures. First, we will discuss the nucleotide adenosine which is released in a non-vesicular fashion. Second, we will describe the cholinergic system which is noteworthy because it acts on two different neuromodulatory systems, the fast nicotinic acetylcholine (ACh) receptor channels (nAChRs) and the slow, G-protein coupled muscarinic ACh receptors (mAChRs). Third, we will address the dopaminergic system as an example of neuromodulation by a monoamine and finally peptidergic modulation by orexin/hypocretin. The underlying biophysical and biochemical mechanisms of the function of these neuromodulator systems will only be discussed in the context of their effects in different cortical layers and on different neuron types. We will mainly concentrate here on data from functional, mostly electrophysiological studies which allow a cell-specific examination of neuromodulator action and its underlying mechanisms such as the coupled G-Protein type and ion channel types activated via intracellular enzyme cascades as well as the coupled ionotropic nAChR channel subtypes. However, this data will be put in context with earlier *in situ* hybridisation, immunohistochemical, receptor autoradiography and electronmicroscopy studies whenever necessary or possible.

BRIEF OVERVIEW OF G-PROTEIN SIGNALING MECHANISMS

The effects of most of the neuromodulator systems reviewed here are mediated via G-protein coupled receptors (GPCRs). G-proteins can be broadly subdivided into four different groups with different signaling pathways, namely the $G_{i/o}$-, G_s-, and $G_{q/11}$- and $G_{12/13}$ G-protein families (for a review see Oldham and Hamm, 2008). Neuromodulator receptors can be coupled to the first three G-protein types but not to $G_{12/13}$ proteins which have mainly cytoskeletal function by regulating actin dynamics.

G-proteins are membrane-bound proteins consisting of three different subunits, the large α- and the smaller β- and γ-subunits, the latter of which form a dimeric β/γ-complex. In its inactive form, the G-protein α-subunit binds GDP which upon activation of the GPCR is exchanged for GTP. This results in a dissociation of the α-subunit from the β/γ-complex and the receptor molecule and in turn initiates many different signaling cascades of which only a few are shown in **Figure 2**. The α-subunit affects downstream second messenger cascades. Basically, the $G_{i/o}$ α-subunit inhibits while the G_s α-subunit activates the adenylate cyclase (AC) – phosphokinase A (PKA) pathway that is involved in the phosphorylation of target enzymes and ion channels such as voltage-gated L-type Ca^{2+} channels (Ca_v1) (Dittmer et al., 2014; Murphy et al., 2014). The G_q α-subunit activates phospholipidase C (PLC) which hydrolyses membrane-bound phosphatidylinositol 4,5-bisphosphate to inositol trisphosphate (IP_3) and diacyl glycerol (DAG). IP_3 will open IP_3-sensitive Ca^{2+} channels of the endoplasmic reticulum and cause intracellular Ca^{2+} release. DAG, on the other hand, in combination with an increase in intracellular Ca^{2+} activates protein kinase C (PKC) which leads to the activation of many downstream signaling cascade including, e.g., an increased neuronal excitability by up regulating a persistent Na current (Astman et al., 1998) and an enhancement of synaptic transmission via the phosphorylation of AMPA-type glutamate receptors (Lee et al., 2000; McDonald et al., 2001).

In addition to its α-subunit mediated effects, β/γ-subunit complex of $G_{i/o}$ proteins affects the G-protein coupled, inwardly rectifying K^+-channels (GIRK or $K_{ir}3$) (for reviews see Doupnik, 2008; Lüscher and Slesinger, 2010; Dascal and Kahanovitch, 2015) and voltage-gated Ca^{2+} channels of the N-, P/Q and R-type ($Ca_v2.2$, $Ca_v2.1$, $Ca_v2.3$) (Zamponi et al., 2015; Huang and Zamponi, 2017). The modulation via the β/γ-subunit complex is direct (i.e., not via a second messenger pathway) and thus significantly faster (<1 s) than that initiated by α-subunits. It is a so-called membrane-delimited step because the β/γ-subunit complex diffuses over a short distance within the cell membrane (for reviews see Doupnik, 2008; Lüscher and Slesinger, 2010; Dascal and Kahanovitch, 2015; Zamponi et al., 2015; Huang and Zamponi, 2017).

ADENOSINE RECEPTORS

Adenosine is an almost ubiquitous endogenous neuromodulator and has been implicated in sleep homoeostasis and energy metabolism of neurons (Ribeiro et al., 2002; Porkka-Heiskanen and Kalinchuk, 2011). It is generated during high neuronal activity, e.g., by ATP-dependent ion transporters that are necessary to maintain intracellular ionic homeostasis (for reviews see Fredholm et al., 2005; Sebastião and Ribeiro, 2009). Adenosine is a metabolite of the intracellular ATP degradation; it is transported into the extracellular space by nucleoside

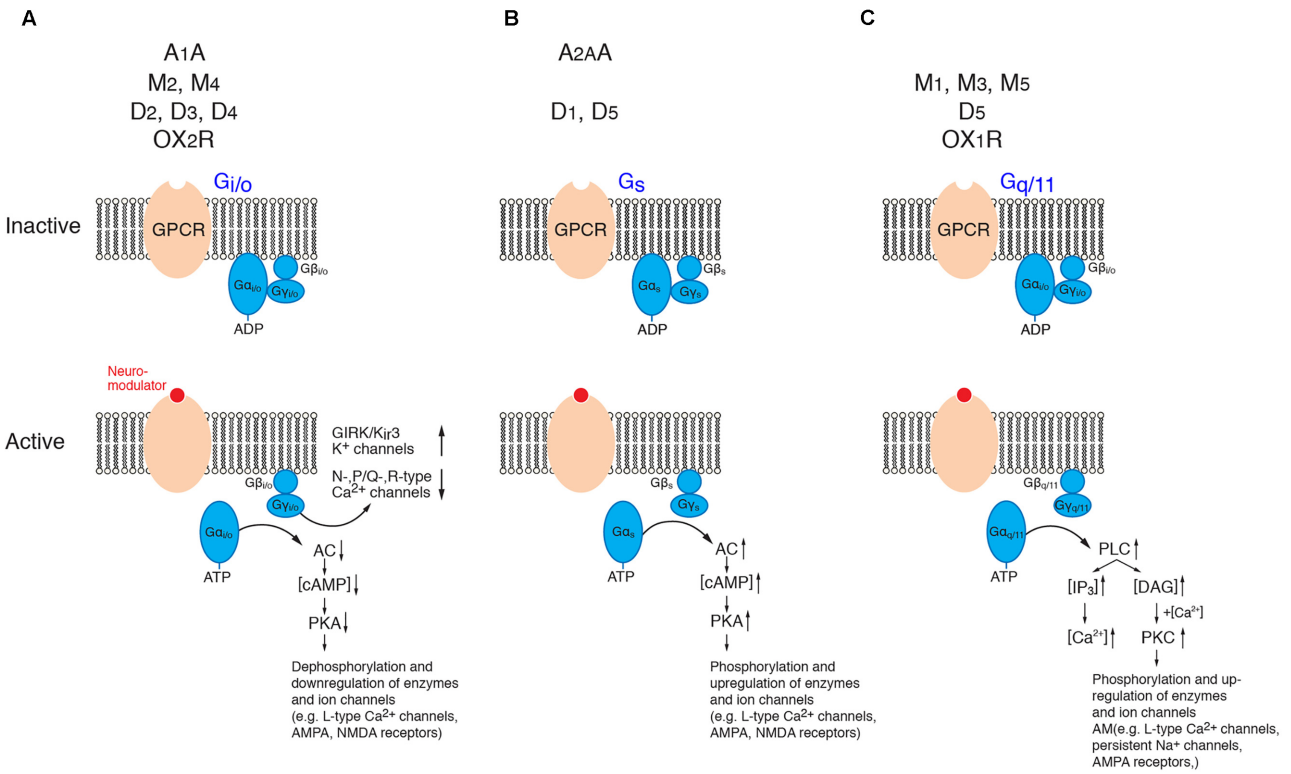

FIGURE 2 | Signaling cascades of neuromodulator-coupled G-proteins. Signaling pathways of the G-protein coupled receptors (GPCRs) discussed in this review (top row). **(A)** $G_{i/o}$ signaling, **(B)** G_s signaling and **(C)** $G_{q/11}$ signaling pathways. Signaling occurs via the dissociated and phosphorylated Gα subunit or via direct interaction between the βγ subunit complex and the effector (K^+- and Ca^{2+} channels). See text for details. It should be noted that the downstream signaling pathways of PKA, PKC and PLC are significantly more diverse than shown here. (AC, adenylate cyclase; ADP, adenosine diphosphate; ATP, adenosine trisphosphate; cAMP, cyclic adenosine monophosphate; DAG, diacylglycerol; GIRK, G-protein coupled, inwardly rectifying K^+ channel; IP_3, inositol trisphosphate; PKA, phosphokinase A; PKC, phosphokinase C; PLC; phospholipase C). For the abbreviation of receptor subtypes see text.

transporters which are located in all cellular compartments of a neuron, i.e., dendrites, soma and axon. In addition, membrane bound ATPase (EctoATPase) can catalyze the formation of adenosine extracellularly by degrading ATP that diffused from the cytoplasm of neurons and glia in the perisynaptic space. Thus, in contrast to the other neuromodulator systems discussed below, adenosine is not a classical neurotransmitter because it is not stored in synaptic vesicles from which it is released.

Of the four different adenosine receptor subtypes that exist, i.e., the A_1, A_{2A}, A_{2B}, and A_3 receptors, only the A_1 and A_{2A} adenosine receptors (A_1AR and A_{2A}AR) are highly expressed in the CNS. Both have high but different adenosine affinities, activate either $G_{i/o}$ (A_1AR) or G_s (A_{2A}AR) proteins and have opposite effects on synaptic transmission (Fredholm et al., 2001, 2005, 2011; Sebastião and Ribeiro, 2009; Chen et al., 2014). They show a differential and partly complementary distribution in different brain regions (Fredholm et al., 2001; Ribeiro et al., 2002). Autoradiography studies demonstrated that the A_1AR mRNA expression is abundant in the neocortex, cerebellum, hippocampus and the dorsal horn of the spinal cord and is enriched at synaptic sites; no apparent layer-specificity was found (Cremer et al., 2011). On the other hand, A_{2A}AR mRNA is strongly expressed in striato-pallidal GABAergic neurons and the olfactory bulb but only weakly so in the neocortex; only a suppressive effect of A_1AR on inhibitory transmission in layer 2/3 has been reported (Bannon et al., 2014). Therefore, only the laminar- and cell-specific effects of A_1ARs will be discussed below. It should be noted that adenosine receptors are not only expressed in neurons but also in glial cells such as astrocytes and microglia.

Adenosine binding to A_1ARs activates $G_{i/o}$ proteins. This results in an increased open probability of $K_{ir}3$ channels and a decrease in the open probability of Ca^{2+} channels via the fast, direct interaction with the Gβ/γ subunit complex (see **Figure 2A**). The activation of $K_{ir}3$ channels by adenosine will result in a hyperpolarisation of the resting membrane potential in the majority of excitatory neurons but was not found in inhibitory neocortical interneurons (van Aerde et al., 2015).

The A_1AR-mediated hyperpolarizing response shows clear and significant layer- and cell-dependent differences in amplitude. Notably, in both prefrontal cortex (PFC) and primary somatosensory (S1) barrel cortex, L2 pyramidal cells showed no adenosine-induced hyperpolarisation at all (van Aerde et al., 2015), thereby defining this layer by its functional properties. It was found that PFC L3 pyramidal cells displayed mixed and cell type-specific adenosine effects (as defined by their morphological

and electrophysiological properties). L3 pyramidal cells that showed a regular firing pattern (about a quarter of the total) were unresponsive to adenosine, with all others showing a weak to strong hyperpolarisation. In layer 4 of the S1 barrel cortex, all excitatory neurons were hyperpolarised by adenosine. L5 pyramidal cells showed also a hyperpolarisation in response to A_1AR activation. However, the response amplitude was significantly larger in slender-tufted (L5A) pyramidal cells than thick-tufted (L5B) pyramidal cells and largest in PFC L5 pyramidal cells with long basal dendrites (see **Figure 3** and van Aerde et al., 2015). It has been demonstrated that thick-tufted pyramidal cells project mainly sub-cortically while slender-tufted pyramidal cells show dense axonal collaterals in superficial layers 2 and 3 (Molnár and Cheung, 2006; Oberlaender et al., 2011) suggesting a target-specificity in the A_1AR density in these neuron types. This finding was comparable for both S1 barrel cortex and PFC indicating that the A_1AR response is conserved between different cortical areas.

PFC L6 pyramidal neurons showed an adenosine response that was comparable to that of slender-tufted L5 pyramidal neurons. In addition, A_1AR activation decreases thalamocortical excitation of GABAergic interneurons and excitatory neurons in the neocortex (Fontanez and Porter, 2006). In contrast to excitatory neurons, neocortical GABAergic interneurons did not respond to adenosine application (van Aerde et al., 2015). A summary of the layer- and neuronal cell-type specific distribution of A_1ARs is shown in **Figure 4** and **Table 1**.

Adenosine also affects excitatory synaptic transmission by causing a reduction in the release probability as shown by a decrease in the amplitude of EPSPs and an increase in the failure rate, variability and paired pulse ratio. This is likely due to a reduced Ca^{2+} channel activity at the presynaptic terminal and has been found for intralaminar L2/3, L4 and L5 and translaminar L4-L2/3 connections (Fontanez and Porter, 2006; Kerr et al., 2013; Bannon et al., 2014; van Aerde et al., 2015; Qi et al., 2016). The synaptic adenosine effect is most likely mediated by a reduction in the open probability of presynaptic Ca^{2+} channels involved in triggering the release of neurotransmitters and is already apparent at low endogenous adenosine concentrations (~1–2 μM). This in line with the finding that A_1ARs are predominantly found at synaptic sites (as found in the hippocampus; Rebola et al., 2003) and less so in the dendrites and cell bodies suggesting that the synaptic effect of adenosine is the most prominent and important one.

ACETYLCHOLINE RECEPTORS

Acetylcholine plays a prominent role in arousal, vigilance and attention (for reviews see Hasselmo and Sarter, 2011; Ma et al., 2017). In contrast to adenosine-mediated neuromodulation, acetylcholine (ACh) is released from boutons of axons that originate mainly from neurons in the nucleus basalis of Meynert in the basal forebrain (Mesulam et al., 1983a,b; Yeomans, 2012; Zaborszky et al., 2015). Cholinergic afferents are distributed at very high density throughout all layers of the neocortex, with particularly high axonal bouton densities in layers 6, 5 and 1 (Eckenstein et al., 1988; Henny and Jones, 2008; Kalmbach et al., 2012). ACh may also be (co-)released intracortically from a group of bipolar or fusiform GABAergic

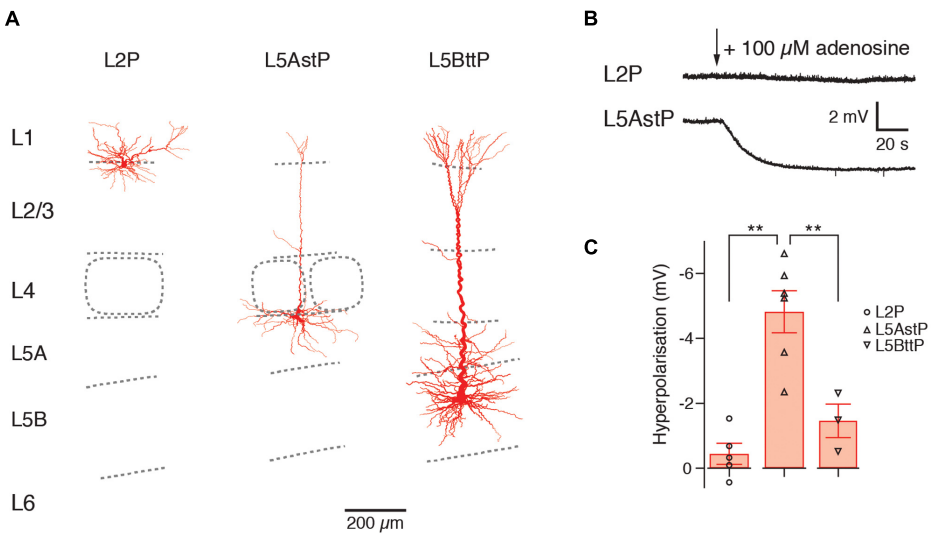

FIGURE 3 | Layer- and cell type-specific difference in the adenosine response in the somatosensory barrel cortex. Significant layer- and cell type-specific differences in the adenosine response in cortical layers 2, 5A and 5B **(A)** Reconstructions of L2, slender-tufted L5A and thick-tufted L5B pyramidal cells in the in the somatosensory barrel cortex. **(B)** Voltage response to adenosine application in L2 and L5A pyramidal cells; L2 pyramidal cells are almost unresponsive to adenosine. **(C)** Comparison of the adenosine response in layers 2, 5A and 5B showing layer-specific differences in the amplitude of the hyperpolarization. This may indicate cell type-specific differences in the density of adenosine A_1ARs. L3, L4, and L6 pyramidal cells show also a hyperpolarizing response to adenosine (not shown). Modified from van Aerde et al. (2015).

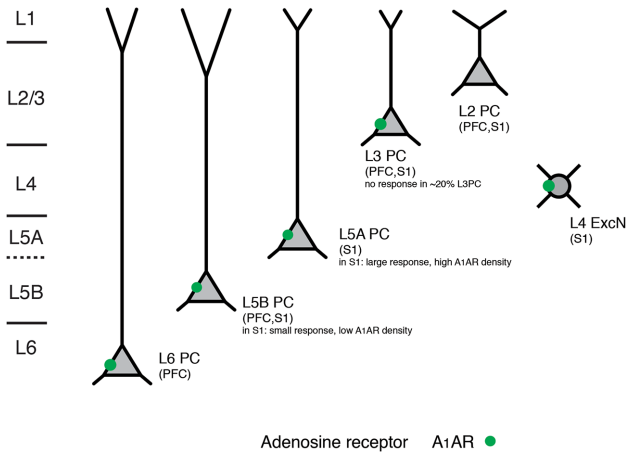

FIGURE 4 | Layer- and cell type-specific A1 adenosine receptor distribution in the prefrontal and primary somatosensory barrel cortex. Adenosine receptors on excitatory neocortical neurons can be found in cortical layers 3–6. Note that in both prefrontal and somatosensory cortex L2 (upper L2/3) pyramidal cells with broad apical tufts were unresponsive to adenosine suggesting no or a very low expression of A_1 adenosine receptors. In layer 5 of somatosensory cortex two pyramidal cell types showed marked differences in their adenosine response that was correlated with their morphology and laminar location; such a clear difference was not found for the prefrontal cortex. All data are from rat.

interneurons [probably vasoactive intestinal peptide (VIP)-positive interneurons] together with the inhibitory transmitter GABA (Parnavelas et al., 1986; Eckenstein et al., 1988; Umbriaco et al., 1994; von Engelhardt et al., 2007). It has been proposed that most of the intracortical ACh is not released at synaptic contacts proper but rather diffusely into the extracellular space, a mechanism termed 'volume transmission' (Descarries et al., 1997; Sarter et al., 2009). However, the presence of intracortical cholinergic synapses has been verified both ultrastructurally (Umbriaco et al., 1994; Turrini et al., 2001; Takács et al., 2013) and functionally (Bennett et al., 2012; Hedrick and Waters, 2015; Hay et al., 2016) for L5 and L6 pyramidal cells as well as for interneurons in layer 1 (Arroyo et al., 2012; Bennett et al., 2012).

The effects of ACh in the neocortex are mediated by two different types of receptors, the G-protein-coupled muscarinic AChRs (mAChRs) and the ionotropic nicotinic AChRs (nAChRs). Both receptor types show cortical layer-specific distributions and effects. These will be discussed separately below.

MUSCARINIC RECEPTORS

Muscarinic AChRs (mAChRs) fall into two different subgroups, the M_1- and the M_2-type receptors. M_1-type receptors comprise M_1, M_3 and M_5 mAChRs that are coupled to $G_{q/11}$ proteins. Following ACh binding, the $G\alpha_{q/11}$ subunit enhances PLC activity resulting in the production of IP_3 and subsequent Ca^{2+} release from intracellular stores and DAG which activates PKC (see **Figure 2C**). M_2 and M_4 mAChRs belong to the M_2-type receptors that are coupled to $G_{i/o}$ proteins (**Figure 2A**) which inhibit the cyclic adenosine monophosphate (cAMP) signaling pathway by blocking AC and in turn decreases the intracellular cAMP concentration and the PKA activity. This will result in a dephosphorylation of K^+, Na^+ and Ca^{2+} and ionotropic GABA and glutamate channels (for reviews see Caulfield and Birdsall, 1998; Thiele, 2013; Muñoz and Rudy, 2014).

The M_1, M_2, and M_4 mAChRs are expressed in the neocortex with the M_1 receptor (M_1R) being the most abundant. M_1Rs show a strong immunoreactivity in layers 2/3 and 6 and a moderate one in layer 5 in both rodent and primate neocortex. Immunoreactivity is associated with both presynaptic axonal boutons and postsynaptic dendritic spines. In contrast, M_2R expression was found to be high in layer 4 and 5 and only moderate in layer 6. M_4R mAChRs on the other hand were only weakly expressed in neocortical layer 4 and some L5 neurons (Levey et al., 1991; Mrzljak et al., 1993; for reviews see Brown, 2010; Thiele, 2013). This suggests marked differences in the response to ACh release in different cortical layers and neuron types.

Application of ACh has been shown to induce long-lasting depolarisations of large neocortical pyramidal neurons (McCormick and Prince, 1986). This has lead to the suggestion that ACh mediates an overall increase in cortical excitability. However, recent studies have revealed a more complex picture by demonstrating that excitatory neuron types in different neocortical layers can be distinguished on the basis of their ACh response amplitude and shape.

Overall, a mAChR response was more common and larger in pyramidal cells located in infragranular than in supragranular layers (McCormick and Prince, 1986; Hedrick and Waters, 2015). Most L2/3 pyramidal cells respond to ACh application with a sustained depolarization while a minor fraction of mostly deep L2/3 pyramidal cells respond with an initial small and transient hyperpolarization followed by a sustained depolarisation. Both the transient hyper- and tonic depolarising responses are exclusively mediated by M_1Rs acting via different K^+ channel types (see below) and have been observed in PFC, S1 and V1 excitatory neurons (Gulledge and Kawaguchi, 2007; Eggermann and Feldmeyer, 2009; see **Figures 5A1,A2,C1,C2**).

In marked contrast, excitatory neurons in layer 4 of sensory cortices are strongly and persistently hyperpolarised by ACh (**Figures 5B1,B2**). This is due to an increase in the open probability of $K_{ir}3$ channels mediated by M_4 mAChR activation. The response is similar in L4 excitatory neurons of different sensory cortices, i.e., the primary auditory, S1 and V1 cortex suggesting that the M_4 AChR response is conserved in sensory cortices. Furthermore, the M_4 AChRs cause also a suppression of the neurotransmitter release probability at excitatory L4-L4 and L4-L2/3 synaptic connections (Eggermann and Feldmeyer, 2009) probably by decreasing the open probability of presynaptic Ca^{2+} channels (Brown, 2010). The exclusive presence of M_4Rs in layer 4 may serve to functionally define this layer in sensory cortices. This finding is, however, in marked contrast to immunohistochemical studies that show only weak M_4R expression in layer 4 (see above).

TABLE 1 | Summary of adenosine receptor, muscarinic and nicotinic ACh receptor, dopamine receptor and orexin receptor effects with respect to cortical layer and cell type.

Layer	Adenosine A_1AR	Muscarinic receptors	Nicotinic receptors	Dopamine receptors	Orexin receptors
Layer 2 Layer 3	*no* A_1AR response (PFC, S1) no A_1AR response in regular spiking L3 PCs (PFC) *weak* hyperpolarizing A_1AR response in broad tufted L3 PCs (PFC) *strong* hyperpolarizing A_1AR response in slender tufted L3 PCs (PFC)	M_1 response transient hyperpolarization and persistent depolarization in L2/3 pyramidal cells (S1, V1) *no/weak* hyperpolarization in layer 2 *moderate* to *strong* transient hyperpolarization in layer 3	no nAChR response in L2/3 pyramidal cells (PFC, S1) but: nicotinic EPSCs in frontal cortical L2/3 pyramidal cells	D1 response Enhancement of glutamatergic transmission in L2/3 pyramidal cells (PFC); mainly postsynaptic effect D1R- and D2R-dependent presynaptic inhibitition of distal glutamatergic synaptic transmission in L3 pyramidal cells (primate PFC) stimulation of PKA activity	Weak OX1R-mediated slowly depolarizing response in L2/3 pyramidal cells (PFC)
Layer 4	*Moderate* hyperpolarising A_1AR response in L4 spiny neurons (S1); strong reduction of exc. transmission; mainly presynaptic effect	M_4 response *strong* persistent hyperpolarization of L4 spiny neurons (S1, V1, A1) strong reduction of exc. transmission; mainly presynaptic effect			
Layer 5A	*strong* hyperpolarizing A_1AR response in st PCs (S1, PFC)	M_1 response persistent depolarization of L5A st pyramidal cells (S1, M_1) enhanced glutamatergic synaptic transmission (S1)	depolarizing, rapidly desensitizing α7 nAChR response in st L5A pyramidal cells	D1 response Depolarization and enhanced excitability of thin-tufted putative CC L5 pyramidal cells (PFC) Enhancement of glutamatergic transmission in L5 pyramidal cells (PFC); mainly postsynaptic effect stimulation of PKA activity	Weak OX1R-mediated slowly depolarizing response in L5 pyramidal cells (PFC)
Layer 5B	*weak* hyperpolarizing A_1AR response in tt PCs (S1, PFC) strong hyperpolarizing A_1AR response in untufted PCs (PFC)	M_1 response transient hyperpolarization and persistent depolarization in L5B tt pyramidal cells (mPFC S1, V1) enhanced glutamatergic synaptic transmission (S1)	depolarizing, rapidly desensitizing α7 nAChR response in tt L5B pyramidal cells, non-α7 (probably α4β2*) nAChRs mediated EPSPs	D2 response Increased after-depolarization, burst AP firing and enhanced excitability of tt putative CT L5 pyramidal cells (PFC) Increase in the AMPA receptor component of EPSPs	
Layer 6	*moderate* hyperpolarizing A_1AR response in PFC L6 PCs	M_1 response depolarization in L6 pyramidal cells, no transient hyperpolarization depolarization in CT L6 pyramidal cells	depolarizing, slowly desensitizing α4β2α5 nAChR response in L6A and L6B pyramidal cellsα4β2α5 nAChR-mediated EPSPs in L6A pyramidal cells	D1 response Depolarization and enhanced excitability of L6 pyramidal cells (PFC) stimulation of PKA activity	OX2R-mediated depolarizing response in L6B excitatory neurons (S1, V1, M1 and cingulate cortex)

The table lists the distribution of the neuromodulator receptor subtypes with respect to cortical layers. Technical datails, cortical area and cell-type specificity is given in brackets. Gray shading indicates layer- and cell-specific differences.

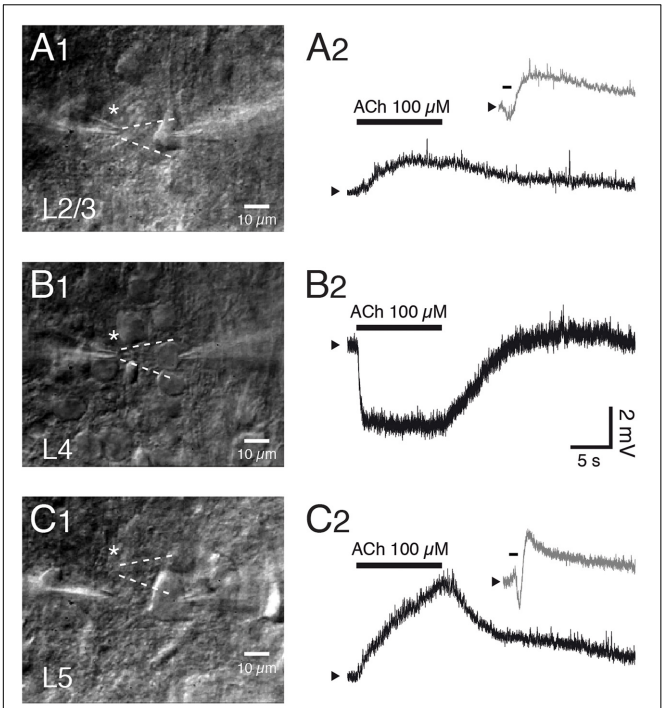

FIGURE 5 | Layer- and cell type-specific muscarinic effects of acetylcholine in the somatosensory barrel cortex. Layer–specific response of excitatory neurons in S1 barrel cortex to rapid application of ACh. **(A1–C1)** Differential interference contrast images of the recorded neurons in layers 2/3, 4 and 5; the profile of the solution ejected by the puff pipette is outlined in white dotted lines. **(A2–C2)** Example responses of L2/3, L4 and L5 excitatory neurons to puff application of ACh. Pyramidal cells in layer 2/3 **(A)** and 5 **(C)** show a depolarization in response to ACh (duration indicated by bar) that is sometimes preceded by a transient hyperpolarization (gray trace in inset). In contrast, all L4 excitatory neurons show a persistent and monophasic hyperpolarizing ACh response.

A large fraction of slender-tufted L5A and thick-tufted L5B pyramidal cells respond to ACh with a rapid transient hyperpolarisation that is followed by a large and tonic depolarisation, as found for L2/3 pyramidal cells (Gulledge and Stuart, 2005; Gulledge et al., 2007; Eggermann and Feldmeyer, 2009; Nuñez et al., 2012; Dasari et al., 2017; see also **Figure 5C2**). This transient ACh-induced hyperpolarisations can be observed more frequently in L5 than in L2/3 pyramidal cells and are mediated by small-conductance, Ca^{2+}-activated K^+ channels (sK_{Ca} channels). The subsequent persistent depolarisation is due to an ACh-induced closure of voltage-gated K^+ channels, K_{ir} channels and other K^+ conductances; all these effects are the result of M_1R activation (Gulledge and Stuart, 2005; Brown, 2010; Thiele, 2013; Dasari et al., 2017). L5B pyramidal cells with either corticocortical or subcortical projection targets (commisural, and corticopontine L5B pyramidal cells, that project to the contralateral cortex and the pons, respectively) have been shown to differ in their response to mAChR activation (Dembrow et al., 2010; see also Dembrow and Johnston, 2014 for a review). Following mAChR activation corticopontine but not commissural pyramidal cells showed a reduced current through hyperpolarization-activated, cyclic nucleotide-gated (HCN) channels and a high probability of shifting into a persistent AP firing mode. Almost all L6 pyramidal cells showed a strong, slowly depolarising M_1R response (McCormick and Prince, 1986; Hedrick and Waters, 2015). In addition, in corticothalamic (CT) L6B pyramidal cells of the visual cortex a depolarising ACh response has been demonstrated that had a slow maintained mAChR- and a faster desensitizing nAChR-component (Sundberg et al., 2017; see also below).

Thus, the muscarinic ACh response shows a layer-specificity in two respects. First, the transient hyperpolarisation is found in L2/3 as well as L5A and L5B pyramidal cells albeit with different strength and frequency of occurrence between layers and cortical areas (Gulledge et al., 2007). Second, the persistent, tonic ACh response is depolarising in layers 2/3, 5 and 6 although the response amplitude and the response probability increases with cortical depth. Layer 4 in sensory cortices stands out in that ACh causes a persistent hyperpolarisation of L4 excitatory neurons, a result of the differential, layer-specific expression of mAChR subtypes. It should also be noted that despite this layer specificity, the ACh response is rather similar between different neocortical areas.

NICOTINIC RECEPTORS

Nicotinic AChRs (nAChRs) are different from all other neuromodulator receptors because they are not coupled to G-proteins but form ligand-gated cation channels permeable to K^+, Na^+ and partially also Ca^{2+}. There are 17 distinct subunits of ionotropic nAChRs, namely the α_{1-10}, β_{1-4}, γ, δ, and ε subunits. Nicotinic AChR channels contain five subunits and may be either homomeric or heteromeric [as pentameric combinations of α and β subunits mainly in the ratio $(\alpha)_2$:$(\beta)_3$ although $(\alpha)_3$:$(\beta)_2$ subunit combinations exist also]. The most abundant nAChR channel subtypes in the neocortex are the homomeric α_7 and the heteromeric $\alpha_4\beta_2$* channels, the latter of which is sometimes associated with an accessory, modulatory subunit (as indicated by the asterisk) such as the α_5 subunit. The α_7 nAChR channels show fast activation and a fast desensitization kinetics, are Ca^{2+}-permeable and have only a low nicotine affinity; $\alpha_4\beta_2$* nAChR currents have a slower onset, are more slowly desensitizing, less permeable to Ca^{2+} and show a high nicotine affinity. If $\alpha_4\beta_2$* nAChRs contain also the accessory α_5-subunit, the desensitization becomes even slower. ACh activates nAChRs either through volume transmission or via cholinergic synapses (Séguéla et al., 1993; Fucile, 2004; Xiao and Kellar, 2004; Dani and Bertrand, 2007; Gotti et al., 2007; see also Hedrick and Waters, 2015; Hay et al., 2016).

In the neocortex, six different nAChR subunits are expressed, namely the α_3, α_4, α_5, α_7, β_2 and β_4 subunits. The α_3 mRNA is strongly and almost exclusively expressed in layer 4 while α_4 mRNA is moderately and β_2-subunit mRNA only weakly expressed in almost all layers. The α_5 subunit is expressed at moderate levels in layer 6B but not at all or only weakly so in other neocortical layers. The α_7 subunit shows a moderate to high expression in layers 1–3, 5, and 6 and no expression in

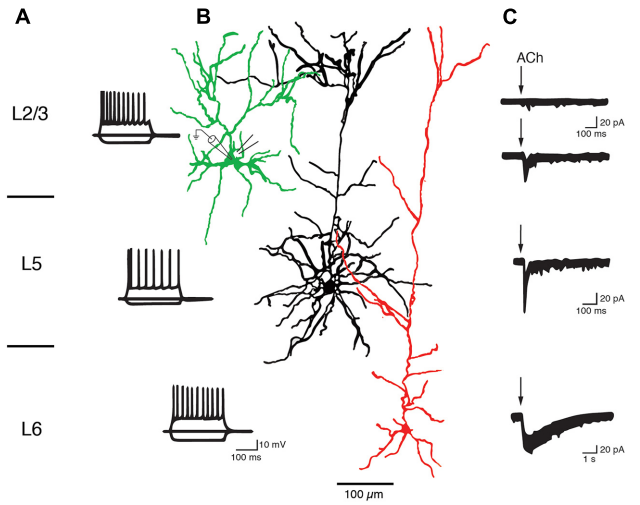

FIGURE 6 | Layer-specific nAChR responses in pyramidal cells of the PFC. Current responses of L2/3, L5, and L6 PFC pyramidal cells to rapid ACh application. **(A)** AP firing pattern elicited by 300 ms current steps in PFC pyramidal cells of cortical layers 2/3, 5, and 6. **(B)** Morphological reconstructions of example L2/3, L5, and L6 pyramidal cells, in green, black and red, respectively. The recording (left) and puff pipette for rapid application) are shown at the soma of the L2/3 pyramidal cell **(C)** Response of pyramidal cells to brief applications of ACh. About 90% of L2/3 pyramidal cells did not display a nicotinergic ACh response (top trace). A small fraction (~10%) of L2/3 and all L5 pyramidal cells showed rapid inward currents following ACh application, a hallmark of α_7 nAChR-mediated currents. L6 pyramidal cells showed very slowly desensitizing ACh-induced currents that are mediated by $\alpha_4\beta_2\alpha_5$ nAChRs (see text for details). After Poorthuis et al. (2013a) with permission from Oxford University Press.

layer 4. The β_4 subunit mRNA shows a strong expression n layer 4 and moderate expression in all other cortical layers (Wada et al., 1989, 1990; Dineley-Miller and Patrick, 1992; Séguéla et al., 1993). It should be noted, however, that in none of these studies the cellular expression of the nAChR subunits was determined so that it is unclear whether the nAChRs are present in either presynaptic terminals of longe-range axons, interneurons or principal excitatory cells.

As found for mAChRs, the distribution of nAChRs is layer- and pyramidal cell type-specific. In both PFC and S1 barrel cortex, almost all L2/3 pyramidal cells show no nicotinic ACh response and therefore do not express nAChRs (Gil et al., 1997; Poorthuis et al., 2013a; Koukouli et al., 2017). In frontal cortex, however, Chu and coworkers recorded cholinergic EPSPs in L2/3 pyramidal cells. This may suggest that at least in some neocortical areas supragranular pyramidal cells are modulated by nAChRs (Chu et al., 2000). In marked contrast, all infragranular pyramidal cells express nAChRs.

Slender-tufted L5A pyramidal cells in S1 cortex respond to ACh application with a rapidly sensitizing inward current and are thus likely to express α_7 nAChRs (Nuñez et al., 2012). Similarly, thick-tufted L5B pyramidal cells in the PFC express α_7 nAChR as indicated by their low sensitivity to nicotine (Couey et al., 2007), fast nAChR response and block by a specific α_7 nAChR antagonist (Poorthuis et al., 2013a; see also **Figure 6**). On the other hand, Hedrick and Waters recorded cholinergic EPSPs in L5 pyramidal cells that were elicited by optical stimulation of the basal forebrain and mediated by non-α_7 (probably $\alpha_4\beta_2$) nAChRs because they were blocked by a specific $\alpha_4\beta_2$ nAChR antagonist. The nAChR-mediated EPSPs were prominent in primary motor (M1) and V1 cortex but rare in PFC (Hedrick and Waters, 2015). Slow ACh EPSPs in M_1 L5 pyramidal cells could only be recorded in the soma and basal dendritic compartments; the apical dendrite and tuft were unresponsive to ACh. In another study a dual component nAChR response was recorded in L5 pyramidal cells of both frontal and somatosensory cortex that was mediated by both α_7 and $\alpha_4\beta_2$ receptors, with the latter becoming more prominent during prolonged ACh application (Zolles et al., 2009). These conflicting results may result from the fact that cholinergic EPSPs and whole cell responses are mediated by different nAChR subtypes as well as neocortical region-specific differences in the expression of nAChR subtypes.

In both L6A and L6B pyramidal neurons, ACh application induces a very slowly desensitizing inward current indicating the presence of $\alpha_4\beta_2$* nAChR combined with the accessory α_5 subunit that further slows down receptor desensitization (Kassam et al., 2008; Alves et al., 2010; Bailey et al., 2012; Poorthuis et al., 2013a,b; Hay et al., 2015; see also Sundberg et al., 2017). In addition, cholinergic EPSPs that were exclusively mediated by $\alpha_4\beta_2\beta_5$ nAChRs and devoid of a α_7-component were also recorded in L6 pyramidal cells (Hay et al., 2016).

Hence, the excitability of L5A, L5B, and L6 pyramidal cells is not only modulated by mAChRs alone but also via nAChRs that preferentially increase the activity of these deep-layer neocortical pyramidal neurons; only a small subset of L2/3 and no L4 excitatory neurons appear to express nAChRs. L6 pyramidal cells show a predominant expression of the slowly desensitizing $\alpha_4\beta_2\alpha_5$ nAChRs which sets them apart from those in other cortical layers. The laminar and cell-specific distribution of these AChR classes is shown in a simplified schematic diagram in **Figure 7** (see also **Table 1**). The fact that both receptor classes act on very different time scales and at different agonist concentrations adds another level of complexity to the ACh modulation of neocortical signaling.

DOPAMINE RECEPTORS

Dopamine is involved in motor control and many higher cognitive functions such as attention, working memory, decision making, and reward. Receptors for dopamine fall into to groups, the D1-class receptors (D1 and D5) of which are mainly coupled to G_s-proteins. D2-class receptors (D2, D3, and D4) on the other hand are coupled to $G_{i/o}$ proteins. Via G_s proteins, D1Rs activate AC, increase intracellular cAMP levels which then results in the stimulation of PKA. PKA suppresses the activity of K_{Ca} channels that mediate the slow afterhyperpolarization (AHP) following an AP (Pedarzani and Storm, 1993; Satake et al., 2008; Yi et al., 2013). In addition, PKA reduces also the open probability of voltage-gated, slowly inactivating K^+ currents (Dong and White, 2003) and K_{ir} channels (Dong et al., 2004). It has also been suggested that PKA enhances a persistent Na^+ current (Yang and Seamans,

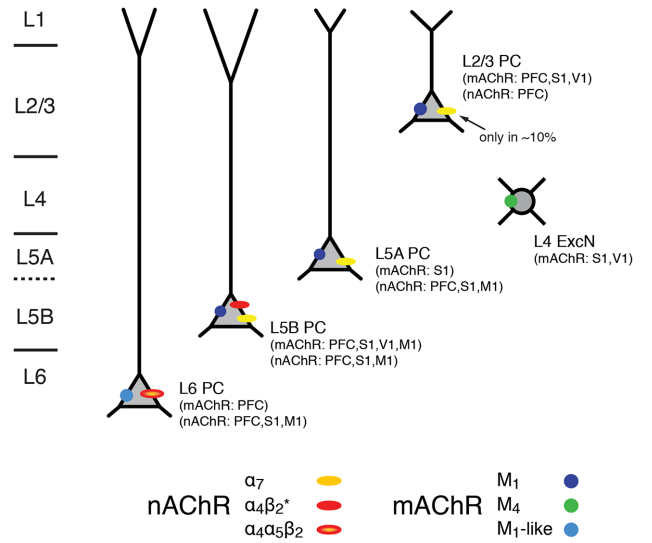

FIGURE 7 | Expression of mAChRs and nAChRs in the neocortex. Schematic diagram of the layer- and cell-type specific distribution of nAChRs and mAChRs in the neocortex. Cortical layering is indicated on the left. Pyramidal cells (PC) in layers 2/3, 5A, 5B and 6 are shown; L5A are generally slender-tufted and L5B thick-tufted pyramidal cells. L4 excitatory neurons (L4 ExcN) include L4 spiny stellate, star pyramids and pyramidal cells. The different brain regions from which the mAChR and nAChR distribution were obtained are given in brackets.

1996) or the rapidly inactivating Na^+ current (Maurice et al., 2001). Furthermore, cAMP directly, i.e., independent of PKA, upregulates HCN channels (Pedarzani and Storm, 1995).

There is also evidence that particularly D5Rs but also D1Rs couple to G_q proteins. Their activation will result in an augmented PLC activity which will trigger intracellular IP_3 production and intracellular Ca^{2+} release. This will potentiate Ca^{2+}-dependent ion conductances such as K_{Ca} channels (for reviews see Beaulieu and Gainetdinov, 2011; Tritsch and Sabatini, 2012).

D2-class receptors on the other hand will decrease the AC activity and cause a reduction in intracellular cAMP levels resulting in a down-regulation of all cAMP-dependent enzymes and ligand- and voltage-gated ion channels. In addition, D2 receptors (D2R) activate K^+ conductances and deactivate N- P/Q- and R-type Ca^{2+} channels via direct interaction with β/γ G-protein subunit complex (see **Figure 2**; Beaulieu and Gainetdinov, 2011; Tritsch and Sabatini, 2012).

In the neocortex, dopamine is released from dopaminergic afferents mostly from the ventral tegmental area (VTA). These afferents project throughout all layers of the frontal, cingulate and rhinal cortices but almost exclusively in deep cortical layers 5 and 6 of most other cortical areas including the M_1, S1 and V1 cortex (Berger et al., 1991; Nomura et al., 2014). In primate neocortex the dopaminergic innervation is much more dense than in rodents and targets all layers in all cortical areas (Berger et al., 1991). Dopaminergic afferents have been shown to establish close appositions with the dendrites of callosally and nucleus accumbens projecting L5 pyramidal cells (i.e., both intracortical and pyramidal tract projecting neurons) and L2, L3, L5, and L6 pyramidal cells in both rat and primate prefrontal cortex (Krimer et al., 1997; Carr et al., 1999; Carr and Sesack, 2000) suggesting a spatially restricted dopamine release. However, the number of dopaminergic appositions is relatively low and the exact signaling mechanisms at these contacts are not known.

Studies of dopaminergic modulation have focussed mostly on pyramidal cells in layers 5 and 6 of the PFC because of the high density of dopaminergic afferents in this brain region and layers. Nevertheless, dopamine receptors have been found in all cortical layers and in many different cortical areas including sensory cortices (see **Figure 8**).

In accordance with the dense dopaminergic innervation of deep cortical layers, both D1R and D2R mRNA expression and immunoreactivity was stronger in layers 5 and 6 than in superficial or intermediate layers in the medial PFC (Weiner et al., 1991; Gaspar et al., 1995; Vincent et al., 1995; Santana et al., 2009; for a review see Santana and Artigas, 2017). D1R mRNA showed a particular abundance in deep layer 6 (i.e., layer 6B); on the other hand, expression of D2R was largely confined to layer 5 where it was higher than that of D1R (Santana et al., 2009). An analysis of the cellular distribution of D2R mRNA showed that it was present mostly in corticocortical (CC), CT and corticostriatal (CStr) projection neurons (Gaspar et al., 1995). In addition, using functional imaging of PKA activity Nomura and coworkers found wide-spread functional expression of D1/5Rs but also D2Rs throughout layers 2/3 and 5 of the frontal, parietal and occipital cortices (Nomura et al., 2014). In this study, only moderate regional and laminar-specific differences in the distribution of the different receptor subtypes were found.

D3R mRNA but no that of D1R or D2R has been detected in layer 4 of rodent S1 barrel cortex. Using receptor autoradiography and *in situ* hybridisation a transient but selective expression of this dopamine receptor type was found until the second postnatal week. D3R expression declined thereafter and was completely absent in the adult (Gurevich and Joyce, 2000; Gurevich et al., 2001). In addition, using immunocytochemistry D3R expression has been reported for pyramidal neurons in layers 3 and 5 of the somatosensory cortex and the PFC (Ariano and Sibley, 1994). Furthermore, D4R immunoreactivity has been shown in L2/3 and L5 pyramidal neurons of PFC, cingulate and parietal cortex as well as in L4 excitatory neurons in M1, S1 and V1 cortex (Mrzljak et al., 1996; Wedzony et al., 2000; Rivera et al., 2008; for a review see Tritsch and Sabatini, 2012).

In most *in vitro* studies in which presynaptic dopamine effects were blocked, dopamine increased the intrinsic excitability of deep layer PFC pyramidal neurons by depolarising the resting membrane potential and/or promoting a slow but long-lasting increase in the number of action potentials elicited by somatic depolarization (Yang and Seamans, 1996; Gulledge and Jaffe, 1998; Gulledge and Jaffe, 2001; Lavin and Grace, 2001; Seamans et al., 2001; Gao and Goldman-Rakic, 2003; Wang and Goldman-Rakic, 2004; Rotaru et al., 2007; Kroener et al., 2009; Moore et al., 2011; Seong and Carter, 2012; Happel et al., 2014; Gorelova and Seamans, 2015; for reviews see Tritsch and Sabatini, 2012; Xing et al., 2016). Generally, these effects are mediated by

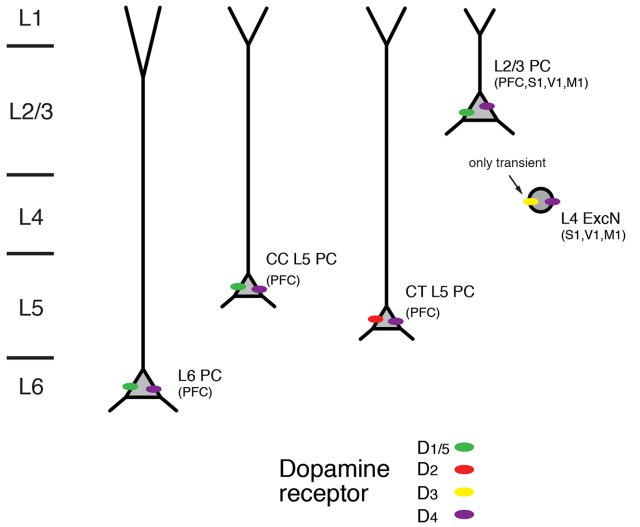

FIGURE 8 | Expression of dopamine receptors in the neocortex. Schematic diagram of the layer- and cell-type specific distribution of dopamine receptor types in different pyramidal cell types in the neocortex. Data were obtained for pyramidal cells (PC) in layers 2/3, 5, and 6; CC and CT denote L5 PC with corticocortical and corticothalamic projection targets. L4 excitatory neurons (L4 ExcN) include L4 spiny stellate, star pyramids and pyramidal cells. Brain regions for which the receptor distribution were obtained are given in brackets. Apart from L4 ExcN all data are from functional, mainly electrophysiological studies (see text for details).

D1R activation and include an enhanced AP firing frequency, a block of K^+ conductances and an increase in a persistent Na^+ current; they are blocked by D1R antagonists and mimicked by D1R agonists. Furthermore, D1R activation has been reported to increase in the amplitude of glutamatergic EPSPs in PFC L2/3 pyramidal cells (Gonzalez-Islas and Hablitz, 2003). Here, the underlying mechanism is probably a G_s-protein-induced phosphorylation of synaptic AMPA and NMDA glutamate receptors (via the AC-cAMP-PKA signaling pathway) that results in a potentiation of the activity both receptor types. Furthermore, a presynaptic D1R- and D2R inhibition of glutamatergic synaptic transmission in L3 pyramidal cells in primate PFC has been reported; this inhibition was found only for distal but not local synaptic inputs (Urban et al., 2002).

Recent studies have shown that dopaminergic modulation in layer 5 of the PFC may depend on the pyramidal cell type and its projection target (Gee et al., 2012; Seong and Carter, 2012; see also Dembrow and Johnston, 2014). CT pyramidal cells differed from CC PFC L5 pyramidal cells in that they had a larger HCN channel current and thick-tufted apical dendrites. While D1Rs were only expressed in thin-tufted putative CC pyramidal cells, D2Rs were present in thick-tufted CT pyramidal cells. An increase in excitability induced by D1R agonist application was found in thin-tufted pyramidal cells (Seong and Carter, 2012). Conversely, in thick-tufted pyramidal cells that projected to the thalamus *but not* to the contralateral cortex, D2R activation resulted in a L-type Ca^{2+} channel- and NMDAR-dependent afterdepolarisation and thus a higher excitability (Gee et al., 2012). This suggests that D2Rs are expressed only in CT L5 pyramidal cells. A D2R-mediated increase in the excitability of thick-tufted PFC L5 pyramidal cells was also observed in another study; here dopamine caused an increase in the AMPA receptor component of EPSPs elicited by layer 2/3 stimulation that led to burst-firing (Wang and Goldman-Rakic, 2004).

Thus, D1Rs are functionally expressed throughout cortical layers 2/3, 5, and 6, with a particularly high expression level in the latter. In contrast, D2Rs are almost exclusively confined to layer 5 and show a cell-specific expression in CT L5 pyramidal cells. It is not known whether the very heterogeneous population of L6 excitatory neurons (see **Figure 1**) shows a similar differential modulation by dopamine. Therefore, more studies on structurally identified neuron types in the different cortical layers are necessary to obtain a detailed picture of the cell-specific distribution of different dopamine receptor subtypes.

OREXIN/HYPOCRETIN RECEPTORS

Orexin/Hypocretin is a peptide that is synthesized in neurons of the lateral hypothalamic area. It plays a pivotal role in the regulation of wakefulness and arousal (for reviews see Sakurai, 2007, 2013; Alexandre et al., 2013; Richter et al., 2014; Kukkonen, 2017). Orexin-releasing neurons synthesize two peptides, orexin A and orexin B (also hypocretin 1 and 2). These peptides act on two G-Protein coupled receptors, the orexin 1 (OX1R; also HCRTR1) and orexin 2 (OX2R; also HCRTR2) receptor. While OX1R has a ∼100-fold higher binding affinity for orexin A than B, OX2R has a similar affinity for both orexins. The OX1R is mainly coupled to a G_q G-protein and causes an increase in intracellular Ca^{2+} (via PLC and IP_3 activation; see above and **Figure 2**). OX2Rs are also coupled to $G_{i/o}$-proteins and thus act by inhibiting K^+ and Ca^{2+} currents. The distribution of mRNA for the OX1R and OX2R is markedly different and often complementary, suggesting that these receptors have distinct functional roles. While OX1R was only weakly expressed in the neocortex, a strong expression of OX2Rs has been found in neocortical layer 6. In addition, weak expression of OX2R has been reported to be present in layers 2/3 and in a few L5 pyramidal cells (Trivedi et al., 1998; Lu et al., 2000; Marcus et al., 2001; Cluderay et al., 2002).

Electrophysiological studies in the S1, V1, M1 and cingulate cortex have shown that in superficial layers of the neocortex orexin did not elicit a response at all and only a minute one in ∼10% of L5 pyramidal cells (Bayer et al., 2004), in line with the immunohistochemical and mRNA expression data. A substantial orexin-response was exclusively observed in L6B neurons where orexin B binds to the OX2R and causes a depolarisation by blocking K^+ currents, a response that is potentiated by activation of $\alpha_4\beta_2\alpha_5$ nAChRs (Bayer et al., 2004; Hay et al., 2015; Wenger Combremont et al., 2016a,b). No orexin-induced response was recorded in L6A neurons (Hay et al., 2015). It has been suggested that the main target neurons of orexin modulation in layer 6B are multipolar spiny neurons, indicating a cell-specific action of orexin (Wenger Combremont et al., 2016b). Excitatory L6B neurons innervate predominantly neurons in infragranular layers

5 and 6 (Clancy and Cauller, 1999; Marx and Feldmeyer, 2013). It has been proposed that one function of the orexin-sensitive L6B neurons is to recruit pyramidal neurons in the thalamorecipient layer 6A. Thus, thalamocortical signaling in layer 6A will be potentiated in an orexin-gated feedforward loop, and become more reliable (Hay et al., 2015). Remarkably, while almost all other neuromodulator systems show functional receptor distributions that extend through almost all layers of the neocortex, the OX2R stands out because it is found almost exclusively in layer 6B excitatory neurons. Therefore, OX2R can be considered as a specific marker for this layer.

While OX2R-mediated depolarisations have only been recorded in L6B neurons of S1, V1, M1 and cingulate cortex, the OX1R receptor appears to be more distributed throughout the cortical layers. It has been shown that in the PFC, orexin acting via OX1R and PKC can increase the excitability of PFC L2/3 and L5 pyramidal cells by inhibiting HCN channels and K^+ conductances (Li et al., 2010; Yan et al., 2012). Thus in contrast to OX2R, OX1R is a less specific marker for cortical lamination.

CONCLUSION

On the basis of the available data the expression pattern of neuromodulator receptors in the neocortex shows a high degree of layer- and cell-specificity (see **Figures 4**, **7**, **8** and **Table 1**). This is probably the result not of a layer-specificity *per se* but due to the fact that neurons with very distinct morphological properties (such as thick-tufted L5 pyramidal cells or L4 spiny stellate cells) are largely or even exclusively confined to a distinct layer.

Differences in the neuromodulator response could be the result of a virtual absence of a neuromodulatory receptor, its exclusive presence or changes in a receptor subtype in a layer and/or cell-type specific fashion. All neuromodulator systems described in this review fulfill at least one if not more of these criteria and may therefore serve to define cortical layers to some extent: An exclusive absence of a response was found for the adenosinergic system for which all superficial L2/3 pyramidal cells were shown to be unresponsive to adenosine while excitatory neurons in all other layers respond to adenosine with a hyperpolarisation. The only layer showing an orexin/hypocretin response is layer 6B. L4 excitatory neurons express the M_4 mAChR while supra- and infra granular pyramidal cells show M_1 mAChR responses. A similar situation was found for ACh acting on nicotinergic receptors where only L6 pyramidal cells showed an $\alpha_4\beta_2\alpha_5$ nAChR response. Furthermore, several studies have demonstrated that the response to a neuromodulator is similar or even identical in different cortical areas, e.g., the tonic ACh-induced hyperpolarisation in L4 excitatory neurons found in the S1, A1 and V1 sensory cortices.

However, it has gradually become apparent, that the expression of neuromodulator receptors can vary between excitatory neurons in a defined layer. Excitatory neurons differ in their intra- and/or subcortical axonal targets, their dendritic morphology, electrophysiological properties and molecular make-up and thus may be subdivided in as many different cell types as GABAergic interneurons (Morishima and Kawaguchi, 2006; Morishima et al., 2011; Oberlaender et al., 2012; Narayanan et al., 2015; Zeisel et al., 2015; Tasic et al., 2016; Luo et al., 2017). Recent studies have demonstrated that this heterogeneity is often reflected in the neuromodulator receptor distribution and their effects (Dembrow et al., 2010; Gee et al., 2012; Seong and Carter, 2012; van Aerde et al., 2015). For the direction of future research it is therefore important that neuromodulation is investigated in identified neuron types, ideally in those for which the axonal projection pattern and target structures have been determined.

AUTHOR CONTRIBUTIONS

Both authors developed the paper concept, wrote the paper and drafted the figures.

FUNDING

For this work funding has been received from the Helmholtz Society and the European Union's Horizon 2020 Research and Innovation Programme under Grant Agreement No. 720270 (HBP SGA1) (to DF).

REFERENCES

Alexandre, C., Andermann, M. L., and Scammell, T. E. (2013). Control of arousal by the orexin neurons. *Curr. Opin. Neurobiol.* 23, 752–759. doi: 10.1016/j.conb.2013.04.008

Alves, N. C., Bailey, C. D., Nashmi, R., and Lambe, E. K. (2010). Developmental sex differences in nicotinic currents of prefrontal layer VI neurons in mice and rats. *PLOS ONE* 5:e9261. doi: 10.1371/journal.pone.0009261

Ariano, M. A., and Sibley, D. R. (1994). Dopamine receptor distribution in the rat CNS: elucidation using anti-peptide antisera directed against D1A and D3 subtypes. *Brain Res.* 649, 95–110. doi: 10.1016/0006-8993(94)91052-9

Arroyo, S., Bennett, C., Aziz, D., Brown, S. P., and Hestrin, S. (2012). Prolonged disynaptic inhibition in the cortex mediated by slow, non-alpha7 nicotinic excitation of a specific subset of cortical interneurons. *J. Neurosci.* 32, 3859–3864. doi: 10.1523/JNEUROSCI.0115-12.2012

Astman, N., Gutnick, M. J., and Fleidervish, I. A. (1998). Activation of protein kinase C increases neuronal excitability by regulating persistent Na+ current in mouse neocortical slices. *J. Neurophysiol.* 80, 1547–1551. doi: 10.1152/jn.1998.80.3.1547

Badin, A. S., Fermani, F., and Greenfield, S. A. (2016). The features and functions of neuronal assemblies: possible dependency on mechanisms beyond synaptic transmission. *Front. Neural Circuits* 10:114. doi: 10.3389/fncir.2016.00114

Bailey, C. D., Alves, N. C., Nashmi, R., De Biasi, M., and Lambe, E. K. (2012). Nicotinic alpha5 subunits drive developmental changes in the activation and morphology of prefrontal cortex layer VI neurons. *Biol. Psychiatry* 71, 120–128. doi: 10.1016/j.biopsych.2011.09.011

Baillarger, J. G. F. (1840). Recherches sur la structure de la couche corticale des circonvolutions du cervau. *Mém. Acad. R. Méd.* 8, 149–183.

Bannon, N. M., Zhang, P., Ilin, V., Chistiakova, M., and Volgushev, M. (2014). Modulation of synaptic transmission by adenosine in layer 2/3 of the rat visual cortex in vitro. *Neuroscience* 260, 171–184. doi: 10.1016/j.neuroscience.2013.12.01

Bayer, L., Serafin, M., Eggermann, E., Saint-Mleux, B., Machard, D., Jones, B. E., et al. (2004). Exclusive postsynaptic action of hypocretin-orexin on sublayer 6b

cortical neurons. *J. Neurosci.* 24, 6760–6764. doi: 10.1523/JNEUROSCI.1783-04.2004

Beaulieu, J. M., and Gainetdinov, R. R. (2011). The physiology, signaling, and pharmacology of dopamine receptors. *Pharmacol. Rev.* 63, 182–217. doi: 10.1124/pr.110.002642

Belgard, T. G., Marques, A. C., Oliver, P. L., Abaan, H. O., Sirey, T. M., Hoerder-Suabedissen, A., et al. (2011). A transcriptomic atlas of mouse neocortical layers. *Neuron* 71, 605–616. doi: 10.1016/j.neuron.2011.06.039

Bennett, C., Arroyo, S., Berns, D., and Hestrin, S. (2012). Mechanisms generating dual-component nicotinic EPSCs in cortical interneurons. *J. Neurosci.* 32, 17287–17296. doi: 10.1523/JNEUROSCI.3565-12.2012

Berger, B., Gaspar, P., and Verney, C. (1991). Dopaminergic innervation of the cerebral cortex: unexpected differences between rodents and primates. *Trends Neurosci.* 14, 21–27. doi: 10.1016/0166-2236(91)90179-X

Bernard, A., Lubbers, L. S., Tanis, K. Q., Luo, R., Podtelezhnikov, A. A., Finney, E. M., et al. (2012). Transcriptional architecture of the primate neocortex. *Neuron* 73, 1083–1099. doi: 10.1016/j.neuron.2012.03.002

Brodmann, K. (1909). *Vergleichende Lokalisationslehre der Grosshirnrinde: in ihren Prinzipien dargestellt auf Grund des Zellenbaues*. Leipzig: Verlag von Johann Ambrosius Barth.

Brown, D. A. (2010). Muscarinic acetylcholine receptors (mAChRs) in the nervous system: some functions and mechanisms. *J. Mol. Neurosci.* 41, 340–346. doi: 10.1007/s12031-010-9377-2

Carr, D. B., O'donnell, P., Card, J. P., and Sesack, S. R. (1999). Dopamine terminals in the rat prefrontal cortex synapse on pyramidal cells that project to the nucleus accumbens. *J. Neurosci.* 19, 11049–11060.

Carr, D. B., and Sesack, S. R. (2000). Dopamine terminals synapse on callosal projection neurons in the rat prefrontal cortex. *J. Comp. Neurol.* 425, 275–283. doi: 10.1002/1096-9861(20000918)425:2<275::AID-CNE9>3.0.CO;2-Z

Caulfield, M. P., and Birdsall, N. J. (1998). International union of pharmacology. XVII. Classification of muscarinic acetylcholine receptors. *Pharmacol. Rev.* 50, 279–290.

Chen, J. F., Lee, C. F., and Chern, Y. (2014). Adenosine receptor neurobiology: overview. *Int. Rev. Neurobiol.* 119, 1–49. doi: 10.1016/B978-0-12-801022-8.00001-5

Chu, Z. G., Zhou, F. M., and Hablitz, J. J. (2000). Nicotinic acetylcholine receptor-mediated synaptic potentials in rat neocortex. *Brain Res.* 887, 399–405. doi: 10.1016/S0006-8993(00)03076-6

Clancy, B., and Cauller, L. J. (1999). Widespread projections from subgriseal neurons (layer VII) to layer I in adult rat cortex. *J. Comp. Neurol.* 407, 275–286. doi: 10.1002/(SICI)1096-9861(19990503)407:2<275::AID-CNE8>3.0.CO;2-0

Cluderay, J. E., Harrison, D. C., and Hervieu, G. J. (2002). Protein distribution of the orexin-2 receptor in the rat central nervous system. *Regul. Pept.* 104, 131–144. doi: 10.1016/S0167-0115(01)00357-3

Couey, J. J., Meredith, R. M., Spijker, S., Poorthuis, R. B., Smit, A. B., Brussaard, A. B., et al. (2007). Distributed network actions by nicotine increase the threshold for spike-timing-dependent plasticity in prefrontal cortex. *Neuron* 54, 73–87. doi: 10.1016/j.neuron.2007.03.006

Cremer, C. M., Lübke, J. H., Palomero-Gallagher, N., and Zilles, K. (2011). Laminar distribution of neurotransmitter receptors in different reeler mouse brain regions. *Brain Struct. Funct.* 216, 201–218. doi: 10.1007/s00429-011-0303-3

Dani, J. A., and Bertrand, D. (2007). Nicotinic acetylcholine receptors and nicotinic cholinergic mechanisms of the central nervous system. *Annu. Rev. Pharmacol. Toxicol.* 47, 699–729. doi: 10.1146/annurev.pharmtox.47.120505.105214

Dasari, S., Hill, C., and Gulledge, A. T. (2017). A unifying hypothesis for M1 muscarinic receptor signalling in pyramidal neurons. *J. Physiol.* 595, 1711–1723. doi: 10.1113/JP273627

Dascal, N., and Kahanovitch, U. (2015). The roles of gbetagamma and galpha in gating and regulation of GIRK channels. *Int. Rev. Neurobiol.* 123, 27–85. doi: 10.1016/bs.irn.2015.06.001

Dembrow, N., and Johnston, D. (2014). Subcircuit-specific neuromodulation in the prefrontal cortex. *Front. Neural Circuits* 8:54. doi: 10.3389/fncir.2014.00054

Dembrow, N. C., Chitwood, R. A., and Johnston, D. (2010). Projection-specific neuromodulation of medial prefrontal cortex neurons. *J. Neurosci.* 30, 16922–16937. doi: 10.1523/JNEUROSCI.3644-10.2010

Descarries, L., Gisiger, V., and Steriade, M. (1997). Diffuse transmission by acetylcholine in the CNS. *Prog. Neurobiol.* 53, 603–625. doi: 10.1016/S0301-0082(97)00050-6

Dineley-Miller, K., and Patrick, J. (1992). Gene transcripts for the nicotinic acetylcholine receptor subunit, beta4, are distributed in multiple areas of the rat central nervous system. *Brain Res. Mol. Brain Res.* 16, 339–344. doi: 10.1016/0169-328X(92)90244-6

Dittmer, P. J., Dell'acqua, M. L., and Sather, W. A. (2014). Ca2+/calcineurin-dependent inactivation of neuronal L-type Ca2+ channels requires priming by AKAP-anchored protein kinase A. *Cell Rep.* 7, 1410–1416. doi: 10.1016/j.celrep.2014.04.039

Dong, Y., Cooper, D., Nasif, F., Hu, X. T., and White, F. J. (2004). Dopamine modulates inwardly rectifying potassium currents in medial prefrontal cortex pyramidal neurons. *J. Neurosci.* 24, 3077–3085. doi: 10.1523/JNEUROSCI.4715-03.2004

Dong, Y., and White, F. J. (2003). Dopamine D1-class receptors selectively modulate a slowly inactivating potassium current in rat medial prefrontal cortex pyramidal neurons. *J. Neurosci.* 23, 2686–2695.

Doupnik, C. A. (2008). GPCR-Kir channel signaling complexes: defining rules of engagement. *J. Recept. Signal Transduct. Res.* 28, 83–91. doi: 10.1080/10799890801941970

Eckenstein, F. P., Baughman, R. W., and Quinn, J. (1988). An anatomical study of cholinergic innervation in rat cerebral cortex. *Neuroscience* 25, 457–474. doi: 10.1016/0306-4522(88)90251-5

Eggermann, E., and Feldmeyer, D. (2009). Cholinergic filtering in the recurrent excitatory microcircuit of cortical layer 4. *Proc. Natl. Acad. Sci. U.S.A.* 106, 11753–11758. doi: 10.1073/pnas.0810062106

Fontanez, D. E., and Porter, J. T. (2006). Adenosine A1 receptors decrease thalamic excitation of inhibitory and excitatory neurons in the barrel cortex. *Neuroscience* 137, 1177–1184. doi: 10.1016/j.neuroscience.2005.10.022

Fredholm, B. B., Ap, I. J., Jacobson, K. A., Linden, J., and Muller, C. E. (2011). International union of basic and clinical pharmacology. LXXXI. Nomenclature and classification of adenosine receptors–an update. *Pharmacol. Rev.* 63, 1–34. doi: 10.1124/pr.110.003285

Fredholm, B. B., Chen, J. F., Cunha, R. A., Svenningsson, P., and Vaugeois, J. M. (2005). Adenosine and brain function. *Int. Rev. Neurobiol.* 63, 191–270. doi: 10.1016/S0074-7742(05)63007-3

Fredholm, B. B., IJzerman, A. P., Jacobson, K. A., Klotz, K. N., and Linden, J. (2001). International union of pharmacology. XXV. Nomenclature and classification of adenosine receptors. *Pharmacol. Rev.* 53, 527–552.

Fucile, S. (2004). Ca2+ permeability of nicotinic acetylcholine receptors. *Cell Calcium* 35, 1–8. doi: 10.1016/j.ceca.2003.08.006

Gao, W. J., and Goldman-Rakic, P. S. (2003). Selective modulation of excitatory and inhibitory microcircuits by dopamine. *Proc. Natl. Acad. Sci. U.S.A.* 100, 2836–2841. doi: 10.1073/pnas.262796399

Gaspar, P., Bloch, B., and Le Moine, C. (1995). D1 and D2 receptor gene expression in the rat frontal cortex: cellular localization in different classes of efferent neurons. *Eur. J. Neurosci.* 7, 1050–1063. doi: 10.1111/j.1460-9568.1995.tb01092.x

Gee, S., Ellwood, I., Patel, T., Luongo, F., Deisseroth, K., and Sohal, V. S. (2012). Synaptic activity unmasks dopamine D2 receptor modulation of a specific class of layer V pyramidal neurons in prefrontal cortex. *J. Neurosci.* 32, 4959–4971. doi: 10.1523/JNEUROSCI.5835-11.2012

Gil, Z., Connors, B. W., and Amitai, Y. (1997). Differential regulation of neocortical synapses by neuromodulators and activity. *Neuron* 19, 679–686. doi: 10.1016/S0896-6273(00)80380-3

Gonzalez-Islas, C., and Hablitz, J. J. (2003). Dopamine enhances EPSCs in layer II-III pyramidal neurons in rat prefrontal cortex. *J. Neurosci.* 23, 867–875.

Gorelova, N., and Seamans, J. K. (2015). Cell-attached single-channel recordings in intact prefrontal cortex pyramidal neurons reveal compartmentalized D1/D5 receptor modulation of the persistent sodium current. *Front. Neural Circuits* 9:4. doi: 10.3389/fncir.2015.00004

Gotti, C., Moretti, M., Gaimarri, A., Zanardi, A., Clementi, F., and Zoli, M. (2007). Heterogeneity and complexity of native brain nicotinic receptors. *Biochem. Pharmacol.* 74, 1102–1111. doi: 10.1016/j.bcp.2007.05.023

Gulledge, A. T., and Jaffe, D. B. (1998). Dopamine decreases the excitability of layer V pyramidal cells in the rat prefrontal cortex. *J. Neurosci.* 18, 9139–9151.

Gulledge, A. T., and Jaffe, D. B. (2001). Multiple effects of dopamine on layer V pyramidal cell excitability in rat prefrontal cortex. *J. Neurophysiol.* 86, 586–595. doi: 10.1152/jn.2001.86.2.586

Gulledge, A. T., and Kawaguchi, Y. (2007). Phasic cholinergic signaling in the hippocampus: functional homology with the neocortex? *Hippocampus* 17, 327–332.

Gulledge, A. T., Park, S. B., Kawaguchi, Y., and Stuart, G. J. (2007). Heterogeneity of phasic cholinergic signaling in neocortical neurons. *J. Neurophysiol.* 97, 2215–2229. doi: 10.1152/jn.00493.2006

Gulledge, A. T., and Stuart, G. J. (2005). Cholinergic inhibition of neocortical pyramidal neurons. *J. Neurosci.* 25, 10308–10320. doi: 10.1523/JNEUROSCI.2697-05.2005

Gurevich, E. V., and Joyce, J. N. (2000). Dopamine D(3) receptor is selectively and transiently expressed in the developing whisker barrel cortex of the rat. *J. Comp. Neurol.* 420, 35–51. doi: 10.1002/(SICI)1096-9861(20000424)420:1<35::AID-CNE3>3.0.CO;2-K

Gurevich, E. V., Robertson, R. T., and Joyce, J. N. (2001). Thalamo-cortical afferents control transient expression of the dopamine D(3) receptor in the rat somatosensory cortex. *Cereb. Cortex* 11, 691–701. doi: 10.1093/cercor/11.8.691

Happel, M. F., Deliano, M., Handschuh, J., and Ohl, F. W. (2014). Dopamine-modulated recurrent corticoefferent feedback in primary sensory cortex promotes detection of behaviorally relevant stimuli. *J. Neurosci.* 34, 1234–1247. doi: 10.1523/JNEUROSCI.1990-13.2014

Hasselmo, M. E., and Sarter, M. (2011). Modes and models of forebrain cholinergic neuromodulation of cognition. *Neuropsychopharmacology* 36, 52–73. doi: 10.1038/npp.2010.104

Hattox, A. M., and Nelson, S. B. (2007). Layer V neurons in mouse cortex projecting to different targets have distinct physiological properties. *J. Neurophysiol.* 98, 3330–3340. doi: 10.1152/jn.00397.2007

Hawrylycz, M. J., Lein, E. S., Guillozet-Bongaarts, A. L., Shen, E. H., Ng, L., Miller, J. A., et al. (2012). An anatomically comprehensive atlas of the adult human brain transcriptome. *Nature* 489, 391–399. doi: 10.1038/nature11405

Hay, Y. A., Andjelic, S., Badr, S., and Lambolez, B. (2015). Orexin-dependent activation of layer VIb enhances cortical network activity and integration of non-specific thalamocortical inputs. *Brain Struct. Funct.* 220, 3497–3512. doi: 10.1007/s00429-014-0869-7

Hay, Y. A., Lambolez, B., and Tricoire, L. (2016). Nicotinic transmission onto layer 6 cortical neurons relies on synaptic activation of non-α7 receptors. *Cereb. Cortex* 26, 2549–2562. doi: 10.1093/cercor/bhv085

Hedrick, T., and Waters, J. (2015). Acetylcholine excites neocortical pyramidal neurons via nicotinic receptors. *J. Neurophysiol.* 113, 2195–2209. doi: 10.1152/jn.00716.2014

Henny, P., and Jones, B. E. (2008). Projections from basal forebrain to prefrontal cortex comprise cholinergic, GABAergic and glutamatergic inputs to pyramidal cells or interneurons. *Eur. J. Neurosci.* 27, 654–670. doi: 10.1111/j.1460-9568.2008.06029.x

Huang, J., and Zamponi, G. W. (2017). Regulation of voltage gated calcium channels by GPCRs and post-translational modification. *Curr. Opin. Pharmacol.* 32, 1–8. doi: 10.1016/j.coph.2016.10.001

Kalmbach, A., Hedrick, T., and Waters, J. (2012). Selective optogenetic stimulation of cholinergic axons in neocortex. *J. Neurophysiol.* 107, 2008–2019. doi: 10.1152/jn.00870.2011

Kassam, S. M., Herman, P. M., Goodfellow, N. M., Alves, N. C., and Lambe, E. K. (2008). Developmental excitation of corticothalamic neurons by nicotinic acetylcholine receptors. *J. Neurosci.* 28, 8756–8764. doi: 10.1523/JNEUROSCI.2645-08.2008

Kerr, M. I., Wall, M. J., and Richardson, M. J. (2013). Adenosine A1 receptor activation mediates the developmental shift at layer 5 pyramidal cell synapses and is a determinant of mature synaptic strength. *J. Physiol.* 591, 3371–3380. doi: 10.1113/jphysiol.2012.244392

Koukouli, F., Rooy, M., Tziotis, D., Sailor, K. A., O'neill, H. C., Levenga, J., et al. (2017). Nicotine reverses hypofrontality in animal models of addiction and schizophrenia. *Nat. Med.* 23, 347–354. doi: 10.1038/nm.4274

Krimer, L. S., Jakab, R. L., and Goldman-Rakić, P. S. (1997). Quantitative three-dimensional analysis of the catecholaminergic innervation of identified neurons in the macaque prefrontal cortex. *J. Neurosci.* 17, 7450–7461.

Kroener, S., Chandler, L. J., Phillips, P. E., and Seamans, J. K. (2009). Dopamine modulates persistent synaptic activity and enhances the signal-to-noise ratio in the prefrontal cortex. *PLOS ONE* 4:e6507. doi: 10.1371/journal.pone.0006507

Kukkonen, J. P. (2017). Orexin/Hypocretin Signaling. *Curr. Top. Behav. Neurosci.* 33, 17–50. doi: 10.1007/7854_2016_49

Lavin, A., and Grace, A. A. (2001). Stimulation of D1-type dopamine receptors enhances excitability in prefrontal cortical pyramidal neurons in a state-dependent manner. *Neuroscience* 104, 335–346. doi: 10.1016/S0306-4522(01)00096-3

Lee, H. K., Barbarosie, M., Kameyama, K., Bear, M. F., and Huganir, R. L. (2000). Regulation of distinct AMPA receptor phosphorylation sites during bidirectional synaptic plasticity. *Nature* 405, 955–959. doi: 10.1038/35016089

Lein, E. S., Belgard, T. G., Hawrylycz, M., and Molnár, Z. (2017). Transcriptomic perspectives on neocortical structure, development, evolution, and disease. *Annu. Rev. Neurosci.* 40, 629–652. doi: 10.1146/annurev-neuro-070815-013858

Levey, A. I., Kitt, C. A., Simonds, W. F., Price, D. L., and Brann, M. R. (1991). Identification and localization of muscarinic acetylcholine receptor proteins in brain with subtype-specific antibodies. *J. Neurosci.* 11, 3218–3226.

Li, B., Chen, F., Ye, J., Chen, X., Yan, J., Li, Y., et al. (2010). The modulation of orexin A on HCN currents of pyramidal neurons in mouse prelimbic cortex. *Cereb. Cortex* 20, 1756–1767. doi: 10.1093/cercor/bhp241

Lodato, S., and Arlotta, P. (2015). Generating neuronal diversity in the mammalian cerebral cortex. *Annu. Rev. Cell Dev. Biol.* 31, 699–720. doi: 10.1146/annurev-cellbio-100814-125353

Lu, X. Y., Bagnol, D., Burke, S., Akil, H., and Watson, S. J. (2000). Differential distribution and regulation of OX1 and OX2 orexin/hypocretin receptor messenger RNA in the brain upon fasting. *Horm. Behav.* 37, 335–344. doi: 10.1006/hbeh.2000.1584

Luo, C., Keown, C. L., Kurihara, L., Zhou, J., He, Y., Li, J., et al. (2017). Single-cell methylomes identify neuronal subtypes and regulatory elements in mammalian cortex. *Science* 357, 600–604. doi: 10.1126/science.aan3351

Lüscher, C., and Slesinger, P. A. (2010). Emerging roles for G protein-gated inwardly rectifying potassium (GIRK) channels in health and disease. *Nat. Rev. Neurosci.* 11, 301–315. doi: 10.1038/nrn2834

Ma, S., Hangya, B., Leonard, C. S., Wisden, W., and Gundlach, A. L. (2017). Dual-transmitter systems regulating arousal, attention, learning and memory. *Neurosci. Biobehav. Rev.* 85, 21–33. doi: 10.1016/j.neubiorev.2017.07.009

Marcus, J. N., Aschkenasi, C. J., Lee, C. E., Chemelli, R. M., Saper, C. B., Yanagisawa, M., et al. (2001). Differential expression of orexin receptors 1 and 2 in the rat brain. *J. Comp. Neurol.* 435, 6–25. doi: 10.1002/cne.1190

Marx, M., and Feldmeyer, D. (2013). Morphology and physiology of excitatory neurons in layer 6b of the somatosensory rat barrel cortex. *Cereb. Cortex* 23, 2803–2817. doi: 10.1093/cercor/bhs254

Maurice, N., Tkatch, T., Meisler, M., Sprunger, L. K., and Surmeier, D. J. (2001). D1/D5 dopamine receptor activation differentially modulates rapidly inactivating and persistent sodium currents in prefrontal cortex pyramidal neurons. *J. Neurosci.* 21, 2268–2277.

McCormick, D. A., and Prince, D. A. (1986). Mechanisms of action of acetylcholine in the guinea-pig cerebral cortex in vitro. *J. Physiol.* 375, 169–194. doi: 10.1113/jphysiol.1986.sp016112

McDonald, B. J., Chung, H. J., and Huganir, R. L. (2001). Identification of protein kinase C phosphorylation sites within the AMPA receptor GluR2 subunit. *Neuropharmacology* 41, 672–679. doi: 10.1016/S0028-3908(01)00129-0

Mesulam, M. M., Mufson, E. J., Levey, A. I., and Wainer, B. H. (1983a). Cholinergic innervation of cortex by the basal forebrain: cytochemistry and cortical connections of the septal area, diagonal band nuclei, nucleus basalis (substantia innominata), and hypothalamus in the rhesus monkey. *J. Comp. Neurol.* 214, 170–197. doi: 10.1002/cne.902140206

Mesulam, M. M., Mufson, E. J., Wainer, B. H., and Levey, A. I. (1983b). Central cholinergic pathways in the rat: an overview based on an alternative nomenclature (Ch1–Ch6). *Neuroscience* 10, 1185–1201.

Meynert, T. (1867). Der Bau der Großhirnrinde und seiner örtlichen Verschiedenheiten, nebst einem pathologisch-anatomischen Collarium. *Vierteljahresschr. Psychiat.* 1, 77–93.

Molnár, Z., and Cheung, A. F. (2006). Towards the classification of subpopulations of layer V pyramidal projection neurons. *Neurosci. Res.* 55, 105–115. doi: 10.1016/j.neures.2006.02.008

Molyneaux, B. J., Goff, L. A., Brettler, A. C., Chen, H. H., Brown, J. R., Hrvatin, S., et al. (2015). DeCoN: genome-wide analysis of In Vivo transcriptional dynamics during pyramidal neuron fate selection in neocortex. *Neuron* 85, 275–288. doi: 10.1016/j.neuron.2014.12.024

Moore, A. R., Zhou, W. L., Potapenko, E. S., Kim, E. J., and Antic, S. D. (2011). Brief dopaminergic stimulations produce transient physiological changes in prefrontal pyramidal neurons. *Brain Res.* 1370, 1–15. doi: 10.1016/j.brainres.2010.10.111

Morishima, M., and Kawaguchi, Y. (2006). Recurrent connection patterns of corticostriatal pyramidal cells in frontal cortex. *J. Neurosci.* 26, 4394–4405. doi: 10.1523/JNEUROSCI.0252-06.2006

Morishima, M., Morita, K., Kubota, Y., and Kawaguchi, Y. (2011). Highly differentiated projection-specific cortical subnetworks. *J. Neurosci.* 31, 10380–10391. doi: 10.1523/JNEUROSCI.0772-11.2011

Mrzljak, L., Bergson, C., Pappy, M., Huff, R., Levenson, R., and Goldman-Rakic, P. S. (1996). Localization of dopamine D4 receptors in GABAergic neurons of the primate brain. *Nature* 381, 245–248. doi: 10.1038/381245a0

Mrzljak, L., Levey, A. I., and Goldman-Rakic, P. S. (1993). Association of m1 and m2 muscarinic receptor proteins with asymmetric synapses in the primate cerebral cortex: morphological evidence for cholinergic modulation of excitatory neurotransmission. *Proc. Natl. Acad. Sci. U.S.A.* 90, 5194–5198. doi: 10.1073/pnas.90.11.5194

Muñoz, W., and Rudy, B. (2014). Spatiotemporal specificity in cholinergic control of neocortical function. *Curr. Opin. Neurobiol.* 26, 149–160. doi: 10.1016/j.conb.2014.02.015

Murphy, J. G., Sanderson, J. L., Gorski, J. A., Scott, J. D., Catterall, W. A., Sather, W. A., et al. (2014). AKAP-anchored PKA maintains neuronal L-type calcium channel activity and NFAT transcriptional signaling. *Cell Rep.* 7, 1577–1588. doi: 10.1016/j.celrep.2014.04.027

Narayanan, R. T., Egger, R., Johnson, A. S., Mansvelder, H. D., Sakmann, B., De Kock, C. P., et al. (2015). Beyond columnar organization: cell type- and target layer-specific principles of horizontal axon projection patterns in rat vibrissal cortex. *Cereb. Cortex* 25, 4450–4468. doi: 10.1093/cercor/bhv053

Narayanan, R. T., Udvary, D., and Oberlaender, M. (2017). Cell type-specific structural organization of the six layers in rat barrel cortex. *Front. Neuroanat.* 11:91. doi: 10.3389/fnana.2017.00091

Nomura, S., Bouhadana, M., Morel, C., Faure, P., Cauli, B., Lambolez, B., et al. (2014). Noradrenalin and dopamine receptors both control cAMP-PKA signaling throughout the cerebral cortex. *Front. Cell Neurosci.* 8:247. doi: 10.3389/fncel.2014.00247

Nuñez, A., Domínguez, S., Buño, W., and Fernández De Sevilla, D. (2012). Cholinergic-mediated response enhancement in barrel cortex layer V pyramidal neurons. *J. Neurophysiol.* 108, 1656–1668. doi: 10.1152/jn.00156.2012

Oberlaender, M., Boudewijns, Z. S., Kleele, T., Mansvelder, H. D., Sakmann, B., and De Kock, C. P. (2011). Three-dimensional axon morphologies of individual layer 5 neurons indicate cell type-specific intracortical pathways for whisker motion and touch. *Proc. Natl. Acad. Sci. U.S.A.* 108, 4188–4193. doi: 10.1073/pnas.1100647108

Oberlaender, M., De Kock, C. P., Bruno, R. M., Ramirez, A., Meyer, H. S., Dercksen, V. J., et al. (2012). Cell type-specific three-dimensional structure of thalamocortical circuits in a column of rat vibrissal cortex. *Cereb. Cortex* 22, 2375–2391. doi: 10.1093/cercor/bhr317

Oldham, W. M., and Hamm, H. E. (2008). Heterotrimeric G protein activation by G-protein-coupled receptors. *Nat. Rev. Mol. Cell Biol.* 9, 60–71. doi: 10.1038/nrm2299

Parnavelas, J. G., Kelly, W., Franke, E., and Eckenstein, F. (1986). Cholinergic neurons and fibres in the rat visual cortex. *J. Neurocytol.* 15, 329–336. doi: 10.1007/BF01611435

Pedarzani, P., and Storm, J. F. (1993). PKA mediates the effects of monoamine transmitters on the K+ current underlying the slow spike frequency adaptation in hippocampal neurons. *Neuron* 11, 1023–1035. doi: 10.1016/0896-6273(93)90216-E

Pedarzani, P., and Storm, J. F. (1995). Protein kinase A-independent modulation of ion channels in the brain by cyclic AMP. *Proc. Natl. Acad. Sci. U.S.A.* 92, 11716–11720. doi: 10.1073/pnas.92.25.11716

Poorthuis, R. B., Bloem, B., Schak, B., Wester, J., De Kock, C. P., and Mansvelder, H. D. (2013a). Layer-specific modulation of the prefrontal cortex by nicotinic acetylcholine receptors. *Cereb. Cortex* 23, 148–161. doi: 10.1093/cercor/bhr390

Poorthuis, R. B., Bloem, B., Verhoog, M. B., and Mansvelder, H. D. (2013b). Layer-specific interference with cholinergic signaling in the prefrontal cortex by smoking concentrations of nicotine. *J. Neurosci.* 33, 4843–4853. doi: 10.1523/JNEUROSCI.5012-12.2013

Porkka-Heiskanen, T., and Kalinchuk, A. V. (2011). Adenosine, energy metabolism and sleep homeostasis. *Sleep Med. Rev.* 15, 123–135. doi: 10.1016/j.smrv.2010.06.005

Qi, G., Van Aerde, K., Abel, T., and Feldmeyer, D. (2016). Adenosine differentially modulates synaptic transmission of excitatory and inhibitory microcircuits in layer 4 of rat barrel cortex. *Cereb. Cortex* 27, 4411–4422. doi: 10.1093/cercor/bhw243

Rebola, N., Pinheiro, P. C., Oliveira, C. R., Malva, J. O., and Cunha, R. A. (2003). Subcellular localization of adenosine A(1) receptors in nerve terminals and synapses of the rat hippocampus. *Brain Res.* 987, 49–58. doi: 10.1016/S0006-8993(03)03247-5

Ribeiro, J. A., Sebastião, A. M., and De Mendonça, A. (2002). Adenosine receptors in the nervous system: pathophysiological implications. *Prog. Neurobiol.* 68, 377–392. doi: 10.1016/S0301-0082(02)00155-7

Richter, C., Woods, I. G., and Schier, A. F. (2014). Neuropeptidergic control of sleep and wakefulness. *Annu. Rev. Neurosci.* 37, 503–531. doi: 10.1146/annurev-neuro-062111-150447

Rivera, A., Penafiel, A., Megias, M., Agnati, L. F., Lopez-Tellez, J. F., Gago, B., et al. (2008). Cellular localization and distribution of dopamine D(4) receptors in the rat cerebral cortex and their relationship with the cortical dopaminergic and noradrenergic nerve terminal networks. *Neuroscience* 155, 997–1010. doi: 10.1016/j.neuroscience.2008.05.060

Rotaru, D. C., Lewis, D. A., and Gonzalez-Burgos, G. (2007). Dopamine D1 receptor activation regulates sodium channel-dependent EPSP amplification in rat prefrontal cortex pyramidal neurons. *J. Physiol.* 581, 981–1000. doi: 10.1113/jphysiol.2007.130864

Sakurai, T. (2007). The neural circuit of orexin (hypocretin): maintaining sleep and wakefulness. *Nat. Rev. Neurosci.* 8, 171–181. doi: 10.1038/nrn2092

Sakurai, T. (2013). Orexin deficiency and narcolepsy. *Curr. Opin. Neurobiol.* 23, 760–766. doi: 10.1016/j.conb.2013.04.007

Santana, N., and Artigas, F. (2017). Laminar and cellular distribution of monoamine receptors in rat medial prefrontal cortex. *Front. Neuroanat.* 11:87. doi: 10.3389/fnana.2017.00087

Santana, N., Mengod, G., and Artigas, F. (2009). Quantitative analysis of the expression of dopamine D1 and D2 receptors in pyramidal and GABAergic neurons of the rat prefrontal cortex. *Cereb. Cortex* 19, 849–860. doi: 10.1093/cercor/bhn134

Sarter, M., Parikh, V., and Howe, W. M. (2009). Phasic acetylcholine release and the volume transmission hypothesis: time to move on. *Nat. Rev. Neurosci.* 10, 383–390. doi: 10.1038/nrn2635

Satake, T., Mitani, H., Nakagome, K., and Kaneko, K. (2008). Individual and additive effects of neuromodulators on the slow components of afterhyperpolarization currents in layer V pyramidal cells of the rat medial prefrontal cortex. *Brain Res.* 1229, 47–60. doi: 10.1016/j.brainres.2008.06.098

Seamans, J. K., Durstewitz, D., Christie, B. R., Stevens, C. F., and Sejnowski, T. J. (2001). Dopamine D1/D5 receptor modulation of excitatory synaptic inputs to layer V prefrontal cortex neurons. *Proc. Natl. Acad. Sci. U.S.A.* 98, 301–306. doi: 10.1073/pnas.98.1.301

Sebastião, A. M., and Ribeiro, J. A. (2009). Adenosine receptors and the central nervous system. *Handb. Exp. Pharmacol.* 193, 471–534. doi: 10.1007/978-3-540-89615-9_16

Séguéla, P., Wadiche, J., Dineley-Miller, K., Dani, J. A., and Patrick, J. W. (1993). Molecular cloning, functional properties, and distribution of rat brain alpha 7: a nicotinic cation channel highly permeable to calcium. *J. Neurosci.* 13, 596–604.

Seong, H. J., and Carter, A. G. (2012). D1 receptor modulation of action potential firing in a subpopulation of layer 5 pyramidal neurons in the prefrontal cortex. *J. Neurosci.* 32, 10516–10521. doi: 10.1523/JNEUROSCI.1367-12.2012

Sundberg, S. C., Lindstrom, S. H., Sanchez, G. M., and Granseth, B. (2017). Cre-expressing neurons in visual cortex of Ntsr1-Cre GN220 mice are corticothalamic and are depolarized by acetylcholine. *J. Comp. Neurol.* 526, 120–132. doi: 10.1002/cne.24323

Taber, K. H., and Hurley, R. A. (2014). Volume transmission in the brain: beyond the synapse. *J. Neuropsychiatry Clin. Neurosci.* 26, iv, 1–4. doi: 10.1176/appi.neuropsych.13110351

Takács, V. T., Freund, T. F., and Nyiri, G. (2013). Neuroligin 2 is expressed in synapses established by cholinergic cells in the mouse brain. *PLOS ONE* 8:e72450. doi: 10.1371/journal.pone.0072450

Tasic, B., Menon, V., Nguyen, T. N., Kim, T. K., Jarsky, T., Yao, Z., et al. (2016). Adult mouse cortical cell taxonomy revealed by single cell transcriptomics. *Nat. Neurosci.* 19, 335–346. doi: 10.1038/nn.4216

Thiele, A. (2013). Muscarinic signaling in the brain. *Annu. Rev. Neurosci.* 36, 271–294. doi: 10.1146/annurev-neuro-062012-170433

Tritsch, N. X., and Sabatini, B. L. (2012). Dopaminergic modulation of synaptic transmission in cortex and striatum. *Neuron* 76, 33–50. doi: 10.1016/j.neuron.2012.09.023

Trivedi, P., Yu, H., Macneil, D. J., Van Der Ploeg, L. H., and Guan, X. M. (1998). Distribution of orexin receptor mRNA in the rat brain. *FEBS Lett.* 438, 71–75. doi: 10.1016/S0014-5793(98)01266-6

Turrini, P., Casu, M. A., Wong, T. P., De Koninck, Y., Ribeiro-Da-Silva, A., and Cuello, A. C. (2001). Cholinergic nerve terminals establish classical synapses in the rat cerebral cortex: synaptic pattern and age-related atrophy. *Neuroscience* 105, 277–285. doi: 10.1016/S0306-4522(01)00172-5

Umbriaco, D., Watkins, K. C., Descarries, L., Cozzari, C., and Hartman, B. K. (1994). Ultrastructural and morphometric features of the acetylcholine innervation in adult rat parietal cortex: an electron microscopic study in serial sections. *J. Comp. Neurol.* 348, 351–373. doi: 10.1002/cne.903480304

Urban, N. N., Gonzalez-Burgos, G., Henze, D. A., Lewis, D. A., and Barrionuevo, G. (2002). Selective reduction by dopamine of excitatory synaptic inputs to pyramidal neurons in primate prefrontal cortex. *J. Physiol.* 539, 707–712. doi: 10.1113/jphysiol.2001.015024

van Aerde, K. I., Qi, G., and Feldmeyer, D. (2015). Cell type-specific effects of adenosine on cortical neurons. *Cereb. Cortex* 25, 772–787. doi: 10.1093/cercor/bht274

Vincent, S. L., Khan, Y., and Benes, F. M. (1995). Cellular colocalization of dopamine D1 and D2 receptors in rat medial prefrontal cortex. *Synapse* 19, 112–120. doi: 10.1002/syn.890190207

Vogt, O. (1906). Über strukturelle Hirnzentra, mit besonderer Berücksichtigung der strukturellen Felder des Cortex pallii. *Anat. Anz.* 20, 74–114.

von Economo, C. (1929). Der Zellaufbau der Grosshirnrinde und die progressive Cerebration. *Ergeb. Physiol.* 29, 83–128. doi: 10.1007/BF02322367

von Engelhardt, J., Eliava, M., Meyer, A. H., Rozov, A., and Monyer, H. (2007). Functional characterization of intrinsic cholinergic interneurons in the cortex. *J. Neurosci.* 27, 5633–5642. doi: 10.1523/JNEUROSCI.4647-06.2007

Wada, E., Mckinnon, D., Heinemann, S., Patrick, J., and Swanson, L. W. (1990). The distribution of mRNA encoded by a new member of the neuronal nicotinic acetylcholine receptor gene family (alpha 5) in the rat central nervous system. *Brain Res.* 526, 45–53. doi: 10.1016/0006-8993(90)90248-A

Wada, E., Wada, K., Boulter, J., Deneris, E., Heinemann, S., Patrick, J., et al. (1989). Distribution of alpha 2, alpha 3, alpha 4, and beta 2 neuronal nicotinic receptor subunit mRNAs in the central nervous system: a hybridization histochemical study in the rat. *J. Comp. Neurol.* 284, 314–335. doi: 10.1002/cne.902840212

Wang, Y., and Goldman-Rakic, P. S. (2004). D2 receptor regulation of synaptic burst firing in prefrontal cortical pyramidal neurons. *Proc. Natl. Acad. Sci. U.S.A.* 101, 5093–5098. doi: 10.1073/pnas.0400954101

Wedzony, K., Chocyk, A., Mackowiak, M., Fijal, K., and Czyrak, A. (2000). Cortical localization of dopamine D4 receptors in the rat brain–immunocytochemical study. *J. Physiol. Pharmacol.* 51, 205–221.

Weiner, D. M., Levey, A. I., Sunahara, R. K., Niznik, H. B., O'dowd, B. F., Seeman, P., et al. (1991). D1 and D2 dopamine receptor mRNA in rat brain. *Proc. Natl. Acad. Sci. U.S.A.* 88, 1859–1863. doi: 10.1073/pnas.88.5.1859

Wenger Combremont, A. L., Bayer, L., Dupre, A., Muhlethaler, M., and Serafin, M. (2016a). Effects of Hypocretin/Orexin and major transmitters of arousal on fast spiking neurons in mouse cortical layer 6B. *Cereb. Cortex* 26, 3553–3562. doi: 10.1093/cercor/bhw158

Wenger Combremont, A. L., Bayer, L., Dupre, A., Muhlethaler, M., and Serafin, M. (2016b). Slow bursting neurons of mouse cortical layer 6b are depolarized by Hypocretin/Orexin and major transmitters of arousal. *Front. Neurol.* 7:88. doi: 10.3389/fneur.2016.00088

Xiao, Y., and Kellar, K. J. (2004). The comparative pharmacology and up-regulation of rat neuronal nicotinic receptor subtype binding sites stably expressed in transfected mammalian cells. *J. Pharmacol. Exp. Ther.* 310, 98–107. doi: 10.1124/jpet.104.066787

Xing, B., Li, Y. C., and Gao, W. J. (2016). Norepinephrine versus dopamine and their interaction in modulating synaptic function in the prefrontal cortex. *Brain Res.* 1641, 217–233. doi: 10.1016/j.brainres.2016.01.005

Yan, J., He, C., Xia, J. X., Zhang, D., and Hu, Z. A. (2012). Orexin-A excites pyramidal neurons in layer 2/3 of the rat prefrontal cortex. *Neurosci. Lett.* 520, 92–97. doi: 10.1016/j.neulet.2012.05.038

Yang, C. R., and Seamans, J. K. (1996). Dopamine D1 receptor actions in layers V-VI rat prefrontal cortex neurons in vitro: modulation of dendritic-somatic signal integration. *J. Neurosci.* 16, 1922–1935.

Yeomans, J. S. (2012). Muscarinic receptors in brain stem and mesopontine cholinergic arousal functions. *Handb. Exp. Pharmacol.* 208, 243–259. doi: 10.1007/978-3-642-23274-9_11

Yi, F., Zhang, X. H., Yang, C. R., and Li, B. M. (2013). Contribution of dopamine d1/5 receptor modulation of post-spike/burst afterhyperpolarization to enhance neuronal excitability of layer v pyramidal neurons in prepubertal rat prefrontal cortex. *PLOS ONE* 8:e71880. doi: 10.1371/journal.pone.0071880

Zaborszky, L., Csordas, A., Mosca, K., Kim, J., Gielow, M. R., Vadasz, C., et al. (2015). Neurons in the basal forebrain project to the cortex in a complex topographic organization that reflects corticocortical connectivity patterns: an experimental study based on retrograde tracing and 3D reconstruction. *Cereb. Cortex* 25, 118–137. doi: 10.1093/cercor/bht210

Zamponi, G. W., Striessnig, J., Koschak, A., and Dolphin, A. C. (2015). The physiology, pathology, and pharmacology of voltage-gated calcium channels and their future therapeutic potential. *Pharmacol. Rev.* 67, 821–870. doi: 10.1124/pr.114.009654

Zeisel, A., Muñoz-Manchado, A. B., Codeluppi, S., Lönnerberg, P., La Manno, G., Juréus, A., et al. (2015). Brain structure. Cell types in the mouse cortex and hippocampus revealed by single-cell RNA-seq. *Science* 347, 1138–1142. doi: 10.1126/science.aaa1934

Zoli, M., Jansson, A., Sykova, E., Agnati, L. F., and Fuxe, K. (1999). Volume transmission in the CNS and its relevance for neuropsychopharmacology. *Trends Pharmacol. Sci.* 20, 142–150. doi: 10.1016/S0165-6147(99)01343-7

Zolles, G., Wagner, E., Lampert, A., and Sutor, B. (2009). Functional expression of nicotinic acetylcholine receptors in rat neocortical layer 5 pyramidal cells. *Cereb. Cortex* 19, 1079–1091. doi: 10.1093/cercor/bhn158

Conflict of Interest Statement: The authors declare that the research was conducted in the absence of any commercial or financial relationships that could be construed as a potential conflict of interest.

frontiers in Neuroanatomy

ORIGINAL RESEARCH
published: 16 February 2018
doi: 10.3389/fnana.2018.00009

Laminar Distribution of Subsets of GABAergic Axon Terminals in Human Prefrontal Cortex

Kenneth N. Fish[1]*, *Brad R. Rocco*[1] and *David A. Lewis*[1,2]

[1]Western Psychiatric Institute and Clinic, Department of Psychiatry, University of Pittsburgh School of Medicine, Pittsburgh, PA, United States, [2]Department of Neuroscience, University of Pittsburgh School of Medicine, Pittsburgh, PA, United States

In human prefrontal cortex (PFC), ∼85% of γ-aminobutyric acid (GABA)-expressing neurons can be subdivided into non-overlapping groups by the presence of calbindin (CB), calretinin (CR) or parvalbumin (PV). Substantial research has focused on the differences in the laminar locations of the cells bodies of these neurons, with limited attention to the distribution of their axon terminals, their sites of action. We previously reported that in non-human primates subtypes of these cells are distinguishable by differences in terminal protein levels of the GABA synthesizing enzymes glutamic acid decarboxylase 65 (GAD65) and GAD67. Here we used multi-label fluorescence microscopy in human PFC to assess: (1) the laminar distributions of axon terminals containing CB, CR, or PV; and (2) the relative protein levels of GAD65, GAD67 and vesicular GABA transporter (vGAT) in CB, CR and PV terminals. The densities of the different CB, CR and PV terminal subpopulations differed across layers of the PFC. PV terminals comprised two subsets based on the presence of only GAD67 (GAD67+) or both GADs (GAD65/GAD67+), whereas CB and CR terminals comprised three subsets (GAD65+, GAD67+, or GAD65/GAD67+). The densities of the different CB, CR and PV GAD terminal subpopulations also differed across layers. Finally, within each of the three calcium-binding protein subpopulations intra-terminal protein levels of GAD and vGAT differed by GAD subpopulation. These findings are discussed in the context of the laminar distributions of CB, CR and PV cell bodies and the synaptic targets of their axons.

Keywords: GAD65, GAD67, glutamic acid decarboxylase, vGAT, human PFC

OPEN ACCESS

Edited by:
Kathleen S. Rockland, School of Medicine, Boston University, United States

Reviewed by:
Kathryn M. Murphy, McMaster University, Canada
Fiorenzo Conti, Università Politecnica delle Marche, Italy

***Correspondence:**
Kenneth N. Fish
fishkn@upmc.edu

Received: *10 November 2017*
Accepted: *24 January 2018*
Published: *16 February 2018*

Citation:
Fish KN, Rocco BR and Lewis DA (2018) Laminar Distribution of Subsets of GABAergic Axon Terminals in Human Prefrontal Cortex. Front. Neuroanat. 12:9. doi: 10.3389/fnana.2018.00009

INTRODUCTION

The questions "Why does the cortex have layers? What is the function of layering? How do cortical neurons integrate information across different layers?" are particularly challenging to answer for the human neocortex because it is not possible to perform the types of tract tracing and electrophysiological studies that have provided key insights in other species. However, important information about human cortical neurons and their axon terminals can be obtained using techniques, such as quantitative fluorescence microscopy, that can be employed in postmortem human brain.

The release of γ-aminobutyric acid (GABA) from the axon terminals of interneurons plays a critical role in regulating the activity of excitatory pyramidal cells (PCs) and thus in determining

the function of cortical networks. Essentially all cortical GABA is synthesized locally in terminals by the 67 and 65 kilodalton isoforms of glutamic acid decarboxylase (GAD), which are products of separate genes and undergo different post-translational modifications. GAD65 is thought to provide the on-demand pool of GABA, whereas GAD67 provides the basal pool. GAD65 has a long half-life (>24 h) and is efficiently trafficked to axonal terminals; in contrast, the half-life of GAD67 is short (∼2 h) and its trafficking to terminals appears to be less efficient as it is distributed throughout interneurons. GAD activity is regulated by a cycle of activation and inactivation, which is determined by the binding and release, respectively, of its co-factor, pyridoxal 5′-phosphate. The activity of GAD65 is co-factor dependent and is highly regulated in response to GABA concentration and neuronal activity, and thus under steady state conditions GAD65 is largely inactive (∼70 to 93%). In contrast, GAD67 is primarily active (∼72%) and is activity-regulated mainly by transcription. In concert, these findings suggest that the two GAD isoforms: (1) provide complementary means for regulating GABA synthesis; and (2) are involved differentially in the spatial and temporal processing of information by GABA-containing neurons (Wilson and Groves, 1981; Contreras et al., 1992; Mercugliano et al., 1992; Feldblum et al., 1993, 1995; Esclapez et al., 1994; Pedneault and Soghomonian, 1994; Soghomonian et al., 1994; Wilson and Kawaguchi, 1996; Bowers et al., 1998; Soghomonian and Martin, 1998).

Based on their functional properties and synaptic targets, different classes of cortical GABAergic neurons play complementary roles in regulating the output of PCs in each cortical layer. Most (∼85%) GABAergic neurons in the primate prefrontal cortex (PFC) can be differentiated into non-overlapping subtypes based on the expression of one of three calcium-binding proteins—parvalbumin (PV; ∼20%), calbindin (CB; ∼20%), or calretinin (CR; ∼45%; Condé et al., 1994; del Río and DeFelipe, 1996; Gabbott and Bacon, 1996; Barinka and Druga, 2010). Terminals from PV neurons target the perisomatic region of PCs and are thought to play an important role in generating gamma oscillations (Gonzalez-Burgos et al., 2015). Terminals from a subset of CB neurons target dendritic compartments of PCs and of other GABAergic, non-CB neuron subtypes (Lewis et al., 2002). Thus, PV and CB neurons provide different strategies for regulating neuronal input-output transformations within cortical circuits as well as feedforward or feedback inhibition within and between cortical layers. Terminals from CR neurons mainly target GABAergic neurons and mediate disinhibitory control of PCs, leading to the selective amplification of local signal processing (Melchitzky and Lewis, 2008). Interestingly, PV, CB and CR interneuron subtypes in monkey PFC can be further subdivided based on the expression of GAD65—some express both GAD65 and GAD67, whereas others express only GAD67 (Fish et al., 2011; Rocco et al., 2016b). Considering the unique role GAD65 and GAD67 play in GABA synthesis within terminals, differential expression of GAD might define functional subsets of PV, CB and CR neurons.

To gain insights about human cortical neurons and their axon terminals in the context of the lamination of the human PFC, the present study capitalized on new quantitative fluorescence microscopy techniques to assess indicators of the amount and type of GABA inhibition each cortical layer receives. Because GAD65 and GAD67 play unique roles in the synthesis of terminal GABA, a major focus of the studies was the assessment of GAD protein levels in terminals immunoreactive (IR) for CB, CR, or PV within each layer.

MATERIALS AND METHODS

Subjects

Brain specimens from 20 subjects (Supplementary Table S1) were recovered during autopsies conducted at the Allegheny County Medical Examiner's Office (Pittsburgh, PA, USA) after obtaining consent from the next of kin. An independent committee of experienced research clinicians confirmed the absence of any psychiatric or neurological diagnoses for each subject using the results of structured interviews conducted with family members, review of medical records and neuropathology exam. Because the length of the postmortem interval (PMI) can affect protein integrity and aging can differentially affect gene expression, only subjects with PMI <16 h and age ≤55 years were used. The University of Pittsburgh's Committee for the Oversight of Research and Clinical Training Involving the Dead and Institutional Review Board for Biomedical Research approved all procedures.

The left hemisphere of each brain was blocked coronally at 1–2 cm intervals, immersed in 4% paraformaldehyde for 48 h at 4°C and then washed in a series of graded sucrose solutions and cryoprotected. Tissue blocks containing the PFC were sectioned coronally at 40 μm on a cryostat and stored in a 30% glycerol/30% ethylene glycol solution at −30°C until processed for immunohistochemistry.

Immunohistochemistry

Four different quadruple-label immunohistochemistry experiments were performed (**Table 1**). For each subject, two sections containing PFC area 9, identified from nearby Nissl-stained sections, and spaced ∼500 μm apart were used in each of the four experiments. A single run containing 40 sections (2 sections/subject) was performed for each experiment. The

TABLE 1 | Antibodies and immunohistochemistry experiments.

Antigen	Species	Dilution	Source	Experiments			
				A	B	C	D
CB	Rabbit	1:1000	Swant	X			X
CR	Rabbit	1:1000	Swant		X		
CR	Goat	1:1000	Swant				X
PV	Rabbit	1:1000	Swant			X	
PV	Guinea pig	1:500	Synaptic systems				X
vGAT	Mouse	1:500	Synaptic systems	X	X	X	X
GAD65	Guinea pig	1:500	Synaptic systems	X	X	X	
GAD67	Goat	1:100	R&D systems	X	X	X	

Rows marked in the experiment column indicates the antigens labeled in each immunohistochemistry assay. See the "Materials and Methods" section for information on how the specificity of each antibody was verified.

sodium citrate antigen retrieval method (Jiao et al., 1999) was performed to enhance immunostaining followed by section permeabilization with 0.3% Triton X-100 in PBS for 30 min at room temperature (RT). Sections were then blocked using 20% donkey serum in PBS for 2 h at RT, and incubated for ∼72 h at 4°C in PBS containing 2% donkey serum and primary antibodies (**Table 1**). The specificity of each antibody was verified as follows: (1) Western blot using human PFC tissue; (2) PV, CB, CR and vesicular GABA transporter (vGAT) antibodies were analyzed by immunolabeling and Western blot using control mouse and knockout tissue; (3) PV (rabbit), CB and CR antibodies were verified using immunolabeling after preadsorption with recombinant protein; and (4) PV (guinea pig), vGAT and GAD antibodies were verified by immunolabeling after preadsorption with the peptide against which each were raised (data not shown, manufacture data sheets, and Celio and Heizmann, 1981; Gottlieb et al., 1986; Kagi et al., 1987; Chang and Gottlieb, 1988; Schwaller et al., 1993; Airaksinen et al., 1997; Guo et al., 2009). Sections were then rinsed for 2 h in PBS and incubated for 24 h in PBS containing 2% donkey serum and secondary antibodies (donkey host) conjugated to biotin (1:250), Alexa 488 (1:500), Alexa 568 (1:500), or Alexa 647 (1:500; Invitrogen, Grand Island, NY, USA for all Alexa secondary antibodies) at 4°C. Next, the sections were rinsed in PBS (2 h), incubated with streptavidin Alexa 405 (1:200) for 24 h, rinsed in PBS (2 h) and mounted (ProLong Gold antifade reagent, Invitrogen) on slides which were stored at 4°C until imaged. Secondary antibody specificity was verified by omitting the primary antibody in control experiments. Multiple pilot studies were performed to determine if any primary/secondary combinations influenced the outcome; results from these studies indicated that the ability to detect each antigen was not dependent on the secondary antibody spectra.

In Situ Hybridization

In situ hybridization probes were designed by Advanced Cell Diagnostics, Inc. (Hayward, CA, USA) to detect mRNAs encoding GAD65 (*GAD2* gene), GAD67 (*GAD1* gene), CB (*CALB1* gene), CR (*CALB2* gene), or PV (*PVALB* gene). Tissue samples were processed using the RNAscope® 2.0 Assay according to the manufacturer's protocol. Briefly, tissue sections (12 μm) from the fresh-frozen right PFC of five subjects were fixed for 15 min in ice-cold 4% paraformaldehyde, incubated in a protease treatment, and then the probes were hybridized to their target mRNAs for 2 h at 40°C. The sections were exposed to a series of incubations that amplified the target probes, and then counterstained with DAPI. GAD65 and GAD67 mRNAs were detected with Alexa 488 and Atto 647, respectively. CB, CR, or PV mRNA was detected with Atto 550.

Microscopy

Data from immunohistochemistry experiments were collected on an Olympus (Center Valley, PA, USA) IX81 inverted microscope equipped with an Olympus spinning disk confocal unit, Hamamatsu EM-CCD digital camera (Bridgewater, NJ, USA), and high precision BioPrecision2 XYZ motorized stage with linear XYZ encoders (Ludl Electronic Products Ltd., Hawthorne, NJ, USA) using a 60× 1.40 N.A. SC oil immersion objective. The equipment was controlled by SlideBook 6.0 (Intelligent Imaging Innovations, Inc., Denver, CO, USA), which was the same software used for post-image processing. 3D image stacks (2D images successively captured at intervals separated by 0.25 μm in the z-dimension) that were 512 × 512 pixels (∼137 × 137 μm; pixel size = 0.267 μm) were acquired over 50 percent of the total thickness of the tissue section starting at the coverslip. Importantly, imaging the same percentage, rather than the same number of microns, of the tissue section thickness controls for the potential confound of storage and/or mounting related volume differences (i.e., *z*-axis shrinkage). The stacks were collected using optimal exposure settings (i.e., those that yielded the greatest dynamic range with no saturated pixels), with differences in exposures normalized during image processing.

Sampling

As determined by measurements made in Nissl-stained sections, the boundaries of the six cortical layers were estimated based on the distance from the pial surface to the white matter: 1 (pia-10%), 2 (10%–20%), 3 (20%–50%), 4 (50%–60%), 5 (60%–80%) and 6 (80%-gray/white matter border). Ten systematic randomly sampled image stacks were taken in each layer per section by applying a sampling grid of 180 × 180 μm^2.

Image Processing

Each fluorescent channel was deconvolved using Autoquant's Blind Deconvolution algorithm. Data segmentation was performed as previously described (Rocco et al., 2016a,b, 2017). Briefly, a Gaussian channel was made for each deconvolved channel by calculating a difference of Gaussians using sigma values of 0.7 and 2. The Gaussian channel was used for data segmentation only. The Ridler-Calvard iterative thresholding algorithm (Ridler and Calvard, 1978) was used to obtain an initial value for iterative segmentation for each channel within each image stack. Multiple iterations with subsequent threshold settings increasing by 25 gray levels were performed in MATLAB (R2015b). After each iteration, the object masks were size-gated within a range of 0.05–0.7 μm^3. For analyses, the image stacks were virtually cropped in the x-, y- and z-dimensions using the center x-, y- and z-coordinates of the IR puncta object masks. In the x- and y-dimensions, the center of each object mask had to be contained in the central 490 × 490 pixels of the image. To select the z-dimension used for analyses, the z-position of each object mask was normalized by the following equation: $Z_{coordinate}$ (# of z-planes for image stack/40).

Next, each object mask was placed in 1 of 40 z-bins based on its normalized z-position. The mean object mask density and mean fluorescence intensity for vGAT and GAD67 were determined within each z-bin, and used for an analysis of variance with *post hoc* comparison via Tukey's honestly significant difference test. The maximum number of adjacent z-bins that were not significantly different for both intensity and object mask number across all channels were used for analyses. By taking this approach we controlled for possible edge effects (i.e., all puncta assessed were fully represented in the virtual space), differences in antibody penetration and differences in

fluorochromes. The final object masks were then used to collect information on the deconvolved channels and to determine terminal density.

Lipofuscin in Human Postmortem Brain Tissue

The major source of native fluorescence in postmortem tissue is from lipofuscin, an intracellular lysosomal protein that accumulates with age (Benavides et al., 2002; Porta, 2002) and fluoresces across the visible spectrum. In previous triple-label studies, we imaged lipofuscin in a fourth visible channel and during processing used information in the lipofuscin channel to exclude signal in the other channels for analysis. This approach has proven to be very effective (Sweet et al., 2010; Curley et al., 2011; Glausier et al., 2014; Rocco et al., 2016a, 2017). In the present studies, all visible channels were needed to separate four different proteins in the same section. Our spectral analysis of lipofuscin revealed that it has a broad Stokes shift such that upon being excited at 402 nm the emission signal can be efficiently collected at 705 nm. Thus, to eliminate this potential confound lipofuscin was imaged using a custom filter combination (402 ex/705 em) in a 5th channel. Lipofuscin was masked using an optimal threshold value, and mask objects made from the other channels that overlapped a lipofuscin mask were eliminated from analyses.

Classification of Terminals

For immunohistochemistry experiments (**Table 1**), PV-IR, CB-IR and CR-IR puncta were classified as a terminal if they also contained vGAT and GAD65 and/or GAD67. A multistep process was used to classify vGAT-IR puncta as GAD65+, GAD67+, or GAD65/GAD67+ terminals. Specifically, mask operations were used to identify GAD65 and vGAT object masks that overlapped each other's centers and did not overlap a GAD67 object mask (GAD65+ terminals). A similar approach was used to define GAD67+ terminals. vGAT object masks that overlapped the centers of both GAD65 and GAD67 object masks were defined as GAD65/GAD67+.

Classification of Somatic GAD mRNA Content

The number of GAD65 and GAD67 mRNA molecules per GABAergic neuron was quantified. GABAergic neurons that contained $\geq$5 GAD65 mRNA or GAD67 mRNA molecules (>2.5X the density of GAD65 mRNA or GAD67 mRNA molecules in the neuropil) were considered to specifically express that transcript.

Statistics

All analyses were performed on the mean values for individual subjects. The density and percentage of each GAD+ terminal subpopulation arising from the different GABAergic neuron subtypes were determined as follows: (1) the values of each measure were averaged for each image stack; (2) the stack means were averaged within layer; (3) layer means were averaged within section; and (4) the section averages were used to generate the mean ($\pm$ standard deviation [SD]) density and percentage of each GAD+ terminal subpopulation per subject. The density of each GAD+ terminal subpopulation was assessed using analysis of variance with *post hoc* comparison via Tukey's honestly significant difference test. For analyses with unequal variances, between groups *post hoc* comparison was performed via the Dunnett T3 test.

RESULTS

The Proportion of vGAT+ Terminals Containing CB, CR, or PV Differs across Cortical Layers

Comparisons of the relative proportions of vGAT terminals in total gray matter of the human PFC (N = 5) revealed that ~50% of the terminals were PV+, ~31% CB+ and ~19% CR+ ($F_{(2,12)} = 74.6$, $p < 0.0005$; **Figure 1A**). A laminar analysis found that these proportions differed for each of the terminal subtypes across the six cortical layers (CB $F_{(5,24)} = 21.58$, $p < 0.0005$; CR $F_{(5,24)} = 7.96$, $p < 0.0005$, and PV $F_{(5,24)} = 38.42$, $p < 0.0005$). The biggest differences from the findings in total gray matter were in layers 1 and 6 where CB+ terminals represented ~57% and ~44% of the terminals, respectively. In addition, CR+ terminals represented ~30% of the total in layer 1. In contrast, on average 64% of the terminals in layers 2–5 were PV+ (**Figure 1B**).

Densities of Three Types of CB Terminals Differ across Layers

Qualitative assessment revealed that terminals containing vGAT and CB contained either GAD65 or GAD67 or both (Rocco et al., 2016b). At the cell level, GABA neurons that expressed CB mRNA contained either both GAD65 and GAD67 mRNAs (**Figures 2A1–A5**) or only GAD67 mRNA (**Figures 2B1–B5**). Quantitative analysis (N = 20) found that the percentage of CB/GAD+ terminals that were GAD65+, GAD67+ or GAD65/GAD67+ differed ($F_{(2,57)} = 15.1$, $p < 0.0005$) (**Figure 3**). Specifically, ~40% of CB GABA terminals contained GAD67, ~35% contained both GAD proteins, and ~25% contained GAD65 in total gray matter. However, a laminar analysis found that these proportions differed for each of the terminal subtypes across the six cortical layers (CB/GAD65+ $F_{(5,114)} = 48.10$, $p < 0.0005$; CB/GAD67+ $F_{(5,114)} = 39.13$, $p < 0.0005$; and CB/GAD65/GAD67+ $F_{(5,114)} = 14.06$, $p < 0.0005$). The biggest differences from the findings in total gray matter were in layers 1 and 6 where CB/GAD67+ terminals represented ~62% and CB/GAD65+ terminals represented ~48% of the terminals, respectively. In addition, in layers 5 and 6 the CB/GAD67+ terminals constituted only 26% and 16%, respectively, of all CB+ GABA terminals.

We next assessed the relative levels of each GAD protein, as reflected in fluorescence intensity, in CB+ axon terminals. The relative amount of GAD65 in CB/GAD65+ terminals (6887 $\pm$ 1726 arbitrary units (a.u.)) was ~34% greater ($t_{(33)} = 3.8$, $p = 0.001$) than in CB/GAD65/GAD67+ terminals (5129 $\pm$ 1146 a.u.), whereas the relative amount of GAD67 was ~24% greater ($t_{(38)} = 3.3$, $p = 0.002$) in

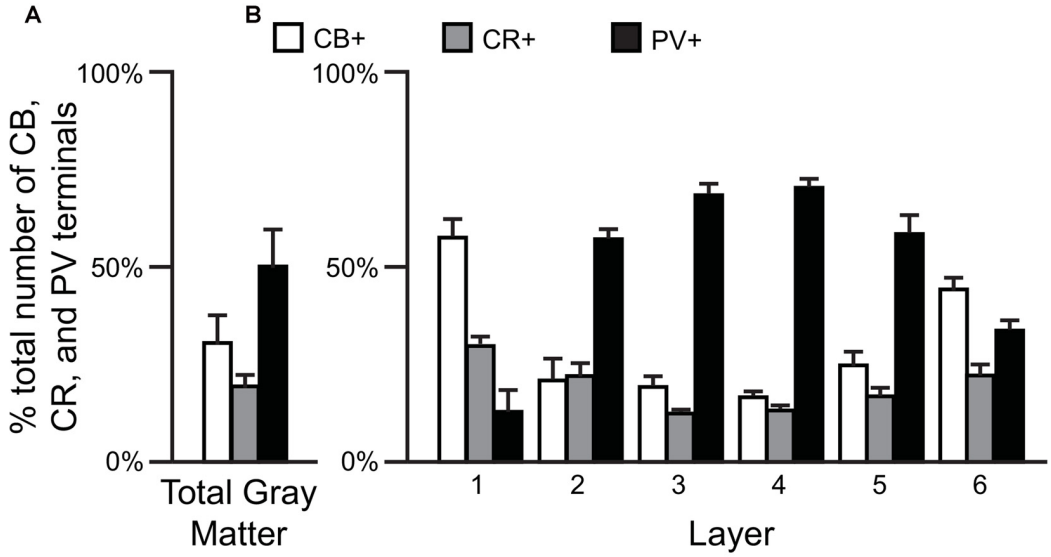

FIGURE 1 | The proportion of GABAergic calbindin+ (CB+), calretinin+ (CR+) and parvalbumin+ (PV+) terminals differs across cortical layers. **(A,B)** Bar graphs showing the relative proportions of vesicular GABA transporter (vGAT) terminals in prefrontal cortex (PFC) that were CB+, CR+ or PV+. Error bars = SEM.

CB/GAD65/GAD67+ terminals (5569 ± 1069 a.u.) than in CB/GAD67+ terminals (4479 ± 1036 a.u.). These relative intensity values might not correspond directly to total protein in a terminal given that larger terminals will generally have more protein content and therefore, a greater amount of total fluorescence intensity. In fact, the volumes of the different subpopulations of terminals were significantly different ($F_{(2,57)}$ = 287, $p < 0.0005$), with mean terminal volume greatest for CB/GAD65/GAD67+ terminals (0.52 ± 0.019 μm^3), intermediate for CB/GAD67+ terminals (0.41 ± 0.033 μm^3) and smallest for CB/GAD65+ terminals (0.32 ± 0.024 μm^3). As is indicative from the above, CB+ terminals containing both GADs contained 32% more total GAD65 than CB/GAD65+ terminals and 60% more total GAD67 than CB/GAD67+ terminals.

Finally, we quantified terminal vGAT levels. The total amount of vGAT protein in the different subpopulations of CB/GAD+ terminals differed significantly ($F_{(2,57)}$ = 79.1, $p < 0.0005$). *Post hoc* analysis showed that the total amount of vGAT in CB/GAD65/GAD67+ terminals was 39% greater ($p < 0.0005$) than in CB/GAD67+ terminals, which contained 48% more ($p < 0.0005$) vGAT protein than CB/GAD65+ terminals.

Densities of Three Types of CR Terminals Differ across Layers

Similar to CB neurons, CR neurons give rise to three distinct terminal subpopulations: CR/GAD65+, CR/GAD67+ and CR/GAD65/GAD67+ terminals (Rocco et al., 2016b). In addition, GABA neurons that expressed CR mRNA expressed both GAD65 and GAD67 mRNAs (**Figures 2C1–C5**) or only GAD67 mRNA (**Figures 2D1–D5**). Quantitative analysis (N = 20) found that the percentage of CR/GAD+ terminals represented by each subpopulation differed ($F_{(2,57)}$ = 34.97, $p < 0.0005$) in total gray matter such that ∼18% of CR GABA terminals contained GAD65, ∼37% contained GAD67, and ∼45% contained both GAD proteins (**Figure 4**). A laminar analysis found no difference in the percentage of CR+ terminals that were GAD65+ between the different cortical layers. In contrast, the percentage of CR+ terminals that contained GAD67 or both GAD proteins differed across the six cortical layers (CR/GAD67+ $F_{(5,114)}$ = 8.63, $p < 0.0005$; CR/GAD65/GAD67+ $F_{(5,114)}$ = 4.88, $p < 0.0005$). These differences were largely due to layers 5–6 where the percentage of CR+ terminals containing GAD67 was lower than in the other layers and the percentage that contained both GAD proteins was higher.

We next assessed the levels of each GAD protein in CR+ axon terminals. The total amount of GAD65 in CR/GAD65/GAD67+ terminals (77366 ± 17181 a.u.) was ∼41% greater ($t_{(38)}$ = 4.7, $p < 0.0005$) than in CR/GAD65+ terminals (55043 ± 12751 a.u.), whereas the total amount of GAD67 was ∼63% greater ($t_{(38)}$ = 7.2, $p < 0.0005$) in CR/GAD65/GAD67+ terminals (58025 ± 11443 a.u.) than in CR/GAD67+ terminals (35638 ± 7783 a.u.). As suggested by these findings, the total amount of vGAT protein in the different subpopulations of CR/GAD+ terminals differed significantly ($F_{(2,57)}$ = 50.1, $p < 0.0005$). Specifically, the total amount of vGAT in CR/GAD65/GAD67+ terminals was 53% greater ($p < 0.0005$) than in CR/GAD67+ terminals, which contained 12% more (p = 0.256) vGAT protein than CR/GAD65+ terminals.

Densities of Two Types of PV Terminals Differ across Layers

Most PV neurons are chandelier or basket cells, which can be differentiated by the cells and perisomatic region they target. A qualitative assessment of GAD protein in PV+ terminals identified two distinct subpopulations: (1) PV/GAD67+; and

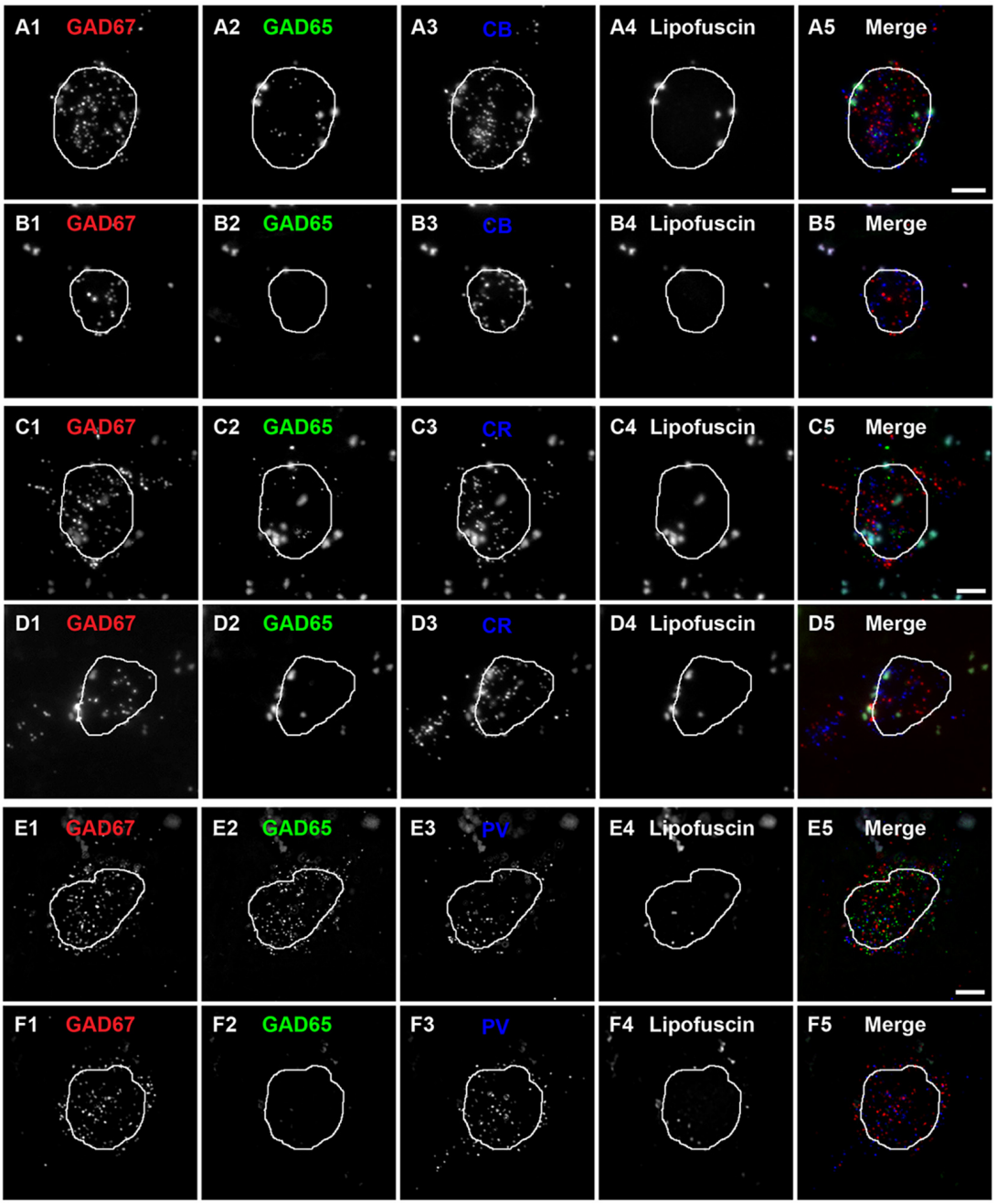

FIGURE 2 | Subtypes of CB, CR and PV neurons are distinguishable by the expression of GAD65 mRNA in human PFC. **(A,B)** Single plane image of a PFC tissue section labeled for CB, GAD65 and GAD67 mRNAs. **(A5)** and **(B5)** are merged images of **(A1–A3)** and **(B1–B3)**, respectively. Lipofuscin autofluorescence is shown in **(A4,B4)**. **(C,D)** Single plane image of a PFC tissue section labeled for CR, GAD65 and GAD67 mRNAs. **(C5)** and **(D5)** are merged images of **(C1–C3)** and **(D1–D3)**, respectively. Lipofuscin autofluorescence is shown in **(C4,D4)**. **(E,F)** Single plane image of a PFC tissue section labeled for PV, GAD65 and GAD67 mRNAs. **(E5)** and **(F5)** are merged images of **(E1–E3)** and **(F1–F3)**, respectively. Lipofuscin autofluorescence is shown in **(E4,F4)**. In all images, the outline of the nucleus, which was visualized using DAPI, is shown. Scale bars = 5 μm.

(2) PV/GAD65/GAD67+ (Fish et al., 2011; Glausier et al., 2014). At the cell level, PV mRNA containing neurons expressed either mRNA encoding both GAD65 and GAD67 or only GAD67 mRNA (**Figures 2E1–E5, F1–F5**, respectively). The percentage of PV+ terminals that contained both GAD proteins (∼78%) differed ($t_{(8)}$ = 5.4, p = 0.001) from the percentage that contained only GAD67 protein (∼22%; **Figure 5**) in total gray matter (N = 5). A laminar analysis, which only assessed layers 2–6 because only a small percentage (∼5%) of all PV+ terminals were in layer 1, found

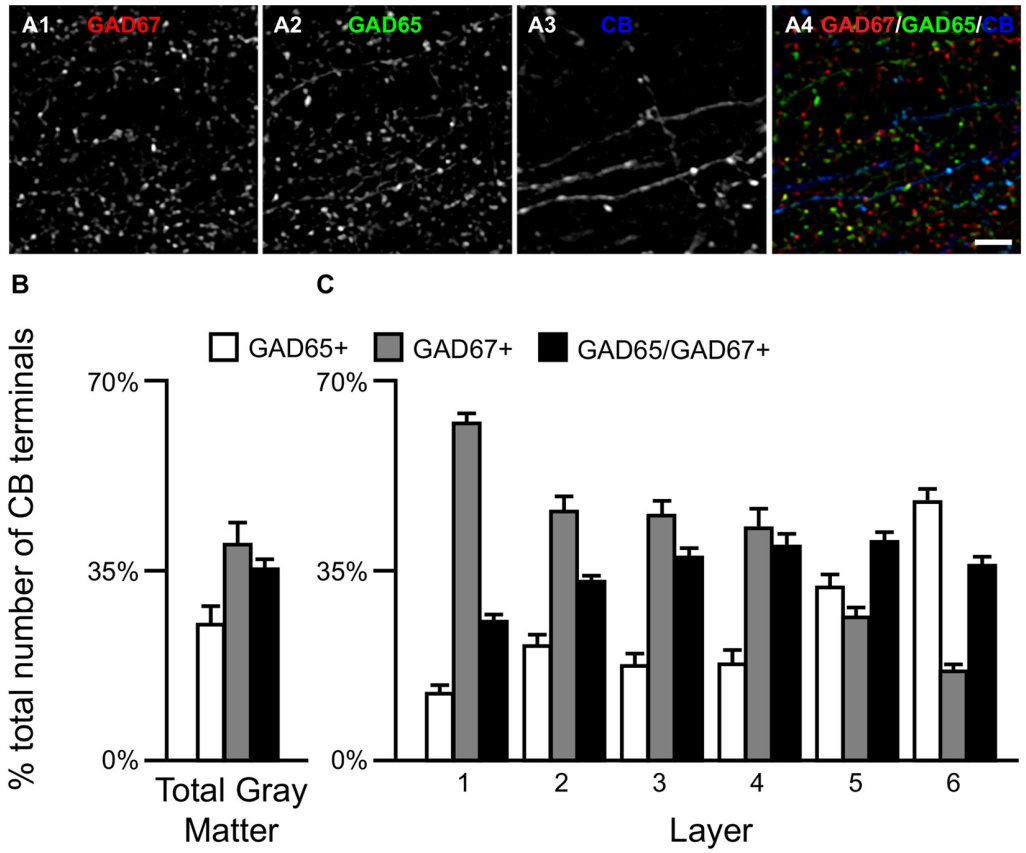

FIGURE 3 | The proportion of three CB/GAD+ terminal subpopulations differs across cortical layers. **(A)** Projection image (6 z-planes separated by 0.25 μm) of a human PFC tissue section immunolabeled for CB, vGAT (not shown), GAD65 and GAD67. Gray scale images **(A1–A3)** are single channel images of the multichannel image **(A4)** and are representative of the immunohistochemistry labeling. Scale bar = 5 μm. **(B,C)** Bar graphs showing the relative proportions of vGAT/CB+ terminals in PFC that were GAD65+, GAD67+, or GAD65/GAD67+. Error bars = SEM.

that this difference was present in layers 3–6 but not in layer 2.

We next assessed the level of GAD67 protein in PV+ axon terminals. The total amount of GAD67 in PV/GAD65/GAD67+ terminals (30277 ± 2693 a.u.) was ∼99% greater ($t_{(8)}$ = 7.7, $p < 0.0005$) than in PV/GAD67+ terminals (15197 ± 3438 a.u.). As suggested by these findings, the total amount of vGAT protein in PV/GAD65/GAD67+ terminals was 157% greater ($t_{(8)}$ = 18.9, $p < 0.0005$) than in PV/GAD67+ terminals.

DISCUSSION

The goal of the present study was to use multi-label immunohistochemistry and quantitative fluorescence confocal microscopy to gain insight into the types and amount of inhibition each cortical layer in the human PFC is likely to receive. Our findings suggest that each cortical layer receives a unique type (based on GAD proteins) and amount (based on the number of inhibitory synapses) of inhibition from GABAergic CB, CR and PV neurons that may reflect the intra- and inter-laminar processing demands required for proper PFC functioning.

Similar to our previous findings in the macaque monkey PFC (Fish et al., 2011, 2013; Rocco et al., 2016b), we found in the human PFC three subpopulations of vGAT terminals based on GAD content: GAD65+, GAD67+ and GAD65/GAD67+. Analyses of CB+, CR+ and PV+ terminals revealed that both CB+ and CR+ terminals comprised all three GAD subsets (GAD65+, GAD67+, or GAD65/GAD67+), whereas PV+ terminals comprised only two subsets (GAD67+ or GAD65/GAD67+). Multiplex mRNA labeling revealed that based on GAD mRNA expression CB, CR, and PV GABA neurons can be divided into two subpopulations: those containing only GAD67 mRNA and those containing both GAD65 and GAD67 mRNAs. Thus, it would appear in human PFC that GAD67+ terminals arise from neurons that express only GAD67 mRNA, whereas GAD65+ and GAD65/GAD67+ terminals arise from neurons expressing both GAD65 and GAD67 mRNAs. Several possibilities might explain the latter finding. First, it is possible that the postsynaptic target influences terminal GAD content. For example, terminals from PV basket cells, which target the soma and proximal dendrites of PCs, contain both GADs. In contrast, terminals from PV chandelier cells, which

exclusively target the axon initial segment of PCs, contain only GAD67 (Fish et al., 2011, 2013; Glausier et al., 2014). The latter finding may be a primate specific event due to hypermethylation of the GAD2 gene (Luo et al., 2017). The lack of GAD67 in some terminals might reflect differences in GAD65 and GAD67 trafficking and half-life. For example, because GAD65 has a very long half-life (>24 h) and is efficiently trafficked to axonal terminals, every terminal from a neuron expressing mRNA for both GADs would be expected to have detectable levels of GAD65. In contrast, the short half-life (∼2 h) of GAD67, along with a trafficking mechanism that is partially dependent on GAD65 (Kanaani et al., 2010), might result in undetectable levels of GAD67 in some terminals. In addition, changes in network activity alter GAD67 protein levels (i.e., decreased activity leads to a decrease in GAD67 protein; Lau and Murthy, 2012). Thus, PC-GABA neuron subnetwork activity might differentially affect GAD67 terminal protein levels within a particular GABA neuron subtype. In support of this latter idea, in all of the three cell types assessed, we found that terminals containing only GAD65 had significantly lower amounts of vGAT protein, whose expression like GAD67 is activity-dependent, relative to those containing both GAD65 and GAD67 protein.

We previously showed that in layer 4 of the monkey PFC terminals arising from cannabinoid receptor 1 expressing basket (CB1rB) neurons contained GAD65, but had undetectable levels of GAD67 and GABA transporter 1 (GAT1). We proposed that lower GAT1 levels in CB1rB neuron terminals allowed for GABA release from them to act on receptors located outside the synaptic cleft. In support of this idea, CB1rB neuron vesicular GABA release can spillover to affect PV synapses in close proximity (Karson et al., 2009) as well as extra-synaptic $GABA_A$ receptors (Alle and Geiger, 2007; Karson et al., 2009). Future studies that assess GAT1 levels in CB+ and CR+ terminals that contain GAD65, but not GAD67, are needed to determine if there is a relationship between GAD and GAT1 terminal expression levels.

CB, CR and PV neurons play different roles in the local cortical network. Thus, the amount and type of GABA inhibition each cortical layer receives directly affects the integration of inputs to that layer (i.e., inhibition provided by CB and CR neurons) or the functional output of neurons located within the layer (i.e., inhibition provided by PV neurons). In primate PFC, CB, CR and PV neurons have distinct laminar distribution

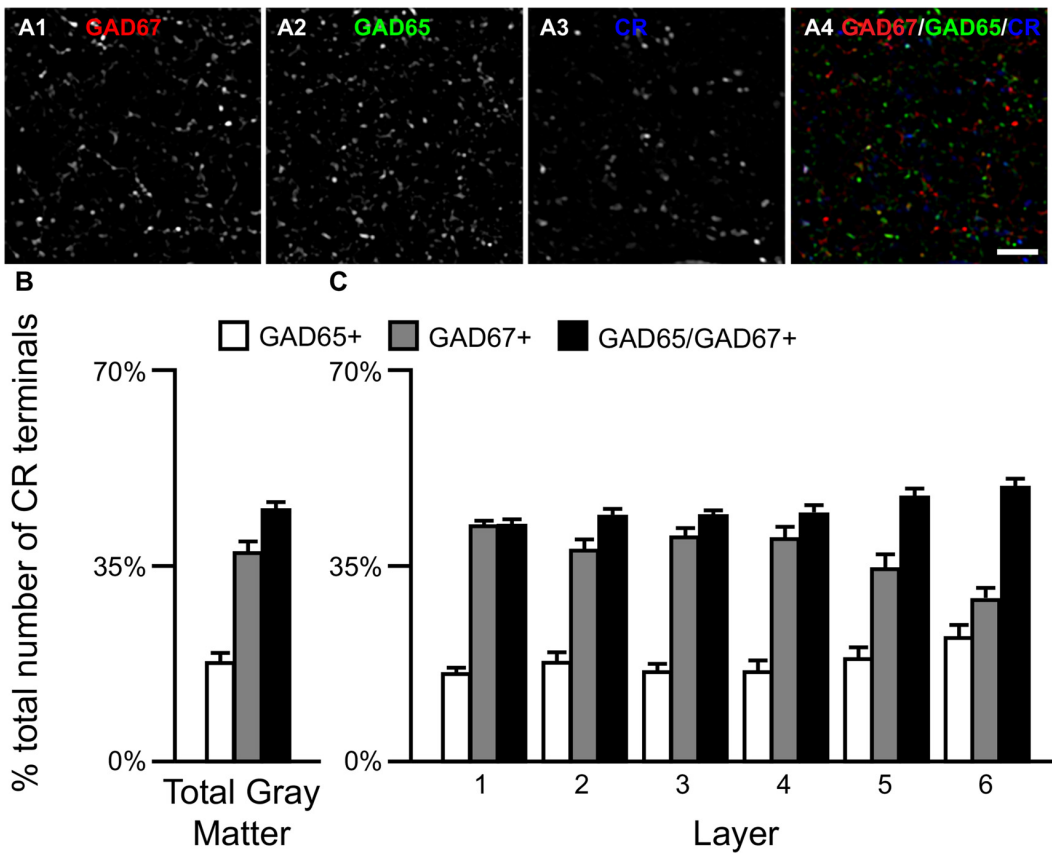

FIGURE 4 | The proportion of three CR/GAD+ terminal subpopulations differs across cortical layers. **(A)** Projection image (7 z-planes separated by 0.25 μm) of a human PFC tissue section immunolabeled for CR, vGAT (not shown), GAD65 and GAD67. Gray scale images **(A1–A3)** are single channel images of the multichannel image **(A4)** and are representative of the immunohistochemistry labeling. Scale bar = 5 μm. **(B,C)** Bar graphs showing the relative proportions of vGAT/CR+ terminals in PFC that were GAD65+, GAD67+, or GAD65/GAD67+. Error bars = SEM.

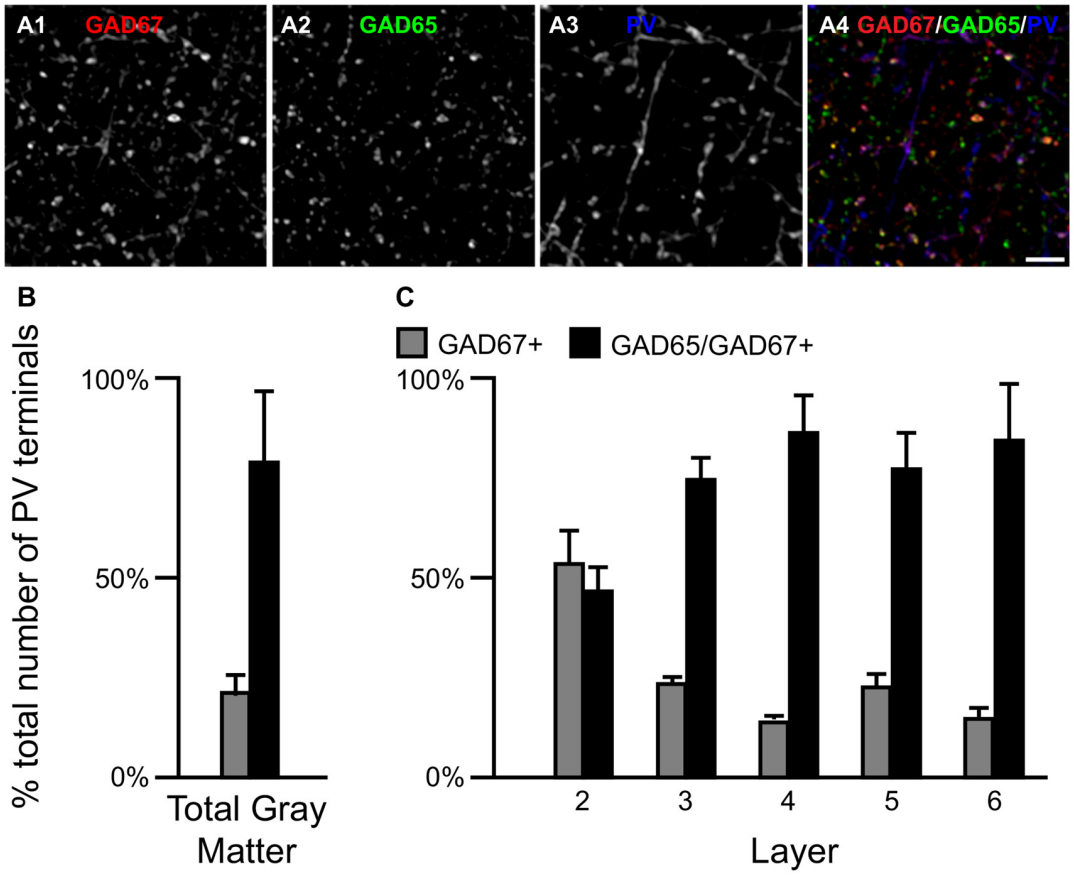

FIGURE 5 | The proportion of two PV/GAD+ terminal subpopulations differs across cortical layers. **(A)** Projection image (5 z-planes separated by 0.25 μm) of a human PFC tissue section immunolabeled for PV, vGAT (not shown), GAD65 and GAD67. Gray scale images **(A1–A3)** are single channel images of the multichannel image **(A4)** and are representative of the immunohistochemistry labeling. Scale bar = 5 μm. **(B,C)** Bar graphs showing the relative proportions of vGAT/PV+ terminals in PFC that were GAD67+ or GAD65/GAD67+. Error bars = SEM.

patterns (see **Figures 1**, **6** and Condé et al., 1994; Hof et al., 1999). The majority (∼65% see **Figure 6**) of CB neurons, which makeup ∼20% of all GABA neurons in primate PFC, are located in cortical layer 2 (Condé et al., 1994; Daviss and Lewis, 1995; Hof et al., 1999). In total gray matter we found that ∼31% of the vGAT terminals assessed contained CB and ∼31% of all CB+ terminals were located in layer 1. This finding suggests that many of the CB+ terminals arise from distal dendrite-targeting Martinotti cells, which are defined by their ascending axonal projections that span multiple layers and ramify in layer 1 (Fairén et al., 1984). Somata of CB-expressing Martinotti cells are found across layers 2–5 (Wang et al., 2004). Martinotti cells have been shown to provide feedback inhibition between neighboring PCs in layer 5 (Silberberg and Markram, 2007), the main cortical output layer, which may serve to synchronize the activity of subtypes of subcortical projecting neurons (Hilscher et al., 2017). Another subtype of CB neuron present in primates, the horse-tail cell, has its somata located in layers 2 through superficial 3. These cells give rise to tightly-bundled descending axonal projections that terminate within a narrow column across multiple deeper layers. Horse-tail cells are distributed at regular intervals and are thought to contribute to the microcolumnar organization within the primate neocortex (Defelipe et al., 1990; del Río and DeFelipe, 1995; Peters and Sethares, 1997); though, their function has been difficult to study due to their apparent absence in other mammalian species (Yáñez et al., 2005). In human cortex >40% of CB cells express the neuropeptide somatostatin (SST) and >80% of SST neurons express CB (González-Albo et al., 2001). SST-expressing neurons are a morphological diverse subtype that includes both Martinotti and horse-tail cells (González-Albo et al., 2001; Wang et al., 2004). In addition to being expressed by neuronal subtypes that terminate across multiple layers, synaptic connections from other subtypes of SST neurons are relatively confined to the same layer where their soma is located (Ma et al., 2006), where they exert control over layer-specific microcircuits, such as those involved in processing thalamic inputs to layer 4 (Xu et al., 2013). Moreover, it was recently demonstrated that their laminar location influences their function (Muñoz et al., 2017).

Although in primate PFC ∼45% of GABAergic neurons contain CR, only 19% of the vGAT terminals assessed contained CR, similar to our finding in monkey PFC (Rocco et al.,

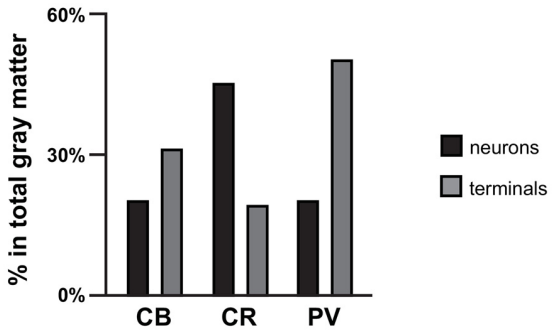

	CB		CR		PV	
Layer	soma	terminals	soma	terminals	soma	terminals
1	1%	31%	22%	19%	0%	<1%
2	65%	15%	50%	19%	12%	12%
3	18%	14%	17%	16%	23%	30%
4	6%	13%	8%	16%	33%	34%
5	10%	13%	3%	16%	23%	15%
6		14%		14%	9%	9%

FIGURE 6 | Summary. Bar graph showing the percentage of all γ-aminobutyric acid (GABA) neurons (black bars) and terminals assessed (gray bars) that is CB+, CR+, or PV+ in PFC total gray matter. Table showing the distribution of soma and terminals for each of the three GABA neuron subtypes across the six cortical layers. The soma data for CB and CR were taken from previously published findings in human PFC (Daviss and Lewis, 1995).

2016b). The greatest density of CR neurons is in PFC layers 2-superficial 3 (Condé et al., 1994; Hof et al., 1999); however, we found that 16%–19% of all CR+ terminals were located in layers 1–5 and 14% were found in layer 6. Considering that CR GABAergic neurons mainly target dendrites of other GABAergic neurons (Melchitzky and Lewis, 2008), which are sparsely located across cortical layers, it is not surprising that CR+ terminals are relatively evenly distributed across cortical layers, and represent the lowest percentage of all GABAergic terminals relative to CB+ and PV+ terminals. In the PFC of monkey, >85% of CR neurons express the neuropeptide vasoactive intestinal polypeptide (VIP) and ∼80% of VIP neurons express CR (Gabbott and Bacon, 1997). Within cortical microcircuits, VIP neurons mainly inhibit SST, and to a lesser extent, PV neurons (Pfeffer et al., 2013; Pi et al., 2013), suggesting that they play a strong role in many of the same microcircuits (Muñoz et al., 2017). By mainly synapsing onto other GABAergic neurons, CR neurons mediate disinhibitory control of PCs, which leads to selective amplification of local signal processing (Pi et al., 2013).

In primate PFC ∼20% of GABAergic neurons express PV. However, in total gray matter we found that ∼50% of terminals expressing a calcium binding protein contained PV. This finding is supported by evidence that on average PV neurons make more contacts with PCs than other GABA neurons and also heavily innervate each other (Markram et al., 2004; Pfeffer et al., 2013). PV neurons provide perisomatic input to PCs in the same layer and to lesser extent to PCs located in layers directly above and below. Considering that approximately half of PV neurons are located in PFC layers 3–4, it is not surprising that we found ∼64% of all PV+ terminals in these layers. The high density of PV innervation within middle cortical layers is important for generating gamma oscillations (Klausberger and Somogyi, 2008; Cardin et al., 2009) and processing feedforward afferent inputs (Xu et al., 2013). Finally, ∼20% of PV+ terminals only contained GAD67 protein (presumed chandelier cell terminals), with the greatest density of these terminals in layer 2. This percentage/distribution is consistent with other studies of chandelier cells (Defelipe et al., 1989).

Feedforward cortico-cortical and thalamo-cortical projections target distinct layers within the PFC (Giguere and Goldman-Rakic, 1988; Barbas and Rempel-Clower, 1997). The innervation pattern of CB+, CR+ and PV+ terminals is apparently well-equipped for regulating these layer-specific inputs, as well as for generating and maintaining synchrony within local networks via feedback inhibition in order to maintain proper PFC functioning. Finally, our findings suggest that the layer-specific distribution of CB+, CR+ and PV+ terminals are likely to differ across cortical regions with distinct laminar cytoarchitectures (e.g., granular vs. agranular regions) in a manner that would provide the needed complement of GABA inputs for the specific functional (e.g., primary sensory, association or motor) properties of each region.

AUTHOR CONTRIBUTIONS

KNF, BRR and DAL contributed intellectually to experimental design, data interpretation and writing of the manuscript. BRR and KNF performed the experiments.

FUNDING

This work was supported by the National Institute of Mental Health (NIMH; MH051234 to DAL; MH096985 to KNF).

ACKNOWLEDGMENTS

The content is solely the responsibility of the authors and does not necessarily represent the official views of the National Institute of Mental Health, the National Institutes of Health, the Department of Veterans Affairs, or the United States Government.

SUPPLEMENTARY MATERIAL

The Supplementary Material for this article can be found online at: https://www.frontiersin.org/articles/10.3389/fnana.2018.00009/full#supplementary-material

REFERENCES

Airaksinen, M. S., Thoenen, H., and Meyer, M. (1997). Vulnerability of midbrain dopaminergic neurons in calbindin-D28k-deficient mice: lack of evidence for a neuroprotective role of endogenous calbindin in MPTP-treated and weaver mice. *Eur. J. Neurosci.* 9, 120–127. doi: 10.1111/j.1460-9568.1997.tb01360.x

Alle, H., and Geiger, J. R. (2007). GABAergic spill-over transmission onto hippocampal mossy fiber boutons. *J. Neurosci.* 27, 942–950. doi: 10.1523/JNEUROSCI.4996-06.2007

Barbas, H., and Rempel-Clower, N. (1997). Cortical structure predicts the pattern of corticocortical connections. *Cereb. Cortex* 7, 635–646. doi: 10.1093/cercor/7.7.635

Barinka, F., and Druga, R. (2010). Calretinin expression in the mammalian neocortex: a review. *Physiol. Res.* 59, 665–677.

Benavides, S. H., Monserrat, A. J., Fariña, S., and Porta, E. A. (2002). Sequential histochemical studies of neuronal lipofuscin in human cerebral cortex from the first to the ninth decade of life. *Arch. Gerontol. Geriatr.* 34, 219–231. doi: 10.1016/s0167-4943(01)00223-0

Bowers, G., Cullinan, W. E., and Herman, J. P. (1998). Region-specific regulation of glutamic acid decarboxylase (GAD) mRNA expression in central stress circuits. *J. Neurosci.* 18, 5938–5947.

Cardin, J. A., Carlen, M., Meletis, K., Knoblich, U., Zhang, F., Deisseroth, K., et al. (2009). Driving fast-spiking cells induces γ rhythm and controls sensory responses. *Nature* 459, 663–667. doi: 10.1038/nature08002

Celio, M. R., and Heizmann, C. W. (1981). Calcium-binding protein parvalbumin as a neuronal marker. *Nature* 293, 300–302. doi: 10.1038/293300a0

Chang, Y. C., and Gottlieb, D. I. (1988). Characterization of the proteins purified with monoclonal antibodies to glutamic acid decarboxylase. *J. Neurosci.* 8, 2123–2130.

Condé, F., Lund, J. S., Jacobowitz, D. M., Baimbridge, K. G., and Lewis, D. A. (1994). Local circuit neurons immunoreactive for calretinin, calbindin D-28k or parvalbumin in monkey prefrontal cortex: distribution and morphology. *J. Comp. Neurol.* 341, 95–116. doi: 10.1002/cne.903410109

Contreras, D., Curró Dossi, R., and Steriade, M. (1992). Bursting and tonic discharges in two classes of reticular thalamic neurons. *J. Neurophysiol.* 68, 973–977. doi: 10.1152/jn.1992.68.3.973

Curley, A. A., Arion, D., Volk, D. W., Asafu-Adjei, J. K., Sampson, A. R., Fish, K. N., et al. (2011). Cortical deficits of glutamic acid decarboxylase 67 expression in schizophrenia: clinical, protein, and cell type-specific features. *Am. J. Psychiatry* 168, 921–929. doi: 10.1176/appi.ajp.2011.11010052

Daviss, S. R., and Lewis, D. A. (1995). Local circuit neurons of the prefrontal cortex in schizophrenia: selective increase in the density of calbindin-immunoreactive neurons. *Psychiatry Res.* 59, 81–96. doi: 10.1016/0165-1781(95)02720-3

Defelipe, J., Hendry, S. H., Hashikawa, T., Molinari, M., and Jones, E. G. (1990). A microcolumnar structure of monkey cerebral cortex revealed by immunocytochemical studies of double bouquet cell axons. *Neuroscience* 37, 655–673. doi: 10.1016/0306-4522(90)90097-n

Defelipe, J., Hendry, S. H., and Jones, E. G. (1989). Visualization of chandelier cell axons by parvalbumin immunoreactivity in monkey cerebral cortex. *Proc. Natl. Acad. Sci. U S A* 86, 2093–2097. doi: 10.1073/pnas.86.6.2093

del Río, M. R., and DeFelipe, J. (1995). A light and electron microscopic study of calbindin D-28k immunoreactive double bouquet cells in the human temporal cortex. *Brain Res.* 690, 133–140. doi: 10.1016/0006-8993(95)00641-3

del Río, M. R., and DeFelipe, J. (1996). Colocalization of calbindin D-28k, calretinin and GABA immunoreactivities in neurons of the human temporal cortex. *J. Comp. Neurol.* 369, 472–482. doi: 10.1002/(sici)1096-9861(19960603)369:3<472::aid-cne11>3.0.co;2-k

Esclapez, M., Tillakaratne, N. J., Kaufman, D. L., Tobin, A. J., and Houser, C. R. (1994). Comparative localization of two forms of glutamic acid decarboxylase and their mRNAs in rat brain supports the concept of functional differences between the forms. *J. Neurosci.* 14, 1834–1855.

Fairén, A., Defelipe, J., Regidon, J., Peters, A., and Jones, E. G. (1984). "Nonpyramidal neurons, general account," in *Cerebral Cortex*, eds A. Peters and E. G. Jones (New York, NY: Plenum), 201–245.

Feldblum, S., Dumoulin, A., Anoal, M., Sandillon, F., and Privat, A. (1995). Comparative distribution of GAD65 and GAD67 mRNAs and proteins in the rat spinal cord supports a differential regulation of these two glutamate decarboxylases *in vivo*. *J. Neurosci. Res.* 42, 742–757. doi: 10.1002/jnr.490420603

Feldblum, S., Erlander, M. G., and Tobin, A. J. (1993). Different distributions of GAD65 and GAD67 mRNAs suggest that the two glutamate decarboxylases play distinctive functional roles. *J. Neurosci. Res.* 34, 689–706. doi: 10.1002/jnr.490340612

Fish, K. N., Hoftman, G. D., Sheikh, W., Kitchens, M., and Lewis, D. A. (2013). Parvalbumin-containing chandelier and basket cell boutons have distinctive modes of maturation in monkey prefrontal cortex. *J. Neurosci.* 33, 8352–8358. doi: 10.1523/JNEUROSCI.0306-13.2013

Fish, K. N., Sweet, R. A., and Lewis, D. A. (2011). Differential distribution of proteins regulating GABA synthesis and reuptake in axon boutons of subpopulations of cortical interneurons. *Cereb. Cortex* 21, 2450–2460. doi: 10.1093/cercor/bhr007

Gabbott, P. L., and Bacon, S. J. (1996). Local circuit neurons in the medial prefrontal cortex (areas 24a,b,c, 25 and 32) in the monkey: II. Quantitative areal and laminar distributions. *J. Comp. Neurol.* 364, 609–636. doi: 10.1002/(sici)1096-9861(19960122)364:4<609::aid-cne2>3.3.co;2-e

Gabbott, P. L., and Bacon, S. J. (1997). Vasoactive intestinal polypeptide containing neurones in monkey medial prefrontal cortex (mPFC): colocalisation with calretinin. *Brain Res.* 744, 179–184. doi: 10.1016/s0006-8993(96)01232-2

Giguere, M., and Goldman-Rakic, P. S. (1988). Mediodorsal nucleus: areal, laminar, and tangential distribution of afferents and efferents in the frontal lobe of rhesus monkeys. *J. Comp. Neurol.* 277, 195–213. doi: 10.1002/cne.902770204

Glausier, J. R., Fish, K. N., and Lewis, D. A. (2014). Altered parvalbumin basket cell inputs in the dorsolateral prefrontal cortex of schizophrenia subjects. *Mol. Psychiatry* 19, 30–36. doi: 10.1038/mp.2013.152

González-Albo, M. C., Elston, G. N., and DeFelipe, J. (2001). The human temporal cortex: characterization of neurons expressing nitric oxide synthase, neuropeptides and calcium-binding proteins, and their glutamate receptor subunit profiles. *Cereb. Cortex* 11, 1170–1181. doi: 10.1093/cercor/11.12.1170

Gonzalez-Burgos, G., Cho, R. Y., and Lewis, D. A. (2015). Alterations in cortical network oscillations and parvalbumin neurons in schizophrenia. *Biol. Psychiatry* 77, 1031–1040. doi: 10.1016/j.biopsych.2015.03.010

Gottlieb, D. I., Chang, Y. C., and Schwob, J. E. (1986). Monoclonal antibodies to glutamic acid decarboxylase. *Proc. Natl. Acad. Sci. U S A* 83, 8808–8812. doi: 10.1073/pnas.83.22.8808

Guo, C., Stella, S. L. Jr., Hirano, A. A., and Brecha, N. C. (2009). Plasmalemmal and vesicular γ-aminobutyric acid transporter expression in the developing mouse retina. *J. Comp. Neurol.* 512, 6–26. doi: 10.1002/cne.21846

Hilscher, M. M., Leão, R. N., Edwards, S. J., Leão, K. E., and Kullander, K. (2017). Chrna2-martinotti cells synchronize layer 5 type a pyramidal cells via rebound excitation. *PLoS Biol.* 15:e2001392. doi: 10.1371/journal.pbio.2001392

Hof, P. R., Glezer, I. I., Condé, F., Flagg, R. A., Rubin, M. B., Nimchinsky, E. A., et al. (1999). Cellular distribution of the calcium-binding proteins parvalbumin, calbindin and calretinin in the neocortex of mammals: phylogenetic and developmental patterns. *J. Chem. Neuroanat.* 16, 77–116. doi: 10.1016/s0891-0618(98)00065-9

Jiao, Y., Sun, Z., Lee, T., Fusco, F. R., Kimble, T. D., Meade, C. A., et al. (1999). A simple and sensitive antigen retrieval method for free-floating and slide-mounted tissue sections. *J. Neurosci. Methods* 93, 149–162. doi: 10.1016/s0165-0270(99)00142-9

Kagi, U., Berchtold, M. W., and Heizmann, C. W. (1987). Ca^{2+}-binding parvalbumin in rat testis. Characterization, localization, and expression during development. *J. Biol. Chem.* 262, 7314–7320.

Kanaani, J., Kolibachuk, J., Martinez, H., and Baekkeskov, S. (2010). Two distinct mechanisms target GAD67 to vesicular pathways and presynaptic clusters. *J. Cell Biol.* 190, 911–925. doi: 10.1083/jcb.200912101

Karson, M. A., Tang, A. H., Milner, T. A., and Alger, B. E. (2009). Synaptic cross talk between perisomatic-targeting interneuron classes expressing

cholecystokinin and parvalbumin in hippocampus. *J. Neurosci.* 29, 4140–4154. doi: 10.1523/JNEUROSCI.5264-08.2009

Klausberger, T., and Somogyi, P. (2008). Neuronal diversity and temporal dynamics: the unity of hippocampal circuit operations. *Science* 321, 53–57. doi: 10.1126/science.1149381

Lau, C. G., and Murthy, V. N. (2012). Activity-dependent regulation of inhibition via GAD67. *J. Neurosci.* 32, 8521–8531. doi: 10.1523/JNEUROSCI.1245-12.2012

Lewis, D. A., Melchitzky, D. S., and Burgos, G. G. (2002). Specificity in the functional architecture of primate prefrontal cortex. *J. Neurocytol.* 31, 265–276. doi: 10.1023/A:1024174026286

Luo, C., Keown, C. L., Kurihara, L., Zhou, J., He, Y., Li, J., et al. (2017). Single-cell methylomes identify neuronal subtypes and regulatory elements in mammalian cortex. *Science* 357, 600–604. doi: 10.1126/science.aan3351

Ma, Y., Hu, H., Berrebi, A. S., Mathers, P. H., and Agmon, A. (2006). Distinct subtypes of somatostatin-containing neocortical interneurons revealed in transgenic mice. *J. Neurosci.* 26, 5069–5082. doi: 10.1523/JNEUROSCI.0661-06.2006

Markram, H., Toledo-Rodriguez, M., Wang, Y., Gupta, A., Silberberg, G., and Wu, C. (2004). Interneurons of the neocortical inhibitory system. *Nat. Rev. Neurosci.* 5, 793–807. doi: 10.1038/nrn1519

Melchitzky, D. S., and Lewis, D. A. (2008). Dendritic-targeting GABA neurons in monkey prefrontal cortex: comparison of somatostatin- and calretinin-immunoreactive axon terminals. *Synapse* 62, 456–465. doi: 10.1002/syn.20514

Mercugliano, M., Soghomonian, J. J., Qin, Y., Nguyen, H. Q., Feldblum, S., Erlander, M. G., et al. (1992). Comparative distribution of messenger RNAs encoding glutamic acid decarboxylases (Mr 65,000 and Mr 67,000) in the basal ganglia of the rat. *J. Comp. Neurol.* 318, 245–254. doi: 10.1002/cne.903180302

Muñoz, W., Tremblay, R., Levenstein, D., and Rudy, B. (2017). Layer-specific modulation of neocortical dendritic inhibition during active wakefulness. *Science* 355, 954–959. doi: 10.1126/science.aag2599

Pedneault, S., and Soghomonian, J. J. (1994). Glutamate decarboxylase (GAD65) mRNA levels in the striatum and pallidum of MPTP-treated monkeys. *Mol. Brain Res.* 25, 351–354. doi: 10.1016/0169-328x(94)90171-6

Peters, A., and Sethares, C. (1997). The organization of double bouquet cells in monkey striate cortex. *J. Neurocytol.* 26, 779–797. doi: 10.1023/A:1018518515982

Pfeffer, C. K., Xue, M., He, M., Huang, Z. J., and Scanziani, M. (2013). Inhibition of inhibition in visual cortex: the logic of connections between molecularly distinct interneurons. *Nat. Neurosci.* 16, 1068–1076. doi: 10.1038/nn.3446

Pi, H. J., Hangya, B., Kvitsiani, D., Sanders, J. I., Huang, Z. J., and Kepecs, A. (2013). Cortical interneurons that specialize in disinhibitory control. *Nature* 503, 521–524. doi: 10.1038/nature12676

Porta, E. A. (2002). Pigments in aging: an overview. *Ann. N Y Acad. Sci.* 959, 57–65. doi: 10.1111/j.1749-6632.2002.tb02083.x

Ridler, T. W., and Calvard, S. (1978). "Picture thresholding using an iterative selection method," in *IEEE Transactions on Systems, Man, and Cybernetics SMC-8*, 630–632. doi: 10.1109/TSMC.1978.4310039

Rocco, B. R., DeDionisio, A. M., Lewis, D. A., and Fish, K. N. (2017). Alterations in a unique class of cortical chandelier cell axon cartridges in Schizophrenia. *Biol. Psychiatry* 82, 40–48. doi: 10.1016/j.biopsych.2016.09.018

Rocco, B. R., Lewis, D. A., and Fish, K. N. (2016a). Markedly lower glutamic acid decarboxylase 67 protein levels in a subset of boutons in Schizophrenia. *Biol. Psychiatry* 79, 1006–1015. doi: 10.1016/j.biopsych.2015.07.022

Rocco, B. R., Sweet, R. A., Lewis, D. A., and Fish, K. N. (2016b). GABA-synthesizing enzymes in calbindin and calretinin neurons in monkey prefrontal cortex. *Cereb. Cortex* 26, 2191–2204. doi: 10.1093/cercor/bhv051

Schwaller, B., Buchwald, P., Blumcke, I., Celio, M. R., and Hunziker, W. (1993). Characterization of a polyclonal antiserum against the purified human recombinant calcium binding protein calretinin. *Cell Calcium* 14, 639–648. doi: 10.1016/0143-4160(93)90089-o

Silberberg, G., and Markram, H. (2007). Disynaptic inhibition between neocortical pyramidal cells mediated by Martinotti cells. *Neuron* 53, 735–746. doi: 10.1016/j.neuron.2007.02.012

Soghomonian, J. J., and Martin, D. L. (1998). Two isoforms of glutamate decarboxylase: why? *Trends Pharmacol. Sci.* 19, 500–505. doi: 10.1016/s0165-6147(98)01270-x

Soghomonian, J. J., Pedneault, S., Audet, G., and Parent, A. (1994). Increased glutamate decarboxylase mRNA levels in the striatum and pallidum of MPTP-treated primates. *J. Neurosci.* 14, 6256–6265.

Sweet, R. A., Fish, K. N., and Lewis, D. A. (2010). Mapping synaptic pathology within cerebral cortical circuits in subjects with Schizophrenia. *Front. Hum. Neurosci.* 4:44. doi: 10.3389/fnhum.2010.00044

Wang, Y., Toledo-Rodriguez, M., Gupta, A., Wu, C., Silberberg, G., Luo, J., et al. (2004). Anatomical, physiological and molecular properties of Martinotti cells in the somatosensory cortex of the juvenile rat. *J. Physiol.* 561, 65–90. doi: 10.1113/jphysiol.2004.073353

Wilson, C. J., and Groves, P. M. (1981). Spontaneous firing patterns of identified spiny neurons in the rat neostriatum. *Brain Res.* 220, 67–80. doi: 10.1016/0006-8993(81)90211-0

Wilson, C. J., and Kawaguchi, Y. (1996). The origins of two-state spontaneous membrane potential fluctuations of neostriatal spiny neurons. *J. Neurosci.* 16, 2397–2410.

Xu, H., Jeong, H.-Y., Tremblay, R., and Rudy, B. (2013). Neocortical somatostatin-expressing GABAergic interneurons disinhibit the thalamorecipient layer 4. *Neuron* 77, 155–167. doi: 10.1016/j.neuron.2012.11.004

Yáñez, I. B., Muñoz, A., Contreras, J., Gonzalez, J., Rodriguez-Veiga, E., and DeFelipe, J. (2005). Double bouquet cell in the human cerebral cortex and a comparison with other mammals. *J. Comp. Neurol.* 486, 344–360. doi: 10.1002/cne.20533

Conflict of Interest Statement: DAL currently receives investigator-initiated research support from Pfizer and has recently served as a consultant in the areas of target identification and validation and new compound development for Merck.

The other authors declare that the research was conducted in the absence of any commercial or financial relationships that could be construed as a potential conflict of interest.

frontiers in Neuroanatomy

REVIEW
published: 12 July 2017
doi: 10.3389/fnana.2017.00054

The Functioning of a Cortex without Layers

Julien Guy[1]* *and Jochen F. Staiger*[1,2]*

[1]*Institute for Neuroanatomy, University Medical Center Göttingen, Georg-August-University, Göttingen, Germany,*
[2]*DFG Center for Nanoscale Microscopy and Molecular Physiology of the Brain (CNMPB), Göttingen, Germany*

A major hallmark of cortical organization is the existence of a variable number of layers, i.e., sheets of neurons stacked on top of each other, in which neurons have certain commonalities. However, even for the neocortex, variable numbers of layers have been described and it is just a convention to distinguish six layers from each other. Whether cortical layers are a structural epiphenomenon caused by developmental dynamics or represent a functionally important modularization of cortical computation is still unknown. Here we present our insights from the reeler mutant mouse, a model for a developmental, "molecular lesion"-induced loss of cortical layering that could serve as ground truth of what an intact layering adds to the cortex in terms of functionality. We could demonstrate that the reeler neocortex shows no inversion of cortical layers but rather a severe disorganization that in the primary somatosensory cortex leads to the complete loss of layers. Nevertheless, the somatosensory system is well organized. When exploring an enriched environment with specific sets of whiskers, activity-dependent gene expression takes place in the corresponding modules. Precise whisker stimuli lead to the functional activation of somatotopically organized barrel columns as visualized by intrinsic signal optical imaging. Similar results were obtained in the reeler visual system. When analyzing pathways that could be responsible for preservation of tactile perception, lemniscal thalamic projections were found to be largely intact, despite the smearing of target neurons across the cortical mantle. However, with optogenetic experiments we found evidence for a mild dispersion of thalamic synapse targeting on layer IV-spiny stellate cells, together with a general weakening in thalamocortical input strength. This weakening of thalamic inputs was compensated by intracortical mechanisms involving increased recurrent excitation and/or reduced feedforward inhibition. In conclusion, a layer loss so far only led to the detection of subtle defects in sensory processing by reeler mice. This argues in favor of a view in which cortical layers are not an essential component for *basic* perception and cognition. A view also supported by recent studies in birds, which can have remarkable cognitive capacities despite the lack of a neocortex with multiple cortical layers. In conclusion, we suggest that future studies directed toward understanding cortical functions should rather focus on circuits specified by functional cell type composition than mere laminar location.

Keywords: neocortex, cortical circuits, reeler mutant mouse, developmental plasticity, optogenetics, lemniscal pathway

OPEN ACCESS

Edited by:
Kathleen S. Rockland, Boston University School of Medicine, United States

Reviewed by:
Andre Goffinet, Université catholique de Louvain, Belgium
Gabriella D'Arcangelo, Rutgers University, The State University of New Jersey, United States

***Correspondence:**
Julien Guy
julien.guy@med.uni-goettingen.de
Jochen F. Staiger
jochen.staiger@med.uni-goettingen.de

Received: *21 April 2017*
Accepted: *20 June 2017*
Published: *12 July 2017*

Citation:
Guy J and Staiger JF (2017) The Functioning of a Cortex without Layers. Front. Neuroanat. 11:54. doi: 10.3389/fnana.2017.00054

THE CONCEPT OF CORTICAL LAYERS

In 1867, Theodor Meynert, the father of cytoarchitectonics, published an account of his microscopic examinations of the mammalian cerebral cortex, the first to propose a subdivision of the cortex in layers based on cellular composition (Meynert, 1867). The concept of cortical layers was not unknown until this point, and had in fact emerged from observations of the cortex by naked eye (Gennari, 1784; Vicq d'Azyr, 1786; Baillarger, 1840). Its gradual historical development is characterized by a great variation, from three to nine, in the number of layers proposed (Meynert, 1867). The practice of defining layering by cellular composition, however, has endured to this day, and largely contributed to our contemporary view of the functional organization of the neocortex. This view subdivides the neocortex into six layers, defined by the morphological cell types they are composed of, their connectivity, developmental origins and patterns of gene expression. This consensus, although fairly well established, is still the subject of ongoing refinements (Zilles and Wree, 1995; Skoglund et al., 1997; Lein et al., 2007; Feldmeyer, 2012; Staiger, 2015; Staiger et al., 2015).

An anatomical description of cortical lamination can hardly ignore the question of laminar function. The fact that cortical layers are composed of distinct neuron types with unique properties and specific connectivity is suggestive of a division of labor among them, whereby each layer carries a fraction of the computational load of a column. For example, a common view is that information is processed in a sequential or feedforward manner in the cortical column, each layer completing its own computation before passing the outcome to the next along the canonical microcircuit. Thus, in the words of Kenneth D. Miller: "*in order to understand the computations being performed by the cortex, we need to understand the nature of the processing undertaken by each layer*" (Miller et al., 2001).

WHAT WOULD BE A SUITABLE DESCRIPTION OF THE FUNCTION OF EACH LAYER?

Ideally, a function that identifies what operations are performed exclusively within one layer, as opposed to operations emerging from the collective action of multiple layers. For example, a recurring statement in the literature considers layer IV of the rodent somatosensory cortex as the main input stage for sensory information, due to its dense innervation by the ventral posterior medial nucleus of the thalamus (Chmielowska et al., 1989; Staiger et al., 1996; Wimmer et al., 2010; Oberlaender et al., 2012) and its vigorous, short latency responses to whisker touch (Simons, 1978; Armstrong-James and Fox, 1987). An imaginary description of the role of individual layers in sensory neocortex could use similar terms: layer IV of the cortex acts as a relay and an amplifier of sensory information (due to the dense reciprocal connections among thalamorecipient excitatory neurons; Feldmeyer et al., 1999; Schubert et al., 2003), perhaps adapting the gain of amplification to behavioral requirements. Layer II/III receives tuned sensory information from layer IV and weaves it together with contextual information (provided by associational cortico-cortical input) to produce the first percept of the external object. Layer II/III informs layer V of the percept; due to its many long range outputs, layer V broadcasts the content of the percept to various locations within the brain, and thus conjures up relevant memories associated with it but stored elsewhere in the cortex. Layer VI, finally, signals back to the sensory thalamus that the ongoing cortical calculation has ended. Although the functions listed here are fictional, an adequate description of laminar function would be of that kind (Schubert et al., 2007; Harris and Mrsic-Flogel, 2013; Harris and Shepherd, 2015).

However desirable it may be, the emergence of such a model has been frustrated by the lack of suitable experimental approaches. Indeed, one can hardly conceive of a reversible surgical or pharmacological inactivation of one layer that would spare all others, although some attempts have been made (Huang et al., 1998; Fox et al., 2003; Wright and Fox, 2010; Constantinople and Bruno, 2013). Similarly, the advent of optogenetics is of limited help here. Because one layer's output is the other's input, reversible optogenetic inactivation of one layer would eventually compromise computation in the entire network, making it difficult to isolate the role of the inactivated layer in generating behavior. In order to determine whether layers are involved in cortical computations *at all*, the field would rather benefit from comparing model organisms possessing laminated vs. non laminated cortices. Ideally, such models would belong to the same species and be identical in all respects expect cortical lamination. The cortices or brain areas to be compared should be composed of similar neurons, forming identical networks performing the same functions.

THE *REELER* NEOCORTEX AS A MODEL SYSTEM

In our opinion, the reeler mutant mouse provides the closest approximation to such a model. The mutation was first documented after it appeared spontaneously at the Institute of Animal Genetics in Edinburgh and results in the loss of expression of the reelin protein (Curran and D'Arcangelo, 1998; Tissir and Goffinet, 2003). This large extracellular protein is expressed by Cajal-Retzius-cells during cortical development (Frotscher et al., 2009). Through signaling via its membrane receptors ApoEr2 and VLDLr (Bock and May, 2016), reelin guides the migration of newborn neurons and orchestrates the development of cortical layers. In the absence of reelin or its receptors, the process of neuronal migration is compromised, which causes severe abnormalities in cortical lamination. The resulting phenotype was initially described as an inversion of the layers, whereby the normal "inside out" pattern was inverted into an "outside in" pattern. There, layer

VI becomes situated below the pia (forming the so called superplate by merging with the marginal zone, representing prospective layer I) and layer II above the white matter (Caviness and Sidman, 1973; Caviness et al., 1988). More recent studies, however, have revealed a far more disorganized pattern (**Figure 1**), where cortical neurons are intermingled in a chaotic manner irrespective of cortical depth, forming patterns which surprisingly seem to vary according to cortical area (Dekimoto et al., 2010; Wagener et al., 2010; Boyle et al., 2011; Pielecka-Fortuna et al., 2015).

How well does the reeler mouse fit as a model with the requirements listed above? The neocortex, hippocampus and cerebellum, the brain structures affected most by reelin deficiency, have received considerable attention over the years. A repeated finding was that all cell types normally found in these regions were all present in reeler (Caviness and Sidman, 1973; Stanfield and Cowan, 1979). The total number of neurons populating the reeler or the wild type cortex is roughly equivalent, although late born (supragranular) neurons are somewhat overrepresented at the expense of early born (infragranular) neurons (Polleux et al., 1998; Wagener et al., 2010, 2016; Boyle et al., 2011). The relative numbers of excitatory and inhibitory neurons are also unchanged (Hevner et al., 2004; Wagener et al., 2016). Furthermore, neurons appear to retain their correct properties despite their ectopic positions. Molecular markers typically expressed in a layer-specific fashion are still expressed by displaced neurons (Katsuyama and Terashima, 2009; Boyle et al., 2011; Wagener et al., 2016), suggesting that their molecular identity is not compromised by the lack of lamination. The morphology of defined neuronal types has been investigated in some detail and is relatively unchanged (Guy et al., 2016), although some excitatory types see a reduction in the number of dendritic spines (Niu et al., 2008), and some inhibitory types have longer dendrites with more branches (Yabut et al., 2007).

One oddity found in reeler is an apparent distortion in the dendritic arbors of some of the ectopic neurons (**Figure 2**). For instance, the apical dendrites of large pyramidal neurons may travel in an oblique fashion towards the pia, they may orient themselves horizontally, and even be inverted (Landrieu and Goffinet, 1981; Simmons et al., 1982; Terashima et al., 1983, 1985; Silva et al., 1991). Similarly distorted dendritic arbors were reported in the hippocampus (Stanfield and Cowan, 1979) and the cerebellum (Heckroth et al., 1989). However, these are better explained by the fact that ectopic cells may find themselves outside of their home structure, where space constraints makes a normal orientation impossible, rather than by an abnormality in their intrinsic morphology—especially in the cerebral cortex. An alternative explanation is that these disorientations result from the attempt of dendritic outgrowth mechanisms to sample from their correct afferent pathways (Pinto Lord and Caviness, 1979), which can be distorted in bizarre manners, best exemplified by lemniscal thalamic projections to the neocortex. The thick myelinated fibers first ascend in an oblique manner to the pial surface before abruptly turning and re-entering the cortical plate where they branch into their terminal arborizations (Caviness and Frost, 1983; Pielecka-Fortuna et al., 2015; Wagener et al., 2016), a phenomenon which has also been observed with *in vivo*-fiber tracking (Harsan et al., 2013). This fiber trajectory could be caused by transient synapses that thalamic synapses form with subplate neurons, which in reeler mice are found just below the pia in the superplate (Higashi et al., 2005). Of course one may wonder whether these morphologically aberrant reeler neurons have also aberrant electrophysiological properties. However, what little evidence exists shows that differences are slim: neurons in the neocortex and the hippocampus retain normal firing patterns and most other intrinsic properties (Silva et al., 1991; Kowalski et al., 2010; Guy et al., 2016).

Neuronal connectivity has also been the subject of scrutiny, and was repeatedly found to be largely intact in reeler (Caviness and Rakic, 1978). Indeed, although thalamocortical fibers follow an unorthodox trajectory through the cortex, they are capable of finding their target areas and cells, especially the layer IV equivalent neurons, in spite of their ectopic positions (Steindler and Colwell, 1976; Terashima et al., 1987; Wagener et al., 2016). Cortico-cortical connectivity is preserved as well in the somatosensory (Guy et al., 2015) and visual cortex (Lemmon and Pearlman, 1981; Simmons et al., 1982). Interhemispheric connections are established in a normal pattern as well (Caviness and Yorke, 1976). Finally, efferent connectivity is also preserved, as shown in the piriform and motor cortices (Terashima et al., 1987; Diodato et al., 2016). Overall, it appears that the mutant and normal cortex are composed of the same elements forming virtually identical circuits. Thus, their main difference resides in the absence of lamination characteristic of the reeler phenotype, making this mutant a fitting model for our endeavor.

FUNCTIONAL PHENOTYPE OF THE *REELER* MOUSE

So what are the functional consequences of a lack of cortical lamination in the reeler mouse? In line with the largely normal connectivity in mutant mice, most studies found little difference in various measures of cortical function. On a circuit level, based on c-fos expression as well as intrinsic signal optical imaging, our group found normal responses to tactile stimulation in the reeler somatosensory cortex as well as in the corresponding subcortical relay stations (Guy et al., 2015; Wagener et al., 2016). Although it had already been shown that some kind of deviant barrels form in the somatosensory cortex of reeler (Caviness et al., 1976; Welt and Steindler, 1977), we also demonstrated that the barrel field retains its proper somatotopic organization, a rather surprising finding in the light of the massive lamination defects (Wagener et al., 2010; Guy et al., 2015). A study using similar approaches found comparable results in the visual cortex, where retinotopic organization and normal visually-evoked responses were observed (Pielecka-Fortuna et al., 2015). The

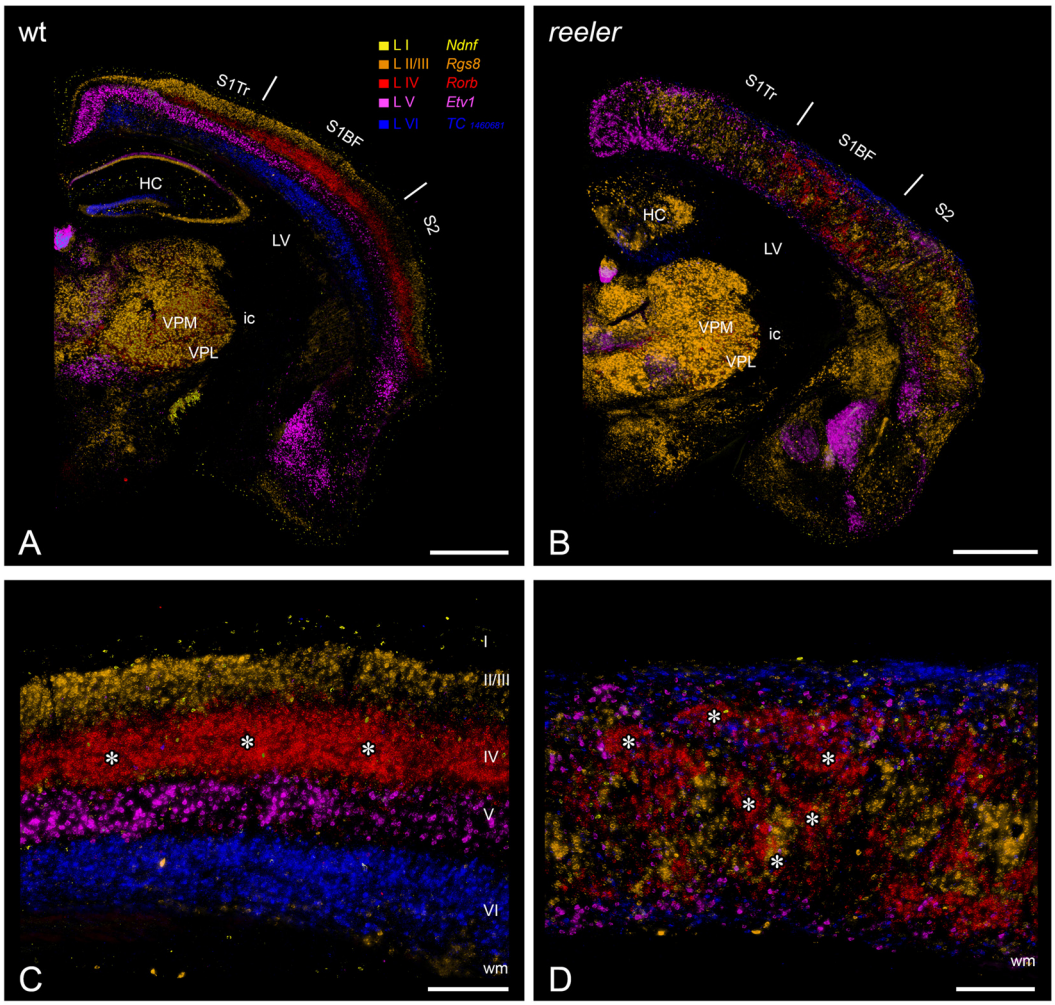

FIGURE 1 | Laminar fate markers show the dramatic disorganization of cortical layers in the reeler brain. **(A,B)** Coronal hemisections through the brain of a wild type **(A)** and a reeler mouse **(B)**, at the level of the primary somatosensory (barrel) cortex. Laminar fate markers (labeled in **A**) have been stained by *in situ*-hybridization in serial sections, false color-coded and overlaid to obtain a comprehensive impression (modified from Wagener et al., 2016). The overview shows that the general anatomical layout of the brain in terms of subcortical nuclei and cortical areas is basically normal. **(C,D)** Higher magnification through the barrel cortex shows a typical layering of a granular cortex **(C)**, with barrel-like clustered L IV-spiny stellates (*asterisks*). In the reeler mutant **(D)**, most cell types can be found anywhere across the cortical depth, with L IV-fated cells also forming cluster, which we called barrel equivalents (*asterisks*). *Roman numerals* mark cortical layers. Abbreviations: HC, hippocampus; ic, internal capsule; LV, lateral ventricle; S1BF, barrel field of the primary somatosensory cortex; S1Tr, trunk region of the primary somatosensory cortex; S2, secondary somatosensory cortex; VPL, nucleus ventralis posterolateralis; VPM, nucleus ventralis posteromedialis. Scale bars: **(A,B)**—1000 μm; **(C,D)**—250 μm.

first electrophysiological study of the reeler brain recorded local field potentials in the mutant hippocampus *in vitro*, and concluded that perforant path input to granule cells, as well as Schaffer collateral input to CA1 pyramidal cells were functional (Bliss and Chung, 1974). The response properties of individual neurons have been investigated as well. Still in the hippocampus *in vitro*, Kowalski et al. (2010) showed that mossy cells of the hilar region of the dentate gyrus receive direct input from granule cells in both mutant and normal mice. Using channelrhodopsin expression to control thalamocortical fiber activity and whole cell recordings *in vitro*, our group provided evidence that spiny stellate neurons, a main constituent of barrels in the somatosensory cortex, receive strong direct input from the ventral posteromedial nucleus in reeler, as they do in normal animals (Guy et al., 2016; Wagener et al., 2016). A few studies investigated the receptive field properties of individual neurons in the reeler visual cortex with single unit, extracellular recordings. Beyond the fact that neurons in the visual cortex respond to various sensory stimuli in the anesthetized reeler mouse, one such study discovered that ocular dominance was largely preserved in the mutant, with similar proportion of cells responding to contra- or ipsilateral stimulation (Dräger, 1981; Simmons and Pearlman, 1983). In addition, in these studies, normal receptive field types were observed in the reeler cortex: both oriented and non-oriented receptive fields, as well as simple

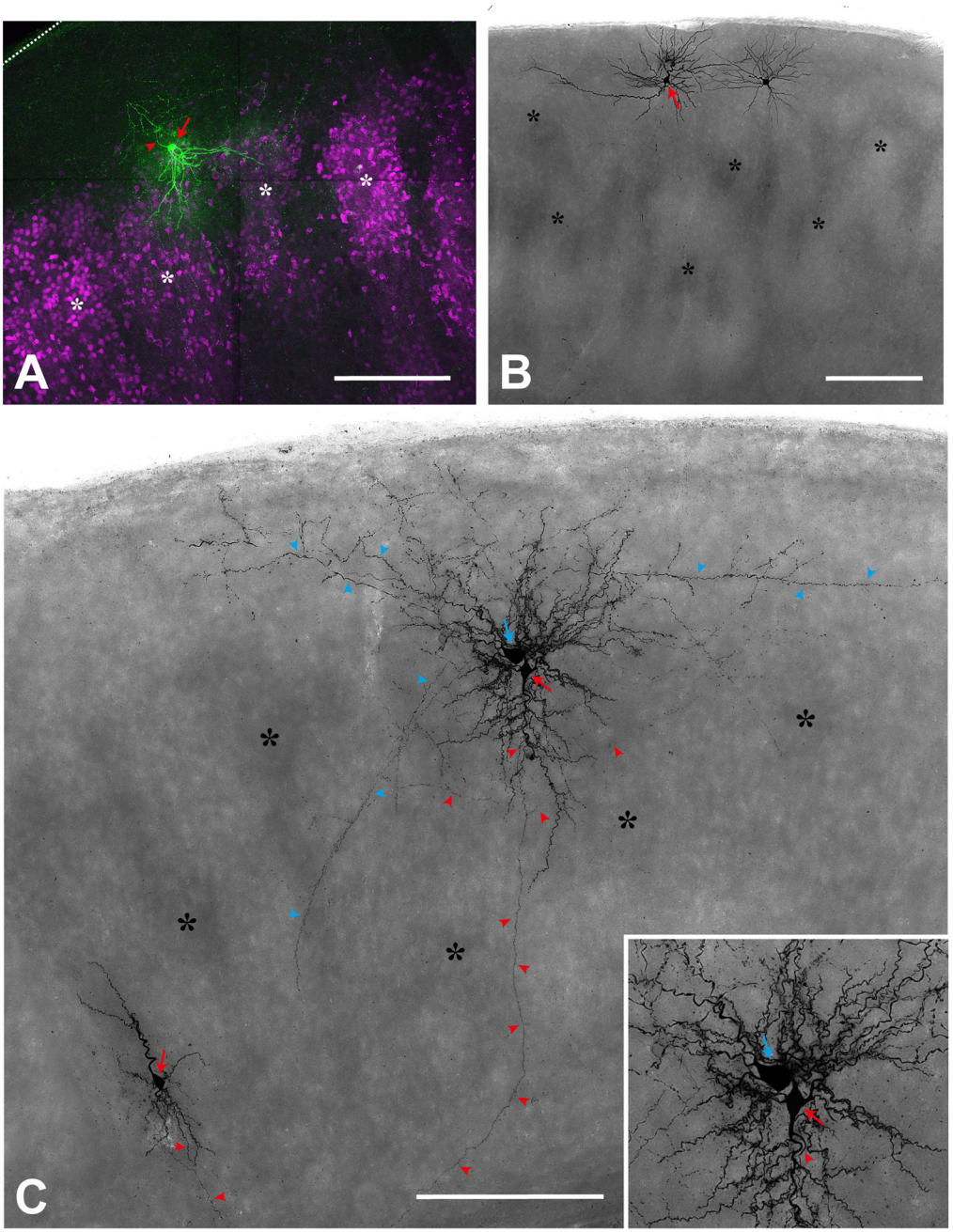

FIGURE 2 | Single cell fillings show the aberrant morphology of several types in the reeler cortex. **(A)** Regular-spiking spiny stellate cell (*red arrow*), located on top of two barrel equivalents (*asterisks*; labeled by Scnn1a-cre/tdTomato; see Guy et al., 2015, 2016). Please note that the dendrites spread out in a V-shaped manner to reach to neighboring cell clusters whereas the axon (*red arrowhead*) initially is directed toward the pial surface (*dashed line*). **(B)** Repetitive-bursting (probably "L Vb") pyramidal cell (*red arrow*) with a horizontally-oriented apical dendrite. **(C)** Cortical slice, in which three neurons have been recorded and labeled. A small up-right, regular-spiking pyramidal cell (*red arrow*; lower left), whose axon (*red arrowheads*) is directed toward the white matter. An inverted regular-spiking pyramidal cell (*red arrow*; see inset for details) shows an axon (*red arrowheads*) originating from the apical dendrite, which points toward the white matter). Directly next to it, a fast-spiking large basket cell (*blue arrow*) is labeled, whose axon (*blue arrowheads*), in addition to many local collaterals, issues divergent axonal projections. Scale bars: **(A)**—100 μm; **(B,C)**—250 μm.

and complex receptive fields, although in somewhat changed relative proportions, with a higher fraction of non-oriented neurons in the mutant. Another noteworthy peculiarity of the mutant visual cortex is its higher proportion of neurons showing very broad receptive fields (Dräger, 1981; Lemmon and Pearlman, 1981). These apparent abnormalities could however be due to differences in the cell populations sampled, as cortical depth is a poor predictor of the cell type recorded in

reeler. Overall, physiological responses to sensory stimulation appear largely preserved in the absence of cortical layers, a good indication that functional connectivity is mostly unchanged.

BEHAVIORAL PERFORMANCE OF THE *REELER* MUTANT MOUSE

A predictable consequence of unaltered functional connectivity is that reeler performs well in tests of perceptual or mnesic capacities. Alas, a hallmark of the reeler phenotype is a severe ataxia (Falconer, 1951; Magdaleno et al., 2002), linked to a well described cerebellar atrophy (Badea et al., 2007), accompanied by cell loss and dispersion (Mariani et al., 1977). Together with the high mortality rate within weeks of birth due to impaired feeding after weaning, this motor impairment has somewhat deterred attempts at investigating behavioral anomalies in the mutant, as many behavioral tests rely on a motor readout. What literature exists is well aligned with our expectation, however. Early observations have reported that reeler mice display a wide and overall normal range of behaviors once adult, including mating (Myers, 1970), in spite of notable delays in sensorimotor and social development (Romano et al., 2013). In what is probably the broadest behavioral study of reeler to date, Salinger et al. (2003) reported that mutant mice can use olfactory cues to find a hidden food pellet; in a separate assay, they were found to have normal depth perception; acoustic responsiveness was found unchanged as well. Although the study reported anomalies in social behavior and reduced anxiety levels, it concluded that sensory function is normal in reeler. Our group has reported that mutant mice normally use their whiskers to explore a novel enriched environment in the dark (Wagener et al., 2010), suggesting proper sensorimotor function. More detailed studies of visual prowess have examined the optokinetic nystagm, the reflex by which mice make head movements to follow a drifting grating. No impairment was found in the mutant either in visual acuity or in their sensitivity to the contrast and spatial frequency of the grating used (Sinex et al., 1979; Pielecka-Fortuna et al., 2015), suggesting that basic visual function is intact as well. On the basis of this largely preserved perception, reeler animals exhibit not only spontaneous exploratory behavior but also seem capable of spatial learning. Goldowitz and Koch (1986) tested the ability of several neurological mutants to learn an 8-arm-radial maze; although the initial performance of reeler was poorer than normal mice, it was equalized by training. Similar results were obtained using a visual water task, in which mice swim to a submerged platform signaled by an oriented grating. Reeler animals were able to learn the task at the same pace as wild type controls, and could recall the task months after the initial training (Pielecka-Fortuna et al., 2015). These results suggest that at least the basic function of sensory cortex and hippocampus is spared. In summary, perception, learning and memory are largely unaffected in the mutant mouse, and although some behavioral anomalies were reported, they seem to relate to social and emotional function rather than sensory acuity (Salinger et al., 2003).

A PUZZLING CONCLUSION: LAYERS HAVE NO APPARENT FUNCTION

Although much of the reeler brain morphology, physiology and behavior remains to be documented, the evidence briefly summarized here is sufficient to form an opinion as to whether or not cortical layers have a function. First, the cortex of the reeler mouse houses "normal" cell types, with their properties mostly unchanged. Second, even though they are ectopic, these neurons form appropriate connections and networks, which is difficult to envisage given the substantial deviation from normal of many neurons types (**Figure 3**). Third, both individual cells and networks respond to sensory input in a seemingly normal way. Fourth, perception, memory and overall behavior are not obviously compromised. It would thus appear that the loss of cortical lamination does not impair cortical function in any recognizable way, and that layers are in fact completely expendable. In other words, we hold the view that *layers as such have no function* in the context of information processing, although we do not exclude that they may serve different purposes. It follows that asking oneself what the role of an individual layer is, in terms of its share of the total computational workload, is misguided. This does not rule out other, supportive roles for layers, for example that they organize neurons into modules in which computation can be run at a lesser metabolic cost. These will be discussed below, after a cautionary note about the reeler mouse and an excursion to another model.

LIMITATIONS OF THE REELER MODEL

Even though the idea that layers have no computational functions is seductive in its simplicity, we must in all fairness acknowledge that the reeler model has limitations that must be mentioned. For one, a few misconnections have been reported in brains areas beyond the neocortex. In the cerebellum of reeler, abnormal synapses were found between mossy fibers and Purkinje cell spines (Mariani et al., 1977; Wilson et al., 1981). In the hippocampus, Kowalski et al. (2010) found aberrant input from the perforant path to mossy cells. Granted, no example of aberrant input was discovered in the neocortex but their existence has been hypothesized (Caviness and Rakic, 1978) and if confirmed, would mean that the reeler model no longer fits the requirement of network equivalence. In addition, reelin expression persists after birth in a heterogeneous subset of GABAergic interneurons (Alcántara et al., 1998; Pohlkamp et al., 2014). The roles of reelin in the adult brain are thought to be multiple and the subject of ongoing research, but some bear potentially significant consequences for our argument. In particular, the protein has been shown to modulate synaptic transmission by various mechanisms. Postsynaptically, reelin mediates an

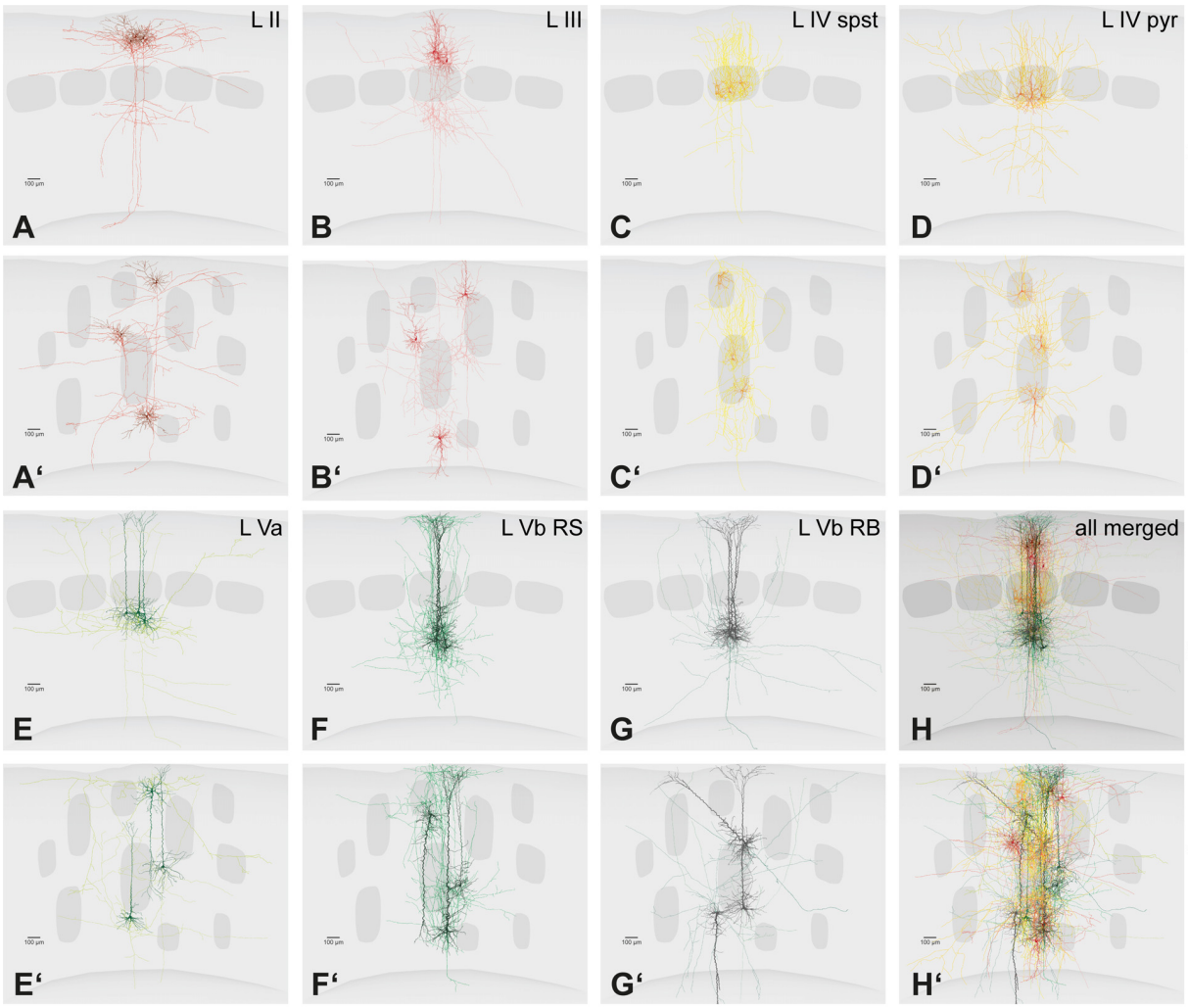

FIGURE 3 | Single cell fillings of excitatory neurons in the wild type and their hypothetical counterparts in the reeler cortex. **(A–H)** Principal cells of the barrel cortex (*n* = 3 overlaid for each type) show typical layer-dependent organization of their dendritic and axonal arbors. Original data published (Schubert et al., 2003, 2006; Staiger et al., 2004, 2015, 2016). **(A′–H′)** Hypothetical schemes showing how reeler equivalent cells could be organized, after rotating and re-distributing them over the cortical depth. *Roman numerals* mark cortical layers. Abbreviations: pyr, pyramidal cell; spst, spiny stellate cell; RB, repetitive-bursting; RS, regular-spiking.

enhancement of Ca^{2+} currents through the NMDA receptor (Chen et al., 2005), and increases AMPA receptor integration in the plasma membrane (Qiu et al., 2006b). Presynaptically, the absence of reelin alters the composition of the SNARE complex and the number of vesicles at hippocampal synapses, an effect accompanied by a decrease in paired pulse facilitation (Hellwig et al., 2011). In line with this role in synaptic transmission, reelin was also shown to enhance hippocampal long-term potentiation (Beffert et al., 2005; Qiu et al., 2006b). In addition, evidence is mounting that GABAergic transmission is weakened by a loss of reelin, resulting in a shift in the excitation-inhibition balance with potentially far-reaching consequences (Qiu et al., 2006a; Guy et al., 2016; Bouamrane et al., 2017). Finally, at least one study reported a slight anomaly in visual perception in reeler mice, namely impairment in orientation discrimination (Pielecka-Fortuna et al., 2015).

Taken together, these results reveal a conundrum: should perceptual or behavioral anomalies be discovered in reeler, how to attribute them to the loss of layers or to abnormalities in synaptic transmission? This problem will predictably limit how much can be learnt from reeler about cortical function, especially with regard to the purpose of cortical lamination. It may be possible to circumvent this problem by utilizing a recently established floxed reelin mouse (Lane-Donovan et al., 2015). For example, one may imagine a conditional reelin knockout (cKO) restricting the loss of reelin during development to specific areas and cell types. Such an approach would in principle enable the creation of a mouse line in which reelin expression is lost in the cortex only, preventing the cerebellar atrophy and ensuing motor deficits as well as all other subcortical abnormalities reported that complicate the behavioral study of the reeler mouse, while preserving the lamination defects. Unfortunately, the necessary cre-driver

line to achieve this high level of specificity so far does not seem to be available. An alternative approach would be to design a cKO animal in which reelin expression is lost in adulthood only, leaving the process of cortical lamination unchanged. By comparing the behavioral phenotype in cortex-dependent tasks of such a cKO mouse with that of the reeler mouse, one may disentangle which aspects of the reeler phenotype are due to lamination defects and which are caused by the loss of the well documented role of reelin in regulating synaptic transmission in the adult brain. Indeed, a phenotype observed in the reeler mutant only but not in cKO animals can be safely assumed to relate to abnormal lamination, while a phenotype shared by both lines is more likely to result from impairments in synaptic modulation. Such an approach was recently used by Lane-Donovan et al. (2015), who generated a reelin cKO mouse that allows for tamoxifen-induced, cre-dependent suppression of reelin expression in normal, fully grown animals. The cKO mouse showed normal lamination of the hippocampus, suggesting that brain development is indeed intact. The density of spines along dendrites of individual hippocampal neurons was also unchanged in cKO mice with respect to control animals receiving vehicle injections, indicating that the reduction in spine density observed in reeler hippocampus may relate to developmental defects rather than reelin dependent spine plasticity in the adult brain (Niu et al., 2008; Lane-Donovan et al., 2015). Conversely, the cKO line exhibits slightly reduced anxiety levels when tested in the open field paradigm (Lane-Donovan et al., 2015), a trait they share with reeler animals (Salinger et al., 2003) and is probably related to the roles of reelin in the adult brain rather than to developmental defects. To our knowledge, no study to date has compared the performance of sensory systems between reeler and reelin cKO animals, but we believe that such approaches hold great promise in solving the conundrum mentioned above. In summary, although the reeler model has limitations that will hopefully be overcome in the near future, we still believe that it largely supports our conclusion that layers do not have essential computational functions.

A GLIMPSE INTO BIRD PALLIUM AS A NON-LAMINATED CORTEX-LIKE STRUCTURE

The reeler mouse is not the only relevant model available, so let us briefly turn to birds. Bird brains lack a laminated neocortex entirely, and for this reason were once thought to be incapable of the finer perceptual and cognitive skills of mammals. Such a view has largely evolved, however, given that some birds in fact possess cognitive abilities that rival those of mammals, including, beyond the obvious capacity for complex social communication: tool use and manufacture (Kenward et al., 2005), abstract numerical skills (Scarf et al., 2011; Ditz and Nieder, 2015), capacity for causal reasoning (Taylor et al., 2012), and anticipation of the future (Clayton et al., 2003; Raby et al., 2007). The fact that birds have cognitive abilities that match those of mammals suggests that mammalian and avian brains must conduct similar operations, in spite of a different organization. The seat of the more advanced capacities of birds is thought to be the pallium, a somewhat cortex-like mantle covering the basal ganglia. For instance, two avian pallial structures, the Wulst and the dorsal ventricular ridge (DVR) were proposed as the avian homolog of the sensory neocortex (Jarvis et al., 2005; Reiner et al., 2005; Butler and Cotterill, 2006). Like the neocortex, the avian pallium exhibits areal functional specialization and receives ascending sensory information from the thalamus (Reiner et al., 2005). Unlike the neocortex, the avian pallium is organized as a set of contiguous nuclei, but remarkable homologies between nuclei and cortical layers were observed (**Figure 4**).

First, thalamorecipient, excitatory interneurons and projection neurons are spatially segregated in the sensory pallium. As an example, the auditory region of the pallium comprises the field L of the nidopallium, the caudal mesopallium and the arcopallium. Field L is subdivided in three subfields named L1, L2 and L3. Thalamorecipient neurons are found primarily in L2 and project to subfields L1, L3 and the caudal mesopallium. These areas are composed of excitatory interneurons, while brainstem projection neurons are located in the arcopallium (Karten, 1997; Jarvis et al., 2005). This mirrors to some extent the segregation of neurons into layers in the neocortex, where thalamorecipient "excitatory interneurons" dwell in layer IV, "intratelencephalic projection neurons" in layer II/III and "subcerebral projection neurons" or "pyramidal tract neurons" in the infragranular layers (Harris and Shepherd, 2015). Second, thalamorecipient and projection neurons in birds can be discriminated on the basis their gene expression pattern, with strong homologies to mammalian neocortex. For instance, thalamorecipient neurons of the auditory pallium express the marker gene RORB, which is also enriched in layer IV of the neocortex, whereas the marker gene ER81 identifies projection neurons in both the avian arcopallium and mammalian layer V (Boyle et al., 2011; Dugas-Ford et al., 2012; Wagener et al., 2016). Third, the spread of sensory information in the avian auditory pallium follows a temporal structure similar to what occurs in a cortical column. Thalamorecipient neurons in field L2 respond with shortest latencies to sensory input, followed by neurons in field L3 and then neurons in field L1 and in the caudal mesopallium; responses in the secondary auditory pallium appear last (Calabrese and Woolley, 2015). This sequence of events matches that of the neocortex, where thalamorecipient neurons of LIV distribute thalamic input to other layers along the canonical microcircuit.

On the basis of these homologies, one is tempted to conclude that avian and mammalian brains possess similar sensory circuits. In fact, a long standing hypothesis is that birds and mammal independently evolved homologous brain structures endowing them with similar sensorimotor and cognitive capabilities, in a stunning example of convergent evolution (Karten, 1997, 2013; Veit and

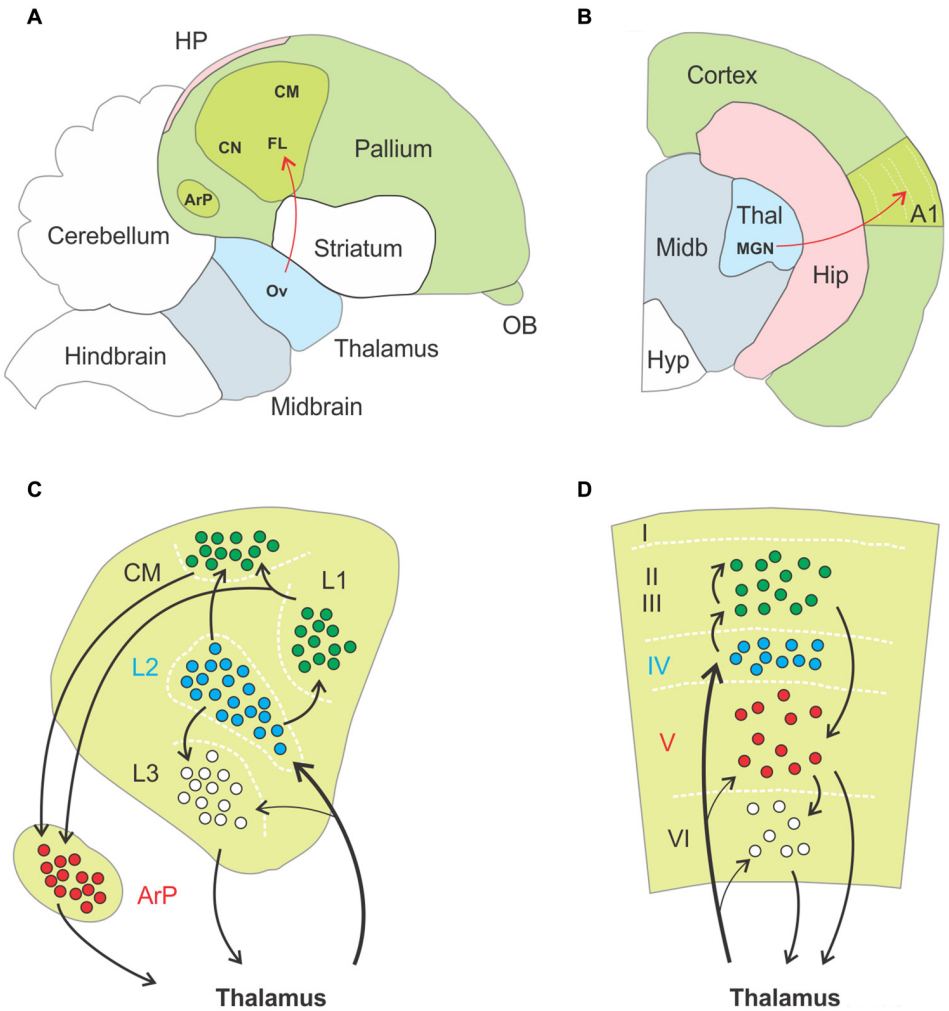

FIGURE 4 | Anatomo-functional homologies between avian and mammalian brain. **(A,B)** Schematic drawings of a parasagittal section through the brain of a zebra finch, **(A**, adapted from Jarvis et al., 2005) and a coronal section through the hemisphere of a mouse **(B)**, respectively. Basic anatomical compartments present on both schematic drawings are color coded (as opposed to white). The primary auditory areas are highlighted in apple green as an example of functional homologies between both species, ascending thalamopallial and thalamocortical pathways indicated in red. Abbreviations: A1, primary auditory cortex; ArP, arcopallium; CM, caudal mesopallium; CN, caudal nidopallium; FL, field L of the nidopallium; HP, hippocampal complex; Hip, hippocampus; Hyp, hypothalamus; MGN, medial geniculate nucleus; Midb, midbrain; OB, olfactory bulb; Ov, nucleus ovoidalis; Thal, thalamus. **(C,D)** Schematic drawings of the functional organization of the auditory pallium **(C)** and primary auditory cortex **(D)**, respectively. Black arrows indicate excitatory connections, dashed white lines highlight approximate borders between pallial nuclei **(C)** and cortical layers **(D)**. Roman numerals label individual layers. Proposed homologies between discrete nuclei and layers are color coded. Thalamorecipient, RORß expressing neurons are labeled in blue, and projection neurons positive for ER81 in red. In both species these populations are linked by intermediate excitatory neurons located more superficially, in subfield L and the caudal mesopallium in birds and in supragranular layers in rodents. Abbreviations: ArP, arcopallium; CM, caudal mesopallium; L1, L2, L3, subfields L1, L2, L3 of the nidopallium.

Nieder, 2013; Ditz and Nieder, 2015). Because the most obvious difference here is laminar vs. nuclear organization, the lesson for us to draw from birds is clear: cortical layers are not required for circuits to perform a refined function.

ALTERNATIVE FUNCTIONS FOR LAYERS

Cortical lamination is a conserved trait across mammalian species. If layers do not participate in cortical processing, what could be their function, if they are not a mere by-product of cortical development (Rakic, 2007)? We know from the reeler model that they do little to help establish specific connections between neuronal populations. Another thought is that they may help optimize synaptic transmission between cell populations. For instance, grouping neurons in layers has the potential advantage of keeping the path length between populations that need to be connected relatively constant. A stable path length ensures synchronous transmission across many synapses, facilitating temporal summation in the

postsynaptic population. The cellular dispersion in the reeler cortex may lead to a more variable average path length and thus a higher temporal jitter in synaptic transmission. Assuming a mean axon conduction velocity of 1.3 m/s in cortical neurons (Swadlow, 1989), an increase in path length of 1000 μm would add nearly a millisecond (0.77 ms) to the total conduction delay. If the neighboring neuron saw its axon shortened by the same distance, a delay of more than 1.5 ms would be introduced between the activation of their synapses, provided they fire synchronously. Such a jitter might appear small at first, but if repeated at every successive synapse along the canonical circuit, could perhaps compromise the synchrony of the entire network. To our knowledge, no data from the reeler neocortex exists that could corroborate this speculation, but it is worth noting that Kowalski et al. (2010) have described an abnormally large temporal jitter in the firing of hippocampal mossy cells in response to a stimulation of the perforant path in reeler. Another possibility is that the precise arrangement of neurons into layers represents a form of optimal solution to the problem of building a highly interconnected network within a limited volume and at a reasonable metabolic cost. The principle that neuronal placement is determined so as to minimize wiring length and space usage without compromising connectivity was initially formulated by Ramon y Cajal. It was since put to the test in quite a number of elegant studies, which showed how this principle can explain the relative positions of cortical areas (Klyachko and Stevens, 2003), the layout of neurons (Chen et al., 2006), the fraction of gray matter volume allotted to dendrites and axons (Chklovskii et al., 2002), and even aspects of neuronal morphology (Chklovskii et al., 2004). Could cortical layers have evolved as an efficient answer to similar challenges? If such an assumption is true, it leads to an interesting prediction about the reeler cortex. If lamination represents an optimal layout of neurons, it follows that the reeler cortex has a suboptimal arrangement, meaning that less space is available to fit the same elements. As a result, it seems likely that less space can be allocated to at least one component of the gray matter, be it cell bodies, neuropil, fibers, glia, or blood vessels, although it seems logical that the elements that develop latest, such as myelin sheaths, would be most affected. To our knowledge, no systematic studies have ever tested such a prediction in sufficient detail, but on first approximation, no obvious difference was reported in the number of oligodendrocytes and astrocytes (Ghandour et al., 1981; Tan et al., 2009), or in the density of blood vessels (Stubbs et al., 2009; Guy et al., 2015). Neurons may provide part of the answer: although their numbers are not significantly changed in reeler, late born neurons, which adopt the compact morphology of supragranular neurons, are overrepresented with respect to early born, large pyramidal neurons (Polleux et al., 1998; Wagener et al., 2016). Determining whether and how cellular dispersion affects the relative space allotted to various components of the gray matter in the reeler brain could shed further light on the function of cortical lamination, and we are looking forward to seeing such studies in the future.

CONCLUDING REMARKS

Whatever the real function of cortical lamination is, the current state of our knowledge is clear: in the span of over 160 years of science, little solid positive evidence that layers participate in cortical computation has emerged, while evidence to the contrary has accumulated. The evidence presented here suggests that the function does not reside in the layer but in the circuit, irrespective of its specific spatial layout (Ye et al., 2016). Although this fact is hardly controversial, we feel that a pervasive ambiguity exists when dealing with layers, in the sense that one can easily, for the sake of convenience, use the terms of "circuits" and "layers" interchangeably. As a result, a function which is in fact carried by a circuit is slowly, by semantic shift, assigned to a layer. A classic example of this is the following statement, now commonplace in the literature: "layer IV is the primary thalamocortical input layer and starts conscious perception of sensory stimuli". While not technically incorrect, the statement is a gross simplification. After all, layer IV is crossed by the dendrites of most pyramidal neurons dwelling elsewhere in the cortical column, so that thalamocortical input is by no means restricted to those neurons whose soma sits there. In addition, excitatory neurons may quickly redistribute input from the thalamus by means of their local axonal collaterals, so that cortical activity nearly instantaneously spreads over several layers and columns to mediate perception of sensory stimuli (Reyes-Puerta et al., 2015). Thus, simplifications such as these can be confusing and quite unhelpful, and we would like to urge us all to use a clear language when writing about layers, so as to not give them functions they do not have.

AUTHOR CONTRIBUTIONS

JFS and JG: conception and drafting of the manuscript; conception and generation of figures.

ACKNOWLEDGMENTS

The authors want to thank Michael Frotscher for his introduction into the fascinating world of the reeler mutant brain. Thus, they want to dedicate this review to him, mourning his untimely passing just before his 70th birthday. The reelin field has lost one of his most innovative and productive figures and we have lost an unreplaceable friend. We also would like to thank Robin Wagener for providing Figure 1 and contributing to much of the ground-laying new data on the reeler somatosensory system. Thanks are also due to the "Barrel Cortical Circuits" group of the Institute for Neuroanatomy, for many fruitful discussions over the years. The author's work is supported by the Deutsche Forschungsgemeinschaft through Sta 431/11-1 and the CNMPB (B1 area). We acknowledge support by the German Research Foundation and the Open Access Publication Funds of the Göttingen University.

REFERENCES

Alcántara, S., Ruiz, M., D'Arcangelo, G., Ezan, F., de Lecea, L., Curran, T., et al. (1998). Regional and cellular patterns of *reelin* mRNA expression in the forebrain of the developing and adult mouse. *J. Neurosci.* 18, 7779–7799.

Armstrong-James, M. A., and Fox, K. (1987). Spatiotemporal convergence and divergence in the rat S1 "barrel" cortex. *J. Comp. Neurol.* 263, 265–281. doi: 10.1002/cne.902630209

Badea, A., Nicholls, P. J., Johnson, G. A., and Wetsel, W. C. (2007). Neuroanatomical phenotypes in the reeler mouse. *Neuroimage* 34, 1363–1374. doi: 10.1016/j.neuroimage.2006.09.053

Baillarger, J. G. F. (1840). *Recherches sur la Structure de la Couche Corticale des Circonvolutions du Cerveau.* Paris: Baillière.

Beffert, U., Weeber, E. J., Durudas, A., Qiu, S., Masiulis, I., Sweatt, J. D., et al. (2005). Modulation of synaptic plasticity and memory by Reelin involves differential splicing of the lipoprotein receptor Apoer2. *Neuron* 47, 567–579. doi: 10.1016/j.neuron.2005.07.007

Bliss, T. V., and Chung, S. H. (1974). An electrophysiological study of the hippocampus of the 'reeler' mutant mouse. *Nature* 252, 153–155. doi: 10.1038/252153a0

Bock, H. H., and May, P. (2016). Canonical and non-canonical reelin signaling. *Front. Cell. Neurosci.* 10:166. doi: 10.3389/fncel.2016.00166

Bouamrane, L., Scheyer, A. F., Lassalle, O., Iafrati, J., Thomazeau, A., and Chavis, P. (2017). Reelin-haploinsufficiency disrupts the developmental trajectory of the E/I balance in the prefrontal cortex. *Front. Cell. Neurosci.* 10:308. doi: 10.3389/fncel.2016.00308

Boyle, M. P., Bernard, A., Thompson, C. L., Ng, L., Boe, A., Mortrud, M., et al. (2011). Cell-type-specific consequences of reelin deficiency in the mouse neocortex, hippocampus, and amygdala. *J. Comp. Neurol.* 519, 2061–2089. doi: 10.1002/cne.22655

Butler, A. B., and Cotterill, R. M. (2006). Mammalian and avian neuroanatomy and the question of consciousness in birds. *Biol. Bull.* 211, 106–127. doi: 10.2307/4134586

Calabrese, A., and Woolley, S. M. N. (2015). Coding principles of the canonical cortical microcircuit in the avian brain. *Proc. Natl. Acad. Sci. U S A* 112, 3517–3522. doi: 10.1073/pnas.1408545112

Caviness, V. S. Jr., Crandall, J. E., and Edwards, M. A. (1988). "The reeler malformation: implications for neocortical histogenesis," in *Cerebral Cortex*, eds A. Peters and E. G. Jones (New York, NY: Plenum Press), 59–89.

Caviness, V. S. Jr., and Frost, D. O. (1983). Thalamocortical projections in the reeler mutant mouse. *J. Comp. Neurol.* 219, 182–202. doi: 10.1002/cne.902190205

Caviness, V. S. Jr., Frost, D. O., and Hayes, N. L. (1976). Barrels in somatosensory cortex of normal and reeler mutant mice. *Neurosci. Lett.* 3, 7–14. doi: 10.1016/0304-3940(76)90091-4

Caviness, V. S. Jr., and Rakic, P. (1978). Mechanisms of cortical development: a view from mutations in mice. *Annu. Rev. Neurosci.* 1, 297–326. doi: 10.1146/annurev.ne.01.030178.001501

Caviness, V. S. Jr., and Sidman, R. L. (1973). Time of origin or corresponding cell classes in the cerebral cortex of normal and reeler mutant mice: an autoradiographic analysis. *J. Comp. Neurol.* 148, 141–151. doi: 10.1002/cne.901480202

Caviness, V. S. Jr., and Yorke, C. H. Jr. (1976). Interhemispheric neocortical connections of the corpus callosum in the reeler mutant mouse: a study based on anterograde and retrograde methods. *J. Comp. Neurol.* 170, 449–459. doi: 10.1002/cne.901700405

Chen, Y., Beffert, U., Ertunc, M., Tang, T. S., Kavalali, E. T., Bezprozvanny, I., et al. (2005). Reelin modulates NMDA receptor activity in cortical neurons. *J. Neurosci.* 25, 8209–8216. doi: 10.1523/JNEUROSCI.1951-05.2005

Chen, B. L., Hall, D. H., and Chklovskii, D. B. (2006). Wiring optimization can relate neuronal structure and function. *Proc. Natl. Acad. Sci. U S A* 103, 4723–4728. doi: 10.1073/pnas.0506806103

Chklovskii, D. B., Mel, B. W., and Svoboda, K. (2004). Cortical rewiring and information storage. *Nature* 431, 782–788. doi: 10.1038/nature03012

Chklovskii, D. B., Schikorski, T., and Stevens, C. F. (2002). Wiring optimization in cortical circuits. *Neuron* 34, 341–347. doi: 10.1016/s0896-6273(02)00679-7

Chmielowska, J., Carvell, G. E., and Simons, D. J. (1989). Spatial organization of thalamocortical and corticothalamic projection systems in the rat SmI barrel cortex. *J. Comp. Neurol.* 285, 325–338. doi: 10.1002/cne.902850304

Clayton, N. S., Bussey, T. J., and Dickinson, A. (2003). Can animals recall the past and plan for the future? *Nat. Rev. Neurosci.* 4, 685–691. doi: 10.1038/nrn1180

Constantinople, C. M., and Bruno, R. M. (2013). Deep cortical layers are activated directly by thalamus. *Science* 340, 1591–1594. doi: 10.1126/science.1236425

Curran, T., and D'Arcangelo, G. (1998). Role of reelin in the control of brain development. *Brain Res. Rev.* 26, 285–294. doi: 10.1016/s0165-0173(97)00035-0

Dekimoto, H., Terashima, T., and Katsuyama, Y. (2010). Dispersion of the neurons expressing layer specific markers in the reeler brain. *Dev. Growth Differ.* 52, 181–193. doi: 10.1111/j.1440-169x.2009.01153.x

Diodato, A., Ruinart de Brimont, M., Yim, Y. S., Derian, N., Perrin, S., Pouch, J., et al. (2016). Molecular signatures of neural connectivity in the olfactory cortex. *Nat. Commun.* 7:12238. doi: 10.1038/ncomms12238

Ditz, H. M., and Nieder, A. (2015). Neurons selective to the number of visual items in the corvid songbird endbrain. *Proc. Natl. Acad. Sci. U S A* 112, 7827–7832. doi: 10.1073/pnas.1504245112

Dräger, U. C. (1981). Observations on the organization of the visual cortex in the reeler mouse. *J. Comp. Neurol.* 201, 555–570. doi: 10.1002/cne.902010407

Dugas-Ford, J., Rowell, J. J., and Ragsdale, C. W. (2012). Cell-type homologies and the origins of the neocortex. *Proc. Natl. Acad. Sci. U S A* 109, 16974–16979. doi: 10.1073/pnas.1204773109

Falconer, D. S. (1951). Two new mutants, 'trembler', and 'reeler', with neurological actions in the house mouse *(Mus musculus* L.). *J. Genet.* 50, 192–201. doi: 10.1007/bf02996215

Feldmeyer, D. (2012). Excitatory neuronal connectivity in the barrel cortex. *Front. Neuroanat.* 6:24. doi: 10.3389/fnana.2012.00024

Feldmeyer, D., Egger, V., Lübke, J., and Sakmann, B. (1999). Reliable synaptic connections between pairs of excitatory layer 4 neurones within a single 'barrel' of developing rat somatosensory cortex. *J. Physiol.* 521, 169–190. doi: 10.1111/j.1469-7793.1999.00169.x

Fox, K., Wright, N., Wallace, H., and Glazewski, S. (2003). The origin of cortical surround receptive fields studied in the barrel cortex. *J. Neurosci.* 23, 8380–8391.

Frotscher, M., Chai, X., Bock, H. H., Haas, C. A., Förster, E., and Zhao, S. (2009). Role of Reelin in the development and maintenance of cortical lamination. *J. Neural Transm.* 116, 1451–1455. doi: 10.1007/s00702-009-0228-7

Gennari, F. (1784). *De Peculiari Structura Cerebri Nonnullisque Ejus Morbis*. Parma: Parmae, Available online at: https://archive.org/details/b2170935x

Ghandour, M. S., Derer, P., Labourdette, G., Delaunoy, J. P., and Langley, O. K. (1981). Glial cell markers in the reeler mutant mouse: a biochemical and immunohistological study. *J. Neurochem.* 36, 195–200. doi: 10.1111/j.1471-4159.1981.tb02395.x

Goldowitz, D., and Koch, J. (1986). Performance of normal and neurological mutant mice on radial arm maze and active avoidance tasks. *Behav. Neural Biol.* 46, 216–226. doi: 10.1016/s0163-1047(86)90696-5

Guy, J., Sachkova, A., Möck, M., Witte, M., Wagener, R. J., and Staiger, J. F. (2016). Intracortical network effects preserve thalamocortical input efficacy in a cortex without layers. *Cereb. Cortex* doi: 10.1093/cercor/bhw281 [Epub ahead of print].

Guy, J., Wagener, R. J., Möck, M., and Staiger, J. F. (2015). Persistence of functional sensory maps in the absence of cortical layers in the somatosensory cortex of reeler mice. *Cereb. Cortex* 25, 2517–2528. doi: 10.1093/cercor/bhu052

Harris, K. D., and Mrsic-Flogel, T. D. (2013). Cortical connectivity and sensory coding. *Nature* 503, 51–58. doi: 10.1038/nature12654

Harris, K. D., and Shepherd, G. M. G. (2015). The neocortical circuit: themes and variations. *Nat. Neurosci.* 18, 170–181. doi: 10.1038/nn.3917

Harsan, L. A., Dávid, C., Reisert, M., Schnell, S., Hennig, J., von Elverfeldt, D., et al. (2013). Mapping remodeling of thalamocortical projections in the living reeler mouse brain by diffusion tractography. *Proc. Natl. Acad. Sci. U S A* 110, E1797–E1806. doi: 10.1073/pnas.1218330110

Heckroth, J. A., Goldowitz, D., and Eisenman, L. M. (1989). Purkinje cell reduction in the reeler mutant mouse: a quantitative immunohistochemical study. *J. Comp. Neurol.* 279, 546–555. doi: 10.1002/cne.902790404

Hellwig, S., Hack, I., Kowalski, J., Brunne, B., Jarowyj, J., Unger, A., et al. (2011). Role for Reelin in neurotransmitter release. *J. Neurosci.* 31, 2352–2360. doi: 10.1523/JNEUROSCI.3984-10.2011

Hevner, R. F., Daza, R. A. M., Englund, C., Kohtz, J., and Fink, A. (2004). Postnatal shifts of interneuron position in the neocortex of normal and reeler mice: evidence for inward radial migration. *Neuroscience* 124, 605–618. doi: 10.1016/j.neuroscience.2003.11.033

Higashi, S., Hioki, K., Kurotani, T., Kasim, N., and Molnár, Z. (2005). Functional thalamocortical synapse reorganization from subplate to layer IV during postnatal development in the reeler-like mutant rat *(Shaking rat Kawasaki)*. *J. Neurosci.* 25, 1395–1406. doi: 10.1523/JNEUROSCI.4023-04.2005

Huang, W., Armstrong-James, M. A., Rema, V., Diamond, M. E., and Ebner, F. F. (1998). Contribution of supragranular layers to sensory processing and plasticity in adult rat barrel cortex. *J. Neurophysiol.* 80, 3261–3271.

Jarvis, E. D., Güntürkün, O., Bruce, L., Csillag, A., Karten, H., Kuenzel, W., et al. (2005). Avian brains and a new understanding of vertebrate brain evolution. *Nat. Rev. Neurosci.* 6, 151–159. doi: 10.1038/nrn1606

Karten, H. J. (1997). Evolutionary developmental biology meets the brain: the origins of mammalian cortex. *Proc. Natl. Acad. Sci. U S A* 94, 2800–2804. doi: 10.1073/pnas.94.7.2800

Karten, H. J. (2013). Neocortical evolution: neuronal circuits arise independently of lamination. *Curr. Biol.* 23, R12–R15. doi: 10.1016/j.cub.2012.11.013

Katsuyama, Y., and Terashima, T. (2009). Developmental anatomy of reeler mutant mouse. *Dev. Growth Differ.* 51, 271–286. doi: 10.1111/j.1440-169x.2009.01102.x

Kenward, B., Weir, A. A., Rutz, C., and Kacelnik, A. (2005). Behavioural ecology: tool manufacture by naive juvenile crows. *Nature* 433:121. doi: 10.1038/433121a

Klyachko, V. A., and Stevens, C. F. (2003). Connectivity optimization and the positioning of cortical areas. *Proc. Natl. Acad. Sci. U S A* 100, 7937–7941. doi: 10.1073/pnas.0932745100

Kowalski, J., Geuting, M., Paul, S., Dieni, S., Laurens, J., Zhao, S. T., et al. (2010). Proper layering is important for precisely timed activation of hippocampal mossy cells. *Cereb. Cortex* 20, 2043–2054. doi: 10.1093/cercor/bhp267

Landrieu, P., and Goffinet, A. (1981). Inverted pyramidal neurons and their axons in the neocortex of reeler mutant mice. *Cell Tissue Res.* 218, 293–301. doi: 10.1007/bf00210345

Lane-Donovan, C., Philips, G. T., Wasser, C. R., Durakoglugil, M. S., Masiulis, I., Upadhaya, A., et al. (2015). Reelin protects against amyloid β toxicity *in vivo*. *Sci. Signal.* 8:ra67. doi: 10.1126/scisignal.aaa6674

Lein, E. S., Hawrylycz, M. J., Ao, N., Ayres, M., Bensinger, A., Bernard, A., et al. (2007). Genome-wide atlas of gene expression in the adult mouse brain. *Nature* 445, 168–176. doi: 10.1038/nature05453

Lemmon, V., and Pearlman, A. L. (1981). Does laminar position determine the receptive field properties of cortical neurons? A study of corticotectal cells in area 17 of the normal mouse and the reeler mutant. *J. Neurosci.* 1, 83–93.

Magdaleno, S. M., Keshvara, L., and Curran, T. (2002). Rescue of ataxia and preplate splitting by ectopic expression of reelin in reeler mice. *Neuron* 33, 573–586. doi: 10.1016/s0896-6273(02)00582-2

Mariani, J., Crepel, F., Mikoshiba, K., Changeux, J. P., and Sotelo, C. (1977). Anatomical, physiological and biochemical studies of the cerebellum from reeler mutant mouse. *Philos. Trans. R. Soc. Lond. B Biol. Sci.* 281, 1–28. doi: 10.1098/rstb.1977.0121

Meynert, T. (1867). Der bau der grosshirnrinde und seiner örtlichen verschiedenheiten, nebst einem pathologisch-anatomischen collarium. *Vierteljahresschr. Psychiat.* 1, 77–93.

Miller, K. D., Pinto, D. J., and Simons, D. J. (2001). Processing in layer 4 of the neocortical circuit: new insights from visual and somatosensory cortex. *Curr. Opin. Neurobiol.* 11, 488–497. doi: 10.1016/s0959-4388(00)00239-7

Myers, W. A. (1970). Some observations on "reeler", a neuromuscular mutation in mice. *Behav. Genet.* 1, 225–234. doi: 10.1007/bf01074654

Niu, S., Yabut, O., and D'Arcangelo, G. (2008). The Reelin signaling pathway promotes dendritic spine development in hippocampal neurons. *J. Neurosci.* 28, 10339–10348. doi: 10.1523/JNEUROSCI.1917-08.2008

Oberlaender, M., de Kock, C. P. J., Bruno, R. M., Ramirez, A., Meyer, H. S., Dercksen, V. J., et al. (2012). Cell type-specific three-dimensional structure of thalamocortical circuits in a column of rat vibrissal cortex. *Cereb. Cortex* 22, 2375–2391. doi: 10.1093/cercor/bhr317

Pielecka-Fortuna, J., Wagener, R. J., Martens, A. K., Goetze, B., Schmidt, K. F., Staiger, J. F., et al. (2015). The disorganized visual cortex in reelin-deficient mice is functional and allows for enhanced plasticity. *Brain Struct. Funct.* 220, 3449–3467. doi: 10.1007/s00429-014-0866-x

Pinto Lord, M. C., and Caviness, V. S. Jr. (1979). Determinants of cell shape and orientation: a comparative Golgi analysis of cell-axon interrelationships in the developing neocortex of normal and reeler mice. *J. Comp. Neurol.* 187, 49–69. doi: 10.1002/cne.901870104

Pohlkamp, T., Dávid, C., Cauli, B., Gallopin, T., Bouché, E., Karagiannis, A., et al. (2014). Characterization and distribution of reelin-positive interneuron subtypes in the rat barrel cortex. *Cereb. Cortex* 24, 3046–3058. doi: 10.1093/cercor/bht161

Polleux, F., Dehay, C., and Kennedy, H. (1998). Neurogenesis and commitment of corticospinal neurons in reeler. *J. Neurosci.* 18, 9910–9923.

Qiu, S., Korwek, K. M., Pratt-Davis, A. R., Peters, M., Bergman, M. Y., and Weeber, E. J. (2006a). Cognitive disruption and altered hippocampus synaptic function in Reelin haploinsufficient mice. *Neurobiol. Learn. Mem.* 85, 228–242. doi: 10.1016/j.nlm.2005.11.001

Qiu, S., Zhao, L. F., Korwek, K. M., and Weeber, E. J. (2006b). Differential reelin-induced enhancement of NMDA and AMPA receptor activity in the adult hippocampus. *J. Neurosci.* 26, 12943–12955. doi: 10.1523/JNEUROSCI.2561-06.2006

Raby, C. R., Alexis, D. M., Dickinson, A., and Clayton, N. S. (2007). Planning for the future by western scrub-jays. *Nature* 445, 919–921. doi: 10.1038/nature05575

Rakic, P. (2007). The radial edifice of cortical architecture: from neuronal silhouettes to genetic engineering. *Brain Res. Rev.* 55, 204–219. doi: 10.1016/j.brainresrev.2007.02.010

Reiner, A., Yamamoto, K., and Karten, H. J. (2005). Organization and evolution of the avian forebrain. *Anat. Rec. A Discov. Mol. Cell. Evol. Biol.* 287, 1080–1102. doi: 10.1002/ar.a.20253

Reyes-Puerta, V., Sun, J. J., Kim, S., Kilb, W., and Luhmann, H. J. (2015). Laminar and columnar structure of sensory-evoked multineuronal spike sequences in adult rat barrel cortex *in vivo*. *Cereb. Cortex* 25, 2001–2021. doi: 10.1093/cercor/bhu007

Romano, E., Michetti, C., Caruso, A., Laviola, G., and Scattoni, M. L. (2013). Characterization of neonatal vocal and motor repertoire of reelin mutant mice. *PloS One* 8:e64407. doi: 10.1371/journal.pone.0064407

Salinger, W. L., Ladrow, P., and Wheeler, C. (2003). Behavioral phenotype of the reeler mutant mouse: effects of RELN gene dosage and social isolation. *Behav. Neurosci.* 117, 1257–1275. doi: 10.1037/0735-7044.117.6.1257

Scarf, D., Hayne, H., and Colombo, M. (2011). Pigeons on par with primates in numerical competence. *Science* 334:1664. doi: 10.1126/science.1213357

Schubert, D., Kötter, R., Luhmann, H. J., and Staiger, J. F. (2006). Morphology, electrophysiology and functional input connectivity of pyramidal neurons characterizes a genuine layer Va in the primary somatosensory cortex. *Cereb. Cortex* 16, 223–236. doi: 10.1093/cercor/bhi100

Schubert, D., Kötter, R., and Staiger, J. F. (2007). Mapping functional connectivity in barrel-related columns reveals layer- and cell type-specific microcircuits. *Brain Struct. Funct.* 212, 107–119. doi: 10.1007/s00429-007-0147-z

Schubert, D., Kötter, R., Zilles, K., Luhmann, H. J., and Staiger, J. F. (2003). Cell type-specific circuits of cortical layer IV spiny neurons. *J. Neurosci.* 23, 2961–2970.

Silva, L. R., Gutnick, M. J., and Connors, B. W. (1991). Laminar distribution of neuronal membrane properties in neocortex of normal and reeler mouse. *J. Neurophysiol.* 66, 2034–2040.

Simmons, P. A., Lemmon, V., and Pearlman, A. L. (1982). Afferent and efferent connections of the striate and extrastriate visual cortex of the normal and reeler mouse. *J. Comp. Neurol.* 211, 295–308. doi: 10.1002/cne.902110308

Simmons, P. A., and Pearlman, A. L. (1983). Receptive-field properties of transcallosal visual cortical neurons in the normal and reeler mouse. *J. Neurophysiol.* 50, 838–848.

Simons, D. J. (1978). Response properties of vibrissa units in rat SI somatosensory neocortex. *J. Neurophysiol.* 41, 798–820.

Sinex, D. G., Burdette, L. J., and Pearlman, A. L. (1979). A psychophysical investigation of spatial vision in the normal and reeler mutant mouse. *Vision Res.* 19, 853–857. doi: 10.1016/0042-6989(79)90018-x

Skoglund, T. S., Pascher, R., and Berthold, C. H. (1997). The existence of a layer IV in the rat motor cortex. *Cereb. Cortex* 7, 178–180. doi: 10.1093/cercor/7.2.178

Staiger, J. F. (2015). "S1 laminar specialization," in *Scholarpedia of Touch*, eds T. J. Prescott, E. Ahissar and E. M. Izhikevich (Paris: Atlantis Press), 507–533.

Staiger, J. F., Bojak, I., Miceli, S., and Schubert, D. (2015). A gradual depth-dependent change in connectivity features of supragranular pyramidal cells in rat barrel cortex. *Brain Struct. Funct.* 220, 1317–1337. doi: 10.1007/s00429-014-0726-8

Staiger, J. F., Flagmeyer, I., Schubert, D., Zilles, K., Kötter, R., and Luhmann, H. J. (2004). Functional diversity of layer IV spiny neurons in rat somatosensory cortex: quantitative morphology of electrophysiologically characterized and biocytin labeled cells. *Cereb. Cortex* 14, 690–701. doi: 10.1093/cercor/bhh029

Staiger, J. F., Loucif, A. J., Schubert, D., and Mock, M. (2016). Morphological characteristics of electrophysiologically characterized layer Vb pyramidal cells in rat barrel cortex. *PLoS One* 11:e0164004. doi: 10.1371/journal.pone.0164004

Staiger, J. F., Zilles, K., and Freund, T. F. (1996). Distribution of GABAergic elements postsynaptic to ventroposteromedial thalamic projections in layer IV of rat barrel cortex. *Eur. J. Neurosci.* 8, 2273–2285. doi: 10.1111/j.1460-9568.1996.tb01191.x

Stanfield, B. B., and Cowan, W. M. (1979). The morphology of the hippocampus and dentate gyrus in normal and reeler mice. *J. Comp. Neurol.* 185, 393–422. doi: 10.1002/cne.901850302

Steindler, D. A., and Colwell, S. A. (1976). reeler mutant mouse: maintenance of appropriate and reciprocal connections in the cerebral cortex and thalamus. *Brain Res.* 113, 386–393. doi: 10.1016/0006-8993(76)90949-5

Stubbs, D., DeProto, J., Nie, K., Englund, C., Mahmud, I., Hevner, R., et al. (2009). Neurovascular congruence during cerebral cortical development. *Cereb. Cortex* 19, i32–i41. doi: 10.1093/cercor/bhp040

Swadlow, H. A. (1989). Efferent neurons and suspected interneurons in S-1 vibrissa cortex of the awake rabbit: receptive fields and axonal properties. *J. Neurophysiol.* 62, 288–308.

Tan, S. S., Kalloniatis, M., Truong, H. T., Binder, M. D., Cate, H. S., Kilpatrick, T. J., et al. (2009). Oligodendrocyte positioning in cerebral cortex is independent of projection neuron layering. *Glia* 57, 1024–1030. doi: 10.1002/glia.20826

Taylor, A. H., Miller, R., and Gray, R. D. (2012). New Caledonian crows reason about hidden causal agents. *Proc. Natl. Acad. Sci. U S A* 109, 16389–16391. doi: 10.1073/pnas.1208724109

Terashima, T., Inoue, K., Inoue, Y., and Mikoshiba, K. (1987). Thalamic connectivity of the primary motor cortex of normal and reeler mutant mice. *J. Comp. Neurol.* 257, 405–421. doi: 10.1002/cne.902570309

Terashima, T., Inoue, K., Inoue, Y., Mikoshiba, K., and Tsukada, Y. (1983). Distribution and morphology of corticospinal tract neurons in reeler mouse cortex by the retrograde HRP method. *J. Comp. Neurol.* 218, 314–326. doi: 10.1002/cne.902180307

Terashima, T., Inoue, K., Inoue, Y., Mikoshiba, K., and Tsukada, Y. (1985). Distribution and morphology of callosal commissural neurons within the motor cortex of normal and reeler mice. *J. Comp. Neurol.* 232, 83–98. doi: 10.1002/cne.902320108

Tissir, F., and Goffinet, A. M. (2003). Reelin and brain development. *Nat. Rev. Neurosci.* 4, 496–505. doi: 10.1038/nrn1113

Veit, L., and Nieder, A. (2013). Abstract rule neurons in the endbrain support intelligent behaviour in corvid songbirds. *Nat. Commun.* 4:2878. doi: 10.1038/ncomms3878

Vicq d'Azyr, F. (1786). *Traité d'anatomie et de Physiologie avec des Planches Coloriées Représentant au Naturel les Divers Organes de l'homme et des Animaux.* Paris: François-Ambroise Didot.

Wagener, R. J., David, C., Zhao, S., Haas, C. A., and Staiger, J. F. (2010). The somatosensory cortex of reeler mutant mice shows absent layering but intact formation and behavioral activation of columnar somatotopic maps. *J. Neurosci.* 30, 15700–15709. doi: 10.1523/JNEUROSCI.3707-10.2010

Wagener, R. J., Witte, M., Guy, J., Mingo-Moreno, N., Kügler, S., and Staiger, J. F. (2016). Thalamocortical connections drive intracortical activation of functional columns in the mislaminated reeler somatosensory cortex. *Cereb. Cortex* 26, 820–837. doi: 10.1093/cercor/bhv257

Welt, C., and Steindler, D. A. (1977). Somatosensory cortical barrels and thalamic barreloids in reeler mutant mice. *Neuroscience* 2, 755–766. doi: 10.1016/0306-4522(77)90029-x

Wilson, L., Sotelo, C., and Caviness, V. S. Jr. (1981). Heterologous synapses upon Purkinje cells in the cerebellum of the reeler mutant mouse: an experimental light and electron microscopic study. *Brain Res.* 213, 63–82. doi: 10.1016/0006-8993(81)91248-8

Wimmer, V. C., Bruno, R. M., de Kock, C. P. J., Kuner, T., and Sakmann, B. (2010). Dimensions of a projection column and architecture of VPM and POm axons in rat vibrissal cortex. *Cereb. Cortex* 20, 2265–2276. doi: 10.1093/cercor/bhq068

Wright, N., and Fox, K. (2010). Origins of cortical layer V surround receptive fields in the rat barrel cortex. *J. Neurophysiol.* 103, 709–724. doi: 10.1152/jn.00560.2009

Yabut, O., Renfro, A., Niu, S. Y., Swann, J. W., Marín, O., and D'Arcangelo, G. (2007). Abnormal laminar position and dendrite development of interneurons in the reeler forebrain. *Brain Res.* 1140, 75–83. doi: 10.1016/j.brainres.2005.09.070

Ye, L., Allen, W. E., Thompson, K. R., Tian, Q. Y., Hsueh, B., Ramakrishnan, C., et al. (2016). Wiring and molecular features of prefrontal ensembles representing distinct experiences. *Cell* 165, 1776–1788. doi: 10.1016/j.cell.2016.05.010

Zilles, K., and Wree, A. (1995). "Cortex: areal and laminar structure," in *The Rat Nervous System*, ed. G. Paxinos (New York, NY: Academic Press), 649–685.

Conflict of Interest Statement: The authors declare that the research was conducted in the absence of any commercial or financial relationships that could be construed as a potential conflict of interest.

Advantages of publishing in Frontiers

OPEN ACCESS
Articles are free to read for greatest visibility and readership

FAST PUBLICATION
Around 90 days from submission to decision

HIGH QUALITY PEER-REVIEW
Rigorous, collaborative, and constructive peer-review

TRANSPARENT PEER-REVIEW
Editors and reviewers acknowledged by name on published articles

Frontiers
Avenue du Tribunal-Fédéral 34
1005 Lausanne | Switzerland

Visit us: www.frontiersin.org
Contact us: info@frontiersin.org | +41 21 510 17 00

REPRODUCIBILITY OF RESEARCH
Support open data and methods to enhance research reproducibility

DIGITAL PUBLISHING
Articles designed for optimal readership across devices

FOLLOW US
@frontiersin

IMPACT METRICS
Advanced article metrics track visibility across digital media

EXTENSIVE PROMOTION
Marketing and promotion of impactful research

LOOP RESEARCH NETWORK
Our network increases your article's readership